

University of Nottingham
UK | CHINA | MALAYSIA

TARGETING DNA REPAIR AND HYPOXIA TO IMPROVE RADIORESPONSE IN BREAST CANCER

Radhika Aiyappa

(BSc, MRes)

Thesis submitted to the University of Nottingham

for the degree of Doctor of Philosophy

July 2020

Abstract

Radiotherapy is an essential treatment modality in the clinical management of breast cancers, with an established role to reduce the risk of local recurrences. However, the repair of radiotherapy-induced DNA damage by cancer cells and the presence of tumour hypoxia reduces the efficacy of radiotherapy as a treatment modality. The present study aimed to assess how agents targeting DNA repair and hypoxia can modulate radioresponse in breast cancer. The aim of the current thesis was to investigate the single agent and radiosensitising efficacy of the FEN-1 inhibitor PTPD, and novel hypoxia-activated prodrug (HAP) KP167, in luminal and triple negative breast cancer models.

The efficacy of PTPD and KP167 were evaluated in two luminal (MCF-7 and T47D) and three triple negative (MDAMB-231, MDAMB-468 and BRCA-1 deficient MDAMB-436) breast cancer cell lines. The well-established DNA repair inhibitors such as the ATM inhibitor, KU-55933 and PARP-1/2 inhibitor, olaparib were used as controls against the FEN-1 inhibitor, PTPD in 2D normoxia cultures. The hypoxia activated prodrug, AQ4N was used as a comparator against its novel analogue KP167 in 3D spheroids, 2D normoxia and 2D hypoxia (1% O_2) cultures. The single agent and radiosensitising efficacy of PTPD and KP167 were assessed by clonogenic survival assays. The expression of cytochrome P450 enzymes, CYP2S1 and CYP2W1, involved in the bio-reductive activation of the HAPs were assessed in breast cancer cells by Western blot and in a large cohort of breast cancer patients (n=1426) by immunohistochemistry.

In vitro results show that PTPD was cytotoxic only in the BRCA-1 deficient MDAMB-436 cells and resulted in a 60% reduction in clonogenic survival, compared to 20-40% and 40-80% reduction across all breast cancer cells with KU-55933 and olaparib. KU-55933 and olaparib induced significant radiosensitisation across all phenotypes of breast cancer cells with sensitiser enhancement ratio's ($SER_{0.01}$) ranging between 1.61-3.42 and 1.60-2.35 respectively. PTPD was effective in radiosensitising only the triple negative cell lines, especially the BRCA-1 deficient MDAMB-436 with $SER_{0.01}$ of 1.50 compared to MDAMB-231 ($SER_{0.01}$ 1.31) and MDAMB-468

($SER_{0.01}$ 1.13) cells. PTPD did not induce any radiosensitisation in the luminal MCF-7 or T47D cells ($SER_{0.01}$ 1.00). The radiosensitisation observed in MDAMB-436 cells may be due, in part, to increased DNA double strand breaks, as assessed by the γH2AX assay, due to PTPD inhibition of single strand repair, along with its inherent double strand break repair deficiency. Such data indicate that PTPD is effective, particularly in the context of BRCA-1 deficiency. PTPD was able to induce some levels of radiosensitisation in the TNBC cell lines, this was however, lower compared to the control DNA repair inhibitors.

In vitro results suggest that AQ4N and KP167 may undergo hypoxia-specific activation as shown by increases in single agent cytotoxicity in 3D spheroid and 2D hypoxia models of breast cancer compared to response obtained in 2D normoxia cultures. KP167 was 2-100 fold more effective in reducing survival with IC_{50} values of (0.14-12.8) μM compared to AQ4N IC_{50} of (0.2–22.8) μM in breast cancer 3D cultures. The luminal MCF-7 and T47D cells were more sensitive to single agent AQ4N and KP167 across all 3 culture conditions and this may be due to the higher expression of CYP2W1 (assessed by Western blot), essential for both estrogen metabolism and HAP activation.

The radiosensitivity induced by HAPs were greater in 3D spheroid and 2D hypoxia models of breast cancer compared to normoxia cultures. Compared to AQ4N $SER_{0.01}$ of 1.30-3.33, a 100-fold increase in radiosensitisation was seen in KP167 treated cells with $SER_{0.01}$ of 1.46-4.55 in 3D spheroid cultures. Greater levels of radiosensitisation with KP167 was also seen in 2D normoxia ($SER_{0.01}$ of 1.21-1.93) and 2D hypoxia ($SER_{0.01}$ of 1.56-2.37) cultures compared to AQ4N $SER_{0.01}$ of 1.11-1.64 and 1.13-1.94 respectively. Such data indicate that KP167 is a potent radiosensitiser across both luminal and triple negative breast cancer cells and may hold promising potential in the treatment of hypoxic breast cancers.

Immunohistochemical studies show that high cytoplasmic CYP2S1 and nuclear CYP2W1 were able to identify a sub-group of ER-positive, HER-2 negative patients, above the age of 50 that may potentially benefit from HAP treatment. Low cytoplasmic CYP2S1 (P=0.034) and nuclear CYP2W1 (P=0.012) were significantly associated with adverse breast cancer specific

survival in the total patient cohort, which retained its significance in multivariate analysis (P=0.002 and P=0.007 respectively). Low cytoplasmic CYP2S1 and nuclear CYP2W1 were also associated with adverse survival in ER-positive (P=0.031) and ER-negative patients (P=0.020) respectively. The association of low CYP2S1 and CYP2W1 with adverse survival may suggest involvement of these enzymes in the metabolism of anti-cancer agents such as tamoxifen and taxanes used in breast cancer treatment. Such data establishes the prognostic significance of CYP2S1 and CYP2W1 in breast cancer.

Collectively, although further confirmation is needed, KP167 appears to be a promising agent, either single or combined with radiation, to target hypoxic breast cancer cells and improve patient outcomes. CYP2S1 and CYP2W1 may be of prognostic significance in breast cancer.

Presentations and awards arising from this thesis

Conference Presentations

Poster Presentation "Improved breast cancer radio-response with novel hypoxia-activated prodrugs". UK Interdisciplinary Breast Cancer Symposium, 2020, January 27-28, Birmingham, UK. Abstract published and selected for poster prize.

Poster Presentation "Improved radiotherapeutic response in breast cancer using novel hypoxia-activated prodrugs". Cancer Research Nottingham 2019, September 16, Nottingham, UK.

Poster Presentation "Improved radiotherapeutic response in breast cancer using novel hypoxia-activated prodrugs". International Congress of Radiation Research 2019, August 26-29, Manchester, UK.

Poster Presentation "Improved radiotherapeutic response in breast cancer using novel hypoxia-activated prodrugs". BACR Tumour Microenvironment conference 2019, July 1-3, Nottingham, UK.

Poster Presentation "Improved breast cancer radioresponse with novel hypoxia-activated prodrugs". 2nd Annual NBCRC Research Day 2019, 14 May, Nottingham, UK.

Poster presentation "Improving radiotherapy outcome in triple negative breast cancer by targeting DNA repair". Annual NBCRC Research Day 2018, March 26, Nottingham, UK.

Poster presentation "Targeting DNA Repair to improve radio therapeutic response." Radiation Research Society (RRS) Annual Meeting 2018, September 23-26, 2018, Chicago, USA.

Manuscripts arising from KP167 and IHC studies are currently in preparation.

Awards

2019	Radiation Research Society (RRS) SIT Travel Award.
2019	Association for Radiation Research (ARR) Travel Bursary.
2018	Sue Watson Postgraduate Oral Presentation Award.
2018	The British Association for Cancer Research (BACR) Student Travel Award.
2018	University of Nottingham School of Medicine Travel Prize.
2018	University of Nottingham Graduate School Travel Prize.

Acknowledgements

I sincerely thank my supervisor, Professor Stewart Martin, for his invaluable guidance, advice, support and encouragement given during the tenure of my study. I am grateful for his excellent supervision which has inspired me to reach my maximum potential.

I thank Professor Srinivasan Madhusudan for the advice and support provided during the DNA repair study. I am grateful to Dr Klaus Pors for supplying the hypoxia-activated prodrugs, and for sharing his knowledge and expertise. I thank Dr Sarah Storr for her supervision, training and support provided during my study. Special thanks to Dr Andrew Green for his guidance and kind help with data analysis.

A special thank you to my colleagues, both past and present at the Academic Unit of Clinical Oncology, especially Bhudsaban Sukkarn, Khaled Al-Hadyan, Nurul Abdullah, Yao Anqi, Richa Vasan, Behnaz Saidy and Martina Quartieri for their support and friendship.

No words can ever be strong enough to express gratitude to my parents, Dr MN Aiyappa and Rajani Aiyappa for their unconditional love and numerous sacrifices. The greatest thanks goes to my dad for inspiring me to choose this path, for believing in me, for his continual support and encouragement. I thank my mum for her kindness, patience, support, and everlasting presence. I thank my brother Bopanna Aiyappa, sister and brother in law, Relica and Arjun Thimmaiah, for those 'laughter-filled' days, for always having my back and keeping me grounded.

I am indebted to my husband Jamie Maudsley, for his love, care, patience and companionship. I thank my in laws, Jasper and Jacqui Maudsley, for their unconditional love and support.

I would like to dedicate this thesis to my dad, without whom, this journey would not be possible.

Abbreviations

2D	2 dimensional
2-OHE_2	2-hydroxyestradiol
3D	3 dimensional
4-OHE2	4-hydroxyestradiol
5-FU	5-fluorouracil
AH	atypical hyperplasia
AI	aromatase inhibitors
AJCC	American Joint Committee on Cancer
ALND	axillary lymph node dissection
AP	apurinic/apyrimidinic
APBI	accelerated partial breast irradiation
APE1	apurinic endonuclease 1
ATCC	American Type Culture Collection
ATM	ataxia telangiectasia mutated
ATR	ataxia-telangiectasia and rad3 related protein
BCS	breast-conserving surgery
BCSS	breast cancer specific survival
BCT	breast-conserving therapy
BER	base excision repair
BMI	body mass index
BRCA-1	Breast Cancer Susceptibility Gene -1
BRCA-2	Breast Cancer Susceptibility Gene -2
CA9	carbonic anhydrase 9
CDK	cyclin dependent kinase
CFRT	conventional multifractionated radiotherapy
CHK-1/2	checkpoint kinase-1/2
CI	confidence interval
CMF	cyclophosphamide, methotrexate, and fluorouracil
CRUK	Cancer Research United Kingdom
CS-CAL	clonogenic survival calculation software
CT	chemotherapy
CYP	cytochrome P450
DCIS	ductal carcinoma *in situ*
DDR	DNA damage response
DM	distant metastasis
DMSO	dimethyl sulfoxide
DNA	deoxyribonucleic acid

DNA-PK	DNA-dependent protein kinase
dRP	deoxyribose-phosphate
DSB	double-strand break
EBC	early breast cancer
EBCTCG	Early Breast Cancer Trialists' Collaborative Group
EBRT	external beam radiotherapy
ECL	enhanced chemiluminescence
ECM	extracellular matrix
EDTA	ethylenediamine tetra acetic acid
EMA	European Medicines Agency
EMR	electromagnetic radiation
EMT	epithelial to mesenchymal transition
EP-HRT	estrogen and progestin HRT
ER	estrogen receptor
EU	European Union
EXO	exonuclease
FACS	fluorescence-activated cell sorting
FDA	Food and Drug Administration
FEN-1	Flap-endonuclease 1
FISH	fluorescent *in situ* hybridisation
FITC	fluorescein isothiocyanate
GEN	GAP endonuclease
GLOBOCAN	global cancer statistics
Gy	gray
H_2O_2	hydrogen peroxide
HAP	hypoxia-activated prodrugs
HDR	high-dose rate
HER-2	human epidermal growth factor receptor-2
HFRT	hypofractionated radiotherapy
HICR	hypoxia-induced chemoresistance
HIF-1α	hypoxia-inducible factor-1α
HNC	head and neck cancer
HNSCC	head and neck squamous cell carcinoma
HR	hazard radio
HRE	hypoxia responsive elements
HRP	horseradish peroxidase
HRR	homologous recombination repair
HRT	hormone replacement therapy
HT	hormonal therapy

IBC	inflammatory breast carcinoma
IC_{50}	half maximal inhibitory concentration
ICC	intraclass correlation co-efficient
ICL	interstrand cross link repair
IDC	invasive ductal carcinoma
IHC	immunohistochemistry
ILC	invasive lobular carcinoma
IMRT	intensity-modulated radiation therapy
IMS	industrial methylated spirit
iNOS	inducible nitric oxide synthase
IORT	intraoperative radiotherapy
IR	ionising radiation
kDa	kilo dalton
LAPC	locally advanced primary breast cancer
LCIS	lobular carcinoma *in situ*
LDR	low-dose rate
LET	Linear energy transfer
LHRH	luteinizing hormone-releasing hormone
LN	lymph-node
LP-BER	long patch-base excision repair
LQ	linear-quadratic
LVI	lymphovascular invasion
MBC	metastatic breast cancer
MDR-1	multi-drug resistance-1
METABRIC	Molecular taxonomy of Breast Cancer International Consortium
MFI	median fluorescence intensity
ml	millilitre
mM	millimolar
MR	mismatch repair
MRN	MRE11/NBS1/RAD5
NACT	Neoadjuvant chemotherapy
NCI-60	National Cancer Institute-60
NHEJ	non-homologous end-joining
NHS	National Health Services
NICE	National Institute for Health and Care Excellence
NPI	Nottingham Prognostic Index
NQO1	NADPH: Quinone oxidoreductase 1
NQO2	NADPH: Quinone oxidoreductase 2
NSCLC	non-small cell lung cancer

OC	oral contraception
OCR	oxygen consumption rate
OER	oxygen enhancement ratio
OFH	oxygen fixation hypothesis
$OH^{\bullet}$	hydroxyl radical
ONS	Office for national statistics
PARP	poly (ADP-ribose) polymerase
PBS	phosphate buffered saline
PCNA	proliferating cell nuclear antigen
pCR	pathological complete response
PE	plating efficiency
PFS	progression free survival
PGE_2	prostaglandin E2
PgR	progesterone receptor
PI3K	phosphoinositide 3-kinase
PMRT	post-mastectomy radiotherapy
Polβ	polymerase β
qRT-PCR	quantitative real time-PCR
RCPath	Royal College of Pathologists
RIPA	radioimmunoprecipitation assay
RNA	ribonucleic acid
ROS	reactive oxygen species
RPA	replication protein A
SABR	stereotactic ablative body radiotherapy
SD	standard deviation
SDS-PAGE	sodium dodecyl sulfate poly-acrylamide gel electrophoresis
SEER	Surveillance, Epidemiology, and End Results
SER	sensitiser enhancement ratios
SERD	selective ER down-regulators
SERM	selective ER modulators
SF	surviving fraction
SLNB	sentinel lymph node biopsy
SP-BER	short patch-base excision repair
SRS	stereotactic radiosurgery
SSB	single-strand break
ssDNA	single-stranded DNA
STR	short tandem repeat
TAM	tumour-associated macrophages

TBS	tris buffered saline
TCGA	The Cancer Genome Atlas
T-DM1	trastuzumab emtansine
T-FAC	taxane-fluorouracil-doxorubicin-cyclophosphamide
TMA	tissue microarray
TNBC	triple negative breast cancer
TOPO II	topoisomerase II
UK	United Kingdom
UK RCPath	Royal College of Pathologists
V	voltage
VEGF	vascular endothelial growth factor
WBI	whole breast irradiation
WHO	World Health Organization
XLF	XRCC 4-like factor
XRCC4	X-ray cross-complementation group 4
µg	microgram
µg/mL	microgram per millilitre
µl	microliter
µM	micromolar
χ^2	Pearson Chi Square test of association

Table of Contents

Abstract ..... **i**
Presentations and awards arising from this thesis ..... **iv**
Acknowledgements ..... **vi**
Abbreviations ..... **vii**
Table of Contents ..... **xii**
List of Tables ..... **xvii**
List of Figures ..... **xix**
Chapter 1 Introduction **1**
1.1 Introduction to Breast Cancer *2*
1.1.1 Epidemiology 2
1.1.2 Risk factors 3
1.1.3 Breast cancer classification 6
1.1.4 Predictive and prognostic factors 12
1.1.5 Treatment options for breast cancer 17
1.2 Radiotherapy *22*
1.2.1 Biological effects of radiotherapy 22
1.2.2 Repair of radiation induced DNA damage 24
1.2.3 Modelling of radiobiological effect 25
1.2.4 Radiotherapy regimens for breast cancer 26
1.2.5 Strategies to improve radiotherapy response 29
1.3 Overall study hypotheses, aims and objectives *30*
Chapter 2 Targeting LP-BER to improve radioresponse in breast cancer **32**
2.1 Abstract *33*
2.2 Introduction and aims *35*
2.2.1 DNA damage response 35
2.2.2 Double strand break repair pathway 37
2.2.3 Single strand break repair pathway-BER 38
2.2.4 Flap endonuclease-1 40
2.2.5 DNA repair inhibitors as novel anticancer therapies 42
2.2.6 FEN-1 inhibitors 43
2.2.7 Hypothesis, aims and objectives 45
2.3 Materials and Methods *46*

2.3.1 Cell lines and culture conditions 46
2.3.2 Sub-culture 47
2.3.3 Cryopreservation and cell recovery 47
2.3.4 Drugs and drug preparation 48
2.3.5 Cell growth curves by proliferation assay 48
2.3.6 Clonogenic survival assay 49
2.3.7 Cell irradiation 51
2.3.8 Drug-radiation combinations 51
2.3.9 Immunofluorescence 52
2.3.10 Statistical analysis 54
2.4 Results 54
2.4.1 Growth characteristics of breast cancer cells 54
2.4.2 Characterisation of positive control drugs – KU-55933 and olaparib 56
2.4.3 Cytotoxicity of PTPD on breast cancer cells 59
2.4.4 Intrinsic radiosensitivity of breast cancer cells 63
2.4.5 Radiosensitisation with KU-55933 and olaparib 65
2.4.6 Radiosensitisation with PTPD 70
2.4.7 RPA and γ-H2AX DNA damage assays 73
2.5 Discussion 79
Chapter 3 Hypoxia-activated prodrugs in 3D and 2D models of breast cancer 91
3.1 Abstract 92
3.2 Introduction and aims 94
3.2.1 Hypoxia 94
3.2.2 Hypoxic radiosensitisers 98
3.2.3 Hypoxia-activated prodrugs 99
3.2.4 AQ4N and novel analogues 103
3.2.5 2D and 3D *in vitro* culture models 107
3.2.6 Hypothesis and aims 108
3.3 Materials and Methods 110
3.3.1 Cell lines and culture conditions 110
3.3.2 Drugs and drug preparation 110
3.3.3 3D spheroid formation, optimisation and culture 111
3.3.4 Plating efficiencies - 2D v 3D 111
3.3.5 Drug penetration experiments 112

3.3.6 Clonogenic survival assays - 3D 113
3.3.7 Proliferation and clonogenic survival assays - 2D.....113
3.3.8 Cell lysis and protein extraction 114
3.3.9 Western blotting 115
3.3.10 Cell irradiation - 2D v 3D.....117
3.3.11 Drug-radiation combinations - 3D and 2D.....117
3.3.12 Statistical analysis.....118
3.4 Results 118
3.4.1 3D spheroid culture 118
3.4.2 Cytotoxicity of AQ4N and KP167 - 3D 124
3.4.3 Cytotoxicity of AQ4N and KP167 on proliferation - 2D 127
3.4.4 Cytotoxicity of AQ4N and KP167 on survival - 2D 131
3.4.5 Endogenous reductase expression 135
3.4.6 Radioresponse of breast cancer cells - 2D v 3D 140
3.4.7 Radiosensitisation with AQ4N and KP167 - 3D 143
3.4.8 Radiosensitisation with AQ4N and KP167 - 2D 149
3.5 Discussion 155
Chapter 4 Hypoxia-activated prodrugs in 2D hypoxia models of breast cancer.....168
4.1 Abstract 169
4.2 Introduction 171
4.2.1 Oxygen effect 171
4.2.2 HIF-1α and radiotherapy 171
4.2.3 Targeting hypoxia 173
4.2.4 Hypothesis and aims.....175
4.3 Materials and Methods 177
4.3.1 Cell lines and culture conditions 177
4.3.2 Drugs and drug preparation.....177
4.3.3 Radioresponse in 0.5% and 1% O_2 177
4.3.4 Western blotting for CA9 178
4.3.5 Cell growth - 2D normoxia v 2D hypoxia 179
4.3.6. Plating efficiencies - 2D normoxia v 2D hypoxia 180
4.3.7 Cytotoxicity assessment of AQ4N and KP167 - 2D hypoxia ...180
4.3.8 Cell irradiation - 2D normoxia v 2D hypoxia.....181
4.3.9 Drug-radiation combinations - 2D hypoxia.....181
4.3.10 Statistical analysis 182

4.4 Results 182
4.4.1 Radioresponse with 0.5% and 1% O_2.....182
4.4.2 Cell growth curves in 2D normoxia v 2D hypoxia.....184
4.4.3 Plating efficiencies in 2D normoxia v 2D hypoxia 186
4.4.4 Cytotoxicity of AQ4N and KP167 in 2D hypoxia 188
4.4.5 Radioresponse of breast cancer cells in 2D normoxia v 2D hypoxia 194
4.4.6 Radiosensitisation with AQ4N and KP167 in 2D hypoxia 196
4.5 Discussion 203
Chapter 5 The expression of CYP2S1 and CYP2W1 in breast cancer 213
5.1 Abstract 214
5.2 Introduction 216
5.2.1 Cytochrome P450 enzymes 216
5.2.2 CYP2S1 and CYP2W1 217
5.2.3 CYP enzymes in estrogen and drug metabolism 218
5.2.4 Hypothesis and aims.....221
5.3 Materials and methods.....223
5.3.1 Patient cohorts.....223
5.3.2 Tissue microarray use.....225
5.3.3 Antibody optimisation 225
5.3.4 Immunohistochemistry 226
5.3.5 Immunohistochemical scoring.....227
5.3.6 Statistical analysis.....228
5.4 Results 229
5.4.1 Optimisation of primary antibodies 229
5.4.2 CYP2S1 staining and frequency 230
5.4.3 CYP2W1 staining and frequency 231
5.4.4 Correlation between CYP2S1 and CYP2W1 protein expression 233
5.4.5 Association of CYP2S1 and clinicopathological variables 234
5.4.6 Association of CYP2W1 and clinicopathological variables.....238
5.4.7 Association of CYP2S1 and overall survival 241
5.4.8 Association of CYP2W1 and overall survival 242
5.4.9 Association of CYP2S1 and CYP2W1 with survival in ER-positive and negative breast cancers 244
5.4.10 Combined cytoplasmic/nuclear CYP2S1 and survival 247

5.4.11 Combined cytoplasmic/nuclear CYP2W1 and survival 249
5.4.12 Association of combined CYP2S1/CYP2W1 and survival 250
5.4.13 Association of CYP2S1 and CYP2W1 mRNA with clinicopathological variables and survival in the METABRIC cohort..253
5.5 Discussion 254
Chapter 6 General discussion, Limitations and Suggestions for future work 264
6.1 General discussion.....265
6.2 Limitations and suggestions for future work.....279
6.3 Conclusions 283
References.....284
Appendix A: Supplementary information for Chapter 2.....333
Appendix B: Supplementary information for Chapter 3.....345
Appendix C: Supplementary information for Chapter 4.....356
Appendix D: Supplementary information for Chapter 5 360

List of Tables

Table 1.1 Subtypes of breast cancer and receptor profile. 9
Table 2.1 Plating efficiencies of breast cancer cell lines. 56
Table 2.2 Radiobiologic parameters of breast cancer cells. 64
Table 2.3 Radiobiologic parameters of breast cancer cells treated with IR and/or KU-55933. 67
Table 2.4 Radiobiologic parameters of breast cancer cells treated with IR and/or olaparib. 69
Table 2.5 Radiobiologic parameters of breast cancer cells treated with IR and/or PTPD. 72
Table 3.1 Buffers for Western blot. 115
Table 3.2 List of antibodies used in Western blot. 116
Table 3.3 Clonogenic IC_{50} values of AQ4N and KP167 in breast cancer spheroids. 126
Table 3.4 Proliferation IC_{50} values of AQ4N and KP167 in 2D normoxia. 130
Table 3.5 Clonogenic IC_{50} values of AQ4N and KP167 in 2D normoxia. 134
Table 3.6 Radiobiologic parameters of breast cancer cells in 2D normoxia and 3D spheroid cultures. 142
Table 3.7 Radiobiologic parameters of breast cancer spheroids treated with IR and/or AQ4N. 145
Table 3.8 Radiobiologic parameters of breast cancer spheroids treated with IR and/or KP167. 147
Table 3.9 Radiobiologic parameters of 2D breast cancer cells treated with IR and/or AQ4N. 151
Table 3.10 Radiobiologic parameters of 2D breast cancer cells treated with IR and/or KP167. 153
Table 3.11 Combined $SER_{0.01}$ values of AQ4N and KP167 in 3D spheroids v 2D normoxic cultures. 154
Table 4.1 List of antibodies used in Western blot. 178
Table 4.2 Radiobiologic parameters of breast cancer cells in 2D normoxia and 2D hypoxia cultures (0.5% and 1% O_2). 183
Table 4.3 Doubling time of 2D breast cancer cells in normoxia (21% O_2) and hypoxia (1% O_2). 186
Table 4.4 Proliferation IC_{50} of AQ4N and KP167 in 2D hypoxia (1% O_2) v 2D normoxia. 190
Table 4.5 Clonogenic IC_{50} of AQ4N and KP167 in 2D hypoxia (1% O_2) v 2D normoxia and 3D spheroids. 192
Table 4.6 Radiobiologic parameters of breast cancer cells in 2D normoxia and hypoxia (1% O_2) cultures. 196
Table 4.7 Radiobiologic parameters of breast cancer cells in 2D hypoxia treated with IR and/or AQ4N. 198
Table 4.8 Radiobiologic parameters of breast cancer cells in 2D hypoxia treated with IR and/or KP167. 200
Table 4.9 Compiled $SER_{0.01}$ values of DNA repair inhibitors and hypoxia-activated prodrugs. 202

Table 5.1 Clinicopathological parameters of breast cancer tissues. 224
Table 5.2 Correlation between CYP2S1 and CYP2W1 protein expression. 233
Table 5.3 Correlation of CYP2S1 with clinicopathological parameters in breast cancer tissues. 235
Table 5.4 Correlation of CYP2W1 with clinicopathological parameters in breast cancer tissues. 238
Table 5.5 Cox proportional hazards analysis for overall survival for cytoplasmic CYP2S1 expression. 242
Table 5.6 Cox proportional hazards analysis for overall survival for cytoplasmic CYP2W1 expression. 243

List of Figures

Figure 1.1 Kaplan Meir survival curves of breast cancer subtypes. 11
Figure 1.2 Direct and indirect effects of ionising radiation. 23
Figure 2.1 Short and long-patch base excision repair. 40
Figure 2.2 Growth curves of breast cancer cells. 55
Figure 2.3 KU-55933 clonogenic survival of breast cancer cells..... 57
Figure 2.4 Olaparib clonogenic survival of breast cancer cells. 58
Figure 2.5 Effect of PTPD on cell proliferation of breast cancer cells. 60
Figure 2.6 PTPD clonogenic survival of breast cancer cells. 62
Figure 2.7 Survival curves of breast cancer cells after single dose irradiation..... 63
Figure 2.8 KU-55933 radiosensitivity in breast cancer cells..... 66
Figure 2.9 Olaparib radiosensitivity in breast cancer cells. 68
Figure 2.10 PTPD radiosensitivity in breast cancer cells..... 71
Figure 2.11 RPA expression in MCF-7 cells following treatment with PTPD and/or radiation. 74
Figure 2.12 Quantified RPA expression in MCF-7, T47D, MDAMB-231, MDAMB-468 and MDAMB-436 cells..... 75
Figure 2.13 γ-H2AX formation in MCF-7 cells following treatment with PTPD and/or radiation. 77
Figure 2.14 Quantified γ-H2AX expression in MCF-7, T47D, MDAMB-231, MDAMB-468 and MDAMB-436 cells. 78
Figure 3.1 Activation of hypoxia-activated prodrugs by one- or two-electron reductases.....100
Figure 3.2 Reductive activation of AQ4N to AQ4. 103
Figure 3.3 Reductive activation of OCT1002 to OCT1001. 105
Figure 3.4 Reductive activation of KP167. 106
Figure 3.5 Morphology of MCF-7, T47D, MDAMB-231, MDAMB-468 and MDAMB-436 spheroids. 119
Figure 3.6 Breast cancer spheroid diameters over an 8-day culture. 120
Figure 3.7 Plating efficiencies of cells grown in 2D normoxia v 3D spheroid culture. 122
Figure 3.8 Visualisation of AQ4N and KP167 penetration in MCF-7 and MDAMB-231 spheroids. 123
Figure 3.9 AQ4N and KP167 spheroid clonogenic survival. 125
Figure 3.10 Effect of AQ4N on proliferation of breast cancer cells in 2D normoxia. 127
Figure 3.11 Effect of KP167 on proliferation of breast cancer cells in 2D normoxia. 129
Figure 3.12 AQ4N clonogenic survival in 2D normoxia. 132
Figure 3.13 KP167 clonogenic survival in 2D normoxia. 133
Figure 3.14 CYP expression in breast cancer cells in normoxia (21% O_2) and hypoxia (0.1% O_2).....137
Figure 3.15 NQO1 and NQO2 expression in breast cancer cells in normoxia (21% O_2) and hypoxia (0.1% O_2). 139
Figure 3.16 Radiation response of cells in 2D v 3D culture.....141

Figure 3.17 AQ4N radiosensitivity in 3D spheroids.....144
Figure 3.18 KP167 radiosensitivity in 3D spheroids.....146
Figure 3.19 AQ4N radiosensitivity in 2D normoxia. 150
Figure 3.20 KP167 radiosensitivity in 2D normoxia. 152
Figure 4.1 HIF-1 mediated effects after radiotherapy. 172
Figure 4.2 Radioresponse of MDAMB-231 cells in 2D normoxia v 2D hypoxia (0.5 and 1% O_2).....183
Figure 4.3 Effect of normoxia and hypoxia (1% O_2) on proliferation of breast cancer cells. 185
Figure 4.4 Plating efficiencies of breast cancer cells in 2D normoxia and hypoxia (1% O_2) culture conditions.....187
Figure 4.5 Effect of AQ4N and KP167 on proliferation in 2D hypoxia (1% O_2). 189
Figure 4.6 AQ4N and KP167 on clonogenic survival in 2D hypoxia (1% O_2). 191
Figure 4.7 Radiation response in 2D normoxia and hypoxia (1% O_2). 195
Figure 4.8 AQ4N radiosensitivity in 2D hypoxia (1% O_2). 197
Figure 4.9 KP167 radiosensitivity in 2D hypoxia (1% O_2). 199
Figure 5.1 Optimisation of CYP2S1 and CYP2W1 antibody in breast tumour composite sections consisting of six stage I breast tumours (grade 1 to 3). 229
Figure 5.2 Distribution histogram of CYP2S1 H-score. 230
Figure 5.3 Representative photomicrographs of CYP2S1 in breast cancer tissues. 231
Figure 5.4 Distribution histogram of CYP2W1 H-score.....232
Figure 5.5 Representative photomicrographs of CYP2W1 in breast cancer tissues. 232
Figure 5.6 Kaplan-Meier survival analysis of CYP2S1 and breast cancer specific survival. 241
Figure 5.7 Kaplan-Meier survival analysis of CYP2W1 and breast cancer specific survival. 243
Figure 5.8 Kaplan-Meier analysis of CYP2S1 and survival in ER-positive and negative breast cancers.....245
Figure 5.9 Kaplan-Meier analysis of CYP2W1 and survival in ER-positive and negative breast cancers. 246
Figure 5.10 Kaplan-Meier analysis of combined cytoplasmic and nuclear CYP2S1 on breast cancer specific survival. 248
Figure 5.11 Kaplan-Meier analysis of combined cytoplasmic and nuclear CYP2W1 on breast cancer specific survival. 250
Figure 5.12 Kaplan-Meier analysis of combined CYP2S1/CYP2W1 and breast cancer specific survival. 251

Chapter 1 Introduction

1.1 Introduction to Breast Cancer

1.1.1 Epidemiology

Breast cancer is the most commonly diagnosed cancer in women in the UK and worldwide. An estimated 2.1 million new cases were diagnosed worldwide in 2018, accounting for 11.6% of all new cancer cases. According to Global Cancer Statistics (GLOBOCAN), about 600,000 (6.6%) women are estimated to have died from breast cancer in 2018 (Bray et al., 2018). In the UK, breast cancer accounts for 15% of all new cancer cases. The latest statistics from Cancer Research United Kingdom (CRUK), report 55,213 new cases and 11,399 deaths, making breast cancer the second leading cause of cancer-related deaths (CRUK, 2019). CRUK estimates that 1 in 8 women and 1 in 870 men in the UK have a lifetime risk of developing breast cancer (CRUK, 2019).

The worldwide incidence of female breast cancer has been estimated to reach approximately 3.2 million new cases/year by 2050 (Hortobagyi et al., 2005). In the UK, breast cancer incidence rates are predicted to rise by 2% between 2014 and 2035 with an estimated 210 cases per 100,000 women (Smittenaar et al., 2016). The incidence of breast cancer is more prevalent in developed countries (71.7 per 100,000) compared to developing countries (29.3 per 100,000), although the corresponding mortality rates are higher in developing countries. Globally, the five-year relative survival ranges from 12% in Africa to 90% in America, Australia and Canada (Abdulrahman and Rahman, 2012, Youlden et al., 2012, Rojas and Stuckey, 2016). Since the early 1970s, breast cancer mortality rates have decreased by almost 39% in the UK (CRUK, 2019). This decrease in breast cancer mortality can be attributed to increased public awareness, better access to population based mammographic screening and improved treatments (Youlden et al., 2012, Rojas and Stuckey, 2016). Early detection (smaller tumours with lower lymph node involvement) through implementation of mammography screening has resulted in higher rates of surgery, ensuring more successful treatment outcomes (Zabicki et al., 2006, Son et al., 2006).

1.1.2 Risk factors

A number of genetic and non-genetic factors contribute to the risk of developing breast cancer. These include age, genetic predisposition (e.g. sporadic/familial mutations in BRCA-1 and BRCA-2 (breast cancer susceptibility genes 1 and 2)), endogenous (early menarche, late menopause) and exogenous (hormone replacement therapy (HRT), oral contraception (OC)) exposure to hormones, high breast density, history of atypical hyperplasia and lifestyle factors (obesity, alcohol and smoking) (Reeves et al., 2012). Some of the important breast cancer risk factors are discussed below.

1.1.2.1 Age

Age is one of the most important risk factors for breast cancer development (Thakur et al., 2017). The American Cancer Society estimates that 1 in 43 women over the age of 50 will develop breast cancer (DeSantis et al., 2019). According to CRUK, breast cancer incidence are highest in women above 90 years of age, and 48% of all breast cancers are diagnosed in women over the age of 50 (CRUK, 2019). However, breast cancer when diagnosed in younger pre-menopausal women are often associated with an aggressive disease and a higher risk of relapse and death (Partridge et al., 2016).

1.1.2.2 Genetic predisposition and family history

Mutations in a number of genes have been shown to be associated with a predisposition to breast cancer. However mutation in one of the two breast cancer susceptibility genes, BRCA-1 and BRCA-2, is the greatest risk factor for breast cancer development (Hawsawi et al., 2019). BRCA-1/2 genes are involved in genome protection and work in different stages of DNA damage response (DDR) and DNA repair (Roy et al., 2011). Germline mutations in the BRCA-1 and BRCA-2 tumour suppressor genes account for 10% of all newly diagnosed breast cancers (Rebbeck et al., 1996). Early-onset breast cancer in immediate relatives is a risk factor for the occurrence of breast cancer in BRCA-1 and BRCA-2 carriers (Narod et al., 2014). Based on a prospective study, the cumulative risk of developing

breast cancer by 80 years of age was 72% for BRCA-1 carriers and 69% for BRCA-2 carriers (Kuchenbaecker et al., 2017). An individual who carries a BRCA-1/2 mutation has a 50-80% lifetime risk of developing breast cancer and 30-50% risk of developing ovarian cancer (Mehrgou and Akouchekian, 2016).

1.1.2.3 Endogenous exposure - Reproductive factors

Reproductive factors that influence hormonal status such as early age at menarche, late menopause, late age at first pregnancy and nulliparity are linked to an increase in the incidence of breast cancer (Kelsey and Bernstein, 1996). Lengthening the reproductive life of a woman, either by an earlier menarche or later menopause, increases the risk of breast cancer suggesting that the overall duration of the exposure to estrogen is the underlying risk factor (Korenman, 1980, Li et al., 2017). Studies by the Collaborative Group on Hormonal Factors show that early age at menarche (<11 years) increases the risk of breast cancer, while a later age at menarche (>14 years) reduces the risk by 18%. Late age at first pregnancy (>35 years) is associated with the risk of developing estrogen receptor (ER)-positive breast cancer compared to women who give birth at a younger age (<19 years) (Ritte et al., 2013). Previous studies have reported that parity provides a life-long protection against breast cancer by up to 50% (MacMahon et al., 1970); however a recent meta-analysis revealed that this protection may only be limited to women with an ER-positive disease (Ursin et al., 2005).

1.1.2.4 Exogenous exposure - Hormone related factors

The use of HRT to reduce menopausal symptoms and the consumption of OC are risk factors (Cogliano et al., 2005), as the estrogens and progestins present in HRT and OC contribute to promotion and acceleration of breast cancer, especially in those tumours that are hormone-dependent (Dall and Britt, 2017). Studies conducted on 16,928 women report that combined use of estrogen and progestin (EP-HRT) preparations increased the risk of breast cancer compared to users of estrogen-only regimens (E-only HRT) (Thorbjarnardottir et al., 2014). However, other studies have found no such associations (Dumeaux et al., 2005).

1.1.2.5 High breast density

Studies have shown that women with high breast density have a four- to six-fold increased risk of developing breast cancer (Vachon et al., 2007, Duffy et al., 2018). A greater amount of epithelial tissue in the breast indicates a greater chance of cancer arising in the epithelial cells (Boyd et al., 2011). Having dense breast tissues also results in false negatives during screening, leading to a higher incidence of breast cancer even in those who were previously screened as being negative (van Gils et al., 1998).

1.1.2.6 Atypical hyperplasia

Atypical hyperplasia (AH) is the accumulation of abnormal epithelial cells in the breast and is a high-risk benign lesion, found in ~10% of patient biopsies (Simpson, 2009). AH lies between a benign and a malignant state because it contains some of the required features for cancer initiation and therefore is considered to be a pre-malignant lesion (Dupont and Page, 1985, Allred et al., 2001). Studies have reported that the incidence of breast cancer after diagnosis of atypical ductal hyperplasia was 29% over 25 years. Increased frequency of mammograms is advised in patients who are diagnosed with AH and a family history of breast cancer (Hartmann et al., 2015).

1.1.2.7 Lifestyle

A strong association exists between lifestyle choices such as obesity, alcohol consumption, and smoking to the risk of developing breast cancer (La Vecchia et al., 2011). Obesity (body mass index (BMI)> 30/kg.m^2) is strongly associated with higher breast cancer risk in post-menopausal women, and a worse disease outcome for women regardless of age (Picon-Ruiz et al., 2017). Data from 12 prospective cohort studies comprising 22,728,674 women reported that every 5 kg/m^2 increase in BMI corresponds to a 2% increased risk in the incidence of breast cancer (Liu et al., 2018). This association between higher BMI and breast cancer risk is related to estrogen production since women with higher amount of body fat have higher levels of circulating estrogens (Cleary and Grossmann, 2009). Epidemiological data show that almost 4% of breast cancer cases

in developed countries can be attributed to alcohol consumption (Hamajima et al., 2002). A prospective study with 105,986 women followed from 1980-2008, reported a 10% increased risk of breast cancer for every 10g of alcohol consumed daily (Smith-Warner et al., 1998, Hamajima et al., 2002, Zhang et al., 2007). Several studies have found a positive association between smoking and breast cancer, especially in women who started smoking at an early age (<17 years) (McTiernan, 2003, Jones et al., 2017).

1.1.3 Breast cancer classification

1.1.3.1 Histological subtypes

Breast cancer can be classified into histological subtypes based on morphological and cytological growth patterns that are consistently associated with distinct clinical presentation and response to therapy (Walker, 2005, Weigelt and Reis-Filho, 2009, Weigelt et al., 2010). Breast cancers arising from the ducts of breast tissues are termed as ductal carcinomas and those that arise from the lobules of the breast are called lobular carcinomas (Malhotra et al., 2010). Ductal and lobular breast cancers can be classified further into non-invasive (*in situ*), locally advanced primary (LAPC) (discussed subsequently) or invasive carcinomas (Ellis et al., 1992). Non-invasive breast carcinomas are a heterogeneous group of tumours which although cancerous, are confined to the ducts and lobules (Allred, 2010). They can be ductal carcinoma *in situ* (DCIS) (20-30%) or lobular carcinoma *in situ* (LCIS) (2%) (Weigelt et al., 2010), and are considered to be immediate precursors of invasive cancers (Wellings and Jensen, 1973, Allred, 2010). Invasive breast cancers occur more frequently, invade surrounding tissue and have the ability to metastasize to different sites (Malhotra et al., 2010). The major invasive tumour types include infiltrating ductal (IDC), invasive lobular, (ILC), mucinous, tubular, medullary and papillary carcinomas (Weigelt and Reis-Filho, 2009, Weigelt et al., 2010). Of these, IDC is the most common (70-80%), followed by ILC which accounts for 10% of all breast cancers (Li et al., 2005, Sinn and Kreipe, 2013). Compared to IDC, patients with ILC have a better 5-year recurrence-free (66% v 87%) and overall survival (70% v 93%)

(Cristofanilli et al., 2005). Tubular, mucinous, and papillary carcinomas usually have excellent clinical outcome compared to IDC and ILC (Ellis et al., 1992, Rosen et al., 1993).

Breast cancers can be classified clinically as early-stage invasive (EBC), locally advanced primary (LAPC) or metastatic (MBC) breast cancer according to the clinical and pathological parameters such as tumour size, tumour type, histological grade, nodal involvement and lymphovascular invasion (LVI). Early-stage invasive breast cancer refers to stage I and stage II breast cancer that have spread beyond the ducts and lobes of the breast and invaded into normal neighbouring tissues (Edge and Compton, 2010). LAPC refers to all stage III non-metastatic breast cancers (Franceschini et al., 2007). LAPC includes disease which is extensive within the breast or in ispilateral nodal areas. LAPC includes: (1) large tumours (>5 cm in diameter); (2) tumours that have spread into the skin or muscles of the chest; (3) tumours with positive lymph nodes and (4) inflammatory breast cancer (IBC) (Garg and Prakash, 2015). IBC is an uncommon and aggressive form of LAPC accounting for 2.5% of all invasive breast cancers (Gordon, 2001, Li et al., 2005, Robertson et al., 2010). IBC is associated with early age at diagnosis, poor nuclear grade, ER-negative tumours and poor prognosis (Hance et al., 2005, Rea et al., 2015). IBC is characterized by rapid progression and visceral metastasis due to a rapid and aggressive hematogenous spread (Gordon, 2001, Lepori, 2015).

Breast cancer metastasis (stage IV) refers to cancer that have spread beyond the breast to distant sites in the body through the blood and lymphatic system. The metastatic lesions colonize vital organs forming multiple foci that subsequently develop resistance to available systemic therapies (Jin and Mu, 2015). Approximately 5-8% of patients present with metastasis at the time of diagnosis, and the 5-year survival of these patients range from only 24% to 39% (DeSantis et al., 2016). The common sites of breast cancer metastasis are bone, liver, lungs and brain (Kennecke et al., 2010). Studies have found a strong association between breast cancer subtypes and sites of metastasis, with influence on the prognosis of patients, which is discussed in section 1.1.3.2 (Gong et al., 2017).

With the onset of mammographic screening the demographics of breast cancer has changed with the majority (83%) of cases comprising EBC (Ward et al., 2015). LAPC comprise 20% of cases (Wang et al., 2017), with stage IV or metastatic cases comprising 5-10% of cases (Cardoso et al., 2012, Kimbung et al., 2015). The 5-year overall survival is 98% for EBC, 85% for LAPC and 24% for MBC (Lord et al., 2012, DeSantis et al., 2016). As discussed below in section 1.1.3.2 and 1.1.4, survival of breast cancer patients decreases with increasing clinical presentation and varies according to subtype (Voduc et al., 2010, DeSantis et al., 2014, Xiao et al., 2018).

1.1.3.2 Breast cancer subtypes

In 2000, genomic analysis (Perou et al., 2000) identified the 4 main molecular subtypes of breast cancer - luminal A, luminal B, human epidermal growth factor receptor-2 (HER-2) enriched and basal-like breast cancers (BLBC) (Perou et al., 2000, Sorlie et al., 2001, Prat and Perou, 2011). In 2011 and 2013, the St. Gallen International Expert Consensus proposed the criteria to identify clinical breast cancer subtypes, based on immunohistochemical detection of 3 protein bio-markers - estrogen and progesterone receptor (ER and PgR), and the tyrosine kinase trans-membrane receptor, HER-2 (Goldhirsch et al., 2011, Goldhirsch et al., 2013). According to this classification, ER status groups breast cancer into ER-positive (luminal), or ER-negative tumours (Perou et al., 2000). ER-positive tumours consist of luminal A and luminal B tumours, HER-2 over-expressing tumours are classified as HER-2 enriched/positive and those absent for ER/PgR/HER-2 are classified as triple negative breast cancers (TNBC). Proliferative activity as determined by Ki-67 index is taken into consideration in the classification and treatment of breast cancer (Goldhirsch et al., 2013). A high Ki-67 index (≥20%) is known to correlate with higher metastatic grade, poorer prognosis and early recurrence (<2 years) (Nishimura et al., 2010). The subtypes of breast cancer, receptor status and prognosis are summarised in Table 1.1.

Table 1.1 Subtypes of breast cancer and receptor profile.

Molecular subtype	Clinical subtype	Receptor profile	Treatment	Prognosis
Luminal A	Luminal A	ER + PgR +/- HER-2 - Ki-67 low (≤20)	Endocrine therapy alone	Good
Luminal B	Luminal B	ER + PgR +/- HER-2 +/- Ki-67 high (≥20)	Endocrine therapy +/- Cytotoxic chemotherapy	Good
HER-2 enriched	HER-2 enriched	HER-2 overexpressed/ amplified ER - PgR - Ki-67 any	HER-2 therapy + Cytotoxic chemotherapy	Intermediate /poor
Basal-like	Triple negative	ER - PgR - HER-2 -	Cytotoxic chemotherapy	Poor

Abbreviations: ER-estrogen receptor; PgR-progesterone receptor; HER-2-human epidermal growth factor receptor-2.

Luminal A tumours account for 50-60% of all breast cancers (Habashy et al., 2012). They are ER- and/or PgR-positive tumours with negative HER-2 and low Ki-67 (<20) index as assessed by immunohistochemistry. They express ER responsive genes or genes characteristic of the luminal epithelium (Sorlie et al., 2001, Yersal and Barutca, 2014). Luminal A tumours respond to endocrine therapy and are considered as a low-risk group since they are associated with better prognosis, low histological grade, and low mitotic index (Inic et al., 2014). Luminal B tumours comprise 15-20% of all breast cancers and are ER or PgR-positive, with a high Ki-67 index (Creighton, 2012). Approximately 30% of HER-2 enriched tumours, defined by immunohistochemistry, are assigned to the luminal B subtype (luminal HER-2) (Loi et al., 2009). Luminal B tumours are associated with higher grade, greater percentage of lymph node positivity, higher mitotic index and higher rates of relapse (Ellis et al., 2008, Creighton, 2012, TCGA, 2012). They have poorer response to endocrine therapy but respond better to neoadjuvant chemotherapy (Paik et al., 2004).

HER-2 enriched breast cancers comprise 15% of all invasive breast carcinomas and are detected clinically by the over-expression of the HER-2 protein assessed by immunohistochemistry and/or HER-2 gene amplification by fluorescent *in situ* hybridisation (FISH) (Prat et al., 2014, Mustacchi et al., 2015). HER-2 enriched tumours are characterized by high expression of genes associated with the HER-2 pathway and/or HER-2 amplicon located in the 17q12 chromosome (Sorlie et al., 2001). The tumours are characterized by a high proliferative index with high grade, p53 mutations, higher rate of recurrence and poor survival (Ross and Fletcher, 1998, Swede et al., 2001). In women with HER-2 positive disease, the addition of trastuzumab to cytotoxic chemotherapy, as discussed in section 1.1.5, increases response rate, time to progression and survival (Slamon et al., 2011).

TNBCs account for 10-15% of all breast cancers and are characterized by the absence of ER, PgR and HER-2 by immunohistochemistry (Cheang et al., 2008). TNBC is a heterogeneous disease which includes basal/non-basal tumours and sub-groups such as claudin-low, molecular apocrine, histological subtypes (medullary, metaplastic, adenoid cystic, squamous-cell), and tumours that demonstrate sporadic BRCAness (BRCA-1/2 mutation) (Diaz et al., 2007, Lehmann et al., 2011, Perou, 2011). TNBCs have the worst prognosis and are associated with younger pre-menopausal women, higher grade, large tumour size, higher risk of local and/or regional relapse and increased mortality (Fulford et al., 2007). Cytotoxic chemotherapy is used in the treatment of patients with TNBCs, along with PARP-inhibitors for the treatment of BRCA-1/2 deficient tumours (Fulford et al., 2007, Tutt et al., 2010). The molecularly defined basal like breast cancers demonstrate an 80% overlap with the clinically defined TNBCs (TCGA, 2012). In addition to the triple negative status, basal-like breast cancers also express high levels of basal cytokeratins such as cytokeratin 4, cytokeratin 14 and cytokeratin 17 (Cheang et al., 2008).

Figure 1.1 shows the association between breast cancer subtypes and survival. The 5-year overall survival for the different subtypes is reported to be 92.6% for luminal A, 88.4%, for luminal B, 83.6%, for HER-2 positive and 82.9% for TNBCs (Zuo et al., 2017).

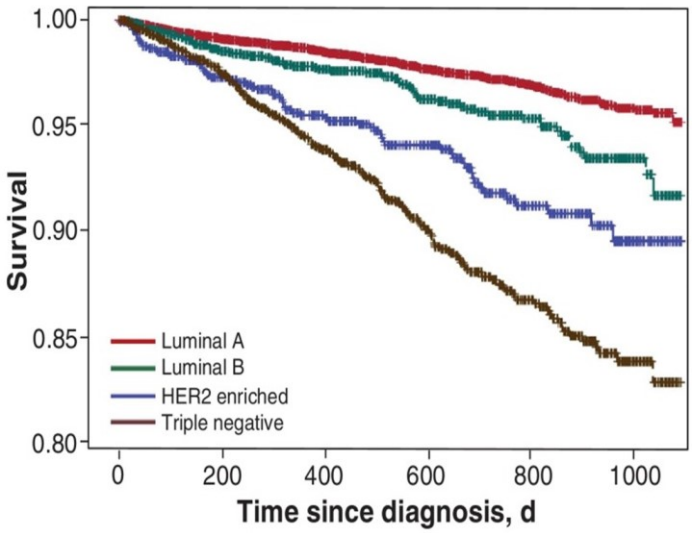


Figure 1.1 Kaplan Meir survival curves of breast cancer subtypes. Luminal A tumours have the best prognosis followed by luminal B, HER-2 enriched and TNBCs. Reproduced from (Fallahpour et al., 2017). Copyright© 2017 by Canadian Medical Association with permission conveyed through Access Copyright.

Luminal A tumours are associated with a lower risk of local or regional recurrence compared to the other subtypes (Voduc et al., 2010). The 15-year rate of distant relapse is 27.8% in luminal A, 42.9% in luminal B, 47.9% in luminal HER-2, 51.4% in HER-2 positive, 43.1% in basal-like and 35.1% in TN non-basal tumours (Kennecke et al., 2010). Breast cancer subtypes are also associated with distinct metastatic patterns which are associated with different prognostic outcomes (Xiao et al., 2018). Patients with ER/PgR-positive tumours have higher incidence of bone metastasis whereas HER-2 enriched tumours demonstrate increased rate of liver metastasis. Higher rates of brain metastasis are commonly seen in HR and HER-2 negative patients and less frequently in luminal tumours (Kennecke et al., 2010, Gong et al., 2017). HER-2 positive and basal like breast cancers are also associated with bone and lung metastases (Kennecke et al., 2010). Metastatic patients with HR and HER-2 positive disease have a better overall survival of 44 months compared to only 13 months in patients with TNBCs (Gong et al., 2017).

1.1.4 Predictive and prognostic factors

Predictive and prognostic factors are used in the clinic to establish associations between clinicopathological parameters and clinical outcome. A predictive factor is one that is capable of providing the likelihood of response or lack of response to a given treatment. A prognostic factor provides information on the outcome of the patient at the time of diagnosis, regardless of treatment (Clark, 2008). In breast cancer, clinical and morphological parameters such as axillary lymph node status, age, tumour size, tumour grade, and LVI are prognostic factors (Cianfrocca and Goldstein, 2004, Schmidt et al., 2010). Status of the hormone receptors - ER/PgR and HER-2 are considered as both predictive and prognostic factors since they determine treatment as well as response of breast cancer patients (Bundred, 2001). Some of the predictive and prognostic factors are discussed below.

1.1.4.1 Axillary lymph node status

Axillary lymph node status has been established as a single most important predictor for disease-free and overall survival (Fisher et al., 1993). Studies have found a direct correlation between the presence of positive lymph nodes and distant metastasis (Cianfrocca and Goldstein, 2004). Approximately, 70% of patients with a node-positive disease develop recurrence within 10 years compared to only 30-40% of patients with a node-negative disease (Fitzgibbons et al., 2000). The 5-year survival is 82.8% for patients with negative lymph nodes compared with 73% in patients with 1-3 positive nodes, 45.7% for 4-12 positive nodes, and 28.4% for ≥13 positive nodes (Fisher et al., 1983). Patients who have a lymph node-positive disease are administered systemic adjuvant therapy to reduce the risk of distant metastasis (Esbah and Oksuzoglu, 2017).

1.1.4.2 Age

Age is a prognostic factor in breast cancer with multiple studies demonstrating a worse prognosis for patients below 35 years of age (Nixon et al., 1994, Albain et al., 1994). Studies conducted by Bonnier et al., 1995 demonstrated higher frequency of undifferentiated grade 3 tumours, lymph

node positivity and negative hormone-receptor status in patients under 35 years of age (Bonnier et al., 1995). The 5-year disease-free survival for patients below 35 years of age is 40% compared to 80% in patients above 35 years of age (Yildirim et al., 2000).

1.1.4.3 Tumour size

Studies show that breast cancer patients with increasing tumour size have a poorer overall survival compared to patients with smaller tumours (Carter et al., 1989). Tumour size correlates with the number of axillary lymph node involvement and is an independent prognostic factor, with the probability of distant recurrence rates increasing with larger tumour size (Cianfrocca and Goldstein, 2004). Data on 24,740 cases recorded in the Surveillance, Epidemiology, and End Results (SEER) show that patients with larger tumour size (>5 cm) with axillary node involvement have a survival rate of only 45.5% compared to 96.3% in patients with smaller tumour size (<2cm) (Carter et al., 1989).

1.1.4.4 Tumour grade

Grading of tumours involves the morphological assessment of tumour biological characteristics which correlates directly to clinical behaviour and patient prognosis (Rakha et al., 2010). The widely accepted method of tumour grading is the Nottingham Grading System (NGS), which is the Nottingham (Elston-Ellis) modification of the Scarff-Bloom Richardson (SBR) classification (Bloom and Richardson, 1957, Elston and Ellis, 1991). NGS is recommended by various professional bodies internationally such as the World Health Organization (WHO), American Joint Committee on Cancer (AJCC), European Union (EU), and the Royal College of Pathologists (UK RCPath) (Walker, 2005, Rakha et al., 2010). Tumour grade is scored based on the mitotic index, nuclear pleomorphism and tubule formation. Using these factors, tumours are scored as grade 1-well differentiated (good prognosis), grade 2-moderately differentiated (intermediate prognosis) and grade 3-poorly differentiated (poor prognosis) tumours (Bloom and Richardson, 1957, Elston and Ellis, 1991). Le Doussal et al., 1989 carried out multivariate analysis on 1262 patients with operable, invasive ductal breast carcinoma and reported that patients with grade 3

tumours were found to have a higher recurrence risk of 4.4 times compared to patients with grade 1 tumours (Le Doussal et al., 1989).

1.1.4.5 Lymphovascular invasion (LVI)

Vascular invasion (VI), consisting of both lymph vessel invasion and blood vessel invasion refers to the invasion of tumour cells into the endothelial lined space of the lymphatic and blood vessels respectively. VI refers to the invasion of tumour emboli into the lymphatic vessels, blood vessels or both, is considered as a prerequisite step in the occurrence of metastasis (Ejlertsen et al., 2009, Song et al., 2011). The recurrence rate for women with LVI-positive stage I disease is 38% compared to only 22% in women with a LVI-negative cancer (Cianfrocca and Goldstein, 2004). Women positive for LVI have a higher rate of mastectomy and higher disease burden compared to LVI-negative patients (Ryu et al., 2018). Studies conducted by our group have shown that the presence of IHC detected LVI is associated with adverse disease-free and poor overall survival (Mohammed et al., 2011). Therefore, patients positive for LVI receive a more intense therapeutic intervention compared to tumours with no LVI. The LVI status can also be used to assist making treatment decisions especially for those patients with lymph node-negative disease (Neville et al., 1992, Lee et al., 2006).

1.1.4.6 ER/PgR and HER-2 status

As discussed in section 1.1.3.2, the hormone receptors, ER and PgR, are routinely used in the clinic to stratify patients into ER-positive or negative breast cancers (Goldhirsch et al., 2013). The presence of ER and PgR can predict response to adjuvant hormonal therapy (Harvey et al., 1999, Dowsett et al., 2010). Its prognostic significance stems from the finding that patients positive for ER and PgR have a 60-70% response rate compared to only 10% in ER/PgR-negative breast cancers (Ravdin et al., 1992). Similar to the hormone receptor status, HER-2 is also used as a prognostic and predictive marker (Ross and Fletcher, 1998, Fitzgibbons et al., 2000). Retrospective analysis conducted on 47 studies, with 15000 women indicated that HER-2 over-expression was an independent predictor of poor prognosis in multivariate analysis (Ross and Fletcher,

1998). Patients with a HER-2 positive disease generally have a lower response to endocrine therapy (Muss et al., 1994, Dowsett et al., 2010) and chemotherapeutic agents like cyclophosphamide, methotrexate, and fluorouracil (CMF) (Gusterson et al., 1992). They respond better to anthracycline based chemotherapy regimen (Paik et al., 1998) and anti-HER-2 treatments (Slamon et al., 2011).

1.1.4.7 Breast cancer staging

The TNM staging as recommended by the American Joint Committee on Cancer (AJCC) divides breast cancer into 5 stages, based on the size of the primary tumour (T), axillary lymph node status (N) and presence or absence of distant metastasis (M) (Edge and Compton, 2010, Cserni et al., 2018). Based on these 3 clinical parameters breast cancer is divided into the following stages - stage 0 comprises of early-stage breast cancers that are non-invasive or localized; stage I and stage II are tumours that have spread beyond the ducts and lobules and invaded into neighbouring tissues; stage III consists of locally advanced cancer and stage IV tumours are those that have already metastasized into distant sites (Edge and Compton, 2010). The 5-year survival in breast cancer patients decreases from stage 0 (100%) to stage I-II (90%) to stage III (72%) and stage IV (26%) (Office for national statistics)(ONS, 2019). In 2018, the AJCC staging system was updated to make breast cancer staging more accurate by adding other characteristics such as ER/PgR and HER-2 status, tumour grade and Oncotype DX (Koh and Kim, 2019).

The Nottingham Prognostic Index (NPI) is a widely used, sensitive and reliable tool for evaluating patient outcome and to support clinical decision making in breast cancer treatment (Kollias et al., 1999). The NPI combines nodal status, tumour size and histological grade at diagnosis to assign patients into one of the six prognostic groups (Galea et al., 1992). NPI is calculated by assembling these 3 parameters in a prognostic index formula: NPI = (lymph node stage (1-3) + histological grade (1-3) + (tumour size (cm) x 0.2) (Haybittle et al., 1982). Using this formula, patient outcomes can be categorised into the following 6 prognostic groups-excellent ($2.02 \leq NPI \leq 2.4$); good ($2.41 \leq NPI \leq 3.4$); moderate

1 (3.41 ≤ NPI ≤ 4.4); moderate 2 (4.41 ≤ NPI ≤ 5.4); poor (5.41 ≤ NPI ≤ 6.4) and very poor (6.41 ≤ NPI ≤ 6.8) (Blamey et al., 2007). Patients who fall into the intermediate or high-risk of relapse categories (>3.41) may be offered treatment with cytotoxic chemotherapy to reduce the risk of recurrence (Kollias et al., 1999, Lee and Ellis, 2008). More recently, NPI+ has been introduced through the addition of more variables to improve prognostic index (Rakha et al., 2014).

1.1.4.8 Adjuvant! Online and NHS PREDICT

Adjuvant! Online and NHS PREDICT are web based tools that help to determine the prognostic benefit of adjuvant therapy which aids clinicians to decide the best course of therapy for patients (Olivotto et al., 2005, Wishart et al., 2010). These tools use computational and mathematical algorithms, developed using clinical outcome data from cancer registries (Wazir et al., 2017). Adjuvant! Online predicts 10-year breast cancer outcomes in patients treated with or without adjuvant systemic therapy (Olivotto et al., 2005). PREDICT is a UK based tool developed to predict overall and breast cancer specific survival in women treated for early-breast cancer in the UK (Wishart et al., 2010, Predict, 2011).

1.1.4.9 Genomic predictors

Multigene-expression based assays that measure a variety of prognostic biomarkers aid in treatment decisions when the commonly used clinical parameters are insufficient to determine prognosis. These assays are useful in cases where patients develop systemic toxicity or fail to respond to treatments (NICE, 2018). Oncotype Dx and Mammaprint have been included in the latest edition of AJCC's prognostic staging system (Byrd and Greene, 2018). Oncotype Dx is a 21 gene based assay that measures the expression of 16 tumour related genes and 5 reference genes by quantitative real time PCR (qRT-PCR), to assess the risk of distant recurrence within 10 years (Cronin et al., 2004, Paik et al., 2004). Mammaprint is a 70-gene signature assay which helps to stratify ER-positive and ER-negative patients below 61 years of age into the high- and low-risk groups (Cardoso et al., 2016). The gene-expression panel assesses 70 genes involved in tumour invasion, metastasis, and

angiogenesis (van de Vijver et al., 2002, Zanotti et al., 2014, Xin et al., 2017).

1.1.5 Treatment options for breast cancer

In the UK, mammography is offered by the NHS breast screening programme to all asymptomatic women between the ages of 47-73. For those with symptoms, specialised units are available for rapid clinical assessment with mammogram, ultrasound and biopsy (Yeo et al., 2014, NICE, 2018). After diagnosis, breast cancer is classified into EBC, LAPC and MBC. The treatment of the three categories of breast cancer can vary between patients and are dependent on clinical and pathological parameters such as tumour size, tumour type, histological grade, nodal involvement and LVI status upon presentation (Shah et al., 2014, NICE, 2018).

1.1.5.1 Early-stage invasive breast cancer

The main treatment for early-stage invasive breast cancer is surgical excision (breast conservation surgery (BCS) or mastectomy) to remove the primary tumour followed by adjuvant chemotherapy or radiotherapy (Fisher et al., 2002). BCS involves excision of the breast tissue that contains the tumour and a small part of the healthy tissues around the tumour (Jatoi and Proschan, 2005), whereas mastectomy involves excision of the whole breast including nearby breast tissues, skin and nipple (Fisher et al., 2002). Lymph nodes are assessed by a sentinel lymph node biopsy (SLNB) or an axillary lymph node dissection (ALND) (Goldhirsch et al., 2011). This procedure clears additional disease and helps maintain local control, in addition to assessing nodal involvement to determine prognosis and plan adjuvant therapies (Yeo et al., 2014). Following surgery, adjuvant therapy is planned only after assessment of prognostic and predictive factors in the pathology report. Based on treatment guidelines for the management of breast cancer by NHS England, adjuvant therapy should start within 31 days post-surgery (Breast Cancer Expert Advisory Group, 2016). The adjuvant therapy options for breast cancer include chemotherapy, radiotherapy, endocrine and/or targeted therapy.

Adjuvant radiotherapy, used either as a single agent or in combination with chemotherapeutics, is prescribed in early-stage breast cancer following BCS to achieve local tumour control and improve breast cancer specific and overall survival (Fisher et al., 2002, Delaney et al., 2003, Delaney et al., 2005, NICE, 2018). Administering post-surgical radiotherapy after mastectomy is not routine clinical practice, but is recommended in patients with higher risk of local recurrence (tumour size >5cm in diameter, axillary lymph nodes >4, positive LVI and positive surgical margins) (Cardoso et al., 2019). The Early Breast Cancer Trialists' Collaborative Group (EBCTCG) report that radiotherapy after BCS leads to significant clinical benefits, with an overall 16% absolute decrease (19% v 35%) in the risk of any breast cancer recurrence (loregional or distant) and a 4% absolute decrease (21% v 25%) in the risk of dying from breast cancer (Darby et al., 2011). These results confirm that radiation is effective in eliminating microscopic disease that may be still present after surgery. Response to radiotherapy, varies according to patient age and also breast cancer subtype, with young women and patients with HER-2 enriched and TNBCs having the highest recurrence rates (Kyndi et al., 2008, He et al., 2019). More recently, studies report that radiotherapy when administered pre-operatively, improves visibility of primary tumour resulting in smaller target volume and minimizing geographical error (van der Leij et al., 2015). The current norm is adjuvant radiotherapy, however surgery conducted after radiotherapy removes the area of irradiated breast leading to decreased fibrosis and improved cosmetic result (Corradini et al., 2019). Clinical trials are currently ongoing (NCT02941835, NCT03359954, NCT03863301) to evaluate the role of pre-operative radiotherapy in breast cancer patients (ClinicalTrials, 2019).

Early-stage invasive breast cancer patients, positive for ER and PgR expression receive treatment with endocrine or hormonal therapy to inhibit the effect of estrogens on ER and/or blocks their synthesis (Ellis et al., 2008, Chang and Fan, 2013). Endocrine therapy can be categorized into selective ER modulators (SERM-e.g. tamoxifen and raloxifene), selective ER down-regulators (SERD-e.g. fulvestrant), aromatase inhibitors (AI-e.g. anastrozole, letrozole and exemestane) and luteinizing hormone-releasing

hormone analogues (LHRH analogues) (Dunbier et al., 2011, Chang and Fan, 2013). In pre and post-menopausal women, treatment with tamoxifen or aromatase inhibitor for 5 years post-surgery remains standard care (Goldhirsch et al., 2005, Dowsett et al., 2010). Several trials (ATLAS and NCIC CTG MA.17) have shown that extended adjuvant endocrine therapy for 10 years instead of 5 years results in improved overall and disease-free survival (Jin et al., 2012, Davies et al., 2013).

Anti-HER-2 therapy with the monoclonal antibody, trastuzumab (Herceptin®) is the standard adjuvant therapy for the treatment for HER-2 positive early-stage breast cancer (Slamon et al., 2011). Studies have reported that administering trastuzumab every 3 weeks for 12 months improves disease-free (218 v 321 recurrence events) and overall survival (59 v 90 deaths) (Piccart-Gebhart et al., 2005, Smith et al., 2007). In patients with tumour size larger than 3 cms in diameter, neoadjuvant chemotherapy with docetaxel and carboplatin is advised before surgery, following which adjuvant trastuzumab is administered for a year (Witherby et al., 2016). T-DMI (KADCYCLA®) is recommended after surgery in HER-2 enriched early-stage breast cancer (high-risk) patients treated with taxane and trastuzumab before surgery (Verma et al., 2012).

Treatment with anthracyclines and taxanes is the standard adjuvant chemotherapy for TNBC following surgery (NICE, 2018). A 15-year meta-analysis conducted by the EBCTCG of long-term outcomes reported that the 10-year breast cancer mortality was reduced by a third in patients who used polychemotherapy regimen consitisting of anthracycline, taxane and alkylator compared to patients who did not receive chemotherapy (Peto et al., 2012).

1.1.5.2 Locally advanced primary breast cancer

Treatment of LAPC is multidisciplinary and includes chemotherapy, surgery, radiotherapy in combination +/- hormonal or targeted therapies (Garg and Prakash, 2015). For large tumours, that are considered inoperable, neoadjuvant chemotherapy with an anthracycline/taxane regimen is administered to a maximum of six cycles to shrink tumour size (Mandilaras et al., 2015). This is usually followed by segmental or modified

radical mastectomy (NICE, 2018). Post-operative radiation therapy may also be recommended after surgery to minimize the risk of local recurrence (Mandilaras et al., 2015).

Following neoadjuvant chemotherapy, women with locally advanced (operable and inoperable) ER-positive tumours receive endocrine therapy according to their menopausal status (tamoxifen for pre-menopausal and AI for post-menopausal women) (Witherby et al., 2016). For HER-2 enriched locally advanced disease, a combination chemotherapy regimen consisting of docetaxel and carboplatin followed by surgery with or without adjuvant radiotherapy is administered. Patients may also receive trastuzumab maintenance therapy for one year to reduce the risk of recurrence (Cardoso et al., 2014). Locally advanced TNBC patients are treated with neoadjuvant chemotherapy containing sequential anthracycline and paclitaxel regimen to shrink tumour size and make them operable (Witherby et al., 2016). The I-SPY 2 (investigation of serial studies to predict your therapeutic response through imaging and molecular analysis 2) trial reported that combination of veliparib-carboplatin added to standard chemotherapy regimen is extremely effective in high-risk TNBC patients and resulted in higher pCR rates (25%), compared to treatment with standard chemotherapy alone (Rugo et al., 2016, Shao et al., 2019).

1.1.5.3 Metastatic breast cancer

The association between breast cancer subtypes and pattern of metastatic relapse has been well-reported with HR-positive tumours likely to have a higher incidence of bone metastasis, whereas HER-2 enriched and TNBC tumours are characterised by visceral metastasis, including liver and lungs (Kennecke et al., 2010, Gong et al., 2017). In the metastatic setting, radiotherapy may be administered to breast cancer patients with bone and brain metastasis to relieve tumour-associated symptoms (Cardoso et al., 2014). More recently, stereotactic radiosurgery (SRS) and stereotactic ablative body radiotherapy (SABR) have been considered as alternatives to surgery for treatment of oligometastasis (Otake and Goto, 2019). A phase I study (NRG-BR001) is currently investigating the recommended

dose of SABR for each metastatic location in patients with breast cancer (ClinicalTrials, 2019).

For metastatic patients who are ER-positive, endocrine therapy forms the first-line of therapy, until disease progression or endocrine resistance occurs. Tamoxifen is used in the treatment of pre-menopausal women. For post-menopausal women, aromatase inhibitor, fulvestrant (SERD), or combination of fulvestrant with AI, or the combination of an AI with the cyclin-dependent kinase (CDK) 4/6 inhibitor palbociclib is administered (Witherby et al., 2016). Biphosphonates (zoledronic acid or sodium clodronate) are currently prescribed for post-menopausal women with a high risk of recurrence (NICE, 2018), with studies reporting a significant reduction in distant recurrence (20.4% v 21.8%), bone recurrence (6.6% v 8.8%) and breast cancer mortality (14.7% v 18%) after treatment (EBCTCG, 2015).

Based on the Cleopatra trial, a combination of pertuzumab, trastuzumab and docetaxel is approved as first line therapy for the treatment of HER-2 enriched metastatic breast cancer (Swain et al., 2015). In the randomized phase III EMILIA study, trastuzumab-DMI (trastuzumab emtansine) conjugate resulted in improved disease control (9.6 v 6.4 months) and overall survival (30.9 v 25.1 months) (Dieras et al., 2017). T-DMI is now administered as second line therapy in metastatic HER-2 enriched breast cancer patients who progress after trastuzumab-taxane therapy (Lewis Phillips et al., 2008).

The first line treatment for patients with metastatic TNBC is standard chemotherapy given sequentially until progression is observed (Dear et al., 2013). It has been demonstrated that anthracyclines or taxanes regimen, such as the taxane-fluorouracil-doxorubicin-cyclophosphamide (T-FAC) regimen used at MD Anderson or doxorubicin-cyclophosphamide-taxane used in the NSABP trials, are effective in a small group of patients (Hudis and Gianni, 2011). The OlympiAD trial reported that in patients treated with olaparib, the risk of disease progression or death was 42% lower and the median progression-free survival was 2.8 months longer compared to standard therapy (Silver et al., 2010). Olaparib has now been approved for treatment of metastatic TNBC (Robson et al., 2017).

1.2 Radiotherapy

1.2.1 Biological effects of radiotherapy

1.2.1.1 Ionising radiation

The main aim of radiotherapy in cancer treatment is to deliver a tumouricidal dose of radiation to a target tumour volume while minimising exposure to healthy tissues, which may be adjacent to tumour cells or in the path of radiation (Emami et al., 1991, Nikjoo et al., 1998). The type of radiation is termed ionising as it produces electrically charged particles, called ions, and free radicals which deposit energy in cellular or biological material as it passes through (Baskar et al., 2012). The deposited energy in critical targets, or production of excessive amounts of ions and free radicals, can kill cancer cells or cause genetic changes that suppress reproductive potential (Baskar et al., 2012).

The therapeutic or biological effects of radiation are dependent on the amount of energy deposited by the radiation, and the damage caused as it interacts with cellular components. Linear energy transfer (LET) describes the amount of energy deposited per unit track length and is measured in units of keV/μm. It is a useful parameter to compare and contrast the different types of ionising radiations, or 'radiation quality'. Ionising radiation (IR) that deposits large amounts of energy per unit track length are termed high-LET radiations (or densely ionising), and those that deposit less energy are called low-LET radiations (or sparsely ionising) (Hunter and Muirhead, 2009, Franken et al., 2011, Hall and Giaccia, 2012). Examples of high LET radiations include α-particles, neutrons and heavy charged ions and examples of low-LET radiations include x-rays, γ-rays, electrons and protons. Clinically, all types of ionising radiation are used to treat cancer, however external beam electromagnetic radiation (EMR) or photon energy (x- and γ-rays), produced by linear accelerators, are more routinely used than charged particle radiations (electrons, protons, neutrons, α-particles and heavy charged ions (carbon)) (Hall and Giaccia, 2012, Baskar et al., 2012). An external photon beam (x-ray) radiation cabinet was used for all radiation experiments in the present study and is discussed in more detail later.

1.2.1.2 Direct and indirect action of radiation

The damage caused by ionising radiation to cells can be direct or indirect as shown in Figure 1.2. In direct action, the radiation track(s) interact directly with the biological material, such as DNA, physically disrupting the molecular structure, which results in cell damage or cell death (Pinto et al., 2005). The action of high-LET charged particle radiations are predominately direct, since the damage they cause is by direct energy transfer to the 'target' molecules (Hall and Giaccia, 2012).

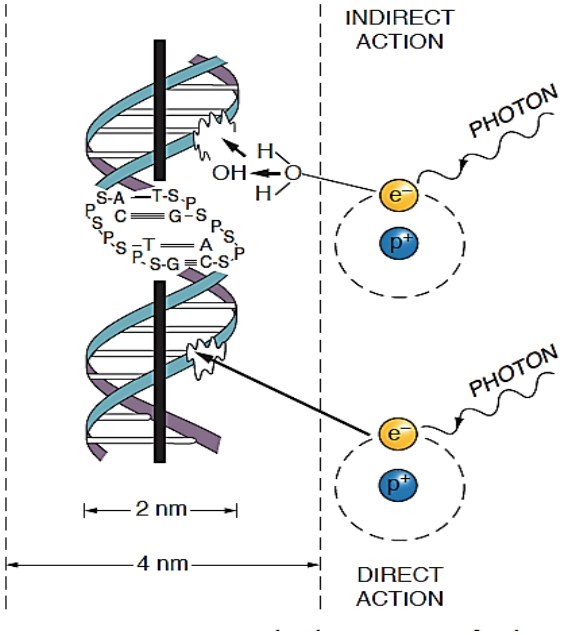


Figure 1.2 Direct and indirect effects of ionising radiation. In direct action, the secondary electron interacts with DNA to produce damage. In the indirect effect, the secondary electron reacts with a water molecule to produce the highly reactive hydroxyl radical that cause oxidative DNA damage to cellular components. Reproduced from (Hall and Giaccia, 2012). Copyright© 2012 by Lippincott Williams & Wilkins (LWW) Inc. with permission conveyed through Copyright Clearance Centre.

The effect of x- and γ-rays, low-LET ionising radiations, is predominately indirect because the damage they cause is by the generation of ions and free radicals, produced via the radiolysis of cellular water, close to the critical target molecules, such as the DNA (Chapman et al., 1973). The ions and free radicals produced in this way have sufficient biological half-lives to be able to diffuse to the critical site(s) and cause damage. About two-third of the damage by low-LET radiations occur when ionising radiation

interacts with cellular water (70% of cell), which results in its ionisation, leading to a cascade of ion and free-radical production. The formation of the water anion and hydrated, or aqueous, electron, H_2O^+ and e^{-aq} respectively (Reaction 1) leads to the production of the highly reactive hydroxyl radical ($OH^\bullet$) (Reaction 2). Two $OH^\bullet$ radicals can react together and produce hydrogen peroxide (H_2O_2) (Reaction 3).

Reaction 1: $H_20 \rightarrow H_20^+ + e^-$

Reaction 2: $H_20^+ + H_20 \rightarrow H_30^+ + OH^\bullet$

Reaction 3: $OH^\bullet + OH^\bullet \rightarrow H_20_2$

The free radicals produced by ionising radiation have a highly reactive unpaired electron, which oxidises proteins, lipids and reacts with cellular DNA to cause structural and biological damage (70% cell killing) (Chapman et al., 1973, Hall and Giaccia, 2012).

Molecular oxygen reacts with low-LET ionising radiation radical-induced DNA damage and leads to the formation of peroxinitrite DNA lesions which are unrepairable and leads to cell damage and death, known as the oxygen fixation hypothesis (OFH) (Oronsky et al., 2011, Grimes and Partridge, 2015). The presence of molecular oxygen is therefore crucial to enhance the therapeutic, or biological, efficacy of ionising radiation and is referred to as the oxygen enhancement ratio (OER)(Rockwell et al., 2009). The magnitude of the OER in model systems depends on the presence of low-molecular-weight solutes, most notably thiols and radical scavengers (Dasu and Denekamp, 1998). Over the years, extensive research has been carried out to improve radiosensitivity by increasing oxygenation in tumours; initially with hyperbaric chambers (Mayer et al., 2005), radiosensitisers, and more recently with agents that target hypoxic tumour cells (Boyle and Travers, 2006, Phillips, 2016). The hypoxia-selective drugs will be discussed in detail in chapter 3.

1.2.2 Repair of radiation induced DNA damage

Radiation induced DNA damage is manifested by single and double strand breaks, in the sugar-phosphate backbone of the DNA molecule (Ward,

1988, Steel, 1996). On average, 1 Gy of clinical radiotherapy produces approximately 40 double and 1000s of single strand breaks and base lesions per diploid genome (Ward, 1985, Alizadeh et al., 2015). Cells respond to DNA damage by activating cell cycle checkpoint arrest and DNA repair pathways, known collectively as the DDR (Ciccia and Elledge, 2010). There are multiple repair pathways in mammalian cells, but physical and biochemical damage induced by ionising radiation are repaired via the base excision repair (BER) (Fortini et al., 2003); non-homologous end joining (NHEJ) and homologous recombination (HR) repair pathways (Mahaney et al., 2009). The majority of DNA double strand DNA breaks induced by low-LET radiations are repaired between 0.5-1 hour, while some repair may take up to 24 hours or more (Schmid et al., 2010). Successful repair of radiation-DNA damage results in radioresistance which allows the cells to survive and replicate (Hoeijmakers, 2001). DNA repair pathways involved in repairing radiation induced DNA damage are discussed in detail in chapter 2.

1.2.3 Modelling of radiobiological effect

1.2.3.1 Dose-response curve

A dose-response curve describes the relationship between the fraction of cells that survive and the absorbed dose of radiation (Puck and Marcus, 1955, Elkind, 1988). Surviving fraction (SF) obtained from radiotherapy experiments are graphically plotted as a function of radiation dose on a log/linear plot, with SF on a logarithmic y-axis and radiation dose on the linear x-axis (Puck and Marcus, 1956). For high-LET radiations, the shape of the survival curve is almost linear indicating an exponential decrease in cell survival. For low-LET radiations, the curves show an initial slope followed by a shoulder region over a low dose range and then become straighter at higher doses (Fowler, 1992). This is because at low doses there is less chance of DNA damage occurring close to each other, giving easily repairable DNA damage. At high doses, there is a higher probability of cluster DNA damage occurring close to each other resulting in a more complex difficult to repair double strand breaks and chromosome aberrations (Jakob et al., 2009). Mammalian cells have differential

sensitivity to radiation, with resistant cell lines showing a large shoulder region (or repair ability) and sensitive cell lines, showing a steeper curve (inherent radiosensitivity), demonstrating less survivors with increasing dose (Hall and Giaccia, 2012).

1.2.3.2 Linear quadratic model

The linear-quadratic (LQ) model is commonly used in the analysis of experimental data and clinically, to conduct treatment planning for cancer in radiotherapy (Joiner, 2009). The LQ model is commonly used to describe the shape of the cell survival curve, assuming there are two components to cell killing - the α-component that is proportional to the radiation dose (D), and the β-component that is proportional to the square of the dose (D2) (Baskar et al., 2012). The SF of cells in this model is represented by the following exponential function:

$$SF(D)=e^{-\alpha \cdot D-\beta \cdot D2}$$

Where S is the surviving fraction of cells after a single radiation dose (D), and α represents the linear and β describes the quadratic component of the survival curve (Joiner, 2009, Hall and Giaccia, 2012). The α and β component in this model represents the intrinsic sensitivity of cells to radiation. The linear component (α), represents single-hit killing and determines response of cells to radiation at low doses; whereas the quadratic component of cell kill (β) represents multiple-hit killing which causes the curve to bend at higher doses. When cell killing obtained from the linear component (α) is equal to the cell kill from quadratic component (β), is known as the α/β ratio (Fowler, 1992). If the shape of the survival curve is linear at low doses, the value of α is higher, which means that the cells are sensitive to radiation (Withers, 1987). In the present study, the LQ model was applied in all radiation experiments to calculate response after radiation.

1.2.4 Radiotherapy regimens for breast cancer

As mentioned previously, adjuvant radiotherapy is used as routine protocol in the treatment of invasive early-stage breast cancer patients following BCS or mastectomy (in the case of high risk patients) (Coates et al., 2015,

Cardoso et al., 2019). The response of the different breast cancer subtypes to radiation is dependent on the intrinsic radiosensitivity, aggressiveness and metastatic potential of the subtypes. Luminal A tumours generally have the most favourable response after radiotherapy compared to the HER-2 enriched and TNBC patients (He et al., 2019). Palliative radiotherapy may be recommended in patients with advanced breast cancer to reduce symptoms associated with advanced disease (Cardoso et al., 2014, Nakamura et al., 2018). Radiation for breast cancer treatment is delivered as external beam radiotherapy (EBRT) and brachytherapy.

1.2.4.1 Conventional fractionated radiotherapy

The standard radiotherapy for patients with early-stage breast cancer and DCIS is the conventional multi-fractionated radiotherapy (CFRT) delivered as EBRT, which administers a total dose of 50 Gy delivered to the whole breast in 25 fractions of 2 Gy each, for up to 6 weeks (Haydaroglu 2012). CFRT reduces the risk of local recurrence by 60-70% in invasive and by 50-60% in non-invasive breast cancer (van Dongen et al., 2000, Fisher et al., 2002, Veronesi et al., 2002). In women with higher risk of local recurrence, an additional boost dose of 10 Gy in 5 fractions or 16 Gy in 8 fractions is administered over a one-week period (Bartelink et al., 2015, Cardoso et al., 2019). The boost continues to be given to high risk patients with at least one of the following risk factors: age up to 50 years, grade 3 tumours, extensive DCIS, vascular invasion, and possibly in cases of non-radical tumour excision (Senkus et al., 2015).

1.2.4.2 Hypofractionated radiotherapy

The currently adopted regimen by most UK centres is the alternative hypofractionated radiotherapy (HFRT), which administers radiotherapy dose with fewer, larger fractions to a total dose of 40 Gy given over 15 fractions in 3 weeks (Haviland et al., 2013). Hypofractionation refers to delivery of radiation doses larger than 2 Gy in fewer fractions over a shorter period of time which shortens treatment time. The adoption of HFRT in UK centres was based on START (Standardisation of Breast Radiotherapy Trials), which demonstrated (10-year follow up) lower recurrence, improved overall survival and lower normal tissue toxicities in patients

treated with HFRT compared to the CFRT regimen (Bentzen et al., 2008, Haviland et al., 2013). This finding, along with cost efficiency and patient preference, has led to most UK centres adopting HFRT over CFRT for the treatment of breast cancer.

1.2.4.3 Intraoperative radiotherapy

Although not in routine practice, Targeted Intraoperative Radiotherapy (TARGIT-IORT) has gained interest as a potential alternative treatment to EBRT for certain patient groups. TARGIT uses a mobile irradiation system to deliver a single large dose (20 Gy) of low energy radiation (50 kV x-rays) for 20-35 minutes, directly to the area of the resected tumour before the incision is closed (Vaidya et al., 2010, Vaidya et al., 2014). Data from a prospective multicentre phase III trial showed a reduction in the overall mortality of patients in the TARGIT group (3.9%) compared to EBRT (5.3%) (Vaidya et al., 2014). Moreover, radiotherapy toxicity was lower in the TARGIT group with only 6 patients (0.5%) presenting with grade 3 radiotherapy-related complications compared to 23 patients (2.1%) in the EBRT group (Vaidya et al., 2010). Currently, TARGIT-IORT is available only in a few UK NHS centres (Coombs et al., 2016).

1.2.4.4 Brachytherapy and accelerated partial breast irradiation

Brachytherapy (BT) and accelerated partial breast irradiation (APBI) are techniques to treat only the tumour site rather than the whole breast in some patients with early-stage breast cancer (Fisher et al., 1993, Vicini et al., 1999). APBI is a novel technique which involves accelerated delivery of radiation doses to the lumpectomy bed, rather than the whole breast (Skowronek et al., 2012). Brachytherapy delivers precision radiation by placing a sealed radioactive source (e.g. iridium-192) at the tumour site after surgery to destroy any microscopic disease, and minimise normal tissue damage (Skowronek and Chicheł, 2014). Using these techniques, ionising radiation can be delivered using low dose rate (LDR-0.4-2 Gy/h), pulsed dose rate (PDR-3Gy/h), or high dose rate (HDR-12 Gy/h), depending on the length of time the radioactive source remains in place (Kauer-Dorner and Berger, 2018). These techniques shortens treatment

time to 4-5 days compared to 5 weeks of treatment with WBI (whole breast irradiation) (Cholewka et al., 2013).

1.2.5 Strategies to improve radiotherapy response

Radiotherapy is an essential component in the multimodality treatment of breast cancer. It is essential for BCT (breast conservation therapy), it reduces locoregional recurrence and mortality and alleviates symptoms in advanced breast cancer patients (Siglin et al., 2012). Studies show that at least 50-60% of cancer patients benefit from radiotherapy, when administered either with a curative or a palliative intent (Delaney et al., 2005). However, local recurrences still occur at a rate of 3-20% (dependent on age and other factors) for patients receiving BCT and 2-12% for patients who have undergone mastectomy, indicating failure of primary treatments (van Dongen et al., 2000, Fisher et al., 2002, Veronesi et al., 2002). One potential way to improve radiation response is to combine ionising radiation with radio-enhancing agents to increase radiotherapeutic efficacy (Raviraj et al., 2014, Lesueur et al., 2017).

Five factors that are important in determining the net effect of radiation therapy on tumours, known as the 5 R's of radiotherapy, are the cancer cell's intrinsic **R**adiosensitivity, DNA **R**epair capacity, the hypoxic fraction in relation to the **R**eoxygenation of surviving cells, **R**edistribution of cells within the cell cycle, and **R**epopulation following radiotherapy (Withers, 1987). Radiosensitisers have been developed to ideally target one or more of these processes but to have minimal, if any, effect on the normal tissue toxicity profile (Brown et al., 2014).

As discussed earlier, a main cytotoxic effect of radiotherapy is via the induction of a large amount of DNA damage to the cancer cells; so one strategy to improve radioresponse is to inhibit DNA repair pathways (Lomax et al., 2013). This finding has led to extensive research on the evaluation of DNA repair inhibitors as radiosensitisers (Mahaney et al., 2009, Vens and Begg, 2010). The presence of hypoxia - pO_2<10 mm Hg (<1% - 2% O_2) in breast cancer is associated with chemo/radiotherapy resistance, metastasis and poor survival (Gilkes and Semenza, 2013). An approach to target tumour hypoxia is to use bioreductive agents and

hypoxia-activated prodrugs (HAPs), that are only activated under conditions of low oxygen into cytotoxic metabolites (Patterson and McKeown, 2000). By combining HAPs with radiotherapy (that efficiently targets oxygenated cells), both the oxygenated and hypoxic compartments of the tumour can be targeted to achieve greater tumour cell radiosensitisation (O'Connor et al., 2016, Phillips, 2016). Several studies suggest that DNA repair pathways and presence of hypoxia can be exploited with beneficial consequences for radiotherapy. Therefore, the present study sought to improve radioresponse in breast cancer cells using novel DNA repair inhibitor and hypoxia-activated prodrug, which are discussed in subsequent chapters.

1.3 Overall study hypotheses, aims and objectives

Hypothesis

The hypothesis framed for the current study was that targeting I) FEN-1 of the long patch-base excision repair (LP-BER) pathway using its inhibitor, PTPD or II) hypoxia using the novel hypoxia-activated prodrug, KP167, will result in radiosensitisation of the luminal and triple negative breast cancer phenotypes. It was also hypothesised that different subtypes of breast cancer, due to their inherently different molecular phenotypes, will show differential response to such treatments.

The overall aim of the thesis was to evaluate the radiation response of breast cancer cell lines and assess how inhibitors of DNA repair, (FEN-1 inhibitor, PTPD) and hypoxia (novel AQ4N analogue, KP167) can alter the radiosensitivity of breast cancer cells. The cytotoxic and radiosensitising effect of PTPD was studied in breast cancer models using various endpoint assays. The cytotoxic and radiosensitising effects of KP167 was studied in breast cancer cells when grown under 3D spheroids and 2D (+/- hypoxia). The efficacy of the novel agents was compared to, and contrasted against, well-characterized agents undergoing, or having undergone, extensive pre-clinical assessments and clinical evaluation.

Objectives for DNA repair inhibitor study

1. Investigate the cytotoxic effect of the novel FEN-1 inhibitor, PTPD as single agent on different breast cancer cell lines using cell proliferation and clonogenic assays (luminal and triple negative breast cancer cells).

2. Examine the potential of PTPD to increase radiosensitivity by altering DNA repair capacity of irradiated cells. Control experiments include assessing radioresponse in breast cancer cells treated with well-established radiosensitisers such as KU-55933 and olaparib to compare radiosensitising efficacy of PTPD.

3. Evaluate the effects of FEN-1 inhibition on DNA damage using single strand (RPA) and double strand (γ-H2AX) DNA damage assays.

Objectives for hypoxia-activated prodrug (HAP) study

1. Assess the single agent anti-cancer effect of the novel HAP, KP167, in luminal and triple negative breast cancer cells, when grown as 3D spheroids and in 2D (+/- hypoxia), with results compared to that obtained with the parental drug, AQ4N.

2. Evaluate protein expression levels of reductases (cytochrome P450, CYP2S1, CYP2W1, NQO1 and NQO2) to gain an initial mechanistic insight into drug activation and differential drug sensitivities in the different subtypes of breast cancer (*in vitro*).

3. Investigate the potential of the novel AQ4N analogue, KP167 to increase radiosensitivity of breast cancer cells (3D and 2D +/- hypoxia) and compare it to radiosensitivity obtained using the parental drug, AQ4N.

4. Assess expression of CYP2S1 and CYP2W1 in a large independent cohort of breast cancer, and determine association with various clinicopathological parameters and survival.

Chapter 2 Targeting LP-BER to improve radioresponse in breast cancer

2.1 Abstract

Background: Breast cancer is often treated by radiotherapy both in the neoadjuvant and adjuvant setting, but may fail in certain patients as indicated by local recurrence rates of up to 15% over 10 years. The efficient repair of radiation-induced DNA damage, by cancer cells, influence recurrence rates with DNA repair inhibitors being trialled, in combination, to improve therapeutic response. FEN-1 of the BER pathway is involved in the repair of single strand breaks and base damages, with previous studies suggesting the involvement of FEN-1 in the repair of radiation-induced DNA damage. The DNA repair inhibitor PTPD, belongs to a class of N-hydroxyurea-based compounds which act as potent and selective inhibitors of FEN-1. The aim of the current chapter was to assess the *in vitro* efficacy of PTPD, as a single agent and in combination with ionising radiation, in luminal and triple negative breast cancer cell models.

Methods: Two luminal (MCF-7 and T47D) and three TNBC (MDAMB-231, MDAMB-468 and the BRCA-1 deficient MDAMB-436) cell lines were chosen as *in vitro* models. The doubling times and plating efficiencies (PEs) were initially assessed using cell growth curves and clonogenic assays, respectively. The well-established DNA repair inhibitors, ATM inhibitor, KU-55933, and PARP-1 inhibitor, olaparib, were used as positive controls and to compare the efficacy of PTPD against. Effects of PTPD on cell proliferation were assessed at different drug concentrations for 24 hours. Single agent clonogenic survival and radiosensitisation were measured by treating pre-plated cells with KU-55933 or olaparib or PTPD and subsequently exposing them to single doses (0-8 Gy) of x-rays. Replication protein A (RPA) and γ-H2AX expression were evaluated, as markers of single and double strand DNA damage respectively, by immunofluorescence microscopy, following PTPD treatment alone or in combination with ionising radiation.

Results: The average doubling times (hours) were approximately 29±4.12 in MCF-7, 32±1.86 in T47D, 20±2.47 in MDAMB-231, 31±1.24 in MDAMB-468 and 41±4.55 in MDAMB-436 cells. The PEs (± standard deviation (SD)) were 41±4.35% in MCF-7, 16±2.82% in T47D, 51±5.70% in

MDAMB-231, 44±1.52% in MDAMB-468 and 19±3.05% in MDAMB-436 cells.

MDAMB-436 cells were substantially more sensitive to treatment with 10 μM KU-55933 with approximately 40% reduced survival compared to 2-20% in MCF-7, T47D, MDAMB-231 and MDAMB-468 cells. Clonogenic survival was greatly reduced with 10 μM olaparib treatment in MCF-7, T47D (40-50%) and MDAMB-436 (80%) cells, compared to a modest 25% decrease in MDAMB-231 and MDAMB-468 cells. Treatment of cells with increasing concentrations (2.5-10 μM) of PTPD, did not affect the rate of cell proliferation (<10%) nor reduce clonogenic survival (<10%) in MCF-7, T47D, MDAMB-231 or MDAMB-468 cells. PTPD treatment was, however, toxic in MDAMB-436 cells and resulted in a dose-dependent reduction in proliferation (IC_{50} 13.97±3.23 μM, P<0.001) and clonogenic survival (IC_{50} 8.06±2.92 μM, P=0.001).

KU-55933 treatment significantly increased radiosensitivity with $SER_{0.01}$ of 1.60±0.23 (P=0.021) in MCF-7, 1.71±0.27 (P=0.007) in T47D, 1.82±0.21 (P=0.020) in MDAMB-231, 1.68±0.33 (P<0.001) in MDAMB-468 and 3.42±0.91 (P=0.003) in MDAMB-436 cells. Significant increase in radiosensitivity was also observed with olaparib treatment with $SER_{0.01}$ of 1.63±0.03 (P<0.00001) in MCF-7, 1.61±0.18, (P=0.011) in T47D, 1.62±0.09 (P=0.002) in MDAMB-231, 1.68±0.33 (P=0.0006) in MDAMB-468 and 2.35±0.13 (P=0.0001) in MDAMB-436 cells.

PTPD treatment resulted in a small but significant radiosensitisation with $SER_{0.01}$ of 1.31±0.07 (P=0.010) in MDAMB-231 and 1.50±0.13 (P=0.025) in MDAMB-436 cells. A marginal but significant increase in radiosensitisation was observed in MDAMB-468 cells at 6 (P=0.016) and 8 Gy (P=0.032) with $SER_{0.01}$ of 1.13±0.08. No radiosensitisation was observed in MCF-7 and T47D cells with $SER_{0.01}$ of 1.00±0.02 (P=0.252) and 1.00±0.01 (P=0.961) respectively.

Treatment with 1 Gy ionising radiation significantly increased single strand DNA damage (RPA expression) in MCF-7 (P=0.001), T47D (P=0.0008), MDAMB-231 (P=0.004), MDAMB-468 (P=0.002) and MDAMB-436 (P<0.0001) cells, and double strand DNA damage (γ-H2AX) in MCF-7 (P=0.0005), T47D (P<0.0001), MDAMB-231 (P<0.0001), MDAMB-468

(*P*=0.0023) and MDAMB-436 (*P*=0.0002) cells. Compared to radiation alone, cells treated with the combination of PTPD and ionising radiation displayed increased single strand DNA damage in MCF-7 (*P*=0.031), T47D (*P*=0.061), MDAMB-231 (*P*=0.020), MDAMB-468 (*P*=0.019) and MDAMB-436 cells (*P*<0.0001), and double strand DNA damage only in MDAMB-436 cells (*P*=0.0003).

Conclusions: Cells behaved as expected with the control DNA repair inhibitors, and although FEN-1 induced some radiosensitisation, at least in TNBCs, it was only slight in comparison to the control/comparator agents. FEN-1 may be suitable target for enhancing radiotherapy in breast cancer but only in the TNBC phenotype, especially those that are BRCA-1 deficient.

2.2 Introduction and aims

Tumour cells are often reliant on particular pathways to repair specific forms of DNA damage induced by either ionising radiation or other cytotoxic agents (Velic et al., 2015). There are at least 6 repair pathways in mammalian cells: non-homologous end-joining (NHEJ), homologous recombination (HR), interstrand cross link repair (ICL), base excision repair (BER), nucleotide excision repair (NER) and mismatch repair (MMR) (Hoeijmakers, 2001, Chatterjee and Walker, 2017). The DNA double strand breaks induced by ionising radiation, that correlate closely with cell lethality, are repaired by the NHEJ and HR pathways (Aparicio et al., 2014). Single strand and base DNA lesions generated by ionising radiation are repaired by the BER pathway, which prevents conversion into a cytotoxic DNA double strand break (Frosina et al., 1996).

2.2.1 DNA damage response

The DDR is a complex network of signalling pathways that sense, signal and repair DNA lesions (Ciccia and Elledge, 2010). Ionising radiation-induced DNA damage initiates a global cellular response to induce transient cell cycle arrest in the G1, S and G2/M phases to allow sufficient time for DNA repair (Helleday et al., 2008, Ciccia and Elledge, 2010). These damage responses are mediated by the master regulators, Ataxia telangiectasia-mutated (ATM) /checkpoint kinase 2 (CHK2) and ataxia

telangiectasia and Rad3-related (ATR) /checkpoint kinase 1 (CHK1) pathways which are activated in response to DNA double strand, and DNA single strand breaks respectively (Smith et al., 2010). ATM mediated phosphorylation of H2AX (Ser139), giving rise to γ-H2AX, is one of the earliest cellular response to DNA double strand breaks (Rogakou et al., 1998). γ-H2AX acts as a platform for the recruitment of repair factors to break site and forms ionising radiation-induced nuclear foci in response to radiation damage (Van Veelen et al., 2005). γ-H2AX is a sensitive biomarker for ionising radiation-induced double strand breaks (Sharma et al., 2012, Valdiglesias et al., 2013), and has been assessed for the same in the current study. Repair pathways are next activated in response to ATM-CHK2 signalling which phosphorylates KU and/or BRCA-1 to promote repair by either NHEJ (Lee et al., 2006) or HR (Gatei et al., 2001) pathways respectively.

The ATR-CHK1 pathway is activated predominantly when replication is blocked in response to single strand DNA (ssDNA) damage (Nam and Cortez, 2011), and signals activation of single strand repair pathways (BER, NER). This results in the uncoupling of DNA polymerase from DNA helicase exposing ssDNA, which is coated by Replication Protein A (RPA) (Zou and Elledge, 2003). RPA is a marker of replication stress and has been used in the current study to assess single strand DNA damage (Namiki and Zou, 2006).

The recruitment of poly (ADP-ribose) polymerase-1 (PARP-1), an important event in DDR response, is central to detecting the presence of damaged DNA and activating signalling pathways that initiate appropriate DNA repair, including both single and double strand breaks (Huambachano et al., 2011). This stimulates the catalytic activity of PARP to generate extensive poly (ADP-ribose) chains (PAR chains) on itself and proteins in the vicinity of DNA damage, a term known as poly(ADP) ribosylation or PARylation (D'Amours et al., 1999). PARP-1 is a crucial first-line sensor of single strand DNA damage induced by ionising radiation (de Murcia and Menissier de Murcia, 1994). It interacts with ATR-CHK1 to induce a S-phase checkpoint (Horton et al., 2007, Kedar et al., 2008), and promotes repair by BER and NER pathways (Chaudhuri and Nussenzweig, 2017).

The clinical use of PARP inhibitors (olaparib for advanced ovarian cancer and metastatic breast cancer) (Bixel and Hays, 2015, Kim et al., 2015) was initially founded on the concept of the 'synthetic lethality' relationship of PARP with BRCA-1/2 proteins. This approach was based on the strategy that tumours with impaired DNA double strand repair pathways, due to BRCA-1/2 deficiency, would rely on PARP-activated BER for survival, and thus inhibition of PARP induces a synthetic lethal phenotype specific to BRCA-1/2 mutant cancer cells with normal, double strand break repair competent cells being spared (Farmer et al., 2005, Bryant et al., 2005, Ashworth, 2008, Tutt et al., 2010). This stategy has now been expanded to include other pathways, for example, if a cancer cell shows deficiency in one pathway, the strategy is to target the remaining main pathway(s) to inhibit the compensatory effect and induce selective lethality, while sparing normal cells (Reaper et al., 2011, Bukhari et al., 2019, Das et al., 2019).

2.2.2 Double strand break repair pathway

It is well established that failure to remove or repair DNA double strand breaks can cause cell death through the generation of lethal chromosomal aberrations or via the direct induction of apoptosis (Jackson and Bartek, 2009). The DNA double strand break repair pathway consists of NHEJ and HR that constitute the fast and slow repair processes with half-lives ranging from 5-30 minutes and 2-5 hours, respectively (Shiloh, 2001, Abraham, 2001, Durant and Nickoloff, 2005, Jeggo et al., 2011).

2.2.2.1 Non homologous end joining

NHEJ is pre-dominant in the G1 phase of the cell cycle when HR is not available (Aparicio et al., 2014). It is initiated when ATM activated KU 70/80 heterodimer recruits DNA-PK to form a functional DNA-PK/KU active complex that allows enzymes to access DNA ends (Mahaney et al., 2009, Ciccia and Elledge, 2010). The DNA ends are digested by nucleases (such as Artemis) and the DNA strand processed by DNA polymerases (such as Polμ or Polλ) to create compatible ends (Goodarzi et al., 2006, Kurosawa et al., 2008). In the last step, a ligation complex consisting of DNA ligase IV, X-ray cross-complementation group 4 (XRCC4) and XRCC 4-like factor

(XLF) ligates the ends of the DNA completing the NHEJ repair process (Ahnesorg et al., 2006, Gu et al., 2007). NHEJ, although a dominant repair process, is considered error prone as it is unable to restore the original sequence of the DNA (Lieber, 2010).

2.2.2.2 Homologous recombination

HR is the error-free repair process, which requires the presence of an intact sister chromatid and can therefore occur only in the S and G2 phases of the cell cycle, when DNA has been replicated (Kadyk and Hartwell, 1992). The HR pathway is initiated when the double strand break is resected by nucleases and helicases resulting in a 3'-single stranded DNA (Sartori et al., 2007). ATM-activated BRCA-1 controls the G2/M checkpoint and prevents cells from entering into mitosis before DNA repair is complete (Deng, 2006). The MRN (MRE11/NBS1/RAD5) complex binds to DNA ends and recruits nucleases to remove damaged bases (Uziel et al., 2003). The ssDNA DNA is coated by RPA to prevent formation of secondary structures and further degradation from nucleases (Sugiyama et al., 1997). BRCA-2 replaces RPA by RAD51, to form a nucleoprotein filament. This structure finds the homologous sequence on the sister chromatid and invades the homologous duplex DNA which serves as a template for DNA synthesis (Kadyk and Hartwell, 1992). After strand invasion, the DNA is polymerised and any lost information is successfully restored by DNA polδ in combination with proliferating cell nuclear antigen (PCNA) (Pardo et al., 2009, Wright et al., 2018).

2.2.3 Single strand break repair pathway-BER

Ionising radiation causes a number of multiple single lesions, including oxidised purine and pyrimidine bases, apurinic abasic sites and single strand breaks on the DNA (Milligan et al., 2000). When two opposing single strand breaks are formed within the cluster, a potentially lethal double strand break can arise (Ward et al., 1987). BER pathway is activated in response to IR-induced DNA damage and has been reported to repair up to ~10000 damaged bases per cell per day (Sun et al., 2017).

2.2.3.1 Short-patch BER

BER can occur via the short-patch (SP-BER) or the long-patch (LP-BER) pathway (Figure 2.1), depending on the length of the region to be repaired and the subset of enzymes involved (Frosina et al., 1996, Asagoshi et al., 2010). The BER pathway is initiated when DNA glycosylases recognise and removes a damaged base to form an apurinic/apyrimidinic (AP) residue. In the case of oxidative damage, oxidised bases are removed by bifunctional glycosylases, such as NTH1, OGG1, NEIL1, NEIL2, and NEIL3 to generate an AP site (Izumi et al., 2003, Hegde et al., 2008). Apurinic endonuclease 1 (APE1) recognizes the AP site and cleaves 5′ to the AP sites generating a nick on which DNA Polβ is loaded. DNA Polβ incorporates the appropriate nucleotide into the gap and eliminates the 5′ AP site via its 5′-deoxyribose-phosphate (dRP) lyase activity (Robertson et al., 2009). A complex of DNA ligase 3 and XRCC1 is recruited to the repair site by PARP-1, which seals the nick completing the SP-BER pathway (Bennett et al., 1997, Krokan and Bjoras, 2013).

2.2.3.2 Long-patch BER

The oxidative stress, such as those caused by ionising radiation, oxidises deoxyribose sugar in the DNA backbone resulting in single strand DNA damage (Nakamura et al., 2003, Asagoshi et al., 2010). The 5′-oxidised deoxyribose lesions are resistant to the dRP lyase activity of Polβ, and can only be excised by the LP-BER sub-pathway (Liu et al., 2005, Liu et al., 2008a). In this pathway, DNA polymerases β/δ/ε incorporate approximately 2-15 nucleotides into the repair patch to remove the 5′-terminal sugar residue. During this process, a flap structure is generated due to strand displacement DNA synthesis. Removal of the flap is essential to prevent strand duplication/deletion events. Flap endonuclease-1 (FEN-1) is recruited to the LP-BER site, which in combination with PCNA excises the flap allowing DNA ligase 1 to seal the nick (Pascucci et al., 1999, Dogliotti et al., 2001). This alternate pathway, which utilises FEN-1 to cleave the damaged base-containing flap structure resulting in a ligatable DNA is the LP-BER pathway (Robertson et al., 2009, Balakrishnan et al., 2009). LP-BER is the dominant pathway used by cells to repair oxidative

base damages, single strand breaks and abasic sites induced by radiotherapy (Dogliotti et al., 2001).

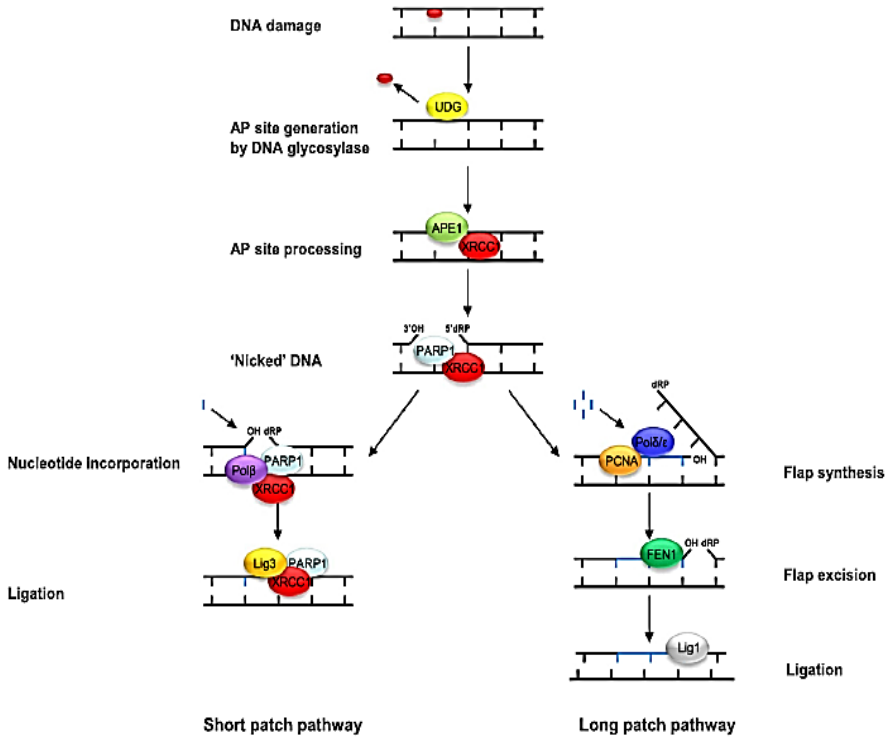


Figure 2.1 Short and long-patch base excision repair. Pathway selection is determined by the type of DNA damage incurred. SP-BER removes damage caused by alkylation and deamination. LP-BER is the dominant pathway for removal of oxidative DNA damage. Reproduced from (Abbotts and Madhusudan, 2010). Copyright© 2010 by Elsevier with permission conveyed through Copyright Clearance Centre Inc.

2.2.4 Flap endonuclease-1

FEN-1 is a multifunctional endonuclease involved in mammalian DNA replication, repair, and recombination (Lieber, 1997). It is a 43 kDA protein located on Chromosome 11 and as a nuclease, FEN-1 recognises and acts on specific DNA structures, irrespective of DNA sequences (Lee and Wilson, 1999, Shen et al., 2005). It functions as a 5'-flap endonuclease (FEN), 5'-3' exonuclease (EXO) and GAP endonuclease (GEN) (Liu et al., 2004). FEN-1 can cleave any DNA or RNA flap structures as long as the unannealed 5'-tail is single stranded (Murante et al., 1996). The major role of FEN-1 is to remove the initiator RNA primers of Okazaki fragments formed during DNA replication and oxidative DNA damage by the LP-BER pathway (Bambara et al., 1997, Liu et al., 2004). Among its other roles, FEN-1 is involved in

the resolution of tri-nucleotide sequence derived secondary structures, restarting stalled replication folks (Singh et al., 2007), fragmenting apoptotic DNA (Shen et al., 2005), and maintenance of telomere stability (Bambara et al., 1997, Shen et al., 2005).

2.2.4.1 FEN-1 in breast cancer

Consistent with its role in DNA replication, FEN-1 is expressed in all proliferative tissues (Warbrick et al., 1998). It is highly expressed in tumours, which links FEN-1 to the hyper-proliferation of cancer cells (Lam et al., 2006). It has been reported that FEN-1 can interact directly with estrogen receptor alpha, (ERα) and influence the expression of estrogen responsive genes to drive proliferation (Moggs et al., 2005, Buterin et al., 2006). In normal breast cells, FEN-1 expression is kept low by hypermethylation of the promoter region, which is abolished during neoplastic transformation (Singh et al., 2008). An extensive study on FEN-1, conducted by a team in Nottingham (Abdel-Fatah et al., 2014), reported that FEN-1 was associated with aggressive breast cancer biology and poor survival of breast cancer patients, irrespective of ER status. In ovarian cancer, FEN-1 was associated with higher grade, higher disease burden after surgery, worst ovarian cancer specific and disease-free survival (Abdel-Fatah et al., 2014).

Several studies have since shown that FEN-1 is upregulated and confers chemotherapy resistance to breast cancer cells (Wang et al., 2015, He et al., 2016). MDAMB-231 cells treated with various chemotherapy agents (mitomycin C, taxol, camptothecin, cytochalasin) and γ-radiation showed a 3-8 fold upregulated FEN-1 expression (Wang et al., 2015). Studies conducted by He et al., 2016 reported that overexpressing FEN-1 in MCF-7 cells prevents apoptosis induced by cisplatin, 5-fluorouracil (5-FU) and temozolomide (TMZ) (He et al., 2016). Such data suggest that FEN-1 is overexpressed in breast cancer cells and provides resistance against cell death induced by various cytotoxic therapies, making it an interesting therapeutic target to increase efficacy of anti-cancer agents in breast cancer.

2.2.5 DNA repair inhibitors as novel anticancer therapies

A strategy to improve radiotherapy in cancer cells is to target proteins involved in the DDR response, to inhibit repair of DNA damages incurred by various cytotoxic therapies (Biau et al., 2019). Some of the recent DNA repair inhibitors undergoing clinical evaluation and therapeutic strategies are discussed below.

KU-55933 was the first potent and selective inhibitor of ATM that induced significant radiosensitisation by inhibiting ATM-mediated phosphorylation of p53, H2AX, and CHK1 (Hickson et al., 2004, Veuger and Durkacz, 2011, Tian et al., 2015, Vavrova et al., 2016). KU-55933 has been shown, in preclinical studies, to be a highly effective radiosensitiser in breast cancer cells (Veuger and Durkacz, 2011), and has been used in the present study as a control drug and comparator. KU-55933 has not progressed in clinical trials due to the high lipophilic nature of the drug which affects solubility, permeability and potency of the agent (Hickson et al., 2004). In clinical trials, the novel oral ATM inhibitor, AZD1390, which is 100-fold more potent in blocking ATM-induced phosphorylation of key DNA repair proteins (Golding et al., 2009) is being evaluated in combination with radiotherapy for the treatment of brain cancer (NCT03423628) and central nervous system malignancies (NCT03423628) (ClinicalTrials, 2019).

As discussed in section 2.2.1, the ATR-CHK1 pathway is involved in suppressing replication stress arising from single strand DNA damage (Fokas et al., 2014). Pre-clinical studies with the ATR inhibitor, M6620, was found to radiosensitise chemo-resistant and chemo-sensitive TNBC patient-derived xenografts (PDX) (Tu et al., 2018), and this inhibitor is currently being evaluated in chemotherapy resistant TNBC and in ER-positive/HER-2 negative patients (NCT04052555) (ClinicalTrials, 2019). M6620 is also being evaluated in combination with radiotherapy for the treatment of patients with locally advanced head and neck squamous cell carcinoma (HNSCC) (NCT02567422). DNA-PK inhibitors have also shown strong radio-sensitisation as inhibition of DNA-PK affects formation of the DNA-PK active complex, which is essential for NHEJ repair (Kashishian et al., 2003). The DNA-PK inhibitor, M3814 is being evaluated as a

radiosensitiser for the treatment of locally advanced solid tumours (NCT02516813), colorectal cancers (NCT03770689) and in patients with advanced metastatic disease (NCT03724890) (ClinicalTrials, 2019).

Several PARP inhibitors (olaparib, talazoparib, rucaparib, veliparib and niraparib) are currently undergoing clinical trials to be used as a single agent or in combination with radiation (Chalmers et al., 2010, Jiang et al., 2019). Olaparib has potent radiosensitising properties in breast cancer (Jang et al., 2015, Bi et al., 2018), and has been used in the current study as a control agent. The RadioPARP trial is investigating olaparib and radiotherapy in patients with inflammatory, loco-regionally advanced or metastatic TNBC or in patients with operated TNBC with residual disease (NCT03109080). Other PARP inhibitors, such as talazoparib and veliparib, are being evaluated in combination with radiation in locally recurrent gynaecologic cancers (NCT03968406) and in patients with brain metastasis (NCT00649207) respectively. Rucaparib is currently undergoing (NCT03542175) phase 1 clinical evaluation with radiotherapy in TNBC patients with an incomplete pathological response after neoadjuvant treatment (ClinicalTrials, 2019).

In addition to PARP inhibitors, APE1, DNA polβ and FEN-1 inhibitors have also focussed on targeting the BER pathway to potentiate effects of chemo/radiotherapy (Sharbeen et al., 2015). Methoxamine is an APE1 inhibitor which prevents recognition of the AP site generated during BER (Qian et al., 2014). It is currently being investigated in combination with cisplatin and radiotherapy in patients with non-small cell lung cancer (NCT02535325) (ClinicalTrials, 2019). Inhibitors of Polβ have also been developed but have demonstrated little efficacy (Barakat et al., 2012), because of the involvement of Polβ in normal functions. FEN-1 inhibitors are discussed below.

2.2.6 FEN-1 inhibitors

FEN-1 is an attractive therapeutic target because deficiencies or deletion in the FEN-1 gene has been found to suppress tumour cell replication and repair of damage induced by various anti-cancer agents (Kucherlapati et al., 2002). These findings prompted the development of N-4 hydroxyurea

based series of FEN-1 inhibitors by Tumey et al., 2005. There are only a few FEN-1 inhibitors reported in the literature and of these, PTPD is the most widely studied (Dorjsuren et al., 2011, Kouichi et al., 2018), and is evaluated in the current thesis as a potential radiosensitiser. Reported FEN-1 inhibitors are discussed below.

JFD00950

Deshmukh et al., 2017 reported a novel FEN-1 inhibitor, JFD00950, a derivative of the N-4 hydroxyurea series published by Tumey et al., 2005 (Deshmukh et al., 2017). The authors carried out a high throughput screening of 53000 compounds which led to the identification of JFD00950 (Deshmukh et al., 2017), which demonstrated maximum inhibition of flap cleavage activity (100%). JFD00950 treatment reduced viability only in the colon cancer DLD-1 cells with an IC_{50} of 16.17±1.17μM with no effect in breast and other cell lines. No other studies have been reported using this compound (Deshmukh et al., 2017).

SC13

He et al., 2018 identified the FEN-1 inhibitor, SC13, based on the N-hydroxyl urea derivative (Tumey et al., 2005) by substituting the hydrophilic hydroxyl groups of urea with the hydrophobic phenyl, benzyl, and *n*-propyl building blocks (He et al., 2018). SC13 was found to specifically inhibit only the FEN activity of FEN-1 with no effects on the EXO or GEN activity. SC13 was reported to inhibit cellular proliferation of NSCLC cells (Zhang et al., 2018) and increase DNA double strand breaks in MCF-7 and MDAMB-231 cells. This agent chemosensitised MCF-7 cells to cisplatin, TMZ, or 5-FU (He et al., 2016) and cervical cancer cells to paclitaxel (He et al., 2018). SC13 has shown promising pre-clinical data, but further evaluation is needed in other cancer models.

PTPD

Tumey et al., 2005 developed an assay based on fluorescently labelled nucleotides screen to identify FEN-1 inhibitors that led to the identification of 3-hydroxy-5-methyl-1-phenylthieno [2,3-d]pyrimidine-2,4(1H,3H)-dion

(PTPD). Drug screening initially identified 9 potential compounds, of which PTPD was the most potent, with an IC_{50} of 0.025 μM using substrate based assays (Tumey et al., 2005). PTPD was found to inhibit FEN-1 cleavage activity by preventing entry of DNA or RNA substrates into the active site of FEN-1 (Exell et al., 2016). Testing PTPD with the kinetic fluorogenic and chemiluminescence AlphaScreen assay showed a strong concentration-dependent inhibition of FEN-1 activity. In combination with chemotherapeutic agents such as TMZ or MMS, PTPD was found to chemosensitise and induce apoptosis of bladder carcinoma cells (Tumey et al., 2005). To date, no studies have assessed the efficacy of PTPD as a radiosensitiser.

2.2.7 Hypothesis, aims and objectives

The requirement of FEN-1 to repair oxidative DNA damage by the LP-BER pathway led to the hypothesis that FEN-1 inhibition would sensitise breast cancer cells to radiotherapy by inhibiting repair of single strand DNA damage. The approach used in the current project was to assess radiosensitisation of breast cancer cells by inhibiting FEN-1, using the FEN-1 inhibitor, PTPD (Tumey et al., 2005, Dorjsuren et al., 2011). The single agent and radiosensitising effects of PTPD were assessed in the different breast cancer phenotypes using a variety of cell lines and various end-points assays. Results obtained with PTPD were compared to well-established DNA repair inhibitors such as KU-55933 and olaparib.

Hypotheses

1. The intrinsic radiosensitivity of breast cancer cells varies between different phenotypes.
2. Inhibiting the LP-BER pathway by PTPD will radiosensitise luminal and triple negative breast cancer cells.
3. The increased radiosensitisation induced by PTPD will be comparable or greater than that induced by control DNA repair inhibitors, KU-55933 and olaparib.

4. PTPD-induced radiosensitisation is due to single strand break repair inhibition and induction of single strand and double strand DNA damage.

Aims

- Characterise the breast cancer cell lines to be used in this study by assessing doubling times and plating efficiencies, comparing to expected values in the literature.
- Assess the intrinsic radiosensitivity of the different breast cancer cells.
- Investigate the *in vitro* efficacy of PTPD, as a single agent against breast cancer cell lines using proliferation and clonogenic survival assays, including control drugs, KU-55933 and olaparib, to help optimise experiments and to compare the efficacy of PTPD against.
- Investigate the *in vitro* radiosensitising effects of PTPD in breast cancer cells, comparing radioresponse in breast cancer cells to those treated with KU-55933 and olaparib.
- Investigate the potential mechanisms underlying any radiosensitising effects of PTPD by quantifying single strand and double strand break DNA damage.

2.3 Materials and Methods

2.3.1 Cell lines and culture conditions

The luminal breast cancer cell lines, MCF-7 and T47D, and TNBC cell lines, MDAMB-231, MDAMB-468 and MDAMB-436 were used in the current study to assess response to FEN-1 inhibition. All cell lines, were initially procured from the American Type Culture Collection (ATCC). Their molecular characteristics are shown in Appendix A-Table A1. All cell lines were used within a passage window of 15, and maintained in a humidified incubator with 5% CO_2 at 37°C. Cell lines were cultured in specific cell culture media listed in Appendix A-Table A2. Iron supplemented donor bovine serum (Gibco, Life Technologies) was heat inactivated at 56°C for 30 minutes before use. Cells were authenticated by multiplex short tandem repeat (STR) DNA profiling analysis (Powerplex 16, Promega)

every 4-6 months. Mycoplasma was tested regularly by technicians every 3-6 months in all breast cancer cell lines using the MycoProbe® Mycoplasma Detection Kit (R&D Systems).

2.3.2 Sub-culture

All tissue culture work was performed in a class II biological safety hood, cleaned with 70% ethanol before and after use. Cells were sub-cultured and grown in normal growth media until reaching 80-90% confluency in a T-75 cm^2 or T-125 cm^2 tissue culture flasks depending on requirement. To passage, media was aspirated and cells gently washed with phosphate buffered saline (PBS) (without Ca^{2+} and Mg^{2+}) (Sigma). 0.5 mg/ml trypsin-EDTA (Sigma) was added, swirled to cover the cell monolayer then aspirated and incubated at 37°C for 1-5 minutes, depending on cell line. Upon detachment, as observed through an inverted phase contrast microscope, trypsin-EDTA was inactivated using complete medium. An appropriate volume (split ratio of 1:5 for MCF-7, MDAMB-468 and MDAMB-436 cells; 1:3 for T47D and 1:10 for MDAMB-231 cells) of cell suspension was transferred into a new tissue culture flask and fresh media added (5ml in T-25 cm^2 flask, 15ml in T-75 cm^2 flask and 25ml in T-125 cm^2 flask). Cells were placed back into the incubator and maintained at 37°C with 5% CO_2.

2.3.3 Cryopreservation and cell recovery

For long-term storage, cells were frozen and preserved in liquid nitrogen to maintain them at low passage number. Cultured cells at 70-80% confluency were brought into suspension using trypsin-EDTA and counted using a haemocytometer. After centrifugation at 170 x g for 5 minutes, $1x10^6$ cells were resuspended in 1 ml of freezing medium (10% dimethyl sulfoxide (DMSO) and 90% complete medium). Cells were transferred into labelled cryovials and frozen overnight at -80 °C freezer in a cell freezing container before transferring into liquid nitrogen (~-180°C) for long-term storage.

To recover cryopreserved cells, cryovials were taken out from liquid nitrogen storage and thawed rapidly using a 37°C water bath. After

disinfecting the vial with 70% ethanol, the cell suspension was transferred into 9 ml of complete medium. The suspension was then centrifuged at 170 x g for 5 minutes. Then supernatant was discarded and the cell pellet was resuspended gently in complete medium, and transferred into a T-25 cm^2 tissue culture flask, and placed in the incubator. Culture medium was replaced the next day to remove any residual DMSO, after which, cells were cultured following routine cell culture procedures.

2.3.4 Drugs and drug preparation

PTPD (AOBIOUS) was reconstituted in DMSO to a stock concentration of 10 mM. KU-55933 (Tocris Biosciences) and olaparib (Santa Cruz Biotechnology) were used as control and comparator drugs. They were reconstituted in DMSO to a stock concentration of 10 mM. Doxorubicin (Sigma) was used as a control for PTPD-treated cell proliferation assays and was prepared in DMSO to a stock concentration of 50 mM. All stock solutions were aliquoted and stored at -20°C for a maximum of 6 months. Stock concentrations were added to complete media to achieve the desired concentrations for use in experiments.

2.3.5 Cell growth curves by proliferation assay

Doubling time is the time taken by cells to double in number during the exponential growth phase (Oraiopoulou et al., 2017). Proliferation assay was initially performed to identify cell line doubling time by monitoring growth of cells over a period of 0-96 hours, in order to establish optimal growth conditions and corroborate with previously published literature. $1x10^6$ cells/well were seeded in triplicate in 6-well culture plates and incubated at 37°C, 5% CO_2 to allow cell adherence. At required time-points, cells were washed with PBS and detached using 500 µl of trypsin-EDTA (section 2.3.2). Once detached, cells were resuspended in 500 µl of complete medium. Cell count was performed in duplicates using the haemocytometer. Cell counts were recorded and growth curves were constructed by plotting average number of cells versus time (hours) on y- and x-axis respectively to identify doubling time of cells. Data presented

graphically represent the average number of cells ± standard deviation (SD) of three independent experiments.

Cell growth curves were also used to determine the effects of PTPD and doxorubicin on proliferation of breast cancer cells. Doxorubicin is a commonly used chemotherapy agent in breast cancer and was used in the current experiment as a positive control agent to compare efficacy of PTPD against, and to ensure cells were responding to toxic insult as expected (Hernandez-Aya and Gonzalez-Angulo, 2013). 1×10^5 cells were seeded in triplicate in 6-well culture plates and incubated overnight to allow cells to attach. The following day, cells were treated with different concentrations of PTPD (2.5, 4, 7.5, 10, 12.5, and 15) μM for 24 hours. At the same time, a parallel set of cells were treated with doxorubicin (0.3 μM for MCF-7and MDAMB-436; 0.6 μM for T47D and 0.4 μM for MDAMB-231 and MDAMB-468 cells) for 24 hours. The ~IC_{50} concentrations of doxorubicin for MCF-7, T47D, MDAMB-231 and MDAMB-468 cells were established by previous PhD students in the lab. The IC_{50} concentration for MDAMB-436 cells were not available at the time of these experiments and therefore these cells were treated with 0.3 μM doxorubicin. Following 24 hours of drug treatment, cells in each well were harvested and counted using a haemocytometer. Cells were also collected and seeded into fresh flasks for determination of clonogenic survival (section 2.3.6). For plots, treated cells were normalised as percentage of untreated control cells at each time point. The dose-response curves were constructed by plotting average percentage of cells versus drug concentration (μM) on y- and x-axis respectively and where possible the IC_{50} of PTPD was calculated. Data presented graphically represent the average percentage of cells ± SD of two or three independent experiments as indicated.

2.3.6 Clonogenic survival assay

The effect of KU-55933, olaparib and PTPD on survival of breast cancer cells were assessed by clonogenic survival assay. 1×10^5 cells were seeded in each well of the 6-well plate and incubated overnight to allow cell adherence. The following day, cells were treated with different concentrations of PTPD (2.5, 4, 7.5, 10, 12.5, and 15) μM and incubated

for 24 hours. In separate experiments cells treated with PTPD were collected from the above proliferation assays, as described in section 2.3.5. For control drug comparator experiments, plated cells were treated with 10 μM of control DNA repair inhibitors, KU-55933 or olaparib for 24 hours. The concentration of 10 μM for control DNA repair inhibitors was chosen based on previously published studies (Hickson et al., 2004, Oplustil O'Connor et al., 2016).

After drug treatment, cells were trypsinized, counted and serially diluted with complete medium to appropriate concentrations and plated into T-25 cm^2 tissue culture flasks. Cells were incubated for 14 (MCF-7, MDAMB-231 and MDAMB-468) or 21 days (T47D and MDAMB-436) at 37°C, 5% CO_2 to allow colony formation. Flasks for clonogenic assays were incubated in an exclusive incubator separated from the routine tissue culture without disturbance. Colonies formed after the incubation period were fixed with 50% methanol in PBS for 15 minutes followed by 100% methanol for another 15 minutes, followed by staining with 0.5% crystal violet. Crystal violet was aspirated and flasks were gently washed under running tap water and allowed to dry before counting colonies. Colonies which contained more than 50 cells were scored as survivors. The plating efficiencies (PEs) of cell lines were initially assessed before applying in further experiments. PEs of untreated controls were calculated using the following equation:

$$PE = \frac{\text{Number of colonies}}{\text{Number of cells plated}} \times 100\%$$

The surviving fraction (SF) of cells following treatment with DNA repair inhibitors were calculated using the equation:

$$SF = \frac{\text{Number of colonies after treatment}}{(\text{Number of cells plated} \times PE)}$$

The dose response curves were constructed by plotting SF versus (v) drug concentration (μM) on y- and x-axis respectively. Where possible, the IC_{50} dose was calculated. Data represent the average SF ± SD of two or three

(as indicated) independent experiments, with each experiment containing six parallel sets.

2.3.7 Cell irradiation

Cells were irradiated using a RS225 Xstrahl x-ray cabinet irradiation system (Xstrahl Limited, UK) with single doses of 2, 4, 6 or 8 Gy. x-rays delivered at 195 kV, 10 mA, with a dose rate of 0.87 Gy/minutes. The cabinet was fitted with a 0.5 mm copper filter and used a 48.4 cm focus-to-skin distance. Sham irradiated cells were used as controls. Dosimetry was routinely assessed by Radiotherapy Physics staff in the Department of Oncology, Nottingham University Hospitals NHS Trust, and City Hospital campus.

Initially, the intrinsic radiosensitivity of breast cancer cells were assessed by irradiating pre-plated breast cancer cells in T-25 cm^2 or T-75 cm^2 flask with single doses of 2, 4, 6 or 8 Gy. After irradiation, cells were returned to the incubator for 14-21 days to allow colony formation. Data represent the average SF ± SD of three independent experiments, with each experiment containing six parallel sets.

2.3.8 Drug-radiation combinations

For drug-radiation combination experiments, cells were plated in T-25 cm^2 or T-75 cm^2 at low seeding densities. It is important that the DNA repair inhibitors are present in cells at the time of radiation to prevent immediate repair of DNA damage (Fok et al., 2019, Lee et al., 2019b). Therefore, the day after seeding, control inhibitors, 10 μM KU-55933 or olaparib was added to the pre-plated cells for 1 hour prior to irradiation. As 10 μM PTPD treatment had no effect on radiosensitivity with 1 hour treatment, cells were treated with PTPD for up to 24 hours prior to irradiation. Treated cells were irradiated with a single doses of 2, 4, 6 or 8 Gy. Sham irradiated cells were used as controls. After irradiation, cells were returned to the incubator for 16-20 hours, as suggested by previously published studies (Oplustil O'Connor et al., 2016, Parsels et al., 2018, Michmerhuizen et al., 2019). Following which, the DNA inhibitor-containing media was replaced with fresh complete medium and flasks transferred to the clonogenic

incubator and allowed to form colonies for appropriate periods of time (section 2.3.6). For survival analysis, the SF of radiation alone was calculated as:

$$SF = \frac{\text{Number of colonies formed after irradiation}}{\text{Number of cells plated} \times PE}$$

The SF of drug-radiation combination experiments were corrected for independent cytotoxic effects of DNA repair inhibitors and was calculated as:

$$SF = \frac{\text{Number of colonies formed after irradiation}}{\text{Number of cells plated} \times PE \times \text{SF of inhibitor}}$$

Dose-response curves were plotted as a function of radiation dose on a log/linear plot using the linear quadratic (LQ) model and calculated using the open source survival calculation programme, CS-CAL developed by the German Cancer Research Centre and available at - http://angiogenesis.dkfz.de/oncoexpress/software/cs-cal/index.htm.

Cellular radioresponse was measured from the radiation survival curves using conventional parameters of α, β, α/β, and SF2 (surviving fraction at 2 Gy). α and β values established from the survival curve assesses the intrinsic radiosensitivity of cells as discussed in chapter 1. The fraction of cells surviving at 2 Gy was also used as a measure of radioresponse between the different cell lines to radiation, +/- DNA repair inhibitor, with greater SF2 values equating to reduced sensitivity (Matthews et al., 1989). The sensitiser enhancement ratio at 1% survival ($SER_{0.01}$) was used to evaluate the degree of radiosensitisation in the presence of the DNA repair inhibitor and was calculated as the ratio of radiation doses in the absence to the presence of the drug which produces the same biological effect (Brown, 1985). SER values greater than 1.00 indicate radiosensitisation. Data represent the mean SF ± SD of three independent experiments, with each experiment containing six parallel sets.

2.3.9 Immunofluorescence

RPA and γ-H2AX protein expression and localisation are often used as an estimate of single strand and double strand DNA damage respectively (Zou

et al., 2006, Sharma et al., 2012). The expression of RPA and γ-H2AX was detected using immunofluorescence and confocal microscopy in response to various treatment conditions (+/- PTPD and radiation). Prior to carrying out PTPD-radiation combination experiments, the optimum radiation dose for RPA and γ-H2AX expression was assessed by immunofluorescence and flow cytometry (FACS) by irradiating representative breast cancer cells (T47D and MDAMB-231) at 0.5, 1 or 1.5 Gy and 1, 2 or 4 Gy respectively. The detailed protocol is given in Appendix A-section A1 for RPA and Appendix A-section A2 for γ-H2AX. After dose selection, cells were fixed at time points of (0, 0.5, 2, 4, 6 and 24) hours to assess time-post irradiation at which RPA (Appendix A-Figure A1 and Figure A2) and γ-H2AX (Appendix A-Figure A3) expression was maximum.

2.3.9.1 PTPD-radiation combination experiments

Sub-confluent cells were trypsinized, and seeded at a density of $2x10^4$ cells onto coated sterile coverslips (Corning™ BioCoat™) in 6-well plates and allowed to adhere overnight. The following day, cells were treated with or without 10 μM PTPD for 24 hours, before being irradiated at a previously optimised dose of 1 Gy for RPA expression and 4 Gy for γ-H2AX detection. At 0.5 hours post-radiation exposure, cells were fixed with 4% paraformaldehyde for 10-20 minutes. Following which, cells were permeabilized and blocked in 0.3% Triton X-100 with 2% serum for 30 minutes at room temperature. Cells were stained with the primary anti-RPA (1:200, Abcam) or primary anti-γ-H2AX antibody (1:500, Merck) and incubated overnight at 4°C. The following day, cells were treated with Alexa 488-conjugated goat anti-mouse secondary antibody (1:200 dilution, Abcam) for 1 hour in the dark, followed by 2-3 washes in 0.05% PBS-Tween-20 buffer. Nuclei were counterstained with mounting media containing DAPI (Vectashield). Imaging was performed at x63 magnification on a confocal microscope (Leica TCS SPE). The number of RPA or γ-H2AX foci per nuclei was counted using ImageJ software and at least 100 nuclei were analysed for each treatment condition. Data represent the mean foci number ± SD of two independent experiments, with each experiment containing three parallel sets.

2.3.10 Statistical analysis

Statistical analyses were conducted using GraphPad Prism 7 software. Data is represented as mean ± SD of two or three (as indicated) independent experiments with each performed in triplicates (or six replicates for clonogenic assays). Data were analysed using the student t-test for comparison between two groups and ANOVA one-way test for comparison between more than two groups. *P* values <0.05 were considered as statistically significant. For combining errors from individual experiments when pooling data, the following formula was used:

$$\text{SD combined} = \sqrt{\frac{\{(n_1 - 1) \times SD_1^2 + (n_2 - 1) \times SD_2^2\}}{(n_1 + n_2 - y)}}$$

Where $SD_{combined}$ is the combined standard deviation from *y* (number of experiments) experiments and SD_1 and SD_2 are the standard deviations in individual experiments and n_1 and n_2 are number of replicates in each experiment (Mukherjee et al., 2007).

2.4 Results

2.4.1 Growth characteristics of breast cancer cells

The growth characteristics, such as doubling times and plating efficiencies, of breast cancer cells used in this study were assessed prior to carrying out experiments to ensure cells were growing as expected. To calculate doubling time, the growth of all cell lines were monitored for a period of 0-96 hours, by performing cell count every 24 hours. Based on the growth curve (Figure 2.2), the average doubling times were 29±4.12 in MCF-7, 32±1.86 in T47D, 20±2.47 in MDAMB-231, 31±1.24 in MDAMB-468 and 41±4.55 hours in MDAMB-436 cells. These results are in agreement with colleagues within the research group and also with previously published literature (Kennedy et al., 1985, Watanabe et al., 2001, Ware et al., 2007). Studies by Watanabe et al., 2001 and Kennedy et al., 1985 demonstrated a similar doubling time of 30.2±0.7 in MCF-7, 31.1±0.6 in T47D, 28.1±1.2 in MDAMB-231, 29.9±0.5 in MDAMB-468 and 44 hours in MDAMB-436 cells.

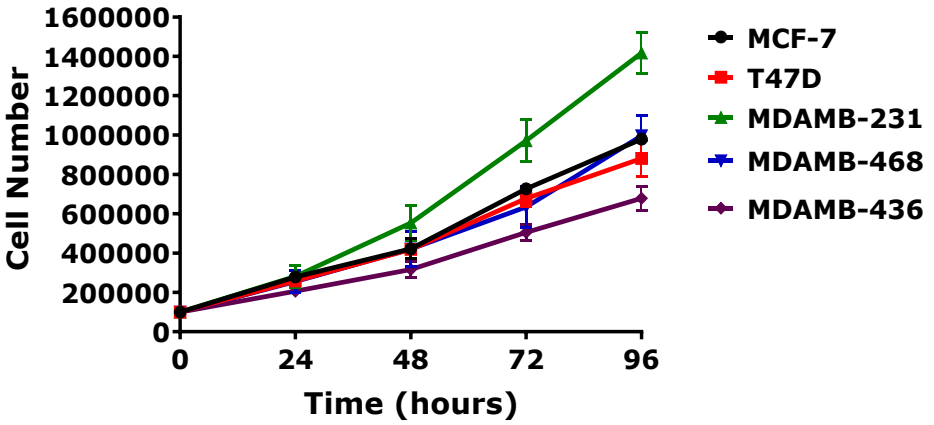


Figure 2.2 Growth curves of breast cancer cells. The average cell number is plotted against the various time-points. Data represent the mean cell number/well ± SD of three independent experiments, with each experiment conducted in triplicate.

The clonogenic assay is a cell survival assay which determines the ability of single cells to form colonies. PE, assessed by clonogenic survival assay, is an inherent characteristic of cells and should be reproducible if growth conditions remain constant (Pomp et al., 1996, Franken et al., 2006).

To assess the PE, sub-confluent cells without any treatment were initially plated for clonogenic survival assays in a series of varying cell densities (100, 200, 400 and 300, 600 and 900) and incubated for 14-21 days to allow colony formation. T47D and MDAMB-436 cells had lower PEs compared to MCF-7, MDAMB-231 and MDAMB-468 cells. As shown in Table 2.1, the PEs were 41±4.35% in MCF-7, 16±2.82% in T47D, 51±5.70% in MDAMB-231, 44±1.52% in MDAMB-468 and 19±3.05% in MDAMB-436 cells. The optimal incubation time for colony formation was 14 days in MCF-7, MDAMB-231 and MDAMB-468 cells with seeding density of 100 or 200 cells/T-25 cm^2 flask. T47D and MDAMB-436 cells required longer incubation period of 21 days with a cell seeding density of 300 and 600 cells/T-25 cm^2 flask.

Table 2.1 Plating efficiencies of breast cancer cell lines.

Cell line	PE (%) obtained in this study	PE (%) published in the literature
MCF-7	41 ± 4.35	46 ± 0.00
T47D	16 ± 2.82	12 ± 13.00
MDAMB-231	51 ± 5.70	56 ± 8.90
MDAMB-468	44 ± 1.52	48 ± 0.00
MDAMB-436	19 ± 3.05	11 ± 1.10

Abbreviations: PE - plating efficiency.

The PE's of cell lines obtained in the current study were comparable to published literature which reported PEs of 46% in MCF-7, 12±13% in T47D, 56±8.90% in MDAMB-231, 48% in MDAMB-468 and 11±1.10% in MDAMB-436 cells (Lagadec et al., 2012, Zhang et al., 2014, Karasawa. K., 2014, Veldwijk et al., 2014, Lindstrom et al., 2017, Su et al., 2018).

Taken together, data indicate that the doubling times and PEs of breast cancer cells used in the current study were similar to published literature, suggesting that the breast cancer cell lines were behaving as expected. The clonogenic assay is the gold standard assay to assess reproductive cell death after treatment with cytotoxic agents, including ionising radiation, and was used in subsequent experiments to assess survival (Franken et al., 2006).

2.4.2 Characterisation of positive control drugs – KU-55933 and olaparib

2.4.2.1 Cytotoxic effect of KU-55933 on breast cancer cells

KU-55933 is a well-established radiosensitiser across multiple cancer models (Tian et al., 2015, Zhang et al., 2015b, Vavrova et al., 2016), and was used as a positive control and comparator in the current study against the FEN-1 inhibitor, PTPD (Hickson et al., 2004). The single-agent cytotoxic effect of KU-55933 on cellular survival of the luminal and TNBC cell lines were evaluated using clonogenic survival assays. A concentration of 10 μM for 24 hours was chosen for treatment based on previously published

studies for the use of DNA repair inhibitors (Kashishian et al., 2003, Hickson et al., 2004, Oplustil O'Connor et al., 2016). Cells without treatment were used as controls in this study. The SF from clonogenic assays were calculated and plotted against the corresponding cell lines as shown in Figure 2.3.

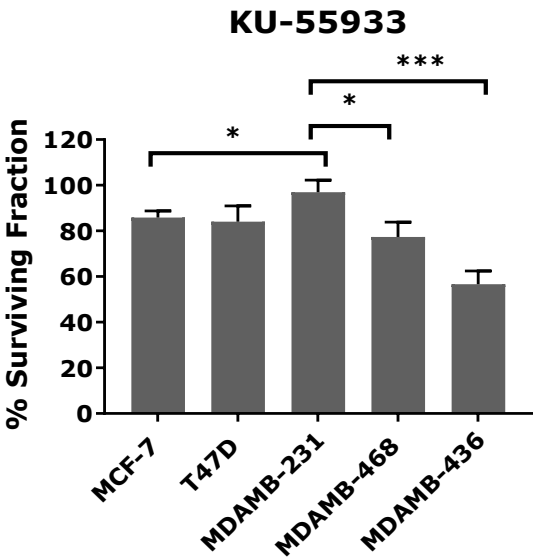


Figure 2.3 KU-55933 clonogenic survival of breast cancer cells.PEs of individual cell lines were: MCF-7 - 45±4.72%; T47D - 15±2.64%; MDAMB-231 - 49±4.72%; MDAMB-468 - 44±2.08%; and MDAMB-436 - 19±2.51%. Data represent the average SF±SD of three independent experiments, with each experiment containing six parallel data sets, which are analysed using the Student's t-test. *P<0.05 and ***P<0.001 for MDAMB-231 v MCF-7, T47D, MDAMB-468 and MDAMB-436.

The MDAMB-231 cells were only slightly affected by treatment with KU-55933 and demonstrated a SF of 96±5.36%. Compared to MDAMB-231 cells, KU-55933 treatment showed a 15-20% decrease in colony formation with SF values of 85±2.92% (P=0.035) in MCF-7, 84±6.87% (P=0.063) in T47D and 77±6.50% (P=0.015) in MDAMB-468 cells. The most sensitive cell line to KU-55933 treatment was MDAMB-436 cells which showed a 44% reduction in clonogenic survival with SF of only 56±5.77% (P<0.001). The above data indicate that KU-55933 is most cytotoxic in the MDAMB-436 cells in comparison to the other breast cancer cell lines. MCF-7, T47D, MDAMB-231 and MDAMB-468 cells are DNA repair-proficient cell lines and therefore this may explain lower levels of cytotoxicity associated with KU-55933 treatment. In contrast, increased cytotoxicity observed in the

MDAMB-436 cells may reflect its inherent BRCA-1 deficient nature, which coupled with ATM inhibition might further decrease or completely inhibit its potential to repair DNA double strand breaks (Chen et al., 2017).

2.4.2.2 Cytotoxic effect of olaparib on breast cancer cells

Olaparib was chosen as a positive control and comparator in the current study, because of its ability to inhibit the single strand break repair pathway, and therefore would provide a more direct comparison to the effects of PTPD (Chen, 2011). As with KU-55933, the single agent cytotoxic effect of olaparib in the luminal and TNBC cell lines was evaluated using clonogenic survival. Cells were treated with 10 μM olaparib (Prasad et al., 2017, Park et al., 2018) for 24 hours and seeded for assessment by clonogenic survival. Cells without drug treatment were used as controls. The SF was calculated and plotted for the respective cell lines as shown in Figure 2.4.

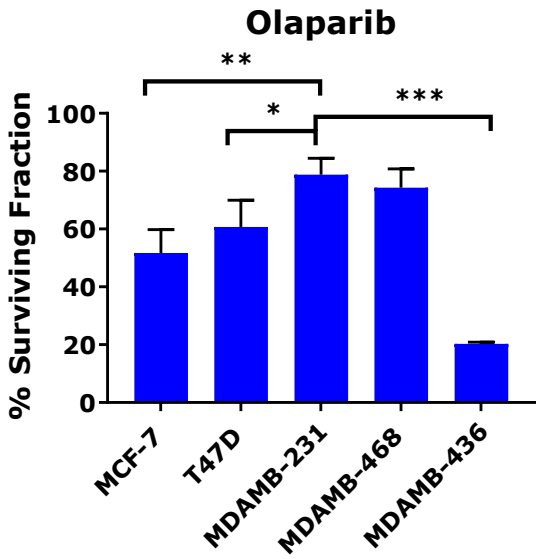


Figure 2.4 Olaparib clonogenic survival of breast cancer cells. PEs of individual cell lines were: MCF-7 - 61±0.57%; T47D - 17±3.21%; MDAMB-231 - 61±3.60%; MDAMB-468 - 47±6.08%; and MDAMB-436 - 23±1.00%. Data represent the average SF±SD of three independent experiments, with each experiment containing six parallel data sets, which are analysed using the Student's t-test. *P<0.05, ** P<0.01 and ***P<0.001 for MDAMB-231 v MCF-7, T47D, MDAMB-468 and MDAMB-436.

Results show that treatment with olaparib was cytotoxic in the luminal MCF-7 and T47D cells and resulted in a 40-50% reduction in colony

formation, with a SF of 51±8.14% (P=0.009) and 60±9.29% (P=0.045) respectively. Compared to the luminal cell lines, the triple negative MDAMB-231 and MDAMB-468 cells were relatively resistant, with 25% reduction in survival with SF values of 78±5.5.67% and 74±6.42% (P=0.421) respectively. As with KU-55933, olaparib was highly cytotoxic in MDAMB-436's and resulted in an 80% decrease in colony formation with SF of 20±0.57% (P<0.001). As mentioned previously, one potential reason for the increase in cytotoxicity observed in MDAMB-436 cells may be because of their inherent BRCA-1/2 deficiency which induces a synthetic lethal phenotype upon PARP inhibition (Bryant et al., 2005, Arun et al., 2015).

2.4.3 Cytotoxicity of PTPD on breast cancer cells

FEN-1 of the LP-BER pathway is involved in the repair of oxidative base damage and single strand breaks induced by ionising radiation (Larsen et al., 2003). In the current study, the radioresponse in PTPD treated breast cancer cells were assessed in subsequent experiments. Initially, the single agent activity of PTPD in the luminal and TNBC cell lines was assessed using proliferation and clonogenic survival assays.

2.4.3.1 Cytotoxic effect of PTPD on proliferation

Breast cancer cell lines were treated with different concentrations of PTPD (0, 2.5, 5, 7.5, 10, 12.5 and 15) μM for 24 hours and proliferation was assessed by cell counting. Doxorubicin, a commonly used chemotherapeutic drug in breast cancer was used as a positive control for proliferation assay (Hernandez-Aya and Gonzalez-Angulo, 2013). Effects of PTPD on cell proliferation of breast cancer cells were assessed by plotting a dose-response curve obtained from cell counts and is presented in Figure 2.5. The half maximal inhibitory dose (IC_{50}) was calculated where possible.

Breast cancer cells treated with doxorubicin showed ~50% reduction in cell number, except in the MDAMB-436 cells which showed an 80% reduction in cell proliferation indicating that they were responding as expected. With doxorubicin (24 hours), breast cancer cells showed a cell proliferation of

61±5.28% in MCF-7, 51.5±3.5% in T47D, 46±1.60% in MDAMB-231, 55±2.82% in MDAMB-468 and 20±1.60% MDAMB-436 cells.

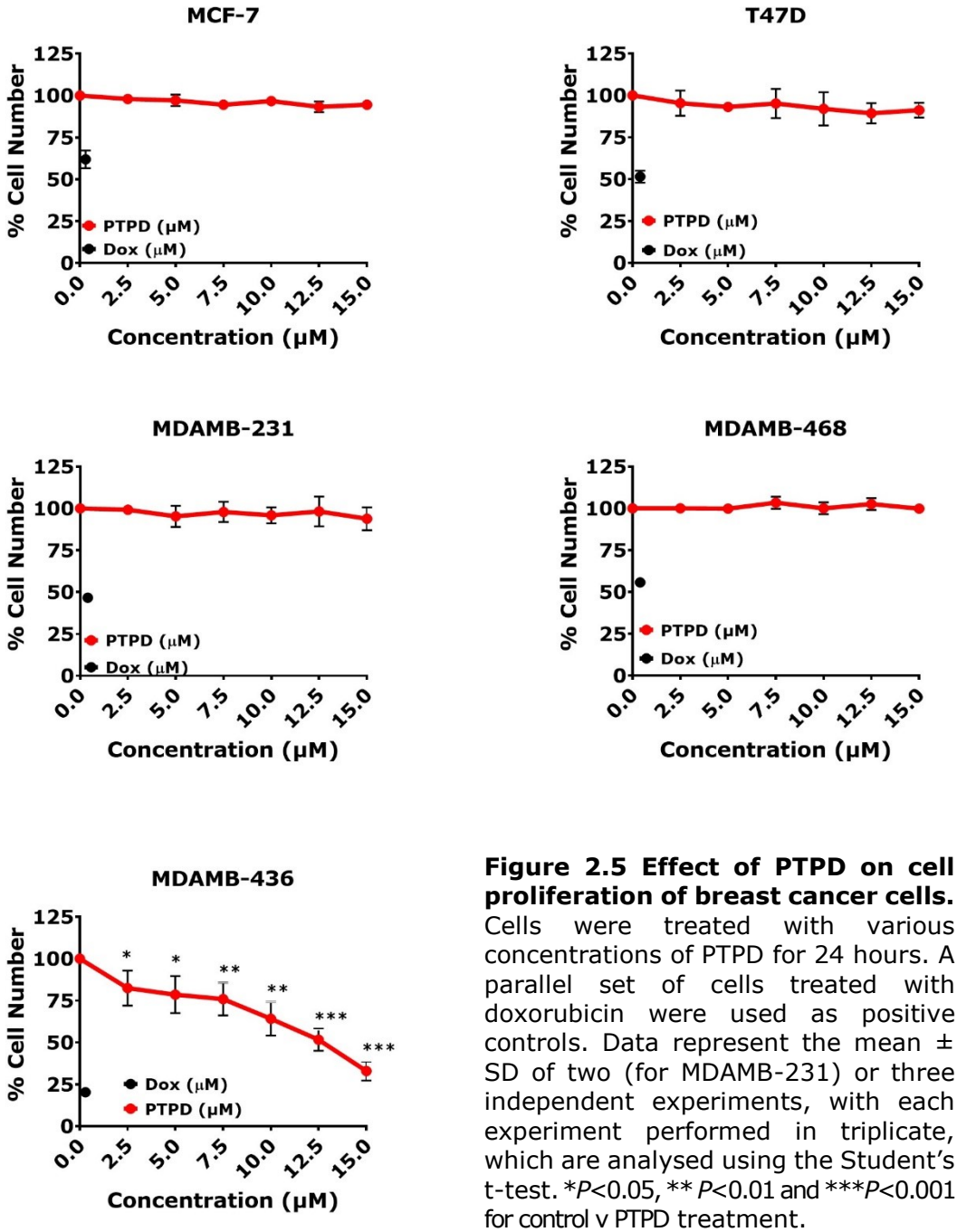


Figure 2.5 Effect of PTPD on cell proliferation of breast cancer cells. Cells were treated with various concentrations of PTPD for 24 hours. A parallel set of cells treated with doxorubicin were used as positive controls. Data represent the mean ± SD of two (for MDAMB-231) or three independent experiments, with each experiment performed in triplicate, which are analysed using the Student's t-test. **P*<0.05, ** *P*<0.01 and ****P*<0.001 for control v PTPD treatment.

Cells were treated with various concentrations of PTPD with results showing no effect of PTPD treatment in all cell lines, but a significant dose dependent reduction in cell number was seen in the MDAMB-436 cells at all concentrations (*P*=0.002 at 10 μM). At 10 μM PTPD, MDAMB-436 cells showed a 36% reduction in proliferation compared to the other breast

cancer cell lines which demonstrated cell proliferation of 96±2.38% in MCF-7, 92±9.90% in T47D, 95±4.80% in MDAMB-231, and 100±3.59% in MDAMB-468 cells. The proliferation IC_{50} of PTPD in MDAMB-436 cells was 13.97±3.23 μM (P<0.001).

In subsequent experiments MDAMB-231 and T47D cells were treated with a higher concentration (50 μM) of PTPD for 24, 48 and 72 hours, to evaluate if increasing concentration and treatment time might change response. The proliferation of both cell lines did not notably change even with increasing concentrations and longer treatment times – data not shown. Taken together, results suggest that PTPD is cytotoxic only in the BRCA deficient MDAMB-436 cells. Clonogenic survival assays were conducted to confirm such findings (section 2.4.3.2).

2.4.3.2 Cytotoxic effect of PTPD on clonogenic survival

Proliferation assays are short-term assays that allows for rapid assessment of tumour cell response to anti-cancer agents and may not necessarily provide information on the long-term effect of cytotoxic treatment (Citrin, 2016). In contrast, clonogenic assay assesses the long-term effect of cytotoxic treatment on cells (Franken et al., 2006, Woolston and Martin, 2011). Cells from the proliferation assays, as described in section 2.4.3.1, were used to assess clonogenic survival following PTPD treatment (0, 2.5, 5, 7.5, 10, 12.5 and 15) μM. Effects of PTPD on clonogenic survival of breast cancer cells were assessed by plotting dose-response curves as shown in Figure 2.6. The clonogenic IC_{50} was calculated where possible.

In the current set of experiments, cells treated with the concentrations of doxorubicin used for proliferation assay were all killed (MCF-7 and MDAMB-436 with 0.3 μM; T47D with 0.6 μM; MDAMB-231 and MDAMB-468 with 0.4 μM) indicating substantial differences in response between IC_{50}'s from short term proliferation assays v longer term clonogenic survival assays. Such data reinforce the need to always conduct both assay types when evaluating novel agents.

Unlike doxorubicin, PTPD treatment had only marginal, or no, effects on the survival of MCF-7, T47D, MDAMB-231 and MDAMB-468 cells, but, as

with proliferation data, MDAMB-436 cells demonstrated a dose dependent reduction in colony formation with clonogenic IC_{50} value of 8.06±2.92 μM (*P*=0.001), which was lower than that achieved for proliferation assay (13.97±3.23 μM). In all other cell lines, 10 μM PTPD treatment, resulted only in a marginal reduction of <10% in clonogenic survival.

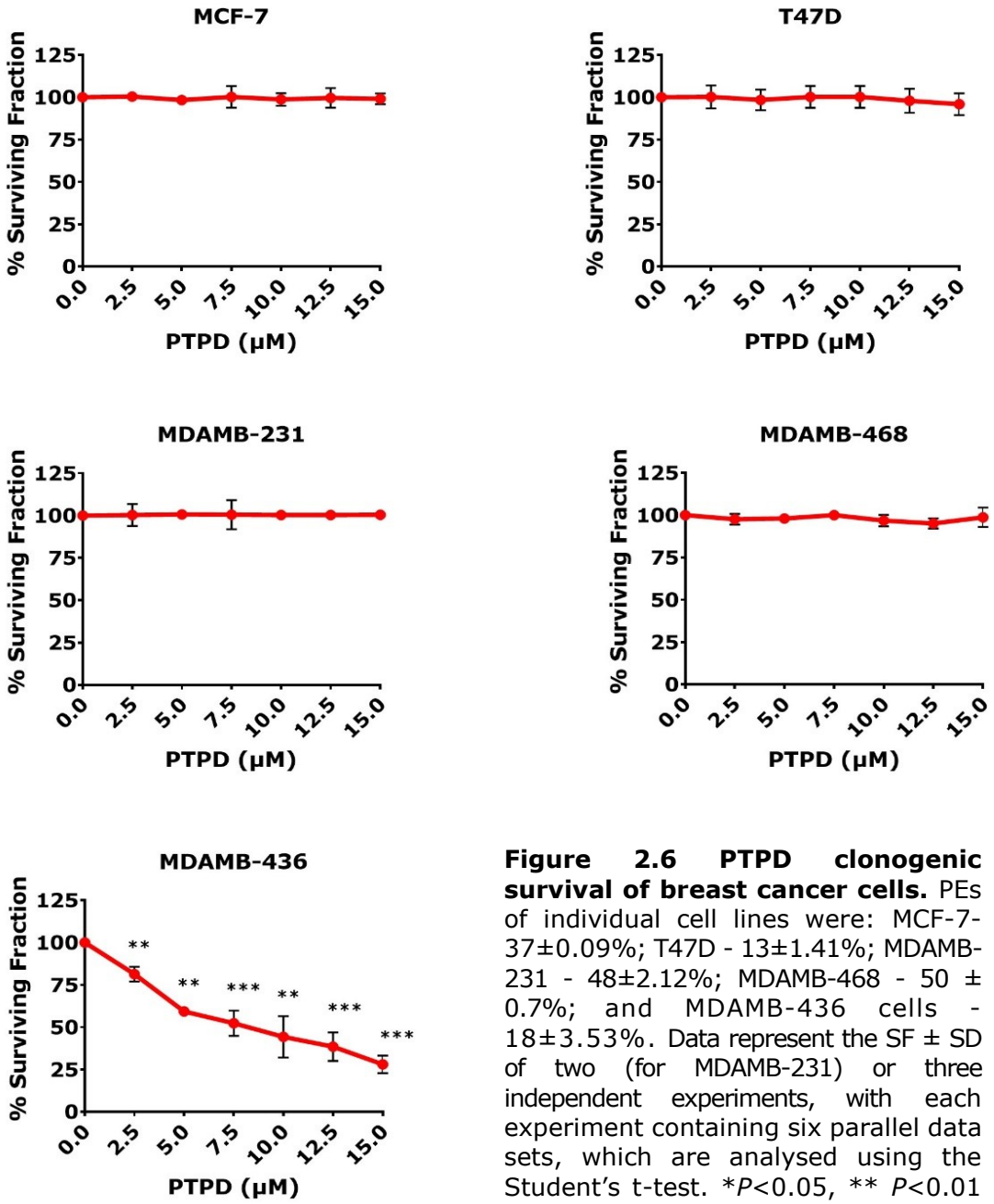


Figure 2.6 PTPD clonogenic survival of breast cancer cells. PEs of individual cell lines were: MCF-7- 37±0.09%; T47D - 13±1.41%; MDAMB-231 - 48±2.12%; MDAMB-468 - 50 ± 0.7%; and MDAMB-436 cells - 18±3.53%. Data represent the SF ± SD of two (for MDAMB-231) or three independent experiments, with each experiment containing six parallel data sets, which are analysed using the Student's t-test. **P*<0.05, ** *P*<0.01 and ****P*<0.001 for control v PTPD treatment.

Data suggest that PTPD is non-cytotoxic to MCF-7, T47D, MDAMB-231 and MDAMB-468 cells when assessed by proliferation or clonogenic survival

assays. The cytotoxic effect of PTPD was observed only in the MDAMB-436 cells. As with olaparib treatment, this may be due to inhibition of FEN-1 inducing a synthetic lethal phenotype (Bryant et al., 2005). The BRCA-1 deficient cell line has a dysfunctional double strand break repair pathway and therefore may be more reliant on the FEN-1 mediated single strand repair pathway to repair DNA damage (Mengwasser et al., 2019). Since PTPD was non-toxic to most cell lines, a concentration of 10 μM was used for all cell lines in subsequent experiments.

2.4.4 Intrinsic radiosensitivity of breast cancer cells

The intrinsic radiosensitivity of a cell line is an important factor that determines its radioresponse (Hall et al., 2014). Prior to carrying out drug-radiation combination experiments, the radioresponse of breast cancer cells following exposure to single dose irradiation with 2, 4, 6 or 8 Gy was assessed using clonogenic survival assays. The SF's were plotted as a function of radiation dose on a log/linear plot and data fitted using the linear quadratic (LQ) model as shown in Figure 2.7.

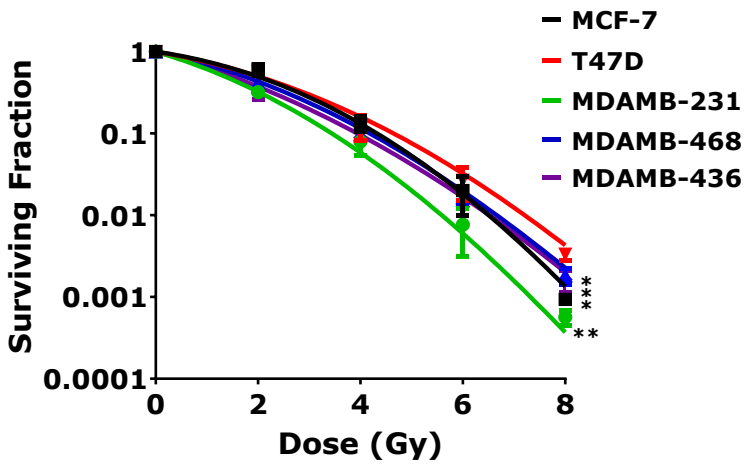


Figure 2.7 Survival curves of breast cancer cells after single dose irradiation. The PEs of individual cell lines were: MCF-7 - 45±4.72%; T47D - 15±2.64%; MDAMB-231 - 49±4.72%; MDAMB-468 - 44±2.08%; MDAMB - 436 - 19±2.51%. Data represent the mean SF ± SD of three independent experiments, with each experiment containing six parallel data sets, which are analysed using the Student's t-test. *P<0.05 and ***P<0.001 for T47D v MCF-7, MDAMB-231. MDAMB-468 and MDAMB-436 cells.

SF2's were assessed, with higher values indicating greater survival and reduced sensitivity (Hall et al., 2014). All lines demonstrated a dose

dependent reduction in surviving fraction, with differential radiosensitivity noted between the different breast cancer phenotypes. Luminal cells were relatively more radioresistant compared to TNBC lines. At 2 Gy, the luminal MCF-7 and T47D cells were the most resistant to radiation with SF values of 0.49±0.01, and 0.49±0.10 respectively. TNBC lines, MDAMB-231 and MDAMB-436, were more sensitive with SF2 values of 0.31±0.04, and 0.35±0.08 respectively, whereas the MDAMB-468 cells were moderately sensitive with an SF2 value of 0.43±0.02. MDAMB-231 cells were the most radiosensitive with this being particularly evident at the highest dose of 8 Gy, with an SF8 of 0.0003 (P=0.003) compared to 0.004 in T47D cells, the most resistant. MCF-7, MDAMB-468 and MDAMB-436 showed intermediate sensitivity with SF8 values of 0.001 (P=0.005), 0.002 (P=0.045) and 0.002 (P=0.015) respectively. The radioresponse of cancer cells used in this study were similar to previous studies that reported SF2's of 0.51 in MCF-7, 0.46 in T47D (El-Awady et al., 2003); 0.53 in MDAMB-231 (Torres-Roca et al., 2005), 0.49 in MDAMB-468 cells (Mehta et al., 2016) and 0.26 in MDAMB-436 cells (Zhao et al., 2016). Separate survival curves for luminal and TNBC cells shown in Appendix A-Figure A4. Radiobiologic parameters (α, β, and α/β ratio), are summarised in Table 2.2.

Table 2.2 Radiobiologic parameters of breast cancer cells.

Cell line	α (Gy^{-1})	β (Gy^{-2})	α/β (Gy)	SF2
MCF-7	0.17±0.01	0.08±0.08	2.61±2.22	0.49±0.01
T47D	0.24±0.12	0.05±0.01	5.12±3.82	0.49±0.10
MDAMB-231	0.49±0.06	0.06±0.01	7.77±2.67	0.31±0.04
MDAMB-468	0.30±0.06	0.05±0.01	5.81±3.37	0.43±0.02
MDAMB-436	0.42±0.11	0.04±0.01	10.70±5.65	0.35±0.08

Parameters were calculated from clonogenic data fitted to a LQ model. Abbreviation: SF2, surviving fraction at 2Gy. α represents the initial slope and β refers to the terminal slope of the dose-response curve. α/β ratio refers to the dose where the linear and quadratic components are equal.

In the LQ model, a higher α/β ratio represents a more linear survival curve which indicates increased radiosensitivity (van Leeuwen et al., 2018). The

α-value and α/β ratio of MDAMB-231 (0.49±0.06 and 7.77±2.67) and MDAMB-436 (0.42±0.11 and 10.70±5.65) cells were higher in comparison to MCF-7 (0.17±0.01 and 2.61±2.22), T47D (0.24±0.12 and 5.12±3.82) and MDAMB-468 (0.30±0.06 and 5.81±3.37) cells respectively. This indicates that MDAMB-231 and MDAMB-436 cell lines are intrinsically more sensitive to radiation compared to the other cell lines. Although the *in vitro* radioresponse obtained in the current study are in agreement with previously published literature, these contradict the response of clinical subtypes to radiation. Clinically, the TNBCs are more radioresistant with a 2-fold increase in the risk of local recurrence following radiotherapy, compared to luminal breast cancers (Tramm et al., 2014, Sjöström et al., 2017). Such data indicate that the vitro behaviour of cells does not always mimic *in vivo* tumour response, reasons for which will be discussed later.

2.4.5 Radiosensitisation with KU-55933 and olaparib

2.4.5.1 KU-55933 radiosensitises breast cancer cells

To test the radiosensitising properties of the control agent, KU-55933, pre-plated breast cancer cells were treated with 10 μM KU-55933 for 1 hour pre- and 16 hour-post-irradiation exposure. The effect of KU-55933 on radiosensitivity of breast cancer cells was assessed by clonogenic survival. As shown in Figure 2.8, KU-55933 substantially increased radiosensitivity across all breast cancer phenotypes.

Mean SF2 values were significantly higher in control cells than in KU-55933 treated cells i.e. 0.41±0.13 v 0.19±0.04 (P=0.02) in MCF-7, 0.55±0.10 v 0.21±0.04 (P=0.007) in T47D, 0.36±0.01 v 0.10±0.01 (P=0.020) in MDAMB-231, 0.43±0.02 v 0.15±0.03 (P<0.001) in MDAMB-468, and 0.35±0.08 v 0.03±0.02 (P=0.003) in MDAMB-436 cells. KU-55933 treatment significantly enhanced radiosensitivity in all breast cancer cells with $SER_{0.01}$ of 1.60±0.23 in MCF-7, 1.71±0.27 in T47D, 1.82±0.21 in MDAMB-231, 1.68±0.33 in MDAMB-468 and 3.42±0.91 in MDAMB-436 cells. Such SER values equate to the survival of cells at 8 Gy decreasing from 0.001 to 0.0001 in MCF-7, 0.003 to 0.0004 in T47D, 0.0005 to 0.00003 in MDAMB-231, 0.002 to 0.0002 in MDAMB-468 and 0.001 to

0.000009 in MDAMB-436 cells treated with KU-55933. Other radiobiologic parameters are summarised in Table 2.3.

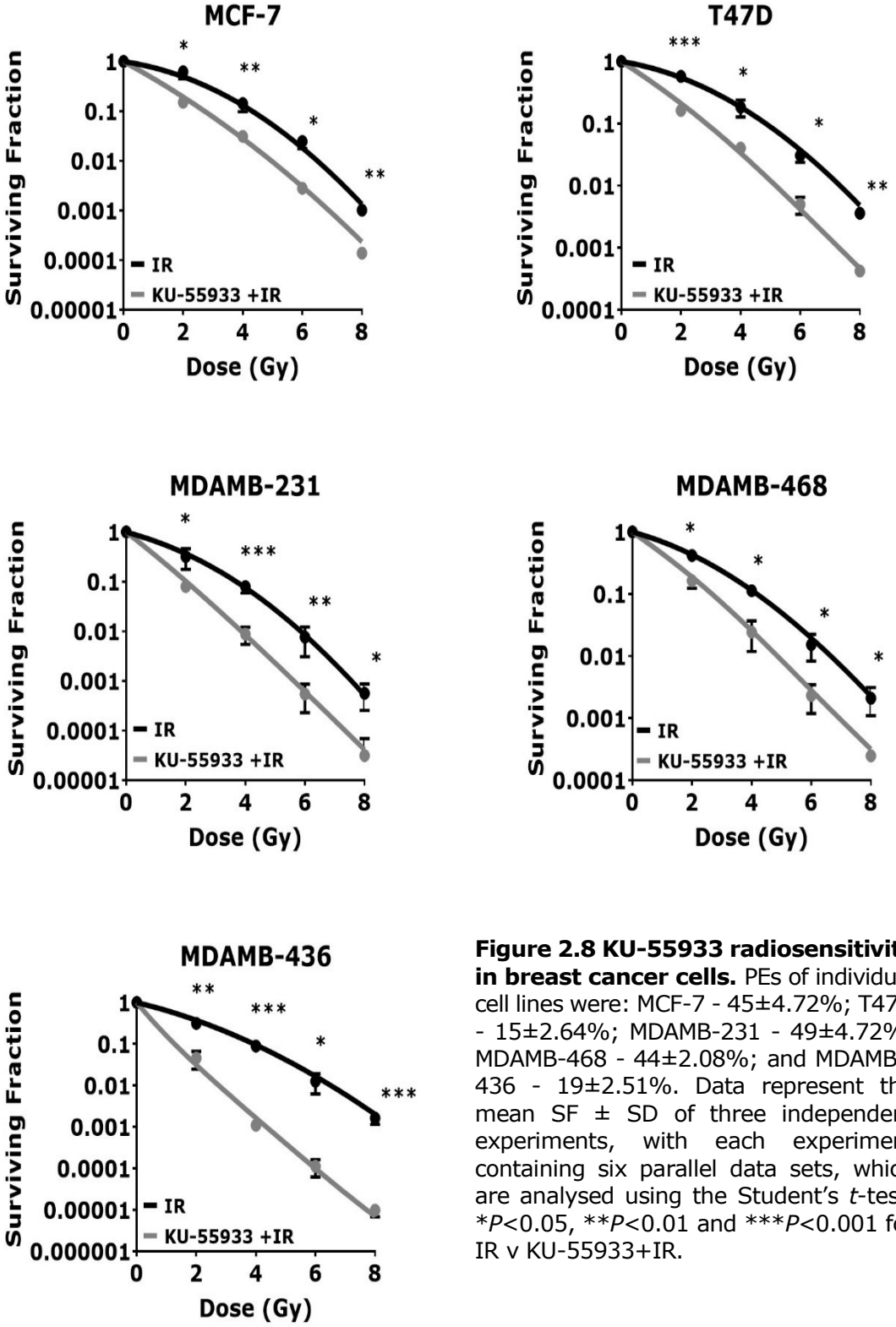


Figure 2.8 KU-55933 radiosensitivity in breast cancer cells. PEs of individual cell lines were: MCF-7 - 45±4.72%; T47D - 15±2.64%; MDAMB-231 - 49±4.72%; MDAMB-468 - 44±2.08%; and MDAMB - 436 - 19±2.51%. Data represent the mean SF ± SD of three independent experiments, with each experiment containing six parallel data sets, which are analysed using the Student's *t*-test. **P*<0.05, ***P*<0.01 and ****P*<0.001 for IR v KU-55933+IR.

Table 2.3 Radiobiologic parameters of breast cancer cells treated with IR and/or KU-55933.

Cell line	α (Gy^{-1})	β (Gy^{-2})	α/β (Gy)	SF2	$SER_{(0.01)}$
MCF-7					
IR	0.22±0.18	0.08±0.02	4.32±3.76	0.41±0.13	
KU-55933+IR	0.76±0.12	0.03±0.01	20.68±7.56	0.19±0.04	1.60±0.23
t test	***P*=0.013**	***P*=0.034**	***P*=0.022**	***P*=0.021**	
T47D					
IR	0.17±0.11	0.06±0.01	2.93±2.04	0.55±0.10	
KU-55933+IR	0.63±0.09	0.05±0.01	12.79±5.36	0.21±0.04	1.71±0.27
t test	***P*=0.006**	*P*=0.33	***P*=0.04**	***P*=0.007**	
MDAMB-231					
IR	0.37±0.24	0.07±0.02	6.81±7.03	0.36±0.12	
KU-55933+IR	1.08±0.04	0.03±0.02	61.27±53.49	0.102±0.01	1.82±0.21
t test	***P*=0.007**	*P*=0.13	*P*=0.143	***P*=0.020**	
MDAMB-468					
IR	0.30±0.06	0.05±0.01	5.81±3.37	0.43±0.02	
KU-55933+IR	0.91±0.11	0.01±0.00	91.08±68.67	0.15±0.03	1.68±0.33
t test	***P*=0.005**	***P*=0.012**	*P*=0.098	***P*<0.001**	
MDAMB-436					
IR	0.39±0.00	0.04±0.01	10.70±5.65	0.35±0.08	
KU-55933+IR	1.37±0.47	0.01±0.00	43.17±18.06	0.03±0.02	3.42±0.91
t test	***P*=0.028**	***P*=0.020**	***P*=0.041**	***P*=0.003**	

Statistical significance was determined by Student's *t*-test. The *P*-values are bold where they are ≤ 0.05. Abbreviations: IR, irradiation; $SER_{0.01}$, sensitiser enhancement ratio at 1% survival; SF2, surviving fraction at 2Gy.

Treatment with KU-55933 significantly increased the α-value in MCF-7 (*P*=0.013), T47D (*P*=0.006), MDAMB-231 (*P*=0.007), MDAMB-468 (*P*=0.005) and MDAMB-436 (*P*=0.028) cells, which consequently raised the α/β ratio in these cell lines indicating the potency of KU-55933 as a radiosensitiser. The above data show that KU-55933 increases radiosensitivity across all the breast cancer phenotypes. Such data reinforce the importance of DNA double strand repair in mediating radiation response and cell survival. The greatest radiosensitisation was seen in MDAMB-436 cells perhaps due to inhibition of ATM adding to the already compromised repair competency due to their BRCA-1 deficiency, resulting in intolerable levels of DNA damage which manifests in greater levels of radiosensitisation (Cuadrado et al., 2006).

2.4.5.2 Olaparib radiosensitises breast cancer cells

To assess the radiosensitising effects of olaparib, breast cancer cells were pre-plated and treated with olaparib for 1 hour pre- and 16 hours post-irradiation exposure before incubation for clonogenic survival. As seen in Figure 2.9, olaparib treatment resulted in significant radiosensitisation across all the breast cancer cell lines.

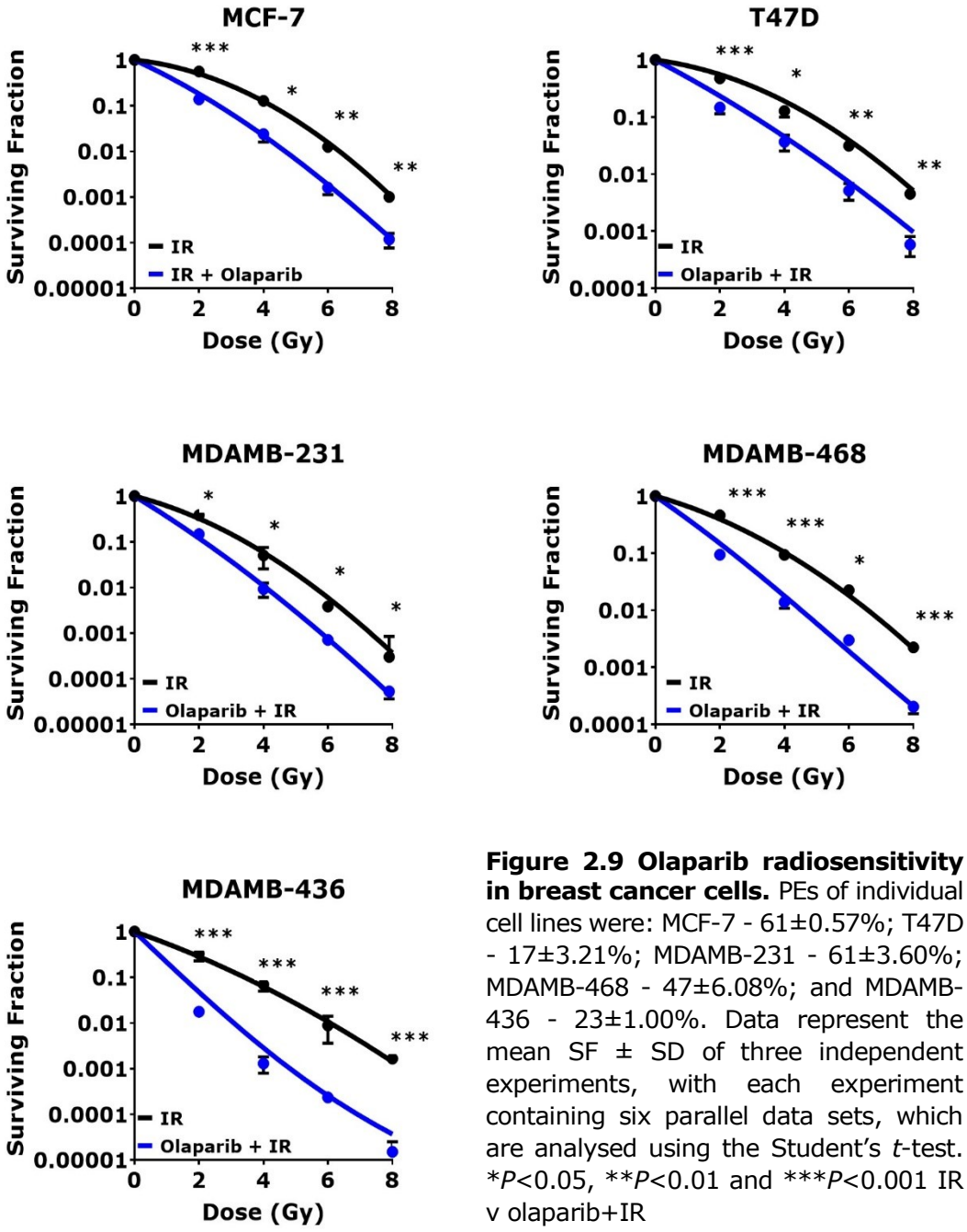


Figure 2.9 Olaparib radiosensitivity in breast cancer cells. PEs of individual cell lines were: MCF-7 - 61±0.57%; T47D - 17±3.21%; MDAMB-231 - 61±3.60%; MDAMB-468 - 47±6.08%; and MDAMB-436 - 23±1.00%. Data represent the mean SF ± SD of three independent experiments, with each experiment containing six parallel data sets, which are analysed using the Student's *t*-test. **P*<0.05, ***P*<0.01 and ****P*<0.001 IR v olaparib+IR

.

Mean SF2 values were significantly higher in control cells compared to olaparib treated cells i.e. 0.49±0.00 v 0.18±0.02 (*P*<0.00001) in MCF-7, 0.49±0.10 v 0.22±0.02 (*P*=0.011) in T47D, 0.31±0.04 v 0.10±0.02 (*P*=0.002) in MDAMB-231, 0.38±0.04 v 0.13±0.02 (*P*=0.0006) in MDAMB-468, and 0.28±0.02 v 0.02±0.017 (*P*=0.0001) in MDAMB-436 cells. The mean $SER_{0.01}$ were 1.63±0.03, 1.61±0.18, 1.62±0.09, 1.68±0.33 and 2.35±0.13 in MCF-7, T47D, MDAMB-231, MDAMB-468 and MDAMB-436 cells respectively. Such SER values equate to the survival of cells decreasing from 0.001 to 0.0001 in MCF-7, 0.005 to 0.0005 in T47D, 0.0003 to 0.00005 in MDAMB-231, 0.002 to 0.0002 in MDAMB-468 and 0.001 to 0.00001 in MDAMB-436 cells treated with olaparib. Other radiobiologic parameters are summarised in Table 2.4.

Table 2.4 Radiobiologic parameters of breast cancer cells treated with IR and/or olaparib.

Cell line	α (Gy^{-1})	β (Gy^{-2})	α/β (Gy)	SF2	$SER_{(0.01)}$
MCF-7					
IR	0.17±0.01	0.08±0.00	2.20±0.37	0.49±0.00	
Olaparib+IR	0.75±0.06	0.05±0.01	16.38±5.66	0.18±0.02	1.63±0.03
t test	***P*=0.0001**	***P*=0.021**	***P*=0.012**	***P*<0.00001**	
T47D					
IR	0.24±0.12	0.05±0.01	5.12±3.82	0.49±0.10	
Olaparib+IR	0.70±0.06	0.02±0.00	26.10±2.27	0.22±0.02	1.61±0.18
t test	***P*=0.005**	***P*=0.043**	***P*=0.001**	***P*=0.011**	
MDAMB-231					
IR	0.49±0.06	0.06±0.01	7.77±2.67	0.31±0.04	
Olaparib+IR	0.99±0.06	0.03±0.01	31.75±16.50	0.10±0.02	1.62±0.09
t test	***P*=0.0007**	***P*=0.045**	*P*=0.067	***P*=0.002**	
MDAMB-468					
IR	0.36±0.05	0.04±0.00	7.52±1.70	0.38±0.04	
Olaparib+IR	1.00±0.09	0.01±0.00	164.67±79.19	0.13±0.02	1.68±0.33
t test	***P*=0.0005**	***P*=0.0001**	***P*=0.026**	***P*=0.0006**	
MDAMB-436					
IR	0.54±0.06	0.04±0.01	15.62±1.00	0.28±0.02	
Olaparib+IR	1.56±0.06	0.04±0.06	38.25±6.91	0.02±0.017	2.35±0.13
t test	***P*=0.00002**	0.493	***P*=0.004**	***P*=0.0001**	

Statistical significance was determined by Student's *t*-test. The *P*-values are bold where they are ≤ 0.05. Abbreviations: IR, irradiation; $SER_{0.01}$, sensitiser enhancement ratio at 1% survival; SF2, surviving fraction at 2Gy.

Olaparib uniformly radiosensitised MCF-7, T47D, MDAMB-231 and MDAMB-468 cells with greater levels of radiosensitivity observed in the MDAMB-436 cells. Significant increases in the α-value were observed in MCF-7 (*P*=0.0001), T47D (*P*=0.005), MDAMB-231 (*P*=0.0007), MDAMB-468 (*P*=0.0005) and MDAMB-436 (*P*=0.00002) cells. This led to a significant increase in the α/β value which indicated that cell killing obtained with olaparib was linear. Taken together, the above results indicate that inhibition of PARP enzyme enhances radiosensitivity across all breast cancer phenotypes regardless of BRCA-1 status.

2.4.6 Radiosensitisation with PTPD

The current study hypothesised that inhibiting FEN-1 using its specific inhibitor, PTPD, would result in abrogation of the LP-BER pathway, and increase sensitivity of the cancer cells to radiation. To assess this, pre-plated cells were treated with 10 μM PTPD for 24 hours pre- and 16 hours post-irradiation exposure before incubation for clonogenic survival. As seen in Figure 2.10, PTPD increased radiosensitivity in the triple negative MDAMB-231 and MDAMB-436 cells, but, although significant differences were observed, the increased radiosensitisation was modest, especially in comparison to the control drug comparators (KU-55933 and olaparib).

Treatment with PTPD induced a differential radioresponse in the different breast cancer cell lines (Figure 2.10). In comparison to control cells, PTPD treatment did not result in any significant change in the SF2 values i.e. 0.52±0.06 v 0.46±0.03 (*P*=0.252) in MCF-7, 0.66±0.08 v 0.66±0.07 (*P*=0.961) in T47D or 0.45±0.10 v 0.35±0.09 (*P*=0.289) in MDAMB-468's. Increased radiosensitisation was seen in MDAMB-468 cells only at higher doses of 6 (*P*=0.016) and 8 Gy (*P*=0.032). Only MDAMB-231 and MDAMB-436 cells were radiosensitised by PTPD treatment which resulted in a small but significant reduction in their SF2 values i.e. 0.41±0.05 v 0.23±0.04 (*P*=0.010) and 0.40±0.10 v 0.18±0.03 (*P*=0.025) respectively.

The $SER_{0.01}$ values were 1.00±0.02 in MCF-7, 1.00±0.01 in T47D, 1.31±0.07 in MDAMB-231, 1.13±0.08 in MDAMB-468 and 1.50±0.13 in MDAMB-436 cells. Such SER values equate to the survival of cells at 8 Gy decreasing from 0.0004 to 0.0002 in MDAMB-231, 0.002 to 0.001 in

MDAMB-468 and 0.001 to 0.0001 in MDAMB-436 cells treated with PTPD. No change in the SF8 of MCF-7 (0.001 and 0.001) and T47D (0.006 and 0.006) cells were observed with PTPD treatment. Other radiobiologic parameters are summarised in Table 2.5.

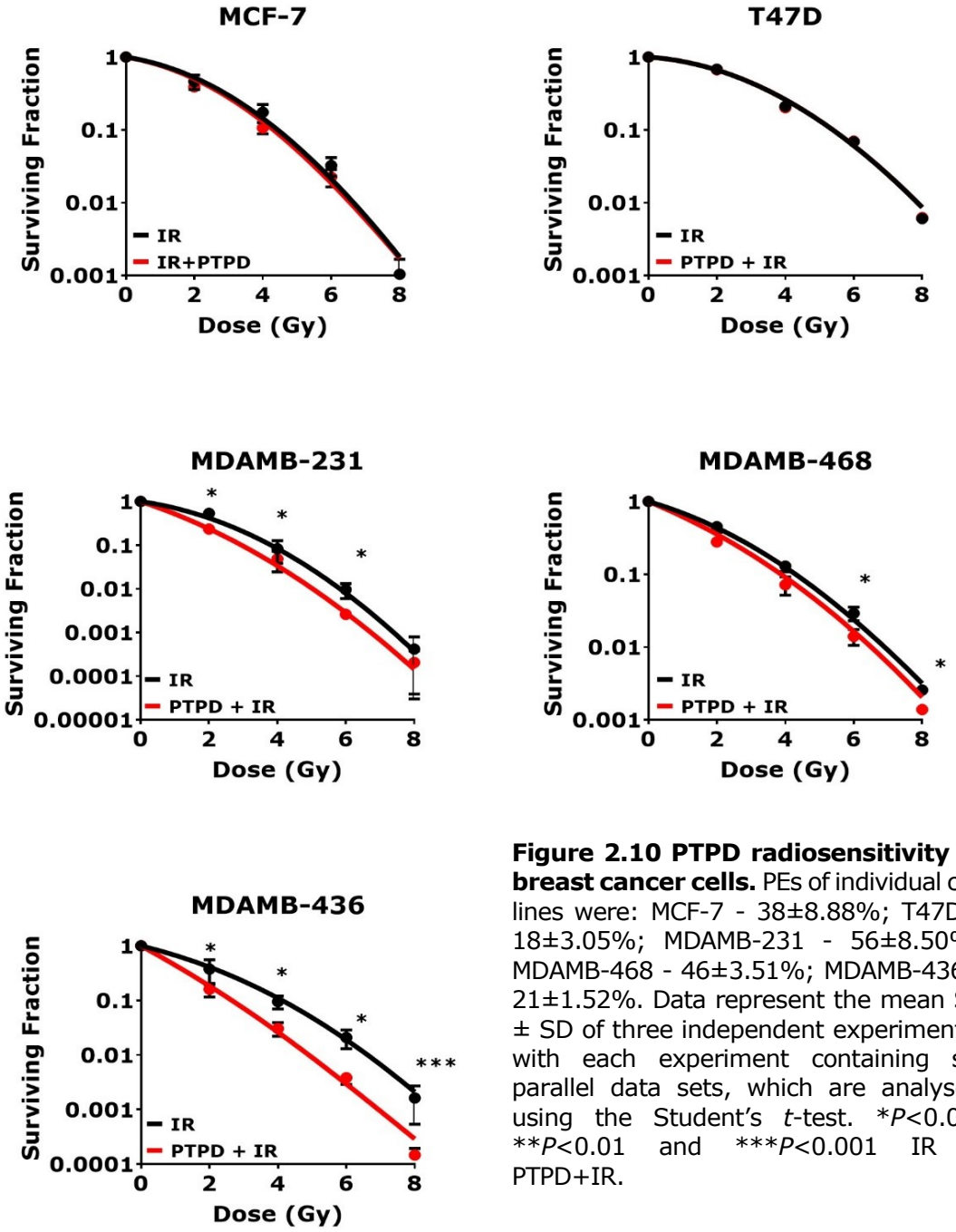


Figure 2.10 PTPD radiosensitivity in breast cancer cells. PEs of individual cell lines were: MCF-7 - 38±8.88%; T47D - 18±3.05%; MDAMB-231 - 56±8.50%; MDAMB-468 - 46±3.51%; MDAMB-436 - 21±1.52%. Data represent the mean SF ± SD of three independent experiments, with each experiment containing six parallel data sets, which are analysed using the Student's *t*-test. **P*<0.05, ***P*<0.01 and ****P*<0.001 IR v PTPD+IR.

Table 2.5 Radiobiologic parameters of breast cancer cells treated with IR and/or PTPD.

	α (Gy^{-1})	β (Gy^{-2})	α/β (Gy)	SF2	$SER_{(0.01)}$
MCF-7					
IR	0.17±0.10	0.08±0.01	2.30±1.61	0.52±0.06	
PTPD+IR	0.19±0.10	0.08±0.02	2.60±2.26	0.46±0.03	1.00±0.02
t test	*P*=0.878	*P*=0.900	*P*=0.859	*P*=0.252	
T47D					
IR	0.07±0.07	0.06±0.01	1.24±1.29	0.66±0.08	
PTPD+IR	0.07±0.07	0.06±0.01	0.45±0.38	0.66±0.07	1.00±0.01
t test	*P*=0.990	*P*=0.988	*P*=0.370	*P*=0.961	
MDAMB-231					
IR	0.25±0.09	0.09±0.01	2.95±1.54	0.416±0.05	
PTPD+IR	0.59±0.12	0.06±0.01	10.07±3.97	0.23±0.04	1.31±0.07
t test	***P*=0.018**	*P*=0.077	***P*=0.044**	***P*=0.010**	
MDAMB-468					
IR	0.30±0.14	0.05±0.01	6.2±3.80	0.45±0.10	
PTPD+IR	0.45±0.18	0.04±0.01	13.10±10.86	0.35±0.09	1.13±0.08
t test	*P*=0.321	*P*=0.378	*P*=0.356	*P*=0.289	
MDAMB-436					
IR	0.35±0.17	0.05±0.01	8.57±7.41	0.40±0.10	
PTPD+IR	0.79±0.16	0.03±0.02	27.42±26.02	0.18±0.03	1.5±0.13
t test	***P*=0.033**	*P*=0.333	*P*=0.293	***P*=0.025**	

Statistical significance was determined by Student's *t*-test. The *P*-values are bold where they are ≤ 0.05. Abbreviations: IR, irradiation; $SER_{0.01}$, sensitiser enhancement ratio at 1% survival; SF2, surviving fraction at 2Gy.

The α-value was significantly increased only in the MDAMB-231 (*P*=0.018) and MDAMB-436 (*P*=0.033) cells, suggesting radiosensitising effect of PTPD in these cell lines. In the MDAMB-468 cells, α-value and α/β ratio were increased, although not significantly, suggesting a marginal radiosensitising effect that supports radiosensitivity observed in MDAMB-468 cells at higher doses. These parameters were not altered in the MCF-7 and T47D which indicate that PTPD did not offer any significant radiosensitivity in these cell lines. The radiosensitivity observed in MDAMB-231, MDAMB-436 and MDAMB-468 (at higher doses) cells could be due to the inability of these particular cell lines to effectively repair double strand breaks induced by ionising radiation (TCGA, 2012, Lee et al., 2019a), as opposed to repair-proficient luminal cells. Compared to radiosensitivity observed with control inhibitors, KU-55933 and olaparib, the above results

indicate that PTPD was not as effective across the different breast cancer phenotypes. DNA damage assays were next carried out to examine the reasons for the differential radiosensitivity seen between the cell lines, following PTPD treatment.

2.4.7 RPA and γ-H2AX DNA damage assays

2.4.7.1 RPA expression following PTPD in combination with ionising radiation

In order to assess if PTPD treatment either as a single agent or in combination with radiation increases DNA single strand damage, the expression of RPA was assessed in breast cancer cells by immunofluorescence microscopy. Breast cancer cells were treated with 10 μM PTPD for 24 hours, then irradiated with 1 Gy, before assessing RPA expression at 30 minutes post-IR (optimisation experiments given in Appendix A-Figure A1 and A2). Control DNA repair inhibitors were not assessed for RPA and γH2AX expression, since potent radiosensitisation was observed with these agents, which is indicative of DNA double strand breaks (Mladenov et al., 2013). Therefore, in the current study with PTPD, cells without treatment were used as negative controls. Figure 2.11 shows representative immunofluorescence micrograph for MCF-7 cells. Immunofluorescent micrographs for all other cell lines are presented in Appendix A-Figure A5. Figure 2.12 shows quantified RPA expression in MCF-7, T47D, MDAMB-231, MDAMB-468 and MDAMB-436 cells.

As shown in Figure 2.12, base levels of single strand DNA damage were found in all untreated control cells (~20 RPA foci/nucleus). PTPD treatment resulted in a small but non-significant increase in single strand DNA damage in MCF-7, T47D, MDAMB-231 and MDAMB-468 cells with 33±1.17, 30±5.42, 38±5.14 and 40±4.63 foci/nucleus respectively. Treatment with PTPD significantly increased single strand DNA damage only in the MDAMB-436 cells which showed increased RPA foci of 50±0.21/nucleus (P=0.0021 (statistics performed on n=2 each experiment with 3 replicates)). As expected, treatment with ionising radiation significantly increased single strand DNA damage with RPA foci of 88±12.80 (P=0.001) in MCF-7,

80±13.29 (*P*=0.0008) in T47D, 105±18.77 (*P*=0.004) in MDAMB-231, 95±7.07 (*P*=0.002) in MDAMB-468 and 106±3.54 (*P*<0.0001) in MDAMB-436 cells (statistics performed on n=2 each experiment with 3 replicates). When combining PTPD treatment with radiation, RPA foci generation was increased to an even greater extent compared to radiation alone with 117±9.89 (*P*=0.031) in MCF-7, 105±4.03 (*P*=0.061) in T47D, 161±12.75 (*P*=0.020) in MDAMB-231, 134±14.30 (*P*=0.019) in MDAMB-468 and 181±16.67 (*P*<0.0001) foci/nucleus in MDAMB-436 cells (statistics performed on n=2 each experiment with 3 replicates).

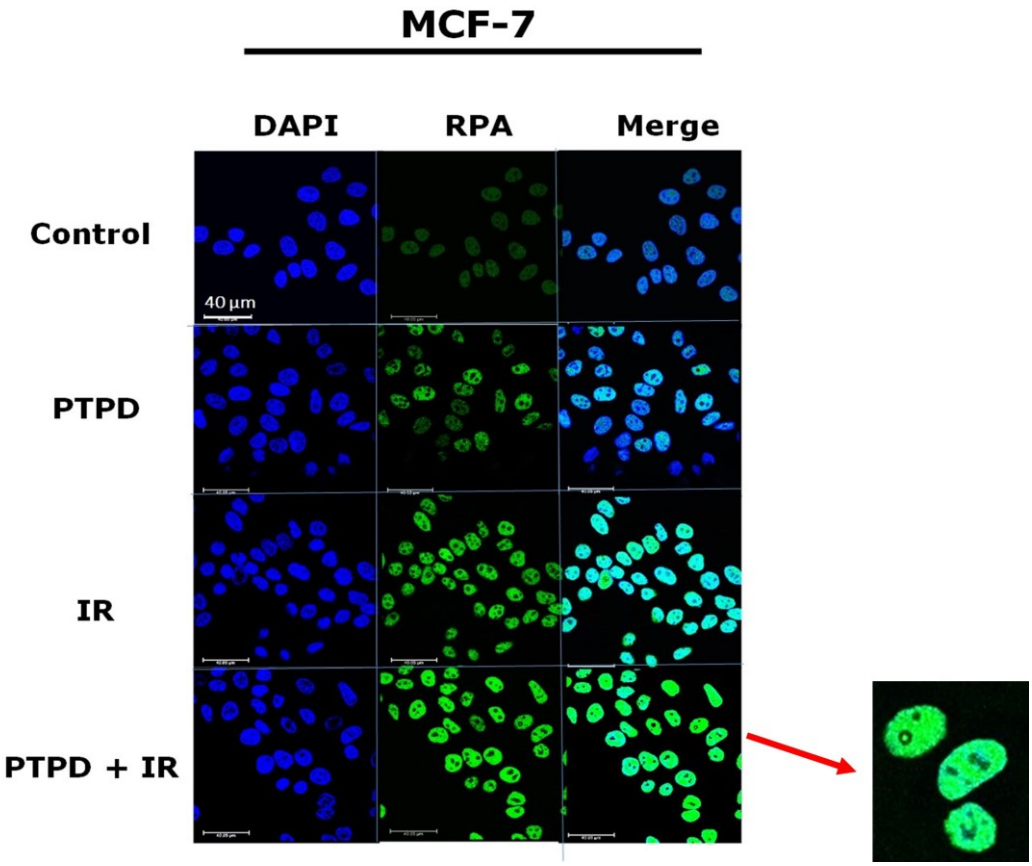


Figure 2.11 RPA expression in MCF-7 cells following treatment with PTPD and/or radiation. Representative images of RPA immunofluorescent staining in MCF-7 cells. 63x magnification. Blue - DAPI fluorescent stain. Green - RPA; Scale bar - 40 µm.

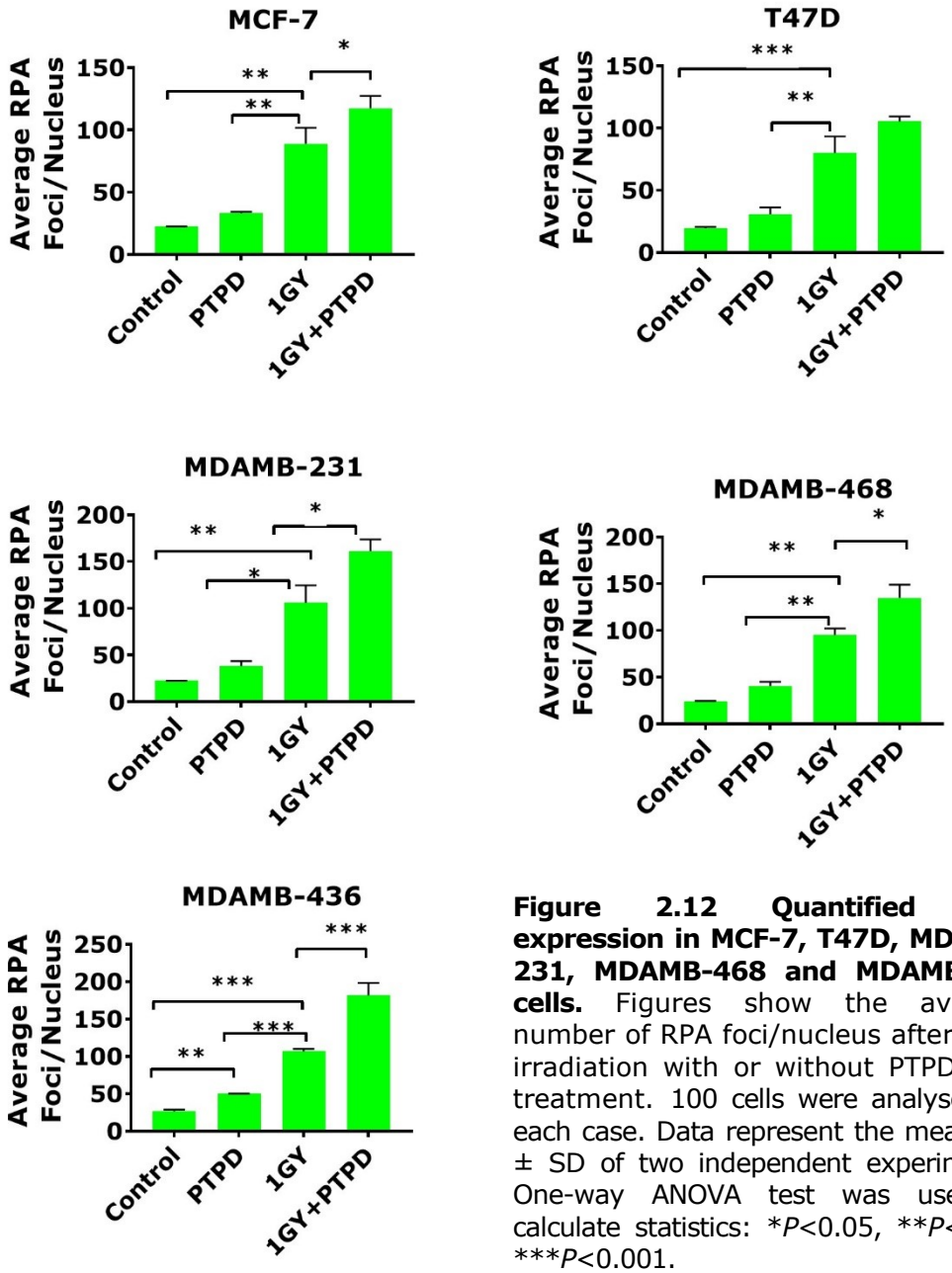


Figure 2.12 Quantified RPA expression in MCF-7, T47D, MDAMB-231, MDAMB-468 and MDAMB-436 cells. Figures show the average number of RPA foci/nucleus after 1 Gy irradiation with or without PTPD pre-treatment. 100 cells were analysed for each case. Data represent the mean foci ± SD of two independent experiments. One-way ANOVA test was used to calculate statistics: **P*<0.05, ***P*<0.01, ****P*<0.001.

When comparing between cell lines, the effects of this combination treatment on RPA foci formation were more pronounced in MDAMB-436 cells, but a similar response was seen in all cell lines. Data suggest that PTPD treatment can cause DNA single strand damage and enhance the amount of DNA damage induced by radiation across all breast cancer cells.

In terms of cell lethality DNA double strand breaks are the principle cytotoxic lesions that induce cell death. Single strand breaks can also

contribute to cell lethality if repair pathways are compromised, allowing conversion into the cytotoxic double strand breaks (Cantoni et al., 1996). Therefore, in order to assess if PTPD +/- radiation had any effect on DNA double strand induction, the expression of γ-H2AX was next assessed.

2.4.7.2 γ-H2AX expression following PTPD in combination with ionising radiation

As with RPA methodology pilot experiments were conducted in the representative breast cancer cell line, MDAMB-231 using FACS to optimise γ-H2AX expression in response to different doses of radiation (Appendix A-Figure A3). Increase in γ-H2AX was noted at 4 Gy of ionising radiation, with maximum expression at 0.5 hours post-irradiation. Based on these experiments, γ-H2AX expression was assessed in response to PTPD treatment + 4 Gy IR. Figure 2.13 shows representative immunofluorescence micrograph for γ-H2AX expression in MCF-7 cells. Immunofluorescence micrographs for all other cell lines are presented in Appendix A-Figure A6. Figure 2.14 shows quantified γ-H2AX expression in MCF-7, T47D, MDAMB-231, MDAMB-468 and MDAMB-436 cells.

As shown in Figure 2.14, base levels of γ-H2AX expression (spontaneous DNA DSBs) was found in all untreated control cells (~4-5 γ-H2AX foci/nucleus). Breast cancer cells treated with PTPD alone demonstrated only a marginal increase in DNA double strand breaks with (9±0.15, 7±0.43, 8±2.91, 7±0.92, and 15±1.13) γ-H2AX foci/nucleus in MCF-7, T47D, MDAMB-231, MDAMB-468 and MDAMB-436 cells respectively. As expected, treatment with ionising radiation significantly (statistics performed on n=2 each experiment with 3 replicates) increased the amount of DNA double strand breaks with average γ-H2AX foci of 30±2.96 (P=0.0005) in MCF-7, 37±0.26 (P<0.0001) in T47D, 39±0.64 (P<0.0001) in MDAMB-231, 31±4.27 (P=0.0023) in MDAMB-468 and 35±4.57 (P=0.0002) in MDAMB-436 cells.

Compared to radiation alone, cells treated with both PTPD and radiation displayed only marginal increase in foci expression in MCF-7 (33±0.02), T47D (37±0.26), MDAMB-231 (42±0.76), and MDAMB-468 cells

(37±4.28). In MDAMB-436 cells, γH2AX foci was increased to an even greater extent than achieved by irradiation alone. A significant increase in γ-H2AX expression was found in MDAMB-436 cells with average foci of 59±6.94 (*P*=0.0003 (statistics performed on n=2 each experiment with 3 replicates)).

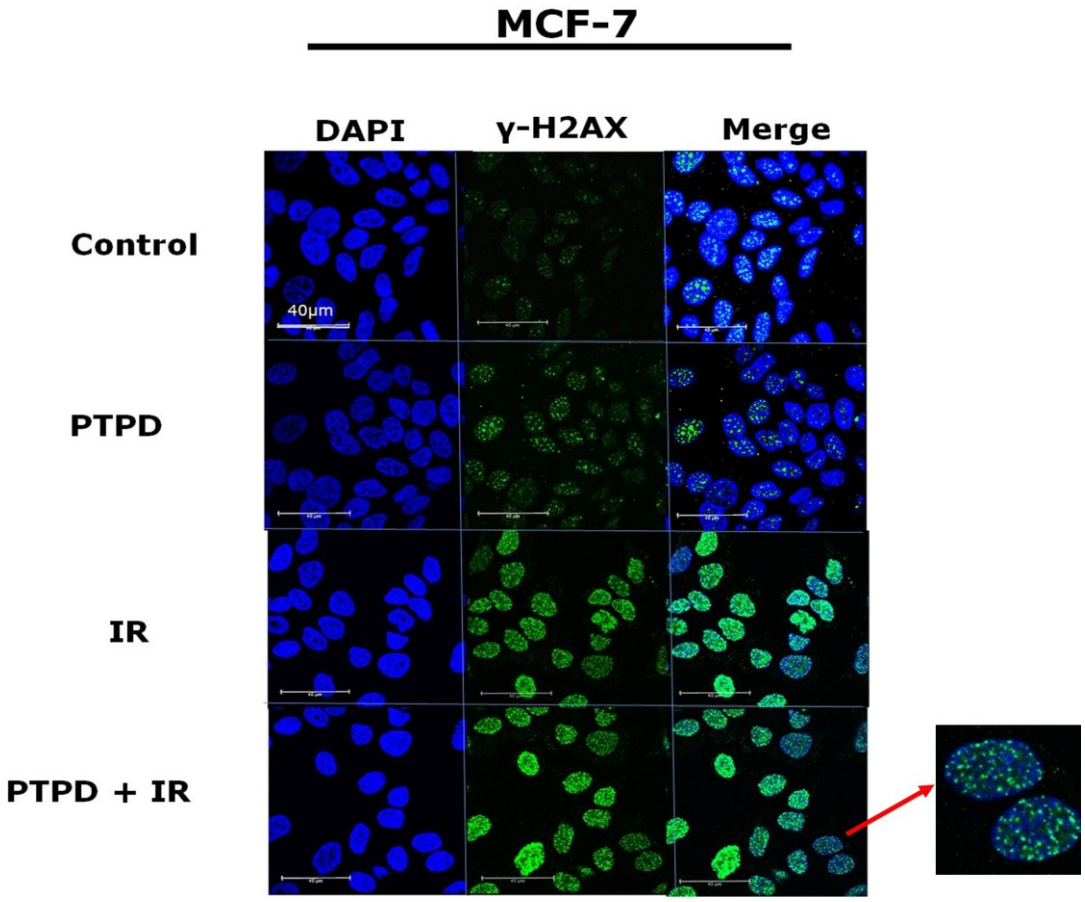


Figure 2.13 γ-H2AX formation in MCF-7 cells following treatment with PTPD and/or radiation. Representative images of γ-H2AX immunofluorescent staining in MCF-7 cells. 63x magnification. Blue - DAPI fluorescent stain. Green - γ-H2AX; Scale bar - 40 μm.

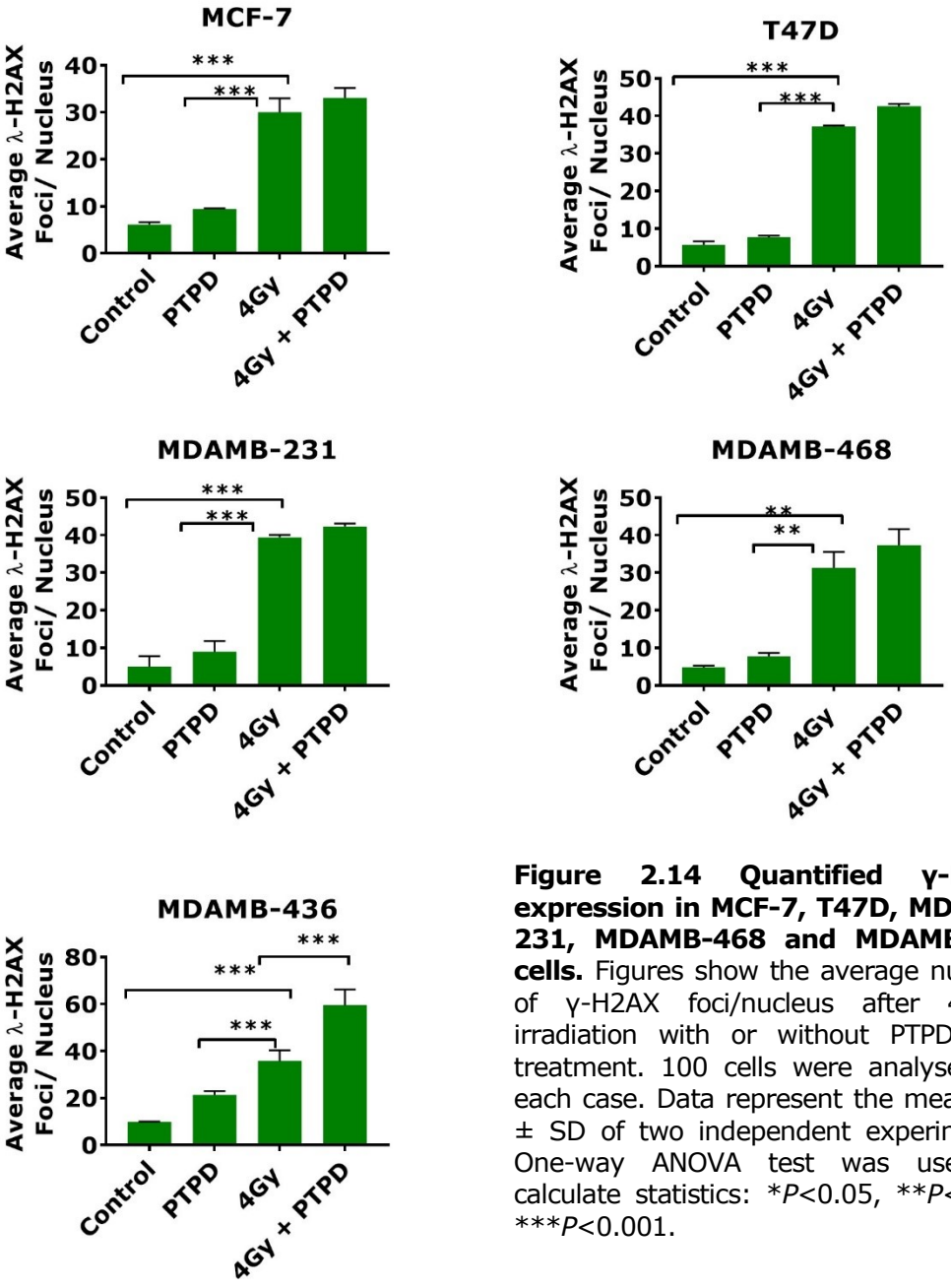


Figure 2.14 Quantified γ-H2AX expression in MCF-7, T47D, MDAMB-231, MDAMB-468 and MDAMB-436 cells. Figures show the average number of γ-H2AX foci/nucleus after 4 Gy irradiation with or without PTPD pre-treatment. 100 cells were analysed for each case. Data represent the mean foci ± SD of two independent experiments. One-way ANOVA test was used to calculate statistics: **P*<0.05, ***P*<0.01, ****P*<0.001.

Such data suggests that treatment with PTPD in combination with radiation induces DNA double strand breaks only in the BRCA-1 deficient MDAMB-436 cells. In MCF-7, T47D, MDAMB-231 and MDAMB-468 cells, the damage induced by PTPD and radiation is not significantly different to that induced by radiation alone. The enhancement in the number of DNA double strand breaks resulting from unrepaired single strand breaks due to FEN-1 inhibition, in the already double strand repair deficient MDAMB-436 cells may be one of the underlying mechanisms responsible for the PTPD

induced radiosensitisation in these cell lines. Above data suggest that FEN-1 might be a suitable target to enhance radiotherapy in BRCA-1 deficient tumours.

2.5 Discussion

As indicated above, FEN-1 is an important nuclease in mammalian replication and repair, and is responsible for cleaving DNA/RNA flap structures that arise during these processes (Lieber, 1997). Studies have shown that the highly selective FEN-1 inhibitor PTPD, inhibits the cleavage activity of FEN-1 with an IC_{50} of 0.025 μM in substrate based assays (Tumey et al., 2005, Dorjsuren et al., 2011). PTPD out-competes DNA/RNA substrates in binding to the active site of FEN-1, and in this way inhibits the cleavage activity preventing cell replication and repair (Dorjsuren et al., 2011, Exell et al., 2016, Kouichi et al., 2018). Previous studies report that FEN-1 accumulates rapidly at ionising radiation-induced damaged sites to repair DNA damage by the LP-BER pathway (Asagoshi et al., 2010, Kleppa et al., 2012, Sun et al., 2017). Therefore, it was hypothesised that inhibiting the LP-BER pathway using PTPD may improve radioresponse in breast cancer cells. The single agent and radiosensitising effect of PTPD were assessed across luminal and TN breast cancer phenotypes. Results were compared to that obtained with well-established DNA repair inhibitors such as the ATM inhibitor, KU-55933 and PARP-1/2 inhibitor, olaparib.

Cell doubling time and plating efficiencies are the commonly used estimates to determine growth characteristics of cells in culture (Deschavanne, 1999). These were initially assessed in all breast cancer cells used in the current study to understand their growth patterns and compare with previously published literature. To assess doubling time, the growth of cells were monitored over a period of 0-96 hours and cell counts were recorded every 24 hours. Based on their respective growth curves, MCF-7, MDAMB-231 and MDAMB-468 cells had faster doubling time ranging 20-31 hours, compared to 32-41 hours in T47D and MDAMB-436 cells. The results obtained are in accordance with colleagues within the department and with published studies which report doubling time of 28-30 hours in MCF-7, MDAMB-231 and MDAMB-468 cells compared to 31-44

hours in T47D and MDAMB-436 cells (Kennedy et al., 1985, Watanabe et al., 2001).

In the current study, the cytotoxic effect of DNA repair inhibitors and ionising radiation were assessed by clonogenic survival assays. The clonogenic assay has been established as the gold standard method to assess reproductive cell death after exposure to ionising radiation and/or determine effectiveness of chemotherapeutic agents (Franken et al., 2006). A lethally irradiated cell may not show any morphological evidence of damage/death and may even undergo one or two rounds of cell division, before undergoing metabolic death and its subsequent loss from the population (Woolston and Martin, 2011). So when assessing response to radiation, it is important to measure the effects on long-term survival (Munshi, 2005). A cell that forms a colony is classified as a 'survivor' or a resistant cell that has survived the cytotoxic insult. The cell survival curve obtained from clonogenic assays describes the relationship between the dose of cytotoxic agent used and the fraction of cells that remain unaffected by treatment (Munshi, 2005, Woolston and Martin, 2011).

Plating efficiency, an intrinsic characteristic of cells, determines the ability of single cells to form colonies (Rafehi et al., 2011). Breast cancer cells without any treatment were seeded for clonogenic survival assays in order to assess their colony forming ability. MCF-7, MDAMB-231 and MDAMB-468 cells formed colonies in 14 days as opposed to T47D and MDAMB-436 cells which required a 21 day incubation period. The time for colony formation was dependent on the doubling time of cells in T47D and MDAMB-436 cell lines. Several other studies have also found that the slowest growing clones have longer doubling times (Beer and Szumiel, 1994). MCF-7, MDAMB-231 and MDAMB-468 cells had PEs ranging 41-51% compared to lower PEs ranging 16-19% in T47D and MDAMB-436 cells. These findings were supported by literature which report PE of 46-56% in MCF-7, MDAMB-231 and MDAMB-468 cells; and lower PEs of 12-11% in T47D and MDAMB-436 cells (Lagadec et al., 2012, Zhang et al., 2014, Karasawa. K., 2014, Veldwijk et al., 2014, Lindstrom et al., 2017, Su et al., 2018).

The ATM inhibitor, KU-55933 was one of the positive control drugs used in the current study. KU-55933 is a small molecule inhibitor (2-morpholin-4-yl-6-thianthren-1-yl-pyran-4) that has been shown to specifically inhibit kinase activities of ATM in the low nanomolar range (IC_{50} - 12.9 nM) (Hickson et al., 2004, Li and Yang, 2010). In response to DNA double strand breaks, ATM induces cell cycle arrest and ensures repair of DNA damage, primarily by the HR pathway (Hickson et al., 2004, Li and Yang, 2010). The ability of KU-55933 to prevent phosphorylation or activation of ATM, has been found to result in radiosensitive phenotypes in multiple cancer models (You et al., 2007, Smith et al., 2010). In the current study, single agent cytotoxicity of KU-55933 was assessed in both luminal and TNBC cells by clonogenic assay. Treatment resulted in a marginal reduction in colony formation in MCF-7 and T47D (<15%), MDAMB-231 (<4%), and MDAMB-468 (25%) cells. In support of this finding, studies by Crescenzi et al., 2008 reported that ATM inhibition by KU-55933 can induce senescence in breast, lung, and colon carcinoma cells via the p21 pathway (Crescenzi et al., 2008). Other studies have found that treatment with KU-55933 does not affect cell plating or viability of breast cancer cells (Rainey et al., 2008). Taking into consideration the above mentioned findings, it appears that response of cell lines to KU-55933 as a single agent, is cell-line dependent. Compared to the above mentioned cell lines, KU-55933 treatment was more cytotoxic in the BRCA-1 deficient MDAMB-436 cells which demonstrated a 44% reduction in colony formation. This observation suggests that inhibition of ATM in the context of BRCA-1 deficiency induces cell lethality in MDAMB-436 cells.

ATM and BRCA-1 are implicated in DDR and HR pathways (Cuadrado et al., 2006). It was shown that in the absence of BRCA-1, ATM becomes essential for supporting the residual levels of HR necessary to carry out DNA double strand repair (Chen et al., 2017). Genetic analysis in BRCT (BRCA1 C-terminal) mutant mice studies have shown that ATM has a role in homology-directed repair (HDR) pathway, independent of BRCA-1 function. HDR is not important for normal DNA double strand repair, but becomes critical when functions of BRCA-1 are compromised. ATM inhibition was further associated with synthetic lethality of BRCT mutant

mice models (Abida et al., 2018). In the current study, the BRCA-1 deficient MDAMB-436 cells demonstrated reduced survival after treatment with the ATM inhibitor, KU-55933, further providing evidence for the synthetic lethal association that exists between ATM and BRCA-1.

The oral PARP-1/2 inhibitor, olaparib is a selective and potent inhibitor of PARP enzymes inhibiting PARP-1 and PARP-2 with IC_{50} of 5 nM and 1 nM in cell-free assays respectively (Menear et al., 2008). PARP-1 is a well-recognized member of the DDR pathway and is predominantly involved in the repair of single strand breaks via the BER pathway (Allinson et al., 2003, Farmer et al., 2005). Olaparib inhibits the enzymatic activity of PARP and traps PARP with the DNA, increasing formation of trapped PARP-DNA complexes, resulting in unrepaired DNA damage and cell death (Farmer et al., 2005). In the current study, olaparib was used as a control and a comparator, to provide a direct comparison against PTPD, as both PARP-1 and FEN-1 are critical components in the BER pathway (Hegde et al., 2008, Asagoshi et al., 2010). Treatment with olaparib reduced colony formation in all breast cancer cell lines regardless of BRCA-1 status. The luminal MCF-7 and T47D cells were sensitive to olaparib treatment with a 40-50% reduction in colony formation. The triple negative cell lines, MDAMB-231 and MDAMB-468 cells were the most resistant with only a 20-25% decrease and MDAMB-436 cells were the most sensitive, with an 80% reduction in overall cell survival.

One of the reasons for the therapeutic use of olaparib in clinical oncology, is because it exploits the synthetic lethal relationship between PARP and BRCA-1. Synthetic lethality exists when the loss of two genes results in cell lethality, but loss in either one of these genes does not affect cell survival (Bryant et al., 2005, Bryant et al., 2009). This finding formed the basis for the recommendation of olaparib in the treatment of BRCA-1 deficient tumours (Tutt et al., 2010). The reduced survival observed in the BRCA-1 deficient MDAMB-436 cells with olaparib treatment is because of its inability to repair both single strand and double strand DNA damage when both BRCA-1 and PARP-1 are non-functional (Arun et al., 2015). Similar to results obtained in our study, Arun et al., 2015 reported that BRCA-1 deficient cell lines - HCC-1947, MDAMB-436, and SUM-149, treated with

varying concentrations of olaparib showed a dose dependent reduction in cell survival. This study also reported that MDAMB-231 cells when transfected with BRCA-1 mutant allele showed significant growth inhibition with olaparib, which suggests that patients without BRCA-1 mutations can also benefit from PARP inhibitors (Arun et al., 2015).

In the current study, treatment with olaparib also resulted in reduced survival in the BRCA-1 proficient MCF-7, T47D, MDAMB-231 and MDAMB-468 cell lines. Studies conducted by Michmerhuizen et al., 2019, found that olaparib has modest single agent anti-cancer activity in breast cancer cells outside of BRCA-1 deficient cells (Michmerhuizen et al., 2019). Similar to observations in the current study, Pierce et al., 2013 found that olaparib treatment resulted in decreased survival of breast cancer cells, independent of molecular subtype and BRCA-1 status (Pierce et al., 2013). They reported similar trends as that observed in the current study with luminal cell lines, MCF-7 and T47D being more sensitive to treatment with 60% reduced survival compared to 40% in MDAMB-231 and MDAMB-468 triple negative cells (Pierce et al., 2013). The role of PARP-1 inhibition in luminal cancers are not very well reported, but the toxicity observed in TNBC cell lines may be because of its shared characteristics with BRCA-1 deficient tumours, commonly known as sporadic BRCAness (Hartman et al., 2012). TNBCs may be susceptible to PARP-1/2 inhibitors, because these tumours have lower expression of BRCA-1/2 or genes involved in DNA repair pathways (Turner et al., 2004). Such findings indicate that PARP-1 inhibition is cytotoxic in both BRCA-1 proficient and deficient cells; with greater levels of growth inhibition observed in BRCA-1 deficient cell lines.

Doxorubicin, a commonly used chemotherapeutic agent in breast cancer (Beslija et al., 2007, Buzdar, 2007), was used as a positive control to compare efficacy of single agent PTPD in breast cancer cells. The proliferation IC_{50} (0.3-0.8) μM of doxorubicin resulted in a ~50% decrease in cell proliferation, but when applied in clonogenic survival resulted in total cell-kill, which indicate that doxorubicin has different potencies in proliferation and clonogenic survival assays – a trend that has been observed previously by colleagues (Dr Nurul Abdullah) in the department

and with published literature (Maass et al., 2015, Wen et al., 2018). The clonogenic IC_{50} of doxorubicin has been reported to range between 0.01-0.08 μM in breast cancer cells which is 10 times lower than the proliferation IC_{50} values, which may explain the increase in cytotoxicity observed in clonogenic survival (Costantini et al., 2010, Zhang et al., 2012, Fang et al., 2014).

Treatment with PTPD had only marginal effects (<10%) on proliferation and clonogenic survival in MCF-7, T47D, MDAMB-231 and MDAMB-468 cells suggesting that PTPD is unable to exert cytotoxic effect in these cell lines. The role of FEN-1 is to remove oxidative DNA damage through the single strand LP-BER pathway (Liu et al., 2008a). In the absence of a DNA damaging agent, FEN-1 inhibition in breast cancer cell lines may not be significant enough to affect cell proliferation and survival. Additionally, single strand DNA damage is not considered as cytotoxic, as lesions can be easily repaired by alternative DNA repair pathways (Robertson et al., 2009). However, FEN-1 inhibition in the context of BRCA-1 deficiency was able to induce cytotoxic effects in MDAMB-436 cells. PTPD treatment demonstrated a reduction of 36% in proliferation and 66% in clonogenic survival in the BRCA-1 deficient MDAMB-436 cells. One of the reasons for the increased cytotoxicity observed in this cell line upon FEN-1 inhibition, may be because of dual inhibition of both single and double strand repair pathways. This suggests that FEN-1 inhibition may function similarly to PARP-1 inhibition in the MDAMB-436 cells (Arun et al., 2015). Studies conducted by Ward et al., 2017 reported that cells deficient for double strand repair pathway proteins were sensitive to FEN-1 inhibition. For example, down-regulating FEN-1 using siRNA in ATM deficient cells was found to result in cell death, indicating a synthetic lethal relationship between ATM and FEN-1 (Ward et al., 2017). More recently, studies by Mengwasser et al., 2019 reported that BRCA-deficient cells are more reliant on FEN-1 to repair DNA compared to BRCA wild-type cells (Mengwasser et al., 2019). Such studies provide an explanation for the increase in sensitivity observed in the BRCA-1 deficient MDAMB-436 cells to FEN-1 inhibition.

Radiotherapy is an integral part of breast cancer treatment, either to treat residual cancer after surgery, to shrink tumour size in locally advanced disease or to extend survival/relieve symptoms in the case of metastatic breast cancer patients (NICE, 2018). Agents that increase efficacy of radiotherapy are under pre-clinical and clinical evaluation (Raleigh and Haas-Kogan, 2013, Biau et al., 2019). Prior to assessing radio-response of DNA repair inhibitors, the intrinsic radiosensitivity of luminal and TNBC cell lines used in this study were assessed via clonogenic survival assays. The surviving fraction at 2 Gy was calculated from the radiation dose response curve fitted to the LQ model. All cell lines demonstrated dose dependent reduction in survival following exposure to radiation. The most sensitive cell lines to radiation were the triple negative MDAMB-231 and MDAMB-436 cells followed by MDAMB-468 cells compared to the luminal MCF-7 and T47D cells. The SF2 values in MCF-7, T47D and MDAMB-468 cells were higher ranging between 43-49% compared to 31-35% in MDAMB-231 and MDAMB-436 cells.

In the current study, the response of breast cancer cells to radiation was differential between the different breast cancer phenotypes. Clinically, patients who are positive for the expression of ER and PgR are more radiosensitive compared to ER and HER-2 negative patients (Wang et al., 2011, Kyndi et al., 2008, Nguyen et al., 2008). Studies by Kyndi et al., 2008 reported a significant improvement in overall survival in patients who were ER and PgR-positive compared to ER, PgR-negative and HER-2 positive tumours treated with post-mastectomy radiotherapy (Kyndi et al., 2008). Another study conducted in 793 invasive breast cancer patients who received BCS followed by radiotherapy, reported lower local recurrence of 0.8% and 1.5% in luminal A and B tumours respectively compared to higher recurrence of 8.4% and 7.1% in HER-2 and TNBC patients (Nguyen et al., 2008). In contrast, Speers et al., 2015 reported no significant association (P=0.48) between the radiosensitivity of breast cancer cell lines and their respective intrinsic subtype (Speers et al., 2015). Taken together, data suggests that intrinsic radiosensitivity in pre-clinical breast cancer models varies between different cell lines with no clear association to the clinical patterns of response in the different phenotypes. Several

factors may also influence the differential radioresponse of cells *in vitro* compared to *in vivo* responses. 2D cell culture does not adequately take into account the natural 3D environment of cells (Baharvand et al., 2006). *In vivo* models examine both the inherent radiosensitivity of tumour cells and environmental influences, such as hypoxia and host immunity (Barker et al., 2015). The lack of these factors in a 2D cell culture system may explain the discrepancy observed between *in vitro* and *in vivo* radioresponses.

The radioresponse of control DNA repair inhibitors were assessed, prior to assessing radioresponse in PTPD treated cells. Treatment with KU-55933 resulted in significant radiosensitisation across all breast cancer phenotypes with $SER_{0.01}$ ranging from 1.6-3.4. Similar to results obtained in our study, Rainey et al., 2008 reported that inhibiting ATM transiently for 4 hours was sufficient to sensitise cells to ionising radiation and suggested that clinical radiosensitisation may only require ATM inhibition for short periods of time (Rainey et al., 2008). KU-55933 was found to radiosensitise glioma cells with SER values of 1.6 (Biddlestone-Thorpe et al., 2013). Another study reported that inhibition of ATM by KU-55933 inhibits the enhanced double strand break repair proficiency observed in glioblastoma cancer stem cells resulting in potent radiosensitisation with SERs ranging from 2.6-3.5. (Carruthers et al., 2015), similar to that observed in the current study with the BRCA-1 deficient MDAMB-436 cells.

A suggested model for radiosensitisation by PARP inhibition involves inhibition of BER or single strand repair pathway, leading to persistent radiation-induced single strand breaks that are converted into cytotoxic 1-ended double strand breaks (Chalmers et al., 2010). Additionally, trapping of PARP-DNA complexes by inhibitors interferes with cellular replication (Pommier et al., 2016), as a result of which, radiosensitisation with PARP is more pronounced in replicating cells (Noel et al., 2006, Chan et al., 2010) and in cells that are HR-deficient (synthetic lethality) (Loser et al., 2010, Verhagen et al., 2015). As both of these characteristics are specific to tumours compared to normal cells, radiosensitisation is expected to occur preferentially in tumour cells. A second model for tumour-specific cell killing relies on the ability of PARP inhibitors to increase tumour blood

flow which reduces the radioresistant hypoxic population of cells and promotes efficient drug delivery (Liu et al., 2008b, Borst et al., 2017). All these characteristics make PARP inhibitors ideal radiosensitisers and many of which are undergoing clinical evaluation (ClinicalTrials, 2019). In the current study, treatment with olaparib significantly increased radiosensitivity in both BRCA-1 proficient and deficient cells with $SER_{0.01}$ ranging from 1.6-2.3. In support of this finding, studies conducted previously have reported that olaparib when combined with radiation enhances radiosensitivity of breast cancer cells with SERs ranging from 1.12-1.76. The radiosensitivity obtained with olaparib treatment was attributed to delayed repair of double strand DNA damage which was present even at 12-16 hours after treatment, compared to irradiated cells (Michmerhuizen et al., 2019).

The levels of radiosensitisation seen with KU-55933 ($SER_{0.01}$ 3.42) was much greater than that observed with olaparib ($SER_{0.01}$ 2.35) in the BRCA-1 deficient MDAMB-436 cells. It has been reported that cells deficient for BRCA-1 driven HR pathways are dependent on ATM-mediated homology-directed repair pathway to repair DNA double strand breaks (Abida et al., 2018). Therefore, dual inhibition of both these proteins could result in complete abrogation of homology-directed repair pathways which might explain the greater levels of radiosensitivity achieved with ATM inhibition in the MDAMB-436 cells. In contrast, dual inhibition of both PARP-1 and BRCA-1, would still result in an intact ATM-driven HDR pathway, to repair DNA double strand damage. This may explain the increased radiosensitivity observed with ATM inhibition compared to PARP 1/2 inhibition in the MDAMB-436 cells.

The FEN-1 inhibitor, PTPD was investigated as a potential radiosensitiser in breast cancer cells. Data from clonogenic survival demonstrate that treatment with PTPD induced differential radioresponses between luminal and TNBC cells. PTPD induced radiosensitivity was specific to the triple negative MDAMB-231, MDAMB-468 and MDAMB-436 cells with $SER_{0.01}$ of 1.31, 1.13 and 1.50 respectively. However, no PTPD-induced radiosensitisation was observed in the luminal MCF-7 or T47D cells ($SER_{0.01}$ 1.00). From such data, it appears that PTPD was able to induce

radiosensitisation only in the intrinsically radiosensitive phenotypes (MDAMB-231 and MDAMB-436) compared to the radioresistant MCF-7 and T47D cells, which suggest that the intrinsic radiosensitivity of cells might be a factor in PTPD induced radiosensitisation (Franken et al., 2006). Secondly, TNBCs are characterised by higher rates of genomic instability, higher mutation burden and altered DNA repair pathways (Bianchini et al., 2016, Hubalek et al., 2017, Ali et al., 2018). TCGA analysis reveals that the most frequent loss-of-function alterations in TNBC involves genes associated with DNA damage repair such as p53, BRCA-1 and RB1, which impairs DNA repair capacity in this breast cancer subtype (TCGA, 2012). Other studies have also reported that the expression of BER pathway genes such as XRCC1 and Polβ is altered in TNBCs (Lee et al., 2019a), which might explain the radiosensitivity observed in TNBC cells as opposed to the luminal cell lines. The increased radiosensitisation observed in MDAMB-436 cells may be due to the inherent BRCA-1 deficiency and the synthetic lethal relationship that exists between FEN-1 and BRCA-1 (Mengwasser et al., 2019).

RPA is a single strand DNA binding protein that binds to damaged DNA and helps in the recruitment of genome maintenance factors to regulate DNA repair (Marechal and Zou, 2015). RPA nuclear foci measurement was assessed in the current study as a marker of ss-DNA damage (Bélanger et al., 2018) using fluorescent antibodies, and detected by immunofluorescent microscopy. From initial optimisation experiments, RPA expression was maximum at 0.5 hour post-1 Gy radiation, which is in agreement with published literature which report that RPA co-localises with DNA within 20-30 minutes of irradiation exposure (Kobayashi et al., 2002, Stephan et al., 2009). In order to assess if PTPD induced DNA damage in the breast cancer phenotypes, the levels of RPA were assessed in response to PTPD treatment and ionising radiation. Compared to radiation alone, combined treatment of PTPD in combination with radiation, increased RPA expression by 1-2 fold in all cell lines (MCF-7 (P=0.031), T47D (P=0.061), MDAMB-231 (P=0.020), MDAMB-468 (P=0.019) and MDAMB-436 (P<0.0001) cells), suggesting that addition of PTPD increases the amount of single strand DNA damage caused by ionising radiation. Single strand

DNA damage does not necessarily result in cell lethality, unless it is left unrepaired and gets converted into DNA double strand breaks. In order to assess if PTPD in combination with radiation induced DNA double strand breaks, the levels of γ-H2AX was also assessed.

Phosphorylation of the histone variant H2AX at Ser139 (γ-H2AX) by the ATM protein is one of the initial cellular response to DNA double strand breaks (Rogakou et al., 1998). In response to radiation damage, γ-H2AX serves as a platform for the recruitment of DNA repair proteins to the damage site forming nuclear ionising radiation-induced foci (IRIF) (Paull et al., 2000). γ-H2AX foci can be detected microscopically, by using fluorescent gamma-H2AX-specific antibodies (Nakamura et al., 2006). Based on optimization experiments, γ-H2AX expression was maximum between 0-0.5 hours post-exposure to 4 Gy of ionising radiation. In agreement with this finding, it has been previously reported that γ-H2AX phosphorylation is detectable in minutes following irradiation and reaches maximum levels within the first 30 minutes (Nakamura et al., 2006, Tu et al., 2013). In order to identify if treatment with PTPD and radiation increased DNA double strand breaks, the levels of γ-H2AX expression was assessed. With combined PTPD and radiation treatment, only marginal increases in γ-H2AX foci formation was observed in MCF-7, T47D, MDAMB-231 and MDAMB-468 cells. A significant ~2-fold increase in the number of DNA double strand damage was observed only in the MDAMB-436 cell line (P=0.0003). Such results suggest that PTPD treatment in combination with radiation is effective only in the context of BRCA-1 deficiency. The lack of significant induction of DNA double strand damage by PTPD treatment may explain marginal levels or lack of radiosensitisation observed upon PTPD treatment in MCF-7, T47D, MDAMB-231 and MDAMB-468 cells.

In conclusion, the FEN-1 inhibitor, PTPD was found to selectively radiosensitise TNBC cell lines and therefore this inhibitor might hold potential as a radiosensitiser in the treatment of TNBC patients. The radiosensitisation seen upon FEN-1 inhibition in the BRCA-1 deficient cell line is significant, but may warrant further study in other BRCA-1 deficient cells. However, the levels of radiosensitisation obtained with PTPD were lower than that achieved with the ATM inhibitor, KU-55933, and the PARP

inhibitor, olaparib, and so the clinical utility of this approach may be questionable. Further experiments with PTPD were not carried out due to the low levels of radiosensitisation seen. Rather, attention was focused on novel hypoxia-activated prodrugs, with experiments discussed in subsequent chapters.

Conclusions

All the hypothesis proposed at the beginning of this chapter were answered:

The luminal and triple negative breast cancer cell lines exhibit differential intrinsic radiosensitivities.

Inhibition of FEN-1 radiosensitises triple negative breast cancer cells but not luminal cell lines.

Radiosensitisation achieved with PTPD was lower than that induced by control DNA repair inhibitors, KU-55933 and olaparib.

PTPD induced single strand breaks was associated with radiosensitisation only in the triple negative, but not in luminal cells.

The induction of DNA double strand breaks by PTPD treatment was associated with radiosensitivity only in MDAMB-436 cells.

Chapter 3 Hypoxia-activated prodrugs in 3D and 2D models of breast cancer

3.1 Abstract

Background: Hypoxia is often found in breast cancer and is associated with radiotherapy resistance, metastasis and poor survival. The presence of molecular oxygen is essential to enhance the therapeutic efficacy of radiation. Tumour hypoxia, therefore, is a barrier to efficient treatment. A strategy to eradicate hypoxic tumour cells and improve radioresponse is by hypoxia-activated prodrugs (HAPs) that are activated in, and therefore cytotoxic to hypoxic tumour cells. AQ4N was one such bioreductive prodrug - TOPO II inhibitor that showed promising results as a hypoxia-activated radiosensitiser in phase I clinical trials. Unfortunately, development of this agent has not progressed further. The novel AQ4N analogue, KP167, developed by Dr Klaus Pors at the University of Bradford is a hypoxia-activated - TOPO II inhibitor, with additional DNA alkylating properties. The aim of the current chapter was to investigate the *in vitro* efficacy of KP167, as single agent and in combination with ionising radiation, in 3D spheroids and 2D normoxic models of luminal and triple negative breast cancer.

Methods: 3D spheroid (>500 µm diameter) and 2D (21% O_2) monolayer cultures of two luminal (MCF-7 and T47D) and three triple negative (MDAMB-231, MDAMB-468 and BRCA-1 deficient MDAMB-436) breast cancer cell lines were chosen as *in vitro* models. AQ4N was used as a comparator against the novel agent, KP167. The cellular cytotoxicity of single agent AQ4N and KP167 were evaluated using growth curves in 2D and clonogenic survival assays in both 3D spheroid and 2D normoxic models. Expression of various endogenous reductases (cytochrome P450, CYP2S1, CYP2W1, NQO1 and NQO2), involved in the bioreductive-activation of HAPs, were evaluated by Western blot of cell lysates to assess if endogenous reductase expression may reflect any difference in sensitivity observed between the different breast cancer phenotypes. Radiosensitisation was measured by treating cells (3D and 2D) with single agent 3D IC_{50} doses of AQ4N or KP167 for 96 hours and subsequently exposing them to single doses (0-8 Gy) of x-rays and examined via clonogenic survival assays.

Results: Clonogenic data shows that both AQ4N and KP167 reduce survival of breast cancer spheroids in a dose-dependent manner. Overall, the luminal cell lines MCF-7 and T47D were more sensitive to single agent AQ4N and KP167 treatment compared to the triple negative MDAMB-231 and MDAMB-468 cells, in both 3D and 2D cultures. Compared to AQ4N IC_{50} of (0.2-22.8) μM, KP167 demonstrated a 2-100 fold increase in potency with IC_{50} values ranging between (0.14-12.8) μM. As expected AQ4N and KP167 were less potent in 2D normoxia conditions with AQ4N IC_{50} (24 hour) ranging from (10.5 - >45) μM for proliferation and (<5 - >45) μM in clonogenic survival. The IC_{50} values of KP167 ranged from (21 - >45) μM for proliferation and (<5 - >45) μM in clonogenic survival.

Higher endogenous expression of cytochrome P450 (MCF-7>T47D>MDAMB-468>MDAMB-231>MDAMB-436 cells) and CYP2W1 (MCF-7>T47D>MDAMB-436>MDAMB-231>MDAMB-468 cells) was observed in luminal cells compared to TNBC cell lines. Compared to MCF-7 cells, the expression of cytochrome P450 was significantly reduced in MDAMB-231 (P=0.044) and MDAMB-436 (P=0.032) cells. CYP2W1 was significantly reduced in MDAMB-231 (P=0.023), MDAMB-468 (P=0.003) and MDAMB-436 (P=0.025) cells, compared to MCF-7 cells. CYP2S1 was expressed in all cell lines with marginal increase in TNBC cells (MDAMB-436>MDAMB-468>MDAMB-231>MCF-7>T47D cells). Compared to MDAMB-436, CYP2S1 was significantly reduced in MCF-7 (P=0.032), T47D (P=0.021) and MDAMB-231 (P=0.041) cells. NQO1 expression was higher in MDAMB-436 compared to MCF-7 (P=0.001), but undetected in T47D, MDAMB-231 and MDAMB-468 cells. The expression of NQO2 (MDAMB-231>MDAMB-468>MCF-7>MDAMB-436>T47D cells) was significantly greater in MDAMB-231 cells compared to MCF-7 (P=0.047), T47D (P=0.001), and MDAMB-436 (P=0.005) cells. Higher expression of cytochrome P450 and CYP2W1 in MCF-7 and T47D cells, compared to the triple negative cell lines, may have contributed to the increase in cytotoxicity observed in luminal cells with single agent AQ4N and KP167 treatment.

AQ4N was an effective radiosensitiser of breast cancer spheroids with $SER_{0.01}$ of 1.30±0.08 in MCF-7, 1.58±0.06 in T47D, 1.44±0.04 in MDAMB-231, 1.64±0.08 in MDAMB-468 and 3.33±0.18 in MDAMB-436 cells.

Increased radiosensitisation was also observed with KP167 in all breast cancer spheroids, with 100-fold increase in radiosensitivity noted at 8 Gy in T47D and TNBC cell lines. KP167 radiosensitised spheroids with $SER_{0.01}$ of 1.46±0.66 in MCF-7, 1.76±0.20 in T47D, 2.53±0.06 in MDAMB-231, 2.28±0.24 in MDAMB-468 and 4.55±0.24 in MDAMB-436 cells.

AQ4N and KP167 induced lower levels of radiosensitisation in 2D normoxia compared to 3D spheroid cultures. AQ4N radiosensitised breast cancer cells with $SER_{0.01}$ of 1.17±0.06 in MCF-7, 1.64±0.27 in T47D, 1.29±0.28 in MDAMB-231, 1.11±0.44 in MDAMB-468 and 1.19±0.12 in MDAMB-436 cells. KP167 was more effective than AQ4N in normoxia cultures with $SER_{0.01}$ of 1.21±0.05 in MCF-7, 1.93±0.09 in T47D, 1.43±0.46 in MDAMB-231, 1.32±0.19 in MDAMB-468 and 1.68±0.08 in MDAMB-436 cells.

Conclusion: KP167 is a highly potent radiosensitiser, especially in 3D models of TNBC. KP167 appears to be a promising new drug, either as a single agent and especially when combined with radiation, to target hypoxic cancer cells.

3.2 Introduction and aims

3.2.1 Hypoxia

The cellular microenvironment contains different concentrations of oxygen that can be divided into normoxia (21% O_2), physoxia (1–13% O_2) and hypoxia (0.1–1% O_2). Normoxia is a term which refers to 'normal' atmospheric levels of 20-21% (160mmHg) oxygen, that cells are routinely cultured in (McKeown, 2014). This physiological concentration of oxygen in tissues is referred to as physoxia or physiological hypoxia (Vaupel et al., 2007, Carreau et al., 2011). Certain studies have reported that, depending on tissue type, the oxygen concentration in normal tissues can vary between 10 (2% O_2) and 80mmHg (10% O_2), while tumour cells can contain <5mmHg (<0.5% O_2) (Vaupel et al., 2007). The lower level of physoxia is approx. 3%, below which pathological hypoxia sets in. Hypoxia pO_2<10mmHg (<1%-2% O_2) in tumours arises due to the uncontrolled proliferation of cancer cells in the absence of an efficient blood supply. The rapidly proliferating tumour cells become distanced from the vasculature

(>100-200 µm), and quickly exhaust available nutrients and oxygen, creating an imbalance between oxygen demand and supply (Yu et al., 2014). This results in oxygen depletion creating a hypoxic tumour microenvironment (Brown and Wilson, 2004).

Chronic and acute hypoxia

Hypoxia is a characteristic of solid tumours (Brown and Wilson, 2004) with most containing regions of acute (low O_2 levels for minutes to hours) and chronic hypoxia (low O_2 levels for hours to days) or anoxia (0% O_2), that is deleterious for cancer treatment as it promotes drug resistance and drives malignant progression (Kato et al., 2011, Bayer and Vaupel, 2012). Acute hypoxia or perfusion-limited hypoxia can arise as a result of temporary perturbations in blood supply (Brown, 1979). It is also known as intermittent or cycling hypoxia and can occur when blood supply is cut-off due to vessel obstruction by tumour cells, blood cells or fibrin aggregates (Dewhirst, 2009). Chronic hypoxia or diffusion-limited hypoxia is thought to arise due to the inability of the vasculature to reach tumours that lie beyond the diffusion capacity of oxygen (>150-200 µm) (Cai et al., 2015). This occurs when the increasing tumour mass creates large diffusion distance between itself and the oxygen-supplying blood vessels (Gulledge and Dewhirst, 1996, Lanzen et al., 2006).

3.2.1.1 Hypoxia in cancer

Hypoxia is an independent predictor of poor clinical outcome and tumours that exhibit significant hypoxia have been associated with an increased risk of mortality, independent of prognostic factors such as grade, histology, nodal status and size (Vaupel et al., 2007). Tumour hypoxia leads to radio- and chemotherapy resistance, as well as selection of tumour clones with increased metastatic potential (Brown, 2007). The presence of hypoxia upregulates hypoxia-inducible factor (HIF) - the main transcription factor that promotes adaptive response of cells by transcribing a number of hypoxia-related genes such as vascular endothelial growth factor (VEGF) carbonic anhydrase 9 (CA9), Bcl-2 etc that drive pro-angiogenic pro-survival and pro-apoptotic pathways (Swinson et al., 2003). Studies have

shown that hypoxia drives metastasis by upregulating metastasis-related genes, such as osteopontin, lysyl oxidase, CXCR4, IL8 and VEGF (Rofstad, 2000, Erler et al., 2006).

Hypoxia occurs in approximately 40% of breast cancers and is more commonly seen in locally advanced primary breast cancer (Vaupel et al., 2003, Vaupel et al., 2005). Hypoxic regions have been found to occur in all breast cancer stages, from *in situ* carcinomas to both lobular and ductal invasive cancers (Hohenberger et al., 1998). Studies have reported that the mean pO_2 in breast cancer ranges between 2.5 to 28mmHg (0.3-3.5% O_2), with a median value of 10mmHg (1.3% O_2), in comparison to 65mmHg (8% O_2) in normal breast (Vaupel et al., 1991). The presence of hypoxia in breast cancer also decreases the effectiveness of hormonal therapy due to loss of ERα (Kurebayashi et al., 2001). In patients with DCIS, the presence of hypoxia or necrosis is associated with a shorter time to recurrence (Cornfield et al., 2004). Van den Eynden et al., 2005 reported that the presence of hypoxia in primary breast cancers was associated with hypoxia markers in their lymph node metastases, indicating that the hypoxia phenotype is maintained even in metastatic lesions (Van den Eynden et al., 2005).

3.2.1.2 Hypoxia and therapy resistance

Multiple reasons have been put forward over the years, to explain why the presence of tumour hypoxia is associated with resistance to anti-cancer therapies (Kinoshita et al., 2001, Teicher, 1994). These include but not limited to: 1. Hypoxic tumour cells can be quiescent, non-proliferative and therefore non-reactive to most anti-cancer agents that target the rapidly proliferating tumour cells (Butturini et al., 2019); 2. Chemotherapy drugs may not be able to reach hypoxic regions due to the increasing inter-vascular distance (Gulledge and Dewhirst, 1996); 3. The presence of molecular oxygen is critical for radiation induced cell lethality (described in detail below in section 3.2.1.3) (Wang et al., 2019); 4. Hypoxic tumour cells have upregulated DNA repair and anti-apoptotic pathways, which increases the rate of DNA repair and prevents cell death induced by various anti-cancer agents (Sermeus et al., 2012, Jongen et al., 2017); 5. Hypoxia

promotes acidosis due to a shift from oxidative phosphorylation to glycolysis, which affects drug delivery and cellular uptake of pH sensitive anti-cancer agents (DeClerck and Elble, 2010); 6. Hypoxia upregulates expression of multidrug transport P-glycoprotein encoded by the MDR-1 (multi-drug resistance-1) gene, an ATP dependent efflux pump that actively exports drugs out of cells, conferring resistance to a broad range of chemotherapeutics (Muredda et al., 2003, Lv et al., 2015). In support of the aforementioned reasons, several chemotherapeutic drugs used in breast cancer treatment such as 5-FU (Wouters et al., 2007) and methotrexate, platinum agents such as cisplatin and carboplatin, alkylating agents such as docetaxel and doxorubicin, have demonstrated to be less effective under hypoxic conditions-termed as hypoxia-induced chemoresistance (HICR) (Teicher et al., 1981, Wouters et al., 2007, Baker et al., 2008, Notte et al., 2013).

3.2.1.3 Hypoxia and radiotherapy response

It is known that the presence of intratumoural hypoxia severely compromises radiotherapy efficacy (Graham and Unger, 2018). Gray and colleagues, in 1953, were the first to identify a decrease in oxygen between the periphery and the centre of tumours; and reported that killing hypoxic cells required up to a three-fold higher dose of radiation compared to oxic cells. This difference in radiation response between oxygenated and hypoxic cells is known as the oxygen enhancement ratio (OER) (Gray et al., 1953, Roots and Smith, 1974). Oxygen is a highly electron-affinic molecule that chemically modifies radiation-induced free radical DNA damage creating lesions that are non-restorable, termed as the oxygen fixation hypothesis (Roots and Smith, 1974, Brown and Wilson, 2004). In the absence of oxygen, the DNA based free radicals are reduced by compounds containing sulfhydryl groups, which reverts DNA back to the undamaged form, resulting in radiotherapy resistance (Brown, 1999, Brown and Wilson, 2004). Furthermore, defects in DNA repair pathways such as mismatch repair and homologous recombination repair have been reported in cells exposed to hypoxia, which further alters sensitivity of hypoxic cells to radiotherapy (Bristow and Hill, 2008).

3.2.2 Hypoxic radiosensitisers

Overcoming radioresistance in hypoxic tumours has been attempted by various means, including hyperbaric oxygen therapy, hyperthermia and carbogen breathing combined with nicotinamide to improve tumour oxygenation (Jordan and Sonveaux, 2012). Hyperbaric oxygen therapy is the breathing of 100% oxygen to increase systemic oxygen tension which was shown to improve tumour local control by 10% (Daruwalla and Christophi, 2006). However, this technique increases radiation-induced tissue injury and the chance of oxygen-related seizures during therapy (Overgaard and Horsman, 1996). Hyperthermia is the elevation of body temperatures to higher than normal levels (~45°C) (Song et al., 2001). When combined with radiation, hyperthermia can act as a radiosensitiser, since heat can damage various cellular components (van der Zee et al., 2000), and dilate blood vessels which increases blood flow to hypoxic regions of tumours (Wust et al., 2002). Clinical trials have shown significant improvement in survival when combined with radiation (41% v 59%) in the treatment of recurrent breast (Vernon et al., 1996), pelvic (van der Zee et al., 2000), prostate (Hurwitz et al., 2011) and other cancers (Peeken et al., 2017). However, the widespread use of hyperthermia may be limited due to technical complications, such as maintenance of homogenous heating and monitoring of temperatures.

Compared to the traditional hyperbaric approach, a more recent approach is the use of accelerated radiotherapy (68 Gy over 5.5 weeks) in combination with carbogen (95% oxygen, 5% CO_2) breathing and oral nicotinamide (ARCON), a vasodilator (Kaanders et al., 2002), to decrease diffusion-limited and perfusion-limited hypoxia respectively. A phase III clinical trial (NCT00147732) with 345 laryngeal cancer patients reported a significant improvement in regional control in patients treated with ARCON (93%) than with accelerated radiotherapy (86%) (Janssens et al., 2012). Promising results from a phase III BCON trial in bladder cancer recently reported a significant improvement in 5 year recurrence-free survival (41% vs 33%), which was also maintained at 10 years (27% vs 20%) in patients treated with ARCON (Song et al., 2019).

The development of oxygen-mimetic nitroimidazole radiosensitisers that substitute for oxygen in fixing radiation-induced DNA damage was another approach to target radiation-resistant hypoxic tumour cells (Jackson et al., 2019). These agents are less rapidly metabolised by tissues, enabling better diffusion and penetration compared to oxygen which is readily metabolised in respiring tissues. The nitroimidazoles are enzymatically reduced by nitroreductase enzymes leading to the production of highly reactive anion radicals that cause irreversible damage to cellular components (Edwards, 1993, Oronsky et al., 2011). From the many that have been examined over the years, nimorazole is well tolerated in patients and is approved as a radiosensitiser in Denmark for the treatment of HNSCC patients (Timothy et al., 1984, Overgaard et al., 1998). The NIMRAD trial (NCT01950689) is currently evaluating nimorazole in combination with radiotherapy in patients with locally advanced HNSCC (ClinicalTrials, 2019). An additional approach, to overcome hypoxic radioresistance is the use of drugs that selectively target hypoxic cells (Guise et al., 2014, Jackson et al., 2019)

3.2.3 Hypoxia-activated prodrugs

A hypoxia-activated prodrug (HAP) is specifically designed to be activated by cellular reductases only in hypoxic tissues and thus selectively kill hypoxic cells (Denny, 2000). A prodrug is a compound that is initially inactive, but can only be converted into its pharmacologically active cytotoxic counterpart via specific metabolic pathways (Guise et al., 2014). Bio-reduction of HAPs into their respective cytotoxins can occur via a one- or two-electron reduction catalysed by cellular reductases as shown in Figure 3.1.

In the one-electron pathway, the prodrug undergoes reduction to form the prodrug radical in the absence of oxygen. In the presence of oxygen, the radical species can be reverted back (back-oxidised) to generate the parental drug and ROS (Mistry et al., 2017). The free radicals generated during this process are neutralised by anti-oxidant systems in cells, which reduces the toxic effects in oxygenated tissues (Wilson and Hay, 2011, Phillips, 2016).

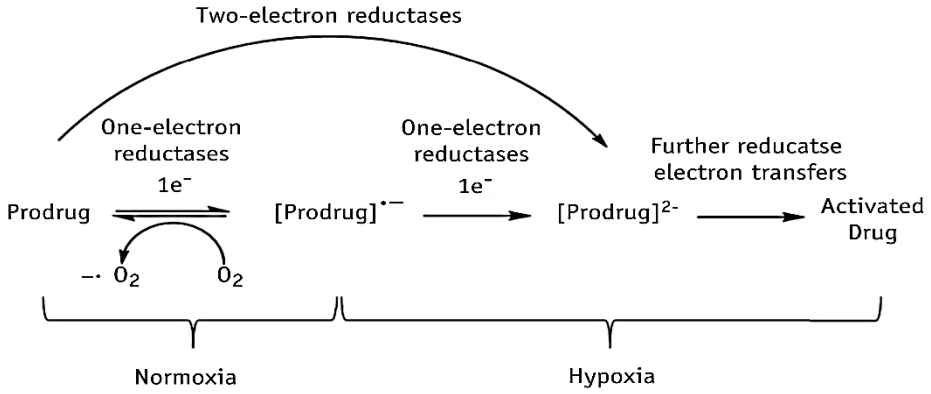


Figure 3.1 Activation of hypoxia-activated prodrugs by one- or two-electron reductases. In the presence of oxygen the radical species reverts back to the parental drug. In hypoxia, further reduction occurs activating the prodrug (one-electron). The two-electron reduction results in oxygen independent activation of the prodrug. Reproduced from (Mistry et al., 2017). Copyright© 2017 by Elsevier with permission conveyed through Copyright Clearance Centre Inc.

In the absence of oxygen, the prodrug radical can undergo further enzyme-mediated reduction to generate the active cytotoxic drug. In contrast, the two-electron reduction bypasses the oxygen sensitive intermediate step to generate the active cytotoxic metabolite. These reactions are usually oxygen insensitive and selectivity is largely determined by the presence of endogenous reductases (Workman, 1994).

However, certain HAPs such as AQ4N, undergo the oxygen sensitive, sequential two-electron reduction which are catalysed by the cytochrome P450 family of endogenous reductases (Wilson and Hay, 2011, Phillips, 2016). Cytochrome P450 family of monooxygenase enzymes are involved in metabolising a wide variety of drugs, and can carry out both the one- and two-electron reduction reactions (Guengerich, 2008). NAD(P)H:quinone oxidoreductase 1 (NQO1) and NRH:quinone oxidoreductase 2 (NQO2) are cytosolic enzymes that catalyse the two-electron metabolic reduction of quinones and derivatives (Iskander et al., 2006). HAPs are more effective when combined with conventional chemo/radiation therapy that target the oxygenated tumour cells (Mistry et al., 2017). Despite extensive pre-clinical and clinical research over several years, HAPs have still not found clinical utility, but many are

currently undergoing or have undergone phase I and phase II clinical evaluation – these are discussed below.

TH-302 (Evofosfamide)

TH-302 is a 2-nitroimidazole hypoxia-activated prodrug of bromo-isophosphoramide mustard. It undergoes a one-electron reduction catalysed by cytochrome P450 enzymes to yield the cytotoxic metabolite that results in DNA cross linking and induces cell cycle arrest (Meng et al., 2012). TH-302 targets hypoxic cells and reduces its ability to repopulate following re-oxygenation (Liapis et al., 2015). Positive results were obtained from phase II clinical trials in combination with doxorubicin in sarcoma patients (Chawla et al., 2014) and gemcitabine in pancreatic cancer (Borad et al., 2015). Currently, most phase III clinical trials (NCT02047500, NCT01864538, NCT02093962, NCT02598687, and NCT02255110) (ClinicalTrials, 2019), have been withdrawn or terminated as TH-302 failed to demonstrate any improvement in progression-free or overall survival (Lee et al., 2017).

EO9 (Apaziquone)

EO9 is an indolequinone analogue of mitomycin C, and can undergo either the one-or two-electron reduction to generate the cytotoxic metabolite in both aerobic and hypoxic conditions (Phillips et al., 2013). In the absence of oxygen, NQO1 plays a central role in the reductive activation via the two-electron reduction pathway. In the absence of NQO1, EO9 undergoes a one-electron reduction catalysed by cytochrome P450 (Plumb and Workman, 1994, Robertson et al., 1994, Workman, 1994). The short biological half-life led to a clinical trial to study the effects of intra-vesical administration of EO9 into the bladder and eight complete responses were obtained out of a total of 12 patients (Puri et al., 2006). However, phase III clinical studies were terminated due to insufficient efficacy (NCT01475266, NCT01469221, NCT01410565) (ClinicalTrials, 2019). Currently no new trials are recruiting, so clinical development of EO9 seems to have stalled. Researchers are, however, continuing investigations with new generations of such agents in pancreatic (Inman et al., 2014)

and brain cancers, in combination with radiation (S Martin, unpublished data).

PR-104

PR-104 is a phosphate ester 'pre-prodrug' that belongs to the nitroaromatic compound of HAPs. PR-104 is hydrolysed by systemic phosphatases to generate the intermediate PR-104A compound that is further metabolised by one- or two-electron reduction to the para-hydroxylamine PR-104H and para-amine PR-104M metabolites, which causes DNA cross-links (Patterson et al., 2007). A wide variety of reductases catalyse the reduction in PR-104A including the cytochrome P450 reductase (Guise et al., 2007). Phase 1 clinical trials have been completed, but progression of this agent has stopped as a result of severe dose-limiting myelotoxicity (McKeage et al., 2012). A new nitrobenzamide mustard analogue CP-506, has been reported to be potent in the killing of hypoxic triple negative breast cancer, lung and pancreatic cancer cells, and is currently undergoing pre-clinical evaluation (Niemans et al., 2018, thiolloy et al., 2018).

Tirapazamine (TPZ)

TPZ is an aromatic N-oxide that can undergo a one-electron reduction catalysed by cytochrome P450 reductase or a two-electron reduction catalysed by NQO1 to form the DNA damaging metabolite (Patterson et al., 1994). TPZ entered phase I and phase II clinical trials and generated positive results when used in combination with cisplatin, etoposide and/or radiotherapy (Miller et al., 1997, Le et al., 2009). However, phase III trials failed to demonstrate any survival advantage by adding TPZ to chemotherapy or radiotherapy in non-small cell lung cancer (Williamson et al., 2005), head and neck cancer (Rischin et al., 2010) and cervical cancer (DiSilvestro et al., 2014). Recently, a novel analogue of TPZ, SN30000 is undergoing extensive pre-clinical evaluation in combination with chemo and radiotherapy in colorectal cancer and has shown better efficacy than the parental compound (Mao et al., 2018, Mao et al., 2019).

3.2.4 AQ4N and novel analogues

AQ4N (Banoxantrone), is a di-N-oxide aliphatic amino anthracenedione, (1,4-bis{[2(dimethylamino)ethyl]amino}-5,8-hydroxyanthracene-9,10-dione bis-N-oxide), metabolised by the cytochrome P450 (CYP) family of reductases and inducible nitric oxide synthase (iNOS) to AQ4, a potent inhibitor of topoisomerase II (TOPO II), in the absence of oxygen (Patterson, 1993, Patterson and McKeown, 2000, Nishida and Ortiz de Montellano, 2008). AQ4N undergoes an initial two-electron reduction reaction to yield the mono-N-oxide (AQ4M), followed by a further two-electron reduction to generate the DNA binding toxin AQ4, as shown in Figure 3.2.

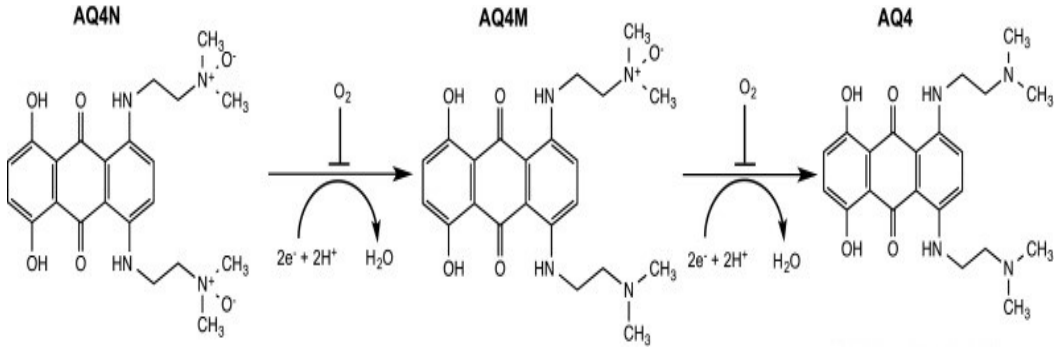


Figure 3.2 Reductive activation of AQ4N to AQ4. AQ4N undergoes sequential two-electron reduction to yield AQM and a further two-electron reduction to yield AQ4, catalysed by cytochrome P450 enzymes and iNOS in the absence of oxygen. Reproduced from (Phillips, 2016). Copyright© 2016 by Springer with permission conveyed through Copyright Clearance Centre Inc.

AQ4N is more potent in hypoxic conditions, because in normoxia, oxygen outcompetes AQ4N in binding to the haem-centred active site of CYP enzymes (Raleigh et al., 1998). The presence of oxygen therefore inhibits the efficient reduction of AQ4N (Patterson and McKeown, 2000). Studies by Nishida et al., 2010 reported that the orphan CYP enzymes, CYP2S1 and CYP2W1 are expressed in high levels in hypoxic cells and catalyse the reduction of AQ4N to AQ4, more efficiently compared to all other P450 enzymes (Nishida et al., 2010). CYP2S1 and CYP2W1 have been found to reduce AQ4N to AQ4 at a rate of approximately 12 mole of substrate per mole of enzyme per minute (Nishida et al., 2010). After reduction, the highly stable AQ4 binds DNA non-covalently, and inhibits TOPO II of

hypoxic cells, as they re-enter the cell cycle during reoxygenation (Patterson and McKeown, 2000). Inhibition of TOPO II prevents unwinding of DNA during replication and repair, resulting in stalled replication forks that can lead to cell death through the generation of cytotoxic DNA double strand breaks (Salceda et al., 2006, McClendon and Osheroff, 2007).

AQ4N is an ideal HAP, as it can penetrate deep into tumour tissues, localise to hypoxic regions and exert bystander effects in proximate tumour cells (Albertella et al., 2008, Tredan et al., 2009). Furthermore, AQ4N enhances the efficacy of radio- (McKeown et al., 1995, Patterson et al., 2000) and chemotherapy (cyclophosphamide, mitoxantrone, and cisplatin) (Friery et al., 2000, Patterson et al., 2000, Tredan et al., 2009), due to the targeting of the therapy-resistant hypoxic population during reoxygenation. Promising results from several pre-clinical studies established AQ4N as a potent radiosensitiser (Patterson et al., 2000, McErlane et al., 2005) which progressed AQ4N to clinical trials as an adjuvant to chemo/radiotherapy in glioblastoma multiforme (NCT00394628), chronic lymphocytic leukemia, small lymphocytic leukemia (NCT00109356), advanced solid tumours and non-Hodgkin's lymphoma (NCT00090727) (Mistry et al., 2017). In a phase I clinical trial of glioblastoma and head and neck tumours, AQ4N was found to be selectively activated in Glut-1 positive hypoxic regions of solid tumours (Albertella et al., 2008). Early clinical trials have shown that AQ4N did not result in major systemic toxicities and was well tolerated in patients at doses up to 768 mg/m^2 given weekly as a single agent (Benghiat et al., 2004, Papadopoulos et al., 2008) or 447 mg/m^2 when given in combination with radiation (Steward et al., 2007). In a study of 22 oesophageal carcinoma patients, AQ4N in combination with fractionated radiotherapy resulted in 50% reduction in tumour volume in 3 patients and stable disease in 9. Biopsies taken from AQ4N treated patients demonstrated higher concentration of AQ4 in tumour tissues compared to normal tissues (tumour: normal tissue ratio >3.7) (Steward et al., 2007). Although trials yielded promising results, AQ4N was not progressed by the pharma company that purchased the rights and AQ4N has now gone off patent – it is still, however, being investigated scientifically by a number of groups, as an agent that can be rationally combined with conventional therapies to

improve therapeutic efficacy (O'Connor et al., 2016, Feng et al., 2017). Additional analogues have been developed as described below.

OCT1002

As shown in Figure 3.3, like AQ4N, OCT1002 is a hypoxia-activated prodrug that is reduced into its cytotoxic counterpart OCT1001 in hypoxic conditions (Nesbitt et al., 2017a). With OCT1002, the 12 hydrogen atoms within the two N-oxide side chains of AQ4N are substituted with deuterium (McKenna et al., 2018). This modification lowers the rate of OCT1001 metabolism, which results in persistence of the drug intracellularly, increasing its effectiveness (Nesbitt et al., 2017a). Reduction is unidirectional. A single dose (30mg/kg) of OCT1002 was found to control tumour growth in castrate-resistant prostate cancer for 42 days and increased efficacy of abiraterone, cabazitaxel, and docetaxel. Studies have shown promising anti-cancer activity when combined with bicalutamide in prostate cancer (Nesbitt et al., 2017b). The drug is currently undergoing commercialisation by OncoTherics (Nesbitt et al., 2017a).

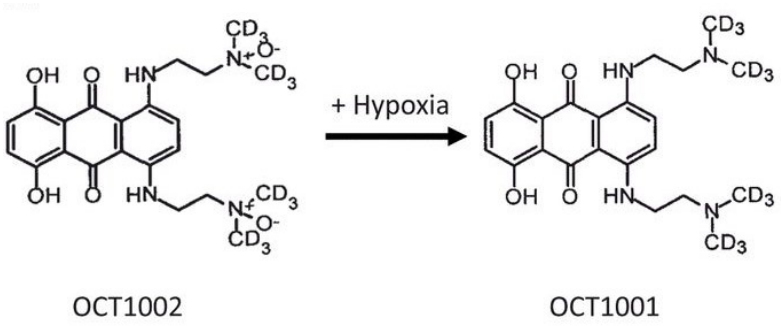


Figure 3.3 Reductive activation of OCT1002 to OCT1001. OCT1002 undergoes sequential 2 electron reduction catalysed by cytochrome P450 family of enzymes. Reproduced from (Nesbitt et al., 2017a). Copyright© 2017 by American Association for Cancer Research with permission conveyed through Copyright Clearance Centre Inc.

KP167

KP167, used in the current project, is a newly developed AQ4N analogue, synthesised by Dr Klaus Pors at the University of Bradford. It differs from AQ4N through substitution of one CH3 group with a Cl group, and deletion of the 3 CH3 groups within the two N-oxide side chains. In the absence of

oxygen, KP167 undergoes the oxygen sensitive two-electron reduction to yield an intermediate product that further undergoes a two-electron reduction to yield the cytotoxic metabolite - a bicyclic electrophile as shown in Figure 3.4.

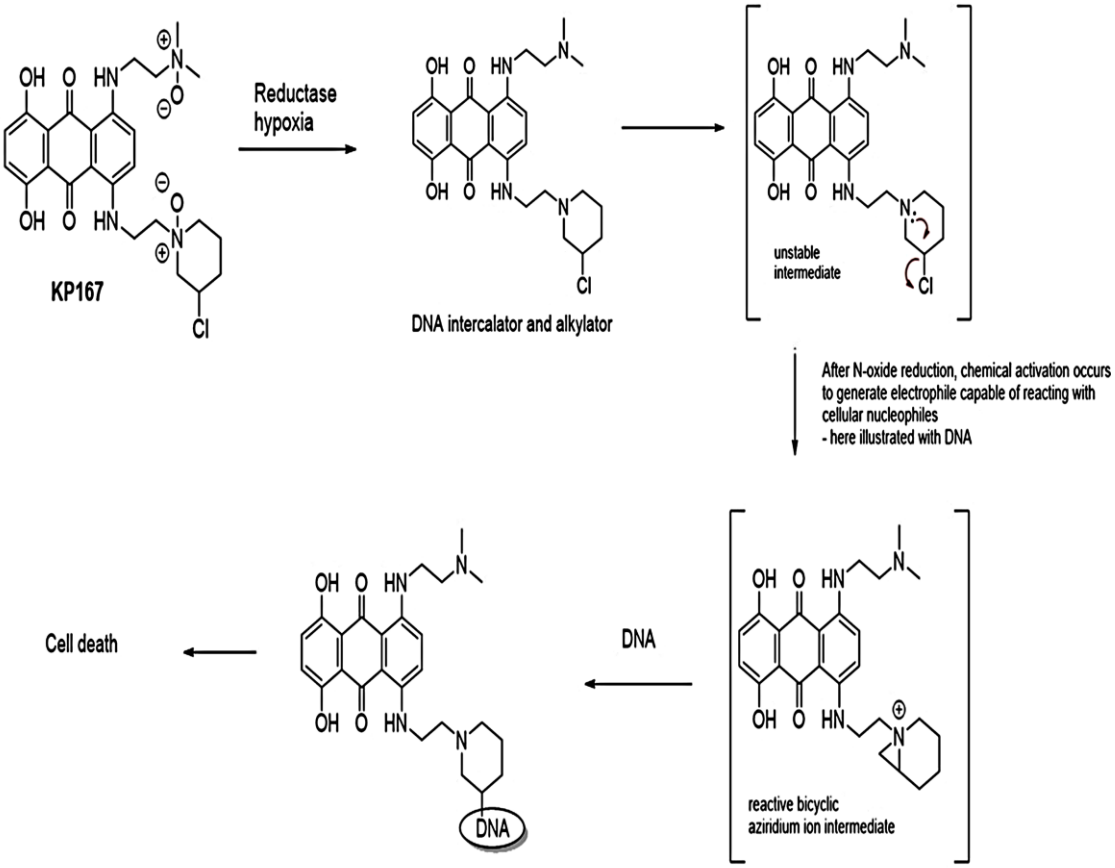


Figure 3.4 Reductive activation of KP167. In the absence of oxygen, KP167 undergoes sequential two electron reduction catalysed by cytochrome P450 family enzymes, to yield the highly reactive DNA binding metabolite (Klaus Pors, personal communication of unpublished data).

Following N-oxide reduction, KP167 interacts with cellular components such as proteins and nucleic acids leading to cellular toxicity. The highly reactive metabolite binds to DNA covalently, as opposed to AQ4N or OCT1002 that binds DNA non-covalently. Covalent binding of the drug to the DNA causes irreversible DNA damage subsequently resulting in cell death (Alotaibi and Momen, 2019).

The active metabolite of KP167 not only functions as a DNA intercalator and a TOPO II inhibitor, but also as a potent DNA alkylator. As an alkylating agent, KP167 induces formation of DNA adducts as well as intra- and inter-

strand DNA cross-links which blocks DNA replication, leading to DNA strand breaks, chromatid breaks and chromosomal aberrations (La et al., 2010). Preliminary studies conducted at the University of Bradford show that KP167 enhances efficacy of oxaliplatin (38% survival v 58% survival with oxaliplatin alone) in human colorectal cancer cells (Klaus Pors, personal communication of unpublished data). As mentioned previously, the parental AQ4N has been established as a potent radiosensitiser across multiple cancer models but the effectiveness of KP167 in breast cancer, and as a hypoxia-activated radiosensitiser has not been investigated till date. It is this that the current study primarily sought to investigate. In addition, although AQ4N has been evaluated in multiple cancer models there is little information regarding its effectiveness in breast cancer (Albertella et al., 2008), with no information on its ability to radiosensitise breast cancer – the current chapter also sought to address this.

3.2.5 2D and 3D *in vitro* culture models

In the current study the effect of HAPs, AQ4N and KP167, were studied in two-dimensional (2D) and three dimensional (3D) cell culture systems. *In vitro* experiments usually use traditional 2D culture where cells in monolayers are cultured on flat surfaces (Breslin and O'Driscoll, 2013). Loss of tissue architecture and cell-cell contact in a 2D system, means that growth in 2D does not replicate *in vivo* growth conditions (Edmondson et al., 2014). 3D culture with multicellular tumour spheroids are an ideal *in vitro* model to study the hypoxic tumour microenvironment and drug response, as they provide physiologically relevant and more predictive information of *in vivo* cellular responses compared to 2D assays (Leek et al., 2016, Durand and Olive, 1992, Riffle and Hegde, 2017). Spheroids (>200 µm), like tumours, contain proliferating cells in normoxic areas, quiescent cells in hypoxic areas and dying cells in necrotic zones (Kim, 2005, Khaitan et al., 2006, Kapałczyńska et al., 2018), compared to monolayer cultures, which mostly contain proliferating cells (Mehta et al., 2012). In the current chapter, the cytotoxic effects of AQ4N and KP167 were studied in 3D spheroid culture systems, as this class of agents require hypoxia to undergo chemical reduction into their respective DNA binding cytotoxic metabolites (Patterson and McKeown, 2000, Patterson, 2002).

The effects of AQ4N and KP167 were also assessed in 2D normoxia to assess response in the presence of oxygen.

3.2.6 Hypothesis and aims

Hypoxia occurs in all stages of breast cancer, from *in situ* carcinomas to high grade invasive carcinomas (Hohenberger et al., 1998). Breast cancers with adverse prognostic characteristics such as the absence of the hormone receptors and lymph node positivity have lower pO_2 and higher areas of hypoxic and anoxic tissues, which are associated with shorter time to recurrence (Cornfield et al., 2004). The presence of tumour hypoxia also hinders efficacy of radiotherapy in breast cancer (Cuisnier et al., 2003, Graham and Unger, 2018).

Neoadjuvant therapy (preoperative treatment of tumours) is usually administered to LAPC patients, but recent evidence suggest that it is as effective as adjuvant therapy in the treatment of early stage invasive breast cancer (Zardavas and Piccart, 2015, Rubovszky and Horvath, 2017), with some agents being assessed in a neoadjuvant setting with radiotherapy (Poleszczuk et al., 2017, Brackstone et al., 2017). As discussed previously, surgery followed by radiotherapy is the current norm. But studies have demonstrated that administering neoadjuvant radiotherapy to the bulk of tumours activates a robust antitumor immune response which does not occur post-operatively (Formenti and Demaria, 2012, Burnette and Weichselbaum, 2013). Furthermore, Liapis et al., 2016 reported that the hypoxia-prodrug, TH-302, in combination with paclitaxel was able to suppress breast cancer growth in the mammary gland and bone of osteolytic breast cancer murine models, which indicate that combining a HAP with an anti-cancer agent has the potential to target even breast cancer metastasis (Liapis et al., 2016).

Such data suggest that combining a hypoxia-prodrug with radiotherapy in breast cancer may result in the eradication of both hypoxic and oxic cells in early stage invasive, LAPC and/or metastatic breast cancer which may hold potential for tumour suppression and reduction of metastatic clones. The novel AQ4N analogue, KP167 is a newly developed hypoxia-activated prodrug with additional anti-cancer properties in comparison to the

parental AQ4N (known radiosensitiser). The current study hypothesised that KP167 would be an effective radiosensitiser across the different breast cancer phenotypes. It was also hypothesised that radiosensitivity achieved with KP167 would be comparable or greater than that achieved with the parental drug AQ4N. The single agent anti-cancer and radiosensitising effects of KP167 were assessed across 3D and 2D models of breast cancer, with results compared to the experimental comparator, AQ4N.

Hypotheses

1. Single-agent AQ4N and KP167 treatment will be more cytotoxic in 3D spheroids compared to cells grown under 2D normoxia.
2. Endogenous reductase levels influence response of breast cancer cells to AQ4N and KP167.
3. Differential radiosensitivity will be observed between cells grown in 2D normoxia v 3D spheroids.
4. Radiosensitivity achieved with AQ4N and KP167 will be higher in 3D spheroids compared to 2D normoxia cultures.
5. Radiosensitivity achieved with KP167 will be comparable or greater that that induced by the parental AQ4N, in both 3D spheroid and 2D normoxia cultures.

Aims

- To assess single agent anti-cancer effect of KP167 and AQ4N in luminal and triple negative breast cancer cells in 3D spheroids and 2D normoxia culture conditions.
- To examine protein expression levels of reductases to gain an initial mechanistic insight into activation and differential drug sensitivities.
- To assess radioresponse in breast cancer cells grown in 3D spheroid and 2D normoxia.
- To investigate KP167 as a radiosensitiser in breast cancer cells (3D spheroids and 2D normoxia), comparing results against the parent drug, AQ4N.

3.3 Materials and Methods

3.3.1 Cell lines and culture conditions

The luminal breast cancer cell lines, MCF-7 and T47D, TNBC cell lines, MDAMB-231 MDAMB-468 and BRCA-1 deficient MDAMB-436, and the normal mammary epithelial cell line, MCF-10A were used in the current chapter to assess response to HAP treatment. General growth conditions and media formulations for MCF-7, T47D, MDAMB-231, MDAMB-468 and MDAMB-436 cells have been described in chapter 2 (Appendix A-Table A1 and Table A2). The normal mammary epithelial cell line, MCF-10A, was included to assess potential therapeutic differences between cancer and 'normal' cells. Experiments with MCF-10A were carried out by an Erasmus placement student, Martina Quartieri under my supervision. The molecular characteristics and cell culture media formulation for MCF-10A cells is shown in Appendix B-Table B1 and Table B2 respectively. Due to lack of KP167 supply from collaborator, who experienced problems during synthesis, experiments in MCF-10A were only conducted for the comparator drug AQ4N, and therefore all results for this cell line is presented in Appendix B.

3.3.2 Drugs and drug preparation

The novel drug, KP167 was synthesised and supplied by Dr Klaus Pors based at the Institute of Cancer Therapeutics, University of Bradford, UK. AQ4N (Sigma) was used as a drug comparator against its analogue, KP167. AQ4N and KP167 were reconstituted in distilled water to a stock concentration of 10 mM. All stock solutions were aliquoted and stored at -20°C for a maximum of 3 months, and repeated freeze thaw cycles were avoided. Stock concentrations were added to complete media to achieve the desired concentrations for use in experiments. A new batch of drugs received was always tested for similar response between new and old to ensure consistency and to minimise batch-batch variability.

3.3.3 3D spheroid formation, optimisation and culture

Spheroids >200 µm have regions of hypoxia and therefore this model served as an ideal platform to study the effects of hypoxia-activated prodrugs (Hirschhaeuser et al., 2010). To culture spheroids, sub-confluent breast cancer cells were trypsinized, counted using haemocytometer and seeded in 96-well ultra-low attachment round-bottomed plates (Corning), at different seeding densities (5000, 10,000 and 20,000 cells/well) in 100 µl of culture media. To assist spheroid formation in MDAMB-231 and MDAMB-468 cells, culture media was supplemented with matrigel (BD) at a concentration of 5 µl/well. The plates were centrifuged at 2000 r.p.m for 10 minutes to aggregate cells into a single spheroid structure and incubated at 37°C, 5% CO_2. The following day, 100 µl of fresh culture media was added, and spent media was replaced every 48 hours. Spheroid growth was monitored over a period of 8 days and images of the 6 replicate spheroids for each cell seeding density was captured using an inverted phase contrast microscope (Leica) with a 10x objective. The haemocytometer was used as a reference to determine the scale of images. Spheroid area (S) was calculated using ImageJ software. The measured area (S) of the 2D projection of spheroids was used to calculate the diameter ($D = 2\sqrt{S/\pi}$) (McIntyre et al., 2012, Voissiere et al., 2017). Data presented graphically represent the average diameter calculated from measurements of 6 spheroids in one experiment.

3.3.4 Plating efficiencies - 2D v 3D

In order to compare PEs of breast cancer cells grown in 2D v 3D cultures, spheroids from the above experiments were pooled on day 7 and centrifuged at 1000 r.p.m for 5 minutes. The supernatant was discarded and spheroids were washed twice with PBS, followed by incubation with 500 µl trypsin-EDTA for 5 min at 37°C. Spheroids were dissociated with the help of a pipette into single-cell suspensions. Following dissociation into single cells, complete media was added to inactivate tryspin-EDTA. Cells were counted using a haemocytometer and serially diluted with complete medium to appropriate concentrations and plated into T-25cm^2 tissue culture flasks for conventional 2D clonogenic assay as described in section

2.3.6. At the same time, parallel experiments were also carried out with 2D grown cells (section 2.3.6) to compare PE between 2D and 3D culture conditions. PE was calculated as described in section 2.3.6. Data represent the mean ± SD of three independent experiments, with each experiment containing six parallel sets.

3.3.5 Drug penetration experiments

Before conducting drug exposure experiments in spheroid models, it was important to ensure that drugs could penetrate across all layers of the spheroid structure. Therefore, to assess drug penetration, MCF-7 and MDAMB-231 spheroids on day 3 (>500 µm) were treated with 5 µM of AQ4N and KP167 for 8, 24 and 48 hours. AQ4N and KP167 are fluorescent drugs due to the presence of the anthraquinone chromophore which can be detected both *in vitro* and *in vivo* (Feng et al., 2017, Williams et al., 2009). For all breast spheroids, drug penetration was also assessed by treatment with 10 µM doxorubicin (representative fluorescent drug comparator) for 24 hours. Breast cancer spheroids treated with DMSO were used as a negative control. Following treatment with AQ4N/KP167/DOX, spheroids were washed twice with PBS and fixed in 4% PFA for 10 minutes. Following which, spheroids were washed twice, and fixation was stopped by adding 100 mM glycine for 10 minutes. Following wash, spheroids were resuspended in ice-cold methanol and pipetted onto slides, allowed to air dry and mounted in ProLongTM antifade mounting medium (Invitrogen). Images to investigate drug penetration at 10x magnification was obtained by performing Z stack by laser scanning confocal microscopy (Leica TCS SPE), which records images at different focal planes, allowing visualization of the entire sample. AQ4N and KP167 was visualised between 650–800 nm (λ excitation-647 nm) (Patterson and McKeown, 2000) and doxorubicin was visualised at 550nm (λ excitation-468 nm). A total of 15 images were generated across the whole spheroid at step size of 15 µm, across difference focal planes, examining the top, middle and bottom for fluorescence intensity. Negative controls with DMSO did not give any detectable signals. Data represent two independent experiments, with each containing 30 spheroids.

3.3.6 Clonogenic survival assays - 3D

The single-agent anti-cancer effect of AQ4N and KP167 was assessed by clonogenic assays using breast cancer spheroids. 6 replicate spheroids per treatment were produced and allowed to grow before being treated on day 3 with various concentrations of AQ4N (0.1-50) μM or KP167 (0.01-45) μM for 96 hours. Based on initial optimization experiments (given in Appendix B-Figure B3) and those reported in the literature (McKeown et al., 1996), a treatment time of 96 hours was chosen for all experiments. Drug-media was refreshed at the 48 hour time-point. Following drug treatment, spheroids from the same treatment were collected and disaggregated by tryspin/EDTA into single cell suspensions as described in section 3.3.4. Following dissociation, culture media was added to neutralise trypsin-EDTA. Cells were counted using a haemocytometer and plated into T-25cm^2 tissue culture flasks for conventional 2D clonogenic assay (section 2.3.6). Cells were incubated for 14 (MCF-7, MDAMB-231, MDAMB-468 and MCF-10A) or 21 days (T47D and MDAMB-436) at 37°C, 5% CO_2 to allow colony formation. PE and SF were calculated as described in section 2.3.6. The dose response curves were constructed by plotting SFs versus drug concentration (μM) on y- and x-axis respectively and the IC_{50} dose was calculated using GraphPad Prism 7 software. Data represent the mean SF ± SD of three independent experiments, with each experiment containing six parallel sets.

3.3.7 Proliferation and clonogenic survival assays - 2D

Previous studies report that cells exhibit minimal or no toxicity to AQ4N in the presence of oxygen (Patterson and McKeown, 2000, McKeown et al., 2007). Therefore in order to assess the single-agent effect of AQ4N or KP167 on breast cancer cells grown in 2D normoxia, proliferation and clonogenic assays were conducted.

3.3.7.1 Proliferation assay in 2D normoxia

To assess the anti-proliferative effect of AQ4N and KP167 on breast cancer cells, 1x10^6 cells/well were seeded in triplicate in 6-well culture plates and incubated at 37°C, 5% CO_2 to allow cell adherence. The following day, cells

were treated with various concentrations of AQ4N or KP167 (5, 15, 25, 35, 45) μM for 24, 48 and 72 hours. Following drug treatment, cells in each well were harvested and counted using a haemocytometer. Cells were also collected and seeded into fresh flasks for determination of clonogenic survival (section 3.3.7.2). Cell counts obtained after treatment were normalised as percentage of untreated control cells at each time-point. The dose-response curves were constructed by plotting average percentage of cells versus drug concentration (μM) on y- and x-axis respectively. The IC_{50} doses were calculated using GraphPad Prism 7 software. Data presented graphically represent the average percentage of cells ± standard deviation (SD) of three independent experiments.

3.3.7.2 Clonogenic survival assay in 2D normoxia

The effect of AQ4N and KP167 on survival of breast cancer cells were assessed by clonogenic survival assay. 1×10^5 cells treated with various concentrations of AQ4N or KP167 (5, 15, 25, 35, 45) μM for 24, 48 and 72 hours were collected from proliferation assay as described in section 3.3.7.1. Cells were counted using a haemocytometer, serially diluted with complete media and plated into fresh T-25cm^2 tissue culture flasks for assessment of clonogenic survival as described in section 2.3.6. The SF was calculated as described in section 2.3.6 and the IC_{50} doses were calculated using GraphPad Prism 7 software. Data represent the mean SF ± SD of three independent experiments, with each experiment containing six parallel sets.

3.3.8 Cell lysis and protein extraction

The expression of endogenous reductases (cytochrome P450, CYP2S1, CYP2W1, NQO1 and NQO2) involved in bioreducing HAPs were assessed by Western blotting of breast cancer cell lysates obtained from normoxic (21% O_2) and hypoxic (1% O_2) cultured cells. Sub-confluent cells, grown in 2D normoxia and 2D hypoxia (Cells were made hypoxic at 1% O_2 for 48 hours; methodology described in detail in chapter 4 section 4.3.3) were harvested and pelleted by centrifugation at 1000 r.p.m for 5 minutes. Following wash with PBS, 5x10^6-10^7 cells were resuspended in 1 ml of RIPA

Buffer (Sigma), supplemented with 1 X phosphatase inhibitor cocktail, protease inhibitor cocktail and EDTA (ThermoFisher Scientific). Microcentrifuge tubes containing cell lysates were incubated on ice for 15 minutes and centrifuged at 13000 r.p.m for 15 minutes at 4°C. The supernatant (total protein) was collected and transferred to a fresh tube and stored at -20°C for short-term or -80°C for long-term storage. Thawed lysates were kept on ice before use and repeated freeze-thaw cycles were avoided.

3.3.9 Western blotting

13 µl of cell lysate (section 3.3.8) was mixed with 5µl of Bolt™ LDS Sample Buffer (ThermoFisher), and 2µl Bolt™ Sample Reducing Agent (ThermoFisher). The lysate was boiled at 100°C for 5 minutes on a heat block and centrifuged at 10000 x g for 2 minutes and placed on ice until loading. Buffers were prepared as described in Table 3.1.

Table 3.1 Buffers for Western blot.

Buffer	Preparation
Running	50ml Bolt™ MES Running Buffer (20X) to 950ml distilled H_2O
Transfer	25ml Bolt™ Transfer Buffer (20X), 50ml methanol to a total volume of 500ml distilled H_2O.
Blocking	2.5g milk powder (Marvel Original dried skimmed milk powder) dissolved in 50ml 0.1% PBS/Tween.

Abbreviations: SDS, sodium dodecyl sulfate; PBS, phosphate buffered saline.

A precast polyacrylamide Bolt™ 4-12% Bis-Tris Plus gel was used. The gel was loaded into Bolt™ mini gel tank (ThermoFisher), filled with 1X Bolt™ MES SDS Running Buffer (20X) according to the manufacturer's instructions. 20 µl of prepared sample was loaded per well along with 3µL of a standard pre-stained molecular weight protein marker (MagicMark™ XP, Novex life Technology) and 5µl of See Blue™ Plus2 Pre-Stained Standard (GE Healthcare). SDS-PAGE was run at 200V for 25 minutes.

Following separation by SDS-PAGE, the separated proteins were electroblotted onto a nitrocellulose membrane (Whatman GE Healthcare) using Bolt™ transfer buffer at 10V for 90 minutes. Membranes were blocked for one hour in 0.05% PBS/Tween containing 5% non-fat milk and probed with a primary antibody at 4°C overnight. Membranes probed with the primary antibody for β-actin, were used as a loading control. The antibodies used in this study, are listed in Table 3.2.

Table 3.2 List of antibodies used in Western blot.

Antibodies	Host species	Dilution	Molecular Weight (kDA)	Catalogue Number	Source
Anti-P450	Rabbit	1:2000	77	ab180597	Abcam
Anti-CYP2S1	Rabbit	1:500	55	ab69650	Abcam
Anti-CYP2W1	Rabbit	1:50	54	ab76666	Abcam
Anti-NQO1	Mouse	1:500	29	3187	Cell signalling
Anti-NQO2	Rabbit	1:250	26	ab137612	Abcam
Anti-β-actin	Mouse	1:1000	42	ab8226	Abcam
Anti-β-actin	Rabbit	1:2000	42	ab8227	Abcam
Donkey anti-mouse	Donkey	1:10000	-	926-68072	Li-COR IRDye
Donkey anti-rabbit	Donkey	1:10000	-	926-32213	Li-COR IRDye

After incubation, membranes were washed for 3 x 5 minutes in 0.1% PBS/Tween. Membranes were probed with appropriate secondary antibodies and incubated for 1 hour at room temperature. After incubation, membranes were washed for 3 x 5 minutes in 0.1% PBS/Tween. Following which, blots were scanned using an Odyssey® FC Imager (LI-COR Biosciences). The bands were quantified using Image Studio Version 4.1 (LI-COR Biosciences) and normalised against the signals of β-actin, which was used as an internal loading control. Data presented graphically represent the mean of normalised protein expression to β-actin ± SD of three independent experiments, with separate cell lysates from different passage numbers of cells.

3.3.10 Cell irradiation - 2D v 3D

Initially, the intrinsic radiosensitivity of breast cancer cells when grown as 3D spheroids v 2D normoxia cultures were assessed in order to investigate the difference in radiosensitivity between the two culture conditions. To assess radioresponse in 3D cultures, spheroids were irradiated at a single dose of 2, 4, 6, or 8 Gy. Cells with sham irradiation were set as 0 Gy. Immediately following irradiation, cells were disaggregated from their spheroid structure (section 3.3.4) and plated for assessment of clonogenicity using the conventional clonogenic survival assay as described in section 2.3.6. Parallel experiments were also carried out with 2D normoxic cells (section 2.3.7) to compare the intrinsic radiosensitivity between 2D and 3D cultures. SF of radiotherapy experiments were calculated as described in section 2.3.8. Data represent the mean SF ± SD of three independent experiments, with each experiment containing six parallel sets.

3.3.11 Drug-radiation combinations - 3D and 2D

3.3.11.1 Drug-radiation combinations in 3D spheroids

To assess the effects of AQ4N and KP167 on radiosensitivity of cells in 3D, spheroids (>500 µm) were treated on day 3 with the clonogenic IC_{50} of AQ4N or KP167 for 96 hours. Drug-media was refreshed at 48 hours. Following treatment, spheroids were irradiated with a single dose of 2, 4, 6, or 8 Gy (cells with sham irradiation were set as 0 Gy). Following irradiation, cells were disaggregated and seeded for clonogenic survival. Data was processed as described in section 2.3.8. Data represent the mean SF ± SD of three independent experiments, with each experiment containing six parallel sets.

3.3.11.2 Drug-radiation combinations in 2D cultures

In order to assess if the 3D IC_{50} doses of AQ4N and KP167 were able to radiosensitise breast cancer cells in 2D normoxia, $3x10^5$ cells/ml were seeded in T-25cm^2 tissue culture flasks and allowed to attach for 24 hours. The following day, cells were treated with the 3D clonogenic IC_{50} of AQ4N

and KP167 for 96 hours. Drug-media was refreshed at 48 hour time-point. Cells were irradiated at single doses of 2, 4, 6 or 8 Gy. After irradiation, cells were plated for clonogenic survival and data processed as described previously (section 2.3.8). Data represent the mean SF ± SD of three independent experiments, with each experiment containing six parallel sets.

3.3.12 Statistical analysis

Statistical analyses were conducted using GraphPad Prism 7 software. Data were represented as mean ± SD of three independent experiments with each performed in triplicate. For comparing two variables, the Student's *t*-test was used. *P* values < 0.05 were considered as having reached statistical significance. Errors from individual experiments were calculated as described in section 2.3.10.

3.4 Results

3.4.1 3D spheroid culture

3.4.1.1 Spheroid growth assay

To culture spheroids, breast cancer cells were seeded at various densities and aggregated by centrifugation to form cells into a single 3D spheroid structure. Initially all cell lines were grown as spheroids without any additional supplements. MCF-7, T47D and MDAMB-436 cells formed spheroids, whereas MDAMB-231 and, particularly, MDAMB-468 cells were unable to form spheroid structures. Matrigel was added to the media of these two cell lines to aid spheroid formation with Figure 3.5 showing the representative growth patterns (no matrigel for MCF-7, T47D and MDAMB-436 cells; matrigel supplementation for MDAMB-231 and MDAMB-468 cells). The average spheroid diameter in the three groups over an 8-day culture is shown in Figure 3.6.

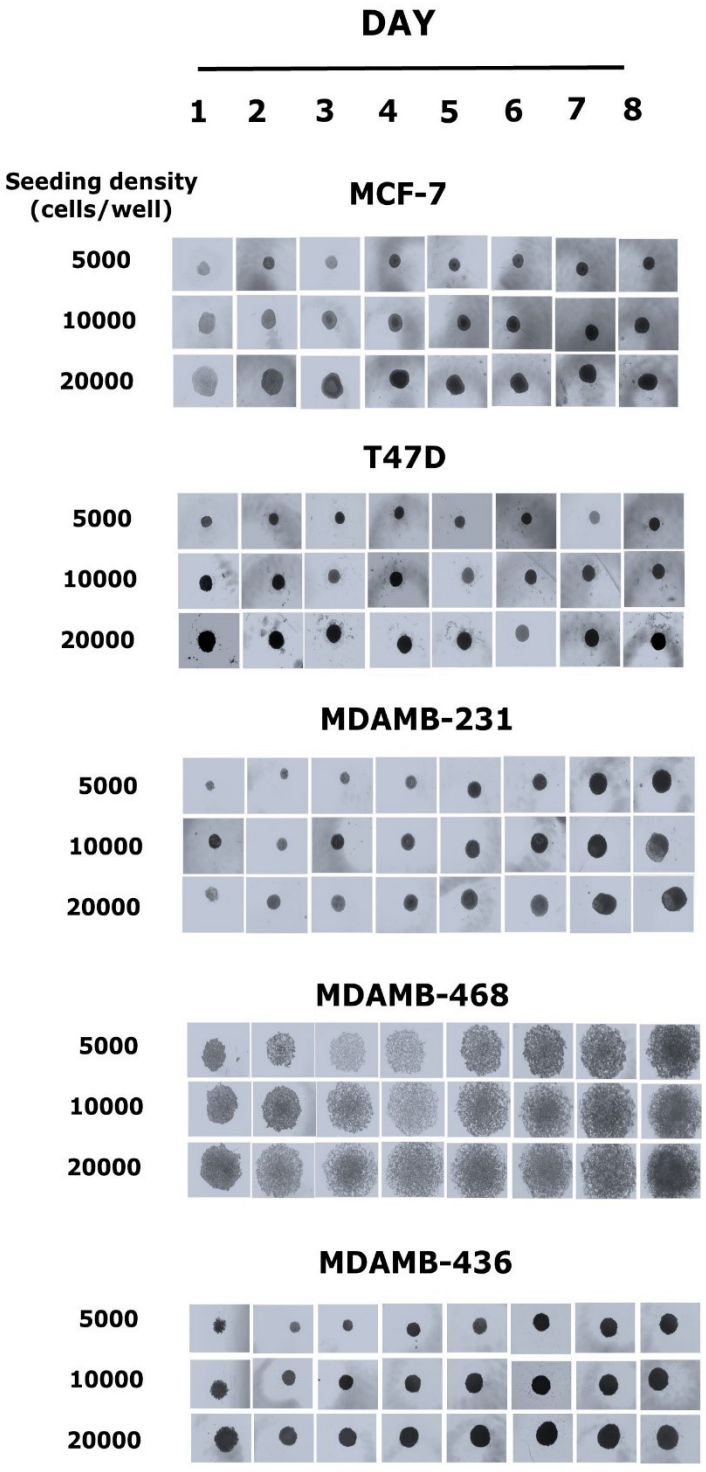


Figure 3.5 Morphology of MCF-7, T47D, MDAMB-231, MDAMB-468 and MDAMB-436 spheroids. Representative phase contrast micrographs of breast cancer spheroids from Day 1 to 8 with seeding density of 5000, 10,000 and 20,000 cells/well in 96-well ultra-low attachment plates (10x magnification). Images represent spheroids from one experiment.

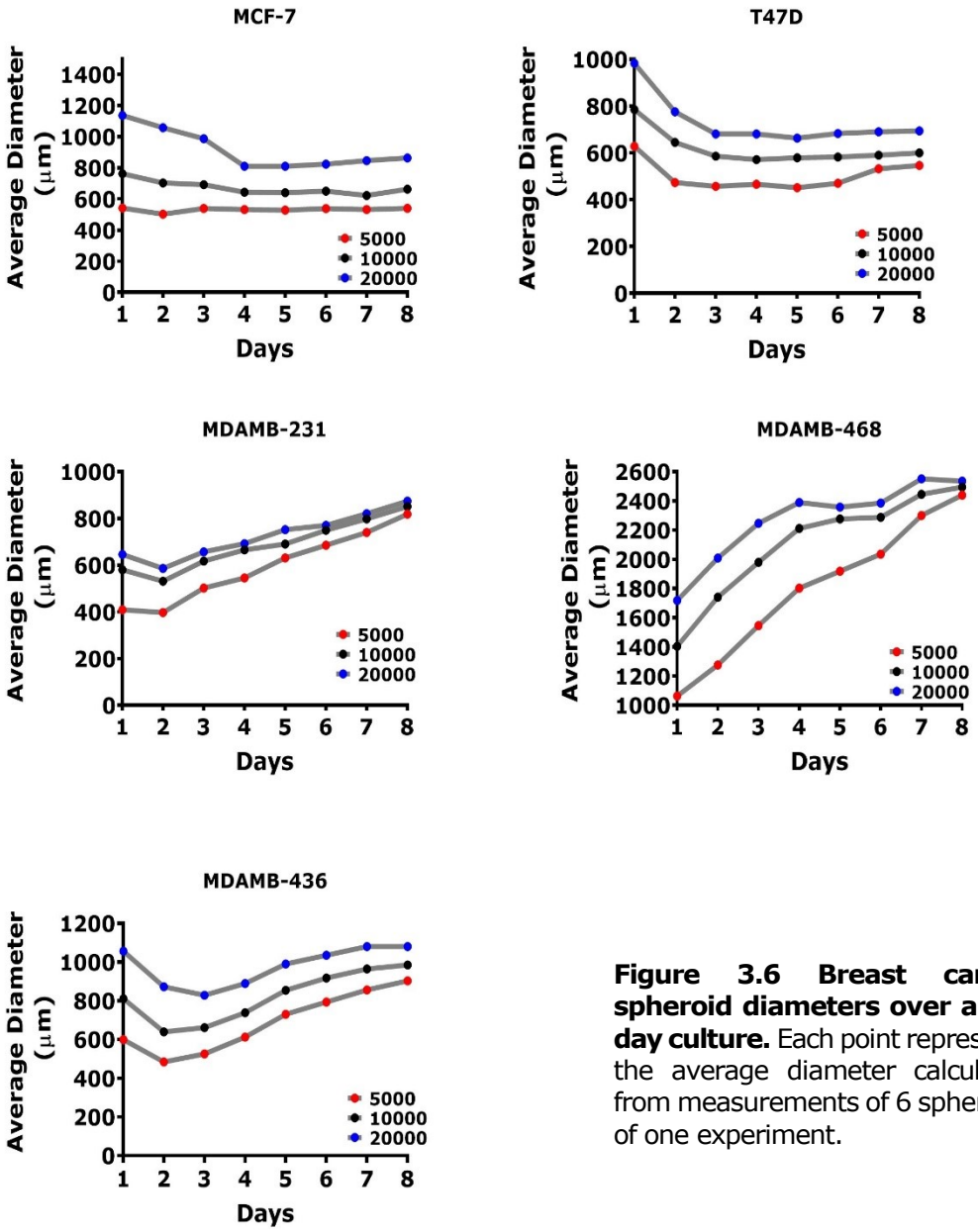


Figure 3.6 Breast cancer spheroid diameters over an 8-day culture. Each point represents the average diameter calculated from measurements of 6 spheroids of one experiment.

Even with matrigel supplementation, the spheroids formed by MDAMB-231 and MDAMB-468 cells were loosely aggregated compared to tight and compact structures formed in MCF-7, T47D and MDAMB-436 cells. Compared to the triple negative cells, growth in luminal breast cancer spheroids remained constant and showed only marginal increase in spheroid diameter over a period of 8 days.

As seen in Figure 3.6, the average spheroid diameters on day 3, with a cell seeding density of 10,000 cells/well was 692 μm in MCF-7, 586 μm in T47D, 671 μm in MDAMB-231, 1979 μm in MDAMB-468 and 985 μm in

MDAMB-436 cells. On day 8 (10,000 cells/well), MFC-7 and T47D cells did not demonstrate any change in size with average diameters of 663 and 600 µm respectively. Exponential increases of spheroid size was observed in the triple negative lines with average spheroid diameters of 851 µm in MDAMB-231, 2494 µm in MDAMB-468 and 985 µm in MDAMB-436 cells.

These results perhaps suggest that luminal cell lines are more sensitive to growth in a 3D environment compared to the TNBC cell lines. However, results must be interpreted with caution as the cell number per spheroid was not assessed, and it is possible that the cell number may have increased without any change in spheroid diameter. As all spheroids formed diameters of >500 µm on day 3, a cell seeding density of 10,000/well was chosen for all subsequent experiments. Spheroids were allowed to grow and form compact structures for 48 hours before initiating drug treatments on day 3 of spheroid formation.

The normal mammary epithelial cell line, MCF-10A formed small and compact spheroids (day 3 - 412 µm), with a slight decrease in spheroid size noted over a period of 8 days (395 µm). Similar to luminal cells, the MCF-10A cells appeared to be sensitive to growth in a 3D environment. MCF-10A spheroid growth data is shown in Appendix B-Figure B1.

3.4.1.2 Plating efficiency of spheroids

The PEs of breast cancer cells grown in 2D normoxia were assessed in chapter 2 and corroborated to previously published data in the literature. To identify if growth in a 3D environment affected the PE of breast cancer cells, a total of 6 spheroids on day 7 were collected from the above experiment, then disaggregated by trypsinization and plated to allow colony formation. Parallel experiments were also carried out on cells grown in 2D normoxia to compare PE obtained between the two culture methods. The PEs obtained for 2D and 3D cultures are plotted against the respective cell lines and presented in Figure 3.7.

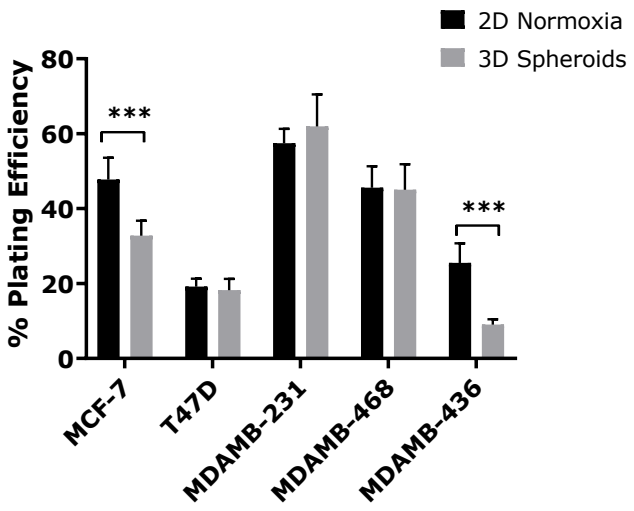


Figure 3.7 Plating efficiencies of cells grown in 2D normoxia v 3D spheroid culture. Data represent the mean ± SD of three independent experiments, with each experiment containing six parallel data sets. ***P<0.001 2D v 3D (student's t-test).

Significant reductions in the PE of MCF-7 (P=0.0004) and MDAMB-436 (P<0.0001) cells were observed in 3D as opposed to 2D cultures. There was no significant difference in the PE of T47D (P=0.55), MDAMB-231 (P=0.26) or MDAMB-468 (P=0.88) cells. In 2D v 3D, MCF-7 had PE's of 47±5.83 and 32±4.02; T47D with 19±2.12% and 18±3.01; MDAMB-231 with 57±3.86% and 61±8.53%; MDAMB-468 with 45%±5.74% and 45±6.80%; MDAMB-436 with 25%±5.74% and 9±1.48% and MCF-10A cells with 23±0.28% and 34±2.30% respectively.

3.4.1.3 Drug penetration experiments in 3D spheroids

To assess if drugs pentrated equally and fully throughout spheroids, a total of 30 representative MCF-7 and MDAMB-231 spheroids were treated with 5 μM of AQ4N or KP167. The distribution of the HAPs were qualitatively visualized for fluorescence using a laser scanning confocal microscope. Figure 3.8 show drug penetration in MCF-7 and MDAMB-231 spheroids at 8, 24 and 48 hours.

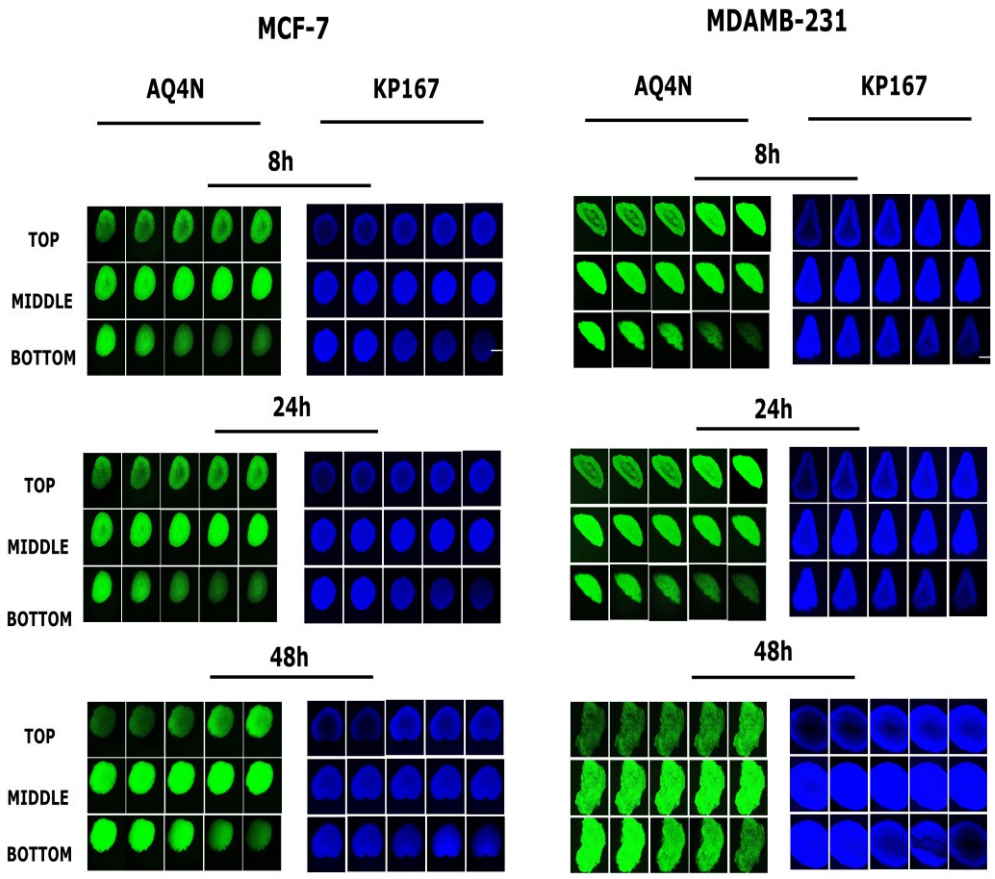


Figure 3.8 Visualisation of AQ4N and KP167 penetration in MCF-7 and MDAMB-231 spheroids. Representative images of spheroid cross-sections obtained using confocal microscope (10x magnification, step size 15 µm) are shown above. Experiments were repeated twice, with each containing 30 spheroids. Scale bar represents 200 µm.

A total of 15 images/treatment were taken across each whole spheroid at step sizes of 15 µm, across different focal planes, examining the top, middle and bottom for fluorescence intensity. As shown in Figure 3.8, fluorescent Z-stack imaging of spheroid cross-sections show that AQ4N and KP167 were able to penetrate across all layers of spheroid structure at 8, 24, and 48 hours, regardless of size or matrigel inclusion. Even at the shortest treatment time of 8 hours, AQ4N and KP167 penetrated across all layers of the spheroid structure in both the tightly formed MCF-7 and loosely aggregated MDAMB-231 spheroids.

Such data suggest that drug penetration should not, therefore, be a factor that might affect efficacy of AQ4N and KP167, and that any observed effects were not due to differences in drug penetration across different

spheroid cultures. All breast cancer spheroids were also treated with the representative fluorescent drug doxorubicin to assess drug penetration, images of which are given in Appendix B-Figure B2.

3.4.2 Cytotoxicity of AQ4N and KP167 - 3D

The potency of both AQ4N and KP167 were initially tested in a 3D spheroid culture system, as spheroids (>500 μm) contain regions of hypoxia (Leek et al., 2016, Riffle and Hegde, 2017), which would ensure that the HAPs were efficiently bioreduced by the cytochrome P450 family of enzymes into their respective cytotoxic metabolites (Raleigh et al., 1998, Nishida et al., 2010). Treatment times of 96 hours were chosen based on optimisation experiments (Appendix B-Figure B3) conducted in HT-29 spheroids. Clonogenic assays in these cells demonstrated that treatment time of 48 hours resulted in only ~10-20% reduction in survival, with SF of 94% (AQ4N) and 81% (KP167). However, when treatment time was increased to 96 hours, a greater reduction in cell survival was obtained with SF of 54% (AQ4N) and 46% (KP167). These findings were further supported by previous studies which report that administering AQ4N for 4 days prior to irradiation maximises its efficacy (McKeown et al., 1995). Therefore, based on data obtained with HT-29 cells and those reported in literature, all breast cancer spheroids were treated with AQ4N and KP167 for 96 hours in all subsequent experiments.

Figure 3.9 shows the surviving fraction of cells obtained against the corresponding concentrations of AQ4N (0.1-50) μM and KP167 (0.1-45) μM. The x-axis (drug concentration) varies between cell lines due to the differential response of cells to drug treatment, with sensitive cell lines requiring lower doses to achieve IC_{50} concentrations. AQ4N and KP167 treatment was cytotoxic in all breast cancer spheroids and resulted in a dose dependent reduction in clonogenic survival.

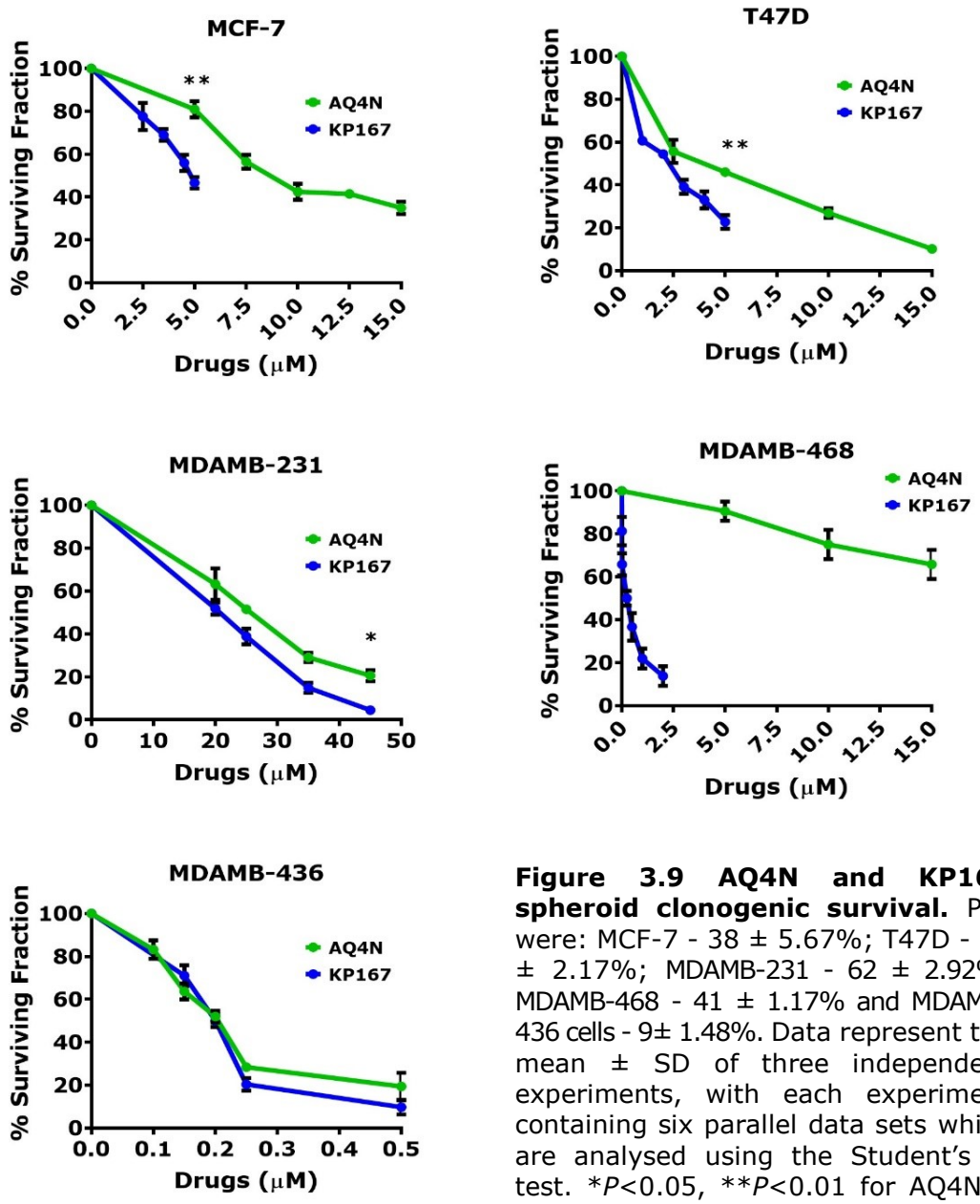


Figure 3.9 AQ4N and KP167 spheroid clonogenic survival. PEs were: MCF-7 - 38 ± 5.67%; T47D - 29 ± 2.17%; MDAMB-231 - 62 ± 2.92%; MDAMB-468 - 41 ± 1.17% and MDAMB-436 cells - 9± 1.48%. Data represent the mean ± SD of three independent experiments, with each experiment containing six parallel data sets which are analysed using the Student's *t*-test. **P*<0.05, ***P*<0.01 for AQ4N v KP167.

.

Table 3.3 shows the IC_{50} values of AQ4N (0.2-22.8) μM and KP167 (0.14-12.8) μM. Compared to AQ4N, clonogenic survival was significantly reduced with 5 μM KP167 treatment in MCF-7 (P=0.004), T47D (P=0.007) and with 45 μM in MDAMB-231 (P=0.033) cells.

Table 3.3 Clonogenic IC_{50} values of AQ4N and KP167 in breast cancer spheroids.

Cell line	AQ4N (μM)	KP167 (μM)
MCF-7	8.5±2.9	6.1±0.4
T47D	4.4±0.5	1.9±0.6
MDAMB-231	21.1±4.9	12.8±1.3
MDAMB-468	22.8±1.1	0.2±0.01
MDAMB-436	0.2±0.01	0.14±0.01
MCF-10A	8.8±2.6	-

The IC_{50} values were calculated using Graphpad prism software. Abbreviations: μM - micromolar; - not available.

As can be seen, KP167 IC_{50} values were ~1-2 fold lower than the parental drug AQ4N in all cell lines, with the MDAMB-468 cells showing a 100-fold greater potency of KP167 than AQ4N. This increase in the single-agent cytotoxic effect of KP167 may be due to its ability to bind DNA covalently and kill both proliferating and quiescent tumour cells by DNA alkylation and TOPO II inhibition, as opposed to AQ4N which functions only as a TOPO II inhibitor in proliferating cells (Patterson and McKeown, 2000). The normal-like MCF-10A cells were included in the current study to assess for potential difference in the response of cancer v normal cells to HAP treatment. Similar response to the luminal MCF-7 cells were observed in MCF-10A cells which also demonstrated a dose dependent reduction in clonogenic survival with AQ4N IC_{50} of 8.8±2.6 μM. The cytotoxicity observed in the normal cell line, may be because of the presence of hypoxia in spheroid cultures, which may not be seen *in vivo*, as hypoxia is a characteristic only of solid tumours (Semenza, 2010). Data for MCF-10A is only available for AQ4N and therefore graph is presented in Appendix B-Figure B4.

Data suggest that both AQ4N and KP167 may undergo hypoxia-selective activation which results in its ability to exert cytotoxic effect in breast cancer spheroids – to determine the validity of this, and the importance of hypoxic activation, cytotoxicity was also assessed in 2D normoxic conditions (next section). The current data show that KP167 was more effective than the parental compound, AQ4N.

3.4.3 Cytotoxicity of AQ4N and KP167 on proliferation - 2D

3.4.3.1 Assessment of AQ4N on cell proliferation

The effect of AQ4N on proliferation of breast cancer cells in 2D normoxia was assessed by treating cells with varying concentrations (5-45) μM of AQ4N for a period of 24, 48 or 72 hours. The anti-proliferative effect was assessed by plotting average percentage of cells (y-axis) versus drug concentration (x-axis) as shown in Figure 3.10. Untreated cells were used as controls in the current study.

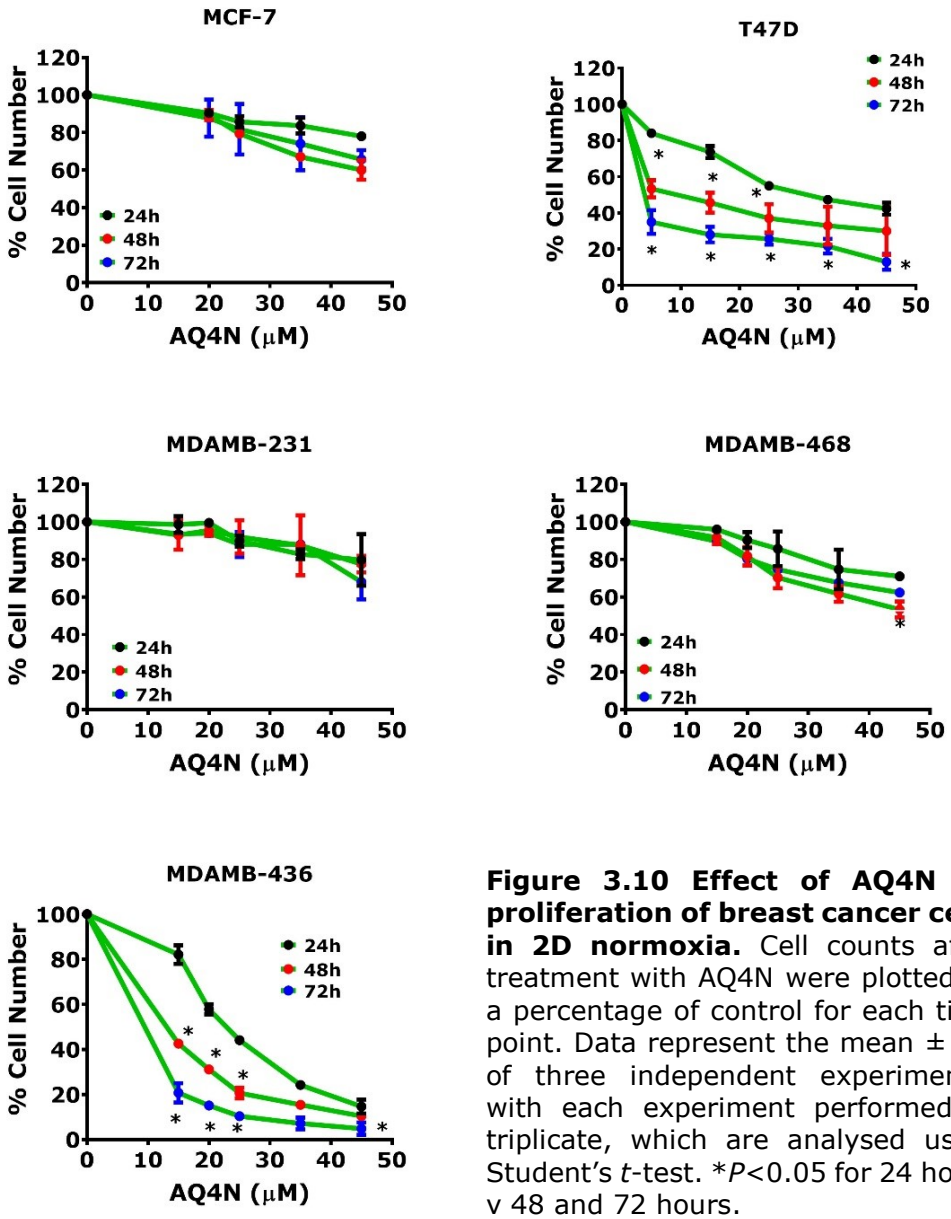


Figure 3.10 Effect of AQ4N on proliferation of breast cancer cells in 2D normoxia. Cell counts after treatment with AQ4N were plotted as a percentage of control for each time point. Data represent the mean ± SD of three independent experiments, with each experiment performed in triplicate, which are analysed using Student's *t*-test. **P*<0.05 for 24 hours v 48 and 72 hours.

The range of concentrations used were higher than those tested in spheroid cultures as it was considered that the presence of oxygen might lower the potency of the HAPs (Nishida et al., 2010, Manley and Waxman, 2013). As shown in Figure 3.10, treatment with the highest concentration of AQ4N (45 μM) decreased cell proliferation by 30-40% in MCF-7, 60-80% in T47D, 20-30% in MDAMB-231, 30-50% in MDAMB-468 and 85-90% in MDAMB-436 cells. The IC_{50} doses for proliferation were not achieved in the concentrations tested for MCF-7, MDAMB-231 and MDAMB-468 cells. Compared to 24 hours, cell proliferation was significantly reduced with AQ4N treatment at 48 and 72 hours in T47D (P=0.0003 and P=0.0002) and MDAMB-436 (P=0.014 and P=0.0003) cells respectively. T47D cells showed IC_{50} values of 34.6±10.1 μM (P=0.001) (24 hours), 13.2±5.9 μM (P<0.0001) (48 hours), and <5 μM (P=0.0001) (72 hours), and MDAMB-436 cells with IC_{50} values of 10.5±7.6 μM (P=0.001) (24 hours), 5.0±1.5 μM (P=0.0001) (48 hours) and <5 μM (P=0.002) (72 hours).

The above data indicate that at high concentrations, breast cancer cells treated with AQ4N demonstrate a dose dependent reduction in cellular proliferation, with varying levels of sensitivity observed between the different phenotypes of breast cancer. The luminal cell line, T47D and BRCA-1 deficient MDAMB-436 cells were more sensitive to treatment with AQ4N. AQ4N treatment was also cytotoxic to the normal MCF-10A cells which showed reduced proliferation with IC_{50} values of 34.1±6.5 μM (P<0.0001) (24 hours), 15.8±5.8 μM (P=0.0002) (48 hours), and 9.4±4.6 μM (P=0.0002) (72 hours). Dose response data for MCF-10A is given in Appendix B-Figure B5.

3.4.3.2 Assessment of KP167 on cell proliferation

The effect of the novel agent, KP167 on cell proliferation was assessed by treatment with varying concentrations (5-45) μM of KP167 for 24, 48 or 72 hours. Cell counts obtained after treatment with KP167 were plotted as a percentage of control for each time point and is presented in Figure 3.11.

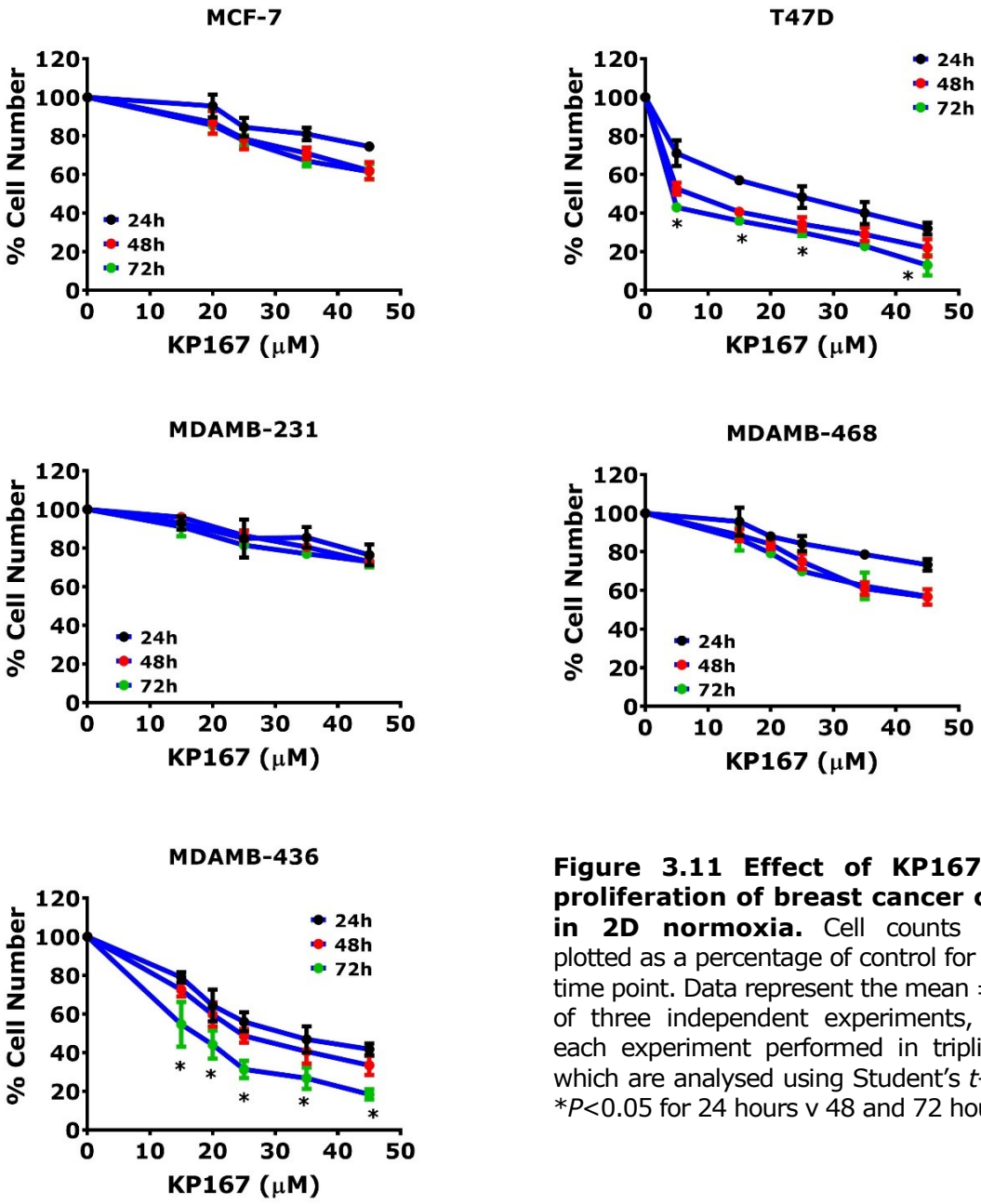


Figure 3.11 Effect of KP167 on proliferation of breast cancer cells in 2D normoxia. Cell counts were plotted as a percentage of control for each time point. Data represent the mean ± SD of three independent experiments, with each experiment performed in triplicate, which are analysed using Student's *t*-test. **P*<0.05 for 24 hours v 48 and 72 hours.

KP167 treatment reduced proliferation by 25-40% in MCF-7 and 70-90% in T47D cells compared to 15-20% in MDAMB-231, 30-45% in MDAMB-468 and 60-80% in MDAMB-436 cells at 45 μM. The IC_{50} doses for proliferation were not achieved in the concentrations tested for MCF-7, MDAMB-231 and MDAMB-468 cells. T47D cells showed IC_{50} values of 21.2±7.7 μM (*P*=0.001) (24 hours), 11.4±8.8 μM (*P*=0.001) (48 hours), and 9.7±0.9 μM (*P*=0.0002) (72 hours) and MDAMB-436 cells showed IC_{50} values of 30±6.6 μM (*P*=0.0002) (24 hours), 21.9±2.5 μM (*P*<0.0001) (48 hours)

and 10±2.9 μM (P=0.0002) (72 hours). Significant reductions in proliferation were observed in T47D (P<0.05) and MDAMB-436 cells (P<0.05) at 72 hours compared to 24 hour treatment.

The above results suggest that, as with AQ4N, KP167 treatment results in decreased proliferation of breast cancer cells even in the presence of oxygen, albeit at high drug concentrations. The luminal T47D cells and the BRCA-1 deficient MDAMB-436 cells were the most sensitive, MCF-7 and MDAMB-468 cells were moderately sensitive and MDAMB-231 cells were the most resistant to treatment with KP167 in 2D normoxic cultures. Tabulated IC_{50} doses for both AQ4N and KP167 are presented below in Table 3.4.

Table 3.4 Proliferation IC_{50} values of AQ4N and KP167 in 2D normoxia.

Cell line	AQ4N (μM)			KP167 (μM)		
	24h	48h	72h	24h	48h	72h
MCF-7	>45	>45	>45	>45	>45	>45
T47D	34.6±10.1	13.2±5.9	<5	21.2±7.7	11.4±8.8	9.7±0.9
MDAMB-231	>45	>45	>45	>45	>45	>45
MDAMB-468	>45	>45	>45	>45	>45	>45
MDAMB-436	10.5±7.6	5.0±1.5	<5	30±6.6	21.9±2.5	10±2.9
MCF-10A	34.1±6.5	15.8±5.8	9.4±4.6	-	-	-

The IC_{50} values were calculated using Graphpad prism software. Abbreviations: μM - micromolar; - not available.

As shown in the above table, breast cancer cell lines demonstrated similar response to both AQ4N and KP167 in 2D normoxia cultures. The IC_{50} doses for proliferation were not achieved in MCF-7, MDAMB-231 or MDAMB-468 cells, within the concentrations (5-45 μM) tested. Both AQ4N and KP167 were found to reduce proliferation in the luminal T47D and BRCA-1 deficient MDAMB-436 cells. AQ4N reduced proliferation in the MCF-10A cell lines which demonstrated similar response to T47D cells. Greatest

reduction in proliferation was observed in the luminal T47D, BRCA-1 deficient MDAMB-436 and the normal MCF-10A cells.

3.4.4 Cytotoxicity of AQ4N and KP167 on survival - 2D

3.4.4.1 Assessment of AQ4N on clonogenic survival

AQ4N (5-45) μM treated cells from the above described proliferation assay were seeded for clonogenic assays in order to assess the effects of AQ4N on long-term cell survival. The SFs obtained after treatment were plotted against the dose and is presented in Figure 3.12.

Similar trends to that observed with the AQ4N proliferation assay were noticed in clonogenic survival, although the concentrations required to achieve 50% cell killing were lower in clonogenic assays. Treatment with 45 μM AQ4N reduced clonogenic survival by 60% in MCF-7 and 90% in T47D cells compared to 30% in MDAMB-231 and 45-55% in MDAMB-468 cells. AQ4N treatment was highly toxic in the MDAMB-436 cells which demonstrated total cell kill, even at the lowest doses used. For all drug-radiation combination experiments (3D and 2D), cells were treated only with the 3D clonogenic IC_{50} values and therefore lower doses of AQ4N were not tested in 2D.

The IC_{50} concentrations in MCF-7 cells were 43.6±18.7 μM (P=0.004) (24 hours), 34.4±7.4 μM (P=0.002) (48 hours), and 31.2±7.2 μM (P=0.044) (72 hours) and in T47D cells were <5 μM (P<0.05) (24 hours), <5 μM (P<0.05) (48 hours) and 7.2±1.5 μM (P<0.05) (72 hours). The IC_{50} doses were not achieved for MDAMB-231 (>45 μM) and MDAMB-436 (<5 μM) cells within the concentrations of AQ4N tested. In MDAMB-468, the IC_{50} values were >45 μM (24 hours), 39.4±9.6 μM (P=0.001) (48 hours) and 31.5±0.9 μM (P<0.0001) (72 hours). Significant reduction in proliferation was noted in MDAMB-436 cells at 48 (P=0.002) and 72 (P=0.0003) hours compared to 24 hours.

In clonogenic survival, AQ4N treatment was very cytotoxic in the normal MCF-10A cells which demonstrated IC_{50} values (Appendix B-Figure B5) of 10.2±3.5 μM (P<0.0001) (24 hours), 5.4±0.6 μM (P<0.0001) (48 hours), and <5 μM (P<0.0001) (72 hours). Tabulated clonogenic IC_{50} doses for

AQ4N at different time points is presented in Table 3.5. Above data indicate that higher concentrations of AQ4N can decrease survival in breast cancer cells even in normoxic conditions.

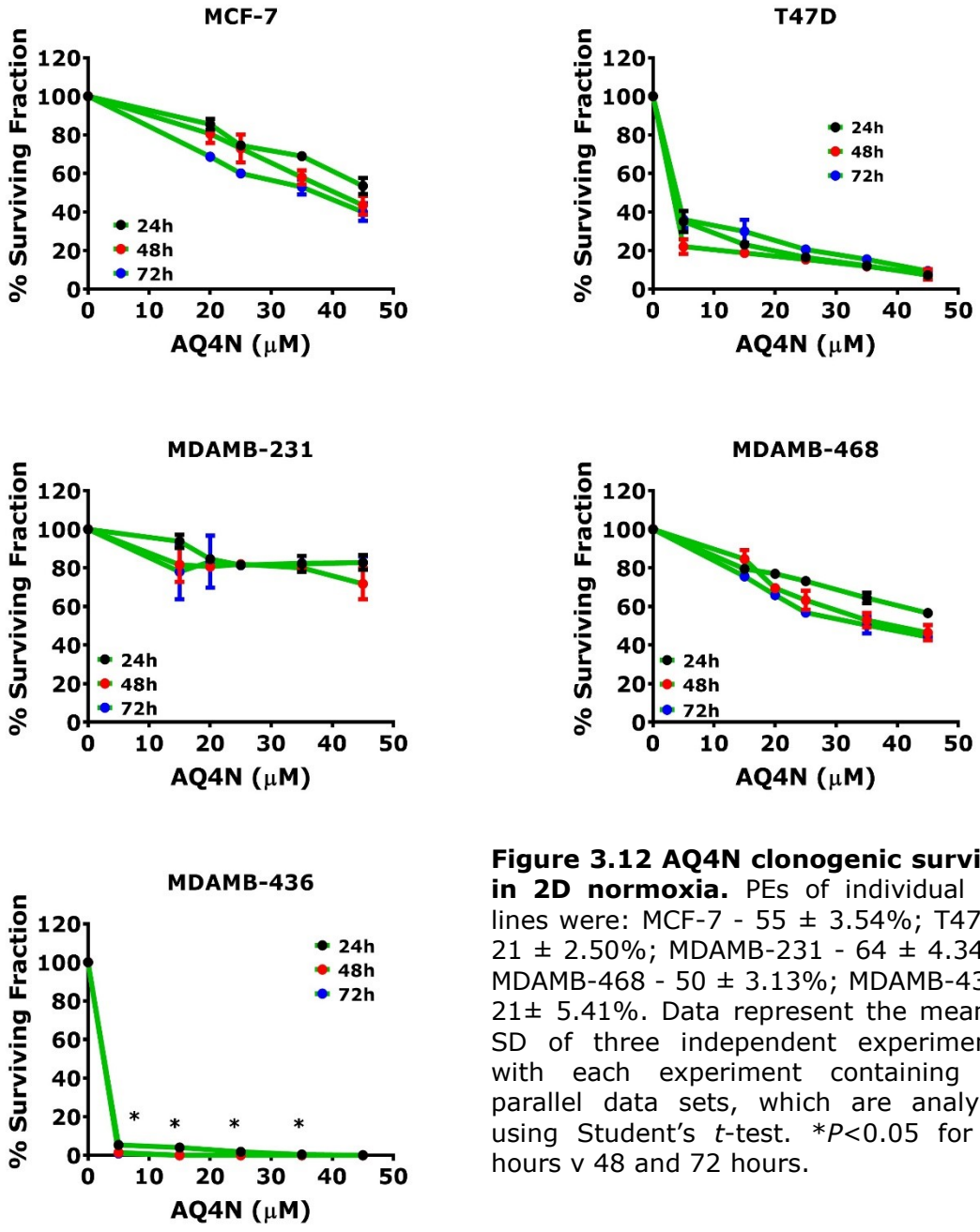


Figure 3.12 AQ4N clonogenic survival in 2D normoxia. PEs of individual cell lines were: MCF-7 - 55 ± 3.54%; T47D - 21 ± 2.50%; MDAMB-231 - 64 ± 4.34%; MDAMB-468 - 50 ± 3.13%; MDAMB-436 - 21± 5.41%. Data represent the mean ± SD of three independent experiments, with each experiment containing six parallel data sets, which are analysed using Student's *t*-test. **P*<0.05 for 24 hours v 48 and 72 hours.

3.4.4.2 Assessment of KP167 on clonogenic survival

Breast cancer cells were treated with various concentrations (5-45) μM of KP167 for 24, 48 or 72 hours and effect on cell survival was assessed by clonogenic survival assays. As seen in Figure 3.13, KP167 treatment reduced survival and resulted in a differential response between the different subtypes, with luminal cells demonstrating increase in sensitivity compared to the triple negative cell lines.

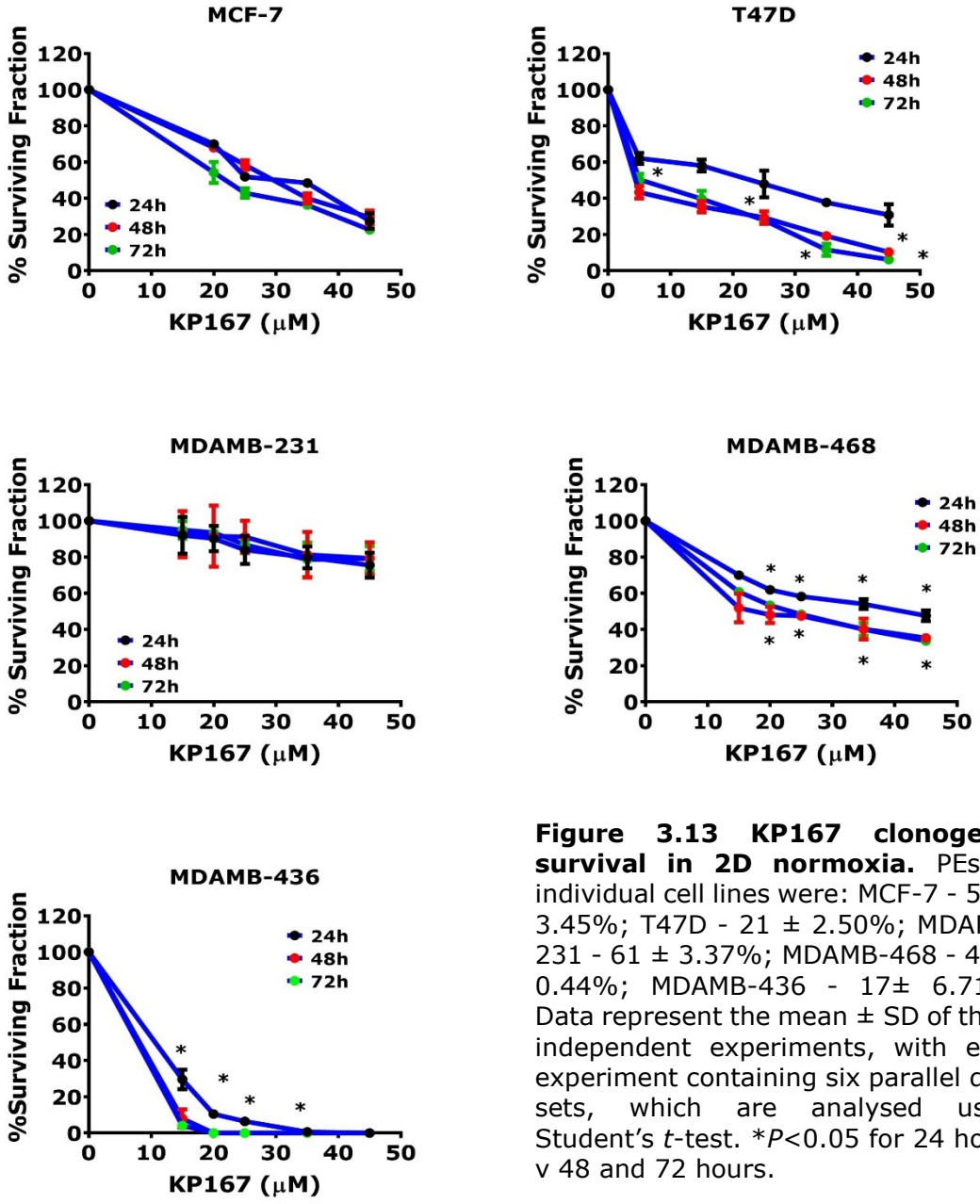


Figure 3.13 KP167 clonogenic survival in 2D normoxia. PEs of individual cell lines were: MCF-7 - 54 ± 3.45%; T47D - 21 ± 2.50%; MDAMB-231 - 61 ± 3.37%; MDAMB-468 - 46 ± 0.44%; MDAMB-436 - 17± 6.71%. Data represent the mean ± SD of three independent experiments, with each experiment containing six parallel data sets, which are analysed using Student's *t*-test. **P*<0.05 for 24 hours v 48 and 72 hours.

Treatment with 45 μM KP167 reduced survival by 70-80% in MCF-7 and 70-95% in T47D cells, compared to 20-25% in MDAMB-231, 55-70% in MDAMB-468 and 100% in MDAMB-436 cells. The IC_{50} concentrations (Table 3.5) were 26.2±10.0 μM (*P*=0.004) (24 hours), 22.7±12.9 μM (*P*=0.010) (48 hours), and 22.0±14.2 μM (*P*=0.015) (72 hours) in MCF-7 and 19.4±6.9 μM (*P*=0.005) (24 hours), 6.5±2.2 μM (*P*<0.0001) (48 hours) and 6.9±2.4 μM (*P*=0.0008) (72 hours) in T47D cells. The IC_{50} doses in MDAMB-231 and MDAMB-436 cells were >45 and <5 μM respectively. In MDAMB-468 cells, IC_{50} values were 32.6±4.2 μM (*P*<0.0001) (24 hours), 16.3±2.2 μM (*P*<0.0001) (48 hours), and 18.6±1.8 μM (*P*<0.0001) (72 hours). Significant reduction in survival was observed at 48 and 72 hours compared to treatment time of 24 hours in T47D (*P*=0.031 and *P*=0.0002), MDAMB-468 (*P*=0.007 and *P*=0.012) and MDAMB-436 (*P*=0.001 and *P*=0.001) cells. Above mentioned data indicate that the luminal cell lines, MCF-7 and T47D along with the BRCA-1 deficient MDAMB-436 cells were more sensitive to treatment with KP167 as demonstrated by reduced survival compared to the triple negative cells.

Table 3.5 Clonogenic IC_{50} values of AQ4N and KP167 in 2D normoxia.

Cell line	AQ4N (μM)			KP167 (μM)		
	24h	48h	72h	24h	48h	72h
MCF-7	43.6±18.7	34.4±7.4	31.2±7.2	26.2±10.0	22.7±12.9	22.0±14.2
T47D	<5	<5	7.2±1.5	19.4±6.9	6.5±2.2	6.9±2.4
MDAMB-231	>45	>45	>45	>45	>45	>45
MDAMB-468	>45	39.4±9.6	31.5±0.9	32.6±4.2	16.3±2.2	18.6±1.8
MDAMB-436	<5	<5	<5	<5	<5	<5
MCF-10A	10.2±3.5	5.4±0.6	<5	-	-	-

The IC_{50} values were calculated using Graphpad prism software. Abbreviations: μM - micromolar; - not available.

As seen in Table 3.5, MDAMB-231 cells were the most resistant to treatment with both AQ4N and KP167 in 2D normoxia compared to the MDAMB-436 cell lines which were the most sensitive. The clonogenic IC_{50} values were not achieved in MDAMB-231 cells in the range of drug concentrations used. MDAMB-468 and MCF-7 cells were moderately sensitive to treatment with both AQ4N and KP167, with KP167 showing greater reduction in survival compared to AQ4N. T47D and MDAMB-436 cells were the most sensitive cell lines to treatment with AQ4N in comparison to KP167 at the 24 hour time-point.

AQ4N appeared to be cytotoxic in the normal MCF-10A cells in 2D normoxia with similar IC_{50} values as that obtained in 3D cultures. Response of the normal cell line was similar to the luminal T47D cells. Taken together, data indicate that the hypoxia-activated prodrugs are cytotoxic to breast cancer cells in 2D normoxia, at much higher concentrations than that required to achieve similar effects in 3D cultures, in most cell lines. Similar response to the agents under 2D normoxia and 3D spheroids were observed in the highly sensitive BRCA-1 deficient MDAMB-436 and normal MCF-10A cells.

3.4.5 Endogenous reductase expression

Experiments to assess the effects of AQ4N and KP167 on breast cancer cell lines in 3D spheroids (section 3.4.3) and 2D normoxia (section 3.4.4), show that ER-positive cell lines (MCF-7 and T47D) showed a greater reduction in clonogenic survival (lower IC_{50} values in 3D and 2D) compared to TNBC lines (with the exception of BRCA-1 deficient cells). It has been previously reported that cytochrome P450 family of proteins, CYP2S1 and CYP2W1 are the main CYP enzymes involved in bioreducing AQ4N (Nishida et al., 2010). The cytochrome P450 family of enzymes are also involved in the metabolism and oxidation of estrogen in luminal cells (Tsuchiya et al., 2005, Cheng et al., 2001). Therefore, the expression of various endogenous reductases (cytochrome P450, CYP2S1, CYP2W1, NQO1 and NQO2) was investigated in the luminal and TNBC cell lines, to identify if endogenous reductase expression may reflect the difference in sensitivity between the different phenotypes. The protein levels of reductases were assessed in breast cancer cell lysates obtained from normoxic and hypoxic

cells (1% O_2 for 48 hours). Figure 3.14 (cytochrome P450, CYP2S1 and CYP2W1) and Figure 3.15 (NQO1 and NQO2) show the representative Western blot images and average quantified results of reductase expression from three independent experiments using lysates from different isolations.

As seen in Figure 3.14-B, cytochrome P450 expression was highest in luminal MCF-7 and T47D cells, compared to the triple negative MDAMB-231, MDAMB-468, MDAMB-436 and normal MCF-10A cells (MCF-7>T47D>MDAMB-468>MDAMB-231>MDAMB-436>MCF-10A). Compared to MCF-7 cells, expression of cytochrome P450 in MDAMB-436 (P=0.032 and P=0.044) and MCF-10A (P=0.014 and P=0.038) cells was significantly reduced under both normoxia and hypoxia respectively, and only under hypoxia in the MDAMB-231 cells (P=0.044). In all the breast cell lines, hypoxia did not affect expression of cytochrome P450 compared to the endogenous levels present in normoxic cells.

CYP2S1 expression (Figure 3.14-C) was present in both luminal and triple negative breast cancer cells. The pattern of CYP2S1 expression was highest in MDAMB-436>MDAMB-468>MDAMB-231>MCF-7>T47D>MCF-10A cells. Compared to MDAMB-436 cells, the expression of CYP2S1 in normoxia was significantly reduced in MCF-7 (P=0.032), T47D (P=0.021), MDAMB-231 (P=0.041) and MCF-10A (P=0.044) cells. There was no significant difference in the endogenous expression of CYP2S1 between normoxia and hypoxia across all cell lines.

CYP2W1 (Figure 3.14-D) expression was highest in MCF-10A>MCF-7>T47D>MDAMB-436>MDAMB-231>MDAMB-468 cells. Expression was significantly reduced in MDAMB-468 (P=0.003), MDAMB-231 (P=0.023) and MDAMB-436 (P=0.025) cells compared to MCF-7 cells. Compared to MCF-10A cells, the expression of CYP2W1 was significantly lower in MDAMB-231 (P=0.0008), MDAMB-468 (P=0.003) and MDAMB-436 (P=0.001) cells. No significant difference in the expression of reductases was observed between normoxia and hypoxia.

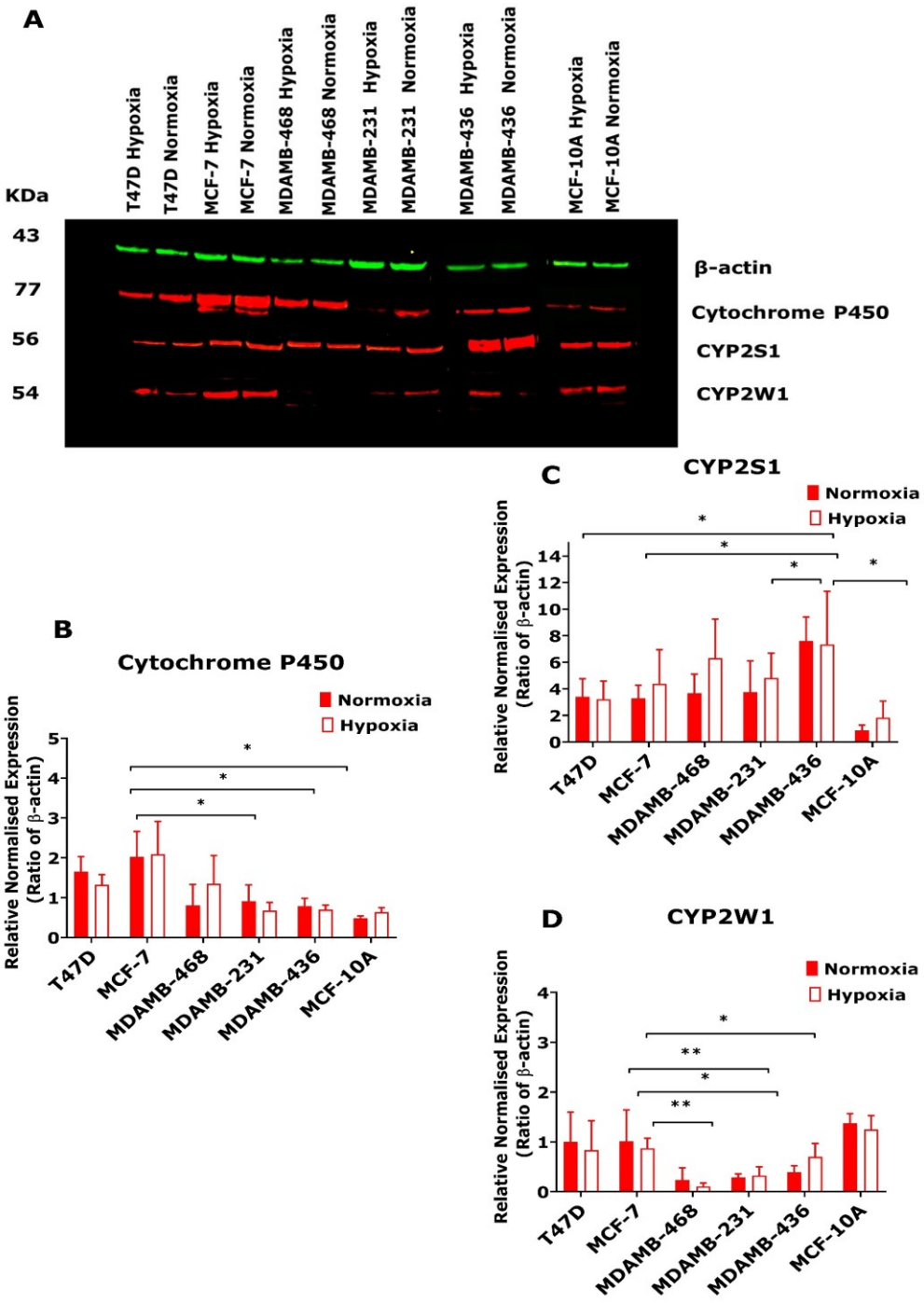


Figure 3.14 CYP expression in breast cancer cells in normoxia (21% O_2) and hypoxia (0.1% O_2). (A) Representative Western blot images for cytochrome P450, CYP2S1 and CYP2W1. Quantified expression of (B) Cytochrome P450 (C) CYP2S1 and (D) CYP2W1. Red bands indicate cytochrome P450, CYP2S1, CYP2W1 expression and green bands represent β-actin. Data in the bar charts represent the mean of normalised protein expression to β-actin ± SD of three independent experiments, with separate cell lysates from different passage numbers of cells, which are analysed using Student's *t*-test. **P*<0.05, ***P*<0.01.

Data indicate that expression of cytochrome P450 and CYP2W1 were higher in the luminal MCF-7 and T47D cells compared to the triple negative MDAMB-231 and MDAMB-468 cell lines. Highest expression of CYP2W1 was present in the normal MCF-10A cells followed by the luminal MCF-7 and T47D cells. The higher expression of reductases in these cell lines, may explain, at least in part, the increased cytotoxicity observed in this phenotype with single agent AQ4N and KP167 in 3D and 2D cultures. Higher expression of CYP2S1 in the BRCA-1 deficient MDAMB-436 cells along with the inherent double strand repair deficiency, may explain the increase in sensitivity to AQ4N and KP167 in these cell lines. Such data suggest that the endogenous levels of CYP enzymes in breast cancer cells may influence treatment response to AQ4N and KP167. The expression of CYP2S1 and CYP2W1 in breast cancer subtypes was further investigated in breast cancer patient tumour tissues by immunohistochemistry and is discussed in chapter 5.

The cytosolic enzymes, NQO1 and NQO2, bio-reduce a wide variety of drugs including quinones and derivatives (Nemeikaitė-Čėnienė et al., 2019). To assess if these were differentially expressed across the breast cancer phenotypes, their expression was also assessed by Western blot with results shown in Figure 3.15.

There was no consistent difference in expression seen between the phenotypes. Greater expression of NQO1 (Figure 3.15-B) was observed in MDAMB-436, MCF-7 and MCF-10A cells. Normalised data of 3 independent experiments show increased expression in response to hypoxia in MCF-7 (P=0.029), and MDAMB-436's (P=0.020), but not in MCF-10A cells (P=0.443), although this may not be seen clearly in the representative Western blot image. NQO1 expression was completely absent in T47D, MDAMB-231 and MDAMB-468 cell lines. The expression of NQO1 was significantly higher in MDAMB-436 cells compared to MCF-7 (P=0.001 and P<0.0001) and MCF-10A (P=0.008 and P<0.0001) cells both under normoxia and hypoxia respectively.

Unlike NQO1, the expression of NQO2 (Figure 3.15-C) was present across all breast cancer cell lines. The pattern of NQO2 expression was highest in MDAMB-231>MCF-10A>MDAMB-468>MCF-7>MDAMB-436>T47D cells.

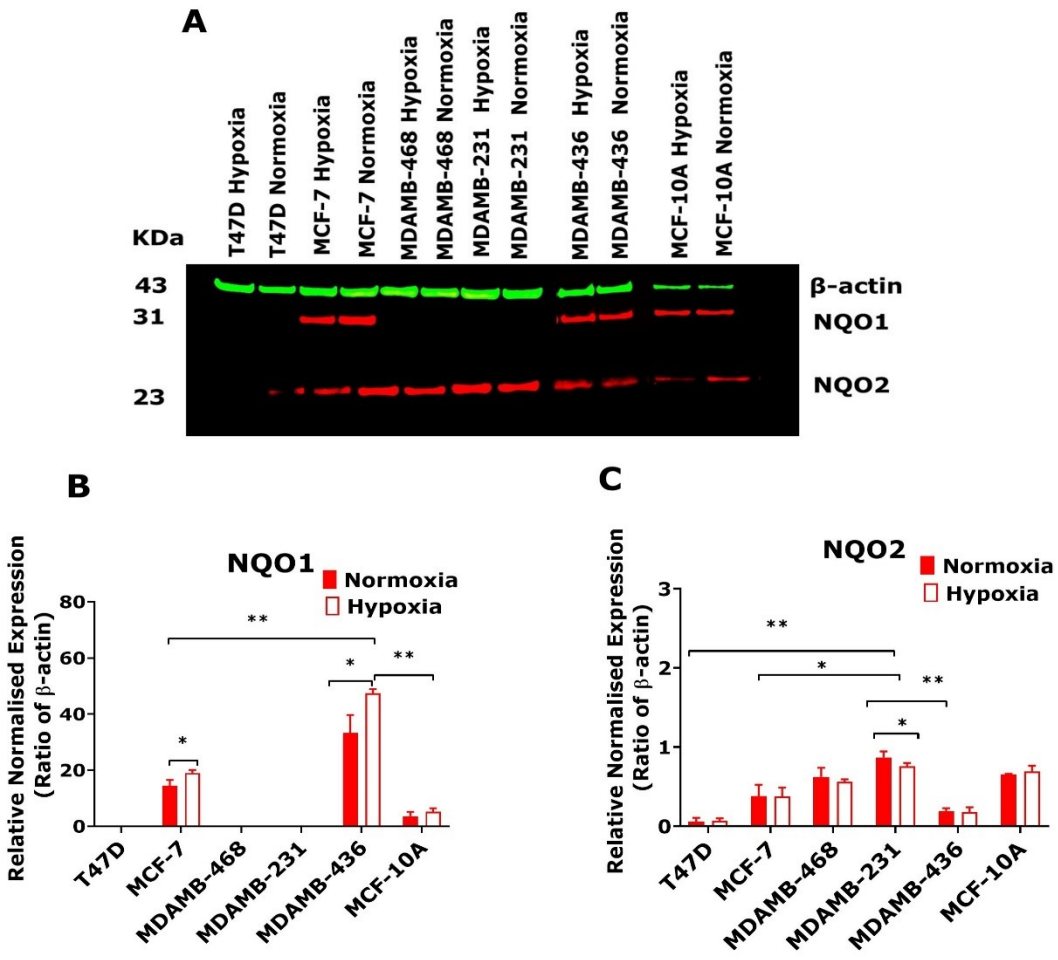


Figure 3.15 NQO1 and NQO2 expression in breast cancer cells in normoxia (21% O_2) and hypoxia (0.1% O_2). (A) Representative Western blot images for NQO1 and NQO2. Red bands indicate NQO1 and NQO2 expression and green bands represent β-actin. Quantified expression of (B) NQO1 and (C) NQO2. Data in the bar charts represent the mean of normalised protein expression to β-actin ± SD of three independent experiments, with separate cell lysates from different passage numbers of cells, which are analysed using Student's *t*-test. **P*<0.05, ***P*<0.01.

The expression of NQO2 was significantly reduced under hypoxia in MDAMB-231 cells (*P*=0.029). Expression was higher in MDAMB-231 cells compared to T47D (*P*=0.001 and *P*=0.001), and MDAMB-436 (*P*=0.005 and *P*=0.049) cells both under normoxia and hypoxia cultures respectively, and in normoxic MCF-7 cells (*P*=0.047).

NQO1 data suggest that expression is cell line, rather than phenotype, specific, whereas the expression of NQO2 is present in all cell lines. In light

of such data, and as these enzymes have not previously been associated with bioreducing AQ4N (Manley and Waxman, 2013), these enzymes were not investigated further.

3.4.6 Radioresponse of breast cancer cells - 2D v 3D

Before progressing to drug-radiation combination experiments, the intrinsic radioresponse of breast cancer spheroids were assessed. Cells were grown as spheroids and irradiated with single dose of 2, 4, 6 or 8 Gy. Parallel experiments were also carried out on cells grown in 2D normoxia to compare radiosensitivity obtained between 2D and 3D cultures. Surviving fraction (SF) was plotted as a function of radiation dose on a log/linear plot using the linear quadratic (LQ) model as shown in Figure 3.16.

There was little difference in the radioresponse between 2D and 3D cultures. A slight, but significant, increase in 3D SF2 value was observed only in the luminal MCF-7 (P=0.010) cells, but not in T47D (P=0.517) MDAMB-231 (P=0.958) and MDAMB-468 (P=0.419) cells compared to 2D cultures. The BRCA-1 deficient MDAMB-436 cells were radioresistant with significantly higher SF2 values (P<0.001) in 3D compared to 2D cultures. The mean SF2 values in 2D v 3D culture were 0.50±0.04 v 0.36±0.02 in MCF-7, 0.44±0.10 v 0.26±0.07 in T47D, 0.33±0.10 v 0.25±0.02 in MDAMB-231, 0.34±0.02 v 0.32±0.03 in MDAMB-468 and 0.30±0.03 v 0.64±0.01 in MDAMB-436 cells. MCF-10A cells were more sensitive to radiation under 3D cultures with SF2 of 0.20 compared to 0.38 in 2D cultures (Appendix B-Figure B6). Radiobiological parameters are given in Appendix B-Table B3.

The radioresponse of breast cancer cells obtained in 2D were similar to those obtained in chapter 2, and to previous studies (also reported in chapter 2), indicating that cells were behaving as expected compared to published *in vitro* literature. Table 3.6 summarises various radiobiologic parameters including α, β, and α/β ratios.

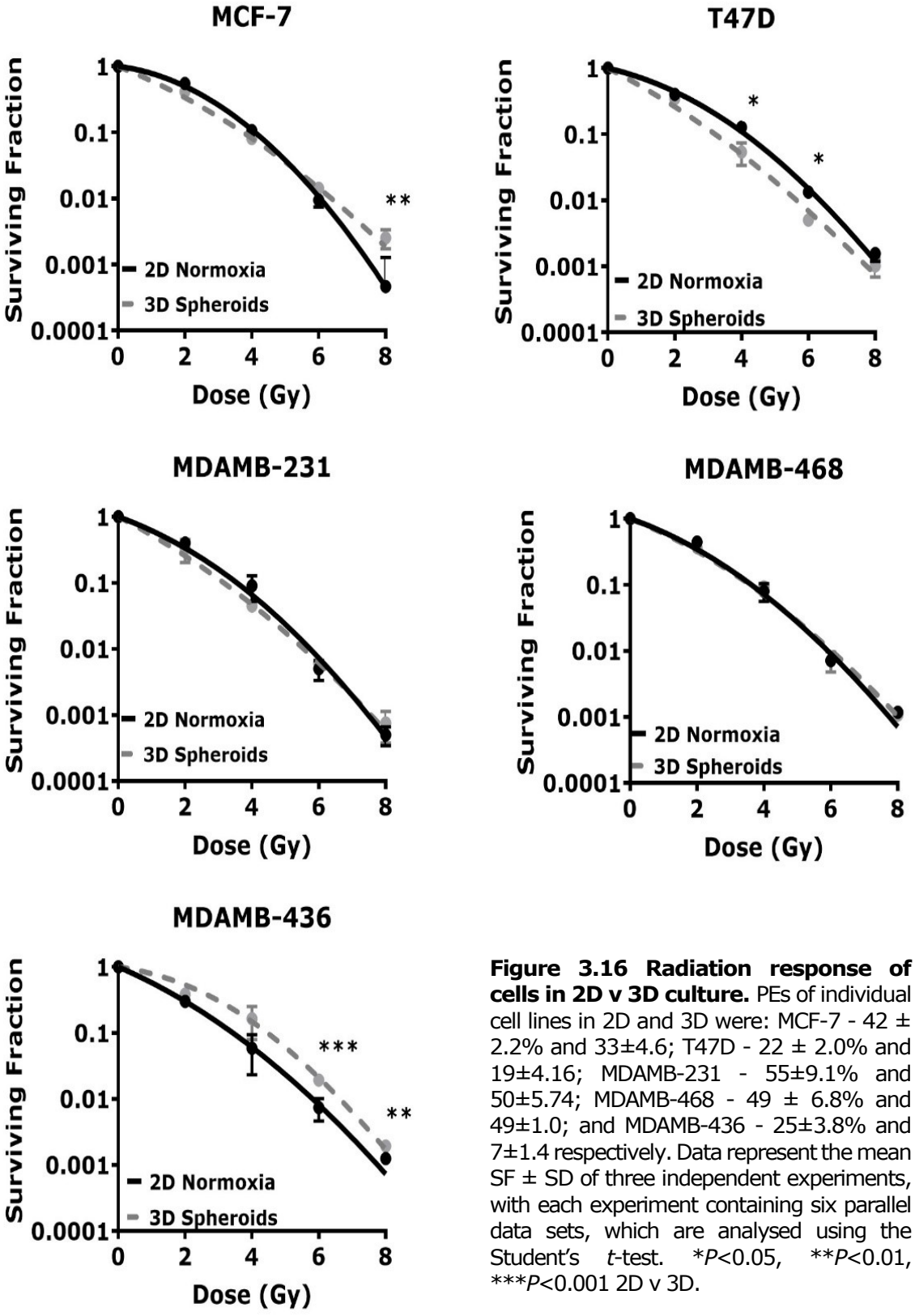


Figure 3.16 Radiation response of cells in 2D v 3D culture. PEs of individual cell lines in 2D and 3D were: MCF-7 - 42 ± 2.2% and 33±4.6; T47D - 22 ± 2.0% and 19±4.16; MDAMB-231 - 55±9.1% and 50±5.74; MDAMB-468 - 49 ± 6.8% and 49±1.0; and MDAMB-436 - 25±3.8% and 7±1.4 respectively. Data represent the mean SF ± SD of three independent experiments, with each experiment containing six parallel data sets, which are analysed using the Student's *t*-test. **P*<0.05, ***P*<0.01, ****P*<0.001 2D v 3D.

Table 3.6 Radiobiologic parameters of breast cancer cells in 2D normoxia and 3D spheroid cultures.

Cell line	α (Gy^{-1})	β (Gy^{-2})	α/β (Gy)	SF2
MCF-7				
2D Normoxia	0.14±0.05	0.10±0.01	1.40±0.55	0.50±0.04
3D Spheroids	0.46±0.08	0.03±0.01	12.89±5.46	0.36±0.02
*t*test	***P*=0.004**	***P*<0.001**	***P*=0.022**	***P*=0.010**
T47D				
2D Normoxia	0.23±0.23	0.07±0.02	4.40±5.35	0.44±0.10
3D Spheroids	0.60±0.18	0.03±0.02	26.09±19.73	0.26±0.07
*t*test	*P*=0.097	*P*=0.114	*P*=0.611	*P*=0.517
MDAMB-231				
2D Normoxia	0.42±0.19	0.06±0.02	7.50±4.73	0.33±0.10
3D Spheroids	0.60±0.06	0.15±0.19	8.83±7.98	0.25±0.02
*t*test	*P*=0.224	*P*=0.125	*P*=0.476	*P*=0.958
MDAMB-468				
2D Normoxia	0.40±0.06	0.06±0.01	6.85±2.79	0.34±0.02
3D Spheroids	0.46±0.06	0.04±0.01	9.95±3.29	0.32±0.03
*t*test	*P*=0.316	*P*=0.211	*P*=0.281	*P*=0.419
MDAMB-436				
2D Normoxia	0.50±0.24	0.05±0.00	10.26±3.05	0.30±0.03
3D Spheroids	0.03±0.01	0.09±0.01	0.34±0.06	0.64±0.01
*t*test	***P*=<0.001**	***P*<0.001**	***P*=0.004**	***P*<0.001**

Statistical significance was determined by Student's *t*-test. The *P*-values are bold where they are ≤ 0.05. Abbreviations: IR, irradiation; SF2, surviving fraction at 2Gy.

MCF-7 spheroids demonstrated a significant increase in the α-value (*P*=0.004), which increased the α/β ratio (*P*=0.022) suggesting that MCF-7 cells were sensitive to radiation when grown as 3D spheroids. MDAMB-436 cells were more radioresistant when grown as 3D spheroids and showed a significant reduction in the α-value (*P*<0.001) and α/β (*P*=0.004) ratio compared to 2D cultures. Increase in the α-value and α/β ratio were observed in T47D, MDAMB-231 and MDAMB-468 cells, albeit not significantly, suggesting a small radiosensitising effect in 3D spheroid cultures. As mentioned, data indicate only marginal differences in radioresponse between 2D and 3D cultures in the current study.

3.4.7 Radiosensitisation with AQ4N and KP167 - 3D

3.4.7.1 Effect of AQ4N on radiosensitivity - 3D

Previously published studies have reported the radiosensitising effects of AQ4N and its progression to clinical trials as an adjuvant to radiotherapy (Benghiat et al., 2004, Mehibel et al., 2016). In the current study, the radiosensitising effects of AQ4N were assessed in breast cancer spheroids. Radiation survival curve data from AQ4N-radiation combination experiments were fitted to the LQ model and various radiobiological parameters such as α, β, α/β value and SF2 were ascertained as previously described. Sensitiser enhancement ratios (SER's) were calculated at 1% survival ($SER_{0.01}$) and was used to assess any radiosensitising effect of AQ4N. As shown in Figure 3.17, AQ4N increased radiosensitivity across all breast cancer phenotypes, with effects more pronounced in the MDAMB-436 cells.

Mean SF2 values in control cells were significantly higher compared to AQ4N treated cells i.e. 0.36±0.02 v 0.22±0.02 (P=0.002) in MCF-7, 0.26±0.07 v 0.10±0.03 (P=0.027) in T47D, 0.25±0.02 v 0.13±0.01 (P=0.007) in MDAMB-231, 0.32±0.03 v 0.27±0.03 (P=0.0008) in MDAMB-468 and 0.62±0.02 v 0.12±0.01 (P=0.006) in MDAMB-436 cells. AQ4N treatment enhanced radiosensitivity in all breast cancer cells with $SER_{0.01}$ of 1.30±0.08 (MCF-7), 1.58±0.06 (T47D), 1.44±0.04 (MDAMB-231), 1.64±0.08 (MDAMB-468) and 3.33±0.18 (MDAMB-436). Such $SER_{0.01}$ values equate to the survival of cells at 8 Gy decreasing from 0.002 to 0.001 in MCF-7, 0.001 to 0.00006 in T47D, 0.0007 to 0.0002 in MDAMB-231, 0.001 to 0.00004 in MDAMB-468 and 0.001 to 0.00006 in MDAMB-436 cells with AQ4N treatment.

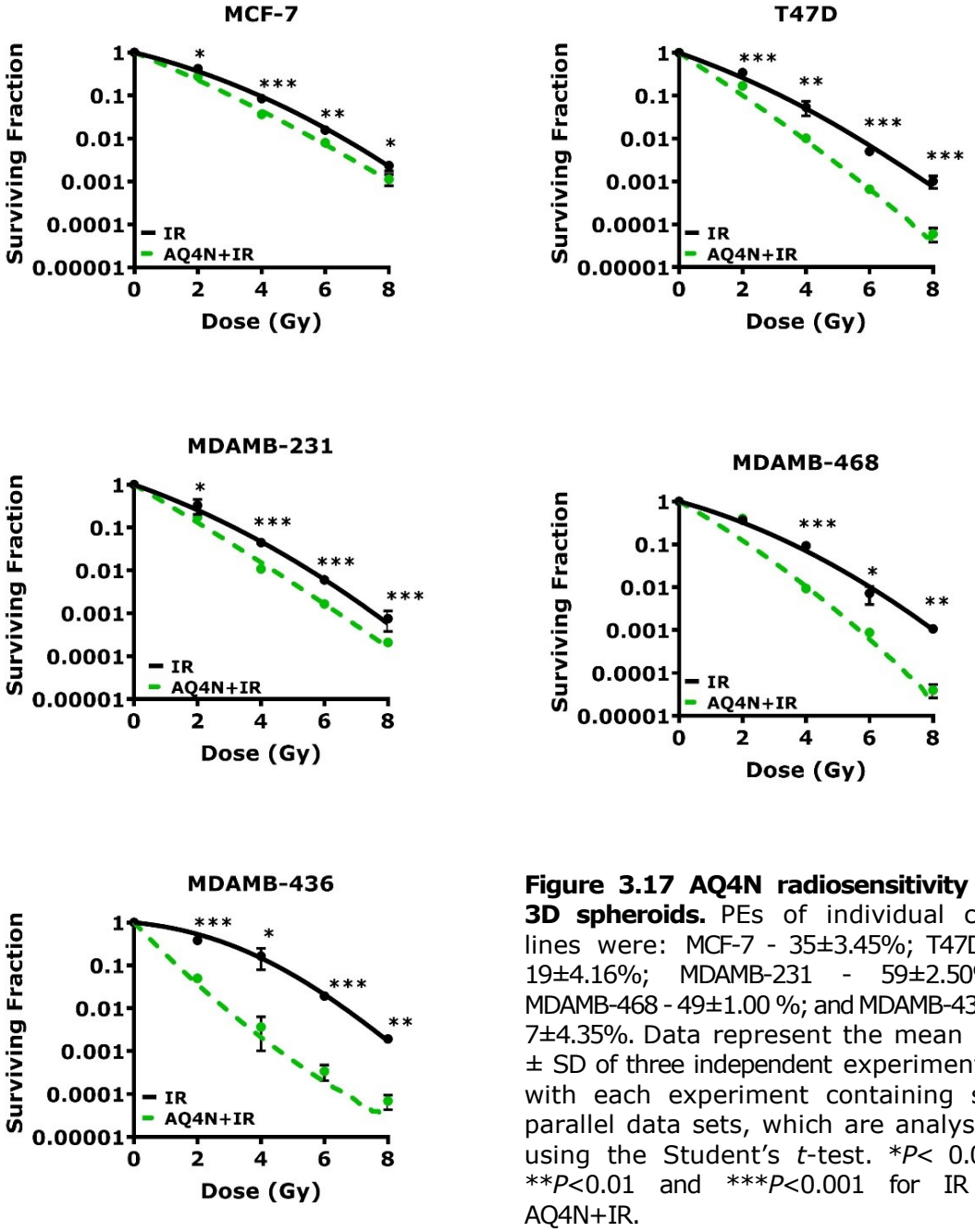


Figure 3.17 AQ4N radiosensitivity in 3D spheroids. PEs of individual cell lines were: MCF-7 - 35±3.45%; T47D - 19±4.16%; MDAMB-231 - 59±2.50%; MDAMB-468 - 49±1.00 %; and MDAMB-436 - 7±4.35%. Data represent the mean SF ± SD of three independent experiments, with each experiment containing six parallel data sets, which are analysed using the Student's *t*-test. **P*< 0.05, ***P*<0.01 and ****P*<0.001 for IR v AQ4N+IR.

A modest increase in radiosensitisation, similar to luminal MCF-7 cells, was observed in AQ4N treated MCF-10A cells with $SER_{0.01}$ 1.36±0.12 (Appendix B-Figure B7 and radiobiologic parameters in Appendix B-Table B4). The radiobiologic parameters of breast cancer spheroids treated with IR and/or AQ4N are shown in Table 3.7.

Table 3.7 Radiobiologic parameters of breast cancer spheroids treated with IR and/or AQ4N.

Cell line Spheroids	α (Gy^{-1})	β (Gy^{-2})	α/β (Gy)	SF2	$SER_{(0.01)}$
MCF-7					
IR	0.46±0.08	0.03±0.01	12.89±5.46	0.36±0.02	
AQ4N+IR	0.57±0.15	0.03±0.01	25.69±22.32	0.22±0.02	1.30±0.08
t test	*P*=0.326	*P*=0.527	*P*=0.389	***P*=0.002**	
T47D					
IR	0.60±0.18	0.01±0.02	26.09±19.73	0.26±0.07	
AQ4N+IR	1.12±0.21	0.01±0.02	280.15±36.3	0.10±0.03	1.58±0.06
t test	***P*=0.035**	*P*=0.396	*P*=0.295	***P*=0.027**	
MDAMB-231					
IR	0.6±0.06	0.15±0.19	8.83±7.98	0.25±0.02	
AQ4N+IR	0.99±0.04	0.01±0.01	95.89±50.00	0.13±0.01	1.44±0.04
t test	***P*=0.008**	*P*=0.276	***P*=0.040**	***P*=0.007**	
MDAMB-468					
IR	0.46±0.06	0.04±0.01	9.95±3.29	0.32±0.03	
AQ4N+IR	0.95±0.10	19.03±4.89	19.03±4.89	0.27±0.03	1.64±0.08
t test	***P*=0.002**	*P*=0.77	*P*=0.056	***P*=0.0008**	
MDAMB-436					
IR	0.03±0.03	0.09±0.01	0.35±0.38	0.62±0.02	
AQ4N+IR	1.73±0.14	0.05±0.01	32.75±2.15	0.12±0.01	3.33±0.18
t test	***P*=0.0005**	*P*=0.415	***P*=0.004**	***P*=0.006**	

Statistical significance was determined by Student's *t*-test. The *P*-values are bold where they are ≤ 0.05. Abbreviations: IR, irradiation; $SER_{0.01}$, sensitiser enhancement ratio at 1% survival; SF2, surviving fraction at 2Gy.

AQ4N treatment increased the α-value in MCF-7 (*P*=0.326), T47D (*P*=0.035), MDAMB-231 (*P*=0.008), MDAMB-468 (*P*=0.002) and MDAMB-436 (*P*=0.0005) compared to control cells. Increases in the α-value raised the α/β ratio in all cell lines suggesting that the cell killing obtained with AQ4N treatment was linear. Greater radiosensitisation was induced in the BRCA-1 deficient MDAMB-436 cells and the underlying double strand repair deficiency may contribute towards the increase in radiosensitivity observed in these cell lines to AQ4N treatment (Song et al., 2013, Arun et al., 2015). Above data indicate that AQ4N is an efficient radiosensitiser across all breast cancer spheroids. The efficacy of KP167 as a radiosensitiser was next assessed.

3.4.7.2 Effect of KP167 on radiosensitivity - 3D

Figure 3.18 shows that KP167 substantially increased radiosensitivity in all breast cancer spheroids, with greatest increase seen in the triple negative cell lines.

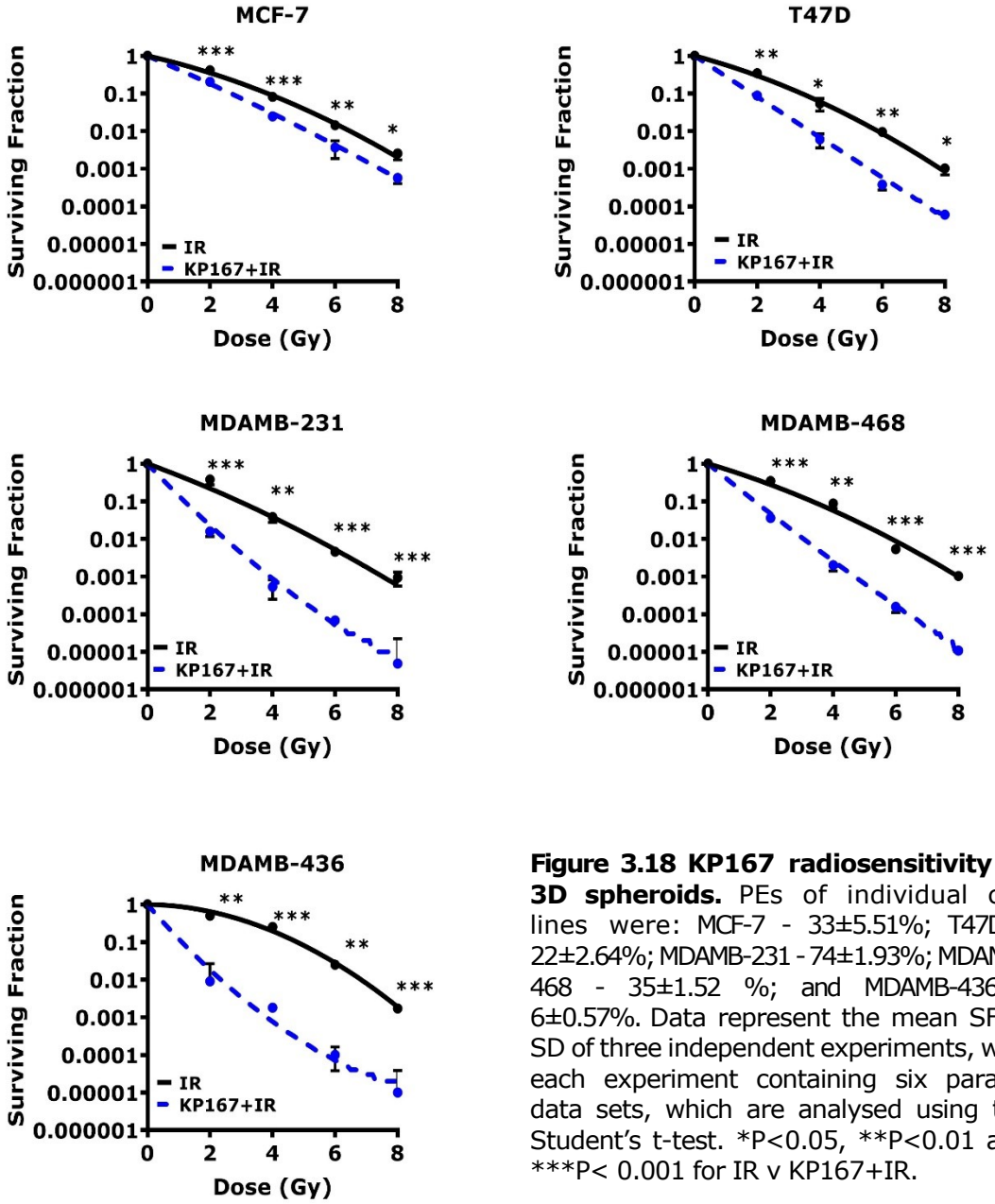


Figure 3.18 KP167 radiosensitivity in 3D spheroids. PEs of individual cell lines were: MCF-7 - 33±5.51%; T47D - 22±2.64%; MDAMB-231 - 74±1.93%; MDAMB-468 - 35±1.52 %; and MDAMB-436 - 6±0.57%. Data represent the mean SF ± SD of three independent experiments, with each experiment containing six parallel data sets, which are analysed using the Student's t-test. *P<0.05, **P<0.01 and ***P< 0.001 for IR v KP167+IR.

Compared to control cells, the mean SF2 values in KP167 treated breast cancer spheroids were significantly lower i.e. 0.35±0.02 v 0.18±0.03 (*P*=0.002) in MCF-7, 0.23±0.05 v 0.06±0.01 (*P*=0.009) in T47D, 0.21±0.04 v 0.02±0.01 (*P*=0.001) in MDAMB-231, 0.27±0.03 v

0.04±0.01 (*P*=0.0002) in MDAMB-468 and 0.64±0.00 v 0.01±0.01 (*P*=0.0001) in MDAMB-436 cells. KP167 treatment enhanced radiosensitivity in all breast cancer cells with $SER_{0.01}$ of 1.46±0.66 in MCF-7, 1.76±0.20 in T47D, 2.53±0.06 in MDAMB-231, 2.28±0.24 in MDAMB-468 and 4.55±0.24 in MDAMB-436 cells. Compared to controls, the SF8 in KP167 treated cells decreased from 0.002 to 0.0005 in MCF-7, 0.001 to 0.00006 in T47D, 0.0009 to 0.000004 in MDAMB-231, 0.001 to 0.00001 in MDAMB-468 and 0.001 to 0.00001 in MDAMB-436 cells. Data indicate that KP167 resulted in a ~100-fold increase in radiosensitivity in T47D, MDAMB-231, MDAMB-468 and MDAMB-436 cells. Other radiobiologic parameters including α, β, and α/β ratios are given in Table 3.8.

Table 3.8 Radiobiologic parameters of breast cancer spheroids treated with IR and/or KP167.

Cell line Spheroids	α (Gy^{-1})	β (Gy^{-2})	α/β (Gy)	SF2	$SER_{(0.01)}$
MCF-7					
IR	0.43±0.04	0.04±0.01	10.51±2.31	0.35±0.02	
KP167+IR	0.83±0.11	0.01±0.01	102.04±70.49	0.18±0.03	1.46±0.66
t test	***P*=0.004**	***P*=0.026**	*P*=0.087	***P*=0.002**	
T47D					
IR	0.69±0.15	0.02±0.01	20.83±26.73	0.23±0.05	
KP167+IR	1.38±0.12	0.01±0.01	165.50±184.86	0.06±0.01	1.76±0.20
t test	***P*=0.004**	*P*=0.626	*P*=0.250	***P*=0.009**	
MDAMB-231					
IR	0.70±0.12	0.02±0.01	14.81±4.38	0.21±0.04	
KP167+IR	2.04±0.25	0.06±0.03	35.91±13.03	0.02±0.01	2.53±0.06
t test	***P*=0.001**	*P*=0.202	*P*=0.056	***P*=0.001**	
MDAMB-468					
IR	0.46±0.06	0.04±0.008	9.95±3.29	0.27±0.03	
KP167+IR	1.57±0.06	0.01±0.01	87.16±75.79	0.04±0.01	2.28±0.24
t test	***P*=0.00003**	***P*=0.016**	*P*=0.152	***P*=0.0002**	
MDAMB-436					
IR	0.03±0.01	0.09±0.00	0.34±0.06	0.64±0.00	
KP167+IR	2.22±0.19	0.10±0.02	-21.58±2.86	0.01±0.01	4.55±0.24
t test	***P*=0.004**	*P*=0.595	***P*=0.008**	***P*=0.0001**	

Statistical significance was determined by Student's *t*-test. The *P*-values are bold where they are ≤ 0.05. Abbreviations: IR, irradiation; $SER_{0.01}$, sensitiser enhancement ratio at 1% survival; SF2, surviving fraction at 2Gy.

Spheroids treated with KP167 demonstrated a significant increase in α-value in MCF-7 (P=0.004), T47D (P=0.004), MDAMB-231 (P=0.001), MDAMB-468 (P=0.00003) and MDAMB-436 (P=0.004) cells. Increase in the α-value raised the α/β ratio suggesting that KP167 was an extremely potent radiosensitiser across all breast cancer phenotypes. Greater increases in radiosensitivity were observed in the triple negative MDAMB-231, MDAMB-468 and MDAMB-436 cells. The level of radiosensitisation achieved in all cell lines was greater than the parental drug AQ4N. Combined graphs for radiosensitivity obtained with AQ4N and KP167 in 3D spheroids is given in Appendix B-Figure B8.

In some studies, matrigel has been found to alter sensitivity to drugs, with previous studies reporting that addition of an ECM can either enhance drug efficacy or promote drug resistance (Langhans, 2018, Sebens and Schafer, 2012, Bonnans et al., 2014). In order to assess whether the addition of matrigel altered response in MDAMB-231 and MDMAB-468 spheroids to KP167, an additional experiment was conducted in MCF-7 cells. The radiation response in MCF-7 cells formed into spheroids with matrigel (MCF-7+M), treated with AQ4N or KP167 (Appendix B-Figure B9), was compared against the response of MCF-7 cells formed into spheroids without matrigel as shown above in section 3.3.7.1 (AQ4N) and 3.3.7.2 (KP167). Data show that although matrigel inclusion increased sensitivity of MCF-7 cells (SF2 value of 0.25±0.02 (MCF-7+M) v 0.35±0.02 (MCF-7)) to radiation alone, there was no difference in the radiosensitivity of MCF-7 cells to AQ4N or KP167 between +/- matrigel. MCF-7 cells demonstrated similar radioresponse with $SER_{0.01}$ values of 1.2 (AQ4N) and 1.5 (KP167) in both treatment conditions (+/- matrigel). These experiments indicate that matrigel did not alter radiosensitivity in MDAMB-231 or MDAMB-468 cells to KP167 treatment. This data is presented in Appendix B-Figure B9 with radiobiological parameters supplied in Appendix B-Table B5. Taken together, data suggest that the greater increase in radiosensitivity observed in MDAMB-231 and MDAMB-468 cells is due to the effectiveness of KP167 as a radiosensitiser. Moreover, TNBC cells, in general are known to have defective DNA repair pathways (Alli et al., 2009), which may have enhanced the cytotoxic effects of KP167 in these cell lines.

The level of radiosensitivity obtained with KP167 in the triple negative breast cancer cells (MDAMB-231, MDAMB-468 and MDAMB-436) was greater than that achieved with gold standard radiosensitisers such as KU-55933 and olaparib investigated in chapter 2 (section 2.4.5). Such data indicate that KP167 may be promising in the treatment of TNBCs.

3.4.8 Radiosensitisation with AQ4N and KP167 - 2D

Initial experiments to assess the effect of single agent AQ4N and KP167 in 2D culture, demonstrated that the HAPs caused a dose dependent reduction in proliferation (section 3.4.4.1) and clonogenic survival (section 3.4.4.2) of breast cancer cells even in the presence of oxygen. Given this finding, the radio-response of breast cancer cells treated with AQ4N and KP167 were assessed in 2D normoxia. These experiments were carried out to investigate if doses that were cytotoxic in spheroid cultures, were able to induce radiosensitivity in normoxic cells. Therefore, cells grown in normoxia were treated with the spheroid IC_{50} concentration of AQ4N or KP167 for 96 hours, following which cells were irradiated and seeded for assessment of clonogenic survival.

3.4.8.1 Effect of AQ4N on radiosensitivity – 2D

The effects of AQ4N on radioresponse of breast cancer cells in 2D normoxia were assessed by plotting a dose response curve and is presented in Figure 3.19. Data show that compared to controls, the SF2 values in AQ4N treated cells were significantly reduced in MCF-7 - 0.50±0.04 v 0.36±0.05 (P=0.024) and T47D - 0.44±0.10 v 0.16±0.04 (P=0.013), but not in MDAMB-231 - 0.33±0.10 v 0.20±0.04 (P=0.125), MDAMB-468 - 0.34±0.02 v 0.27±0.03 (P=0.068) and MDAMB-436 - 0.30±0.03 v 0.23±0.07 (P=0.252) cells. AQ4N marginally increased radiosensitivity with $SER_{0.01}$ of 1.17±0.06 in MCF-7, 1.29±0.28 in MDAMB-231, 1.11±0.44 in MDAMB-468 and 1.19±0.12 in MDAMB-436 cells. A greater increase in radiosensitisation was seen in T47D cells with an $SER_{0.01}$ of 1.64±0.27.

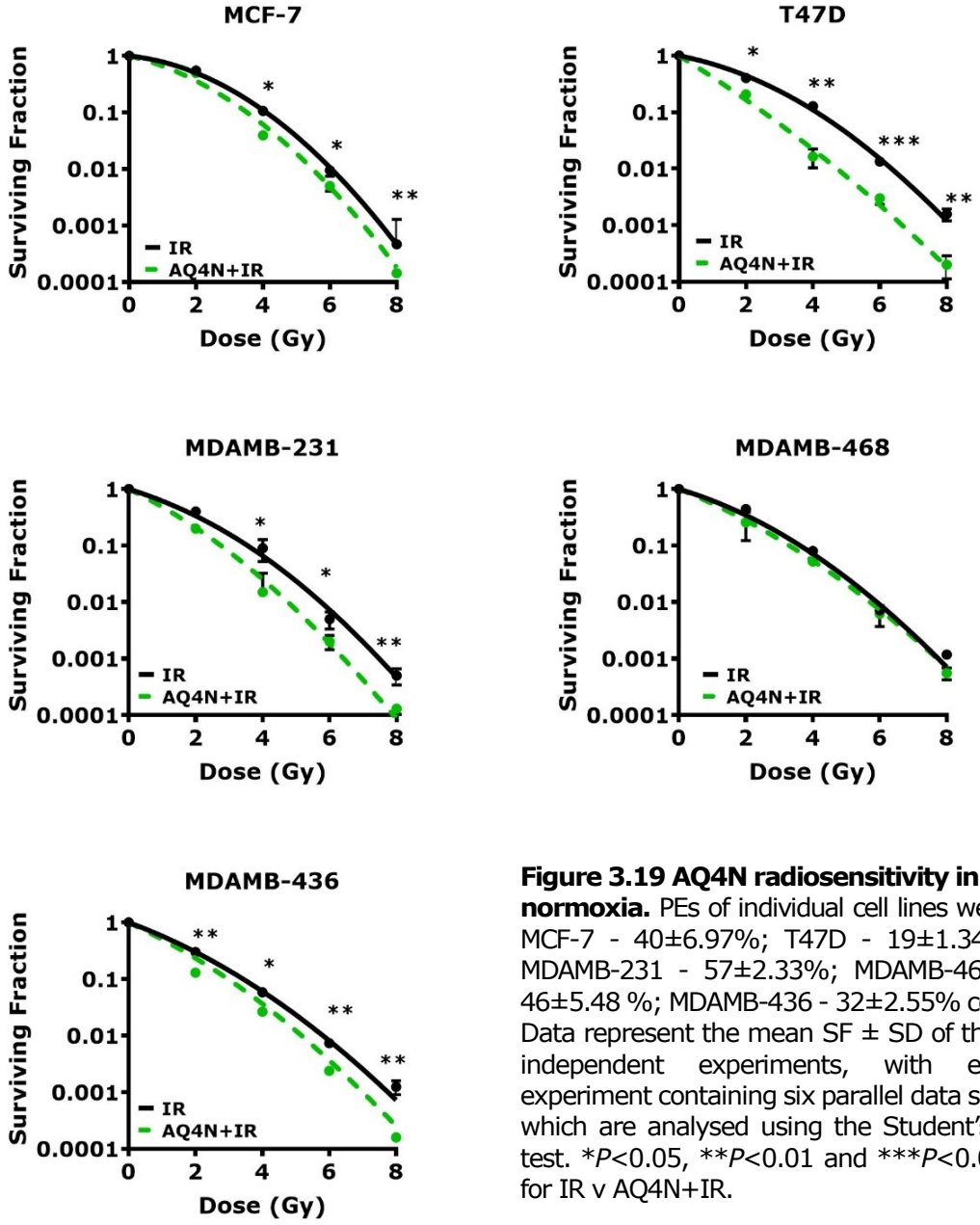


Figure 3.19 AQ4N radiosensitivity in 2D normoxia. PEs of individual cell lines were: MCF-7 - 40±6.97%; T47D - 19±1.34%; MDAMB-231 - 57±2.33%; MDAMB-468 - 46±5.48 %; MDAMB-436 - 32±2.55% cells. Data represent the mean SF ± SD of three independent experiments, with each experiment containing six parallel data sets, which are analysed using the Student's *t*-test. **P*<0.05, ***P*<0.01 and ****P*<0.001 for IR v AQ4N+IR.

Such values equate to the survival of AQ4N treated cells at 8 Gy decreasing from 0.0004 to 0.0001 in MCF-7, 0.001 to 0.0002 in T47D, 0.0005 to 0.0001 in MDAMB-231, 0.001 to 0.0005 in MDAMB-468 and 0.001 to 0.0001 in MDAMB-436 cells. Radiobiologic parameters including α, β, and α/β ratios are summarised in Table 3.9.

Treatment with AQ4N increased the α-value in all cell lines, but significant increase was only noted in MCF-7 (*P*=0.050) and T47D (*P*=0.019) cells (Table 3.9). Such data suggest that AQ4N marginally increases

radiosensitivity in MCF-7, MDAMB-231, MDAMB-468 and MDAMB-436 cells, with greater radiosensitivity observed in the T47D cells.

Table 3.9 Radiobiologic parameters of 2D breast cancer cells treated with IR and/or AQ4N.

Cell line Normoxia	α (Gy^{-1})	β (Gy^{-2})	α/β (Gy)	SF2	SER $_{(0.01)}$
MCF-7					
IR	0.14±0.05	0.10±0.00	1.40±0.55	0.50±0.04	
AQ4N+IR	0.32±0.10	0.09±0.01	3.58±1.52	0.36±0.05	1.17±0.06
t test	***P*=0.050**	*P*=0.455	*P*=0.080	***P*=0.024**	
T47D					
IR	0.23±0.23	0.07±0.02	4.40±5.35	0.44±0.10	
AQ4N+IR	0.85±0.15	0.02±0.01	32.72±19.54	0.16±0.04	1.64±0.27
t test	***P*=0.019**	*P*=0.043	*P*=0.072	***P*=0.013**	
MDAMB-231					
IR	0.42±0.19	0.06±0.02	7.50±4.73	0.33±0.10	
AQ4N+IR	0.66±0.02	0.06±0.02	12.15±6.87	0.20±0.04	1.29±0.28
t test	*P*=0.174	*P*=0.904	*P*=0.389	*P*=0.125	
MDAMB-468					
IR	0.40±0.06	0.06±0.01	6.85±2.79	0.34±0.02	
AQ4N+IR	0.55±0.01	0.04±0.01	13.95±7.25	0.27±0.03	1.11±0.44
t test	*P*=0.094	*P*=0.172	*P*=0.189	*P*=0.068	
MDAMB-436					
IR	0.50±0.24	0.05±0.00	10.26±3.05	0.30±0.03	
AQ4N+IR	0.65±0.24	0.04±0.03	24.81±28.02	0.23±0.07	1.19±0.12
t test	*P*=0.366	*P*=0.932	*P*=0.422	*P*=0.252	

Statistical significance was determined by Student's *t*-test. The *P*-values are bold where they are ≤ 0.05. Abbreviations: IR, irradiation; $SER_{0.01}$, sensitiser enhancement ratio at 1% survival; SF2, surviving fraction at 2Gy.

Radiosensitivity induced by AQ4N in 2D normoxia was substantially lower than that observed in 3D spheroid cultures, suggesting that the radiosensitising effect of AQ4N is more reliant on hypoxia. In 2D normoxia, only marginal radiosensitisation was observed in the normal MCF-10A cells, with an $SER_{0.01}$ of 1.15 suggesting that the radiosensitising effect of AQ4N may only be minimal in normal cells. Although further studies are required to confirm such findings, data from these experiments indicate only minimal radiosensitisation in normal cells which offers HAPs a potential therapeutic advantage over the targeting of hypoxic cells. Data for MCF-10A is shown in Appendix B-Figure B10 with radiobiological parameters supplied in Appendix B-Table B6.

3.4.8.2 Effect of KP167 on radiosensitivity – 2D

The SF obtained from KP167–radiation combination experiments in 2D normoxia is presented in Figure 3.20.

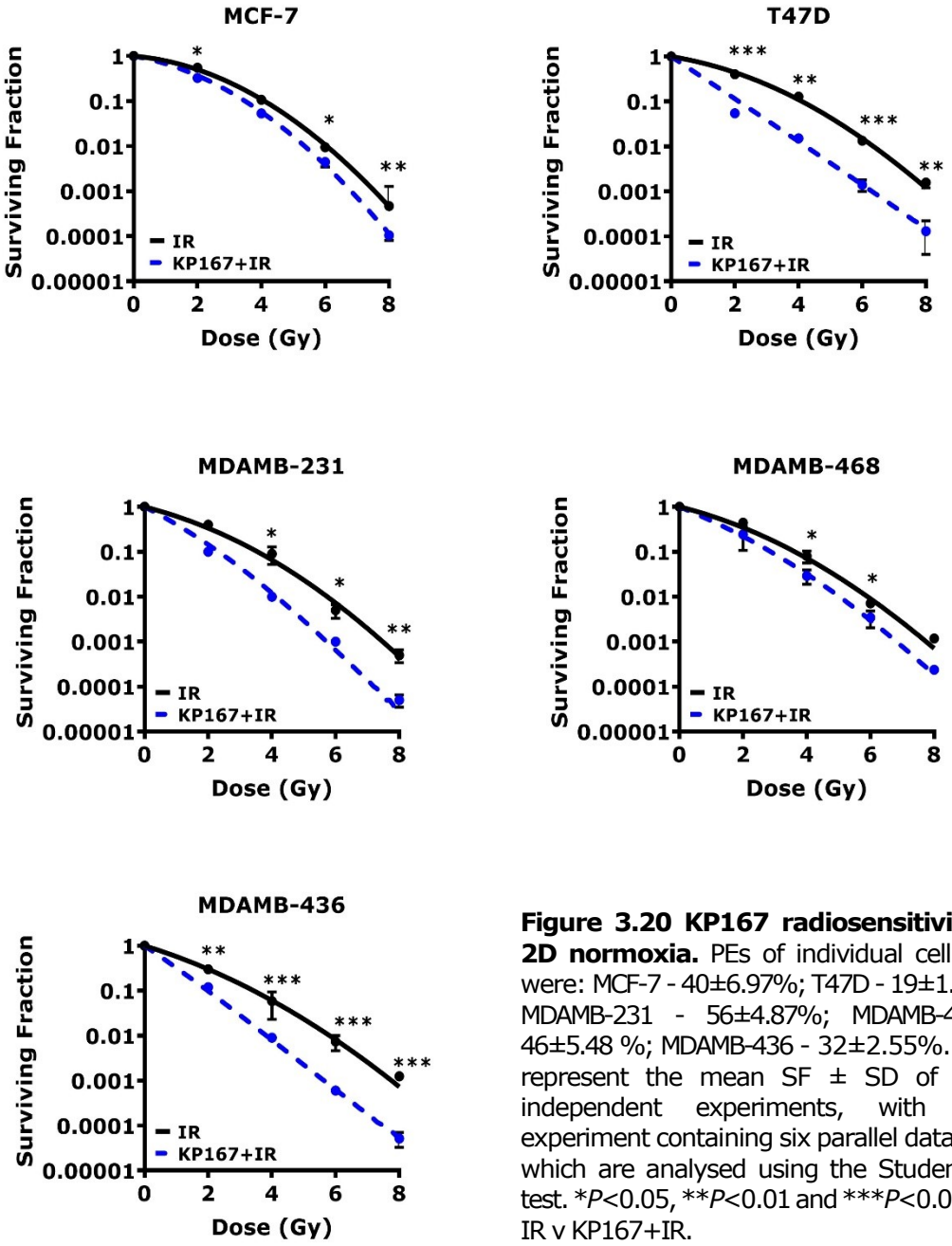


Figure 3.20 KP167 radiosensitivity in 2D normoxia. PEs of individual cell lines were: MCF-7 - 40±6.97%; T47D - 19±1.34%; MDAMB-231 - 56±4.87%; MDAMB-468 - 46±5.48 %; MDAMB-436 - 32±2.55%. Data represent the mean SF ± SD of three independent experiments, with each experiment containing six parallel data sets, which are analysed using the Student's *t*-test. **P*<0.05, ***P*<0.01 and ****P*<0.001 for IR v KP167+IR.

As seen from the graphs, KP167 treatment resulted in significant decrease in the SF2 values in MCF-7 (*P*=0.045), T47D (*P*=0.006), MDAMB-231 (*P*=0.038), MDAMB-468 (*P*=0.043) and MDAMB-436 (*P*=0.00002) cells compared to control cells. Mean SF2 values in control cells were higher i.e. 0.50±0.04 v 0.36±0.06 in MCF-7, 0.44±0.10 v 0.02±0.02 in T47D,

0.33±0.10 v 0.14±0.02 in MDAMB-231, 0.34±0.02 v 0.21±0.06 in MDAMB-468 and 0.23±0.01 v 0.08±0.01 in MDAMB-436 cells compared to KP167 treated cells. Enhanced radiosensitivity was observed with KP167 treatment in all breast cancer cells with $SER_{0.01}$ of 1.21±0.05 in MCF-7, 1.93±0.09 in T47D, 1.43±0.46 in MDAMB-231, 1.32±0.19 in MDAMB-468 and 1.68±0.08 in MDAMB-436 cells. Compared to control cells, KP167 treatment decreased SF8 of breast cancer cells from 0.0004 to 0.0001 in MCF-7, 0.001 to 0.0001 in T47D, 0.0005 to 0.00005 in MDAMB-231, 0.001 to 0.0002 in MDAMB-468, and 0.001 to 0.00005 in MDAMB-436 cells. Some of the radiobiologic parameters are summarised in Table 3.10.

Table 3.10 Radiobiologic parameters of 2D breast cancer cells treated with IR and/or KP167.

Cell line Normoxia	α (Gy^{-1})	β (Gy^{-2})	α/β (Gy)	SF2	$SER_{(0.01)}$
MCF-7					
IR	0.14±0.05	0.10±0.01	1.40±0.55	0.50±0.04	
KP167+IR	0.29±0.13	0.10±0.02	3.04±2.16	0.36±0.06	1.21±0.05
t test	*P*=0.148	*P*=0.778	*P*=0.270	***P*=0.045**	
T47D					
IR	0.23±0.23	0.05±0.01	5.12±3.82	0.44±0.10	
KP167+IR	1.07±0.12	0.01±0.01	175.47±79.57	0.02±0.02	1.93±0.09
t test	***P*=0.005**	***P*=0.005**	***P*=0.020**	***P*=0.006**	
MDAMB-231					
IR	0.42±0.19	0.06±0.02	7.50±4.73	0.33±0.10	
KP167+IR	0.84±0.16	0.06±0.03	21.75±23.00	0.14±0.02	1.43±0.46
t test	***P*=0.050**	*P*=0.991	*P*=0.352	***P*=0.038**	
MDAMB-468					
IR	0.40±0.06	0.06±0.01	6.85±2.79	0.34±0.02	
KP167+IR	0.67±0.21	0.04±0.02	19.54±17.57	0.21±0.06	1.32±0.19
t test	*P*=0.108	*P*=0.499	*P*=0.284	***P*=0.043**	
MDAMB-436					
IR	0.64±0.00	0.01±0.00	32.94±7.02	0.23±0.01	
KP167+IR	1.09±0.02	0.03±0.03	71.23±73.24	0.08±0.01	1.68±0.08
t test	***P*<0.00001**	*P*=0.412	*P*=0.271	***P*=0.00002**	

Statistical significance was determined by Student's *t*-test. The *P*-values are bold where they are ≤ 0.05. Abbreviations: IR, irradiation; $SER_{0.01}$, sensitiser enhancement ratio at 1% survival; SF2, surviving fraction at 2Gy.

Treatment with KP167 increased the α-value across all breast cancer cells, but significance was established in T47D (P=0.005), MDAMB-231 (P=0.050) and MDAMB-436 cells (P<0.00001). Increases in α/β ratios were also noted in all breast cancer cells treated with KP167, which indicate that the cell killing induced by KP167 was linear. These results indicate that KP167 is an efficient radiosensitiser across all breast cancer phenotypes even in 2D normoxic conditions. The radiosensitisation achieved with KP167 was higher compared to AQ4N under 2D normoxia. However, lower levels of radiosensitisation were achieved in 2D normoxia compared to 3D spheroid cultures, suggesting that KP167, like AQ4N, is more effective in 3D and reliant on hypoxia. Compiled dose response curves for AQ4N and KP167 in 2D normoxia are given in Appendix B-Figure B11. Compiled $SER_{0.01}$ values of AQ4N and KP167 in both 3D and 2D cultures are presented in Table 3.11.

Table 3.11 Combined $SER_{0.01}$ values of AQ4N and KP167 in 3D spheroids v 2D normoxic cultures.

Cell line	AQ4N (SER $_{0.01}$)		KP167 (SER $_{0.01}$)	
	3D Spheroids	2D Normoxia	3D Spheroids	2D Normoxia
MCF-7	1.30±0.08	1.17±0.06	1.46±0.66	1.21±0.05
T47D	1.58±0.06	1.64±0.27	1.76±0.20	1.93±0.09
MDAMB-231	1.44±0.04	1.29±0.28	2.53±0.06	1.43±0.46
MDAMB-468	1.64±0.08	1.11±0.44	2.28±0.24	1.32±0.19
MDAMB-436	3.33±0.18	1.19±0.12	4.55±0.24	1.68±0.08
MCF-10A	1.36±0.12	1.15	-	-

Abbreviations: $SER_{0.01}$, sensitiser enhancement ratio at 1% survival.

Data from the above experiments indicate that both AQ4N and KP167 are highly effective as radiosensitisers in 3D spheroid cultures compared to radiosensitivity obtained in 2D normoxia, suggesting that the presence of hypoxia may enhance the cytotoxic effects of these agents. Compared to all other cell lines, T47D cells maintained similar levels of radiosensitivity

in both 3D spheroids and 2D normoxic cultures. Higher expression of endogenous reductases such as cytochrome P450 and CYP2W1 in the luminal T47D cells may explain, in part, the increase in drug sensitivity even in the presence of oxygen. Only moderate-marginal increase in radiosensitisation was seen in the normal MCF-10A cells between 2D and 3D cultures, which suggests that the HAPs have greater cytotoxic effect in cancer cells as opposed to normal cells. Future experiments should assess the radiosensitising effect of KP167 in MCF-10A cell lines to determine if similar response is observed. Compared to AQ4N, the radiosensitivity obtained with KP167 was higher in both 3D spheroids and 2D normoxic cultures as seen by greater KP167 $SER_{0.01}$ values. The radiosensitivity obtained with KP167 in TNBC 3D spheroid cultures were greater in comparison to well-established DNA repair inhibitors such as olaparib and KU-55933 investigated in chapter 2. Table comparing $SER_{0.01}$ values of DNA repair inhibitors and HAPs is presented in chapter 4-Table 4.9. Taken together, data from the above experiments indicate that KP167 is an effective anti-cancer agent and a potent radiosensitiser across both luminal and triple negative breast cancer models.

3.5 Discussion

Hypoxia-activated prodrugs are designed to be cytotoxic to hypoxic cancer cells which are largely associated with radiotherapy failure and reduced response to various breast cancer chemotherapeutic agents (Wouters et al., 2007). The newly developed novel AQ4N analogue KP167, binds DNA covalently and functions as a DNA alkylator, in addition to being a TOPO II inhibitor. Such properties in the novel drug suggests that KP167 may be highly effective in the targeting of hypoxic cells, both quiescent and proliferative, as opposed to the parental AQ4N which is cytotoxic only in proliferating cells (Patterson and McKeown, 2000). Therefore, the current study set out to investigate the single-agent and radiosensitising effect of KP167 in 3D and 2D models of breast cancer, with the parental AQ4N used as a comparator.

In the current chapter, the efficacy of the hypoxia-activated prodrugs, AQ4N and KP167 was studied in a 3D spheroid culture system as these

agents require hypoxia to form stable DNA binding cytotoxins (O'Connor et al., 2016). Cells in spheroids grow naturally in a 3D environment, which allows them to interact with other cells, the extracellular matrix and the microenvironment (Kim, 2005, Nunes et al., 2019). Spheroids, similar to tumours, have proliferative cells on the outer layers, and those cells in the inner layers become hypoxic or necrotic (Vinci et al., 2012). The presence of hypoxic and necrotic areas developed as a consequence of oxygen and nutrient gradients, promote growth of aggressive, therapy-resistant and metastatic tumour clones (Kim et al., 2011, Mehta et al., 2012, Kapałczyńska et al., 2018). The presence of acidosis (low intracellular pH) in hypoxic areas of the tumour, which occurs due to a metabolic switch to glycolysis as an energy source in the absence of oxygen, results in a heterogeneous population of metabolically diverse cells in hypoxic v oxic areas of the tumour, with differential response to treatment (Cardone et al., 2005, Eales et al., 2016). Furthermore, the lack of or decreasing levels of oxygen present in a 3D environment decreases radiotherapeutic efficacy (Grimes et al., 2014, Horsman and Overgaard, 2016). For all the aforementioned reasons, the multicellular tumour spheroids are considered as one of the best established 3D models to bridge the gap between the conventional 2D cell cultures and *in vivo* studies (Pampaloni et al., 2007).

In the current study, spheroids were formed using the pellet culture method (Sutherland et al., 1971, Li et al., 2011), which promotes formation of a single spheroid of reproducible size (Vinci et al., 2012). Similar to tumours, hypoxia in spheroid cultures occur over time, with early studies indicating that spheroids <200 μm in diameter contain mostly proliferating and normoxic cells (Mueller-Klieser et al., 1986). Increase in spheroid diameter ~ 200-300 μm results in zonation with proliferating cells on the outer layers, co-existing with hypoxic cells at the core. With an increase in spheroid diameter to ≥500 μm, the formation of hypoxic and necrotic core is frequently observed (Khaitan et al., 2006, Olive et al., 1992, Milotti et al., 2017). Since the presence of hypoxia in 3D cultures were not assessed in the current study, all subsequent experiments utilised spheroids with ≥500 μm in diameter (to ensure hypoxic core), to determine efficacy of the hypoxia-activated prodrugs.

Spheroid formation was straightforward in the luminal MCF-7 and T47D cells which readily formed tight and compact spheroids. One of the reasons for this observation may be due to, luminal cells in general, maintain apical-basal polarity and retain most of the epithelial cell characteristics such as the presence of tight junction protein, E-cadherin, which enables them to maintain cell-cell adhesion and form tight compact structures (Bazzoun et al., 2013). MDAMB-436 cells formed regular spherical structures which were not as compact as those formed by luminal cells. The MDAMB-231 and MDAMB-468 cells formed loose aggregates and required the addition of matrigel to bind cells into a compact structure (Vinci et al., 2012, Tevis et al., 2017). Clinically, the triple negative/basal like breast cancers show unfavourable prognosis and high rates of distant metastasis to visceral organs like the liver, lungs and brain (Bianchini et al., 2016). Therefore, gain of an EMT (epithelial-mesenchyme transition) phenotype is highly characteristic of triple negative cell lines (Sarrio et al., 2008). Moreover, loss of tight junction proteins and gain of mesenchymal markers such as fibronectin, vimentin, and N-cadherin (Sarrio et al., 2008), may be one of the reasons for their inability to form tight and compact structures, compared to luminal cells which retain most of its epithelial characteristics (Guarino et al., 2007, Martin and Jiang, 2009)

It was also noted that the luminal cell lines, MCF-7 and T47D, did not demonstrate an increase in spheroid size compared to the triple negative cell lines, MDAMB-231, MDAMB-468 and MDAMB-436 cells which demonstrated an exponential increase in spheroid size over an 8-day culture. Compared to luminal cancers, the TNBCs are inherently more aggressive and associated with increased risk of local or regional recurrence, as discussed previously (Voduc et al., 2010, Bianchini et al., 2016). They also share similar characteristics to cancer initiating cells that have metabolic plasticity, which allows them to switch between metabolic pathways to cater to the energetic demand for rapid cell growth and survival in harsh conditions (Park et al., 2019). Therefore, compared to luminal cell lines, TNBCs may be better adapted to growing in an oxygen and nutrient deficient microenvironment which might explain the increase in spheroid size observed only in the TNBC cells (Kennecke et al., 2010).

It is important to note that in the above discussed study only the spheroid diameter was assessed, and therefore results have to be interpreted with caution. Future experiments can assess spheroid diameter as well as the cell number/spheroid to identify cells that are sensitive v resistant to growth in a 3D environment. Also, the presence of hypoxia in spheroid cultures may be assessed by staining for hypoxic markers such as pimonidazole, CA9 etc (Voissiere et al., 2017).

The single agent efficacy of AQ4N and KP167 was initially assessed in breast cancer spheroids by treating cells with various concentrations of HAPs before seeding for assessment of clonogenic survival. Clonogenic survival assays demonstrated that AQ4N treatment was cytotoxic with IC_{50} values ranging 0.2-22.8 μM and resulted in a dose-dependent reduction in survival, with varying levels of sensitivity observed between the different breast cancer phenotypes. The more sensitive cell lines to treatment were the luminal MCF-7, T47D and the BRCA-1 deficient MDAMB-436 cells, with lower IC_{50} values compared to the MDAMB-231 and MDAMB-468 cells. Several other studies have also reported that AQ4N induces differential levels of sensitivity, which can range from low - sub μM concentrations, across different cell line models. For example, the IC_{50} values of AQ4N ranged from 0.4 μM in the HT1080 fibrosarcoma cell lines to 28.9 μM in the HCT116 colon carcinoma cells lines (Mehibel et al., 2016).

The MCF-10A human mammary epithelial cell line is a widely used non-tumorigenic cell line model to study normal breast function (Soule et al., 1990). Experiments with MCF-10A cells were included to look for differential effects between normal and cancer cell lines, in response to treatment with AQ4N and KP167. However, due to supply issues with KP167, experiments for MCF-10A cells were only conduced for AQ4N. Data show that MCF-10A cells were sensitive to treatment with AQ4N and demonstrated a dose dependent reduction in cellular survival with IC_{50} value of 8.8 μM, similar to that observed in the luminal MCF-7 cells. It is important to note that in the current study, the MCF-10A cells were formed into spheroids in order to have a hypoxic core. In the presence of hypoxia, AQ4N will undergo reductive activation by CYP enzymes and target hypoxic

cells (Raleigh et al., 1998), which may explain the cytotoxicity observed in the normal MCF-10A 3D cultures.

The novel agent, KP167, with lower IC_{50} (0.14-12.8 μM) concentrations, was more effective in reducing the survival of breast cancer cells compared to AQ4N, and demonstrated a 2-100 fold increase in potency. The MDAMB-468 cells which were the most resistant cell-line to AQ4N treatment (IC_{50} of AQ4N - 22.8 μM), demonstrated a 100-fold increase in sensitivity with KP167 IC_{50} value of 0.2 μM. The reasons for this observation is unclear, but it appears that MDAMB-468 cells are inherently sensitive to agents that target replication. Studies by Tassone et al., 2005 reported similar findings where a 100-fold increase in sensitivity was observed in MDAMB-468 cells treated with docetaxel with IC_{50} values of 0.08 μM compared to 1-5 μM in MCF-7 and BRCA-1 deficient HCC1937 cells (Tassone et al., 2005). As expected, the most sensitive cell-line to KP167 treatment was the BRCA-1 deficient MDAMB-436 cells, with KP167 IC_{50} value of 0.14 μM. The fanconi anaemia (FA)/BRCA pathway is implicated in the repair of chromosomal defects that arise during homologous recombination. Disruption of this pathway due to BRCA-1 mutation, as in the case of MDAMB-436 cells, have been found to result in extreme chromosomal instability and hypersensitivity of these cells to DNA alkylating agents (D'Andrea and Grompe, 2003). The inherent double strand repair deficiency (Farmer et al., 2005, Treszezamsky et al., 2007), along with hypersensitivity to DNA alkylating agents may explain, in part, the increase in sensitivity observed in MDAMB-436 cells to KP167 treatment.

Overall, the increase in KP167 potency observed in breast cancer 3D cultures may be due to its DNA alkylating properties in addition to the double strand breaks induced by TOPO II inhibition. The covalent binding of KP167 to DNA may also enable it to be cytotoxic to even non-proliferating/ quiescent tumour cells. All these properties in the novel agent may increase its cytotoxic effect compared to the parental AQ4N. If time had allowed, it would have been interesting to examine levels of DNA damage induction and repair across the various lines, in response to these agents. Equally, it would have been interesting to have compared effects of AQ4N v KP167 in quiescent cells.

The effects of AQ4N and KP167 in the presence of oxygen were also assessed in 2D breast cancer cells by proliferation and clonogenic survival assays. Data show that both AQ4N and KP167 resulted in a dose dependent reduction in proliferation and clonogenic survival in all breast cancer cell lines. However higher concentrations of HAPs were required to induce 50% cell killing in most cell lines. The triple negative MDAMB-231 and MDAMB-468 cells were resistant to treatment with AQ4N and KP167 and demonstrated the least reduction in survival at 24 hours (MDAMB-231 IC_{50} - >45 μM for AQ4N and KP167; MDAMB-468 IC_{50} - >45 μM for AQ4N and 32 μM for KP167). This finding is in agreement with previous studies which report minimal or no toxicity when AQ4N was tested against the NCI (National Cancer Institute) panel of 60 cell lines in normoxic conditions, where most cell lines had IC_{50} >100 μM (Patterson and McKeown, 2000). In contrast, potent cytotoxicity was observed when AQ4N was bioreduced under hypoxic conditions, which suggests that efficient conversion of the drug into the DNA binding metabolite occurs in the absence of oxygen (Patterson, 1993, Wilson et al., 1996). For example, Mehibel et al., 2009 reported that under normoxic conditions the IC_{50} of AQ4N in macrophages was 40 μM, but gets reduced to 3.9 μM under hypoxic conditions, which suggests that AQ4N is bioreduced at a high rate in hypoxic cells (Mehibel et al., 2009).

Compared to the triple negative cells, the luminal cell lines demonstrated reduced survival with IC_{50} values of (43 and 26) μM in MCF-7 and (<5 and 19.4) in T47D cells for AQ4N and KP167 respectively. A possible explanation for this observation is that the cytochrome P450 family of enzymes which are involved in bioreducing AQ4N and KP167 are active in luminal cell lines as these enzymes are also involved in the metabolism and oxidation of estrogen (Tsuchiya et al., 2005). Therefore, in order to identify if the differential expression of reductases contributes to differential sensitivity observed between the luminal and triple negative cells, the expression of reductases were evaluated by Western blot. Data show that the expression of cytochrome P450 and CYP2W1 were greater in the luminal MCF-7 and T47D cells compared to the TN MDAMB-231, MDAMB-468 and MDAMB-436 cells, which may explain, in part, the

increase in cytotoxicity observed in these cell lines as opposed to the TNBC cells.

As seen with spheroid data, the BRCA-1 deficient MDAMB-436 cells were the most sensitive, even in 2D cultures, with lower IC_{50} values of <5 μM (AQ4N) and <5 μM (KP167). The inherent BRCA-1 deficient nature and sensitivity to alkylating agents, may lead to higher levels of irreparable DNA damage, which may reduce survival in the MDAMB-436 cells (Song et al., 2013, Arun et al., 2015). Furthermore, the expression of CYP2S1, as assessed by Western blot, was greater in the MDAMB-436 cells, which may have increased HAP metabolism, contributing to the increased cytotoxicity observed in these cell lines.

Similar to results obtained in the current study, Manley et al., 2013 reported that the intrinsic sensitivity of cells to AQ4N under normoxia varies widely between cell lines ranging from 3 μM in A549 and U251 cells to 130-160 in FaDu and HT-29 cells. The pancreatic cell lines, BxPC-3 and PC3 cells were insensitive to AQ4N under normoxic conditions even at higher doses of 250 and 500 μM (Manley and Waxman, 2013). While comparing data obtained under normoxia to those obtained using spheroid cultures, both AQ4N and KP167 were more potent to cells in 3D. Such experiments further support previous observations that activation of these agents occur more effectively, and therefore are more cytotoxic to cells, under hypoxic conditions (Albertella et al., 2008, Nishida et al., 2010). Time-permitting, it would have been interesting to determine endogenous expression of cytochrome P450, CYP2S1 and CYP2W1 (endogenous and in response to treatment) in breast cancer 3D spheroid cultures, and compare it to levels obtained in 2D normoxia, to assess if the reductases are expressed differently between the different culture conditions.

AQ4N was also cytotoxic to the normal MCF-10A cells, which demonstrated a reduction in proliferation and clonogenic survival in normoxic cultures with IC_{50} (24 hours) of 34.1±6.5 μM and 10.2±3.5 μM respectively. The response observed in these cell lines were similar to the luminal breast cancer cells. AQ4N has been previously reported to be systemically non-toxic to normoxic cells (Patterson and McKeown, 2000). However, increase in the cytotoxic effects observed in the normal MCF-10A cells to AQ4N,

may be due to an increase in the expression of CYP2W1, as demonstrated by Western blot, which may have resulted in drug activation under normoxic conditions. Moreover the reliability of the MCF-10A cells as 'normal' cell lines has been questioned with studies reporting a basal- like and mesenchymal cancer cell features in these cell lines (Qu et al., 2015, Neve et al., 2006). It is therefore important to assess the effect of AQ4N on another normal breast cell line to further confirm such findings. The response of normal breast cancer cell lines to KP167 treatment may also be assessed in the future. It is also important to assess the *in vivo* safety, tolerability and side effects of single agent KP167 treatment.

Cellular radiosensitivity measures the ability of irradiated cells to produce colonies which determines radioresponse of a particular cell line (Puck and Marcus, 1956). In the current study, breast cancer cells demonstrated only marginal differences in radiation response between 2D and 3D cultures. The luminal MCF-7, T47D and normal MCF-10A cells were more radiosensitive in 3D cultures compared to the BRCA-1 deficient MDAMB-436 cells which demonstrated radioresistance. The triple negative MDAMB-231 and MDAMB-468 cells did not demonstrate any variation in their radiation response between 2D and 3D cultures. Such data suggest that the luminal cells are more radiosensitive in 3D, compared to their 2D counterparts.

However, when comparing the intrinsic radiosensitivity between luminal and triple negative breast cancer cells in 3D, the luminal MCF-7 and T47D cells demonstrated similar levels of radiosensitivity in comparison to the triple negative MDAMB-231 and MDAMB-468 cells (SF2 - 0.26-0.36). This observation contradicts clinical response of breast cancer subtypes to radiation, wherein the luminal cancers are more radiosensitive compared to the triple negative subtype (Wang et al., 2011, Kyndi et al., 2008, Nguyen et al., 2008). The radiation response of *in vivo* tumours are dependent on various biological factors such as, but not limited to, the repair capacity of cells, the level of intracellular sulfhydryls (neutralises free radical DNA damage induced by radiation), the intrinsic radiosensitivity, the number of clonogenic stem cells along with various micro-environmental and host influences such as the presence of oxygen,

pH changes, ability of cells to repopulate after irradiation, cellular kinetics and host immune response (Barendsen, 1987, Bristow et al., 1990). The *in vitro* generated 3D models, although a more accurate representation of *in vivo* tumours compared to 2D monolayer cultures will still lack the complexity of the original tumours, stroma and other cells present in a tumour microenvironment (Kim et al., 2005), which may explain the discrepancies observed between clinical and *in vitro* behaviour of cell lines.

Studies conducted by a previous PhD student in the group (Dr Yimin Zhang) found that the luminal cell line, MCF-7 was more radiosensitive compared to the triple negative MDAMB-231 cells irradiated in 3D 'on top' culture model with matrigel. Such data suggest that the type of *in vitro* 3D culture (+/- matrigel) may also influence the response of cells to radiation. For example, ECM (extracellular matrix) components are mostly used in 3D cultures to provide structural support as in the case of the present study (matrigel used in MDAMB-231 and MDAMB-468 spheroids). However, ECM components consists of, but are not limited to, a wide array of matrix proteins, growth factors, glycoproteins and other secreted proteins. Changes in any of these components have been found to influence cell differentiation, proliferation, survival and response to radio and chemotherapy (Sebens and Schafer, 2012, Bonnans et al., 2014, Langhans, 2018) – all of these indicate that the presence of ECM may alter cell behaviour which may also contribute to the inconsistency in 3D response observed between different studies.

One of the major reasons for failure of radiotherapy in breast cancer is the presence of tumour hypoxia (Graham and Unger, 2018). As mentioned previously, hypoxia is a common occurrence in both carcinoma *in situ* and invasive breast cancers (Hohenberger et al., 1998). Therefore agents that target hypoxia and improve radioresponse offer the possibility to improve local tumour control and reduce metastasis. Using breast cancer cells and *in vivo* animal models of osteolytic breast cancer, Liapis et al., 2016 reported that the hypoxia-activated prodrug TH-302, was able to destroy ~50-90% of hypoxic cancer cells in bone tissue. When used in combination with paclitaxel, TH-302 was found to reduce tumour growth in the mammary gland and bone (common site of breast cancer metastasis)

(Liapis et al., 2016), which indicate that combining a HAP with conventional therapies has the potential to target both the primary tumour as well as its metastatic deposits. Furthermore, promising results from another pre-clinical study demonstrated that in combination with radiation, the HAPs, PR-104 and TH-302 sensitises BRCA-2 knockout mutants to radiation, indicating that these agents have the potential to exploit hypoxia as well as HR defects in breast cancer cells (Hunter et al., 2014). This strategy holds true not only for BRCA-1/2 deficient tumours, but studies report that hypoxic cancer cells demonstrate defective HR pathways, which can be therapeutically exploited to induce greater radiosensitisation (Chan et al., 2008, Chan et al., 2010) .

In the present study, the radiosensitising effect of AQ4N and KP167 was assessed in breast cancer 3D spheroid models. Data indicate that AQ4N resulted in significant radiosensitisation across both the luminal and triple negative breast cancer spheroids with $SER_{0.01}$ ranging (1.30 - 3.33). Such data support the observation made by previous studies which report the radio-enhancing properties of AQ4N (McKeown et al., 1996, Mehibel et al., 2016). For example, studies by Mehibel et al., 2016 reported that the dose required to achieve 10% cell survival in the HT1080 fibrosarcoma in combination with radiation was only 0.38 μM compared to 0.75 μM with single agent AQ4N treatment. In mice models, combined AQ4N-radiation treatment reduced tumour growth by 40% compared to treatment with radiation alone (McKeown et al., 1996, Patterson et al., 2000). DNA damage assays demonstrated that compared to damage induced by radiation alone, a prolonged second peak of DNA damage was observed with combined treatment. This was due to the killing of hypoxic cells by AQ4N (by TOPO II inhibition) which re-entered the cell cycle when the surrounding oxic cells were killed by radiation (Hejmadi et al., 1996). Such data indicate that AQ4N potentiates effects of radiotherapy which may be due to the induction of greater levels of DNA damage compared to damage induced by radiation alone.

In addition to the TOPO-II inhibiting role, KP167 has additional DNA alklyating properties which led to the hypothesis that radiosensitivity observed with KP167 would be comparable, if not greater than AQ4N. Data

show that KP167 induced greater increases in radiosensitivity compared to AQ4N, across all breast cancer spheroids with $SER_{0.01}$ ranging 1.46 - 4.55. Compared to all other radiosensitisers investigated in this thesis, KP167 showed the greatest increase in radiosensitivity (100-fold) in the triple negative MDAMB-231 ($SER_{0.01}$ 2.53), MDAMB-468 ($SER_{0.01}$ 2.28) and MDAMB-436 ($SER_{0.01}$ 4.55) spheroids. A possible explanation for the increase in cytotoxicity may be because TNBC cells in general, are characterised by defects in the double strand DNA repair pathways (Song et al., 2013). Studies show that while MDAMB-436 cells are BRCA-1 mutated, both MDAMB-231 and MDAMB-468 cells are characterised by BRCA-1 allelic loss (Elstrodt et al., 2006). Such findings suggest that the impaired/deficient DNA double strand repair capacity in the TNBC cell lines, along with TOPO II inhibition and DNA alkylation induced by KP167, may have enhanced the cytotoxic effect in TNBCs in response to KP167 treatment.

Clinically, TNBCs are characterised by increased rates of locoregional recurrence (Zhang et al., 2015a), distant metastasis and poor overall survival (Dent et al., 2007, Liedtke et al., 2008). Resistance to radiotherapy is a major factor for local recurrence of breast cancer after breast-conserving therapy (Komoike et al., 2005), with clinical findings indicating greater radioresistance in TNBCs compared to luminal breast cancers, as previously discussed (Lowery et al., 2012). Several studies report that the proportion of hypoxic and necrotic areas are higher in ER-negative tumours in comparison to ER-positive cancers (Hohenberger et al., 1998, Rundqvist and Johnson, 2013). The radiosensitivity obtained with KP167 in the TNBC cells were higher in comparison to well-established radiosensitisers such as KU-55933 ($SER_{0.01}$ 1.60-3.42) and olaparib ($SER_{0.01}$ 1.61-2.35) (which is being clinically assessed as a radiosensitiser in TNBCs (NCT03109080), investigated in chapter 2. Although further studies are required to confirm efficacy of KP167, both *in vitro* and *in vivo*, results from the current study demonstrates that KP167 may be effective as a hypoxia-activated radiosensitiser in breast cancers, especially in the TNBC cells.

As mentioned previously HAPs are designed such that they are minimally or non-toxic in oxygenated cells (Patterson and McKeown, 2000). Current experiments assessing single agent cytotoxicity revealed that the HAPs are anti-proliferative and reduce survival in most breast cancer cells, albeit at high doses. Therefore, in order to investigate if the concentrations that results in 50% cell killing in spheroid cultures could radiosensitise normoxic cells, breast cancer cells grown in 2D normoxia were treated with the IC_{50} doses obtained using spheroid cultures. Data show that in the presence of oxygen, AQ4N induced only marginal increases in radiosensitivity with $SER_{0.01}$ of 1.11 - 1.29 in all, except T47D cells with higher $SER_{0.01}$ of 1.64. As with 3D spheroids, greater increase in radiosensitisation was obtained with KP167 with $SER_{0.01}$ ranging 1.21 - 1.68, with greater increases noted in T47D cells with $SER_{0.01}$ of 1.93. From the data described above and in previous sections, it appears that T47D cells are sensitive to HAP treatment both under 3D and 2D cultures. Apart from higher reductase activity (cytochrome P450 and CYP2W1) in these cell lines, a plausible explanation for this observation may be because T47D cells contain high levels of PgR and are responsive to progestin (Nardulli and Katzenellenbogen, 1988). Studies conducted by Atif et al., 2015 reported that the addition of progesterone enhanced the anti-cancer efficacy of TMZ in glioblastoma cells. Combined therapy of progesterone with TMZ was found to reduce cell proliferation, increase apoptosis and decrease migration of glioblastoma cells (Atif et al., 2015). Progesterone has been found to exert anti-proliferative and apoptotic effects in many cancers including breast (Formby and Wiley, 1999), ovarian (Bu et al., 1997) and endometrial cancers (Medina et al., 2007). This increase in radiosensitivity in T47D cells may be due to high levels of progesterone in these cell lines which somehow enhances efficacy of both AQ4N and KP167, irrespective of oxygen presence. Taken together, results indicate that AQ4N marginally radiosensitises most breast cancer cells in 2D normoxia, while enhanced radiosensitivity was conferred upon KP167 treatment.

Only marginal increase in radiosensitisation was observed with AQ4N in the normal MCF-10A cells with $SER_{0.01}$ of 1.15 in 2D normoxia compared to $SER_{0.01}$ of 1.36 in 3D spheroid cultures. Slight increase in radiosensitivity

observed in 3D, may be due to the presence of hypoxic cells in 3D cultures, which may have resulted in drug activation. Although further experiments are needed to assess the effects of AQ4N and KP167 in normal breast cells, at least from these experiments it appears that AQ4N in combination with radiation may be minimally toxic to normal cells, similar to previously reported studies (Mehibel et al., 2016).

In conclusion, the novel AQ4N analogue KP167, investigated in this study was found to be an effective anti-cancer agent and a potent radiosensitiser across both luminal and triple negative breast cancer phenotypes. The radiosensitivity achieved with KP167 in the triple negative 3D cultures were higher than that achieved with clinically approved agents such as olaparib and well-established radiosensitisers such as KU-55933 and AQ4N. This study provides the first evidence for the use of KP167 as a radiosensitiser in breast cancer. The next chapter examines the efficacy of AQ4N and KP167 on breast cancer cells grown in 2D hypoxia (1% O_2) conditions to assess the effects of HAPs on uniformly hypoxic breast cancer cells.

Conclusions

All the hypothesis postulated at the beginning of this chapter were successfully answered:

AQ4N and KP167 were more potent to breast cancer cells grown in 3D compared to 2D normoxic conditions.

Higher endogenous reductase expression in MCF-7 and T47D may explain the increase in sensitivity of luminal cells to single agent HAP treatment.

Radiosensitivity obtained with AQ4N and KP167 was higher in 3D breast cancer spheroids compared to cells grown in 2D normoxia.

KP167 was a potent radiosensitiser across all breast cancer phenotypes, both under 3D spheroids and 2D normoxia conditions.

Radiosensitivity obtained with KP167 was higher than the parental drug AQ4N, in both culture conditions.

Chapter 4 Hypoxia-activated prodrugs in 2D hypoxia models of breast cancer

4.1 Abstract

Introduction: The novel hypoxia-activated prodrug, KP167, investigated in chapter 3, demonstrates potent radiosensitising effect in 3D models of luminal and triple negative breast cancer cells. The presence of hypoxia in 3D spheroids was presumed to be the reason for the enhancement in cytotoxicity observed in 3D cultures compared to normoxia-grown cells. In order to further investigate the efficacy of the hypoxia-activated prodrugs, the single-agent and radiosensitising effect of KP167 was assessed in breast cancer cells grown in 2D hypoxia culture. The parental drug AQ4N was used as a comparator against its novel analogue, KP167.

Methods: 2D hypoxia experiments were conducted using a HypoxyLab™ benchtop hypoxia workstation, flushed with 1% O_2, 5% CO_2 and 94% N_2 to maintain 1% O_2 levels. 2D monolayer cultures (21% and 1% O_2) of two luminal (MCF-7 and T47D) and three triple negative (MDAMB-231, MDAMB-468 and BRCA-1 deficient MDAMB-436) breast cancer cell lines were chosen as *in vitro* models. The doubling times, plating efficiencies (PEs) and radiation response of breast cancer cells grown in 2D hypoxia (1% O_2 for 48 hours) were initially assessed using cell growth curves and clonogenic assays respectively. The cellular cytotoxicity of single agent AQ4N and KP167 in 2D hypoxia were evaluated using growth curves and clonogenic survival assays. Radiosensitisation was measured by culturing cells under hypoxia for 24 hours, treating them with single agent IC_{50} doses of AQ4N or KP167 for 24 hours, whilst maintaining hypoxia, then subsequently exposing them to single doses (0-8 Gy) of x-rays and examined via clonogenic survival assays.

Results: Compared to 2D normoxia, cells grown in 2D hypoxia had significantly longer doubling times of (19-38 hours normoxia) v (49-117 hours hypoxia) in MCF-7 (P=0.022), T47D (P=0.011), MDAMB-231 (P=0.009) MDAMB-468 (P=0.001) and MDAMB-436 cells (P=0.020). Decreases in PEs between normoxic and hypoxic cells (18-60% normoxia) v (13-43% hypoxia), were observed in MCF-7 (P=0.0007), T47D (P=0.090), MDAMB-231 (P=0.008), MDAMB-468 (P=0.012), and MDAMB-

436 (*P*=0.109) cells. Maintenance of hypoxia was confirmed by assessing CA9 expression by Western blotting.

AQ4N and KP167 treatment was cytotoxic to cells grown in 2D hypoxia and demonstrated a dose dependent reduction in proliferation and clonogenic survival, with lower IC_{50} values compared to 3D spheroid and 2D normoxia cultures (chapter 3). The single agent clonogenic IC_{50} values of AQ4N and KP167 were 5.2±1.9 μM and 4.9±0.95 μM in MCF-7, 2.0±0.1 μM and 2.2±0.49 μM in T47D, 6.1±2.7 μM and 3.4±1.24 μM in MDAMB-231, 9.5±0.8 μM and 4.8±0.31 μM in MDAMB-468, and 0.15±0.03 μM and 0.37±0.01 μM in MDAMB-436 cells respectively.

As expected, hypoxia (1% O_2 for 48 hours) increased radioresistance in MCF-7 (*P*=0.019), T47D (*P*=0.050), MDAMB-231 (*P*=0.002), MDAMB-468 (*P*=0.002) and MDAMB-436 (*P*=0.013) cells, compared to cells grown under normoxia. Hypoxia enhanced radioresistance with $OER_{0.01}$ of 1.69±0.22 in MCF-7, 1.44±0.20 in T47D, 1.55±0.01 in MDAMB-231, 1.53±0.07 in MDAMB-468 and 1.30±0.03 in MDAMB-436 cells.

AQ4N treatment induced significant radiosensitisation of the hypoxic cells in MCF-7 (*P*=0.020), T47D (*P*<0.0001), MDAMB-231 (*P*=0.008), MDAMB-436 (*P*=0.0003), but not in MDAMB-468 cells (*P*=0.225). AQ4N treatment resulted in $SER_{0.01}$ of 1.30±0.08 in MCF-7, 1.74±0.32 in T47D, 1.69±0.11 in MDAMB-231, 1.13±0.10 in MDAMB-468 and 1.94±0.25 in MDAMB-436 cells.

A greater increase in radiosensitisation was observed with KP167 treatment in MCF-7 (*P*=0.032), T47D (*P*=0.001), MDAMB-231 (*P*=0.003), MDAMB-468 (*P*=0.0002) and MDAMB-436 (*P*=0.003) cells. KP167 treatment increased radiosensitivity in all breast cancer cells with $SER_{0.01}$ of 1.56±0.12 in MCF-7, 2.37±0.11 in T47D, 1.75±0.04 in MDAMB-231, 1.72±0.02 in MDAMB-468 and 1.81±0.33 in MDAMB-436 cells.

Conclusions: Data confirms the hypoxia-selective activation of AQ4N and KP167. KP167 shows anti-cancer and potent radiosensitisation in breast cancer 2D hypoxia cultures, and appears to be a promising hypoxia-activated radiosensitiser in breast cancer.

4.2 Introduction

4.2.1 Oxygen effect

Oxygen is a potent radiosensitiser as the presence of molecular oxygen enhances the cytotoxic effects of ionising radiation (Thoday and Read, 1947), known as the oxygen fixation hypothesis (Roots and Smith, 1974, Ewing, 1998). It has been reported that oxygen fixation increases the number of single and double strand breaks in irradiated DNA, providing evidence that the amount of DNA damage produced between oxic v hypoxic cells contributes to the difference in radiosensitivity (Prise et al., 1993). The oxygen effect also causes the mitochondria to produce higher amount of ROS that can indirectly cause additional levels of DNA damage (Richardson and Harper, 2016). This enhancement in radiotherapeutic efficacy (2.5-3-fold) (Rockwell et al., 2009) is only observed when molecular oxygen is present during irradiation (Howard-Flanders and Moore, 1958). The presence of oxygen after irradiation has no effect on radiosensitisation because the essential chemical reactions are completed within a few milliseconds after exposure (Rockwell et al., 2009). The full radiosensitising effect of oxygen is observed at concentrations >3% O_2, while at lower levels of 0.1% O_2 and 1% O_2, a decrease in radiosensitivity occurs (Palcic and Skarsgard, 1984).

4.2.2 HIF-1α and radiotherapy

The ability of hypoxia to alter radioresponse in tumour cells is not only due to the 'oxygen effect', but also because of the ability of HIF-1α to promote expression of genes that allow cell survival under conditions of oxygen deprivation (<10mmHG) (Semenza, 2003, Williams et al., 2005). It is known that reoxygenation occurs in hypoxic tumour cells after radiotherapy (Gregoire et al., 1999). This effect occurs due to a combination of reduced oxygen consumption rate (OCR), brought about by the killing of the more radiosensitive oxygenated tumour cells, along with an increase in oxygen perfusion (Bussink et al., 2000). The expression of HIF-1α is upregulated within 24 hours of radiation exposure and lasts up

to one week post-irradiation (Moeller and Dewhirst, 2006). Figure 4.1 shows HIF-1α mediated effects following irradiation.

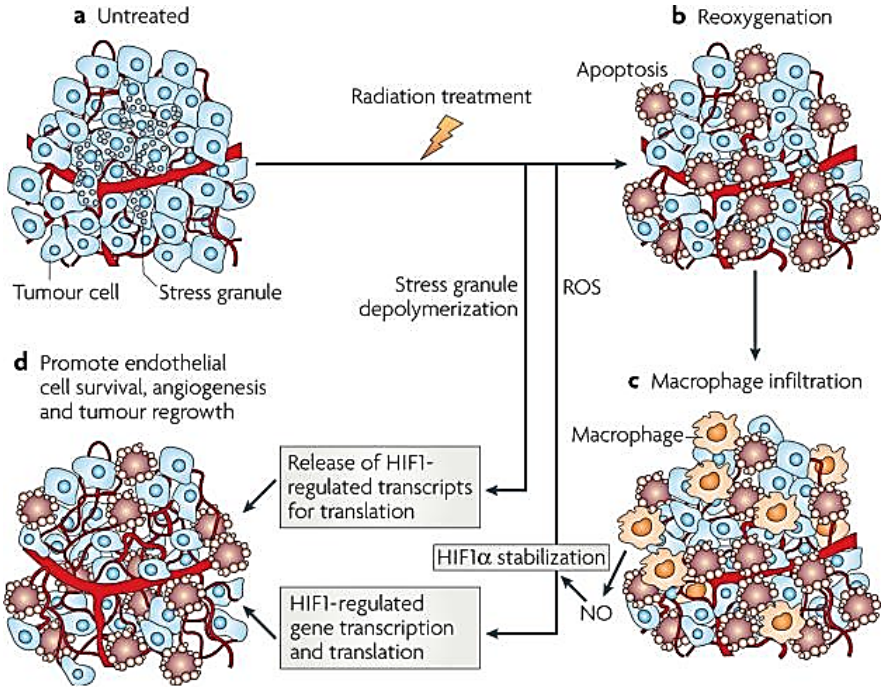


Figure 4.1 HIF-1 mediated effects after radiotherapy. Following reoxygenation of hypoxic cells after radiotherapy, HIF-1α is stabilised by ROS, stress granules and NO released by macrophage infiltration. Stabilised HIF-1α induces expression of genes involved in cell survival, angiogenesis and tumour regrowth. Reproduced from (Dewhirst et al., 2008). Copyright© 2008 Nature Reviews Medicine with permission conveyed through Copyright Clearance Centre.

The ROS and stress granules (molecules released during cellular stress which prevents use of energy for translation) that are produced during irradiation promotes HIF-1α stabilisation after reoxygenation (Kedersha et al., 1999, Moeller et al., 2004). A second peak of HIF-1α stabilisation occurs on day 6-7 post-irradiation, due to macrophage infiltration which releases nitric oxide (NO) (promotes vasodilation and anaerobic metabolism) (Sonveaux, 2017). Once stabilised, HIF-1α can bind to HREs (hypoxia responsive elements) in promoter regions of target genes to upregulate several downstream effectors such as VEGF, plasminogen activator inhibitor-1 (PAI-1), CA9 (assessed as the endogenous marker of hypoxia in the current chapter), glycolytic pathway enzymes etc, all of which contribute to cell survival by promoting angiogenesis, anaerobic glycolysis, and tumour regrowth (Semenza, 2003). HIF-1α mediated activity can also offer protection against oxidative stress, anti-cancer

agents and increase the invasiveness and metastatic potential of cancer cells (Moeller et al., 2004, Dewhirst et al., 2008)

4.2.3 Targeting hypoxia

Over the past 3 decades many techniques (carbogen breathing, radiation sensitisers, blood transfusions, hemoglobin-oxygen affinity modifiers, HIF-1 inhibitors and nicotinamide) were developed in attempts to increase tumour oxygenation and/or target hypoxic cells, several of which were clinically trialled (Overgaard and Horsman, 1996, Brown, 2007). One of the reasons for the lack of success in clinical trials may have been the lack of accurate identification of patient tumours that contain hypoxic cell populations (Hunter et al., 2016). Although clinical trials failed to demonstrate overall benefit, these trials demonstrated that specifically targeting hypoxic tumours significantly improved loco-regional control after radiotherapy. For example, a phase II trial in HNSCC patients comparing tirapazamine plus chemoradiation to chemoradiation alone, showed significant benefit in patients who were identified as having hypoxia using [18F]-misonidazole positron emission tomography. In this study only 1 in 19 patients had a loco-regional failure compared to 8 out of 13 patients who received only chemoradiation (Rischin et al., 2006). Bhandari et al., 2019 quantified hypoxia in ~8000 tumours across 19 cancers and reported that hypoxic tumours were characterised by extreme genomic instability, copy number alterations, TP53 mutations, allelic loss of PTEN, dysregulated miRNA profiles etc. Such hypoxia-associated mutational signatures will aid in the development of biomarkers and identify patients that may benefit from hypoxia-driven therapy (Bhandari et al., 2019). For example, promising results were obtained in the DAHANCA trial which used a 15-gene hypoxic signature (Toustrup et al., 2011) to classify head and neck cancer patients into 'more' hypoxic and 'less' hypoxic groups - the use of nimorazole increased loco-regional control from 18 to 49% only in patients classified into the 'more' hypoxic group (Toustrup et al., 2012).

An alternative approach is to reduce the oxygen demand by decreasing the OCR in hypoxic cells, which may be a more effective strategy compared to

previous methods aimed at increasing oxygen delivery (Lin and Maity, 2015). Metformin, used in the treatment of diabetes, is the only FDA approved agent that was shown to reduce hypoxia and OCR in tumours. However, at pharmacological concentrations, only a 20-30% reduction in OCR was observed (Zannella et al., 2013, Wheaton et al., 2014). The anti-malarial drug atovaquone, was found to reduce hypoxia by decreasing the OCR (by inhibition of mitochrondrial complex III) in colorectal and lung cancer spheroids (Ashton et al., 2016). In combination with radiation, atovaquone caused a significant growth delay in nude mice models and this agent has recently completed clinical evaluation with results to follow (NCT02628080). Other strategies that have shown great promise in targeting hypoxia includes exploiting the HR-deficiency in hypoxic cells (contextual synthetic lethality) by treatment with the PARP inhibitor, olaparib. In combination with radiation, olaparib was found to increase levels of unrepaired DNA double strand breaks and apoptosis in hypoxic NSCLC cells with no significant effect on DNA damage in non-hypoxic cells (Jiang et al., 2016). A phase I study with 21 advanced non-small cell lung carcinoma patients reported that the phosphoinositide 3-kinase (PI3K) inhibitor, buparlisib in combination with thoracic radiotherapy was well tolerated in patients and decreased hypoxia by 20% in 10 out of 15 patients (67%) (McGowan et al., 2019). Pre-clinical evaluation of the HAP, CH-01, a CHK1/Aurora A inhibitor has been reported to reduce survival in colon carcinoma cancer cells exposed to hypoxia, with minimal effect in oxygenated cells (Cazares-Korner et al., 2013).

Because of the significant impact hypoxia causes to anti-cancer therapies and patient survival, there is an urgent need to develop agents that target hypoxia to improve response. Thus, several hypoxia-targeting agents are in various stages of pre-clinical and clinical development. Data from chapter 3 shows the potent radiosensitising effect of KP167 in breast cancer 3D cultures, indicating that this agent may hold promising potential as a hypoxia-activated radiosensitiser. In order to further confirm the hypoxia-specific activation of KP167, the efficacy of this agent was assessed in breast cancer 2D hypoxia cultures.

4.2.2.1 2D hypoxia culture

One of the simplest ways to study the effects of hypoxia is in a 2D cell culture system with modifiable oxygen levels to reduce oxygen concentrations ranging 0.1%-1%. This method is advantageous to study the effects of reduced oxygen levels in 2D grown cells. A range of information such as the effect of hypoxia on cell proliferation, cell survival, gene and protein expression and response to chemo and radiotherapy can be gauged and interpreted (Leek et al., 2016). In the current study, 2D hypoxia experiments were conducted using the HypoxyLab™ hypoxia incubator from Oxford Optronix. It is a bench-top work station that mimics *in vivo* oxygen state by precisely controlling levels of oxygen, carbon dioxide, temperature and humidity to achieve accurate hypoxic conditions (Hypoxylab™, 2020).

4.2.4 Hypothesis and aims

It has been well-established that most breast cancers contain hypoxic cells that influence the response of tumours to radiotherapy. As demonstrated in chapter 3, KP167 was found to be a potent radiosensitiser in breast cancer 3D spheroid models. It was speculated that the presence of hypoxic cell populations in 3D spheroids (≥500 µM in diameter) (Khaitan et al., 2006, Riffle and Hegde, 2017) may have been a main reason for the increased effectiveness in 3D cultures compared to 2D normoxic culture. In order to further investigate the efficacy of these agents under hypoxia, the current chapter investigates the effects of KP167 in 2D hypoxia-cultured breast cancer cells. The hypothesis framed in the current chapter was that KP167 is a potent hypoxia-activated radiosensitiser across luminal and triple negative breast cancer cells. It was also hypothesised that radiosensitisation obtained with KP167 will be greater than that achieved with the parental drug, AQ4N. The efficacy of AQ4N and KP167 were assessed in two luminal (MCF-7 and T47D) and three triple negative (MDAMB-231, MDAMB-468 and BRCA-1 deficient MDAMB-436) breast cancer cell lines.

Hypotheses

1. Hypoxia (0.5% and 1% O_2) increases radioresistance in MDAMB-231 cells, with 0.5% inducing greater resistance than 1%.
2. Hypoxia (1% O_2) alters proliferation and clonogenic survival in luminal and triple negative breast cancer cells.
3. Single-agent AQ4N and KP167 treatment is cytotoxic to breast cancer cells grown in hypoxic conditions (1% O_2), with the level of cytotoxicity greater than when cells are cultured under normoxia.
4. Exposure to 1% O_2 increases radioresistance of both luminal and triple negative breast cancer cells.
5. AQ4N and KP167 are highly effective hypoxic radiosensitisers in 2D breast cancer cultures (1% O_2) with radiosensitisation greater under hypoxia than normoxia.
6. Radiosensitisation achieved with KP167 will be greater than AQ4N in both luminal and triple negative breast cancer models.

Aims

- To identify the optimal concentration of oxygen for 2D hypoxia experiments, by assessing radioresponse in the representative breast cancer cell line, MDAMB-231, cultured in various hypoxic conditions (0.5% and 1% O_2). Response was compared to those obtained under 2D normoxia (21% O_2) cultures.
- To confirm presence of hypoxia (1% O_2) by assessing CA9 expression in luminal and triple negative breast cancer cells.
- To investigate the influence of hypoxia (1% O_2) on proliferation and clonogenic survival of breast cancer cells and compare it to results obtained with 2D normoxia culture conditions.
- To assess single agent anti-cancer effect of KP167 and AQ4N in luminal and triple negative breast cancer cells in 2D hypoxia (1% O_2) and compare it to results obtained with 2D normoxia culture conditions.
- To compare radioresponse between 2D hypoxia (1% O_2) and 2D normoxia cultures.

- To investigate KP167 as a radiosensitiser in 2D hypoxic breast cancer cells and compare results against the parent drug AQ4N, and to results obtained with 2D normoxic culture conditions.

4.3 Materials and Methods

4.3.1 Cell lines and culture conditions

The luminal breast cancer cell lines, MCF-7 and T47D, TNBC cell lines, MDAMB-231, MDAMB-468 and MDAMB-436, and the normal mammary epithelial cell line, MCF-10A were used in the current study to assess response to AQ4N and KP167 treatment. Culture conditions and media recipes have been described in detail in Appendix A-Table A1 and Table A2 for MCF-7, T47D, MDAMB-231, MDAMB-468 and MDAMB-436 cells and in Appendix B-Table B1 and Table B2 for MCF-10A cells. Experiments with MCF-10A were carried out by Martina Quartieri under my supervision. Experiments with MCF-10A were completed only for AQ4N, due to lack of KP167 supply. Therefore all AQ4N data for this cell line is presented in Appendix C.

4.3.2 Drugs and drug preparation

AQ4N and KP167 were reconstituted and used as described in section 3.3.2.

4.3.3 Radioresponse in 0.5% and 1% O_2

In order to identify the O_2 concentration for 2D hypoxia experiments, that was non-cytotoxic, but still induced radioresistance, MDAMB-231 cells were used as a representative breast cancer cell line to assess radioresponse between the three different hypoxia conditions i.e. 0.5% O_2 for 24 hours and 1% O_2 for either 24 or 48 hours. For hypoxia experiments, $4x10^5$ MDAMB-231 cells were seeded into T-25 cm^2 tissue culture flasks and allowed to adhere in a normoxic incubator (21% O_2) for 3 hours. Following which, cells for hypoxia experiments were placed in a HypoxyLab™ hypoxia work station (Oxford Optronix) for 24 or 48 hours. The work station was continuously flushed with 0.5% O_2, 5% CO_2 and 94.5% N_2 to maintain

0.5% O_2 levels and with 1% O_2, 5% CO_2 and 94% N_2 to maintain 1% O_2 levels. Parallel experiments were also carried out in 2D normoxic (21% O_2) cells (section 2.3.7) to compare radioresponse between 2D normoxia and 2D hypoxia culture conditions. After normoxia/hypoxia incubation for either 24 hours and/or 48 hours, cells were immediately irradiated with a single dose of 2, 4, 6, or 8 Gy (cells with sham irradiation were set as 0 Gy). After irradiation, cells were trypsinized, counted using haemocytometer and serially diluted with complete medium to appropriate concentrations and plated into T-25 cm^2 tissue culture flasks for the conventional 2D clonogenic assays as described in section 2.3.6. SF of radiotherapy experiments were calculated as described in section 2.3.8. The OER, defined as the ratio of radiation doses in oxic and hypoxic conditions which produce the same biological effect (Hall and Cox, 2010), was used to assess difference in radioresponse between oxic v hypoxic cells. OER was calculated at 1% survival as follows-

$$\text{OER} = \frac{\text{Radiation dose in hypoxia to give 1\% SF}}{\text{Radiation dose in normoxia to give 1\% SF}}$$

4.3.4 Western blotting for CA9

CA9 is upregulated in hypoxic conditions and is often used as an endogenous marker to assess hypoxia in cells (Olive et al., 2001). In order to confirm presence of hypoxia by CA9 expression, lysates from hypoxic (1% O_2 for 48 hours) and normoxic (21% O_2 for 48 hours) cells were obtained as described in section 3.3.8 and Western blot was performed as described in section 3.3.9. The antibodies used are listed in Table 4.1.

Table 4.1 List of antibodies used in Western blot.

Antibodies	Host species	Dilution	Molecular Weight (kDA)	Catalogue Number	Source
Anti-CA9	Mouse	1:1000	49	ab00414-1.1	2BScientific
Anti-β-actin	Rabbit	1:2000	42	ab8227	Abcam
Rabbit anti-mouse HRP	Rabbit	1:1000	-	P0260	Dako
Goat anti-rabbit HRP	Goat	1:1000	-	P0448	Dako

Following SDS-PAGE, membranes were blocked for one hour in 0.05% PBS-Tween-20 containing 5% non-fat milk and probed with primary antibody for CA9 at 4°C overnight. Membranes probed with the primary antibody for β-actin was used as a loading control. The following day, membranes were probed with the appropriate (horse radish peroxidase (HRP)-conjugated) antibody (DAKO), and incubated for 1 hour at room temperature. After incubation, the membranes were washed for 3 x 5 minutes in 0.1% PBS/Tween and blots were developed using the Enhanced Chemiluminescence (ECL) detection method (Amersham). The chemiluminescence of the membrane was detected using Image Studio Version 4.1 (LI-COR Biosciences) by exposing membranes for 30 seconds to 2 minutes depending on the intensity of the signal. CA9 expression was assessed in three independent experiments, with separate cell lysates obtained from different passage numbers of cells.

4.3.5 Cell growth - 2D normoxia v 2D hypoxia

The effect of hypoxia (1% O_2) on proliferation of breast cancer cells were assessed by monitoring growth of cells for 0-96 hours. $1x10^5$ cells/well were seeded in triplicate in 6-well culture plates and allowed to adhere at 37°C, 5% CO_2 for 3 hours in a normoxic incubator. Following which, cells for hypoxia experiments were placed in a HypoxyLab™ hypoxia work station as described in section 4.3.3. Parallel experiments were conducted in 2D normoxic cells to compare cell proliferation against hypoxic cells. For control 2D normoxia experiments, cells were seeded as described above and allowed to remain in the normoxic incubator for (0-96) hours. At different time points of 24, 48, 72 and 96 hours, control 2D normoxic cells and 2D hypoxic cells were washed with PBS and detached using 500 µl of trypsin-EDTA (section 2.3.2). Once detached, cells were resuspended in a further 500 µl of complete medium. Cell counts were performed in duplicate using a haemocytometer. Cell counts were recorded and growth curves constructed by plotting average number of cells versus time (hours) on y- and x-axis respectively to identify doubling time of cells. Data represent the average cell number ± SD of three independent experiments.

4.3.6. Plating efficiencies - 2D normoxia v 2D hypoxia

The PEs of breast cancer cells grown in 1% O_2 (48 hours) were assessed to investigate if hypoxia affects the colony forming potential of breast cancer cell lines. To compare PE between normoxia and hypoxia conditions, cells from the above proliferation assay (section 4.3.5) were counted and serially diluted with complete medium to appropriate concentrations. Cells were plated into T-25 cm^2 tissue culture flasks for conventional 2D clonogenic assay as described in section 2.3.6. PE was calculated as described in section 2.3.6. Data represent the mean PE ± SD of three independent experiments, with each experiment containing six parallel sets.

4.3.7 Cytotoxicity assessment of AQ4N and KP167 - 2D hypoxia

4.3.7.1 Proliferation assay

Proliferation assays were carried out to assess the anti-proliferative effect of AQ4N and KP167 on breast cancer cells grown in 2D hypoxia (1% O_2). $1x10^5$ cells/well were seeded in triplicate in 6-well culture plates and incubated in the normoxic incubator for 3 hours to allow cell adherence. Following attachment, cells were transferred into the HypoxyLab™ hypoxia work station maintained at 1% O_2 for 24 hours and treated with various concentrations of AQ4N (0.01-10) µM or KP167 (0.15-10) µM for a further 24 hours under hypoxia. Following HAP treatment, cells in each well were harvested and cell count was performed using a haemocytometer (cells were collected and seeded for clonogenic survival assays - section 4.3.7.2). The dose-response curves were constructed by plotting average percentage of cells versus drug concentration (µM) on y- and x-axis respectively. The IC_{50} doses were calculated where possible. Data presented graphically represent the average percentage of cells ± standard deviation (SD) of three independent experiments.

4.3.7.2 Clonogenic survival assay

Hypoxic conditioned cells treated with various concentrations of AQ4N or KP167 were collected from the above described proliferation assays

(section 4.3.7.1) and seeded for assessment of clonogenic survival as described in section 2.3.6. IC_{50} doses were calculated for AQ4N and KP167. Data represent the mean SF ± SD of three independent experiments for AQ4N and two independent experiments for KP167, with each experiment containing six parallel sets.

4.3.8 Cell irradiation - 2D normoxia v 2D hypoxia

The radioresponse of breast cancer cells when grown as 2D normoxia v 2D hypoxia were assessed in order to investigate the difference in radiosensitivity between the two culture conditions. For hypoxia experiments, $4x10^5$ breast cancer cells were seeded into T-25 cm^2 tissue culture flasks and allowed to adhere in a normoxic incubator for 3 hours. Following which, cells for hypoxia experiments were incubated in a hypoxia work station (HypoxyLab™) for 48 hours, which was maintained at 1% O_2. Flasks were always examined to ensure that cells were still sub-confluent and in the logarithmic growth phase. Following hypoxic exposure of 48 hours, a flask of cells was used immediately to conduct Western blot analysis of CA9 expression to confirm hypoxia (as described in section 4.3.4). Parallel experiments were conducted in 2D normoxic cells as described in section 2.3.7. After normoxia/hypoxia incubation for 48 hours, cells were irradiated at a single dose of 2, 4, 6, or 8 Gy (cells with sham irradiation were set as 0 Gy) and seeded for assessment of clonogenic survival. Survival data was processed as described previously (section 2.3.8). Data represent the mean SF ± SD of three independent experiments, with each experiment containing six parallel sets.

4.3.9 Drug-radiation combinations - 2D hypoxia

To assess the effects of AQ4N and KP167 on radiosensitivity of cells grown in 2D hypoxia, $4x10^5$ breast cancer cells were seeded into T-25 cm^2 tissue culture flasks and allowed to adhere in a normoxic incubator for 3 hours. Cells were transferred into the HypoxyLab™ hypoxia work station maintained at 1% O_2 for 24 hours, prior to treatment with the clonogenic IC_{50} of AQ4N or KP167 for a further 24 hours in 1% O_2. Following drug treatment, cells were irradiated at single doses of 2, 4, 6 or 8 Gy. Sham

irradiated cells were used as controls. After irradiation, cells were immediately plated and survival data was processed as described previously (section 2.3.8). Western blot analysis of CA9 expression was performed after 48 hours of hypoxic exposure to confirm hypoxia (as described in section 4.3.4). Data represent the mean SF ± SD of three independent experiments for AQ4N and two independent experiments for KP167, with each experiment containing six parallel sets.

4.3.10 Statistical analysis

Statistical analyses were conducted using GraphPad Prism 7 software. Data is represented as mean ± SD of two or three, as indicated, independent experiments with each performed in triplicate. For comparing two variables, the Student's *t*-test was used. *P* value < 0.05 were considered to be statistically significant. Errors from individual experiments were calculated as described in section 2.3.10.

4.4 Results

4.4.1 Radioresponse with 0.5% and 1% O_2

To identify the optimal oxygen concentration for 2D hypoxia experiments, MDAMB-231 cells were grown in 0.5% O_2 for 24 hours and 1% O_2 for 24 and 48 hours, then irradiated before seeding for assessment of clonogenic survival. Parallel experiments were carried out on cells grown in 2D normoxia (21% O_2) to compare and contrast radiosensitivity obtained with hypoxic cultures. The resultant survival curves, fitted using the linear quadratic (LQ) model, are shown in Figure 4.2.

SF2 and $OER_{0.01}$ values were used to compare radiation response between the different treatment conditions and are shown, along with other radiobiologic parameters including α, β, and α/β ratios in Table 4.2. MDAMB-231 cells exposed to the different hypoxic conditions demonstrated significant radioresistance compared to cells grown in normoxia. The SF2 values in 2D normoxic cells were 0.25±0.02 compared to 0.58±0.09 (P=0.004) in 0.5% O_2 (24 hours), 0.61±0.01 (P=0.035) in 1% O_2 (24 hours) and 0.55±0.01 (P=0.002) in 1% O_2 (48 hours). Hypoxic

exposure increased radioresistance with OERs at 1% survival ($OER_{0.01}$) of 1.66±0.11 in 0.5% O_2 (24 hours), 1.40±0.06 in 1% O_2 (24 hours) and, 1.62±0.38 in 1% O_2 (48 hours).

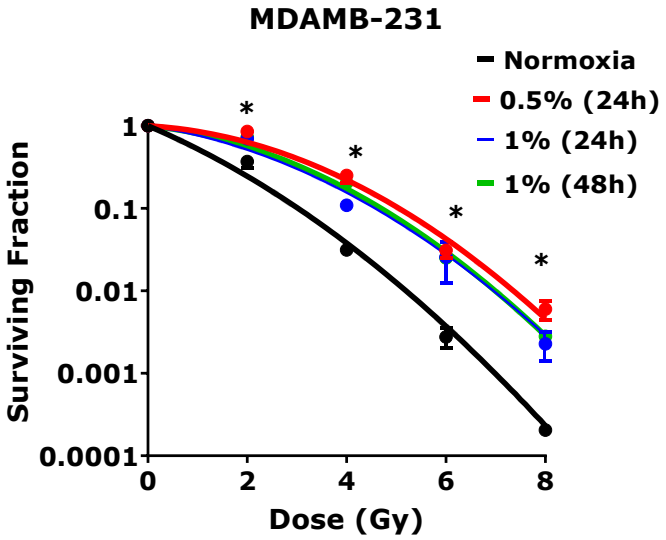


Figure 4.2 Radioresponse of MDAMB-231 cells in 2D normoxia v 2D hypoxia (0.5 and 1% O_2). Radiation survival curves were fitted to LQ model. PEs of MDAMB-231 cell lines were 56±4.0% in 21% O_2, 32±9.4% in 0.5% O_2 (24h), 61±3.7% in 1% O_2 (24h) and 43±2.6% in 1% O_2 (48h). Data represent the mean SF ± SD of three independent experiments, with each experiment containing six parallel data sets which are analysed using the Student's t-test. *P<0.05 for normoxia v hypoxia.

Table 4.2 Radiobiologic parameters of breast cancer cells in 2D normoxia and 2D hypoxia cultures (0.5% and 1% O_2).

Cell line	α (Gy^{-1})	β (Gy^{-2})	α/β (Gy)	SF2	$OER_{(0.01)}$
Normoxia	0.56±0.06	0.06±0.01	9.58±2.85	0.25±0.02	
0.5% Hypoxia (24h) *t*test	0.10±0.06 ***P*<0.001**	0.07±0.01 *P*=0.198	1.48±0.83 ***P*=0.009**	0.58±0.09 ***P*=0.004**	1.66±0.11
1% Hypoxia (24h) *t*test	0.24±0.05 ***P*=0.004**	0.06±0.01 *P*=0.798	3.69±0.91 *P*=0.191	0.61±0.10 ***P*=0.035**	1.40±0.06
1% Hypoxia (48h) *t*test	0.14±0.01 ***P*=0.002**	0.07±0.01 ***P*=0.02**	1.98±0.01 ***P*=0.001**	0.55±0.01 ***P*=0.002**	1.62±0.38

Statistical significance was determined by Student's *t*-test. The *P*-values are bold where they are ≤ 0.05. Abbreviations: IR, irradiation; $OER_{0.01}$, oxygen enhancement ratio at 1% survival; SF2, surviving fraction at 2Gy.

Such $OER_{0.01}$ values equate to the SF8 of MDAMB-231 cells increasing 10-fold from 0.0002 to 0.005 in 0.5% O_2, 0.0002 to 0.002 in 1% O_2 (24 hours) and 0.0002 to 0.003 in 1% O_2 (48 hours) compared to normoxic (21% O_2) cells. The data confirms the ability of hypoxia to induce radioresistance in breast cancer cells. Since no significant difference in radioresponse was observed between 0.5% (24 hours) and 1% O_2 (48 hours) (P=0.954), all subsequent experiments were carried out at 1% O_2 for 48 hours.

A significant decrease in the α-value of MDAMB-231 cells grown in 0.5% O_2 (24 hours) (P<0.001), 1% O_2 (24 hours) (P=0.004) and 1% O_2 (48 hours) (P=0.002) was observed, which led to a decrease in the α/β ratio. The decreased α-value and α/β ratios reflects that the absence of oxygen allows radiation-induced DNA damage to be more easily repaired, contributing to radioresistance (Skarsgard and Harrison, 1991, Dasu and Denekamp, 1998, Rockwell et al., 2009).

4.4.2 Cell growth curves in 2D normoxia v 2D hypoxia

Hypoxia has been shown to inhibit proliferation in a variety of tumour cell types, and the role of HIF-α as a direct inhibitor of replication has been published previously (Hubbi et al., 2013). Therefore, the effect of hypoxia (1% O_2) on proliferation of breast cancer cells were initially assessed by monitoring growth of cells for a period of 0-96 hours and comparing response to those obtained in 2D normoxia. Doubling times in normoxic v hypoxic conditions were obtained from cell growth curves plotted using cell counts and presented in Figure 4.3.

The expression of CA9 was present in all breast cancer cells exposed to hypoxia and absent in cells grown in normoxic culture conditions, confirming a hypoxic response as seen in Figure 4.3. Marginal decreases in breast cancer cell proliferation were noted at 48 hours of hypoxic exposure, following which a significant reduction in proliferation was noted at 72 and 96 hours in all cell lines. Compared to 2D normoxia, cells in 2D hypoxia had significantly longer doubling times of 31.5±1.1 v 52.2±0.5 (P=0.002) in MCF-7, 33.1±8.9 v 117.4±66.2 (P=0.011) in T47D, 19.1±3.3 v 49.0±10.5 (P=0.009) in MDAMB-231, 33.5±4.6 v 57.4±1.2 (P=0.001)

in MDAMB-468 and 38.2±5.7 v 109.1±32.3 (P=0.020) hours in MDAMB-436 cells. Tabulated doubling time of breast cancer cells under normoxia and hypoxic is presented in Table 4.3.

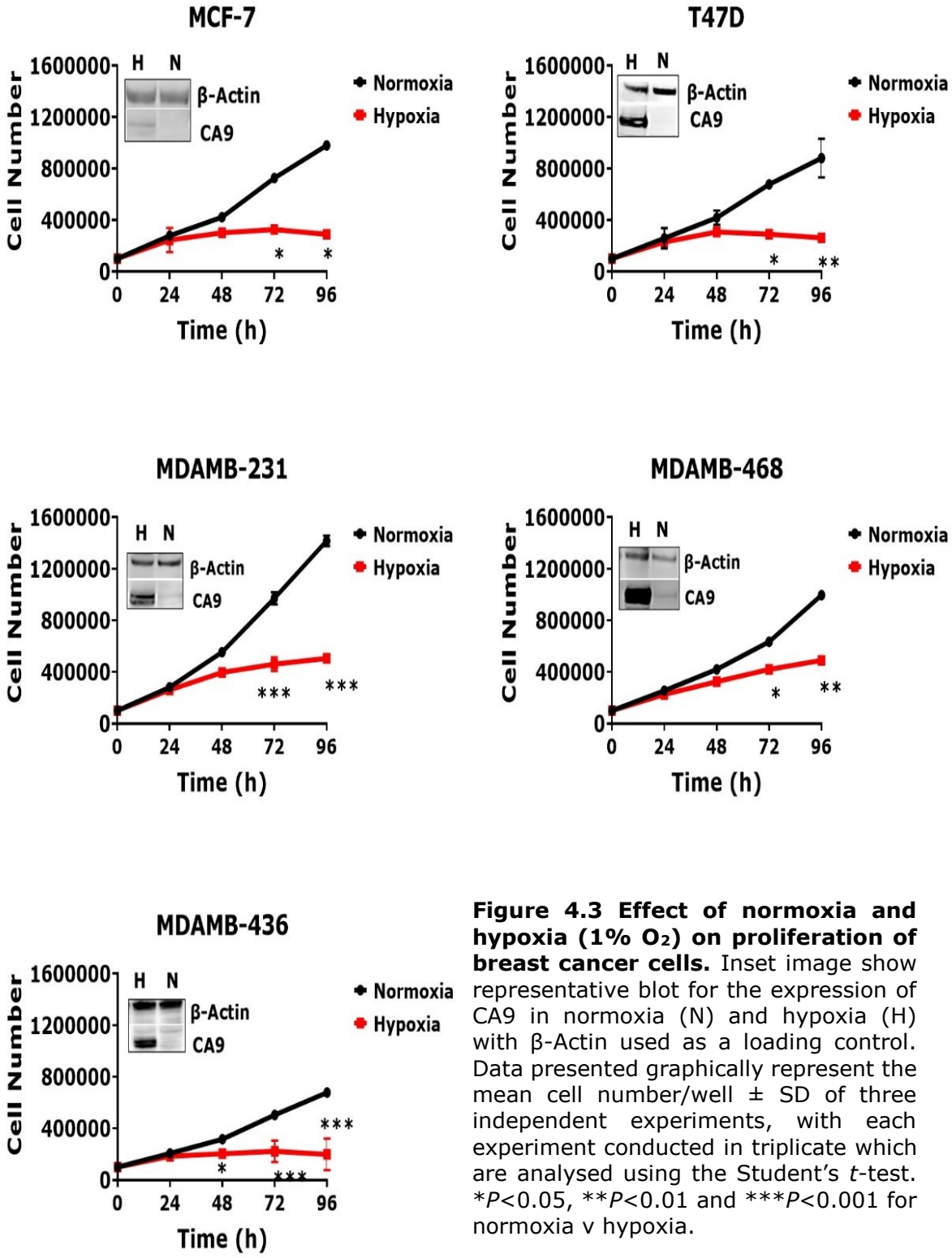


Figure 4.3 Effect of normoxia and hypoxia (1% O_2) on proliferation of breast cancer cells. Inset image show representative blot for the expression of CA9 in normoxia (N) and hypoxia (H) with β-Actin used as a loading control. Data presented graphically represent the mean cell number/well ± SD of three independent experiments, with each experiment conducted in triplicate which are analysed using the Student's *t*-test. **P*<0.05, ***P*<0.01 and ****P*<0.001 for normoxia v hypoxia.

Table 4.3 Doubling time of 2D breast cancer cells in normoxia (21% O_2) and hypoxia (1% O_2).

Cell line	Doubling time (hours)	
	Normoxia	Hypoxia
MCF-7	31.5±1.1	52.2±0.5
T47D	33.1±8.9	117.4±66.2
MDAMB-231	19.1±3.3	49.0±10.5
MDAMB-468	33.5±4.6	57.4±1.2
MDAMB-436	38.2±5.7	109.1±32.3
MCF-10A	22.5±6.2	51.6±7.3

The doubling times obtained under 2D normoxia are in agreement with previous chapters and published literature (section 2.4.1). A similar response was observed in MCF-10A cells with a doubling time of 22.5±6.2 hours in 2D normoxia compared to 51.5±7.3 hours in 2D hypoxia. Graphs for MCF-10A are supplied in Appendix C-Figure C1. In all subsequent experiments drug treatment with the HAPs were initiated at 24 hours of hypoxia treatment to ensure cells were in the exponential growth phase.

Data are in agreement with previously published literature, that hypoxia decreases proliferation and increases doubling time in all breast cancer cell lines (Song et al., 2018). Hypoxia is a modulator of cell proliferation because the increase in the number of cells increases the oxygen demand which would further aggravate hypoxic stress; so cells respond by reducing the rate of cellular proliferation (Hubbi et al., 2013, Ortmann et al., 2014, Hubbi and Semenza, 2015). Furthermore, reduced cell proliferation is one of the mechanisms by which hypoxic tumour cells demonstrate radio- and chemoresistance (discussed subsequently) (Teicher, 1994).

4.4.3 Plating efficiencies in 2D normoxia v 2D hypoxia

Cells from the above experiments were also plated for clonogenic survival assays to examine if hypoxia (1% O_2 for 48 hours) affects the colony forming potential in breast cancer cells. The PEs obtained are presented in Figure 4.4.

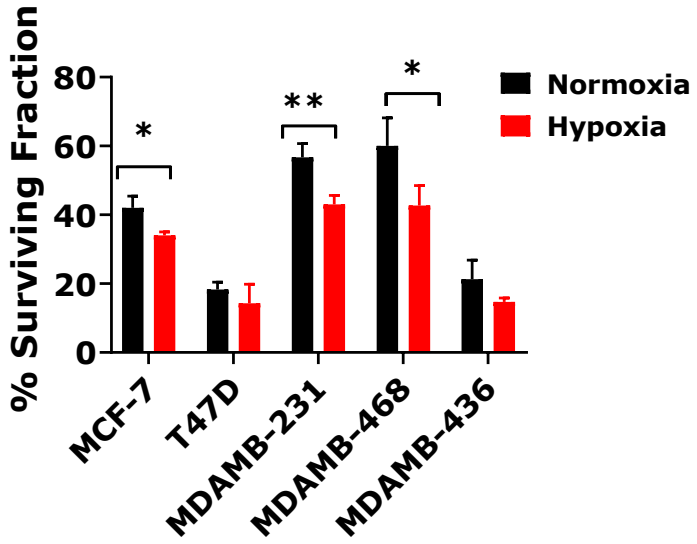


Figure 4.4 Plating efficiencies of breast cancer cells in 2D normoxia and hypoxia (1% O_2) culture conditions. Data represent the mean ± SD of three independent experiments, with each experiment containing six parallel data sets which are analysed using student's *t*-test. **P*<0.05, ***P*<0.01 for normoxia v hypoxia.

Marginal decreases in plating efficiencies were observed in all breast cancer cells exposed to hypoxia for 48 hours, with significance observed in MCF-7 (*P*=0.022), MDAMB-231 (*P*=0.008) and MDAMB-468 (*P*=0.012) cells. There was no significant difference in the PEs between normoxia and hypoxia grown T47D (*P*=0.090) and MDAMB-436 (*P*=0.109) cells. The PEs in 2D normoxia v hypoxia grown cells were 42.0±3.46% v 34.0±1.00% in MCF-7, 18.3±2.08% v 13.0±3.60% in T47D, 56.6±4.04% v 43.0±2.64% in MDAMB-231, 60.0±3.60% v 42.6±5.85% in MDAMB-468 and 21.3±5.50% v 14.6±1.15% in MDAMB-436 cells respectively. In MCF-10A cells, the PEs in 2D normoxia v 2D hypoxia were 49±7.07% and 27±1.41% respectively. The PE's of cell lines obtained under 2D normoxia were comparable to PEs obtained in chapter 2 and 3, and to published literature as referred to in chapter 2 section 2.4.1. Previous studies indicate that exposure to hypoxia decreases plating efficiencies in cancer cell lines (Spiro et al., 1984, Papandreou et al., 2005, Wu and Yotnda, 2011, Ma et al., 2012), which may be in response to cellular stress caused by oxygen deprivation (Degenhardt et al., 2006, Guo et al., 2019). Hypoxia has been reported to promote apoptosis by inducing mitochondrial damage,

upregulating apoptotic markers, increasing production of ROS and expression of HIF-1α - all of which may contribute to the reduction in clonogenic survival, as seen in the current experiment (Semenza, 2012).

4.4.4 Cytotoxicity of AQ4N and KP167 in 2D hypoxia

The efficacy of AQ4N and KP167 was studied in 2D hypoxia-cultured breast cancer cells by proliferation and clonogenic survival assays and compared to response obtained in 2D normoxia (data from chapter 3), to confirm the hypoxia-specific activation of these agents.

4.4.4.1 Effect of AQ4N and KP167 on proliferation

To assess the anti-proliferative effect of AQ4N and KP167, breast cancer cells were grown as monolayers in 1% O_2 for 24 hours and treated with varying concentrations of AQ4N (0.01-10) μM and KP167 (0.15-10) μM for 24 hours. The anti-proliferative effect of AQ4N and KP167 was assessed by plotting a dose-response obtained from cell counts (%) and is presented in Figure 4.5. It should be noted that the x-axis (drug concentration) varies between different cell lines, reflecting the differential sensitivity of cells to these agents.

Breast cancer cells treated with AQ4N and KP167 showed a dose dependent reduction in cellular proliferation. The IC_{50} doses of AQ4N and KP167 were not obtained from the range of concentrations tested (0-10) μM for proliferation assay, except in the T47D cells with KP167 IC_{50} of 3.3±0.04 μM and MDAMB-436 cells with AQ4N IC_{50} of 0.25±0.08 μM. Treatment with varying concentrations of AQ4N significantly reduced proliferation in MCF-7 cells compared to KP167 treatment at 2.5 (P=0.017 (statistics performed on n=2, each experiment with 6 replicates)), 5 (P=0.035 (statistics performed on n=2, each experiment with 6 replicates)) and 7.5 μM (P=0.033 (statistics performed on n=2, each experiment with 6 replicates)). In T47D cells, KP167 treatment resulted in reduced proliferation compared to AQ4N at 1 (P=0.024 (statistics performed on n=2, each experiment with 6 replicates)), 1.5 (P=0.048 (statistics performed on n=2, each experiment with 6 replicates)) and 2 μM (P=0.023 (statistics performed on n=2, each experiment with 6 replicates)).

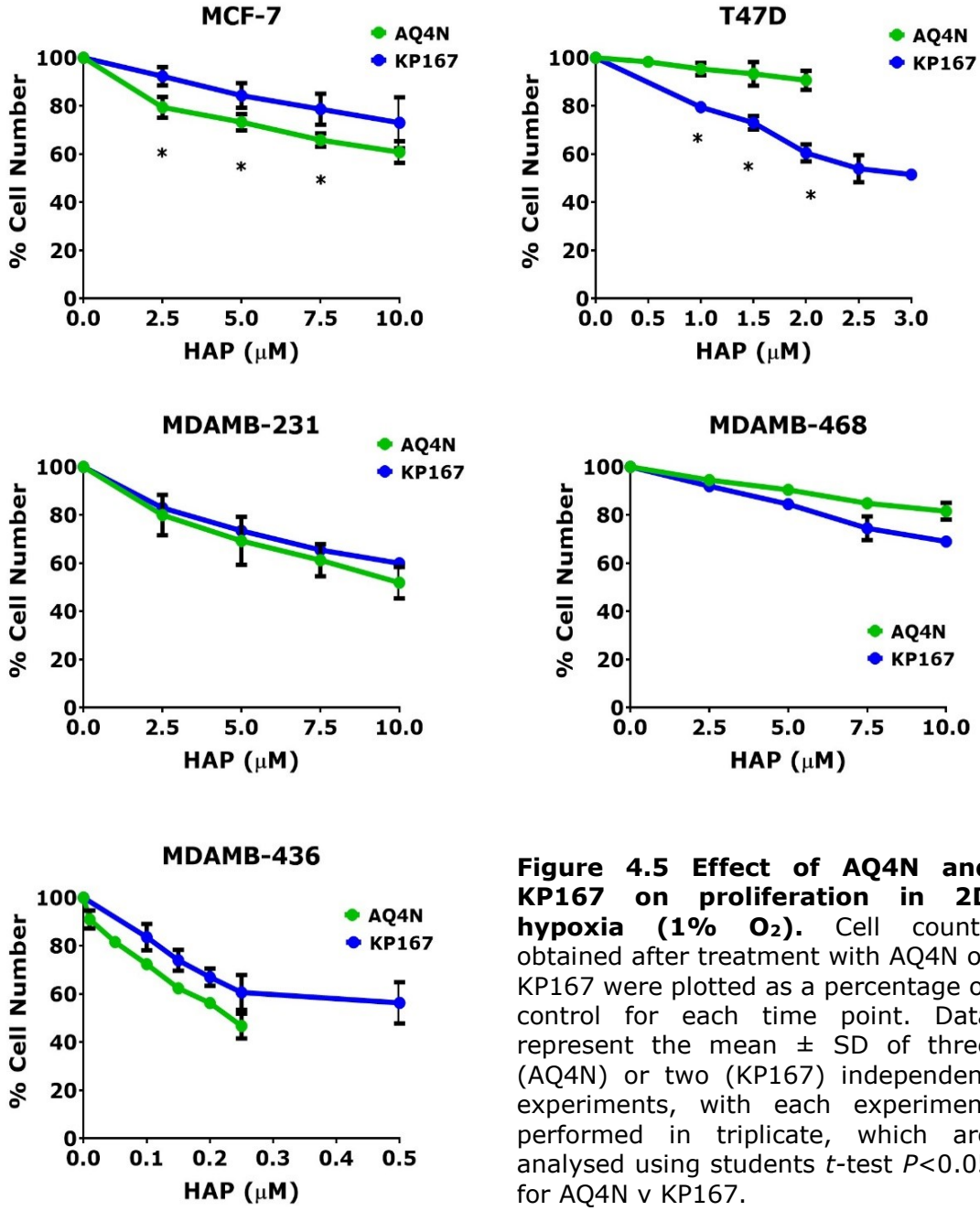


Figure 4.5 Effect of AQ4N and KP167 on proliferation in 2D hypoxia (1% O_2). Cell counts obtained after treatment with AQ4N or KP167 were plotted as a percentage of control for each time point. Data represent the mean ± SD of three (AQ4N) or two (KP167) independent experiments, with each experiment performed in triplicate, which are analysed using students *t*-test $P<0.05$ for AQ4N v KP167.

Decreased proliferation was also observed in MCF-10A cells with AQ4N IC_{50} values of 9.8±4.0 μM as shown in Appendix C-Figure C2. Tabulated proliferation IC_{50} doses for both AQ4N and KP167 in 2D hypoxia v 2D normoxia (data taken from chapter 3) are presented in Table 4.4.

Table 4.4 Proliferation IC_{50} of AQ4N and KP167 in 2D hypoxia (1% O_2) v 2D normoxia.

Cell line	AQ4N (μM) 24 hours		KP167 (μM) 24 hours	
	2D Hypoxia	2D Normoxia	2D Hypoxia	2D Normoxia
MCF-7	>10	>45	>10	>45
T47D	>3	34.6±10.1	3.3±0.04	21.2±7.7
MDAMB-231	>10	>45	>10	>45
MDAMB-468	>10	>45	>10	>45
MDAMB-436	0.25±0.08	10.5±7.6	>0.5	30±6.6
MCF-10A	9.8 ±4.0	34.1±6.5	-	-

IC_{50} values were calculated using Graphpad prism software.
Abbreviations: μM - micromolar; - not available.

As seen in the above table, the most sensitive cell lines to treatment with both AQ4N and KP167 in 2D hypoxia and 2D normoxia were the luminal T47D, BRCA-1 deficient MDAMB-436 and the normal MCF-10A (data for AQ4N only) cells. In MCF-7, MDAMB-231 and MDAMB-468 cells, the IC_{50} doses for proliferation were not achieved within the concentrations tested in each culture condition. In T47D, MDAMB-436 and MCF-10A cells, the IC_{50} doses achieved were lower in 2D hypoxia when compared to 2D normoxia, suggesting that the HAPs are more effective when used in hypoxic cultures. For drug-radiation combination experiments, breast cancer cells were treated with the clonogenic IC_{50} values and therefore higher doses of AQ4N and KP167 were not assessed for proliferation in MCF-7, MDAMB-231 and MDAMB-468 cells.

4.4.4.2 Effect of AQ4N and KP167 on clonogenic survival

The effect of AQ4N and KP167 on survival of breast cancer cells grown in 2D hypoxia were next assessed by clonogenic survival assays. Dose response curves are presented in Figure 4.6.

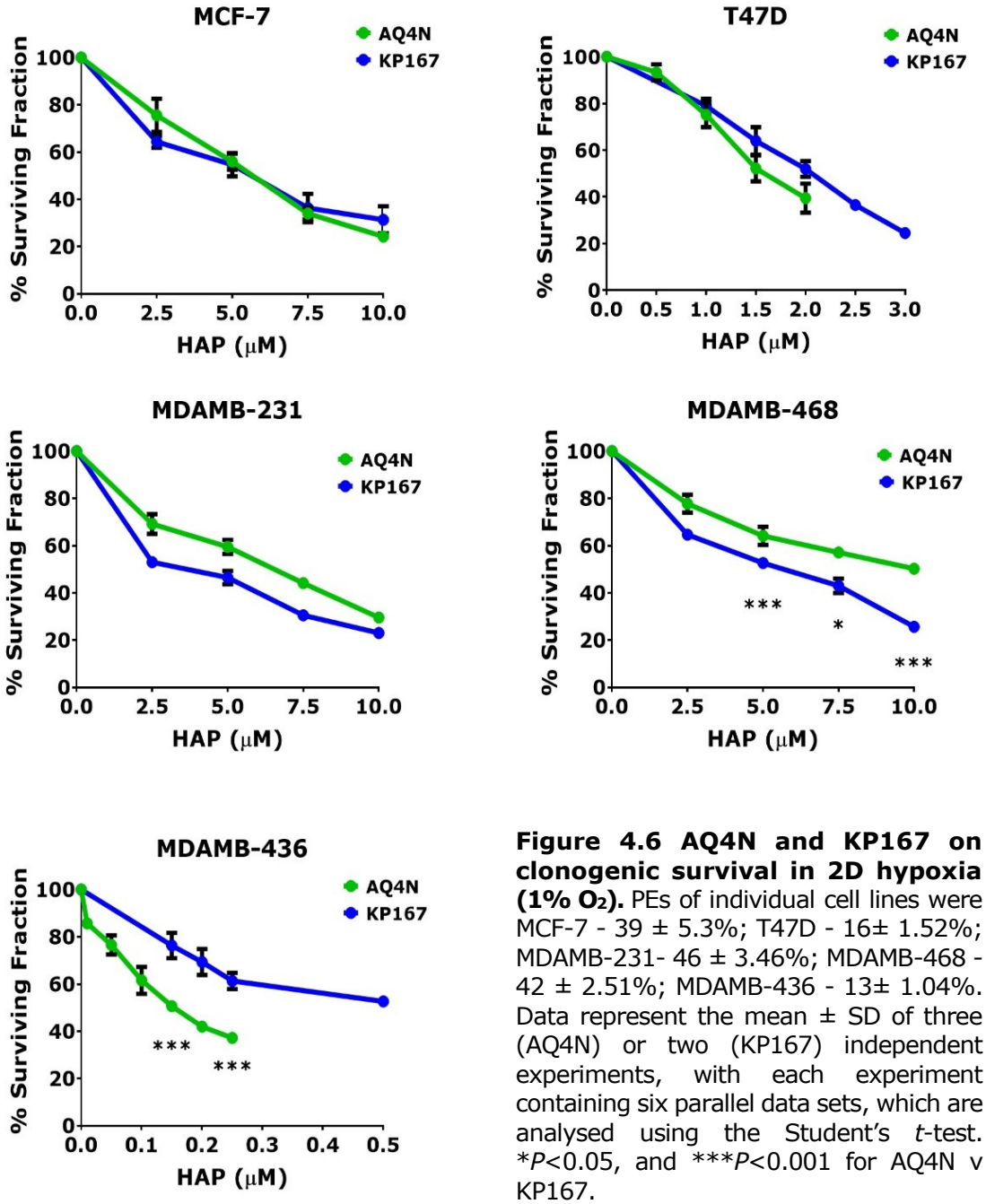


Figure 4.6 AQ4N and KP167 on clonogenic survival in 2D hypoxia (1% O_2). PEs of individual cell lines were MCF-7 - 39 ± 5.3%; T47D - 16± 1.52%; MDAMB-231- 46 ± 3.46%; MDAMB-468 - 42 ± 2.51%; MDAMB-436 - 13± 1.04%. Data represent the mean ± SD of three (AQ4N) or two (KP167) independent experiments, with each experiment containing six parallel data sets, which are analysed using the Student's *t*-test. **P*<0.05, and ****P*<0.001 for AQ4N v KP167.

The same concentrations of AQ4N and KP167 tested for proliferation assay resulted in a dose dependent reduction in clonogenic survival in all breast cancer cells in 2D hypoxia. The IC_{50} doses of AQ4N and KP167 were 5.2±1.9 μM and 4.9±0.95 μM in MCF-7, 2.0±0.1 μM and 2.2±0.49 μM in T47D, 6.1±2.7 μM and 3.4±1.24 μM in MDAMB-231, 9.5±0.8 μM and 4.8±0.31 μM in MDAMB-468, and 0.15±0.03 μM and 0.37±0.01 μM in MDAMB-436 cells. AQ4N treatment was also cytotoxic in MCF-10A cells and

resulted in reduced survival with IC_{50} values of 6.1 ±1.3 μM. The effect of AQ4N on clonogenic survival of MCF-10A cells is given in Appendix C-Figure C2.

MDAMB-468 cells were significantly more sensitive to KP167 treatment compared to AQ4N and demonstrated lower survival at 5 (P=0.0003 (statistics performed on n=2, each experiment with 6 replicates)), 7.5 (P=0.010 (statistics performed on n=2, each experiment with 6 replicates)) and 10 μM (P=0.0001 (statistics performed on n=2, each experiment with 6 replicates)). MDAMB-436 cells demonstrated significantly reduced survival with AQ4N treatment compared to KP167 at 0.2 (P=0.0001, (statistics performed on n=2, each experiment with 6 replicates)) and 0.25 μM (P<0.0001, (statistics performed on n=2, each experiment with 6 replicates)). Table 4.5 compares IC_{50} values of AQ4N and KP167 in 2D hypoxia (24 hour treatment), 2D normoxia (24 hour treatment) and 3D spheroids (data taken from chapter 3).

Table 4.5 Clonogenic IC_{50} of AQ4N and KP167 in 2D hypoxia (1% O_2) v 2D normoxia and 3D spheroids.

Cell line	AQ4N (μM)			KP167 (μM)		
	2D Hypoxia	2D Normoxia	3D Spheroids	2D Hypoxia	2D Normoxia	3D Spheroids
MCF-7	5.2±1.9	43.6±18.7	8.5±2.9	4.9±0.95	26.2±10.0	6.1±0.4
T47D	2.0±0.1	<5	4.4±0.5	2.2±0.49	19.4±6.9	1.9±0.6
MDAMB-231	6.1±2.7	>45	21.1±4.9	3.4±1.24	>45	12.8±1.3
MDAMB-468	9.5±0.8	>45	22.8±1.1	4.8±0.31	32.6±4.2	0.2±0.01
MDAMB-436	0.15±0.03	<5	0.2±0.01	0.37±0.01	<5	0.14±0.01
MCF-10A	6.1 ±1.3	10.2±3.5	8.8±2.61	-	-	-

The IC_{50} values were calculated using Graphpad prism software. Abbreviations: μM - micromolar; - not available.

Overall, the luminal MCF-7 and T47D cells demonstrated similar IC_{50} values for both AQ4N and KP167 under 2D hypoxia culture conditions. The triple negative MDAMB-231 and MDAMB-468 cells were more sensitive to KP167

and demonstrated ~50% reduction in KP167 IC_{50} values compared to AQ4N. The opposite effect was observed in the BRCA-1 deficient MDAMB-436 cells with ~50% reduction in AQ4N IC_{50} values compared to KP167. Such results indicate that efficient reduction of AQ4N and KP167 occurs in hypoxic conditions, as demonstrated by reduced survival and lower IC_{50} values in breast cancer cells when compared to response in normoxic conditions (chapter 3). Increases in the single agent cytotoxic effect of AQ4N and KP167 were observed in breast cancer cells grown in 2D hypoxia and 3D spheroids compared to response in 2D normoxia cultures as seen in the above table. The ability of these agents to undergo hypoxia-selective conversion into their cytotoxic metabolites in the absence of oxygen, explains the increase in cytotoxicity observed in hypoxia and spheroid cultures (Raleigh et al., 1998, Nishida et al., 2010). When comparing response between 2D hypoxia and 3D spheroids, most cell lines demonstrate lower IC_{50} values in 2D hypoxia cultures, suggesting that these agents are more efficiently metabolised in uniformly hypoxic monolayer cells compared to 3D spheroids which consists of both normoxic and hypoxic cell populations (Riffle and Hegde, 2017), which may demonstrate differential drug sensitivities.

The luminal T47D, BRCA-1 deficient MDAMB-436 and normal MCF-10A (for AQ4N) cells demonstrated similar sensitivity to HAPs across all 3 platforms which suggests that these cell lines are sensitive to AQ4N or KP167, regardless of oxygen availability and culture conditions. Although further studies are required to identify reasons for these observations, the inherent double strand deficiency in the BRCA-1 deficient MDAMB-436 cells and increased CYP2S1 expression (assessed by Western blot in chapter 3) may explain, in part, the sensitivity of these cell lines to TOPO II inhibitors such as AQ4N and KP167. Higher expression of reductases such as cytochrome P450 and CYP2W1 in T47D cells along with higher levels of progesterone (known to enhance efficacy of HAPs such as TPZ as discussed in chapter 3) (Nardulli and Katzenellenbogen, 1988, Atif et al., 2015), may increase sensitivity of T47D cells to AQ4N and KP167. MCF-10A cells demonstrated greater expression of CYP2W1 which may have enhanced the cytotoxicity profile of AQ4N in the normal MCF-10A cells. Taken together, data from

current experiments further confirm the hypoxia-specific cytotoxicity of AQ4N and KP167 in breast cancer cells.

4.4.5 Radioresponse of breast cancer cells in 2D normoxia v 2D hypoxia

Prior to drug-radiation combination experiments, the radioresponse of breast cancer cells grown in 2D hypoxia were assessed, in order to identify if hypoxia influences radiosensitivity of cell lines. As shown in Figure 4.7 hypoxia substantially increased radioresistance in both luminal and triple negative breast cancer cells.

Compared to cells grown in normoxia, SF2 values (Table 4.6) were significantly increased in hypoxia i.e. 0.24±0.05 v 0.58±0.03 (P=0.019) in MCF-7, 0.35±0.49 v 0.66±0.09 (P=0.05) in T47D, 0.24±0.01 v 0.55±0.01 (P=0.002) in MDAMB-231, 0.30±0.01 v 0.71±0.02 (P=0.002) in MDAMB-468 and 0.28±0.04 v 0.44±0.05 (P=0.013) in MDAMB-436 cells. Hypoxia enhanced radiosensitivity in all breast cancer cells with $OER_{0.01}$ of 1.69±0.22 in MCF-7, 1.44±0.20 in T47D, 1.55±0.01 in MDAMB-231, 1.53±0.07 in MDAMB-468 and 1.30±0.03 in MDAMB-436 cells. Such values equate to the survival of cells at 8 Gy increasing from 0.0002 to 0.005 in MCF-7, 0.002 to 0.012 in T47D, 0.0002 to 0.002 in MDAMB-231, 0.001 to 0.005 in MDAMB-468, and 0.0002 to 0.001 in MDAMB-436 cells. MCF-10A cells exposed to hypoxia also demonstrated significant radioresistance with $OER_{0.01}$ of 1.55±0.16. Graphs for MCF-10A are supplied in Appendix C-Figure C3.

Compared to 2D normoxia, a significant decrease in the α-value of MCF-7 (P=0.05), T47D (P=0.07), MDAMB-231 (P=0.002), MDAMB-468 (P=0.005) and MDAMB-436 (P=0.029) cells was noted which decreased the α/β ratio in these cells. Such data indicate that hypoxic cells were more radioresistant compared to cells in 2D normoxia.

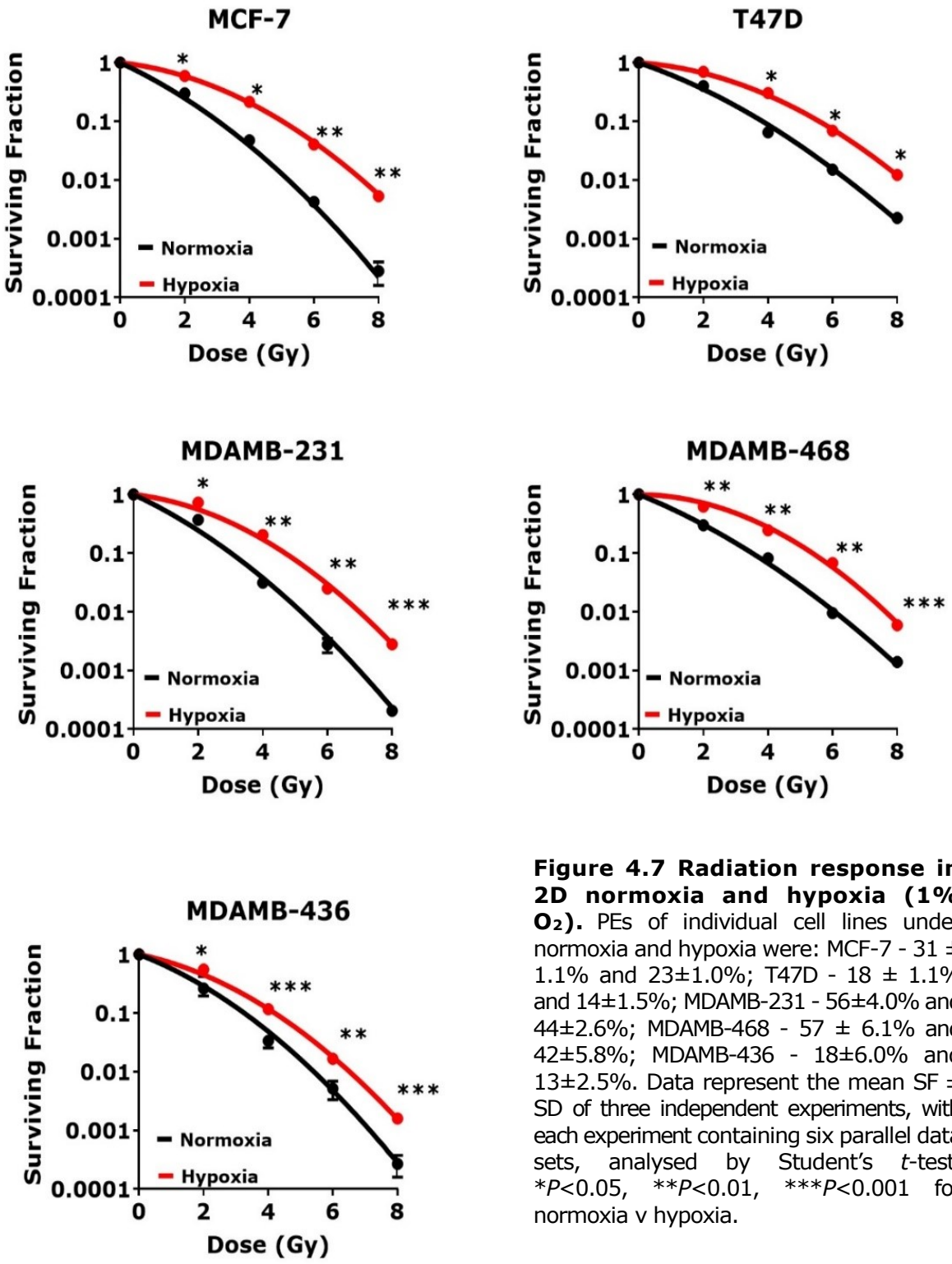


Figure 4.7 Radiation response in 2D normoxia and hypoxia (1% O_2). PEs of individual cell lines under normoxia and hypoxia were: MCF-7 - 31 ± 1.1% and 23±1.0%; T47D - 18 ± 1.1% and 14±1.5%; MDAMB-231 - 56±4.0% and 44±2.6%; MDAMB-468 - 57 ± 6.1% and 42±5.8%; MDAMB-436 - 18±6.0% and 13±2.5%. Data represent the mean SF ± SD of three independent experiments, with each experiment containing six parallel data sets, analysed by Student's *t*-test. **P*<0.05, ***P*<0.01, ****P*<0.001 for normoxia v hypoxia.

Table 4.6 Radiobiologic parameters of breast cancer cells in 2D normoxia and hypoxia (1% O_2) cultures.

Cell line	α (Gy^{-1})	β (Gy^{-2})	α/β (Gy)	SF2	OER $_{(0.01)}$
MCF-7					
2D Normoxia	0.58±0.14	0.05±0.01	10.8±5.07	0.24±0.05	
2D Hypoxia	0.11±0.07	0.08±0.03	3.56±1.06	0.58±0.03	1.69±0.22
t test	***P*=0.05**	*P*=0.317	*P*=0.187	***P*=0.019**	
T47D					
2D Normoxia	0.43±0.11	0.04±0.02	12.41±8.49	0.35±0.49	
2D Hypoxia	0.09±0.08	0.05±0.01	1.70±2.87	0.66±0.09	1.44±0.20
t test	*P*=0.07	*P*=0.43	*P*=0.22	***P*=0.05**	
MDAMB-231					
2D Normoxia	0.59±0.02	0.05±0.00	10.31±0.51	0.24±0.01	
2D Hypoxia	0.14±0.00	0.07±0.01	1.98±0.01	0.55±0.01	1.55±0.01
t test	***P*=0.002**	***P*=0.022**	***P*=0.001**	***P*=0.002**	
MDAMB-468					
2D Normoxia	0.52±0.04	0.04±0.01	12.11±1.96	0.30±0.01	
2D Hypoxia	0.03±0.02	0.08±0.01	0.51±0.24	0.71±0.02	1.53±0.07
t test	***P*=0.005**	***P*=0.010**	***P*=0.014**	***P*=0.002**	
MDAMB-436					
2D Normoxia	0.49±0.09	0.06±0.01	7.72±2.51	0.28±0.04	
2D Hypoxia	0.26±0.06	0.06±0.00	3.95±1.35	0.44±0.05	1.30±0.03
t test	***P*=0.029**	*P*=0.844	*P*=0.084	***P*=0.013**	

Statistical significance was determined by Student's *t*-test. The *P*-values are bold where they are ≤ 0.05. Abbreviations: IR, irradiation; $OER_{0.01}$, oxygen enhancement ratio at 1% survival; SF2, surviving fraction at 2Gy.

4.4.6 Radiosensitisation with AQ4N and KP167 in 2D hypoxia

4.4.6.1 Radiosensitisation with AQ4N

The radiosensitising efficacy of AQ4N was assessed by treating 2D hypoxia cultured breast cancer cells with the clonogenic IC_{50} values obtained previously in section 4.4.4.2. Figure 4.8 shows that the radiosensitisation by AQ4N ranged from marginal to substantial across the different breast cancer phenotypes, with effects more pronounced in the luminal T47D cells.

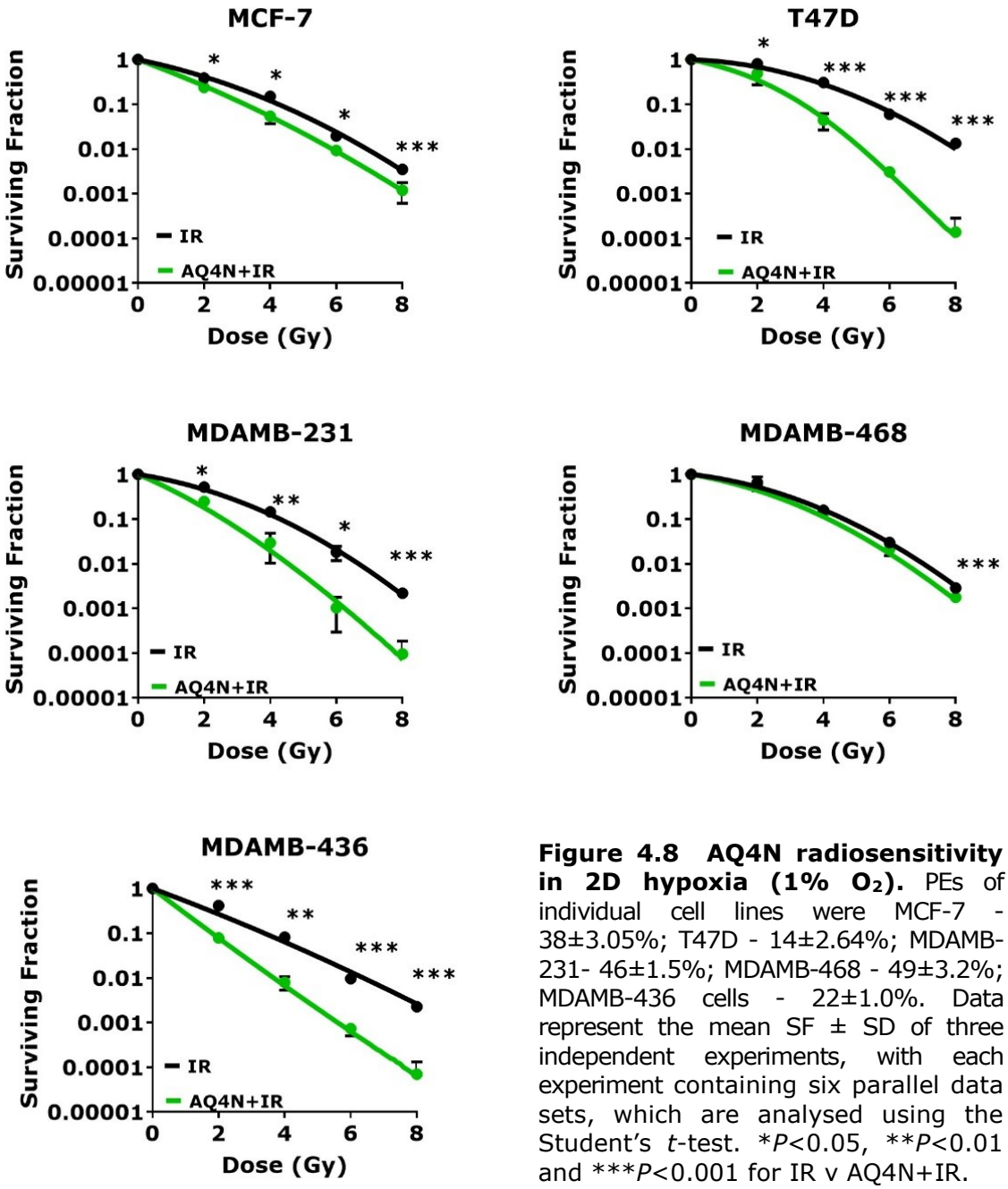


Figure 4.8 AQ4N radiosensitivity in 2D hypoxia (1% O_2). PEs of individual cell lines were MCF-7 - 38±3.05%; T47D - 14±2.64%; MDAMB-231- 46±1.5%; MDAMB-468 - 49±3.2%; MDAMB-436 cells - 22±1.0%. Data represent the mean SF ± SD of three independent experiments, with each experiment containing six parallel data sets, which are analysed using the Student's *t*-test. **P*<0.05, ***P*<0.01 and ****P*<0.001 for IR v AQ4N+IR.

Compared to control cells, the mean SF2 values (Table 4.7) were significantly reduced in AQ4N treated cells i.e. 0.41±0.05 v 0.25±0.04 (*P*=0.020) in MCF-7, 0.68±0.05 v 0.35±0.17 (*P*<0.0001) in T47D, 0.45±0.09 v 0.18±0.03 (*P*=0.008) in MDAMB-231, and 0.26±0.01 v 0.07±0.02 (*P*=0.0003) in MDAMB-436 cells, but not in MDAMB-468 cells with SF2 of 0.52±0.03 v 0.43±0.10 (*P*=0.225).

AQ4N treatment increased radiosensitivity in all lines with $SER_{0.01}$ of 1.30±0.08 in MCF-7, 1.74±0.32 in T47D, 1.69±0.11 in MDAMB-231,

1.13±0.10 in MDAMB-468 and 1.94±0.25 in MDAMB-436 cells. Such values equate to the survival of cells at 8 Gy decreasing from 0.003 to 0.001 in MCF-7, 0.013 to 0.0001 in T47D, 0.002 to 0.00007 in MDAMB-231, 0.002 to 0.001 in MDAMB-468, and 0.002 to 0.00007 in MDAMB-436 cells. MCF-10A cells were also significantly radiosensitised with AQ4N. Graphs for MCF-10A are supplied in Appendix C-Figure C4 and radiobiologic parameters summarised in Appendix C-Table C2.

Table 4.7 Radiobiologic parameters of breast cancer cells in 2D hypoxia treated with IR and/or AQ4N.

Cell line	α (Gy^{-1})	β (Gy^{-2})	α/β (Gy)	SF2	$SER_{(0.01)}$
MCF-7					
IR	0.35±0.09	0.04±0.01	8.24±3.29	0.41±0.05	
AQ4N+IR	0.62±0.10	0.02±0.01	27.86±18.73	0.25±0.04	1.30±0.08
t test	***P*=0.028**	*P*=0.092	*P*=0.148	***P*=0.020**	
T47D					
IR	0.06±0.05	0.06±0.01	1.01±0.94	0.68±0.05	
AQ4N+IR	0.33±0.34	0.11±0.06	6.71±9.74	0.35±0.17	1.74±0.32
t test	*P*=0.088	***P*=0.0001**	***P*=0.0006**	***P*<0.0001**	
MDAMB-231					
IR	0.27±0.13	0.06±0.01	4.77±3.61	0.45±0.09	
AQ4N+IR	0.72±0.10	0.07±0.03	12.19±6.93	0.18±0.03	1.69±0.11
t test	***P*=0.010**	*P*=0.764	*P*=0.175	***P*=0.008**	
MDAMB-468					
IR	0.19±0.04	0.06±0.01	2.98±1.01	0.52±0.03	
AQ4N+IR	0.29±0.16	0.06±0.02	5.93±5.77	0.43±0.10	1.13±0.10
t test	*P*=0.360	*P*=0.873	*P*=0.433	*P*=0.225	
MDAMB-436					
IR	0.63±0.03	0.24±0.40	52.15±23.91	0.26±0.01	
AQ4N+IR	1.29±0.16	0.01±0.01	270.76±365.19	0.07±0.02	1.94±0.25
t test	***P*=0.002**	*P*=0.390	*P*=0.359	***P*=0.0003**	

Statistical significance was determined by Student's *t*-test. The *P*-values are bold where they are ≤ 0.05. Abbreviations: IR, irradiation; $SER_{0.01}$, sensitiser enhancement ratio at 1% survival; SF2, surviving fraction at 2Gy.

Compared to control cells, a significant increase in the α-value was observed in MCF-7 (*P*=0.028), MDAMB-231 (*P*=0.010) and MDAMB-436 (*P*=0.002) cells, but not in T47D (*P*=0.088) and MDAMB-468 (*P*=0.360) cells. Increase in α-value led to an increase in the α/β ratio in all cell lines suggesting that AQ4N radiosensitises all breast cancer cells under 2D

hypoxic conditions. The BRCA-1 deficient MDAMB-436, the luminal cell line, T47D and the triple negative MDAMB-231 cells were the most radiosensitised by AQ4N treatment.

4.4.6.2 Radiosensitisation with KP167

The radioresponse of KP167 treated cells, grown in 2D hypoxia is presented in Figure 4.9.

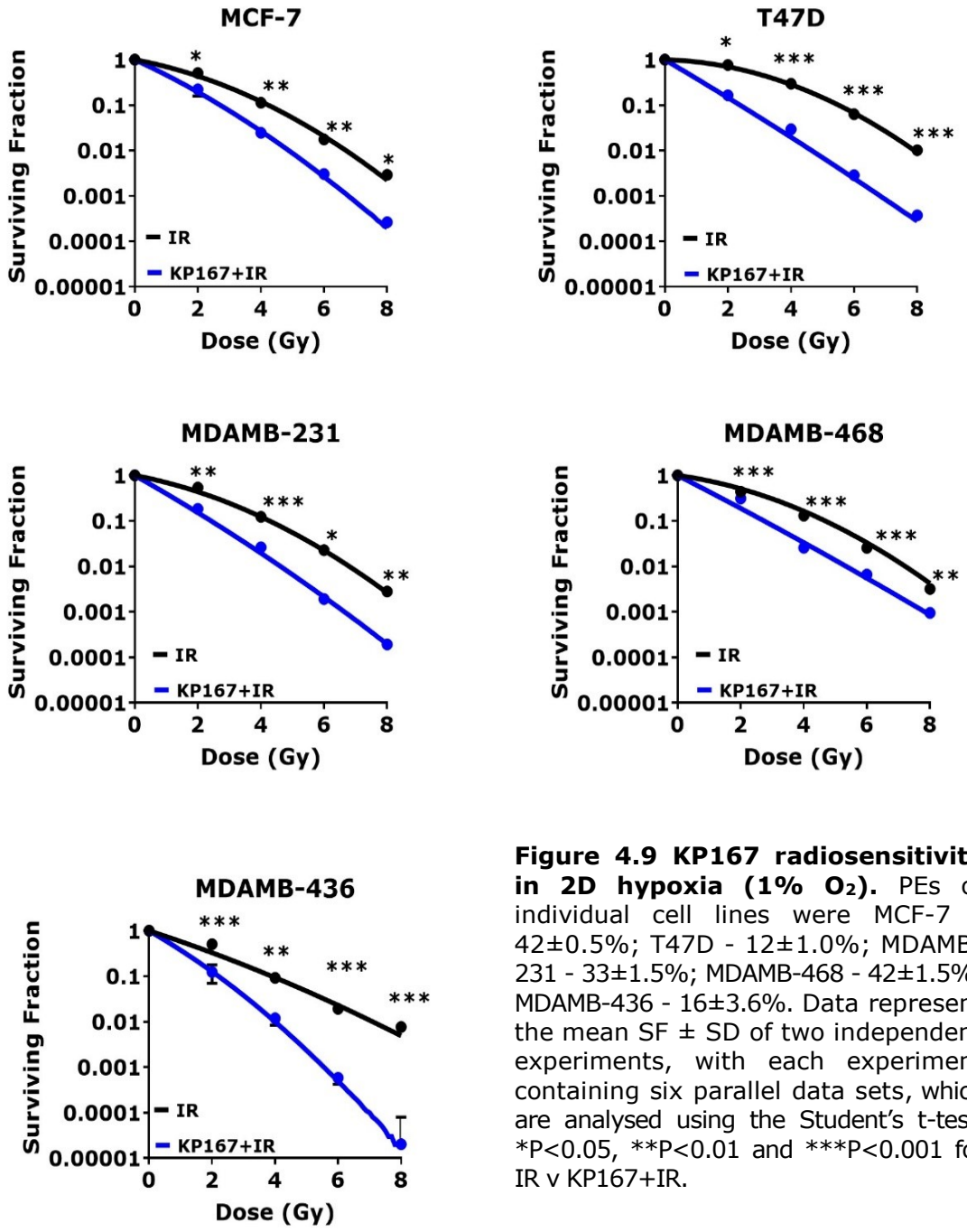


Figure 4.9 KP167 radiosensitivity in 2D hypoxia (1% O_2). PEs of individual cell lines were MCF-7 - 42±0.5%; T47D - 12±1.0%; MDAMB-231 - 33±1.5%; MDAMB-468 - 42±1.5%; MDAMB-436 - 16±3.6%. Data represent the mean SF ± SD of two independent experiments, with each experiment containing six parallel data sets, which are analysed using the Student's t-test. *P<0.05, **P<0.01 and ***P<0.001 for IR v KP167+IR.

As shown in Figure 4.9, cells treated with KP167 demonstrated enhanced radiosensitivity across both luminal and triple negative breast phenotypes. Compared to controls, mean SF2 values (Table 4.8) in KP167 treated cells were significantly reduced i.e. 0.43±0.06 v 0.19±0.13 (*P*=0.032) in MCF-7, 0.69±0.02 v 0.14±0.02 (*P*=0.001) in T47D, 0.43±0.01 v 0.15±0.01 (*P*=0.003) in MDAMB-231, 0.50±0.00 v 0.18±0.00 (*P*=0.0002) in MDAMB-468 and 0.32±0.03 v 0.12±0.03 (*P*=0.003) in MDAMB-436 cells. (Statistics performed on n=2, each experiment with 6 replicates).

Table 4.8 Radiobiologic parameters of breast cancer cells in 2D hypoxia treated with IR and/or KP167.

Cell line	α (Gy^{-1})	β (Gy^{-2})	α/β (Gy)	SF2	$SER_{(0.01)}$
MCF-7					
IR	0.30±0.09	0.05±0.01	5.52±2.75	0.43±0.06	
KP167+IR	0.73±0.06	0.04±0.01	19.44±10.13	0.19±0.13	1.56±0.12
t test	***P*=0.034**	*P*=0.445	*P*=0.201	***P*=0.032**	
T47D					
IR	0.04±0.01	0.06±0.01	0.63±0.29	0.69±0.02	
KP167+IR	0.94±0.09	0.01±0.01	384.44±476.85	0.14±0.02	2.37±0.11
t test	***P*=0.006**	***P*=0.021**	*P*=0.372	***P*=0.001**	
MDAMB-231					
IR	0.30±0.01	0.05±0.00	53.98±34.91	0.43±0.01	
KP167+IR	0.90±0.06	0.02±0.00	44.44±13.48	0.15±0.01	1.75±0.04
t test	***P*=0.005**	***P*=0.009**	***P*=0.055**	***P*=0.003**	
MDAMB-468					
IR	0.22±0.01	0.05±0.00	3.83±0.19	0.50±0.00	
KP167+IR	0.81±0.00	0.01±0.00	106.01±42.31	0.18±0.00	1.72±0.02
t test	***P*=0.0001**	***P*=0.002**	*P*=0.076	***P*=0.0002**	
MDAMB-436					
IR	0.52±0.08	0.01±0.01	39.36±26.23	0.32±0.03	
KP167+IR	0.93±0.22	0.05±0.03	29.05±29.24	0.12±0.03	1.81±0.33
t test	***P*=0.04**	*P*=0.168	*P*=0.672	***P*=0.003**	

Statistical significance was determined by Student's *t*-test. The *P*-values are bold where they are ≤ 0.05. Abbreviations: IR, irradiation; $SER_{0.01}$, sensitiser enhancement ratio at 1% survival; SF2, surviving fraction at 2Gy.

KP167 treatment increased radiosensitivity in all breast cancer cells with $SER_{0.01}$ of 1.56±0.12 in MCF-7, 2.37±0.11 in T47D, 1.75±0.04 in MDAMB-231, 1.72±0.02 in MDAMB-468 and 1.81±0.33 in MDAMB-436 cells. 8 Gy, following KP167 treatment decreased survival from 0.002 to 0.0002 in

MCF-7, 0.001 to 0.0003 in T47D, 0.002 to 0.0001 in MDAMB-231, 0.003 to 0.0009 in MDAMB-468, 0.007 to 0.00002 in MDAMB-436 cells. Such data indicate that KP167 effectively radiosensitised both luminal and triple negative breast cancer cells in 2D hypoxia. The radiosensitivity obtained with KP167 was greater than AQ4N in all lines, apart from MDAMB-436 cells with marginally higher AQ4N induced radiosensitisation.

All breast cancer cells treated with KP167 demonstrated significant radiosensitisation with increased α-value and α/β ratio, which indicates a more linear cell killing. The α-value was significantly increased in MCF-7 (P=0.034), T47D (P=0.006), MDAMB-231 (P=0.005), MDAMB-468 (P=0.0001) and MDAMB-436 (P=0.04) cells (Statistics performed on n=2, each experiment with 6 replicates). With KP167 treatment, the greatest increase in radiosensitisation was seen in the T47D cells followed by the triple negative MDAMB-436, MDAMB-231 and MDAMB-468 cells. Taken together, data indicate that KP167 is a highly potent radiosensitiser across all phenotypes of breast cancer when grown in 2D hypoxia culture conditions. The above experiments were conducted only twice and therefore results have to be interpreted with caution. Compiled $SER_{0.01}$ values of DNA repair inhibitors and HAPs (2D hypoxia, 2D normoxia and 3D spheroids) is given in Table 4.9.

Table 4.9 Compiled $SER_{0.01}$ values of DNA repair inhibitors and hypoxia-activated prodrugs.

Cell line	Sensitiser Enhancement Ratio								
	KU-55933	Olaparib	PTPD	AQ4N			KP167		
	2D Normoxia	2D Normoxia	2D Normoxia	2D Normoxia	2D Hypoxia	3D Spheroids	2D Normoxia	2D Hypoxia	3D Spheroids
MCF-7	1.60±0.23	1.63±0.03	1.00±0.02	1.17±0.06	1.30±0.08	1.30±0.08	1.21±0.05	1.56±0.12	1.46±0.66
T47D	1.71±0.27	1.61±0.18	1.00±0.01	1.64±0.27	1.74±0.32	1.58±0.06	1.93±0.09	2.37±0.11	1.76±0.20
MDAMB-231	1.82±0.21	1.62±0.09	1.31±0.07	1.29±0.28	1.69±0.11	1.44±0.04	1.43±0.46	1.75±0.04	2.53±0.06
MDAMB-468	1.68±0.33	1.68±0.33	1.13±0.08	1.11±0.44	1.13±0.10	1.64±0.08	1.32±0.19	1.72±0.02	2.28±0.24
MDAMB-436	3.42±0.91	2.35±0.13	1.5±0.13	1.19±0.12	1.94±0.25	3.33±0.18	1.68±0.08	1.81±0.33	4.55±0.24
MCF-10A	-	-	-	1.15	1.71±0.31	1.36±0.12	-	-	-

The pooled data from chapter 3 and 4, suggest that in most cell lines, radiosensitisation observed with both AQ4N and KP167 were lower in 2D normoxia compared to radiosensitivity obtained in 2D hypoxia and 3D spheroid cultures. Such observations confirm the hypoxia-selective cytotoxicity of AQ4N and KP167. It has been previously reported that cells grown in 3D demonstrate higher levels of cytochrome P450 enzymes, and decreased expression of genes involved in DNA repair, cell cycle and DNA replication (Schmidt et al., 2016). In light of such data, it appears that efficient metabolism of drugs in 3D by the cytochrome P450 enzymes followed by the inability of cells to repair DNA damage may have contributed to the increase in radiosensitivity observed in 3D v 2D cultures, especially in the TNBC cell lines. In all of the culture conditions investigated, KP167 was able to induce greater levels of radiosensitisation compared to the parental AQ4N. The greatest increase in radiosensitisation was seen especially in the triple negative breast cancer 3D models of MDAMB-231, MDAMB-468 and MDAMB-436 cells with KP167 treatment. This increase in radiosensitivity was even greater compared to radiosensitivity obtained with well-established radiosensitisers such as KU-55933 and olaparib investigated in chapter 2.

The normal MCF-10A cells were only marginally radiosensitised in 2D normoxia, compared to response in 2D hypoxia and 3D cultures. Such data suggests that AQ4N may target only the tumour cell population as opposed to the well-oxygenated normal cells *in vivo*. In conclusion, data indicate that KP167 is a highly effective and potent radiosensitiser in 3D spheroid, 2D normoxia and 2D hypoxia models of breast cancer.

4.5 Discussion

Radiotherapy is an essential treatment modality in the management of breast cancers. Studies over the years have shown that the presence of tumour hypoxia reduces local tumour control after radio and chemotherapy (Hohenberger et al., 1998, Vaupel et al., 2005). Therefore, hypoxia-selective cytotoxins that target the hypoxic fraction of tumour cells and increase efficacy of chemo and radiotherapy are under extensive pre-clinical evaluation (Jackson et al., 2019). The novel hypoxia-activated

prodrug, KP167 investigated in chapter 3 was found to exert anti-cancer and potent radiosensitising effect across luminal and triple negative breast cancer cells. Continuing from chapter 3, the current chapter set out to assess the single-agent and radiosensitising effect of KP167 under 2D hypoxia, with the parental drug AQ4N, used as a comparator.

As mentioned previously, HIF-1α is a master regulator that controls cellular response to hypoxia by regulating the expression of a wide variety of genes involved in proliferation, apoptosis, angiogenesis, metastasis and invasion (Kumar and Choi, 2015, Jiang et al., 2015). HIF-1 target genes include mediators of angiogenesis such as VEGF and its receptors, CA9, enzymes involved in the glycolytic pathway such as lactate dehydrogenase, hexokinase 2 and glucose transporters (GLUT-1, GLUT-3) (Harris, 2002). Many of these gene products also act to alter the radioresponse of cells, e.g. VEGF (Chan and Camphausen, 2003). CA9 is considered as a robust marker for the presence of tumour hypoxia, as it is quickly and extensively upregulated under hypoxic conditions (Potter and Harris, 2004). CA9 promotes tumour growth and metastasis by reducing intracellular pH levels in hypoxia (acidosis), that can activate proteases which break down extracellular matrix to facilitate EMT and aid migration, alter metabolism, and promote inflammation and angiogenesis (Giatromanolaki et al., 2001, Pastorekova and Gillies, 2019). Previous studies conducted in breast cancer tissues report that CA9 is undetectable in normal breast, but upregulated in hyperplastic tissues, with the highest expression found in hypoxic areas (Jiang et al., 2015, Daly et al., 2018). In the current study, all breast cell lines, including the normal MCF-10A cells maintained in 1% O_2 expressed CA9, which was undetectable in cells grown in 21% O_2. This observation confirmed that the breast cells grown in 1% O_2 were indeed hypoxic.

The primary adaptive response of cells to conditions of oxygen and nutrient deprivation is to decrease the cellular need for oxygen demand (Greijer and van der Wall, 2004). Cellular proliferation requires cells to enter the cell cycle which is known to be a highly energy demanding process that may be restricted under hypoxic conditions (Hubbi and Semenza, 2015). Therefore, in order to assess the effect of hypoxia on proliferation, breast

cancer cells were grown in 1% O_2 for 0-96 hours, and the effects were assessed by cell counting. Compared to cells in normoxia, similar levels of proliferation were observed at 24 hours, with gradual reductions noted at the 48-hour time-point. Following which, significant reduction in cell proliferation was noted at 72 and 96 hours. In comparison to 2D normoxia, breast cancer cells in 2D hypoxia (1% O_2) had significantly longer doubling times i.e. (19-38 normoxia) v (49-117 hypoxia) hours. These cellular adaptations are regulated by HIF-1α, which induces cell cycle arrest in hypoxic cells by directly repressing cell cycle genes (Ortmann et al., 2014). In addition, prolyl hydroxylases (PHD) which is the inhibitor of HIF-1α promotes breast cancer cell proliferation by regulating levels of Cyclin D. However, under hypoxia, PHD is inactivated resulting in decreased Cyclin D1 levels which reduces proliferation in breast cancer cells (Zhang et al., 2009). Furthermore, depletion of median oxygen concentrations below 10 mmHg results in acidosis, ATP depletion and reduced energy supply (Hockel et al., 1991), all of which may affect proliferation in hypoxic cultures.

The reduced proliferation often seen in hypoxic cells has been associated with resistance to a number of anti-cancer agents (Teicher et al., 1981, Teicher, 1994, McKeown, 2014). Most chemotherapeutic drugs target the rapidly dividing cells. Therefore, slowly dividing cells present in hypoxic areas of the tumour demonstrate reduced response to anti-cancer agents that are reliant on preferential drug uptake by rapidly proliferating cancer cells (Amadori et al., 1997). In the current study, significant reductions in cell proliferation were observed only at 72 and 96 hours of hypoxic exposure. Therefore, in all subsequent experiments, breast cancer cells were treated with AQ4N and KP167 at the 24-hour time-point, which ensured that cells were rapidly proliferating at the time of drug treatment. Since AQ4N is cytotoxic by TOPO II inhibition only in proliferating cells, the reduced proliferation seen in hypoxic cells at 72 and 96 hours may have affected the potency of AQ4N as a TOPO II inhibitor. This however, may not be the case for KP167, due to its covalent binding to DNA and additional alkylating properties, which may enable it to be cytotoxic to even quiescent cancer cells. Future experiments can assess the efficacy of AQ4N and

KP167 in quiescent v proliferating cells to determine if the cytotoxic effects of HAPs are differential in the quiescent cell population.

The plating efficiencies of cells grown in 2D hypoxia were also assessed and compared to normoxic cultures in order to investigate if the presence of hypoxia affects the ability of breast cancer cells to form colonies. Slight decreases in PEs of cell lines were observed in T47D and MDAMB-436 cells, and significant reductions seen in MCF-7, MDAMB-231, MDAMB-468 and normal MCF-10A cells. Since ATP production is restricted under conditions of hypoxia, many cell types respond by inducing cell cycle arrest and/or activating cell death pathways (Iida et al., 2002, Koshiji et al., 2004). HIF-1α is known to be a key regulator in this process and initiates apoptosis by stimulating expression of pro-apoptotic proteins (BNIP3) (Greijer and van der Wall, 2004), and inhibiting expression of apoptotic markers (cleaved caspase-3) (Daly et al., 2018). It has been reported that overexpression of BNIP3 in MCF-7 cells binds to and inhibits the anti-apoptotic proteins, Bcl-2 and Bcl-xL (Boyd et al., 1994). HIF-1α has also been reported to interact with the inhibitor of p53, MDM2, which allows stabilisation of p53 protein to promote programmed cell death in hypoxic cells (Chen et al., 2003). Time permitting, it would have been interesting to investigate the apoptotic response of the different breast cell lines in response to AQ4N and KP167 treatment under oxic and hypoxic conditions.

Hypoxia is also known to induce acidosis (low intracellular pH) which can affect delivery and cellular uptake of certain pH sensitive anti-cancer agents such as doxorubicin (Lankelma et al., 1999, Patel and Tannock, 2009). This may not be the case for AQ4N and possibly KP167 as it has been previously demonstrated that decreasing the pH of the cell culture media to 6.5 had only minimal effect on the cytotoxicity of AQ4, which indicates persistence of its anti-cancer activity even in low pH conditions (Patterson et al., 2000). In addition, studies have shown that following a 2-hour incubation with AQ4N, ~26% of the active metabolite AQ4 was retained in cells, suggesting that AQ4 may be able to diffuse into proximate tumour cells and exert bystander effects, potentially targeting even the oxic tumour cell population (Smith et al., 1997). Furthermore, macrophage infiltration into hypoxic regions releases NOS which stabilises HIF-1α to

promote cellular adaptations (as discussed previously in section 4.2.2) (Dewhirst et al., 2008). However studies have shown an increase in AQ4N metabolism and tumour cell cytotoxicity in response to iNOS induction by macrophages (Mehibel et al., 2009). Such results indicate that iNOS commonly present in a hypoxic tumour microenvironment also activates AQ4N, which further enhances the hypoxia-selective toxicity of this agent (Fitzpatrick et al., 2008, Mehibel et al., 2016).

Most often, anti-cancer agents are unable to reach hypoxic areas because of the increasing distance from the nearest capillary (Vaupel and Mayer, 2007). Both pre-clinical and clinical studies have shown that the active metabolite AQ4 is stable, and localises to hypoxic regions efficiently (Albertella et al., 2008, Williams et al., 2009). Using immunofluorescence techniques, Tredan et al., 2009 demonstrated that AQ4N has the ability to rapidly penetrate and localise to hypoxic tumour tissues *in vivo*, and in combination with agents such as mitoxantrone which has limited drug penetration, delays tumour growth (Tredan et al., 2009). The cytotoxic effect of AQ4N has been reported to be ≥8-fold higher in hypoxia when compared to normoxic cultures in rat glioblastoma cells and human NSCLC cell lines (Manley and Waxman, 2013). Similar results were obtained from patient biopsies in a phase I study, wherein >3.4-fold higher concentration of AQ4 was found in hypoxic v normal tissues (Steward et al., 2007). Studies have also demonstrated that increasing tumour hypoxia by blocking blood flow into the tumour using a clamp or by the use of drugs such as hydralazine was also found to increase the anti-tumour efficacy of AQ4N in a tumour xenograft model (Patterson et al., 2000). Such evidence indicate that the anti-tumour efficacy of AQ4N (and possibly KP167) are unaffected by hypoxia-induced cellular adaptations which makes AQ4N and analogues ideal to target hypoxic cells.

In chapter 3, the hypoxia-activated prodrugs, AQ4N and KP167 were highly effective in breast cancer 3D cultures compared to cells grown in 2D normoxia. This may be because efficient reduction of these agents into their DNA binding cytotoxins may have occurred in hypoxic cells present in breast cancer spheroids (Raleigh et al., 1998). Therefore, in order to confirm the hypoxia-specific activation of AQ4N and KP167, breast cancer

cells in 2D monolayers were made hypoxic at 1% O_2, following which they were treated with various doses of AQ4N and KP167. Data show that both AQ4N and KP167 were highly cytotoxic to breast cancer cells in 2D hypoxia compared to response in 2D normoxia cultures (chapter 3). Treatment in 2D hypoxia, reduced survival in breast cancer cells with lower AQ4N (0.15-9.5) μM and KP167 (0.37-4.9) μM IC_{50} values compared to those obtained in 2D normoxia.

Compared to 3D, an increase in cytotoxicity in most cell lines, was observed in 2D hypoxic cultures and this may be because 2D hypoxic cells were grown as monolayers and uniformly subjected to hypoxia (1% O_2), which may have enabled efficient conversion of AQ4N and KP167 into their respective cytotoxic metabolites. This is in contrast to 3D spheroids, wherein normoxic, hypoxic and necrotic cells, all co-exist in different layers of the spheroid structure and may demonstrate differential drug sensitivities (Mueller-Klieser et al., 1986). For example, the oxygenated cells present in a 3D spheroid may not be adequately targeted as opposed to a 2D culture where cells were made uniformly hypoxic, enabling efficient drug activation. Summarising data obtained from chapter 3 and 4, it appears that the single-agent AQ4N and KP167 treatment were more cytotoxic in breast cancer cells grown in 2D hypoxia and 3D spheroid cultures when compared to response obtained in 2D normoxia, which confirms the hypoxia-specific activation of these agents.

The radioresponse in the breast cancer cell lines under 2D hypoxia (1% O_2 for 48 hours) were next investigated in order to assess if exposure to hypoxia increased radioresistance. As expected, hypoxia enhanced radioresistance in all breast cancer cells with $OER_{0.01}$ of 1.30-1.69. One of the reasons for the increase in radioresistance is due to lack of molecular oxygen in hypoxic tissues as discussed previously. Oxygen is a known radiosensitiser which chemically modifies radiation-induced free radical DNA damage and enhances the cell killing efficiency of radiation known as the oxygen fixation hypothesis (Gatenby et al., 1988, Williams et al., 2005). In support of this, studies conducted by Metsala et al., 2018 reported that the increased radioresistance seen in HeLa cells at 1% hypoxia was due to a reduction in the number of DNA double strand breaks

compared to cells grown in 21% O_2 (Metsälä et al., 2018). Studies have also reported upregulated DNA repair pathways and accumulation of γH2AX (involved in recruitment of DNA repair proteins) in cancer cells and mouse embryonic fibroblasts exposed to chronic hypoxia, even in the absence of detectable levels of DNA damage (Wrann et al., 2013).

In addition, the expression of HIF-1α in hypoxic cells promote chemo or radioresistance by regulating genes involved in apoptosis, DNA repair and cellular metabolism (Unruh et al., 2003, Meijer et al., 2012, Takasaki et al., 2016). In hypoxia, HIF-1α functions to enhance glycolysis, serine synthesis pathway, and pentose phosphate pathways, all of which increase production of antioxidants that neutralise free radicals or ROS generated by radiation (Guzy and Schumacker, 2006, Wu and Wei, 2012, Koritzinsky and Wouters, 2013). Moreover, hypoxia also sustains cells in a non-proliferative, quiescent state that protects them from the cytotoxic effects of radiation (Fidoamore et al., 2016). It would be interesting to assess and compare the levels of DNA damage (γH2AX assay) induced in response to AQ4N and KP167 under different oxygen conditions, if time had permitted. Future work may assess this.

Previous experiments that assessed the single-agent efficacy of AQ4N and KP167 demonstrated increased potency in 2D hypoxia cultures compared to efficacy under 2D normoxia (chapter 3). Therefore, the radioresponse of AQ4N and KP167 were also assessed in breast cancer cells grown in 2D hypoxia to determine if levels of radiosensitisation achieved would be greater than 2D normoxia cultures. For these experiments, cells were made hypoxic for 24 hours, then treated with the clonogenic IC_{50} dose of AQ4N and KP167 for a further 24 hours before irradiation. Data show that AQ4N was able to induce greater levels of radiosensitisation across all breast cancer cells compared to response observed in 2D normoxic cultures. The level of radiosensitisation induced by AQ4N ranged from marginal to significant with $SER_{0.01}$ of 1.13-1.94. Compared to 3D cultures, greater increase in radiosensitisation was noted only in the luminal T47D, triple negative MDAMB-231 and normal MCF-10A cells.

An ideal anti-cancer drug must be selective and exert cytotoxicity specific to cancer cells, while sparing normal tissues. AQ4N has been reported to

exhibit minimal or no cytotoxicity to normal cells (McKeown et al., 1996). Therefore, in order to identify if AQ4N could preferentially kill breast cancer cells, the single agent and radiosensitising effect were assessed in the normal MCF-10A cells. Compiled data from chapter 3 and chapter 4 show that AQ4N was cytotoxic and reduced survival in MCF-10A cells in all of the 3 culture conditions tested. However, when assessing radiosensitivity under normoxia, AQ4N seemed to only marginally radiosensitise the normal MCF-10A cells ($SER_{0.01}$ 1.15), which suggest that AQ4N in combination with radiation may reduce the normal tissue toxicity profile *in vivo*. The increase in radiosensitivity observed in 2D hypoxia ($SER_{0.01}$ 1.71) and 3D spheroids ($SER_{0.01}$ 1.36) may only be because of the presence of hypoxia when cells were grown under these conditions. Also, it should be noted that previous studies report the presence of basal/mesenchymal features (Neve et al., 2006), and absence of markers such as β-casein and α-lactalbumin, (commonly present in breast tissues) (Qu et al., 2015), which questions the validity of MCF-10A as a suitable 'normal' breast cell line model. Therefore, future experiments may assess the radiosensitising effects of both AQ4N and KP167 in another normal breast cell line to confirm such findings.

Lastly, the radiosensitising effects of KP167 were assessed in breast cancer cells grown in 2D hypoxia. Data show that, compared to AQ4N, greater increases in radiosensitisation was observed with the novel KP167 across all breast cancer phenotypes with $SER_{0.01}$ of 1.56-2.37. The radiosensitivity obtained in 2D hypoxia were greater compared to response observed in 2D normoxia cultures, which suggest that these agents undergo hypoxia-selective activation and therefore are more potent in hypoxic cultures. Compared to radiosensitivity observed in 3D spheroids, the luminal MCF-7, T47D and normal MCF-10A cells demonstrated greater increases in radiosensitivity in 2D hypoxia culture conditions. The presence of active CYP enzymes (involved in estrogen metabolism) and efficient drug metabolism in 2D monolayer hypoxic cultures of luminal and MCF-10A cells (Western blot data in chapter 3), may explain to some extent, the increased radiosensitivity observed in 2D compared to 3D cultures.

As demonstrated in the previous chapter, greater levels of KP167-induced radiosensitivity was observed in 3D spheroid cultures of TN MDAMB-231, MDAMB-468 and MDAMB-436 cells. However, these cell lines demonstrated reduced levels of radiosensitisation in 2D hypoxia compared to response seen in 3D. The reasons for this observation is unclear, although other studies have also reported similar findings. For example, Flader et al., 2000 reported that the benzimidazolequinone analogues were 46-fold more potent in 2D hypoxic HeLa cells and 65-fold more potent in 3D spheroids compared to normoxic controls (Flader et al., 2000). Further investigation led to the finding that under hypoxic conditions, the prodrug localised to both mitochondria (50%) and the nucleus (32%), as opposed to normoxic cells where 60% of localization was in the mitochondria and 28% was in the nuclear compartments. These studies indicate that the sub-cellular localization of the drug, the cellular uptake and hydrophobicity may have contributed to differential drug sensitivities in 2D v 3D cells (Sharma et al., 2019). Furthermore, Schmidt et al., 2016, studied gene expression in the HLaC78 spheroids and reported increase in levels of drug metabolising cytochrome P450 enzymes and downregulation of genes involved in cell cycle and DNA repair in 3D cultures compared to 2D grown cells (Schmidt et al., 2016). From the above mentioned studies, it appears that the increased levels of cytochrome P450-mediated drug metabolism and downregulated DNA repair pathways, along with the already repair-compromised nature of TNBC cell lines may have contributed to the increase in cytotoxic effects observed in 3D cultures.

In conclusion, data suggest greater increases in AQ4N/KP167 induced radiosensitivity was achieved in 3D spheroid and 2D hypoxia cultures compared to 2D normoxia models, which confirms the hypoxia-selective potency of these agents. The novel AQ4N analogue, KP167 was a highly effective anti-cancer agent and potent radiosensitiser across both luminal and triple negative breast cancer cells. These studies provide preliminary evidence for the use of KP167 as a hypoxia-activated radiosensitiser in breast cancer, especially in triple negative breast cancer models. The next chapter investigates the expression of CYP2S1 and CYP2W1 in a large independent cohort of breast cancer patients.

Conclusions

All the hypotheses framed at the beginning of the study were addressed:

Similar levels of radioresistance were observed between 0.5% and 1% O_2.

Hypoxia was found to alter proliferation and clonogenic survival in luminal and triple negative breast cancer cells.

AQ4N and KP167 were cytotoxic to breast cancer cells grown in hypoxia (1% O_2) compared to normoxia grown cells.

Hypoxia increased radioresistance in both luminal and triple negative breast cancer cells.

AQ4N and KP167 were highly effective hypoxic radiosensitisers in 2D breast cancer cultures (1% O_2) compared to radiosensitivity obtained with 2D normoxia.

Overall, the radiosensitivity obtained with KP167 was greater compared to AQ4N in 2D hypoxia.

Chapter 5 The expression of CYP2S1 and CYP2W1 in breast cancer

5.1 Abstract

Background: The cytochrome P450 (CYP) family of enzymes have important roles in breast cancer pathogenesis due to their involvement in estrogen metabolism and the production of carcinogenic metabolites during this process. They are also involved in the metabolism of anti-cancer agents such as tamoxifen and taxanes used in breast cancer treatment. The 'orphan' CYP enzymes, CYP2S1 and CYP2W1 are involved in the reductive activation of the hypoxia-activated prodrug, AQ4N (and possibly KP167). AQ4N and KP167 were shown in previous chapters to be highly effective anti-cancer agents and potent radiosensitisers in breast cancer cells. *In vitro* data from chapter 3 suggest that greater expression of CYP2W1 (assessed by Western blot) in luminal breast cancer cell lines may make them more responsive to single agent AQ4N or KP167 treatment. Assessing the expression of CYP2S1 and CYP2W1 in breast cancers may therefore help identify patient subgroups that could potentially benefit from HAP treatment. The current chapter investigates the expression of CYP2S1 and CYP2W1 by immunohistochemistry in a large independent cohort of breast cancer. The prognostic significance of CYP enzymes and their correlation with clinical and pathological parameters were also assessed.

Methods: A total of 1426 patients were assessed for the expression of CYP2S1 and CYP2W1 on tissue microarrays using immunohistochemistry. Correlation between CYP2S1 and CYP2W1 was determined using Spearman's correlation. The association between CYP2S1 and CYP2W1 (cytoplasmic and nuclear) protein expression with clinical and pathological parameters were assessed using Pearson's chi-square (χ^2) test. To assess the relationship between protein expression and survival outcomes in the total patient cohort and ER-positive/negative breast cancers, survival curves were plotted using the Kaplan-Meier method and statistical significance was determined using the Log-rank test. For multivariate survival analysis, Cox proportional hazards regression model was used to test the statistical independence and significance of the predictors on overall survival.

Result: Spearman's rank order correlation demonstrated significant, albeit weak, positive correlation between cytoplasmic and nuclear CYP2S1 (r^2=0.288, *P*<0.001) and between cytoplasmic and nuclear CYP2W1 (r^2=0.326, *P*<0.001). Significant positive correlations were also observed between cytoplasmic CYP2S1 and cytoplasmic CYP2W1 (r^2=0.288, *P*<0.001) and nuclear CYP2W1 (r^2=0.180, *P*<0.001), suggesting that the enzymes may have overlapping functions in drug metabolism, hypoxia and breast cancers. However, the expression of nuclear CYP2S1 was negatively correlated with cytoplasmic (r^2=-0.174, *P*<0.001) and nuclear CYP2W1 (r^2=-0.119, *P*<0.001), potentially indicating involvement in different pathways.

High cytoplasmic CYP2S1 and nuclear CYP2W1 were commonly present in ER-positive compared to ER-negative cancers. 35.5% of cases with high cytoplasmic CYP2S1 was present in ER-positive (*P*=0.011), and only 5.2% and 7.7% of cases with high cytoplasmic CYP2S1 were present in HER-2 positive (*P*=0.001) and triple negative breast cancers (*P*=0.0910) respectively. 39.7% of cases with high nuclear CYP2W1 were present in ER-positive (*P*=0.405), with only 4.3% and 6.9% of cases with high nuclear CYP2W1 belonging to the HER-2 positive (*P*=0.464) and triple negative (*P*=0.187) breast cancers respectively.

High cytoplasmic CYP2S1 was significantly associated with various clinicopathological parameters such as patients age of 50 years or above (*P*<0.001), grade 3 tumours (*P*<0.001), intermediate NPI prognostic group (*P*=0.002), high nuclear pleomorphism (*P*=0.003), mitosis (*P*<0.001), and ductal carcinoma (*P*=0.022). High nuclear CYP2S1 expression was associated with absence of HER-2 positive disease (*P*=0.011), grade 3 tumours (*P*=0.009), intermediate NPI prognostic group (*P*=0.025), high mitosis (*P*=0.002), and ductal carcinoma (*P*=0.007).

The expression of high cytoplasmic CYP2W1 was significantly associated with patients aged 50 years or above (*P*=0.002), absence of HER-2 positive disease (*P*=0.003), intermediate NPI prognostic group (*P*=0.013) and high mitosis (*P*=0.009). Nuclear CYP2W1 did not show association with any clinicopathological variables.

Univariate Kaplan-Meier survival analysis show that low expression of cytoplasmic CYP2S1 was significantly associated with adverse breast cancer specific survival (*P*=0.034), which remained so in multivariate analysis (hazard ratio (HR): 0.639; 95% confidence interval (CI): 0.483-0.846; *P*=0.002). Low expression of nuclear CYP2W1 was significantly associated with adverse breast cancer specific survival (*P*=0.012), and was also maintained in multivariate analysis (hazard ratio (HR): 0.677; 95% confidence interval (CI): 0.510-0.898; *P*=0.007). Low expression of cytoplasmic CYP2S1 and nuclear CYP2W1 were also associated with poor breast cancer specific survival in ER-positive (*P*=0.031) and ER-negative patients (*P*=0.020) respectively.

Conclusions. High cytoplasmic CYP2S1 and nuclear CYP2W1 expression were specific to ER-positive tumours, and identifies a subgroup of ER-positive, HER-2 negative breast cancers that may potentially benefit from single agent HAP treatment. The cytochrome P450 enzymes, CYP2S1 and CYP2W1 may be important as prognostic markers in breast cancer.

5.2 Introduction

5.2.1 Cytochrome P450 enzymes

The cytochrome P450 (CYP) isoenzymes are a large family of constitutive and inducible heme-containing enzymes that are located in the lipid bilayer of the endoplasmic reticulum (Slaughter and Edwards, 1995, Murray, 2000). Most of the CYP enzymes are predominantly expressed in the liver, but are also found in other organs such as lungs, placenta, kidneys and small intestine (Furge and Guengerich, 2006). The human genome project identified ~57 CYP genes which are classified into 18 families based on sequence similarity, most of which are significantly involved in carcinogenesis and metabolism of drugs and xenobiotics (Estabrook, 2003). Of the 57 identified, the metabolic functions of 13 have not been elucidated till date, and these are often referred to as the 'orphan' CYPs (Ingelman-Sundberg, 2005). Overall, the main biological functions of CYP enzymes involve oxidation/metabolism of endogenous compounds such as vitamin A, D, steroids, fatty acid, and eicosanoid; and detoxification of

exogenous agents such as natural products, drugs, and carcinogens (Cheng et al., 2001, Coon, 2005, Guengerich, 2008). They are important in the synthesis of steroid hormones such as estrogen and testosterone and sterols such as cholesterol and bile acids (Cheng et al., 2001, Niwa et al., 2015).

5.2.2 CYP2S1 and CYP2W1

5.2.2.1 CYP2S1

Cytochrome P450 2S1 (CYP2S1), is an orphan CYP enzyme that is mostly present in epithelial cells of tissues that are exposed to the environment such as skin, respiratory, gastrointestinal, and urinary tracts (Saarikoski et al., 2005a). Certain studies have reported mRNA expression of CYP2S1 in breast, kidney, placenta, and liver (Pelkonen and Raunio, 1997, Smith et al., 2003, Du et al., 2004). CYP2S1 is associated with the synthesis and metabolism of lipids including prostaglandins (PGE_2) and retinoids (Smith et al., 2003). The increased expression of CYP2S1 is commonly found in cancers of epithelial origin as well as in the chronic hyper-proliferative disease, psoriasis (Saarikoski et al., 2005a). Immunohistochemical analysis in 170 breast cancers previously demonstrated that high expression of CYP2S1 was associated with shorter survival of patients, although this trend was not observed in multivariate analysis. No other correlations with clinical and pathological parameters were reported in the study (Murray et al., 2010). CYP2S1 is reported to be expressed in hypoxic cells (Downie et al., 2005) and effectively metabolises drugs such as AQ4N (Nishida et al., 2010) and benzothiazoles (GW610 and SF203) (Tan et al., 2011).

5.2.2.2 CYP2W1

Cytochrome P450 2W1 (CYP2W1), is another 'orphan' CYP which is endogenously expressed in foetal colon and normally silenced after birth (Karlgren et al., 2006). The expression of CYP2W1 is minimal or absent in normal tissues, but demonstrates a tumour-specific expression pattern, especially in epithelial-derived tumours (Choudhary et al., 2005, Karlgren and Ingelman-Sundberg, 2007). CYP2W1 mRNA is reportedly upregulated

in breast cancer, and associated with response to neoadjuvant chemotherapy (Hlaváč et al., 2014). mRNA has also been detected in colon and adrenal tumours (Karlgren et al., 2006, Ronchi et al., 2014), and has been verified as a prognostic marker in patients with stage II or stage III colon cancer (Edler et al., 2009). To date, no studies have reported the prognostic significance of CYP2W1 in breast cancer. CYP2W1 is associated with metabolising lysophospholipids, and a variety of exogenous agents, such as AQ4N (Nishida et al., 2010), benzphetamine, several polycyclic aromatic hydrocarbon dihydrodiols (Wu et al., 2006), indoles (Yoshioka et al., 2006), indolines (2-methyl-5-nitroindoline or 5-bromoindoline) (Gomez et al., 2010) and benzothiazoles (Tan et al., 2011, Wang and Guengerich, 2012).

5.2.3 CYP enzymes in estrogen and drug metabolism

5.2.3.1 CYPs in estrogen metabolism

Estrogens play a crucial role in the development of hormone-associated cancers such as breast, ovarian, endometrial, prostate, colon, and lung (Cavalieri et al., 2000, Russo et al., 2003, Folkerd and Dowsett, 2010). As mentioned in chapter 1, prolonged exposure to estrogen is an important risk-factor in the development of hormone-associated cancers (Ritte et al., 2013). Estrogen-mediated carcinogenesis has been reported to occur through 3 distinct mechanisms - ER mediated hormonal activity to drive transcription of genes involved in tumour progression; production of toxic metabolites by cytochrome P450 enzymes during estrogen metabolism; and through estrogen induced aneuploidy (Frasor et al., 2003, Russo et al., 2003).

The CYP enzymes are involved in eliminating estrogens from the body by converting them into inactive metabolites in the liver that are subsequently excreted (Cheng et al., 2001). These enzymes catalyse the first step in the metabolism of estrogens, i.e. hydroxylation of estrogens into 2-hydroxy (2-OHE_2) and 4-hydroxyestradiol (4-OHE_2) metabolites (Lakhani et al., 2003, Tsuchiya et al., 2005). The 2- and 4-hydroxy derivatives (and other metabolites) are then converted into 2- and 4-methoxy metabolites by

catechol-O-methyltransferase (COMT) (Lakhani et al., 2003). Oxidation of catechol estrogens to semiquinones and quinones generates carcinogenic forms of estrogen metabolites which are implicated in breast cancer progression (Dwivedy et al., 1992). Furthermore, conversion of semiquinones to quinones occurring through the redox cycles generates superoxide anion radicals (O_2^-) that can cause oxidative damage to cellular components (Jakovcevic et al., 2015).

The expression of CYP enzymes is induced by estrogen itself, resulting in increased metabolism and elimination from the body (Tsuchiya et al., 2005). Prolonged exposure to estrogen promotes chromosomal instability, centrosome amplifications and aneuploidy (Fernandez et al., 2006, Hontz et al., 2007), all of which contributes to breast cancer progression. Changes in levels of CYP enzymes leading to prolonged estrogen exposure not only results in carcinogenesis, but also affects liver and other organs contributing adversely towards health and physiology (Modugno et al., 2003).

5.2.3.2 CYPs in drug metabolism

The primary site for drug metabolism is the liver, which facilitates detoxification and excretion of xenobiotics, by enzymatically converting them into water-soluble compounds, which are subsequently excreted. Drug metabolism occurs through phase I and II reactions, of which, oxidation is the most common phase I reaction, catalysed by the cytochrome P450 enzymes (Gibson and Skett, 2001).

The most widely studied role of CYP enzymes (70-80%) is their involvement in drug metabolism i.e. the rate at which drugs are broken down, and the time for which these agents are present in the body (Bibi, 2008). For example, agents that inhibit an enzymatic pathway of CYP enzymes, will result in increased concentrations of drugs that are metabolised by the same pathway, leading to systemic toxicity. On the other hand, agents that induce a specific CYP pathway will enable efficient metabolism and rapid clearance of drugs, which may result in treatment failure (Bibi, 2008, McDonnell and Dang, 2013). Zanger and colleagues previously reported that the majority of prescription drugs sold in the

United States, which are dependent on hepatic clearance are metabolised by the CYP1, CYP2 and CYP3 family of cytochrome P450 enzymes (Zanger et al., 2008). The CYP genes also demonstrate polymorphisms, which can reduce/increase the enzymatic activity and therefore alter potency of agents that are dependent on CYP-mediated metabolism (Miyoshi et al., 2002).

The CYP enzymes are also implicated in the metabolism of tamoxifen, used in the treatment of HR-positive breast cancers (Singh et al., 2011). Tamoxifen is a selective ER modulator that prevents activation of ER by estrogen, and in this way inhibits transcription of genes associated with breast cancer progression (Fugh-Berman and Epstein, 1992, Reinbolt et al., 2015). A number of CYP enzymes such as CYP2D6, are involved in the metabolism of tamoxifen into its potent anti-ER metabolite, endoxifen (Higgins and Stearns, 2010). Polymorphisms in the CYP2D6 genes are associated with either loss or lack of activity, which results in inefficient tamoxifen metabolism. Studies report that patients carrying polymorphisms in the CYP2D6 gene treated with tamoxifen demonstrate impaired formation of anti-estrogen metabolites, which results in increased recurrence rates and shorter relapse-free survival (Schroth et al., 2007, Ramón y Cajal et al., 2010).

The enzymes are also involved in the metabolism of chemotherapeutic agents used in breast cancer especially taxanes, such as docetaxel and paclitaxel (Cresteil et al., 2002, Engels et al., 2004). The metabolism of taxol consists of 19 enzymatic steps, almost half of which have been reported to be catalysed by cytochrome P450 enzymes (Croteau et al., 2006). The CYP enzyme CYP3A4, has been reported to inactivate docetaxel (Guengerich, 1999). Studies in breast cancer demonstrated a higher response rate in tumours negative for CYP3A4 expression, compared to CYP3A4 positive tumours. Furthermore, the expression of the variant CYP3A4 polymorphic allele was found to promote rapid docetaxel clearance from the bloodstream and reduced efficacy of cyclophosphamide in breast cancer (Miyoshi et al., 2002, Miyoshi et al., 2005). The role of CYP enzymes in the metabolism of estrogens, formation of carcinogenic metabolites and metabolism of chemotherapy agents indicate that these enzymes may

have the potential to alter breast cancer aetiology and outcome (Miyoshi et al., 2005).

5.2.3.3 CYP2S1 and CYP2W1 in AQ4N metabolism

Current data suggest that the hypoxia-activated prodrugs, AQ4N and KP167, investigated in chapter 3 and 4, may be effective as anti-cancer agents and radiosensitisers in breast cancer. The HAP, AQ4N (and KP167) undergoes a sequential 2-electron reduction, which is catalysed by the cytochrome P450 enzymes, to yield their respective DNA binding cytotoxins (Raleigh et al., 1998). Using a panel of drug metabolising P450 enzymes, several CYP enzymes were reported to be involved in HAP bio-reduction, out of which CYP3A4 was most effective (Raleigh et al., 1998, Yakkundi et al., 2006) in reducing AQ4N at a rate of 7.2 mole of substrate per mole of enzyme per minute (Shaw et al., 1997). Inducible nitric oxide synthase (iNOS) was also involved in the reductive activation of AQ4N at a rate of 5 mole min^{-1} (Nishida and Ortiz de Montellano, 2008). Following such findings, Nishida et al., 2010 reported that CYP2S1 and CYP2W1 catalyse the hypoxic reduction of AQ4N to AQ4 with the highest turnover rates compared to the previously identified CYP3A4 and iNOS, at a rate of approximately 12 mole of substrate per mole of enzyme per minute. These reactions were inhibited in the presence of oxygen, indicating that activation of AQ4N may be restricted to the more hypoxic regions of the tumour (Nishida and Ortiz de Montellano, 2008, Nishida et al., 2010). In support of these findings, chapter 3 and 4 identified that AQ4N and KP167 were highly effective anti-cancer agents in 2D hypoxia and spheroid cultures compared to their efficacy in normoxia.

5.2.4 Hypothesis and aims

The 'orphan' CYP enzymes, CYP2S1 and CYP2W1 are involved in the reductive-activation of the hypoxia-activated prodrugs, AQ4N (and KP167). *In vitro* data from chapter 3 (Western blot) indicate that CYP2S1 and CYP2W1 are differentially expressed in the different subtypes of breast cancer, with luminal cells having higher CYP2W1 compared to the TNBC cell lines. The differential expression of these enzymes may be responsible

for the increase in single agent cytotoxicity observed in the luminal cells compared to the TNBC subtypes. Therefore, identifying tumours with CYP2S1 and CYP2W1 expression may help in the selection of patients that could potentially benefit from HAP treatments or by other chemotherapeutic agents that require these enzymes for metabolism. The current chapter investigates the expression and prognostic significance of CYP2S1 and CYP2W1 protein expression in a large independent cohort of breast cancer by immunohistochemistry. The expression of CYP2S1 and CYP2W1 protein/mRNA were correlated to various clinicopathological parameters and survival, both in the Nottingham and METABRIC cohort respectively.

Hypotheses

1. CYP2S1 and CYP2W1 are highly expressed in ER-positive tumours compared to the HER-2 positive and TNBC subtypes.
2. High CYP2S1 and CYP2W1 protein expression is associated with improved survival in the total patient cohort and in ER-positive breast cancers.
3. High CYP2S1 and CYP2W1 mRNA expression is associated with improved prognosis in the METABRIC patient cohort.

Aims

- Investigate the cytoplasmic and nuclear expression of CYP2S1 and CYP2W1 in breast cancer tissue microarrays (TMAs) using immunohistochemistry, to evaluate the prognostic value of these proteins in breast cancer patient samples.
- Assess the clinical importance of CYP2S1 and CYP2W1 by correlating protein expression to various clinical and pathological parameters.
- Determine association of CYP2S1 and CYP2W1 with survival by correlating protein expression to breast cancer specific survival in the total patient cohort and within ER-positive or negative breast cancers.
- Investigate the effect of combined CYP expression (CYP2S1+CYP2W1) on survival of breast cancer patients.

- Correlate CYP2S1 and CYP2W1 mRNA to available clinical and pathological parameters and survival in the METABRIC cohort.

5.3 Materials and methods

5.3.1 Patient cohorts

This study is reported according to REMARK (reporting recommendations for tumour marker prognostic studies) criteria (McShane et al., 2005). Ethical approval for this study was granted by Nottingham Research Ethics Committee 2 (REC reference: 19/YH/0293, IRAS project ID: 266925), under the title 'Refining the prognosis of breast cancer and breast cancer precursor lesions for personalised therapy project'.

A total of 1426 primary operable early invasive breast cancer patients, treated surgically in Nottingham City Hospital between 1998 and 2006 were included in this study. Treatment and outcome data were collated and prospectively maintained. The clinical history and tumour characteristics including age, tumour size, tumour stage and grade, NPI index, LVI status, ER, PgR and HER-2 status were assessed. All patients were treated in a standardised manner, by mastectomy or wide local excision, as decided by disease characteristics or patient choice, followed by radiotherapy if indicated. Breast cancer specific survival (BCSS) was calculated as the time-interval (in months) between primary surgery and death resulting from breast cancer and progression-free survival was calculated as the duration (in months) from primary surgery to the occurrence of relapse (including local and regional relapse). Patients were administered systemic adjuvant therapy (hormonal therapy (HT) and CMF (cyclophosphamide, methotrexate and 5-Flourouracil), depending on tumour prognostic and predictive factors including the NPI, lymph node status, menopausal status and ER status. NPI was used to risk stratify and manage patients. Patients stratified into the good prognostic group (NPI ≤3.4) did not receive adjuvant therapy, and all patients with ER-positive tumours with moderate to poor NPI (>3.4) received adjuvant HT. ER-negative patients classified into the poor prognostic NPI group were offered CMF, if fit. ER-positive patients with positive lymph nodes, were given HT

coupled with CMF. Detailed clinicopathological data was recorded at the time of surgery and is shown in Table 5.1.

Table 5.1 Clinicopathological parameters of breast cancer tissues.

Clinicopathological Parameters	Number of patients	Percentage (%)
Age		
< 50 years	436	30.6
≥ 50 years	975	68.4
ND	15	1
Tumour size		
< 2cm	862	60.4
≥2 cm	547	38.4
ND	17	1.2
Nodal stage		
1	877	61.5
2	391	27.4
3	138	9.7
ND	20	1.4
Tumour grade		
1	216	15.1
2	581	40.7
3	613	43
ND	16	1.1
ER status		
Negative	270	18.9
Positive	1141	80
ND	15	1.1
PR status		
Negative	542	38
Positive	765	53.6
ND	119	8.3
NPI		
Good (≤ 3.4)	477	33.5
Intermediate (3.41-5.4)	713	50
Poor (>5.4)	215	15.1
ND	21	1.5
HER2 Status		
Negative	1209	84.8
Positive	109	7.6
ND	108	7.6
Triple Negative Disease		
Negative	1187	83.2
Positive	205	14
ND	34	2.4
LVI		
Negative	415	29.1
Positive	993	69.6
ND	18	1.3
BCSS		
Alive	1041	73
Deceased	247	17.3
Deceased (other causes)	123	8.7
ND	14	1
Distant Metastasis		
Present	293	20.5
Absent	1118	78.4
ND	14	1.1

Abbreviations: ER, estrogen receptor, PR, progesterone receptor; HER-2, human epidermal growth factor receptor-2; NPI, Nottingham Prognostic index; LVI, lymphovascular invasion; BCSS, breast cancer specific survival; DM, distant metastasis; ND, not determined.

The molecular taxonomy of breast cancer international consortium (METABRIC) dataset is a gene expression cohort, which contains sequencing data of 1980 primary breast cancer patients (Curtis et al., 2012). This data set was also used in the current study to assess CYP2S1 and CYP2W1 mRNA associations with available clinicopathological parameters and survival. Information about the data set is published in Curtis et al., 2012. Briefly, patient tumours were collected from 5 centres in the UK and Canada between 1977-2005. Median follow-up was 141 months. Patients who were ER-positive and/or lymph node-negative did not receive adjuvant chemotherapy, whereas all ER-negative and/or lymph node-positive patients were administered adjuvant therapy. In the METABRIC, mRNA was isolated from primary patient tumours and assayed using Illumina HT-12 v 3 platform (Curtis et al., 2012).

5.3.2 Tissue microarray use

CYP2S1 and CYP2W1 protein expression was investigated in a breast cancer tissue microarray (TMA) by immunohistochemical staining. Construction of TMAs were carried out by the Breast Pathology Group at the University of Nottingham (Kariri et al., 2020). A single 0.6 mm tissue core from a representative tumour area (assessed by a specialist breast cancer histopathologist) was used for each patient sample. 4 µm freshly cut TMA sections, mounted onto X-tra adhesive slides (Leica Biosystems), were used for immunohistochemistry. The specificity of antibodies were initially confirmed by Western blot as described below in section 5.3.3.

5.3.3 Antibody optimisation

The specificity of the primary antibodies, rabbit polyclonal anti-CYP2S1 (Abcam Ab69650) and rabbit polyclonal anti-CYP2W1 (Abcam Ab76666), were determined by Western blot in breast cancer cell lysates, as described in Chapter 3 section 3.3.8 and 3.3.9. Antibodies generating expected single bands without non-specific bands were applicable for TMA staining. Representative Western blot images showing antibody specificity is given in Appendix D-Figure D1.

The optimal concentrations of antibodies to be used for immunohistochemistry were initially determined using breast tumour composite sections consisting of six stage I breast tumours (grade 1 to 3), following the procedures described in section 5.3.4. Optimisation of antibody concentration was performed using an immunohistochemical staining kit - Novolink polymer detection kit (Leica). Two different concentrations of each antibody were initially tested (1 in 100 and 1 in 200 for CYP2S1) and (1 in 50 and 1 in 100 for CYP2W1). CDK-5 antibody, previously used in the lab by Dr Sarah Storr, was used as a positive control (Saidy et al., 2020). Sections with omission of the primary antibody were used as negative controls (Woolston et al., 2012).

5.3.4 Immunohistochemistry

Immunohistochemistry was performed using a Novolink Polymer Detection kit (Leica) according to the manufacturers' instructions, as described previously (Davis et al., 2014, Storr et al., 2016). Briefly, slides were deparaffinised in 2 x 5 minutes xylene baths and sequentially rehydrated in 2 x 2 minutes in 100% IMS (industrial methylated spirit) and 1 x 2 minutes in 70% IMS, followed by a 5 minute wash in running tap water. Antigen retrieval was performed in 0.01 M sodium citrate buffer (pH 6.0), heated in a microwave for 10 minutes at 750W followed by another 10 minutes at 450W. Slides were washed immediately under running tap water to stop the antigen retrieval process. The slides were then loaded onto sequenza slide racks (ThermoFisher Scientific). Tissues were treated with 100 µl Novolink Peroxidase Block for 5 minutes at room temperature to neutralise the endogenous peroxidase activity, and washed for 2 x 5 minutes with Tris-buffered saline (TBS) (Tris-Cl (50 mM), NaCl (150 mM), pH 7.6). Following wash, tissues were treated with 100 µl of Novolink Protein Block solution for 5 minutes. Following another wash with TBS as described above, tissues were incubated with the primary antibody, anti-CYP2S1 diluted 1:100, and anti-CYP2W1 diluted 1:50, for one hour at room temperature. The primary antibodies were diluted in bond primary antibody diluent (Leica) and the antibody concentration was optimised as described in section 5.3.3. Following antibody incubation, tissues were washed for 2 x 5 minutes with TBS prior to the application of 100 µl Post

Primary solution (a polymer penetration enhancer) for 30 minutes at room temperature. After wash, slides were incubated with 100 µl of NovoLink Polymer (anti-mouse/rabbit IgG-Poly-horseradish peroxidase (HRP)) for another 30 minutes followed by 2 x 5 minutes TBS wash. Immunohistochemical reactions were developed using 3, 3'-diaminobenzidine (DAB) solution. (1:20 DAB chromogen in DAB substrate buffer) as the chromogenic substrate after which tissues were counterstained with haematoxylin for 6 minutes. Slides were removed from the sequenza trays, and placed in the Leica autostainer. Tissues were dehydrated following a 5 minute wash with running tap water followed by treatment with 3 x 2 minutes IMS baths (1x in 70% IMS and 2x in 100% IMS), followed by fixation in 2 x 5 minutes 100% xylene. Slides were mounted with DPX mounting medium (Sigma) and left to dry overnight. TMA sections were included as positive and negative controls with each run; negative controls had omission of primary antibody in each run, to ensure that the staining observed were not caused by reagents or cross-reactivity of secondary antibodies (Prgomet et al., 2017).

5.3.5 Immunohistochemical scoring

Slides were scanned using a Nanozoomer Digital Pathology Scanner (Hamamatsu Photonics) and staining was assessed at 200x magnification. Cytoplasmic staining was assessed using a semi-quantitative immunohistochemical H score; where the intensity of staining was divided into the following 4 categories; negative (0), weak (1), medium (2) or strong (3). H-scores (0-300) were obtained as the product of staining intensity and percentage of area stained with that intensity (for example 0 x negatively stained tumour % + 1 x weakly stained tumour % + 2 x moderately stained tumour % + 3 x strongly stained tumour %). Nuclear staining was assessed as the percentage of nuclei with any intensity of staining. CYP2S1 and CYP2W1 showed both cytoplasmic and nuclear staining. More than 30% of cores for each TMA were initially double assessed (second scorer – Dr Sarah Storr), with both assessors blinded to clinical outcome and each other's scores. Concordance between scorers were established using the single measure intra-class correlation coefficient (ICC) analysis and if sufficiently robust, the current author then

scored the remaining cores. The single measure ICC values were above 0.7 (cytoplasmic CYP2S1 – 0.80; nuclear CYP2S1 – 0.89; cytoplasmic CYP2W1-0.70; and nuclear CYP2W1-0.74) indicating good concordance between scorers. Damaged/missing cores or those with less than 10% tumour were omitted from scoring. X-tile software was used to determine unbiased cut-points of IHC scores, for stratification into high and low expression (Camp et al., 2004).

5.3.6 Statistical analysis

Statistical analysis was performed using SPSS (v26). Data was stratified based on BCSS using X-Tile software (Camp et al., 2004). Spearman's correlation was used to establish correlation between CYP2S1 and CYP2W1 protein expression, in both nuclear and cytoplasmic compartments. The correlation between categorised protein expression and clinicopathological variables were examined using Pearson's chi-square of association (χ^2). To assess the relationship between protein expression and survival outcomes, survival curves were plotted using the Kaplan-Meier method with statistical significance determined using the Log-rank test. For multivariate survival analysis, Cox proportional hazards regression model was used to test the statistical independence and significance of the predictors on overall survival.

In the METABRIC cohort, X-Tile software was used to dichotomise CYP2S1 and CYP2W1 mRNA into high and low groups, based on BCSS (Camp et al., 2004). As with protein data, correlation between CYP2S1 and CYP2W1 mRNA was established using Spearman's correlation. Association between CYP2S1 and CYP2W1 mRNA and clinicopathological variables were examined using Pearson's chi-square of association (χ^2). Relationship between mRNA expression and survival were plotted using the Kaplan-Meier method with significance determined using the Log-rank test. A *P*-value of <0.05 was considered as having reached statistical significance.

5.4 Results

5.4.1 Optimisation of primary antibodies

The specificity of CYP2S1 and CYP2W1 antibodies were initially assessed by Western blot in luminal and triple negative breast cancer cell lines. Both CYP2S1 and CYP2W1 showed bands at their respective molecular weight of 56 kDa and 54 kDa respectively. There were no non-specific bands detected, providing confirmation that the CYP2S1 and CYP2W1 antibodies were specific and detected the appropriate protein bands. They were considered suitable to be used in IHC for staining of breast cancer tissues. Representative Western blot images are supplied in Appendix D-Figure D1. Figure 5.1 shows representative images of CYP2S1 and CYP2W1 optimisation using two different antibody concentrations, CYP2S1 (1 in 100 and 1 in 200) and CYP2W1 (1 in 50 and 1 in 100). CDK-5 antibody was used as a positive control. As expected, no staining was observed in the negative controls, which had omission of the primary antibody.

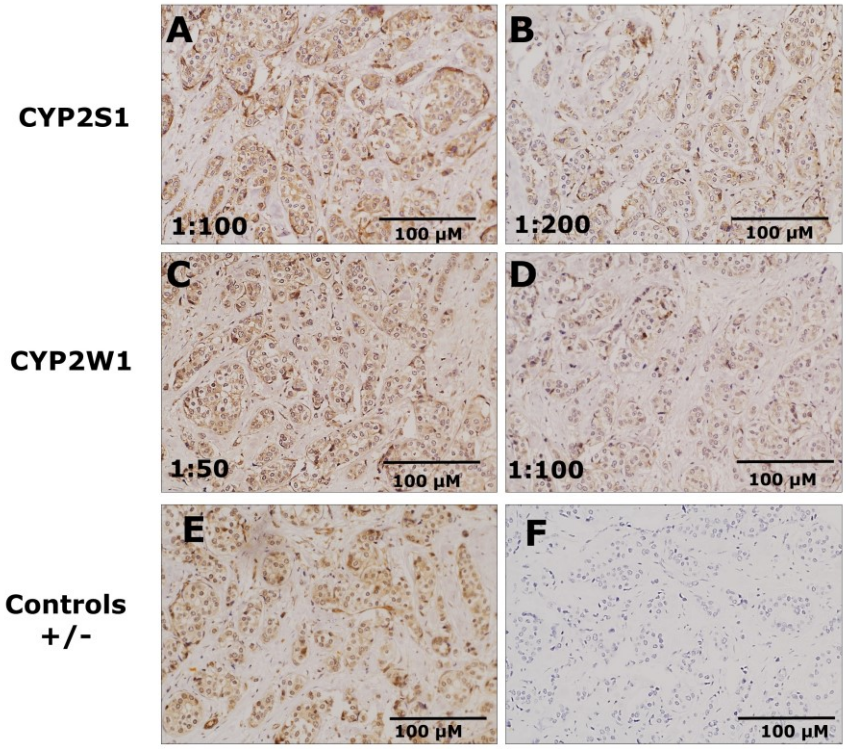


Figure 5.1 Optimisation of CYP2S1 and CYP2W1 antibody in breast tumour composite sections consisting of six stage I breast tumours (grade 1 to 3). (A) CYP2S1 (1 in 100); (B) CYP2S1 (1 in 200); (C) CYP2W1 (1 in 50); (D) CYP2W1 (1 in 100); (E) Positive control-CDK-5; (F) Negative control. Photomicrographs are at 10x magnification. Scale bar represents 100 µm.

Based on data obtained from optimisation experiments, a concentration of 1 in 100 was considered optimal for the detection of CYP2S1 and a dilution of 1 in 50 was chosen for CYP2W1 based on the intensity and clarity of staining. No non-specific staining was observed at these concentrations and therefore these dilutions were selected by agreement with Prof Stewart Martin and Dr Sarah Storr.

5.4.2 CYP2S1 staining and frequency

CYP2S1 expression was observed across all tissues with staining intensity varying from weak to strong in both the cytoplasm and nucleus, and with heterogeneous expression observed between adjacent tumour cells. A total of 1216 patients were assessed for CYP2S1 expression. Cytoplasmic CYP2S1 expression had a median H-score of 150, with values ranging from 0 to 300. Nuclear CYP2S1 expression had a median H score of 0 and ranged from 0 to 100. Cytoplasmic and nuclear H-score distribution histograms are shown in Figure 5.2-A and Figure 5.2-B respectively.

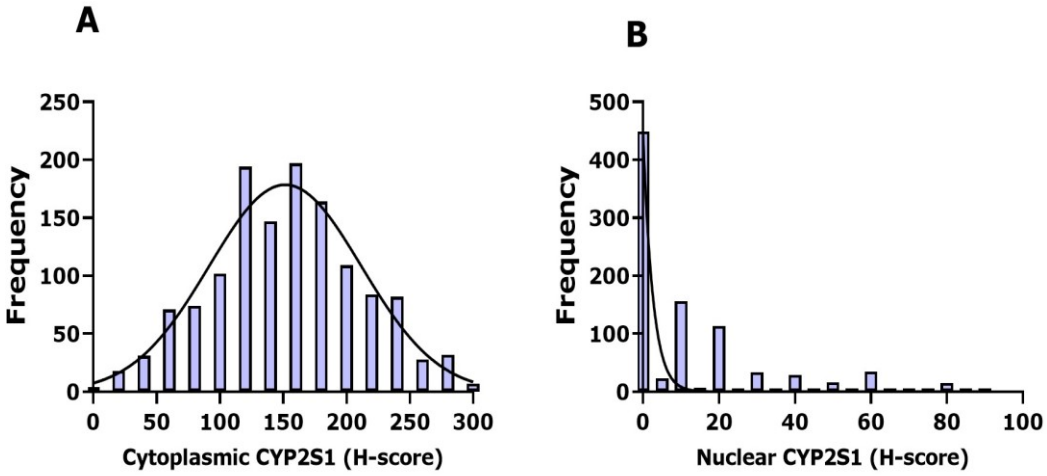


Figure 5.2 Distribution histogram of CYP2S1 H-score. Distribution of (A) Cytoplasmic CYP2S1 ranging 0-300 and (B) Nuclear CYP2S1 ranging 0-100.

Cytoplasmic CYP2S1 expression had an X-tile generated cut-point of 150, with 53.4% of cases (650/1216) demonstrating low expression, and 46.6% of cases (566/1216) with high expression. Nuclear CYP2S1 expression had a cut-point of 30, with 88.4% of cases (1074/1215) demonstrating low expression and 11.6% of cases (141/1215) demonstrating high

expression. Some of the cores within the tissue microarray could not be assessed, due to missing tissue or insufficient tumour cells. Representative photomicrographs of CYP2S1 expression are shown in Figure 5.3.

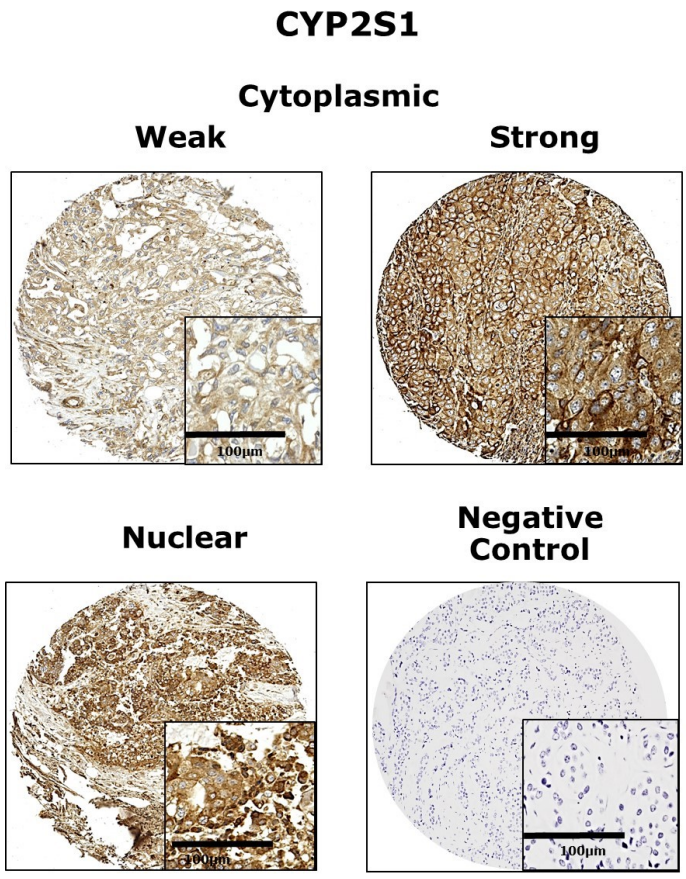


Figure 5.3 Representative photomicrographs of CYP2S1 in breast cancer tissues. Expression levels show weak (top left) and strong (top right) cytoplasmic CYP2S1, nuclear CYP2S1 expression (bottom left) and negative control (bottom right) at 10x magnification with 20x magnification inset panel. Scale bar represents 100 µm.

5.4.3 CYP2W1 staining and frequency

CYP2W1 expression varied from weak to strong in both the cytoplasm and nucleus, with heterogeneous expression observed between adjacent tumour cells. 1193 patients were assessed for CYP2W1. Cytoplasmic expression had a median H-score of 130, and ranged from 0 to 300. Nuclear expression had a median H score of 0 and ranged from 0 to 100. Cytoplasmic and nuclear H-score distribution histograms are shown in Figure 5.4-A and Figure 5.4-B respectively. Representative photomicrographs of CYP2W1 expression are shown in Figure 5.5.

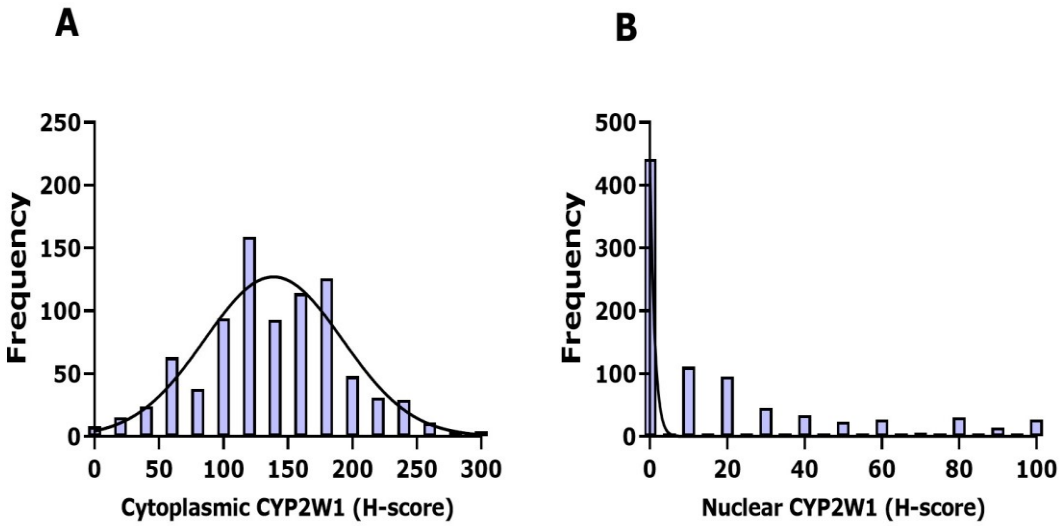


Figure 5.4 Distribution histogram of CYP2W1 H-score. Distribution of (A) Cytoplasmic CYP2W1 ranging 0-300 and (B) Nuclear CYP2W1 ranging 0-100.

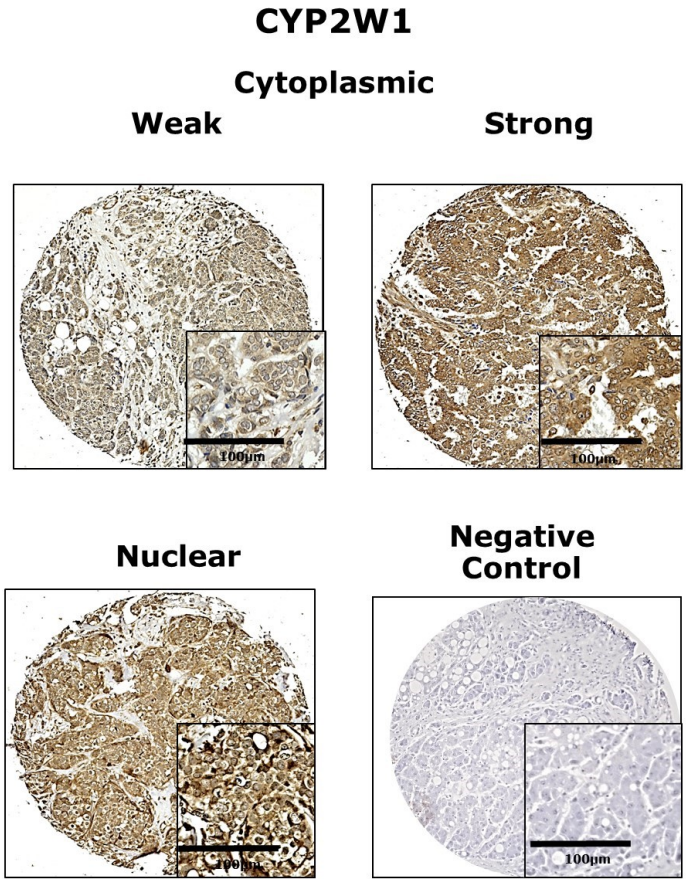


Figure 5.5 Representative photomicrographs of CYP2W1 in breast cancer tissues. Expression levels show weak (top left) and strong (top right) cytoplasmic CYP2W1, nuclear expression (bottom left) and negative control (bottom right) at 10x magnification with 20x magnification inset panel. Scale bar represents 100 µm.

Cytoplasmic CYP2W1 expression had a cut-point of 180, with 84.9% of cases (1014/1193) demonstrating low expression and 15.1% of cases (179/1193) with high expression. Nuclear CYP2W1 expression had a cut-point of 1, with 51.8% of cases (618/1193) demonstrating low expression and 48.2% of cases (575/1193) with high expression. A proportion of cores within the tissue microarray could not be assessed, due to missing tissue or insufficient tumour cells.

5.4.4 Correlation between CYP2S1 and CYP2W1 protein expression

Spearman's correlation is a non-parametric analysis to assess the relationship between two variables using a monotonic function (Joy et al., 2015) and was used to assess association between the CYP enzymes, CYP2S1 and CYP2W1 (Table 5.2).

Table 5.2 Correlation between CYP2S1 and CYP2W1 protein expression.

	Spearman's Correlation		
Variable	**Variable**	**r^2**	**Sig.**
CYP2S1 (Cytoplasmic)	CYP2S1 (Nuclear)	0.288	**<0.001**
	CYP2W1 (Cytoplasmic)	0.288	**<0.001**
	CYP2W1 (Nuclear)	0.180	**<0.001**
CYP2S1 (Nuclear)	CYP2W1 (Cytoplasmic)	-0.174	**<0.001**
	CYP2W1 (Nuclear)	-0.119	**<0.001**
CYP2W1 (Cytoplasmic)	CYP2W1 (Nuclear)	0.326	**<0.001**

Abbreviations: r^2, coefficient of variation; sig, statistical significance, Significant *P*-values (≤0.05) are indicated in bold.

Spearman's rank order correlation demonstrated significant, albeit weak, positive correlation of cytoplasmic CYP2S1 with cytoplasmic CYP2W1 (r^2=0.288, *P*<0.001) and nuclear CYP2W1 (r^2=0.180, *P*<0.001). Interestingly, the expression of CYP2S1 in the nucleus was negatively correlated to cytoplasmic CYP2W1 (r^2=-0.174 *P*<0.001) and nuclear

CYP2W1 (r^2=-0.119, *P*<0.001). As expected the expression of cytoplasmic CYP2S1 was correlated with its expression in the nucleus (r^2=0.288, *P*<0.001). Cytoplasmic CYP2W1 was also correlated to nuclear CYP2W1 (r^2=0.326, *P*<0.001).

The associations noted between cytoplasmic CYP2S1 and CYP2W1 in the above data suggest that these two proteins may have similar roles in breast cancer. CYP2S1 and CYP2W1, both belong to the CYP2 family of cytochrome P450 enzymes and metabolize common substrates (Nishida et al., 2010, Tan et al., 2011). The epithelial and hypoxia-specific expression of both these proteins suggests overlapping/similar functions, which might explain the associations observed in the current data (Karlgren et al., 2005, Szaefer et al., 2019). It is important to note that all the correlations are weak due to the low r values, and may hold only marginal biological relevance.

5.4.5 Association of CYP2S1 and clinicopathological variables

The expression of cytoplasmic and nuclear CYP2S1 protein was correlated with various clinical and pathological parameters using Pearson's chi-square test as shown in Table 5.3.

Table 5.3 Correlation of CYP2S1 with clinicopathological parameters in breast cancer tissues.

Clinicopathological Parameters		CYP2S1					
		Cytoplasmic expression			Nuclear expression		
		Low	High	P value	Low	High	P value
Age	< 50 years	198 (14.9%)	220 (16.5%)	**<0.001**	366 (27.5%)	816 (61.4%)	0.278
	≥ 50 years	523 (39.3%)	389 (29.2%)		52 (3.9%)	95 (7.1%)	
Tumour size	< 20mm	436 (32.8%)	370 (27.9)	0.966	714 (53.8%)	92 (6.9%)	0.627
	≥ 20 mm	283 (21.3%)	239 (18.0%)		466 (35.1%)	57 (4.1%)	
T stage	1	444 (33.9%)	375 (28.3%)		738 (55.7%)	86 (6.5%)	
	2	197 (14.9%)	173 (13%)	0.919	324 (24.5%)	46 (3.5%)	0.592
	3	72 (5.4%)	60 (4.5%)		116 (8.8%)	16 (1.2%)	
Tumour grade	1	110 (8.3%)	87 (6.5%)		183 (13.8%)	15 (1.1%)	
	2	333 (25.1%)	208 (15.7%)	**<0.001**	490 (36.9%)	51 (3.8%)	**0.009**
	3	277 (20.8%)	314 (23.6%)		508 (38.3%)	65 (6.2%)	
ER status	Negative	122 (9.2%)	137 (10.3%)	**0.011**	224 (16.9%)	35 (2.6%)	0.161
	Positive	599 (45%)	472 (35.5%)		957 (72.1%)	112 (8.4%)	
PgR status	Negative	279 (22.4%)	244 (19.6%)	0.947	459 (36.9%)	64 (5.1%)	0.278
	Positive	386 (31%)	335 (26.5%)		646 (52%)	74 (6%)	
NPI category	Good (≤ 3.4)	265 (20.0%)	172 (13.0%)		403 (30.4%)	34 (2.6%)	
	Intermediate (3.41-5.4)	340 (25.7%)	340 (25.7%)	**0.002**	592 (44.7%)	88 (6.6%)	**0.025**
	Poor (>5.4)	112 (8.5%)	96 (7.2%)		182 (13.7%)	25 (1.9%)	

Table continued.

Clinicopathological Parameters		CYP2S1					
		Cytoplasmic expression			Nuclear expression		
		Low	High	P value	Low	High	P value
Tubule formation	1	47 (3.6%)	45 (3.4%)		85 (6.5%)	7 (0.5%)	
	2	209 (15.9%)	172 (13.1%)	0.809	344 (26.2%)	42 (2.7%)	0.200
	3	456 (34.7%)	387 (29.4%)		740 (56.3%)	93 (7.8%)	
Pleomorphism	1	11 (0.8%)	10 (0.8%)		19 (1.4%)	2 (0.2%)	
	2	234 (17.8%)	147 (11.2%)	**0.003**	344 (26.2%)	37 (2.8%)	0.562
	3	467 (35.5%)	447 (34%)		806 (61.3%)	107 (8.1%)	
Mitosis	1	393 (29.9%)	248 (18.9%)		582 (44.3%)	59 (4.5%)	
	2	124 (9.4%)	128 (9.7%)	**<0.001**	231 (17.6%)	21 (1.6%)	**0.002**
	3	194 (14.8%)	227 (17.3%)		355 (27%)	65 (5%)	
HER2 status	Negative	628 (50.6%)	510 (41.1%)	**0.001**	1021(82.3%)	116 (9.3%)	**0.011**
	Positive	40 (3.2%)	64 (5.2%)		85 (6.8%)	19 (1.5%)	
Triple negative disease	Negative	616 (47%)	499 (38%)	0.091	994 (75.8%)	120 (9.2%)	0.869
	Positive	96 (7.3%)	101 (7.7%)		175 (13.3%)	22 (1.7%)	
Vascular invasion	Negative	500 (37.7%)	430 (32.4%)	0.701	353 (26.6%)	44 (3.3%)	0.998
	Positive	218 (16.4%)	179 (13.5%)		826 (62.3%)	103 (7.8%)	
Tumour type	Ductal (including mixed)	608 (45.7%)	537 (40.4%)		1030 (77.6%)	114 (8.6%)	
	Lobular	70 (5.3%)	38 (2.9%)		85 (6.4%)	23 (1.7%)	
	Medullary-like	1 (0.1%)	8 (0.6%)	**0.022**	6 (0.5%)	3 (0.2%)	**0.007**
	Miscellaneous	5 (0.4%)	5 (0.4%)		9 (0.7%)	1 (0.1%)	
	Mixed NST and Lobular	1 (0.1%)	0 (0.0%)		1 (0.1%)	0 (0.0%)	
	Special type	34 (2.6%)	20 (1.5%)		48 (3.6%)	6 (0.5%)	

Abbreviations: ER, estrogen receptor; PgR, progesterone receptor; HER2, human epidermal growth factor receptor-2; NP1, Nottingham prognostic index. The P values are resultant from the Pearson χ^2 test of association or Fisher's Exact test if a cell count was less than five. Significant *P*-values are indicated in bold. The number and percentage of observations for cohort is shown for each clinicopathological variable.

As can be seen, 35.5% of patients with high cytoplasmic CYP2S1 expression were of the ER-positive subtype (χ^2=6.543, df=1, *P*=0.011) and only 5.2% patients with high CYP2S1 demonstrated HER-2 positivity (χ^2=10.721, df=1, *P*=0.001). 7.7% of cases with high cytoplasmic CYP2S1 belonged to the TNBC subtype (*P*=0.091). Such data suggest that high expression of cytoplasmic CYP2S1 is particularly associated with ER-

positive cancers. High cytoplasmic CYP2S1 was also significantly associated with patients aged 50 years or above (χ^2=11.496, df=1, *P*<0.001), grade 3 tumours (χ^2=24.785, df=2, *P*<0.001), intermediate NPI prognostic group (χ^2=12.138, df=2, *P*=0.002), high nuclear pleomorphism (χ^2=11.566, df=2, *P*=0.003), mitosis (χ^2=12.874, df=2, *P*<0.001), and ductal carcinomas (χ^2=14.790, df=6, *P*=0.022).

8.4%, 1.5% and 1.7% of cases with high nuclear CYP2S1 expression were of the ER-positive (*P*=0.161), HER-2 positive (*P*=0.011) and TN (*P*=0.869) breast cancers (*P*=0.889) respectively. As seen with cytoplasmic expression, high nuclear CYP2S1 expression was associated with absence of HER-2 positive disease (χ^2=6.396, df=1, *P*=0.011), grade 3 tumours (χ^2=9.422, df=2, *P*=0.009), intermediate NPI prognostic group (χ^2=7.415, df=2, *P*=0.025), mitosis (χ^2=12.492, df=2, *P*=0.002), and ductal carcinoma (χ^2=17.161, df=6, *P*=0.007).

The high expression of cytoplasmic CYP2S1 in ER-positive cancers is consistent with the role of cytochrome P450 enzymes in the oxidation and metabolism of estrogens (Cheng et al., 2001). The association of both cytoplasmic and nuclear CYP2S1 with higher grade, pleomorphism and mitosis suggest that CYP2S1 may be involved in the proliferation of breast cancer cells, which is in agreement with previous studies reporting the involvement of CYP2S1 in hyper-proliferative disease, psoriasis (Smith et al., 2003). ER-positive patients categorised into the intermediate NPI group have intermediate prognosis and are usually recommended additional cytotoxic therapy in addition to HT, to reduce the risk of recurrence (Lee and Ellis, 2008). In the current study, high CYP2S1 was associated with intermediate NPI category, which suggests that high CYP2S1 may be able to identify HR-positive patients requiring additional therapy.

Current data indicate that high expression of cytoplasmic CYP2S1 may be able to identify a subgroup of ER-positive, HER-2 negative patients, above the age of 50 with intermediate prognosis. Furthermore, patients categorised into this subgroup may be eligible for potential HAP treatment or respond better to chemotherapeutic agents that require CYP2S1 metabolism. *In vitro* data from chapter 3 show CYP2S1 expression across

both luminal and triple negative breast cancer cells, with marginally higher expression in the BRCA-1 deficient triple negative cell line. However, in the current study, expression of CYP2S1 was predominant in ER-positive cancers compared to only a few TNBC cases.

5.4.6 Association of CYP2W1 and clinicopathological variables

The expression of CYP2W1, both cytoplasmic and nuclear, were correlated with various clinicopathological parameters using Pearson's chi-square test with results shown in Table 5.4.

Table 5.4 Correlation of CYP2W1 with clinicopathological parameters in breast cancer tissues.

Clinicopathological Parameters		CYP2W1					
		Cytoplasmic expression			Nuclear expression		
		Low	High	P value	Low	High	P value
Age	< 50 years	335 (25.6%)	81 (6.2%)	**0.002**	206 (15.7%)	210 (16%)	0.39
	≥ 50 years	777 (59.4%)	116 (8.9%)		465 (35.5%)	428 (32.7%)	
Tumour size	< 20mm	665 (50.9%)	130 (9.9%)	0.107	404 (30.9%)	391 (29.9%)	0.74
	≥20 mm	445 (34%)	67 (5.1%)		265 (20.3%)	247 (18.9%)	
T stage	1	686 (52.6%)	127 (9.7%)	0.218	422 (32.3%)	391 (39%)	0.796
	2	303 (23.3%)	57 (4.4%)		181 (13.9%)	180 (13.8%)	
	3	118 (9.0%)	13 (1%)		65 (5.0%)	66 (5.1%)	
Tumour grade	1	161 (12.3%)	26 (2%)	0.185	82 (6.3%)	105 (8%)	0.086
	2	464 (35.5%)	71 (5.4%)		284 (21.7%)	261 (19.2%)	
	3	468 (37.2%)	100 (7.6%)		304 (23.2%)	282 (21.6%)	
ER status	Negative	209 (16%)	47 (3.6%)	0.107	137 (10.5%)	119 (9.1%)	0.405
	Positive	902 (68.9%)	151 (11.5%)		533 (40.7%)	520 (39.7%)	
PgR status	Negative	442 (36.3%)	70 (5.8%)	0.256	254 (20.9%)	258 (21.2%)	0.322
	Positive	592 (48.6%)	113 (9.6%)		370 (30.4%)	335 (27.5%)	
NPI category	Good (≤3.4)	373 (28.6%)	57 (4.4%)	**0.013**	211 (16.2%)	219 (16.8%)	0.518
	Intermediate (3.41-5.4)	550 (42.2%)	119 (9.1%)		352 (27.0%)	317 (24.3%)	
	Poor (>5.4)	184 (14.1%)	21 (1.6%)		105 (8.1%)	100 (7.7%)	

Table continued.

Clinicopathological Parameters		CYP2W1					
		Cytoplasmic expression			Nuclear expression		
		Low	High	P value	Low	High	P value
Tubule formation	1	75 (5.8%)	15 (1.2%)		36 (2.8%)	54 (4.2%)	
	2	303 (23.4%)	59 (4.6%)	0.624	185 (14.3%)	177 (13.7%)	0.081
	3	722 (55.8%)	121 (9.3%)		442 (34.1%)	401 (31%)	
Pleomorphism	1	15 (1.2%)	1 (0.1%)		5 (0.4%)	11 (0.8%)	
	2	332 (25.6%)	44 (3.4%)	0.05	193 (14.9%)	183.5 (14.1%)	0.275
	3	752 (58.1%)	150 (11.6%)		465 (35.9%)	438 (33.8%)	
Mitosis	1	553 (42.8%)	76 (5.9%)		314 (24.3%)	315 (24.4%)	
	2	207 (16%)	40 (3.1%)	**0.009**	124 (9.6%)	123 99.5%)	0.503
	3	338 (26.1%)	79 (6.1%)		223 (17.2%)	194 (15.0%)	
HER2 status	Negative	964 (78.4%)	164 (13.3%)	**0.003**	579 (47.1%)	549 (44.7%)	0.464
	Positive	75 (6.1%)	26 (2.1%)		48 (3.9%)	49.5 (4.3%)	
Triple negative disease	Negative	937 (72.5%)	158 (12.2%)	0.164	550 (42.6%)	545 (42.2%)	0.187
	Positive	161 (12.5%)	36 (2.8%)		109 (8.4%)	88 (6.9%)	
Vascular invasion	Negative	772 (59.1%)	147 (11.3%)	0.156	455 (34.8%)	464 (35.5%)	0.068
	Positive	337 (25.8%)	50 (3.8%)		213 (16.3%)	174 (13.3%)	
Tumour type	Ductal (including mixed	954 (72.9%)	177 (13.5%)		587 (44.9%)	544 (41.6%)	
	Lobular	100 (7.6%)	6 (0.5%)		53 (4.1%)	53 (4.1%)	
	Medullary-like	8 (0.6%)	3 (0.2%)	0.05	5 (0.4%)	6 (0.5%)	0.227
	Miscellaneous	9 (0.7%)	1 (0.1%)		4 (0.3%)	6 (0.5%)	
	Special type	37 (2.8%)	10 (0.8%)		18 (1.4%)	29 (2.2%)	
	Tubular	3 (0.2%)	0 (0.0%)		3 (0.2%)	0 (0.0%)	

Abbreviations: ER, estrogen receptor; PgR, progesterone receptor; HER2, human epidermal growth factor receptor-2; NP1, Nottingham prognostic index. The P values are resultant from the Pearson χ^2 test of association or Fisher's Exact test if a cell count was less than five. Significant *P*-values are indicaed in bold. The number and percentage of observations for cohort is shown for each clinicopathological variable.

As seen above, 11.5% of cases with high cytoplasmic CYP2W1 were present in ER-positive (*P*=0.107), but only 2.1% and 2.8% of cases with high cytoplasmic CYP2W1 were present in HER-2 positive (*P*=0.003) and TN (*P*=0.164) breast cancers respectively. High cytoplasmic CYP2W1 expression was significantly associated with other clinical and pathological parameters such as in patients 50 years or above (χ^2=9.325, df=1,

P=0.002) and absence of HER-2 positive disease (χ^2=8.903, df=1, *P*=0.003). Similar to CYP2S1, high cytoplasmic CYP2W1 was significantly associated with intermediate NPI prognostic group (χ^2=8.678, df=2, *P*=0.013) and high mitosis (χ^2=9.516, df=2, *P*=0.009).

39.7% of patients with high nuclear CYP2W1 belonged to the ER-positive (*P*=0.405) subtype, but only 4.3% and 6.9% of cases with high nuclear CYP2W1 were of the HER-2 positive (*P*=0.464) and TN (*P*=0.187) breast cancers. Nuclear CYP2W1 did not show any association with clinical and pathological variables. Such data indicate that high nuclear CYP2W1 expression was specific to ER-positive cancers compared to HER-2 positive and TNBC cases.

In vitro Western blot data from chapter 3 demonstrated that the expression of CYP2W1 was higher in ER-positive breast cancer cell lines compared to the triple negative cells. Data from the present chapter, show that nuclear CYP2W1 is commonly expressed in ER-positive tumours, which is consistent with the observations observed *in vitro* and with the reported role of CYP2W1 in estrogen metabolism (Zhao et al., 2016).

The association of cytoplasmic CYP2W1 with the intermediate NPI group suggests that high expression of this enzyme could potentially be used as a marker to identify HER-2 negative tumours with intermediate risk of relapse that might be eligible for additional cytotoxic chemotherapy (NICE, 2018). CYP2W1 has been previously reported to be expressed in rapidly proliferating tissues and shows a tumour-specific expression pattern (Zhao et al., 2016), which is consistent with its association in cases with higher mitosis observed in the current study. Such data suggest that CYP2W1 may be involved in the proliferation of breast cancer cells. Current data indicate that high expression of cytoplasmic CYP2W1 could be used as a marker in the identification of HER-2 negative patients above the age of 50 with intermediate risk of recurrence, requiring additional cytotoxic chemotherapy. These subgroups of patients may also benefit from potential HAP treatments.

5.4.7 Association of CYP2S1 and overall survival

The reported role of CYP enzymes in the metabolism of estrogens and anti-cancer agents such as tamoxifen and taxanes, suggest that these enzymes may be involved in breast cancer pathogenesis and response of patients to treatments (Singh et al., 2011, Zhao et al., 2016). Therefore, in the current study the association of CYP2S1 and CYP2W1 protein with breast cancer specific survival were assessed in the total patient cohort.

Analysis show that low cytoplasmic expression of CYP2S1 was, in the total patient cohort, significantly associated with poor breast cancer specific survival (*P*=0.034) as shown by Kaplan-Meier survival analysis in Figure 5.6.

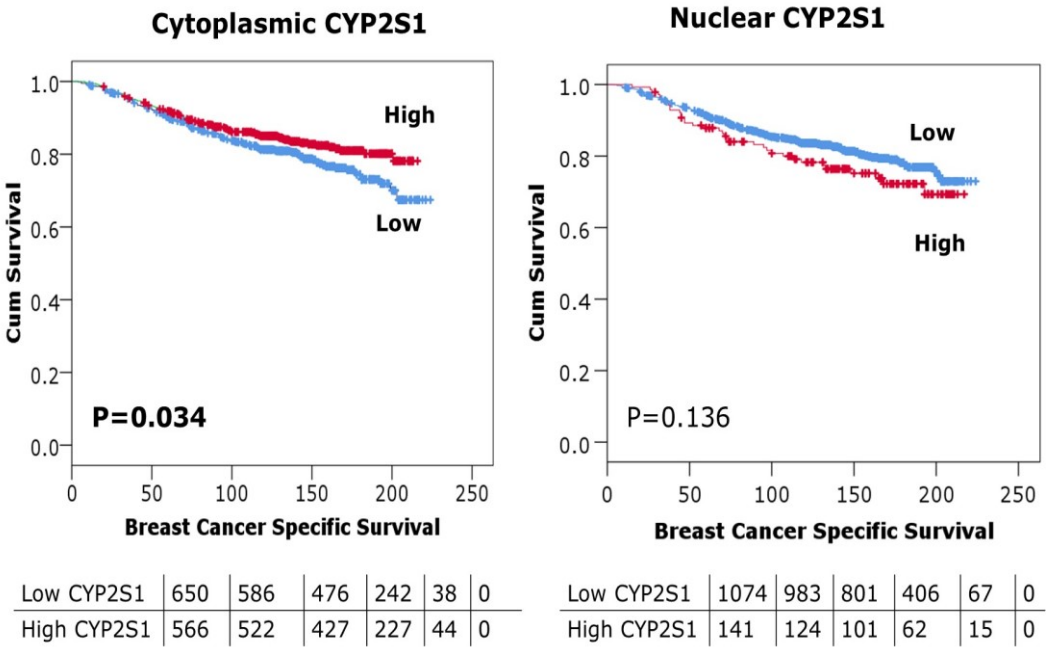


Figure 5.6 Kaplan-Meier survival analysis of CYP2S1 and breast cancer specific survival. Survival curves showing the impact of low (blue line) and high (red line) CYP2S1 expression in cytoplasm and nucleus. Significance was determined using the log-rank test. The numbers shown below the Kaplan-Meier survival curves are the number of patients at risk at the specified month. Significant *P*-values (<0.05) are indicated in bold.

All prognostic variables were individually tested for their association with survival using the Kaplan-Meier with significance determined using the log-rank test. Lower expression of CYP2S1 in the cytoplasm was significantly associated with adverse survival (hazard ratio (HR): 0.639; 95%

confidence interval (CI): 0.483-0.846; *P*=0.002), when potentially confounding factors were included in multivariate assessment (including tumour size, grade, nodal stage, vascular invasion status, ER, PgR and HER2 receptor status) (Table 5.5).

Table 5.5 Cox proportional hazards analysis for overall survival for cytoplasmic CYP2S1 expression.

		95.0% CI for Exp(B)		
Variable	**Sig.**	**Exp (B)**	**Lower**	**Upper**
CYP2S1 (Cytoplasmic)	**0.002**	0.639	0.483	0.846
Tumour size	0.069	0.766	0.575	1.021
Tumour grade	**<0.001**	1.852	1.411	2.432
Nodal stage	**<0.001**	1.783	1.467	2.167
ER status	0.810	0.955	0.654	1.394
PR status	**<0.001**	1.857	1.329	2.593
HER2 status	**0.037**	0.669	0.458	0.976
Vascular invasion	**0.003**	1.594	1.176	2.161

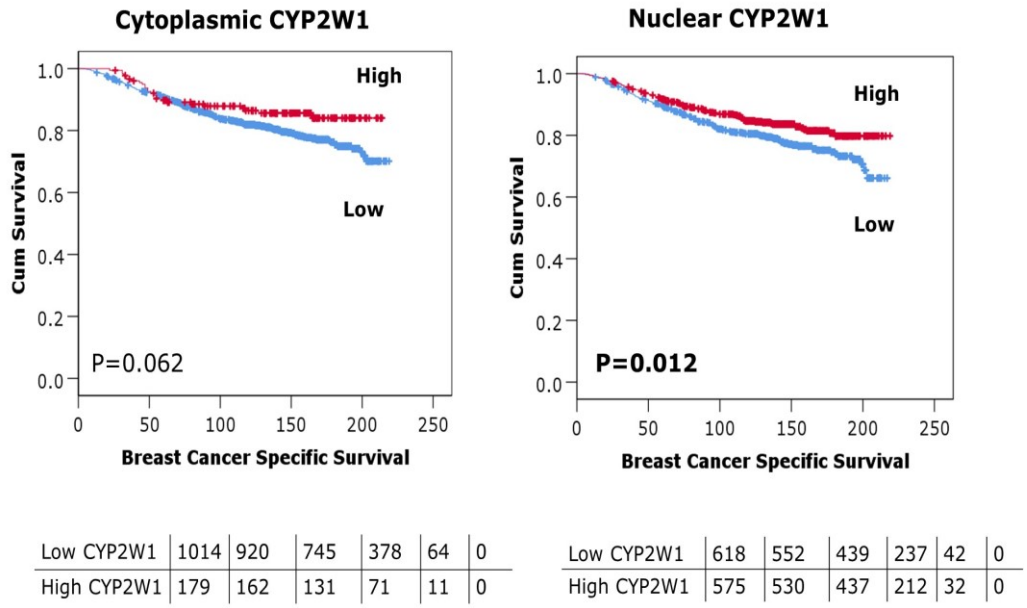
Exp(B) is used to denote hazard ratio and 95% CI is used to denote 95% confidence interval. Significant *P*-values (<0.05) are indicated in bold.

The opposite trend was observed for nuclear CYP2S1 with high expression showing association with adverse survival. Nuclear CYP2S1 expression did not show any statistical significance (*P*=0.136) with breast cancer specific survival, therefore, multivariate analysis was not performed.

5.4.8 Association of CYP2W1 and overall survival

Low nuclear expression of CYP2W1, in the total patient cohort, was significantly associated with adverse breast cancer specific survival (*P*=0.012) as shown by Kaplan-Meier survival analysis in Figure 5.7.

In multivariate analysis, with potentially confounding factors such as tumour size, grade, stage, vascular invasion status, ER, PgR and HER2 receptor status, lower expression of CYP2W1 in the nucleus remained significantly associated with poor survival (hazard ratio (HR): 0.677; 95% confidence interval (CI): 0.510-0.898; *P*=0.007) (Table 5.6). Cytoplasmic CYP2W1 was not significantly associated (*P*=0.062) with survival of breast cancer patients and therefore, multivariate analysis was not conducted.



Low CYP2W1	1014	920	745	378	64	0
High CYP2W1	179	162	131	71	11	0

Low CYP2W1	618	552	439	237	42	0
High CYP2W1	575	530	437	212	32	0

Figure 5.7 Kaplan-Meier survival analysis of CYP2W1 and breast cancer specific survival. Survival curves showing the impact of low (blue line) and high (red line) CYP2W1 expression in cytoplasm and nucleus. Significance was determined using the log-rank test. The numbers shown below the Kaplan-Meier survival curves are the number of patients at risk at the specified month. Significant *P*-values (<0.05) are indicated in bold.

Table 5.6 Cox proportional hazards analysis for overall survival for cytoplasmic CYP2W1 expression.

		95.0% CI for Exp(B)		
Variable	**Sig.**	**Exp (B)**	**Lower**	**Upper**
CYP2W1 (Nuclear)	**0.007**	0.677	0.510	0.898
Tumour size	0.159	0.806	0.598	1.088
Tumour grade	**<0.001**	1.770	1.347	2.326
Nodal stage	**<0.001**	1.852	1.518	2.259
ER status	0.878	0.970	0.660	1.425
PR status	**<0.001**	2.002	1.425	2.813
HER2 status	0.083	0.710	0.483	1.046
Vascular invasion	**0.001**	1.686	1.235	2.302

Exp(B) is used to denote hazard ratio and 95% CI is used to denote 95% confidence interval. Significant P values (<0.05) are indicated in bold.

Current data show that low expression of cytoplasmic CYP2S1 and nuclear CYP2W1 is associated with adverse survival of breast cancer patients in the total cohort. Data also indicate that higher expression of CYP enzymes is associated with improved prognosis, which may be due to the efficient metabolism of chemotherapeutic agents occurring in the presence of these

enzymes (Singh et al., 2011, Ghose et al., 2016). Furthermore low expression of CYP2S1 and CYP2W1 may be able to identify patient subgroups that are unable to efficiently metabolise certain anti-cancer agents. Such insight may help clinicians tailor specific treatments to patients which are not dependent on CYP enzymes for metabolism.

5.4.9 Association of CYP2S1 and CYP2W1 with survival in ER-positive and negative breast cancers

The involvement of cytochrome P450 enzymes in the metabolism and oxidation of estrogen along with its strong association in ER-positive cancers as seen from section 5.4.5 and 5.4.6, suggests that these enzymes may be important as prognostic markers in ER-positive disease. Therefore, the association of cytoplasmic and nuclear CYP2S1 and CYP2W1 with survival were further assessed in ER-positive and ER-negative disease as shown in Figure 5.8 and Figure 5.9 respectively.

5.4.9.1 CYP2S1 and survival in ER-positive and negative cancers

A shown in Figure 5.8, low expression of cytoplasmic CYP2S1 was significantly associated with adverse breast cancer specific survival in ER-positive patients (P=0.031), but not in ER-negative disease (P=0.197). 102/535 ER-positive patients with low CYP2S1 expression had adverse events compared to only 61/435 in the high cytoplasmic CYP2S1 group. There was no significant association between nuclear CYP2S1 and survival in ER-positive (P=0.388) or ER-negative cancers (P=0.314).

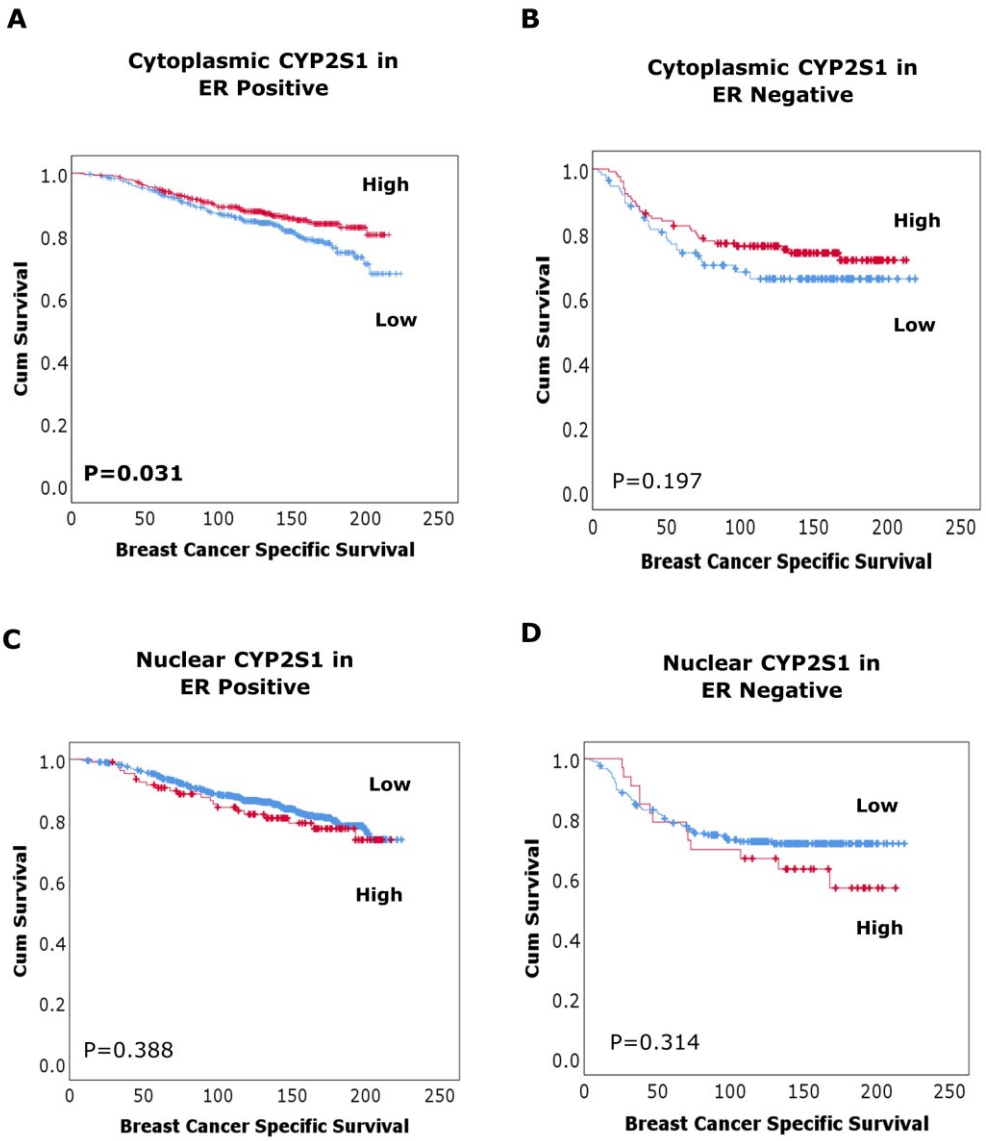


Figure 5.8 Kaplan-Meier analysis of CYP2S1 and survival in ER-positive and negative breast cancers. Cytoplasmic CYP2S1 expression in (A) ER-positive and (B) ER-negative patients. Nuclear CYP2S1 in (C) ER-positive and (D) ER-negative patients. Survival curves showing the impact of low (blue line) and high (red line) CYP2S1 expression in ER-positive and ER-negative patients. Significance was determined using the log-rank test. Significant *P*-values (<0.05) are indicated in bold.

5.4.9.2 CYP2W1 and survival in ER-positive and negative cancers

Kaplan-Meier survival analysis of cytoplasmic and nuclear CYP2W1 in ER-positive and negative subgroups is presented in Figure 5.9.

Low nuclear CYP2W1 was associated with poor survival in ER-negative patients (*P*=0.020), but no significant associations were found between nuclear CYP2W1 and survival in ER-positive patients (*P*=0.177). 46/130 of

ER-negative patients with low nuclear CYP2W1 had an event compared to only 24/111 ER-negative patients with high nuclear CYP2W1 expression. The expression of cytoplasmic CYP2W1 was not associated with survival in ER-positive (*P*=0.156) or ER-negative patients (*P*=0.104).

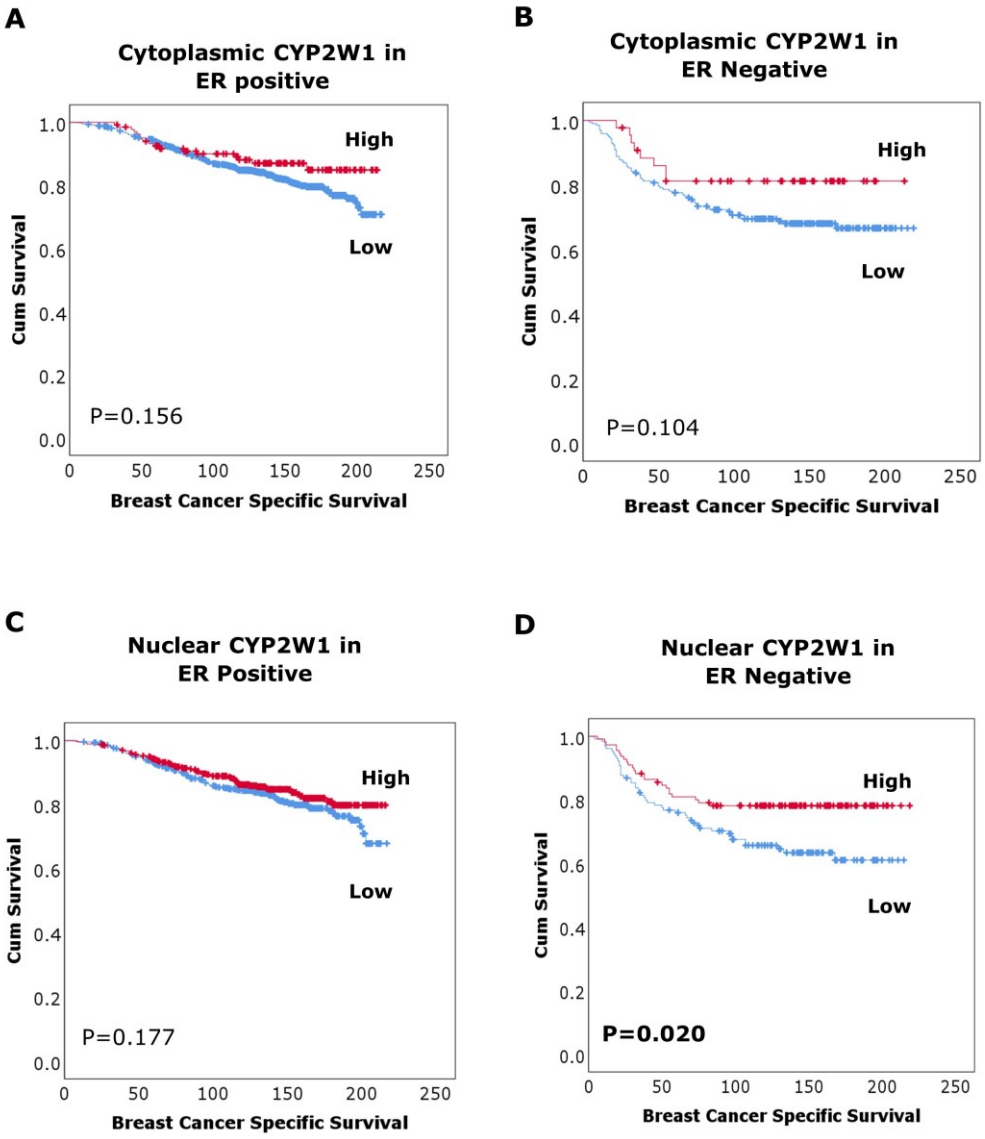


Figure 5.9 Kaplan-Meier analysis of CYP2W1 and survival in ER-positive and negative breast cancers. Cytoplasmic CYP2W1 expression in (A) ER-positive and (B) ER-negative patients. Nuclear CYP2W1 in (C) ER-positive and (D) ER-negative patients. Survival curves showing the impact of low (blue line) and high (red line) CYP2W1 expression in ER-positive and ER-negative patients. Significance was determined using the log-rank test. Significant *P*-values (<0.05) are indicated in bold.

Current data indicate that low cytoplasmic CYP2S1 was associated with shorter survival of ER-positive patients whereas low nuclear CYP2W1 was

associated with poor survival in ER-negative patients. Such data indicate that lower expression of these enzymes contributes to poor survival regardless of ER-status. Although the role of CYP enzymes in ER-negative breast cancers are not fully understood, it appears that high expression of these enzymes are protective and associated with improved prognosis in both ER-positive and negative cancers.

Survival curves showing the association between cytoplasmic CYP2S1 and survival in HER-2 +/- and TNBC +/- patients are supplied in Appendix D-Figure D2. Similar trends to those observed in the above section were noted for HER-2 +/- and TNBC +/-, further suggesting that low expression of these enzymes may be associated with poor survival across all subtypes of breast cancer. Statistical analyses were not carried out in these subgroups due to the smaller number of cases for HER-2 positives (5.2%) and TNBCs (7.7%). The association between CYP2W1 with survival in HER-2 positive/negative and TNBC positive/negative patients were not pursued due to the smaller number of TNBC (6.9%) and HER-2 (4.3%) patients in the cohort. Future experiments may assess the prognostic significance of the orphan CYP enzymes in a large cohort of HER-2 +/- and TNBC +/- patients to confirm such findings.

Due to unavailability of treatment response information for the current cohort, the expression of these enzymes could not be assessed in response to neoadjuvant chemotherapy (NACT), hormonal therapy (HT), chemotherapy (CT) or radiotherapy (RT). Future work may correlate expression of these enzymes to responders of NACT, HT, CT and RT to assess if higher expression of these enzymes is associated with improved prognosis after therapy.

5.4.10 Combined cytoplasmic/nuclear CYP2S1 and survival

Kaplan-Meier analysis of combined cytoplasmic and nuclear CYP2S1 in the total patient cohort, ER-positive and ER-negative patients is shown below in Figure 5.10-A, 5.10-B, and 5.10-C respectively. Marker combinations used in the analysis include low cytoplasmic and low nuclear (blue line), high cytoplasmic and low nuclear (red line), low cytoplasmic and high

nuclear (green line) and high cytoplasmic and high nuclear expression (orange line).

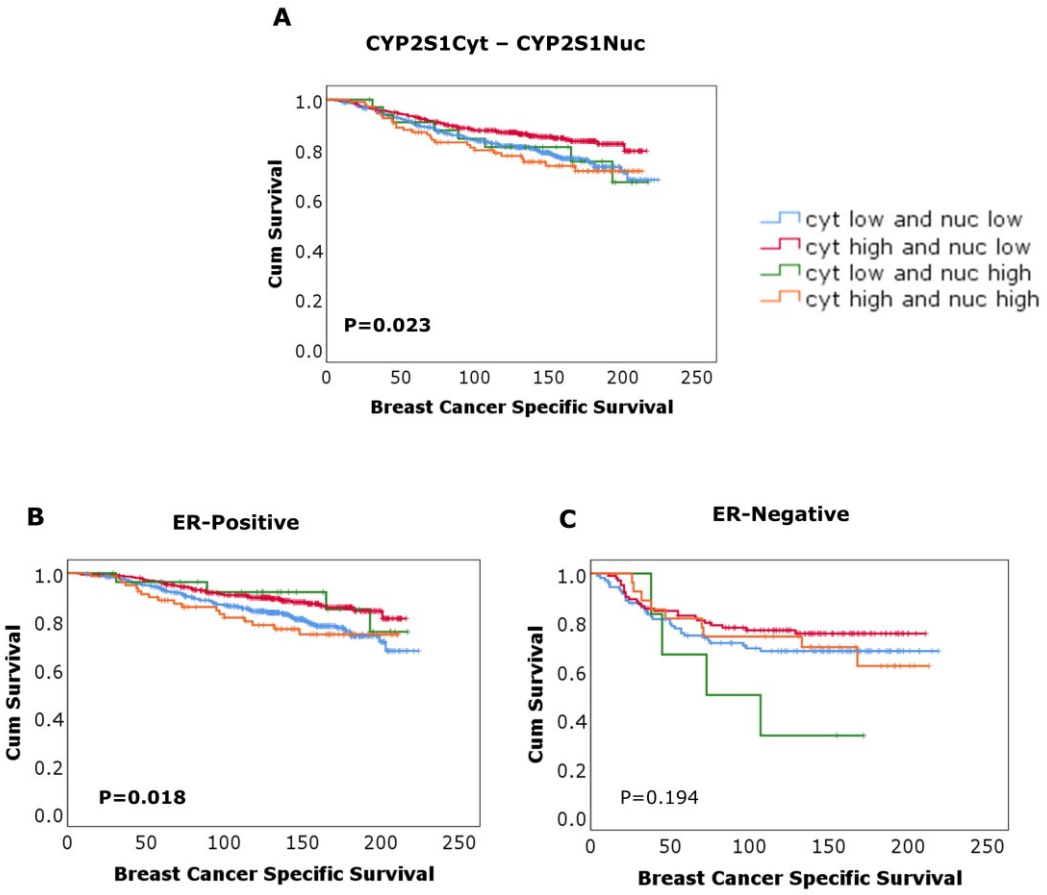


Figure 5.10 Kaplan-Meier analysis of combined cytoplasmic and nuclear CYP2S1 on breast cancer specific survival. The effect of combined cytoplasmic and nuclear CYP2S1 in the (A) Total patient cohort (B) ER-positive and (C) ER-negative patients. Survival curves showing the impact of low cytoplasmic and low nuclear (blue line); high cytoplasmic and low nuclear (red line); low cytoplasmic and high nuclear (green line) and high cytoplasmic and high nuclear (orange line) expression. Significance was determined using the log-rank test. Significant *P* values (<0.05) are indicated in bold.

Interestingly high expression of combined cytoplasmic and nuclear CYP2S1 was significantly associated with adverse survival of breast cancer patients in the total cohort (*P*=0.023) and in ER-positive patients (*P*=0.018). 27/107 of patients in the total cohort with high CYP2S1 (cytoplasmic+nuclear) had adverse events compared to only 65/458 in the low cytoplasmic CYP2S1/high nuclear CYP2S1 group which demonstrated the best survival among the 4 different groups.

The same trend was observed in ER-positive patients, with 18/80 patients with high CYP2S1 (cytoplasmic+nuclear) having events compared to only 45/354 patients belonging to the low cytoplasmic CYP2S1/high nuclear CYP2S1 group. Expression of combined cytoplasmic and nuclear CYP2S1 had no association with survival in the ER-negative subgroup.

It is interesting to note that the presence of high nuclear CYP2S1 is able to reverse the survival trend from low to high contributing to adverse survival in the above mentioned data and in subsequent marker analysis shown in section 5.4.12. Single marker survival analysis of nuclear CYP2S1 in section 5.4.7 demonstrated that high expression was associated with poor survival, although statistical significance was not reached. Data in the current study demonstrate that in combination with high cytoplasmic CYP2S1, high nuclear CYP2S1 identifies a subgroup of patients with adverse survival.

5.4.11 Combined cytoplasmic/nuclear CYP2W1 and survival

Kaplan-Meier survival analysis of combined cytoplasmic and nuclear CYP2W1 in the total patient cohort and in ER-positive and ER-negative patients are shown in Figure 5.11-A, 5.11-B and 5.11-C respectively.

Low expression of combined cytoplasmic and nuclear CYP2W1 was, in the total patient cohort, associated with adverse survival of breast cancer patients (P=0.035). 129/555 patients with low cytoplasmic and nuclear CYP2W1 had adverse events compared to 15/116 in the high cytoplasmic and nuclear CYP2W1 group demonstrating improved patient survival. Low expression of cytoplasmic and nuclear CYP2W1 was also significantly associated with adverse survival in the ER-negative subgroup (P=0.040), with 42/109 events in the low subgroup compared to only 4/23 events in the high subgroup. Cytoplasmic and nuclear CYP2W1 did not demonstrate any such association in ER-positive breast cancers (P=0.354).

Such data indicate that combined expression of low cytoplasmic and nuclear CYP2W1 in the total patient cohort, and in ER-negative breast cancers is associated with poor survival of patients. Data indicate that CYP2W1 may be of prognostic significance in ER-negative breast cancers.

However, caution must be taken while interpreting this data as the cohort used in the study was predominantly ER-positive. Analysis on a large cohort of ER-negative patients should be conducted before reaching any firm conclusions.

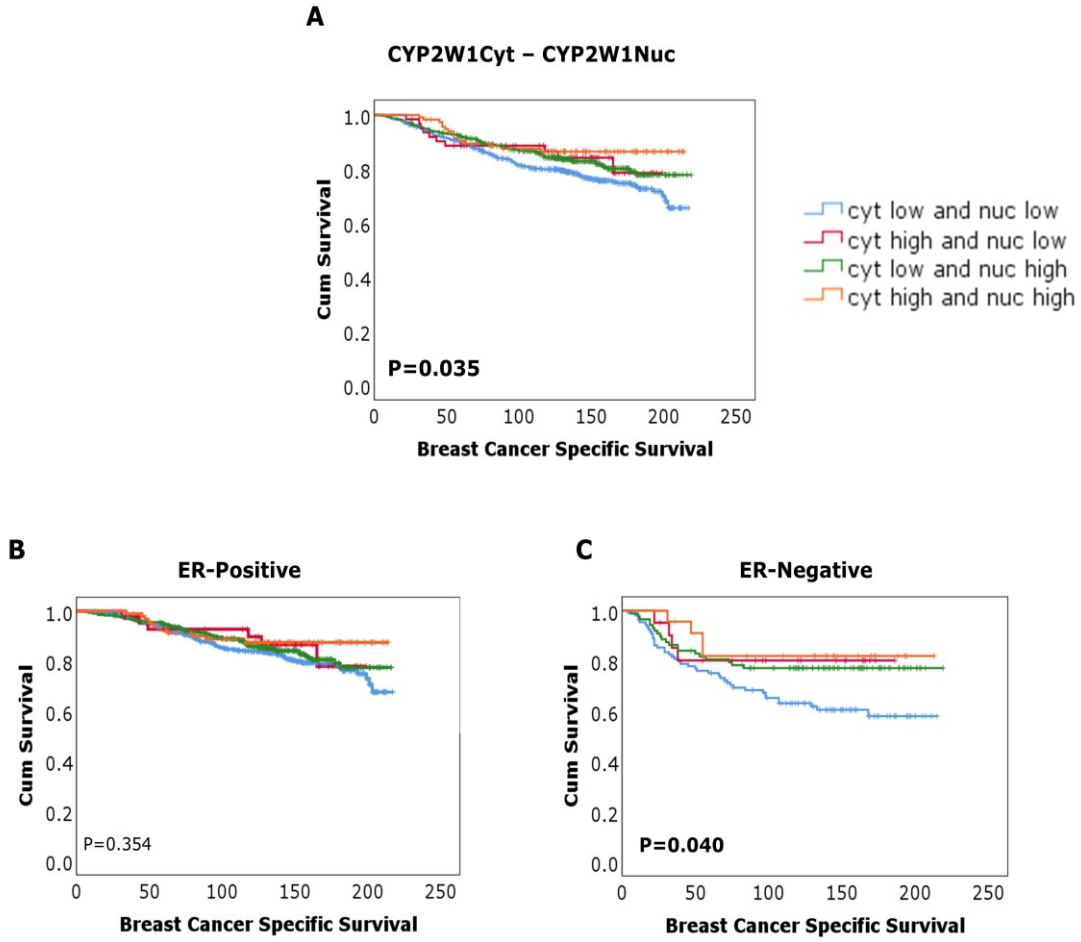


Figure 5.11 Kaplan-Meier analysis of combined cytoplasmic and nuclear CYP2W1 on breast cancer specific survival. Effect of combined cytoplasmic and nuclear CYP2W1in the (A) Total patient cohort (B) ER-positive and (C) ER-negative patients. Survival curves showing the impact of low cytoplasmic and low nuclear (blue line); high cytoplasmic and low nuclear (red line); low cytoplasmic and high nuclear (green line) and high cytoplasmic and high nuclear (orange line) expression. Significance was determined using the log-rank test. Significant *P* values (<0.05) are indicated in bold.

5.4.12 Association of combined CYP2S1/CYP2W1 and survival

Association of marker combinations such as cytoplasmic CYP2S1 and nuclear CYP2W1 (Figure 5.12-A), nuclear CYP2S1 and cytoplasmic CYP2W1 (Figure 5.12-B), cytoplasmic CYP2S1 and cytoplasmic CYP2W1, (Figure 5.12-C) and nuclear CYP2S1 and nuclear CYP2W1 (Figure 5.12-D) were

also analysed to assess the effects of marker combinations on breast cancer specific survival in the total patient cohort.

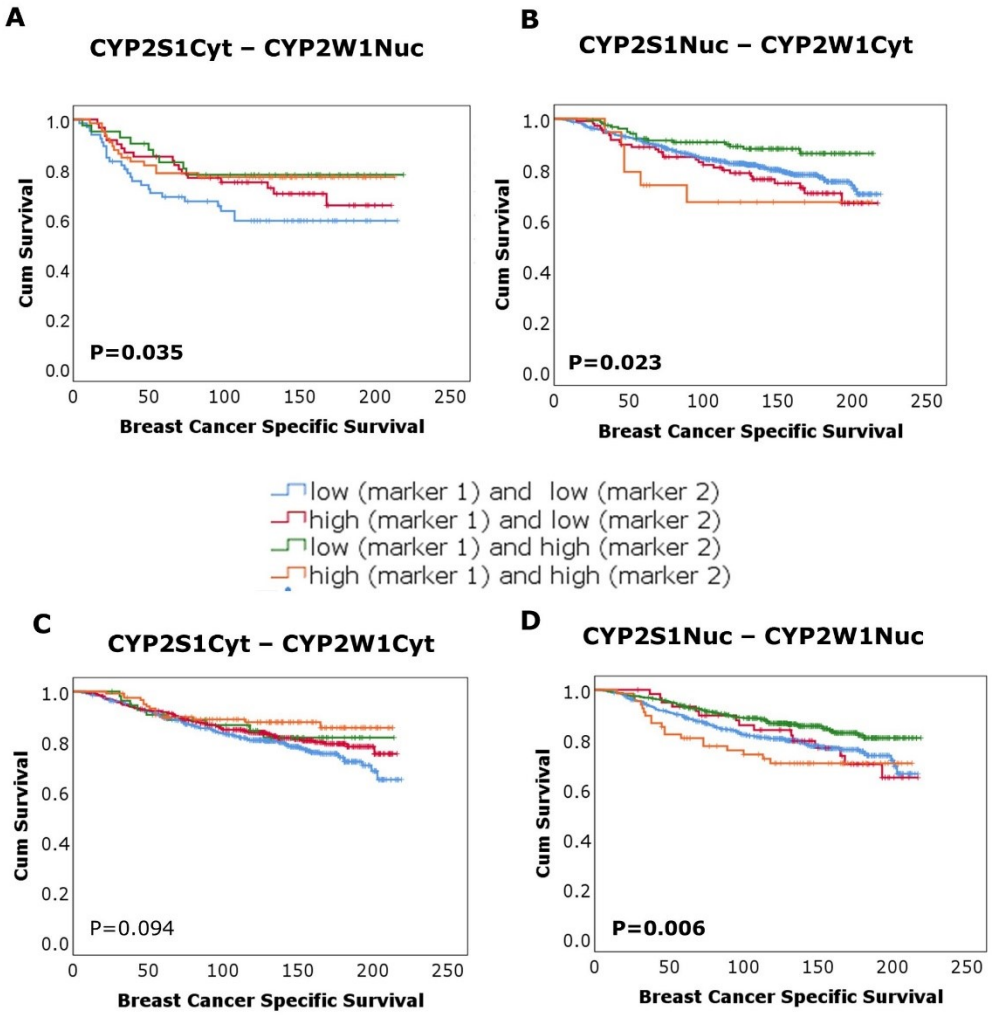


Figure 5.12 Kaplan-Meier analysis of combined CYP2S1/CYP2W1 and breast cancer specific survival. Survival curves showing the impact of (A) Cytoplasmic CYP2S1 and nuclear CYP2W1 (B) Nuclear CYP2S1 and cytoplasmic CYP2W1 and (C) Cytoplasmic CYP2S1 and CYP2W1 and (D) Nuclear CYP2S1 and CYP2W1 in the total patient cohort. Low-low expression of both markers is depicted as blue line; high and low as red line; low and high as green line and; high and high as orange line. Significance was determined using the log-rank test. Significant *P*-values (<0.05) are indicated in bold.

Single marker analysis in previous sections demonstrated that cytoplasmic CYP2S1 (section 5.4.7) and nuclear CYP2W1 (section 5.4.8) were associated with poor survival of breast cancer patients and remained so in multivariate analysis. Combination of both these markers as seen in Figure 5.12-A was also associated with shorter breast cancer specific survival (*P*=0.035) in the total patient cohort. 84/348 patients in the low

cytoplasmic CYP2S1/low nuclear CYP2W1 had adverse events compared to only 42/298 patients in the high-high subgroup. Such data further reiterates the prognostic importance of these enzymes in breast cancer.

Kaplan-Meier survival curves for combined cytoplasmic CYP2S1 and nuclear CYP2W1 in ER+/-, HER-2+/- and for TNBC+/- is given in Appendix D-Figure D3. Similar trends as that obtained in the total patient cohort (Figure 5.12) is observed i.e. the association of low cytoplasmic CYP2S1 and nuclear CYP2W1 with adverse survival was seen in ER+/-, HER-2 negative and TNBC+/- subtype, indicating that absence of these markers results in poor survival, irrespective of subtype. Further assessment is required in a larger number of HER-2 positive and TNBC patients to confirm such findings.

Figure 5.12-C shows that low expression of both cytoplasmic CYP2S1 and CYP2W1 was associated with adverse survival in the total patient cohort (P=0.094), although statistical significance was not reached. 84/348 patients with low expression had adverse survival compared to only 15/119 events in the high expression group. Figure 5.12-B show that high expression of nuclear CYP2S1 and cytoplasmic CYP2W1 was associated with poor survival (P=0.023) in the total patient cohort. 6/19 patients with high expression had adverse events compared to only 18/155 patients in the low nuclear CYP2S1 and high cytoplasmic CYP2W1 group. Similarly high expression of nuclear CYP2S1 and CYP2W1 (Figure 5.12-D), was associated with adverse breast cancer specific survival (P=0.006) with 19/67 patients experiencing adverse events compared to 70/473 events in the low nuclear CYP2S1 and high nuclear CYP2W1 group, which demonstrated the best survival trends.

It is important to note that high expression of nuclear CYP2S1 is consistently associated with shorter survival of patients as seen in section 5.4.10 and combined marker analysis in Figure 5.12-B and Figure 5.12-D. It appears to be a powerful marker in that the presence of high nuclear CYP2S1 has the ability to change survival from the consistently observed low expression-poor survival trend to high expression-poor survival. Future experiments should investigate further the prognostic significance and

functions of nuclear CYP2S1 in the different subtypes of breast cancer and this may help identify subgroups of patients with adverse prognosis.

5.4.13 Association of CYP2S1 and CYP2W1 mRNA with clinicopathological variables and survival in the METABRIC cohort

In the METABRIC cohort, CYP2S1 mRNA expression ranged from 5.3-8.58 (median - 6.02), and had an X-tile generated cut-point of 6.74, with 94.5% of cases (1873/1980) demonstrating low expression and 5.4% of cases (107/1980) with high expression. CYP2W1 mRNA expression ranged from 4.81-6.29 (median - 5.42), and had a cut-point of 5.54, with 51.4% of cases (623/1212) demonstrating low expression and 48.5% of cases (589/1212) with high expression. Spearman's correlation demonstrated that the expression of CYP2S1 mRNA was negatively correlated to CYP2W1 mRNA (r^2=-0.063, *P*=0.005). This observation is similar to data obtained with nuclear CYP2S1 protein expression which was negatively correlated to both cytoplasmic and nuclear CYP2W1 protein, as demonstrated in section 5.4.4.

Table showing association of CYP2S1 and CYP2W1 with clinicopathological parameters is shown in Appendix D-Table D1 and Table D2 respectively. High expression of CYP2S1 mRNA was significantly associated with absence of HER-2 positive disease (χ^2=11.652, df=1, *P*=0.001), absence of PgR (χ^2=10.400, df=1, *P*=0.001) and basal-like breast cancers (χ^2=15.377, df=5, *P*=0.009). The expression of high CYP2W1 was significantly associated with tumour size ≥20 cm (χ^2=6.919, df=1, *P*=0.009) and luminal A cancers (χ^2=13.431, df=5, *P*=0.020). The association of high CYP2S1 mRNA with absence of HER-2 status, and high CYP2W1 with Luminal A tumours is in agreement with results obtained in the Nottingham cohort protein assessments.

Kaplan-Meier survival analysis demonstrated that unlike protein expression, the mRNA expression of both CYP2S1 (*P*=0.279) and CYP2W1 (*P*=0.121) were not significantly associated with survival in the METABRIC cohort, although similar trends (low expression resulting in poor survival) to that observed in the Nottingham cohort, with protein expression, was noted. Survival curves are presented in Appendix D-Figure D4.

In conclusion, the current chapter demonstrates the prognostic importance of CYP2S1 and CYP2W1 protein expression in both single marker and combined marker analysis. Future studies should assess the predictive power of the protein expression by examining association between CYP2S1/CYP2W1 and overall survival by treatment, to particularly identify their role in the chemotherapeutic response of breast cancer patients.

5.5 Discussion

The cytochrome P450 family of enzymes have important roles in the progression of cancer by activating pre-carcinogens and in response to chemotherapy, where they participate in the activation or inactivation of anti-cancer agents (Danielson, 2002). The 'orphan' CYP enzymes, CYP2S1 and CYP2W1 show upregulated expression in breast cancer tissues (Hlaváč et al., 2014). They are also involved in the reductive activation of AQ4N, and possibly KP167 into their respective cytotoxic metabolites (Nishida et al., 2010). Therefore, identifying their expression in breast cancer may help identify patient tumours that can potentially benefit from prodrug treatment (following confirmation of hypoxia). The aim of the current chapter was to investigate the clinical expression of CYP2S1 and CYP2W1 in a large independent cohort of breast cancer patients by immunohistochemistry. The cytoplasmic and nuclear expression of these proteins were assessed and correlated to various clinicopathological parameters and survival. The expression of CYP2S1 and CYP2W1 mRNA were also correlated to clinicopathological parameters and survival in the METABRIC cohort, in order to assess if similar trends would be observed between protein (Nottingham cohort) and mRNA expression (METABRIC cohort).

Immunohistochemical staining indicated that the expression of both CYP2S1 and CYP2W1 were present in the majority of breast cancer tissues. Both markers demonstrated localisation in the cytoplasm and nucleus, which is in accordance with previously reported studies (Saarikoski et al., 2005b, Ronchi et al., 2014, Wang et al., 2020). On assessing correlation between the markers, the expression of cytoplasmic CYP2S1 demonstrated a significantly positive, but weak correlation to cytoplasmic and nuclear

CYP2W1. This may be because both CYP2S1 and CYP2W1 belong to the CYP2 family of cytochrome P450 enzymes and share 40% sequence homology (Kumarakulasingham et al., 2005, Saarikoski et al., 2005b, Guengerich, 2008). They share common substrates and are expressed specifically in epithelial cells (Saarikoski et al., 2005b, Zhao et al., 2016, Szaefer et al., 2019). They are both upregulated in breast cancer cells treated with anti-cancer agents such as 5F-203 and GW-610 (Tan et al., 2011). Both these proteins are also upregulated in hypoxia by HIF-1α (Rivera et al., 2007, Chung et al., 2015), and involved in the bio-reduction of AQ4N (Nishida et al., 2010). Such data suggest that these proteins may have overlapping or similar functions in breast cancer which may explain the correlations observed between the two 'orphan' CYP enzymes. As expected, the expression of cytoplasmic CYP2S1 and CYP2W1 were correlated to their expression in the nucleus. It has been reported that although the majority of CYP enzymes are cytoplasmic, they can also be nuclear to take part in the metabolism of nuclear substrates (Muskhelishvili et al., 2001). However, the expression of nuclear CYP2S1 demonstrated a significant negative correlation with cytoplasmic and nuclear CYP2W1. Similar results were obtained in the METABRIC cohort, wherein the mRNA expression of CYP2S1 and CYP2W1 were negatively correlated. Such observations indicate that CYP2S1 and CYP2W1 may also be involved in different processes. It is important to note that all the correlations found in the present study were weak associations, and may not necessarily be biologically relevant.

It is well-established that the cytochrome P450 family of enzymes are involved in the aetiology of hormone-related cancers (Murray et al., 1997, Russo et al., 2003). This is due to their involvement in estrogen and testosterone metabolism (Hayes et al., 1996) and the generation of carcinogenic metabolites during this process (Shimada et al., 1996, Listgarten et al., 2004). The CYP enzymes are involved in the initial hydroxylation step of estrogen metabolism (Tsuchiya et al., 2005). The hydroxylated products such as 4-OHE_2 generated during estrogen metabolism can undergo redox cycling resulting in the formation of reactive quinones and semiquinones that can react with DNA to generate

highly mutagenic sites, all of which may initiate breast, prostate, and other hormone-dependent cancers (Cavalieri et al., 2000, Badawi et al., 2001). Reactive oxygen species such as H_2O_2, generated by the redox cycling of the semiquinone-quinone couple can be reduced by Fe^{2+} and Cu^{+}, to form hydroxyl radicals ($OH^{\bullet}$). In addition to oxidative DNA damage, the hydroxyl radicals also cause lipid peroxidation. The lipid hydroperoxides further stimulate estrogen metabolism, leading to additional semiquinone–quinone redox cycling, generation of ROS and additional DNA damage (Cavalieri et al., 2000), which links cytochrome P450 enzymes to the initiation and progression of several hormone-dependent cancers.

Consistent with the above mentioned involvement of cytochrome P450 enzymes in estrogen metabolism (Cheng et al., 2001), 35.5% of cases with high cytoplasmic CYP2S1 were significantly associated with ER-positive cancers (P=0.011). Although CYP enzymes are involved in estrogen metabolism, no studies have reported the direct involvement of CYP2S1 in the metabolism and oxidation of estrogens. Further studies are required to investigate the role of CYP2S1 in ER-positive tumours. Similarly, 39.7% of cases with high nuclear CYP2W1 were present in ER-positive tumours, which is consistent with *in vitro* data (chapter 3), and with the reported role of CYP2W1 in the metabolism of 17β-estradiol reported by Zhao et al., 2016. In support of this observation, the expression of CYP2W1 mRNA was highly expressed in Luminal A breast cancers in the METABRIC cohort.

5.2% (P=0.001) of patients with high cytoplasmic CYP2S1 and 1.5% (P=0.011) of cases with high nuclear CYP2S1 were present in HER-2 positive breast cancers. Similarly, only 2.1% of patients with high cytoplasmic CYP2W1 belonged to the HER-2 positive subtype (P=0.003). Only 7.7% of cases with high cytoplasmic and 1.7% with high nuclear CYP2S1 expression were present in TNBC patients. *In vitro* data from chapter 3 show that CYP2S1 was present in both luminal and TNBC cell lines, whereas in breast cancer tissues, expression was predominantly in ER-positive tumours. As seen with CYP2S1, only 2.8% with high cytoplasmic and 6.9% cases with high nuclear CYP2W1 expression were present in TNBC cases. Such data suggest that the expression of CYP2S1 and CYP2W1 may be specific to ER-positive cancers, although further

studies are required to confirm such findings. Future work can correlate expression of CYP2S1 and CYP2W1 to the cytochrome P450 enzymes involved in estrogen metabolism such as CYP1A2 and CYP3A4, to understand the role of these enzymes in estrogen metabolism and ER-positive cancers (Cheng et al., 2001). In the current study, high expression of both CYP2S1 ($P<0.001$) and CYP2W1 ($P=0.002$) were identified in patients above the age of 50.

Histological grading of breast cancer is a well-established prognostic factor, wherein tumours are morphologically assessed to determine growth patterns and extent of differentiation (Elston and Ellis, 1991). As discussed in chapter 1, breast tumours are graded on a scale of 1-3, with grade 1 tumours having favourable prognosis and grade 3 tumours being unfavourable with increased risk of growth and spread (Heimann et al., 1997). The 10-year survival of breast cancer patients ranges from 76% in grade 1 tumours to 39% for grade 3 tumours (Pereira et al., 1995). In the present study, high expression of nuclear (6.2%, $P=0.009$) and cytoplasmic (23.6%, $P<0.001$) CYP2S1 was associated with grade 3 tumours. Several studies have demonstrated that tumour grade is an independent prognostic factor in ER-positive breast cancer patients (Wirapati et al., 2008), even in those who received adjuvant endocrine therapy (Ellis et al., 2008), and in patients with lymph node-negative (Rakha et al., 2008) or positive breast cancers (Simpson et al., 2000), regardless of ER status. Studies by Desmedt and colleagues have shown that in ER-positive, HER-2 negative tumours, only proliferation index and tumour grade were significantly associated with clinical outcome in multivariate analysis (Desmedt et al., 2008). Histological grade was also an independent predictor of relapse-free survival in ER-positive, HER-2 negative tumours (Rakha et al., 2007, Rakha et al., 2008). Histological grade can therefore, provide important information regarding the clinical behaviour of tumours, especially in those subgroups (ER-positive, lymph-node-negative) in which the benefit of chemotherapy is uncertain. Such data indicate that CYP2S1 expression may help in the identification of grade 3, ER-positive, HER-2 negative patients above the age of 50 with

unfavourable prognosis that might need additional cytotoxic chemotherapy.

NPI is a prognostic indicator which combines lymph node status, tumour size and histological grade to assess growth rate, metastatic behaviour and genetic instability of breast cancers (Lee and Ellis, 2008). NPI divides patients into the good, intermediate and poor prognostic groups (Galea et al., 1992, Lee and Ellis, 2008). Patients with NPI score of 3.4 or less are considered as low-risk and scores ranging 3.4-5.4 are considered to be at intermediate-risk of relapse. ER-positive patients who fall into the intermediate-risk NPI category may be recommended additional cytotoxic chemotherapy in addition to HR therapy to reduce the risk of recurrence (Goldhirsch et al., 2005). In the present study, the expression of high cytoplasmic (25.7%, P=0.002) and nuclear (6.6% P=0.025) CYP2S1 and high cytoplasmic CYP2W1 (9.1%, P=0.013) were associated with intermediate NPI category, which suggest that high expression of these enzymes may be able to identify tumours that may benefit from additional cytotoxic therapy (NICE, 2018). Furthermore, correlating cases with high expression of CYP2S1 and CYP2W1 to markers of hypoxia such as CA9 or HIF-1α may allow selection of hypoxic tumours that may benefit from potential HAP treatment.

The distinction between benign and malignant tumours is dependent on various factors, such as increased proliferation, invasiveness and metastatic potential (Barry et al., 2001). In breast cancer, assessment of tumour cell proliferation is one of the most integral part of breast cancer grading (Lester et al., 2009). Evaluation of proliferation involves assessing mitotic activity by counting the number of cells present in the M phase of the cell cycle (Fitzgibbons et al., 2000). Higher mitotic figures increases the probability of developing distant metastasis and shorter survival (Medri et al., 2003). Pleomorphism assesses the nuclear-specific changes in nuclei of cells which correlates with clinical aggressiveness and outcome (Elston and Ellis, 1991, Volpi et al., 2004). In the current study, high cytoplasmic CYP2S1 was associated with higher pleomorphism (34%, P=0.003) and higher mitosis (17.3%, P<0.001). High nuclear CYP2S1 was also

associated with mitosis (5%, *P*=0.002). Such correlations suggest that CYP2S1 may be involved in the proliferation of breast cancer cells.

In support of such findings, it has been reviously reported that elevated levels of CYP2S1 is present in psoriasis which is a disease characterised by inflammation and hyper-proliferation of keratinocytes (Valdimarsson et al., 1986). Furthermore, studies by Madanayake et al., 2012, report that CYP2S1 modulates expression of prostaglandin E2 (PGE_2), which stimulates proliferation, migration and inhibits apoptosis in epithelial cell lines (Sheng et al., 2001). Increased expression of PGE_2, modulated by CYP2S1 was found to increase cellular proliferation in the human bronchial epithelial BEAS-2B cell lines (Madanayake et al., 2012). From the above reported findings and data obtained in the current study, it appears that CYP2S1 may alter cell proliferation in breast cancer cells by modulating expression of PGE_2. The association of other CYP enzymes with proliferation of breast cancer cells have also been reported previously. Knockdown of CYP1A1 in the luminal MCF-7 and triple negative MDAMB-231 cells was found to decrease proliferation and clonogenic survival, in addition to inducing apoptosis and cell cycle arrest (Rodriguez and Potter, 2013). Such data indicate the involvement of cytochrome P450 enzymes in the proliferation of breast cancer cells.

As seen with CYP2S1, high cytoplasmic CYP2W1 was also associated with higher mitosis (6.1%, *P*=0.009) in breast cancers. CYP2W1 is also reported to be expressed in rapidly proliferating tissues and shows a tumour-specific expression pattern (Zhao et al., 2016). Studies in embryonic and adult rat tissues demonstrated that the highest levels of CYP2W1 expression was in the embryonic colon, with a steady decrease in expression after birth suggesting a role for this protein during embryonic development (Karlgren et al., 2006, Karlgren et al., 2005). One of the reasons for the association of CYP2W1 with proliferation may be because, retinoid, which has important roles in vision, cell proliferation, differentiation, immune function and development is a well-known substrate of CYP2W1 (Huang et al., 2018). Retinoid has anti-cancer properties and functions to arrest cellular proliferation and induce cell differentiation (Tang and Gudas, 2011). The presence of CYP2W1 in breast cancers inhibits metabolism of retinoid into

retinoic acid, reducing its anti-proliferative effect in tumours (Mongan and Gudas, 2007). In support of this, it has been previously reported that retinoid signalling is compromised during carcinogenesis (Mongan and Gudas, 2007). From the above reported studies, it appears that CYP2W1 has a role in proliferation, higher expression of which is linked to higher pleomorphism and mitosis. Association of CYP enzymes to the various clinical and pathological parameters indicate that expression of CYP2S1 and CYP2W1 could potentially identify tumours with increased proliferative capacity that are of the ER-positive, HER-2 negative subtype, in women above the age of 50.

Inefficient metabolism of tamoxifen (Schroth et al., 2007), taxane and cyclophosphamide (Miyoshi et al., 2002, Miyoshi et al., 2005) by other CYP enzymes have been associated with poor survival in breast cancer patients. Therefore, the expression of CYP2S1 and CYP2W1 were correlated to survival of breast cancer patients to identify their prognostic significance. Kaplan-Meier survival analysis demonstrated that patients with low cytoplasmic CYP2S1 were significantly associated with poor breast cancer specific survival (P=0.034). 130/650 patients with low cytoplasmic CYP2S1 had adverse events compared to only 95/566 patients with high cytoplasmic CYP2S1. Multivariate analysis using Cox proportional hazard regression demonstrated that the independent factors impacting on survival were CYP2S1 (P=0.002), tumour grade (P<0.001), tumour stage (P<0.001), PgR (P<0.001), HER-2 status (P=0.037) and vascular invasion (P=0.003). Opposite trends were observed for nuclear CYP2S1 wherein high expression was associated with poor survival, although statistical significance (P=0.136) was not reached.

The expression of low nuclear CYP2W1 was also associated with adverse survival of breast cancer patients (P=0.012) as shown by Kaplan-Meier survival analysis. 139/618 patients with low nuclear CYP2W1 died compared to 94/574 patients with high nuclear CYP2W1 expression. This trend was also observed in multivariate analysis with independent factors such as CYP2W1 (P=0.007), tumour grade (P<0.001), tumour stage (P<0.001), PgR status (P<0.001) and vascular invasion (P=0.001) affecting survival of patients. The expression of cytoplasmic CYP2W1

showed similar trend (*P*=0.062) of low expression contributing to adverse survival. The correlation observed between cytoplasmic CYP2S1 and nuclear CYP2W1 is consistent with the association of both markers with poor survival of breast cancer patients.

The involvement of CYP enzymes in estrogen metabolism as reported in previous studies and their subtype-specific expression in ER-positive tumours observed in the current study, suggest that these enzymes may have prognostic significance in ER-positive breast cancers. As hypothesised survival analysis demonstrated that low cytoplasmic CYP2S1 was associated with poor survival in ER-positive patients (*P*=0.031), whereas the expression of low nuclear CYP2W1 was associated with poor survival in ER-negative patients (*P*=0.020). The role of these proteins in breast cancer progression is unclear, but the involvement of cytochrome P450 family members in estrogen metabolism and formation of carcinogenic metabolites as by-products of metabolic reactions may contribute to breast cancer pathogenesis (Badawi et al., 2001, Hayes et al., 1996). Lower expression of these proteins may result in inefficient metabolism/activation of chemotherapeutic agents which in turn may indirectly result in poor therapy response contributing to poor survival of patients (Miyoshi et al., 2002, Miyoshi et al., 2005, Schroth et al., 2007). These results are also consistent with previous studies which report that CYP2W1 is low in breast cancer patients with a stable or a progressive disease, but demonstrates increased expression in responders of neoadjuvant therapy (Hlaváč et al., 2014), which suggests that high expression of these enzymes are associated with improved prognosis, as demonstrated in the current study.

The results obtained in the current study with breast cancer contradict data by Kumarakulasingham et al., 2005, where they report that higher expression of CYP2S1 was associated with poor prognosis of colon cancer patients (Kumarakulasingham et al., 2005). Previous studies on 170 breast carcinomas report that high expression of CYP2S1 was associated with shorter survival of breast cancer patients, although this association was not found in multivariate analysis (Murray et al., 2010). Studies in colon cancer demonstrated that high expression of CYP2W1 is associated with poor survival in grade 2 and 3 colon cancers (Thomas et al., 2006, Edler

et al., 2009, Stenstedt et al., 2012). The reasons for discrepancies observed between data obtained in the current study and those reported in the literature may vary because of the differential physiologic functions of these proteins in different tissues (Zanger and Schwab, 2013, Molina-Ortiz et al., 2014). Furthermore, the findings mentioned above were all carried out in smaller numbers of patients in contrast to the current study where the expression was assessed in a large cohort of breast cancer (n=1426).

Various marker combinations were also assessed for effects on survival in the total patient cohort. Low expression of combined cytoplasmic CYP2S1 and nuclear CYP2W1 (P=0.035); high expression of nuclear CYP2S1 and cytoplasmic CYP2W1 (P=0.023); low expression of both cytoplasmic CYP2S1 and CYP2W1 (P=0.094) and high expression of nuclear CYP2S1 and CYP2W1 (P=0.006) were associated with adverse breast cancer specific survival in the total patient cohort. All of these observations reinstate the prognostic significance of CYP2S1 and CYP2W1 in breast cancer. It is important to note that the presence of high nuclear CYP2S1 in the above mentioned combinations has the ability to reverse previously observed trend (low expression – poor survival) to high expression resulting in poor survival. Further studies are required to understand the differential roles of cytoplasmic and nuclear CYP2S1 in breast cancer.

Consistent with protein data obtained in the Nottingham cohort, high expression of CYP2S1 and CYP2W1 mRNA was associated with absence of HER-2 positive disease (P=0.001), and luminal A cancers (P=0.02) respectively, in the METABRIC cohort. Although similar trends were observed (low expression-poor survival), no significant associations between CYP2S1 (P=0.279) and CYP2W1 (P=0.121) mRNA with survival of breast cancer patients were observed, contrary to that observed with protein expression (Nottingham cohort). Such discrepancies may reflect the ability of mRNA to undergo extensive post-transcriptional modifications (eg. methylation) (Greenbaum et al., 2003). RNAs are also subjected to alternative splicing, and not all splice variants may be translated into protein (Koussounadis et al., 2015). Furthermore, the protein expression of CYP2S1 and CYP2W1 were assessed only in tumour cells, whereas mRNA

isolated from tissues contains both tumour and stromal components (Greenbaum et al., 2003). All these may explain, in part, reasons for the lack of correlation observed between mRNA and protein expression with survival in breast cancer patients.

In conclusion, high expression of cytoplasmic CYP2S1 and nuclear CYP2W1 was able to identify a subgroup of ER-positive, HER-2 negative patients above the age of 50 with higher proliferative and metastatic potential. These subgroup of patients can be selected for potential HAP treatment or other chemotherapy agents that are efficiently metabolised by CYP2S1 and CYP2W1. Low expression of cytoplasmic CYP2S1 and nuclear CYP2W1 were associated with adverse survival of breast cancer patients and, from multivariate analyses, were independent prognostic factors. This is the first study to report the prognostic significance of CYP2S1 and CYP2W1 in a large independent cohort of breast cancer.

Conclusions

All the hypotheses postulated at the beginning of the chapter were addressed:

High CYP2S1 and CYP2W1 were expressed in ER-positive tumours compared to the HER-2 positive and TNBC subtypes.

High cytoplasmic CYP2S1 and nuclear CYP2W1 protein were associated with improved survival in the total patient cohort and in ER-positive and negative breast cancers respectively.

High CYP2S1 and CYP2W1 mRNA were not associated with improved prognosis in the METABRIC cohort.

Chapter 6 General discussion, Limitations and Suggestions for future work

6.1 General discussion

Breast cancer is one of the most rapidly increasing cancer in women, and a leading cause of mortality worldwide (Siegel et al., 2018). In the UK, breast cancer is the most commonly diagnosed and second leading cause of cancer related deaths, with more than 11500 deaths reported in 2017 (CRUK, 2019). Although the incidence rates are alarmingly high, the mortality rates have decreased by 39% since the 1970's and by 21% in the last decade (CRUK, 2019). This increase in breast cancer survival over the years can be attributed to increase in breast cancer awareness among women, emergence of novel systemic therapies and implementation of population based mammography screening (Nystrom et al., 2002, EBCTCG, 2005). Breast cancer treatment follows a multimodal approach and includes a combination of surgery (BCS/mastectomy) followed by radiotherapy, chemotherapy (CMF, taxanes), hormonal therapy (tamoxifen/AI), and/or immune/targeted therapies (trastuzumab, olaparib) (NICE, 2018).

Radiotherapy is one of the most effective and necessary treatment modalities in the clinical management of breast cancers (Bartelink et al., 2015). ~50% of breast cancer patients diagnosed worldwide receive radiotherapy as part of their treatment (Delaney et al., 2005). If radiotherapy is not administered after BCS, locoregional recurrences can metastasize and increase the risk of breast cancer mortality (Darby et al., 2011). Although radiotherapy is effective in treating breast cancers, there are a significant proportion of patients that develop local recurrence (10% in 5 years), indicating failure of the primary treatments to provide local tumour control (Bartelink et al., 2001, Min et al., 2011).

Ionising radiation can cause a plethora of DNA damage including both double and single strand breaks (Willers et al., 2004). One of the reasons for radiotherapy failure is due to the ability of tumour cells to repair the bulk of radiation-induced DNA damage through activation of various DNA repair pathways (Jeggo and Lavin, 2009). Therefore combining radiotherapy with DNA repair inhibitors provides an opportunity to increase the efficacy of radiotherapy as a treatment modality (Lesueur et al., 2017).

A number of DNA repair pathways exist in mammalian genomes to repair damage induced by exogenous and endogenous agents (Jackson and Bartek, 2009). In response to oxidative damage induced by radiotherapy, the BER pathway is activated (Vens and Begg, 2010). FEN-1 is a critical component of the LP-BER pathway that is involved in cleaving DNA flap structures that arise during the repair process (Lieber, 1997, Liu et al., 2008a, Vens and Begg, 2010). PTPD is a small molecule FEN-1 inhibitor that binds to and inactivates the cleavage site of FEN-1, disabling its nuclease activity (Tumey et al., 2005, Dorjsuren et al., 2011). Chapter 2 hypothesised that inhibition of FEN-1 by PTPD would radiosensitise breast cancer cells, by increasing levels of unrepaired DNA damage.

The positive control drugs that were used in the DNA repair study to compare efficacy of PTPD were well-established radiosensitisers - the ATM inhibitor, KU-55933 (Hickson et al., 2004), and the clinically approved PARP-1/2 inhibitor, olaparib (FDA, 2018). Initial experiments included assessing the single agent cytotoxicity of PTPD and comparing it to response obtained with control DNA inhibitors. KU-55933 treatment resulted in a modest reduction in colony formation (4-25%) in all breast cancer cells; but greater reduction was observed in the BRCA-1 deficient MDAMB-436 cells (44%). Treatment with olaparib reduced colony formation by 20-50% in all cell lines, compared to 80% in the MDAMB-436 cells. In comparison to control agents, treatment with PTPD had only marginal effects (<10%) on clonogenic survival of MCF-7, T47D, MDAMB-231 and MDAMB-468 cells, but demonstrated increased cytotoxicity in the MDAMB-436 cells with a 66% reduction. All of the 3 DNA repair inhibitors were cytotoxic in the BRCA-1 deficient MDAMB-436 cells, which may be because of the defective DNA double strand repair pathway in these cell lines (Elstrodt et al., 2006).

On assessing radioresponse, KU-55933 treatment resulted in significant radiosensitisation across all the breast cancer phenotypes with $SER_{0.01}$ ranging from 1.6-3.4. As expected, treatment with olaparib significantly increased radiosensitivity in both BRCA-1 proficient and deficient cells with $SER_{0.01}$ ranging from 1.6-2.3. The radiosensitisation obtained in the current study is in agreement with previously reported KU-55933 SER values of

1.6-3.5 and olaparib SER values of 1.12-1.76 (Biddlestone-Thorpe et al., 2013, Carruthers et al., 2015, Michmerhuizen et al., 2019). However, when the radiosensitisation by PTPD was assessed, the luminal cell lines, MCF-7 and T47D did not demonstrate any radiosensitisation ($SER_{0.01}$ 1.00); and only marginal radiosensitivity was observed in the triple negative, MDAMB-231 and MDAMB-468 cells ($SER_{0.01}$ 1.1-1.3). Increased radiosensitivity was observed only in the BRCA-1 deficient MDAMB-436 cells ($SER_{0.01}$ 1.50). The increased cytotoxic effect in the MDAMB-436 cells compared to other cell lines may be because of the impaired double strand repair pathway due to BRCA-1 deficiency, which when combined with FEN-1 inhibition (single strand repair pathway) may inhibit its potential to carry out DNA repair (Mengwasser et al., 2019). These results indicate that while PTPD offered some levels of radiosensitisation in the triple negative cell lines, it was only marginal in comparison to control radiosensitisers such as KU-55933 and olaparib.

DNA damage assays were next conducted by immunofluorescent microscopy to explain the marginal or lack of radiosensitisation by PTPD in the breast cancer cells. Levels of single and double strand DNA damage induced by PTPD were assessed using nuclear foci quantification of RPA and γ-H2AX respectively (Zou et al., 2006, Kinner et al., 2008). Data show that combined treatment of PTPD in combination with radiation increased RPA expression by 1-2 fold in all cell lines, which indicate that addition of PTPD, as expected, increases the amount of single strand DNA damage induced by ionising radiation. However, this did not translate to radiosensitisation. This may be because single strand DNA damage is easily repaired in cells by alternate DNA repair pathways, as opposed to the cytotoxic DNA double strand damage, wherein the prevalence of even one can trigger cell death (Scott and Pandita, 2006, Jackson and Bartek, 2009). Results from the γ-H2AX assay demonstrated that combined treatment of PTPD with radiation increased double strand breaks only in the BRCA-1 deficient MDAMB-436 cells, and not in other cell lines. Such data may help explain the marginal levels, or lack of, PTPD induced radiosensitisation in the luminal and triple negative breast cancer cell lines.

The synthetic lethal association between proteins involved in BER and HR pathways may explain the cytotoxicity observed in the BRCA-1 deficient cell line when FEN-1 was inhibited (Farmer et al., 2005, Bryant et al., 2005). Furthermore, BRCA-1 deficient tumours have been associated with defective BER pathways, as demonstrated by hypersensitivity of these tumours to oxidative DNA damage induced by H_2O_2 (Alli et al., 2009). A functional interaction between BRCA-1 and DNA Polβ have also been reported, which is suggestive of the involvement of DNA Polβ in BRCA-1 mediated HR repair pathways (Masaoka et al., 2013). All these explain the increase in cytotoxicity in MDAMB-436 cells to FEN-1 inhibition compared to the other luminal and TNBC cells. Compared to radiosensitisation obtained with KU-55933 and olaparib, data suggested that PTPD was effective only in the context of BRCA-1 deficiency. Therefore, the study with PTPD was not progressed further in the current thesis due to lack of promising data in other cell lines.

Future work could assess the efficacy of PTPD, olaparib or KU-55933 in hypoxic breast cancer cells to identify if levels of hypoxia can modulate sensitivity of the DNA repair inhibitors. It has been reported that cells exposed to acute or chronic hypoxia have decreased expression of components involved in the HR pathway (Bindra et al., 2007, Chan et al., 2008). It is known that defective HR is synthetically lethal with PARP inhibition (Ashworth, 2008). The concept of 'conceptual synthetic lethality' applies when the decreased HR pathways in hypoxic cells is exploited by treatment with PARP inhibitors. These experiments have resulted in the selective killing of HR-deficient hypoxic cells (Chan et al., 2010). It would be interesting to assess if the efficacy of PTPD changes under hypoxia.

Intratumoural hypoxia arises as a result of diffusion-limited oxygen supply, in which the rapidly proliferating tumour cells become distant from the oxygen supplying blood vessels; and due to perfusion-limited oxygen supply which arises due to the absence of constant blood flow to tumour regions (Vaupel et al., 2004). Hypoxic regions have been found to occur in all breast cancer stages, from *in situ* carcinomas to both lobular and ductal invasive cancers (Hohenberger et al., 1998). Regions of necrosis also occur

in breast cancers and this reflects prolonged periods of oxygen deficit, which is unable to sustain cell survival (Harris, 2002).

Low intracellular oxygen has profound consequences on cancer progression because it results in the tumour cells acquiring a highly invasive and metastatic phenotype that decreases patient survival (Semenza, 2016). Overall, only 6% of patients present with metastatic disease at diagnosis, but ~30% of early-stage breast cancer patients eventually progress to a metastatic disease (O'Shaughnessy, 2005). Hypoxia in primary tumours has been shown to induce expression of lox and lox-like molecules that primes breast cancer cells for metastasis by regulating formation of pre-metastatic niches in target organs (Wong et al., 2011)

The presence of tumour hypoxia is also associated with radiotherapeutic failure (Gray et al., 1953, Brown and Wilson, 2004, Overgaard, 2007) and reduced response to various breast cancer chemotherapeutic agents (Wouters et al., 2007). Radiobiological hypoxia occurs when the radiation-induced DNA damages are more easily repaired in the absence of oxygen, which results in radiotherapy resistance (Jackson et al., 2019). An approach to overcome hypoxia and improve radioresponse in breast cancers is by hypoxia-activated prodrugs (HAPs), which become chemically active in areas of low oxygen, and exert cytotoxic effects in hypoxic cells while remaining non-cytotoxic to the well-oxygenated normal tissues (Patterson and McKeown, 2000, Wilson and Hay, 2011). Therefore targeting the hypoxic fraction of tumours with HAPs will enable efficient delivery of cytotoxic agents into the hypoxic tumour cells. In combination with conventional therapies such as radiation, the HAPs have the potential to eradicate both the oxic and hypoxic tumour cell populations, both in a neoadjuvant and metastatic setting (Patterson and McKeown, 2000, Liapis et al., 2016).

AQ4N is a bio-reductive TOPO II inhibitor that is efficiently bio-reduced in a hypoxic environment into the DNA binding cytotoxic metabolite, AQ4 (Patterson, 2002, Patterson, 1993). The reductive activation of AQ4N to AQ4 is catalysed by the cytochrome P450 enzymes, such as CYP2S1 and CYP2W1 (Nishida et al., 2010). The bioreduced metabolite AQ4, is a persistent anti-cancer agent, which localises to hypoxic tissues and

continues to exert cytotoxic effects, irrespective of tumour reoxygenation (McKeown et al., 1995). AQ4N has been reported in many studies to be an effective enhancer of radiotherapy (McKeown et al., 1996, Hejmadi et al., 1996) as well as chemotherapy (cisplatin, cyclophosphamide, mitoxantrone)(Friery et al., 2000, Patterson et al., 2000, Tredan et al., 2009). Unfortunately, development of this promising hypoxia-selective toxin has not progressed beyond phase I clinical trials.

The novel AQ4N analogue, KP167, is a newly developed HAP that binds DNA covalently and functions as both a DNA alkylator and a TOPO II inhibitor. Preliminary experiments show that KP167 is a highly effective chemosensitiser in colorectal cancer spheroids when used in combination with oxaliplatin (Klaus Pors, personal communication of unpublished data). Several studies have documented the well-established role of AQ4N as a radiosensitiser, but the radiosensitising effects of KP167 had not been assessed prior to this study, nor its efficacy in breast cancer. The novel analogue KP167 has additional anti-cancer properties as mentioned previously, which led to the hypothesis that radiosensitisation observed with KP167 will be comparable if not greater than the parental compound. The single agent and radiosensitising efficacy of KP167 was assessed in 3D spheroid, 2D normoxia and 2D hypoxia models of luminal and triple negative breast cancer cells and compared to the parental drug, AQ4N.

Initially, the efficacy of HAPs were assessed in breast cancer spheroid models, as spheroids which are ≥500 μm in diameter develop a hypoxic core as a result of oxygen and nutrient gradients (Hirschhaeuser et al., 2010). Such agents are more potent in hypoxic conditions because of the efficient bio-reduction of HAPs by the cytochrome P450 family of enzymes in the absence of oxygen (Raleigh et al., 1998). Moreover, these 3D models offer a more accurate representation of *in vivo* tumour responses to anti-cancer agents (Breslin and O'Driscoll, 2013). The single-agent cytotoxic effect of AQ4N and KP167 were assessed by treating spheroids and seeding for assessment of clonogenic survival. Data demonstrated that both AQ4N and KP167 were cytotoxic in all breast cancer spheroids and resulted in a dose dependent reduction in cellular survival. Data indicate that the presence of hypoxia in 3D spheroid cultures may have enabled efficient

activation of AQ4N and KP167 into their DNA binding cytotoxins. Such observations are supported by studies which report that increasing tumour hypoxia by vascular clamping or hydralazine pre-treatment increases the anti-tumour efficacy of AQ4N (Patterson, 1993). Furthermore, the cytotoxic effects of AQ4N was potentiated by a dose enhancement ratio of 5:1 using hypobaric hypoxia in T50/80 tumours *in vivo* (McKeown et al., 1995), all of which indicate the hypoxia-specific activation of these agents.

The novel analogue, KP167 was 2-100 fold more potent in reducing survival of breast cancer cells with IC_{50} values ranging between (0.14-12.8) μM compared to AQ4N IC_{50} of (0.2-22.8) μM. The increased cytotoxic effect observed with the novel analogue KP167, may be due to the targeting of both proliferating and quiescent cell population by TOPO II inhibition and DNA alkylation. This is in contrast to drug action of AQ4N which is cytotoxic only in proliferating cells because of its ability to inhibit the catalytic role of TOPO II, as cells re-enter the cell cycle during reoxygenation (Patterson, 1993, Wilson et al., 1996).

As expected the most sensitive cell line to treatment with AQ4N and KP167 was the BRCA-1 deficient MDAMB-436 cells. This cell line is characterised by a defective HR-pathway due to the BRCA-1 deficiency. This inherent BRCA-1 deficiency coupled with the inability to repair additional DNA double strand breaks induced by TOPO II inhibition (+DNA alkylation in KP167 treated cells), may explain the increase in cytotoxicity compared to the other repair-proficient cell lines (Ashworth, 2008). Overall, the luminal cell lines MCF-7, T47D and the normal epithelial cell line MCF-10A, were sensitive to single agent AQ4N and KP167 treatment with lower IC_{50} values compared to the triple negative MDAMB-231 cells. If time had permitted, the levels of normoxic, hypoxic and necrotic cells in the different breast cancer spheroids could be assessed, and this may explain, to some extent, the differential sensitivity observed in the different breast cell lines to AQ4N and KP167 treatment (Riffle and Hegde, 2017).

Previous studies have reported that AQ4N is minimally toxic to oxygenated cells (Patterson, 1993, Wilson et al., 1996) because of the competitive binding of oxygen to the active haem-centre of cytochrome P450 enzymes, which inhibits the efficient reduction of the HAPs (Raleigh et al., 1998).

Therefore the cytotoxic effects of AQ4N and KP167 were assessed in breast cancer cells grown in 2D normoxia. Data from the current study show that AQ4N and KP167 were able to reduce proliferation and clonogenic survival of breast cancer cells grown in 2D normoxia, albeit at much higher concentrations than those required to induce similar effects in 3D cultures. AQ4N IC_{50} (24 hour) ranged from (0.3->45) μM in clonogenic survival compared to the KP167 IC_{50} value of (1.8->45) μM. The triple negative MDAMB-231 and MDAMB-468 cells were most resistant to treatment with AQ4N and KP167 and demonstrated the least reduction in survival at 24 hours (>32 μM). This finding is in agreement with previous studies which report only minimal toxicity when AQ4N was tested against the NCI panel of 60 cell lines in normoxia (Patterson and McKeown, 2000).

In both 3D spheroid and 2D normoxia cultures, the luminal MCF-7 and T47D cells were more sensitive (with the exception of MDAMB-436 cells) to single agent AQ4N and KP167 treatment, with lower IC_{50} values compared to the triple negative MDAMB-231 and MDAMB-468 cells. The cytochrome P450 enzymes, CYP2S1 and CYP2W1 have been reported to metabolise AQ4N to AQ4 more efficiently compared to the other CYP enzymes (Nishida et al., 2010). Therefore, the endogenous expression of cytochrome P450, CYP2W1 and CYP2S1 were assessed, in order to identify if differential expression of reductases were responsible for the differences in drug sensitivity observed between the luminal and triple negative cells.

The cytochrome P450 family are oxidative enzymes that are involved in the metabolism of many carcinogens and anti-cancer agents (Danielson, 2002). They are important in the development and progression of breast cancer, because of their involvement in the metabolism of estrogen and anti-cancer agents used in breast cancer treatment (Hayes et al., 1996, Tsuchiya et al., 2005). *In vitro* Western blot data demonstrate that the highest expression of cytochrome P450 and CYP2W1 was present in the luminal MCF-7 and T47D cells which may have enhanced the cytotoxicity of AQ4N and KP167 in these cell lines. Such data suggest that determining their expression in breast cancer may help in the identification of patient subgroups that may benefit from potential HAP treatment. Therefore, the expression of CYP2S1 and CYP2W1 were assessed by immunohistochemistry

in breast cancer tissues, and will be discussed subsequently. Although CYP2S1 and CYP2W1 are involved in the hypoxic bio-activation of AQ4N, further experiments are needed to confirm the activation of KP167 by these enzymes. Future experiments could be conducted to assess changes in reductase levels following treatment with AQ4N and KP167 in the different breast cancer cells to identify the main reductases involved in KP167 metabolism. Equally, it would be interesting to compare and contrast endogenous reductase levels between 3D spheroid and 2D normoxic cultures.

In order to further confirm the hypoxia-specific activation of AQ4N and KP167, breast cancer cells in 2D monolayers were made hypoxic at 1% O_2, following which the single agent cytotoxicity of AQ4N and KP167 were assessed. For all experiments in 2D hypoxia (1% O_2 for 48 hours), CA9, the endogenous hypoxia marker (Wykoff et al., 2000, Olive et al., 2001), was initially assessed for positive expression to ensure that the breast cancer cells being used in experiments were truly hypoxic. Clonogenic data show that both AQ4N and KP167 were highly cytotoxic in breast cancer 2D hypoxic cultures with lower IC_{50} values of (0.15-9.5) μM for AQ4N and (0.37-4.9) μM for KP167, compared to those obtained in 2D normoxia cultures. Compared to 3D cultures, increased cytotoxicity with AQ4N and KP167 were observed in 2D cultures and this may be because, 2D hypoxic cells were grown as monolayers and uniformly subjected to hypoxia, which may have enabled efficient CYP-mediated conversion of AQ4N and KP167 into their respective cytotoxic metabolites. This is in contrast to 3D spheroid cultures which contain normoxic, hypoxic and necrotic cells, all co-existing in different layers of the spheroid structure and may demonstrate differential drug sensitivities (Mueller-Klieser et al., 1986). Such data show that AQ4N and KP167 treatment were more cytotoxic in breast cancer cells grown in 2D hypoxia and 3D spheroid cultures when compared to response obtained in 2D normoxia, which confirmed the hypoxia-specific activation of these agents (Patterson and McKeown, 2000, Denny, 2000).

AQ4N has been reported to be an effective enhancer of radiotherapy with studies reporting that AQ4N when administered before radiation results in

a 50% reduction in radiation dose for the same anti-tumour effect (McKeown et al., 1995). A phase I evaluation of AQ4N in combination with fractionated radiotherapy in 18 patients reported that the drug was well-tolerated in patients and tumour concentrations of AQ4 exceeded the normal tissue concentration at a ratio of >3.7. This study reported a >50% decrease in tumour volume in 2 patients, partial response in 1 and stable disease in 9 (Steward et al., 2007).

In the present study, breast cancer spheroids were treated with AQ4N before irradiation and any effects on cell survival were assessed by clonogenic survival assays. In combination with radiation, AQ4N was effective as a radiosensitiser, across all breast cancer phenotypes, with $SER_{0.01}$ of 1.30-3.33. Greater increases in radiosensitisation were observed with KP167 ($SER_{0.01}$ of 1.46-4.55), which was 100 times more potent compared to control cells at 8 Gy in T47D, MDAMB-231, MDAMB-468 and MDAMB-436 cells. Clinically, treatment of TNBCs continues to be a challenge due to the fact that there are no available targeted therapies to treat this particular subtype of breast cancer. Adjuvant therapy in TNBCs rarely leads to remission and the occurrence of metastasis is associated with high resistance to chemotherapy (Somali et al., 2013). Furthermore, regions of hypoxia and necrosis are higher in ER-negative tumours, which also contributes to the local recurrence and radiotherapy resistance observed in this subtype (Generali et al., 2006, Semenza, 2016). Although various agents are currently being evaluated in pre-clinical and clinical studies for the treatment of TNBCs, no targeted agents have been currently approved for clinical use, apart from PARP inhibitors (FDA, 2018).

In the current thesis, radiosensitivity obtained with KP167 in the triple negative MDAMB-231 ($SER_{0.01}$ 2.53), MDAMB-468 ($SER_{0.01}$ 2.28) and MDAMB-436 ($SER_{0.01}$ 4.55) spheroids were greater in comparison to well-established radiosensitisers such as KU-55933 with $SER_{0.01}$ of (1.82-MDAMB-231, 1.68-MDAMB-468, 3.42-MDAMB-436) and olaparib with $SER_{0.01}$ of (1.62-MDAMB-231, 1.68-MDAMB-468, 2.35-MDAMB-436) investigated in the DNA repair study. As seen above, radiosensitivity achieved with KP167 was greater than olaparib, which is currently being evaluated clinically as a radiosensitiser in the RadioParp trial for the

treatment of TNBCs (NCT03109080). Although further studies are required both *in vitro* and *in vivo* to confirm such findings, from the current study, KP167 appears to be a potent radiosensitiser in breast cancer and may hold promising potential, especially in the treatment of TNBCs.

Liapis et al., 2016 studied the anti-cancer efficacy of the HAP, TH-302 in primary breast cancer and metastatic deposits in bone and reported that TH-302 in combination with paclitaxel was able to reduce tumour growth of primary breast cancers and metastatic deposits in bone (Liapis et al., 2016). Such data indicate that the HAPs can potentially be used both in a neoadjuvant and metastatic setting to target hypoxic breast cancers and improve patient outcomes. Other studies have reported that both TH-302 and PR-104 reduced growth and radiosensitised TNBC cell lines, especially BRCA-2 knockout mutants (Hunter et al., 2014). Such data are similar to findings in the current study, wherein the BRCA-1 deficient MDAMB-436 cells were highly radiosensitised by KP167. Such data further indicate that HAPs can be utilised to exploit both hypoxia and HR defects in breast and other cancers.

As expected, the HAPs AQ4N and KP167 demonstrated lower levels of radiosensitisation in breast cancer 2D normoxia cultures. AQ4N resulted in a marginal–modest increase in radiosensitisation with $SER_{0.01}$ of 1.17-1.64. KP167 was more effective than AQ4N even in normoxic conditions with $SER_{0.01}$ of 1.21-1.93. The lower efficacy of the HAPs in normoxia cultures, as previously reported, may be attributed to inefficient reduction of these agents by the cytochrome P450 enzymes in the presence of oxygen (Raleigh et al., 1998).

Lastly, the radiosensitising effect of AQ4N and KP167 were assessed in 2D hypoxia cultures. Similar to results obtained in 3D spheroids, radiosensitisation obtained with KP167 was greater with $SER_{0.01}$ of 1.56-2.37 compared to the AQ4N $SER_{0.01}$ of 1.13-1.94. The radiosensitisation obtained in 2D hypoxia was greater than that obtained in 2D normoxia, further confirming the hypoxia-specific cytotoxicity of these agents. It was expected that cells grown in 2D hypoxia would demonstrate greater levels of radiosensitisation compared to 3D spheroid cultures, since all cells would be hypoxic, which would enable efficient drug activation. Interestingly, the

radiosensitivity obtained in 3D spheroids with KP167 treatment were greater, especially in the TNBC cell lines. Schmidt et al., 2016 analysed the gene expression profile of 12 HNSCC cell line 3D cultures, and reported an increase in the expression of genes involved in cell junctions, adhesion and drug-metabolising cytochrome P450 enzymes. Furthermore, downregulation of genes involved in DNA repair, cell cycle and DNA replication was also observed (Schmidt et al., 2016). Such data suggest that efficient metabolism of drugs in 3D by the cytochrome P450 enzymes followed by the inability of cells to repair DNA damage may have contributed to the increase in cytotoxicity observed in 3D v 2D cultures. In addition, TNBCs are characterised by deficiencies in several DNA repair pathways. For example, defects in HR pathways have been identified in sporadic triple negative tumours independent of BRCA-1/2 deficiency (Telli et al., 2016). All of these may have contributed to the enhanced cytotoxicity profile of AQ4N and KP167 in 3D spheroid cultures, especially in the TNBC cell lines (Song et al., 2013). The radioresponse observed between 3D and 2D cultures may also be dependent on various other factors present in a 3D environment such as gradients of oxygen and nutrition, pH, cell-cell and cell-matrix interactions, differential proliferation rates, altered metabolism etc, compared to 2D cultures (Bristow and Hill, 2008, Rankin et al., 2016, Sharma et al., 2019).

The normal mammary epithelial cell line, MCF-10A was included in the HAP study to assess for potential differential effects between normal and cancer cells. Experiments were only conducted with AQ4N due to lack of KP167 availability. Data show that AQ4N induced modest levels of radiosensitisation in MCF-10A spheroids with an $SER_{0.01}$ of 1.36, greater increases in 2D hypoxia with $SER_{0.01}$ of 1.71 and marginal radiosensitisation in 2D normoxia with $SER_{0.01}$ of 1.15. Increases in AQ4N-induced radiosensitivity was observed in 3D spheroid and 2D hypoxia cultures and this may only be because of the presence of hypoxia in these culture conditions. Such results are promising and demonstrate that the radiosensitising effects of AQ4N is marginal in the presence of oxygen, which suggest that well-oxygenated normal tissues may be spared from the radiosensitising effect of AQ4N. Future work should assess the efficacy

of KP167 in MCF-10A cells to confirm such observations. The effects of the HAPs should also be tested in another normal breast cell lines, and potentially other normal cell types, before firm conclusions can be reached.

As mentioned previously, the CYP enzymes, CYP2S1 and CYP2W1 are expressed in breast tissues and are involved in the reductive activation of AQ4N and may be involved in activating KP167 (Nishida et al., 2010, Hlaváč et al., 2014). *In vitro* Western blot data indicate that the differential expression of these enzymes in the different subtypes of breast cancer may have determined response to AQ4N and KP167 treatment. Therefore, the protein expression of CYP2S1 and CYP2W1 was assessed in a large cohort of breast cancer patients (n=1426) by immunohistochemistry, to assess expression in the different breast cancer phenotypes and to establish any clinical and prognostic significance of these enzymes in breast cancer. CYP2S1 and CYP2W1 mRNA expression was also assessed in a large number of patients (n=1980) in the METABRIC cohort.

The expression of cytoplasmic CYP2S1 and nuclear CYP2W1 protein were specific to ER-positive cancers which is consistent with data obtained *in vitro*, and with the reported role of CYP enzymes in the metabolism and oxidation of estrogens (Zhao et al., 2016). The expression of these enzymes were correlated to various clinical and pathological parameters. This led to the selection of a subgroup of ER-positive, HER-2 negative patients, above 50 years of age, characterised by high grade, pleomorphism, mitosis and intermediate NPI category. Such data suggested that high expression of cytoplasmic CYP2S1 and CYP2W1 protein identifies a subgroup of ER-positive patients with higher proliferative and metastatic potential that may require cytotoxic chemotherapy in addition to hormone-therapy (Rakha et al., 2008, Rakha et al., 2010). Furthermore, this subgroup of patients can potentially become candidates for treatment with the hypoxia-activated prodrugs (following confirmation of hypoxia in tumours).

Estrogen is implicated in breast cancer pathogenesis due to the production of carcinogenic metabolites during its metabolism and oxidation by the cytochrome P450 enzymes (Badawi et al., 2001, Cheng et al., 2001). Cytochrome P450 enzymes are also involved in the metabolism of various

anti-cancer drugs used in the treatment of breast cancer (Fabian et al., 1981, Croteau et al., 2006). For example, tamoxifen, used in the treatment of HR-positive breast cancer, is a prodrug that undergoes metabolic activation, catalysed by the cytochrome P450 enzymes into its active metabolites N-desmethyl-tamoxifen,4–hydroxyl–N-desmethyl-tamoxifen and 4-hydroxy-tamoxifen (Fabian et al., 1981). It has been previously reported that lower expression of CYP enzymes are associated with worse outcome for ER-positive patients treated with tamoxifen due to inefficient drug metabolism (Singh et al., 2011). Similarly, the metabolism of taxol has 19 distinct enzymatic steps, almost half of which are catalysed by the cytochrome P450 enzymes (Croteau et al., 2006). Certain CYP enzymes have the potential to inactivate taxols such as paclitaxel and docetaxel which results in treatment failure (Engels et al., 2004). Cyclophosphamide, used in the CMF regimen to treat breast cancer is a prodrug which also requires bio-activation by the cytochrome P450 enzymes (Bohnenstengel et al., 1996). Studies report that certain polymorphic forms of the CYP enzymes lowers efficiency of cyclophosphamide (El-Serafi et al., 2015). Furthermore, studies have shown an increase in the transcript levels of CYP2W1 in responders of NACT compared to breast cancer patients with a stable or a progressive disease (Hlaváč et al., 2014). These studies provide evidence that tumours with low expression of cytochrome P450 enzymes may not be able to efficiently metabolise certain chemotherapy drugs which may contribute to therapy resistance and impact negatively on the survival of breast cancer patients (Zanger and Schwab, 2013).

All these studies support the findings in the current thesis wherein low expression of cytoplasmic CYP2S1 and nuclear CYP2W1 was associated with shorter survival of breast cancer patients, which was maintained even in multivariate analysis. Low cytoplasmic CYP2S1 and nuclear CYP2W1 were also associated with adverse survival in ER-positive and ER-negative patients respectively. Administering chemotherapy agents that don't require CYP metabolism might lead to better overall survival in the subgroup of patients that demonstrate low levels of CYP2S1 and CYP2W1. Such data emphasise the prognostic significance of CYP enzyme protein expression in breast cancer, regardless of ER status.

METABRIC is a multi-centre cohort which contains mRNA expression of 1980 patients and was used in the present study to assess relationship between the expression of CYP2S1 and CYP2W1 mRNA with clinicopathological parameters and survival (Curtis et al., 2012). High CYP2S1 and CYP2W1 mRNA was associated with absence of HER-2 status and Luminal A tumours respectively, which is in agreement with results obtained with protein expression. However, contrary to results obtained with protein expression in the Nottingham cohort, no significant association between CYP2S1/CYP2W1 mRNA with survival was observed in the METABRIC cohort, although similar trends (low expression – poor survival), were noted. Reasons for discrepancy may be due to various post-transcriptional modification, which may result in a lack of significant correlation between mRNA and translated protein (Greenbaum et al., 2003). A large number of mRNA transcripts can be generated from the same gene via alternative spicing, which may contribute to the discrepant results observed between mRNA and protein expression (Liu et al., 2016). In addition, mRNA isolated from tissues contains admixture of tumour, stromal and immune cells, which may result in diluted effects as opposed to IHC, wherein CYP2S1 and CYP2W1 protein expression were assessed only in tumour cells.

6.2 Limitations and suggestions for future work

The effect of DNA repair inhibitors were only assessed in 2D normoxic models of luminal and TNBC cells. Experiments with additional breast cancer cell lines, such as the HER-2 positives and luminal B subtypes can be carried out in future to assess the radiosensitising effects of PTPD. Although 2D cell culture models are widely used in pre-clinical evaluation of anti-cancer agents, these do not accurately represent *in vivo* tumour responses compared to 3D models (Breslin and O'Driscoll, 2013). Therefore, it may be worthwhile to assess effects of DNA repair inhibitors in 3D spheroid cultures. It has also been reported that DNA repair pathways such as mismatch repair, NER and HR are impaired under hypoxic conditions, due to transcriptional and translational downregulation of proteins involved in DNA repair (Bindra et al., 2007, Scanlon and Glazer,

2015). Future studies could assess the effects of PTPD/DNA repair inhibitors in 2D hypoxia models in order to target the susceptibility of hypoxic cancer cells (Scanlon and Glazer, 2015).

Additional experiments such as combining a double strand and single strand repair inhibitor, such as KU-55933+PTPD could be assessed in combination with radiation as this might allow greater levels of radiosensitisation to be achieved (Fok et al., 2019). In the current study, the effects of PTPD were assessed in combination with single doses of ionising radiation. The hypofractionated radiotherapy, which delivers smaller fractions with large doses are currently used in the treatment of breast cancer (He et al., 2019). It may be interesting to determine the efficacy of PTPD in fractionated radiobiology experiments. If promising data was to be obtained from such experiments, then the effect of PTPD could be tested using *in vivo* animal models to determine dose tolerability and side effects of such treatments.

Data from Chapter 3 show that KP167 was highly effective as a hypoxia-activated radiosensitiser in 3D models of breast cancer, compared to response in 2D normoxia. Future work is needed to confirm the presence of hypoxia in spheroid models. Embedded spheroids can be sectioned to investigate markers of hypoxia, proliferation and apoptosis by immunohistochemistry or immunofluorescence techniques (Tevis et al., 2017). Previous studies have reported the use of pimonidazole as a marker of hypoxia in 3D cultures (Riffle et al., 2017). Pimonidazole undergoes reductive activation in hypoxic cells and binds to form stable adducts with cellular components. It binds to glutathione at concentrations below 1.3% oxygen and can be used in the visualization of severely hypoxic cells (Gross et al., 1995). Clinically, Ki-67 is a commonly used parameter to determine the growth fraction of cells and can be used in the assessment of proliferative cells present in the outer layers of spheroids exposed to nutrition and oxygen (Crispino et al., 1989). The apoptotic marker, cleaved caspase 3 is commonly used as a marker to identify the onset of cell death in 3D cultures (Chen et al., 2015). Assessing levels of hypoxia, cell proliferation and apoptosis, by staining for these markers in breast cancer spheroids might provide further information regarding the differential

sensitivity observed between the different subtypes of breast cancer. For example, greater percentage of hypoxic cells in one cell line as opposed to the other, may enhance the cytotoxic effect of the hypoxia-activated prodrugs.

The cytotoxic effects of AQ4N and KP167 is due to the ability of these agents to cause DNA damage by inhibiting TOPO II, which results in accumulation of DNA double strand breaks in the G2/M phase of the cell cycle. In the present thesis, greater levels of radiosensitivity were observed in KP167 treated cells. In addition to the TOPO II inhibiting role, KP167 may induce higher levels of DNA damage due to its additional DNA alkylating properties, which may induce cell cycle arrests in the G1/S phase (Tu et al., 2004). In addition, the ability of cells to repair DNA damage is subtype specific, with basal triple negative cells generally considered as being repair deficient as opposed to the repair proficient luminal tumours (Guo et al., 2017). Therefore the levels of DNA damage induction and repair in the different cell lines after treatment with AQ4N and KP167 +/- radiation, can be assessed by carrying out γH2AX DNA damage assays by FACS or immunofluorescence (Kinner et al., 2008). The cell cycle distribution of cells in response to AQ4N and KP167 treatment may provide information about differential drug action and sensitivity observed between the different phenotypes of breast cancer. As suggested for PTPD, it would also be of interest to investigate the efficacy of HAP's in fractionated radiation regimes.

Furthermore, the effect of AQ4N and KP167 should also be assessed in proliferating v quiescent cells to determine if KP167, due to its covalent binding and alkylating properties, is cytotoxic to the quiescent cell population. The effect of HAP treatment on various downstream signalling pathways involved in proliferation, apoptosis, DNA repair and metastasis could be examined by measuring protein and mRNA expression of downstream effectors. Using HPLC chromatography techniques, Nishida et al., 2010, demonstrated that CYP2S1 and CYP2W1 was involved in the metabolism of AQ4N to AQ4 under hypoxia with the highest turnover rates compared to the previously identified CYP3A4 and iNOS (Nishida et al.,

2010). Similar experiments could be conducted to determine the specific CYP enzymes involved in the bioreductive metabolism of KP167.

Additional studies may also wish to investigate the efficacy of HAPs in breast cancer primary cells, patient derived xenograft models or murine models to further confirm cell-line data in more clinically relevant settings (Lum et al., 2012). One of the common sites of breast cancer metastasis is the bone, which is characterised by a hypoxic microenvironment (1-6% O_2) (Spencer et al., 2014). Similar to studies conducted by Liapis et al., 2016, the anti-cancer efficacy of KP167 may be tested in primary breast cancers as well in osteolytic breast cancer models to determine if KP167 is effective in targeting both primary and metastatic breast cancer growth. Pharmacokinetics (PK) refers to the movement of drugs in the body (absorption, distribution, bioavailability, metabolism, and excretion), and pharmacodynamic (PD) is the biological response (biochemical or molecular interactions) to a given drug (Meibohm and Derendorf, 1997, Derendorf and Meibohm, 1999). The PK (concentration v time) and PD (effect v time) parameters, dose tolerability and safety of KP167 can be established to better understand drug action. Due to time limitations, experiments with the hypoxia-activated prodrugs were only assessed in luminal A, triple negative and BRCA-1 deficient cell lines. Investigation into the drug responses observed in other subtypes of breast cancers such as luminal B and HER-2 positive cell lines would be interesting, to determine if KP167 is as effective in these subtypes compared to response observed in the TNBCs.

Further studies may also be conducted to determine the role of CYP2S1 and CYP2W1 enzymes in the oxidative metabolism of estrogens and in breast cancer progression. The protein levels of CYP2S1 and CYP2W1 by immunohistochemistry were assessed only in breast tumours and not in corresponding normal tissues. It would be interesting to examine expression in normal breast tissue as a comparator in the future to understand the role of 'orphan' CYP enzymes in breast cancer pathogenesis. In the current study, high expression of cytoplasmic CYP2S1 and nuclear CYP2W1 were able to identify a subgroup of ER-positive, HER-2 negative tumours with increased proliferation, grade and intermediate

prognosis. By assessing hypoxia-markers such as CA9 and HIF-1α in such patient groups, in addition to CYP expression, may result in the identification of patients with hypoxic tumours that may preferentially benefit from potential HAP treatment.

Furthermore, previous studies have reported the association of CYP enzymes in the metabolism of anti-cancer agents used in breast cancer treatment and with responders of NACT (Hlaváč et al., 2014). Future studies may wish to correlate expression of CYP2S1 and CYP2W1 to responders of endocrine therapy, chemotherapy and neoadjuvant chemotherapy in the current cohort to understand the involvement of CYP2S1 and CYP2W1 in drug metabolism and response of patients to treatment.

6.3 Conclusions

In summary, the current thesis evaluated the role of DNA repair inhibitors and hypoxia-activated prodrugs in modulating response of breast cancer cells to radiation. Although the FEN-1 inhibitor, PTPD, failed to demonstrate greater radiosensitisation compared to control agents, the current study provides preliminary evidence for the potential use of PTPD as a radiosensitiser in the treatment of BRCA-1 deficient tumours. In contrast, the novel AQ4N analogue, KP167 was a highly effective hypoxia-activated radiosensitiser across all 3 platforms (3D spheroids, 2D normoxia and hypoxia) investigated. In 3D spheroid cultures, the radiosensitivity obtained in triple negative cell lines were higher than previously observed with well-established radiosensitisers such as KU-55933, AQ4N and clinically approved agents such as olaparib. Although further confirmation is required both *in vitro* and *in vivo*, the current study highlights KP167 as a potentially useful hypoxia-activated radiosensitiser and suggests that it might be a promising agent, either single or combined with radiation, to improve outcome in hypoxic breast cancers. Lastly, the expression of low cytoplasmic CYP2S1 and low nuclear CYP2W1 was associated with adverse survival of breast cancer patients, both in univariate and multivariate analysis, suggesting that these markers may be of prognostic significance in breast cancer.

References

ABBOTTS, R. & MADHUSUDAN, S. 2010. Human AP endonuclease 1 (APE1): from mechanistic insights to druggable target in cancer. *Cancer Treat Rev,* 36**,** 425-35.

ABDEL-FATAH, T. M., RUSSELL, R., ALBARAKATI, N., MALONEY, D. J., DORJSUREN, D., RUEDA, O. M.*, et al.* 2014. Genomic and protein expression analysis reveals flap endonuclease 1 (FEN1) as a key biomarker in breast and ovarian cancer. *Mol Oncol,* 8**,** 1326-38.

ABDULRAHMAN, G. O., JR. & RAHMAN, G. A. 2012. Epidemiology of breast cancer in europe and Africa. *J Cancer Epidemiol,* 2012**,** 915610.

ABIDA, W., BANG, Y. J., CARTER, L., AZARO, A., KREBS, M., IM, S.-A.*, et al.* 2018. Abstract A094: Phase I modular study of AZD0156, a first-in-class oral selective inhibitor of ataxia telangiectasia mutated protein kinase (ATM), in combination with olaparib (AToM Study, Module 1). *Molecular Cancer Therapeutics,* 17**,** A094-A094.

ABRAHAM, R. T. 2001. Cell cycle checkpoint signaling through the ATM and ATR kinases. *Genes Dev,* 15**,** 2177-96.

AHNESORG, P., SMITH, P. & JACKSON, S. P. 2006. XLF interacts with the XRCC4-DNA ligase IV complex to promote DNA nonhomologous end-joining. *Cell,* 124**,** 301-13.

ALBAIN, K. S., ALLRED, D. C. & CLARK, G. M. 1994. Breast cancer outcome and predictors of outcome: are there age differentials? *J Natl Cancer Inst Monogr***,** 35-42.

ALBERTELLA, M. R., LOADMAN, P. M., JONES, P. H., PHILLIPS, R. M., RAMPLING, R., BURNET, N.*, et al.* 2008. Hypoxia-Selective Targeting by the Bioreductive Prodrug AQ4N in Patients with Solid Tumors: Results of a Phase I Study. *Clinical Cancer Research,* 14**,** 1096-1104.

ALI, R., AL-KAWAZ, A., TOSS, M. S., GREEN, A. R., MILIGY, I. M., MESQUITA, K. A.*, et al.* 2018. Targeting PARP1 in XRCC1-Deficient Sporadic Invasive Breast Cancer or Preinvasive Ductal Carcinoma In Situ Induces Synthetic Lethality and Chemoprevention. *Cancer Res,* 78**,** 6818-6827.

ALIZADEH, E., ORLANDO, T. M. & SANCHE, L. 2015. Biomolecular damage induced by ionizing radiation: the direct and indirect effects of low-energy electrons on DNA. *Annu Rev Phys Chem,* 66**,** 379-98.

ALLI, E., SHARMA, V. B., SUNDERESAKUMAR, P. & FORD, J. M. 2009. Defective repair of oxidative dna damage in triple-negative breast cancer confers sensitivity to inhibition of poly(ADP-ribose) polymerase. *Cancer research,* 69**,** 3589-3596.

ALLINSON, S. L., DIANOVA, II & DIANOV, G. L. 2003. Poly(ADP-ribose) polymerase in base excision repair: always engaged, but not essential for DNA damage processing. *Acta Biochim Pol,* 50**,** 169-79.

ALLRED, D. C. 2010. Ductal carcinoma in situ: terminology, classification, and natural history. *J Natl Cancer Inst Monogr,* 2010**,** 134-8.

ALLRED, D. C., MOHSIN, S. K. & FUQUA, S. A. 2001. Histological and biological evolution of human premalignant breast disease. *Endocr Relat Cancer,* 8**,** 47-61.

ALOTAIBI, S. & MOMEN, A. 2019. Anticancer Drugs' Deoxyribonucleic Acid (DNA) Interactions.

AMADORI, D., VOLPI, A., MALTONI, R., NANNI, O., AMADUCCI, L., AMADORI, A.*, et al.* 1997. Cell proliferation as a predictor of response to chemotherapy in metastatic breast cancer: a prospective study. *Breast Cancer Res Treat,* 43**,** 7-14.

APARICIO, T., BAER, R. & GAUTIER, J. 2014. DNA double-strand break repair pathway choice and cancer. *DNA Repair (Amst),* 19**,** 169-75.

ARUN, B., AKAR, U., GUTIERREZ-BARRERA, A. M., HORTOBAGYI, G. N. & OZPOLAT, B. 2015. The PARP inhibitor AZD2281 (Olaparib) induces autophagy/mitophagy in BRCA1 and BRCA2 mutant breast cancer cells. *Int J Oncol,* 47**,** 262-8.

ASAGOSHI, K., TANO, K., CHASTAIN, P. D., 2ND, ADACHI, N., SONODA, E., KIKUCHI, K.*, et al.* 2010. FEN1 functions in long patch base excision repair under conditions of oxidative stress in vertebrate cells. *Molecular cancer research : MCR,* 8**,** 204-215.

ASHTON, T. M., FOKAS, E., KUNZ-SCHUGHART, L. A., FOLKES, L. K., ANBALAGAN, S., HUETHER, M.*, et al.* 2016. The anti-malarial atovaquone increases radiosensitivity by alleviating tumour hypoxia. *Nature Communications,* 7**,** 12308.

ASHWORTH, A. 2008. A synthetic lethal therapeutic approach: poly(ADP) ribose polymerase inhibitors for the treatment of cancers deficient in DNA double-strand break repair. *J Clin Oncol,* 26**,** 3785-90.

ATIF, F., PATEL, N. R., YOUSUF, S. & STEIN, D. G. 2015. The Synergistic Effect of Combination Progesterone and Temozolomide on Human Glioblastoma Cells. *PLoS One,* 10**,** e0131441.

BADAWI, A. F., CAVALIERI, E. L. & ROGAN, E. G. 2001. Role of human cytochrome P450 1A1, 1A2, 1B1, and 3A4 in the 2-, 4-, and 16alpha-hydroxylation of 17beta-estradiol. *Metabolism,* 50**,** 1001-3.

BAHARVAND, H., HASHEMI, S. M., KAZEMI ASHTIANI, S. & FARROKHI, A. 2006. Differentiation of human embryonic stem cells into hepatocytes in 2D and 3D culture systems in vitro. *Int J Dev Biol,* 50**,** 645-52.

BAKER, A. F., KOH, M. Y., WILLIAMS, R. R., JAMES, B., WANG, H., TATE, W. R.*, et al.* 2008. Identification of thioredoxin-interacting protein 1 as a hypoxia-inducible factor 1alpha-induced gene in pancreatic cancer. *Pancreas,* 36**,** 178-86.

BALAKRISHNAN, L., BRANDT, P. D., LINDSEY-BOLTZ, L. A., SANCAR, A. & BAMBARA, R. A. 2009. Long Patch Base Excision Repair Proceeds via Coordinated Stimulation of the Multienzyme DNA Repair Complex. *The Journal of Biological Chemistry,* 284**,** 15158-15172.

BAMBARA, R. A., MURANTE, R. S. & HENRICKSEN, L. A. 1997. Enzymes and reactions at the eukaryotic DNA replication fork. *J Biol Chem,* 272**,** 4647-50.

BARAKAT, K. H., GAJEWSKI, M. M. & TUSZYNSKI, J. A. 2012. DNA polymerase beta (pol beta) inhibitors: a comprehensive overview. *Drug Discov Today,* 17**,** 913-20.

BARENDSEN, G. W. 1987. Differences in radiosensitivity among cells in culture and in experimental tumours: Significance for the effectiveness of human cancer therapy. *Radiotherapy and Oncology,* 8**,** 285-300.

BARKER, H. E., PAGET, J. T. E., KHAN, A. A. & HARRINGTON, K. J. 2015. The tumour microenvironment after radiotherapy: mechanisms of resistance and recurrence. *Nature reviews. Cancer,* 15**,** 409-425.

BARRY, M., SINHA, S. K., LEADER, M. B. & KAY, E. W. 2001. Poor agreement in recognition of abnormal mitoses: requirement for standardized and robust definitions. *Histopathology,* 38**,** 68-72.

BARTELINK, H., HORIOT, J. C., POORTMANS, P., STRUIKMANS, H., VAN DEN BOGAERT, W., BARILLOT, I.*, et al.* 2001. Recurrence rates after treatment of breast cancer with standard radiotherapy with or without additional radiation. *N Engl J Med,* 345**,** 1378-87.

BARTELINK, H., MAINGON, P., POORTMANS, P., WELTENS, C., FOURQUET, A., JAGER, J.*, et al.* 2015. Whole-breast irradiation with or without a boost for patients treated with breast-conserving surgery for early breast cancer: 20-year follow-up of a randomised phase 3 trial. *Lancet Oncol,* 16**,** 47-56.

BASKAR, R., LEE, K. A., YEO, R. & YEOH, K.-W. 2012. Cancer and radiation therapy: current advances and future directions. *International journal of medical sciences,* 9**,** 193-199.
BAYER, C. & VAUPEL, P. 2012. Acute versus chronic hypoxia in tumors: Controversial data concerning time frames and biological consequences. *Strahlenther Onkol,* 188**,** 616-27.
BAZZOUN, D., LELIEVRE, S. & TALHOUK, R. 2013. Polarity proteins as regulators of cell junction complexes: implications for breast cancer. *Pharmacol Ther,* 138**,** 418-27.
BEER, J. Z. & SZUMIEL, I. 1994. Slow clones, reduced clonogenicity, and intraclonal recovery in X-irradiated L5178Y-S cell cultures. *Radiat Environ Biophys,* 33**,** 125-39.
BÉLANGER, F., FORTIER, E., DUBÉ, M., LEMAY, J.-F., BUISSON, R., MASSON, J.-Y.*, et al.* 2018. Replication Protein A Availability during DNA Replication Stress Is a Major Determinant of Cisplatin Resistance in Ovarian Cancer Cells. *Cancer Research,* 78**,** 5561-5573.
BENGHIAT, A., STEWARD, W. P., LOADMAN, P. M., MIDDLETON, M., TALBOT, D., PATTERSON, L. H., FORD, S. & TURNER, A. 2004. Phase 1 dose escalation study of AQ4N, a selective hypoxic cell cytotoxin, with fractionated radiotherapy (RT): First report. *Journal of Clinical Oncology,* 22**,** 2091-2091.
BENNETT, R. A., WILSON, D. M., 3RD, WONG, D. & DEMPLE, B. 1997. Interaction of human apurinic endonuclease and DNA polymerase beta in the base excision repair pathway. *Proc Natl Acad Sci U S A,* 94**,** 7166-9.
BENTZEN, S. M., AGRAWAL, R. K., AIRD, E. G., BARRETT, J. M., BARRETT-LEE, P. J., BLISS, J. M.*, et al.* 2008. The UK Standardisation of Breast Radiotherapy (START) Trial A of radiotherapy hypofractionation for treatment of early breast cancer: a randomised trial. *Lancet Oncol,* 9**,** 331-41.
BESLIJA, S., BONNETERRE, J., BURSTEIN, H., COCQUYT, V., GNANT, M., GOODWIN, P.*, et al.* 2007. Second consensus on medical treatment of metastatic breast cancer. *Ann Oncol,* 18**,** 215-25.
BHANDARI, V., HOEY, C., LIU, L. Y., LALONDE, E., RAY, J., LIVINGSTONE, J.*, et al.* 2019. Molecular landmarks of tumor hypoxia across cancer types. *Nature Genetics,* 51**,** 308-318.
BI, Y., VERGINADIS, II, DEY, S., LIN, L., GUO, L., ZHENG, Y. & KOUMENIS, C. 2018. Radiosensitization by the PARP inhibitor olaparib in BRCA1-proficient and deficient high-grade serous ovarian carcinomas. *Gynecol Oncol,* 150**,** 534-544.
BIANCHINI, G., BALKO, J. M., MAYER, I. A., SANDERS, M. E. & GIANNI, L. 2016. Triple-negative breast cancer: challenges and opportunities of a heterogeneous disease. *Nature reviews. Clinical oncology,* 13**,** 674-690.
BIAU, J., CHAUTARD, E., VERRELLE, P. & DUTREIX, M. 2019. Altering DNA Repair to Improve Radiation Therapy: Specific and Multiple Pathway Targeting. *Frontiers in Oncology,* 9.
BIBI, Z. 2008. Role of cytochrome P450 in drug interactions. *Nutrition & Metabolism,* 5**,** 27.
BIDDLESTONE-THORPE, L., SAJJAD, M., ROSENBERG, E., BECKTA, J. M., VALERIE, N. C., TOKARZ, M.*, et al.* 2013. ATM kinase inhibition preferentially sensitizes p53-mutant glioma to ionizing radiation. *Clin Cancer Res,* 19**,** 3189-200.
BINDRA, R. S., CROSBY, M. E. & GLAZER, P. M. 2007. Regulation of DNA repair in hypoxic cancer cells. *Cancer Metastasis Rev,* 26**,** 249-60.
BIXEL, K. & HAYS, J. L. 2015. Olaparib in the management of ovarian cancer. *Pharmacogenomics and personalized medicine,* 8**,** 127-135.
BLAMEY, R. W., ELLIS, I. O., PINDER, S. E., LEE, A. H., MACMILLAN, R. D., MORGAN, D. A.*, et al.* 2007. Survival of invasive breast cancer according

to the Nottingham Prognostic Index in cases diagnosed in 1990-1999. *Eur J Cancer,* 43**,** 1548-55.
BLOOM, H. J. & RICHARDSON, W. W. 1957. Histological grading and prognosis in breast cancer; a study of 1409 cases of which 359 have been followed for 15 years. *Br J Cancer,* 11**,** 359-77.
BOHNENSTENGEL, F., HOFMANN, U., EICHELBAUM, M. & KROEMER, H. K. 1996. Characterization of the cytochrome P450 involved in side-chain oxidation of cyclophosphamide in humans. *Eur J Clin Pharmacol,* 51**,** 297-301.
BONNANS, C., CHOU, J. & WERB, Z. 2014. Remodelling the extracellular matrix in development and disease. *Nat Rev Mol Cell Biol,* 15**,** 786-801.
BONNIER, P., ROMAIN, S., CHARPIN, C., LEJEUNE, C., TUBIANA, N., MARTIN, P. M. & PIANA, L. 1995. Age as a prognostic factor in breast cancer: relationship to pathologic and biologic features. *Int J Cancer,* 62**,** 138-44.
BORAD, M. J., REDDY, S. G., BAHARY, N., URONIS, H. E., SIGAL, D., COHN, A. L.*, et al.* 2015. Randomized Phase II Trial of Gemcitabine Plus TH-302 Versus Gemcitabine in Patients With Advanced Pancreatic Cancer. *J Clin Oncol,* 33**,** 1475-81.
BORST, G. R., KUMARESWARAN, R., YUCEL, H., TELLI, S., DO, T., MCKEE, T.*, et al.* 2017. Neoadjuvant olaparib targets hypoxia to improve radioresponse in a homologous recombination-proficient breast cancer model. *Oncotarget,* 8**,** 87638-87646.
BOYD, J. M., MALSTROM, S., SUBRAMANIAN, T., VENKATESH, L. K., SCHAEPER, U., ELANGOVAN, B., D'SA-EIPPER, C. & CHINNADURAI, G. 1994. Adenovirus E1B 19 kDa and Bcl-2 proteins interact with a common set of cellular proteins. *Cell,* 79**,** 341-51.
BOYD, N. F., MARTIN, L. J., YAFFE, M. J. & MINKIN, S. 2011. Mammographic density and breast cancer risk: current understanding and future prospects. *Breast Cancer Res,* 13**,** 223.
BOYLE, R. G. & TRAVERS, S. 2006. Hypoxia: targeting the tumour. *Anticancer Agents Med Chem,* 6**,** 281-6.
BRACKSTONE, M., PALMA, D., TUCK, A. B., SCOTT, L., POTVIN, K., VANDENBERG, T.*, et al.* 2017. Concurrent Neoadjuvant Chemotherapy and Radiation Therapy in Locally Advanced Breast Cancer. *Int J Radiat Oncol Biol Phys,* 99**,** 769-776.
BRAY, F., FERLAY, J., SOERJOMATARAM, I., SIEGEL, R. L., TORRE, L. A. & JEMAL, A. 2018. Global cancer statistics 2018: GLOBOCAN estimates of incidence and mortality worldwide for 36 cancers in 185 countries. *CA Cancer J Clin,* 68**,** 394-424.
BREAST CANCER EXPERT ADVISORY GROUP. 2016. *Clinical Guidelines for the Management of Breast Cancer - NHS England* [Online]. Available: https://www.england.nhs.uk/mids-east/wp-content/uploads/sites/7/2018/02/guidelines-for-the-management-of-breast-cancer-v1.pdf [Accessed 20 November 2019].
BRESLIN, S. & O'DRISCOLL, L. 2013. Three-dimensional cell culture: the missing link in drug discovery. *Drug Discov Today,* 18**,** 240-9.
BRISTOW, R. G., HARDY, P. A. & HILL, R. P. 1990. Comparison between in vitro radiosensitivity and in vivo radioresponse of murine tumor cell lines I: parameters of in vitro radiosensitivity and endogenous cellular glutathione levels. *International Journal of Radiation Oncology*Biology*Physics,* 18**,** 133-145.
BRISTOW, R. G. & HILL, R. P. 2008. Hypoxia and metabolism. Hypoxia, DNA repair and genetic instability. *Nat Rev Cancer,* 8**,** 180-92.
BROWN, J. M. 1979. Evidence for acutely hypoxic cells in mouse tumours, and a possible mechanism of reoxygenation. *The British Journal of Radiology,* 52**,** 650-656.
BROWN, J. M. 1985. Sensitizers and protectors in radiotherapy. *Cancer,* 55**,** 2222-8.

BROWN, J. M. 1999. The hypoxic cell: a target for selective cancer therapy--eighteenth Bruce F. Cain Memorial Award lecture. *Cancer Res,* 59**,** 5863-70.
BROWN, J. M. 2007. Tumor hypoxia in cancer therapy. *Methods Enzymol,* 435**,** 297-321.
BROWN, J. M., CARLSON, D. J. & BRENNER, D. J. 2014. The tumor radiobiology of SRS and SBRT: are more than the 5 Rs involved? *International journal of radiation oncology, biology, physics,* 88**,** 254-262.
BROWN, J. M. & WILSON, W. R. 2004. Exploiting tumour hypoxia in cancer treatment. *Nat Rev Cancer,* 4**,** 437-47.
BRYANT, H. E., PETERMANN, E., SCHULTZ, N., JEMTH, A. S., LOSEVA, O., ISSAEVA, N.*, et al.* 2009. PARP is activated at stalled forks to mediate Mre11-dependent replication restart and recombination. *Embo j,* 28**,** 2601-15.
BRYANT, H. E., SCHULTZ, N., THOMAS, H. D., PARKER, K. M., FLOWER, D., LOPEZ, E.*, et al.* 2005. Specific killing of BRCA2-deficient tumours with inhibitors of poly(ADP-ribose) polymerase. *Nature,* 434**,** 913-7.
BU, S. Z., YIN, D. L., REN, X. H., JIANG, L. Z., WU, Z. J., GAO, Q. R. & PEI, G. 1997. Progesterone induces apoptosis and up-regulation of p53 expression in human ovarian carcinoma cell lines. *Cancer,* 79**,** 1944-50.
BUKHARI, A. B., LEWIS, C. W., PEARCE, J. J., LUONG, D., CHAN, G. K. & GAMPER, A. M. 2019. Inhibiting Wee1 and ATR kinases produces tumor-selective synthetic lethality and suppresses metastasis. *The Journal of clinical investigation,* 129**,** 1329-1344.
BUNDRED, N. J. 2001. Prognostic and predictive factors in breast cancer. *Cancer Treat Rev,* 27**,** 137-42.
BURNETTE, B. & WEICHSELBAUM, R. R. 2013. Radiation as an immune modulator. *Semin Radiat Oncol,* 23**,** 273-80.
BUSSINK, J., KAANDERS, J. H., RIJKEN, P. F., RALEIGH, J. A. & VAN DER KOGEL, A. J. 2000. Changes in blood perfusion and hypoxia after irradiation of a human squamous cell carcinoma xenograft tumor line. *Radiat Res,* 153**,** 398-404.
BUTERIN, T., KOCH, C. & NAEGELI, H. 2006. Convergent transcriptional profiles induced by endogenous estrogen and distinct xenoestrogens in breast cancer cells. *Carcinogenesis,* 27**,** 1567-78.
BUTTURINI, E., CARCERERI DE PRATI, A., BORIERO, D. & MARIOTTO, S. 2019. Tumor Dormancy and Interplay with Hypoxic Tumor Microenvironment. *International journal of molecular sciences,* 20**,** 4305.
BUZDAR, A. U. 2007. Preoperative chemotherapy treatment of breast cancer--a review. *Cancer,* 110**,** 2394-407.
BYRD, D. R. & GREENE, F. L. 2018. The Eighth Edition of TNM: Implications for the Surgical Oncologist. *Annals of Surgical Oncology,* 25**,** 10-12.
CAI, Y., ZHANG, J., WU, J. & LI, Z.-Y. 2015. Oxygen transport in a three-dimensional microvascular network incorporated with early tumour growth and preexisting vessel cooption: numerical simulation study. *BioMed research international,* 2015**,** 476964-476964.
CAMP, R. L., DOLLED-FILHART, M. & RIMM, D. L. 2004. X-tile: a new bio-informatics tool for biomarker assessment and outcome-based cut-point optimization. *Clin Cancer Res,* 10**,** 7252-9.
CANTONI, O., SESTILI, P., GUIDARELLI, A., PALOMBA, L., BRAMBILLA, L. & CATTABENI, F. 1996. Cytotoxic impact of DNA single vs double strand breaks in oxidatively injured cells. *Arch Toxicol Suppl,* 18**,** 223-35.
CARDONE, R. A., CASAVOLA, V. & RESHKIN, S. J. 2005. The role of disturbed pH dynamics and the Na+/H+ exchanger in metastasis. *Nat Rev Cancer,* 5**,** 786-95.

CARDOSO, F., COSTA, A., NORTON, L., CAMERON, D., CUFER, T., FALLOWFIELD, L.*, et al.* 2012. 1st International consensus guidelines for advanced breast cancer (ABC 1). *The Breast,* 21**,** 242-252.
CARDOSO, F., COSTA, A., NORTON, L., SENKUS, E., AAPRO, M., ANDRE, F.*, et al.* 2014. ESO-ESMO 2nd international consensus guidelines for advanced breast cancer (ABC2)dagger. *Ann Oncol,* 25**,** 1871-88.
CARDOSO, F., KYRIAKIDES, S., OHNO, S., PENAULT-LLORCA, F., POORTMANS, P., RUBIO, I. T., ZACKRISSON, S. & SENKUS, E. 2019. Early breast cancer: ESMO Clinical Practice Guidelines for diagnosis, treatment and follow-up. *Ann Oncol*.
CARDOSO, F., VAN'T VEER, L. J., BOGAERTS, J., SLAETS, L., VIALE, G., DELALOGE, S.*, et al.* 2016. 70-Gene Signature as an Aid to Treatment Decisions in Early-Stage Breast Cancer. *New England Journal of Medicine,* 375**,** 717-729.
CARREAU, A., EL HAFNY-RAHBI, B., MATEJUK, A., GRILLON, C. & KIEDA, C. 2011. Why is the partial oxygen pressure of human tissues a crucial parameter? Small molecules and hypoxia. *J Cell Mol Med,* 15**,** 1239-53.
CARRUTHERS, R., AHMED, S. U., STRATHDEE, K., GOMEZ-ROMAN, N., AMOAH-BUAHIN, E., WATTS, C. & CHALMERS, A. J. 2015. Abrogation of radioresistance in glioblastoma stem-like cells by inhibition of ATM kinase. *Molecular Oncology,* 9**,** 192-203.
CARTER, C. L., ALLEN, C. & HENSON, D. E. 1989. Relation of tumor size, lymph node status, and survival in 24,740 breast cancer cases. *Cancer,* 63**,** 181-7.
CAVALIERI, E., FRENKEL, K., LIEHR, J. G., ROGAN, E. & ROY, D. 2000. Estrogens as endogenous genotoxic agents--DNA adducts and mutations. *J Natl Cancer Inst Monogr***,** 75-93.
CAZARES-KORNER, C., PIRES, I. M., SWALLOW, I. D., GRAYER, S. C., O'CONNOR, L. J., OLCINA, M. M., CHRISTLIEB, M., CONWAY, S. J. & HAMMOND, E. M. 2013. CH-01 is a hypoxia-activated prodrug that sensitizes cells to hypoxia/reoxygenation through inhibition of Chk1 and Aurora A. *ACS Chem Biol,* 8**,** 1451-9.
CHALMERS, A. J., LAKSHMAN, M., CHAN, N. & BRISTOW, R. G. 2010. Poly(ADP-ribose) polymerase inhibition as a model for synthetic lethality in developing radiation oncology targets. *Semin Radiat Oncol,* 20**,** 274-81.
CHAN, L. W. & CAMPHAUSEN, K. 2003. Angiogenic tumor markers, antiangiogenic agents and radiation therapy. *Expert Rev Anticancer Ther,* 3**,** 357-66.
CHAN, N., KORITZINSKY, M., ZHAO, H., BINDRA, R., GLAZER, P. M., POWELL, S., BELMAAZA, A., WOUTERS, B. & BRISTOW, R. G. 2008. Chronic Hypoxia Decreases Synthesis of Homologous Recombination Proteins to Offset Chemoresistance and Radioresistance. *Cancer Research,* 68**,** 605-614.
CHAN, N., PIRES, I. M., BENCOKOVA, Z., COACKLEY, C., LUOTO, K. R., BHOGAL, N.*, et al.* 2010. Contextual synthetic lethality of cancer cell kill based on the tumor microenvironment. *Cancer Res,* 70**,** 8045-54.
CHANG, J. & FAN, W. 2013. Endocrine therapy resistance: current status, possible mechanisms and overcoming strategies. *Anticancer Agents Med Chem,* 13**,** 464-75.
CHAPMAN, J. D., REUVERS, A. P., BORSA, J. & GREENSTOCK, C. L. 1973. Chemical radioprotection and radiosensitization of mammalian cells growing in vitro. *Radiat Res,* 56**,** 291-306.
CHATTERJEE, N. & WALKER, G. C. 2017. Mechanisms of DNA damage, repair, and mutagenesis. *Environmental and molecular mutagenesis,* 58**,** 235-263.
CHAUDHURI, R. A. & NUSSENZWEIG, A. 2017. The multifaceted roles of PARP1 in DNA repair and chromatin remodelling. *Nat Rev Mol Cell Biol,* 18**,** 610-621.
CHAWLA, S. P., CRANMER, L. D., VAN TINE, B. A., REED, D. R., OKUNO, S. H., BUTRYNSKI, J. E.*, et al.* 2014. Phase II study of the safety and antitumor activity of the hypoxia-activated prodrug TH-302 in combination with

doxorubicin in patients with advanced soft tissue sarcoma. *J Clin Oncol,* 32**,** 3299-306.
CHEANG, M. C., VODUC, D., BAJDIK, C., LEUNG, S., MCKINNEY, S., CHIA, S. K., PEROU, C. M. & NIELSEN, T. O. 2008. Basal-like breast cancer defined by five biomarkers has superior prognostic value than triple-negative phenotype. *Clin Cancer Res,* 14**,** 1368-76.
CHEN, A. 2011. PARP inhibitors: its role in treatment of cancer. *Chinese journal of cancer,* 30**,** 463-471.
CHEN, C.-C., KASS, E. M., YEN, W.-F., LUDWIG, T., MOYNAHAN, M. E., CHAUDHURI, J. & JASIN, M. 2017. ATM loss leads to synthetic lethality in BRCA1 BRCT mutant mice associated with exacerbated defects in homology-directed repair. *Proceedings of the National Academy of Sciences,* 114**,** 7665-7670.
CHEN, D., LI, M., LUO, J. & GU, W. 2003. Direct interactions between HIF-1 alpha and Mdm2 modulate p53 function. *J Biol Chem,* 278**,** 13595-8.
CHEN, D. L., ENGLE, J. T., GRIFFIN, E. A., MILLER, J. P., CHU, W., ZHOU, D. & MACH, R. H. 2015. Imaging caspase-3 activation as a marker of apoptosis-targeted treatment response in cancer. *Molecular imaging and biology,* 17**,** 384-393.
CHENG, Z. N., SHU, Y., LIU, Z. Q., WANG, L. S., OU-YANG, D. S. & ZHOU, H. H. 2001. Role of cytochrome P450 in estradiol metabolism in vitro. *Acta Pharmacol Sin,* 22**,** 148-54.
CHOLEWKA, A., SZLAG, M., BIALAS, B., KELLAS-SLECZKA, S. & SLOSAREK, K. 2013. The importance of the implant quality in APBI - Gliwice experience. Dosimetric evaluation. *J Contemp Brachytherapy,* 5**,** 227-31.
CHOUDHARY, D., JANSSON, I., STOILOV, I., SARFARAZI, M. & SCHENKMAN, J. B. 2005. Expression patterns of mouse and human CYP orthologs (families 1-4) during development and in different adult tissues. *Arch Biochem Biophys,* 436**,** 50-61.
CHUNG, F., MAI, C.-W., NG, P. & LEONG, C.-O. 2015. Cytochrome P450 2W1 (CYP2W1) in colorectal cancers. *Current cancer drug targets,* 16.
CIANFROCCA, M. & GOLDSTEIN, L. J. 2004. Prognostic and predictive factors in early-stage breast cancer. *Oncologist,* 9**,** 606-16.
CICCIA, A. & ELLEDGE, S. J. 2010. The DNA damage response: making it safe to play with knives. *Mol Cell,* 40**,** 179-204.
CITRIN, D. E. 2016. Short-Term Screening Assays for the Identification of Therapeutics for Cancer. *Cancer research,* 76**,** 3443-3445.
CLARK, G. M. 2008. Prognostic factors versus predictive factors: Examples from a clinical trial of erlotinib. *Molecular oncology,* 1**,** 406-412.
CLEARY, M. P. & GROSSMANN, M. E. 2009. Minireview: Obesity and breast cancer: the estrogen connection. *Endocrinology,* 150**,** 2537-42.
CLINICALTRIALS. 2019. *NIH. U.S National Library of Medicine* [Online]. Available: https://clinicaltrials.gov/ [Accessed 1 November 2019].
COATES, A. S., WINER, E. P., GOLDHIRSCH, A., GELBER, R. D., GNANT, M., PICCART-GEBHART, M., THURLIMANN, B. & SENN, H. J. 2015. Tailoring therapies--improving the management of early breast cancer: St Gallen International Expert Consensus on the Primary Therapy of Early Breast Cancer 2015. *Ann Oncol,* 26**,** 1533-46.
COGLIANO, V., GROSSE, Y., BAAN, R., STRAIF, K., SECRETAN, B. & EL GHISSASSI, F. 2005. Carcinogenicity of combined oestrogen-progestagen contraceptives and menopausal treatment. *Lancet Oncol,* 6**,** 552-3.
COOMBS, N., COOMBS, J., VAIDYA, U., SINGER, J., BULSARA, M., TOBIAS, J.*, et al.* 2016. Environmental and social benefits of the targeted intraoperative radiotherapy for breast cancer: Data from UK TARGIT-A trial centres and two UK NHS hospitals offering TARGIT IORT. *BMJ Open,* 6**,** e010703.
COON, M. J. 2005. Cytochrome P450: nature's most versatile biological catalyst. *Annu Rev Pharmacol Toxicol,* 45**,** 1-25.

CORNFIELD, D. B., PALAZZO, J. P., SCHWARTZ, G. F., GOONEWARDENE, S. A., KOVATICH, A. J., CHERVONEVA, I., HYSLOP, T. & SCHWARTING, R. 2004. The prognostic significance of multiple morphologic features and biologic markers in ductal carcinoma in situ of the breast: a study of a large cohort of patients treated with surgery alone. *Cancer,* 100**,** 2317-27.

CORRADINI, S., KRUG, D., MEATTINI, I., MATUSCHEK, C., BOLKE, E., FRANCOLINI, G.*, et al.* 2019. Preoperative radiotherapy: A paradigm shift in the treatment of breast cancer? A review of literature. *Crit Rev Oncol Hematol,* 141**,** 102-111.

COSTANTINI, D. L., VILLANI, D. F., VALLIS, K. A. & REILLY, R. M. 2010. Methotrexate, paclitaxel, and doxorubicin radiosensitize HER2-amplified human breast cancer cells to the Auger electron-emitting radiotherapeutic agent (111)In-NLS-trastuzumab. *J Nucl Med,* 51**,** 477-83.

CREIGHTON, C. J. 2012. The molecular profile of luminal B breast cancer. *Biologics,* 6**,** 289-97.

CRESCENZI, E., PALUMBO, G., DE BOER, J. & BRADY, H. J. 2008. Ataxia telangiectasia mutated and p21CIP1 modulate cell survival of drug-induced senescent tumor cells: implications for chemotherapy. *Clin Cancer Res,* 14**,** 1877-87.

CRESTEIL, T., MONSARRAT, B., DUBOIS, J., SONNIER, M., ALVINERIE, P. & GUERITTE, F. 2002. Regioselective metabolism of taxoids by human CYP3A4 and 2C8: structure-activity relationship. *Drug Metab Dispos,* 30**,** 438-45.

CRISPINO, S., BRENNA, A., COLOMBO, D., FLORES, B., D'AMICO, S., LISSONI, P.*, et al.* 1989. Ki-67 labeling index in breast cancer. *Tumori,* 75**,** 557-62.

CRISTOFANILLI, M., GONZALEZ-ANGULO, A., SNEIGE, N., KAU, S.-W., BROGLIO, K., THERIAULT, R. L.*, et al.* 2005. Invasive Lobular Carcinoma Classic Type: Response to Primary Chemotherapy and Survival Outcomes. *Journal of Clinical Oncology,* 23**,** 41-48.

CRONIN, M., PHO, M., DUTTA, D., STEPHANS, J. C., SHAK, S., KIEFER, M. C., ESTEBAN, J. M. & BAKER, J. B. 2004. Measurement of gene expression in archival paraffin-embedded tissues: development and performance of a 92-gene reverse transcriptase-polymerase chain reaction assay. *The American journal of pathology,* 164**,** 35-42.

CROTEAU, R., KETCHUM, R. E. B., LONG, R. M., KASPERA, R. & WILDUNG, M. R. 2006. Taxol biosynthesis and molecular genetics. *Phytochemistry reviews : proceedings of the Phytochemical Society of Europe,* 5**,** 75-97.

CRUK. 2019. *Breast Cancer Statistics* [Online]. Available: http://www.cancerresearchuk.org/health-professional/cancer-statistics/statistics-by-cancer-type/breast-cancer [Accessed 15 November 2019].

CSERNI, G., CHMIELIK, E., CSERNI, B. & TOT, T. 2018. The new TNM-based staging of breast cancer. *Virchows Arch,* 472**,** 697-703.

CUADRADO, M., MARTINEZ-PASTOR, B., MURGA, M., TOLEDO, L. I., GUTIERREZ-MARTINEZ, P., LOPEZ, E. & FERNANDEZ-CAPETILLO, O. 2006. ATM regulates ATR chromatin loading in response to DNA double-strand breaks. *J Exp Med,* 203**,** 297-303.

CUISNIER, O., SERDUC, R., LAVIEILLE, J. P., LONGUET, M., REYT, E. & RIVA, C. 2003. Chronic hypoxia protects against gamma-irradiation-induced apoptosis by inducing bcl-2 up-regulation and inhibiting mitochondrial translocation and conformational change of bax protein. *Int J Oncol,* 23**,** 1033-41.

CURTIS, C., SHAH, S. P., CHIN, S. F., TURASHVILI, G., RUEDA, O. M., DUNNING, M. J.*, et al.* 2012. The genomic and transcriptomic architecture of 2,000 breast tumours reveals novel subgroups. *Nature,* 486**,** 346-52.

D'AMOURS, D., DESNOYERS, S., D'SILVA, I. & POIRIER, G. G. 1999. Poly(ADP-ribosyl)ation reactions in the regulation of nuclear functions. *Biochemical Journal,* 342**,** 249-268.
D'ANDREA, A. D. & GROMPE, M. 2003. The Fanconi anaemia/BRCA pathway. *Nature Reviews Cancer,* 3**,** 23-34.
DAI, X., CHENG, H., BAI, Z. & LI, J. 2017. Breast Cancer Cell Line Classification and Its Relevance with Breast Tumor Subtyping. *Journal of Cancer,* 8**,** 3131-3141.
DALL, G. V. & BRITT, K. L. 2017. Estrogen Effects on the Mammary Gland in Early and Late Life and Breast Cancer Risk. *Frontiers in Oncology,* 7.
DALY, C. S., FLEMBAN, A., SHAFEI, M., CONWAY, M. E., QUALTROUGH, D. & DEAN, S. J. 2018. Hypoxia modulates the stem cell population and induces EMT in the MCF-10A breast epithelial cell line. *Oncol Rep,* 39**,** 483-490.
DANIELSON, P. B. 2002. The cytochrome P450 superfamily: biochemistry, evolution and drug metabolism in humans. *Curr Drug Metab,* 3**,** 561-97.
DARBY, S., MCGALE, P., CORREA, C., TAYLOR, C., ARRIAGADA, R., CLARKE, M.*, et al.* 2011. Effect of radiotherapy after breast-conserving surgery on 10-year recurrence and 15-year breast cancer death: meta-analysis of individual patient data for 10,801 women in 17 randomised trials. *Lancet,* 378**,** 1707-16.
DARUWALLA, J. & CHRISTOPHI, C. 2006. Hyperbaric oxygen therapy for malignancy: a review. *World J Surg,* 30**,** 2112-31.
DAS, S., CAMPHAUSEN, K. & SHANKAVARAM, U. 2019. Pan-Cancer Analysis of Potential Synthetic Lethal Drug Targets Specific to Alterations in DNA Damage Response. *Frontiers in Oncology,* 9.
DASU, A. & DENEKAMP, J. 1998. New insights into factors influencing the clinically relevant oxygen enhancement ratio. *Radiother Oncol,* 46**,** 269-77.
DAVIES, C., PAN, H., GODWIN, J., GRAY, R., ARRIAGADA, R., RAINA, V.*, et al.* 2013. Long-term effects of continuing adjuvant tamoxifen to 10 years versus stopping at 5 years after diagnosis of oestrogen receptor-positive breast cancer: ATLAS, a randomised trial. *Lancet,* 381**,** 805-16.
DAVIS, J., MARTIN, S. G., PATEL, P. M., GREEN, A. R., RAKHA, E. A., ELLIS, I. O. & STORR, S. J. 2014. Low calpain-9 is associated with adverse disease-specific survival following endocrine therapy in breast cancer. *BMC Cancer,* 14**,** 995.
DE MURCIA, G. & MENISSIER DE MURCIA, J. 1994. Poly(ADP-ribose) polymerase: a molecular nick-sensor. *Trends Biochem Sci,* 19**,** 172-6.
DEAR, R. F., MCGEECHAN, K., JENKINS, M. C., BARRATT, A., TATTERSALL, M. H. & WILCKEN, N. 2013. Combination versus sequential single agent chemotherapy for metastatic breast cancer. *Cochrane Database Syst Rev***,** Cd008792.
DECLERCK, K. & ELBLE, R. C. 2010. The role of hypoxia and acidosis in promoting metastasis and resistance to chemotherapy. *Front Biosci (Landmark Ed),* 15**,** 213-25.
DEGENHARDT, K., MATHEW, R., BEAUDOIN, B., BRAY, K., ANDERSON, D., CHEN, G.*, et al.* 2006. Autophagy promotes tumor cell survival and restricts necrosis, inflammation, and tumorigenesis. *Cancer Cell,* 10**,** 51-64.
DELANEY, G., BARTON, M. & JACOB, S. 2003. Estimation of an optimal radiotherapy utilization rate for breast carcinoma: a review of the evidence. *Cancer,* 98**,** 1977-86.
DELANEY, G., JACOB, S., FEATHERSTONE, C. & BARTON, M. 2005. The role of radiotherapy in cancer treatment: estimating optimal utilization from a review of evidence-based clinical guidelines. *Cancer,* 104**,** 1129-37.
DENG, C.-X. 2006. BRCA1: cell cycle checkpoint, genetic instability, DNA damage response and cancer evolution. *Nucleic acids research,* 34**,** 1416-1426.
DENNY, W. A. 2000. The role of hypoxia-activated prodrugs in cancer therapy. *Lancet Oncol,* 1**,** 25-9.

DENT, R., TRUDEAU, M., PRITCHARD, K. I., HANNA, W. M., KAHN, H. K., SAWKA, C. A., *et al.* 2007. Triple-negative breast cancer: clinical features and patterns of recurrence. *Clin Cancer Res,* 13**,** 4429-34.

DERENDORF, H. & MEIBOHM, B. 1999. Modeling of Pharmacokinetic/Pharmacodynamic (PK/PD) Relationships: Concepts and Perspectives. *Pharmaceutical Research,* 16**,** 176-185.

DESANTIS, C. E., FEDEWA, S. A., GODING SAUER, A., KRAMER, J. L., SMITH, R. A. & JEMAL, A. 2016. Breast cancer statistics, 2015: Convergence of incidence rates between black and white women. *CA Cancer J Clin,* 66**,** 31-42.

DESANTIS, C. E., LIN, C. C., MARIOTTO, A. B., SIEGEL, R. L., STEIN, K. D., KRAMER, J. L., ALTERI, R., ROBBINS, A. S. & JEMAL, A. 2014. Cancer treatment and survivorship statistics, 2014. *CA Cancer J Clin,* 64**,** 252-71.

DESANTIS, C. E., MA, J., GAUDET, M. M., NEWMAN, L. A., MILLER, K. D., GODING SAUER, A., JEMAL, A. & SIEGEL, R. L. 2019. Breast cancer statistics, 2019. *CA: A Cancer Journal for Clinicians,* 69**,** 438-451.

DESCHAVANNE, B. F. P. J. 1999. Relationships between colony forming efficiency and parameters of intrinsic radiosensitivity. *International Journal of Radiation Biology,* 75**,** 1275-1282.

DESHMUKH, A. L., CHANDRA, S., SINGH, D. K., SIDDIQI, M. I. & BANERJEE, D. 2017. Identification of human flap endonuclease 1 (FEN1) inhibitors using a machine learning based consensus virtual screening. *Molecular BioSystems,* 13**,** 1630-1639.

DESMEDT, C., HAIBE-KAINS, B., WIRAPATI, P., BUYSE, M., LARSIMONT, D., BONTEMPI, G., DELORENZI, M., PICCART, M. & SOTIRIOU, C. 2008. Biological processes associated with breast cancer clinical outcome depend on the molecular subtypes. *Clin Cancer Res,* 14**,** 5158-65.

DEWHIRST, M. W. 2009. Relationships between cycling hypoxia, HIF-1, angiogenesis and oxidative stress. *Radiat Res,* 172**,** 653-65.

DEWHIRST, M. W., CAO, Y. & MOELLER, B. 2008. Cycling hypoxia and free radicals regulate angiogenesis and radiotherapy response. *Nature reviews. Cancer,* 8**,** 425-437.

DIAZ, L. K., CRYNS, V. L., SYMMANS, W. F. & SNEIGE, N. 2007. Triple negative breast carcinoma and the basal phenotype: from expression profiling to clinical practice. *Adv Anat Pathol,* 14**,** 419-30.

DIERAS, V., MILES, D., VERMA, S., PEGRAM, M., WELSLAU, M., BASELGA, J., *et al.* 2017. Trastuzumab emtansine versus capecitabine plus lapatinib in patients with previously treated HER2-positive advanced breast cancer (EMILIA): a descriptive analysis of final overall survival results from a randomised, open-label, phase 3 trial. *Lancet Oncol,* 18**,** 732-742.

DISILVESTRO, P. A., ALI, S., CRAIGHEAD, P. S., LUCCI, J. A., LEE, Y. C., COHN, D. E., *et al.* 2014. Phase III randomized trial of weekly cisplatin and irradiation versus cisplatin and tirapazamine and irradiation in stages IB2, IIA, IIB, IIIB, and IVA cervical carcinoma limited to the pelvis: a Gynecologic Oncology Group study. *J Clin Oncol,* 32**,** 458-64.

DOGLIOTTI, E., FORTINI, P., PASCUCCI, B. & PARLANTI, E. 2001. The mechanism of switching among multiple BER pathways. *Prog Nucleic Acid Res Mol Biol,* 68**,** 3-27.

DORJSUREN, D., KIM, D., MALONEY, D. J., WILSON, D. M., 3RD & SIMEONOV, A. 2011. Complementary non-radioactive assays for investigation of human flap endonuclease 1 activity. *Nucleic Acids Res,* 39**,** e11.

DOWNIE, D., MCFADYEN, M. C., ROONEY, P. H., CRUICKSHANK, M. E., PARKIN, D. E., MILLER, I. D., TELFER, C., MELVIN, W. T. & MURRAY, G. I. 2005. Profiling cytochrome P450 expression in ovarian cancer: identification of prognostic markers. *Clin Cancer Res,* 11**,** 7369-75.

DOWSETT, M., CUZICK, J., INGLE, J., COATES, A., FORBES, J., BLISS, J.*, et al.* 2010. Meta-analysis of breast cancer outcomes in adjuvant trials of aromatase inhibitors versus tamoxifen. *J Clin Oncol,* 28**,** 509-18.

DU, L., HOFFMAN, S. M. & KEENEY, D. S. 2004. Epidermal CYP2 family cytochromes P450. *Toxicol Appl Pharmacol,* 195**,** 278-87.

DUFFY, S. W., MORRISH, O. W. E., ALLGOOD, P. C., BLACK, R., GILLAN, M. G. C., WILLSHER, P.*, et al.* 2018. Mammographic density and breast cancer risk in breast screening assessment cases and women with a family history of breast cancer. *European journal of cancer (Oxford, England : 1990),* 88**,** 48-56.

DUMEAUX, V., FOURNIER, A., LUND, E. & CLAVEL-CHAPELON, F. 2005. Previous oral contraceptive use and breast cancer risk according to hormone replacement therapy use among postmenopausal women. *Cancer causes & control : CCC,* 16**,** 537-544.

DUNBIER, A. K., ANDERSON, H., GHAZOUI, Z., SALTER, J., PARKER, J. S., PEROU, C. M., SMITH, I. E. & DOWSETT, M. 2011. Association between breast cancer subtypes and response to neoadjuvant anastrozole. *Steroids,* 76**,** 736-40.

DUPONT, W. D. & PAGE, D. L. 1985. Risk factors for breast cancer in women with proliferative breast disease. *N Engl J Med,* 312**,** 146-51.

DURAND, R. E. & OLIVE, P. L. 1992. Evaluation of bioreductive drugs in multicell spheroids. *Int J Radiat Oncol Biol Phys,* 22**,** 689-92.

DURANT, S. T. & NICKOLOFF, J. A. 2005. Good timing in the cell cycle for precise DNA repair by BRCA1. *Cell Cycle,* 4**,** 1216-22.

DWIVEDY, I., DEVANESAN, P., CREMONESI, P., ROGAN, E. & CAVALIERI, E. 1992. Synthesis and characterization of estrogen 2,3- and 3,4-quinones. Comparison of DNA adducts formed by the quinones versus horseradish peroxidase-activated catechol estrogens. *Chem Res Toxicol,* 5**,** 828-33.

EALES, K. L., HOLLINSHEAD, K. E. R. & TENNANT, D. A. 2016. Hypoxia and metabolic adaptation of cancer cells. *Oncogenesis,* 5**,** e190-e190.

EBCTCG 2005. Effects of chemotherapy and hormonal therapy for early breast cancer on recurrence and 15-year survival: an overview of the randomised trials. *Lancet,* 365**,** 1687-717.

EBCTCG 2015. Adjuvant bisphosphonate treatment in early breast cancer: meta-analyses of individual patient data from randomised trials. *Lancet,* 386**,** 1353-1361.

EDGE, S. B. & COMPTON, C. C. 2010. The American Joint Committee on Cancer: the 7th edition of the AJCC cancer staging manual and the future of TNM. *Ann Surg Oncol,* 17**,** 1471-4.

EDLER, D., STENSTEDT, K., OHRLING, K., HALLSTROM, M., KARLGREN, M., INGELMAN-SUNDBERG, M. & RAGNHAMMAR, P. 2009. The expression of the novel CYP2W1 enzyme is an independent prognostic factor in colorectal cancer - a pilot study. *Eur J Cancer,* 45**,** 705-12.

EDMONDSON, R., BROGLIE, J. J., ADCOCK, A. F. & YANG, L. 2014. Three-dimensional cell culture systems and their applications in drug discovery and cell-based biosensors. *Assay and drug development technologies,* 12**,** 207-218.

EDWARDS, D. I. 1993. Nitroimidazole drugs--action and resistance mechanisms. I. Mechanisms of action. *J Antimicrob Chemother,* 31**,** 9-20.

EJLERTSEN, B., JENSEN, M. B., RANK, F., RASMUSSEN, B. B., CHRISTIANSEN, P., KROMAN, N.*, et al.* 2009. Population-based study of peritumoral lymphovascular invasion and outcome among patients with operable breast cancer. *J Natl Cancer Inst,* 101**,** 729-35.

EL-AWADY, R. A., DIKOMEY, E. & DAHM-DAPHI, J. 2003. Radiosensitivity of human tumour cells is correlated with the induction but not with the repair of DNA double-strand breaks. *Br J Cancer,* 89**,** 593-601.

EL-SERAFI, I., AFSHARIAN, P., MOSHFEGH, A., HASSAN, M. & TERELIUS, Y. 2015. Cytochrome P450 Oxidoreductase Influences CYP2B6 Activity in Cyclophosphamide Bioactivation. *PloS one,* 10**,** e0141979-e0141979.

ELKIND, M. M. 1988. The initial part of the survival curve: does it predict the outcome of fractionated radiotherapy? *Radiat Res,* 114**,** 425-36.

ELLIS, I. O., GALEA, M., BROUGHTON, N., LOCKER, A., BLAMEY, R. W. & ELSTON, C. W. 1992. Pathological prognostic factors in breast cancer. II. Histological type. Relationship with survival in a large study with long-term follow-up. *Histopathology,* 20**,** 479-89.

ELLIS, M. J., TAO, Y., LUO, J., A'HERN, R., EVANS, D. B., BHATNAGAR, A. S.*, et al.* 2008. Outcome prediction for estrogen receptor-positive breast cancer based on postneoadjuvant endocrine therapy tumor characteristics. *J Natl Cancer Inst,* 100**,** 1380-8.

ELSTON, C. W. & ELLIS, I. O. 1991. Pathological prognostic factors in breast cancer. I. The value of histological grade in breast cancer: experience from a large study with long-term follow-up. *Histopathology,* 19**,** 403-10.

ELSTRODT, F., HOLLESTELLE, A., NAGEL, J. H., GORIN, M., WASIELEWSKI, M., VAN DEN OUWELAND, A., MERAJVER, S. D., ETHIER, S. P. & SCHUTTE, M. 2006. BRCA1 mutation analysis of 41 human breast cancer cell lines reveals three new deleterious mutants. *Cancer Res,* 66**,** 41-5.

EMAMI, B., LYMAN, J., BROWN, A., COIA, L., GOITEIN, M., MUNZENRIDER, J. E., SHANK, B., SOLIN, L. J. & WESSON, M. 1991. Tolerance of normal tissue to therapeutic irradiation. *Int J Radiat Oncol Biol Phys,* 21**,** 109-22.

ENGELS, F. K., TEN TIJE, A. J., BAKER, S. D., LEE, C. K., LOOS, W. J., VULTO, A. G., VERWEIJ, J. & SPARREBOOM, A. 2004. Effect of cytochrome P450 3A4 inhibition on the pharmacokinetics of docetaxel. *Clin Pharmacol Ther,* 75**,** 448-54.

ERLER, J. T., BENNEWITH, K. L., NICOLAU, M., DORNHOFER, N., KONG, C., LE, Q. T., CHI, J. T., JEFFREY, S. S. & GIACCIA, A. J. 2006. Lysyl oxidase is essential for hypoxia-induced metastasis. *Nature,* 440**,** 1222-6.

ESBAH, O. & OKSUZOGLU, B. 2017. Prognostic & predictive factors for planning adjuvant chemotherapy of early-stage breast cancer. *The Indian journal of medical research,* 146**,** 563-571.

ESTABROOK, R. W. 2003. A passion for P450s (rememberances of the early history of research on cytochrome P450). *Drug Metab Dispos,* 31**,** 1461-73.

EWING, D. 1998. The oxygen fixation hypothesis: a reevaluation. *Am J Clin Oncol,* 21**,** 355-61.

EXELL, J. C., THOMPSON, M. J., FINGER, L. D., SHAW, S. J., DEBRECZENI, J., WARD, T. A.*, et al.* 2016. Cellularly active N-hydroxyurea FEN1 inhibitors block substrate entry to the active site. *Nature chemical biology,* 12**,** 815-821.

FABIAN, C., TILZER, L. & STERNSON, L. 1981. Comparative binding affinities of tamoxifen, 4-hydroxytamoxifen, and desmethyltamoxifen for estrogen receptors isolated from human breast carcinoma: correlation with blood levels in patients with metastatic breast cancer. *Biopharm Drug Dispos,* 2**,** 381-90.

FALLAHPOUR, S., NAVANEELAN, T., DE, P. & BORGO, A. 2017. Breast cancer survival by molecular subtype: a population-based analysis of cancer registry data. *CMAJ open,* 5**,** E734-E739.

FANG, X., JIANG, H., ZHU, Y., ZHANG, L., FAN, Q. & TIAN, Y. 2014. Doxorubicin induces drug resistance and expression of the novel CD44st via NF-κB in human breast cancer MCF-7 cells. *Oncology reports,* 31.

FARMER, H., MCCABE, N., LORD, C. J., TUTT, A. N., JOHNSON, D. A., RICHARDSON, T. B.*, et al.* 2005. Targeting the DNA repair defect in BRCA mutant cells as a therapeutic strategy. *Nature,* 434**,** 917-21.

FDA. 2018. *FDA approves olaparib for germline BRCA-mutated metastatic breast cancer* [Online]. U.S Food and Drug Administration. Available:

https://www.fda.gov/drugs/resources-information-approved-drugs/fda-approves-olaparib-germline-brca-mutated-metastatic-breast-cancer [Accessed 1 November 2019].
FENG, L., CHENG, L., DONG, Z., TAO, D., BARNHART, T. E., CAI, W., CHEN, M. & LIU, Z. 2017. Theranostic Liposomes with Hypoxia-Activated Prodrug to Effectively Destruct Hypoxic Tumors Post-Photodynamic Therapy. *ACS Nano,* 11**,** 927-937.
FERNANDEZ, S. V., RUSSO, I. H. & RUSSO, J. 2006. Estradiol and its metabolites 4-hydroxyestradiol and 2-hydroxyestradiol induce mutations in human breast epithelial cells. *Int J Cancer,* 118**,** 1862-8.
FIDOAMORE, A., CRISTIANO, L., ANTONOSANTE, A., D'ANGELO, M., DI GIACOMO, E., ASTARITA, C.*, et al.* 2016. Glioblastoma Stem Cells Microenvironment: The Paracrine Roles of the Niche in Drug and Radioresistance. *Stem Cells Int,* 2016**,** 6809105.
FISHER, B., ANDERSON, S., BRYANT, J., MARGOLESE, R. G., DEUTSCH, M., FISHER, E. R., JEONG, J. H. & WOLMARK, N. 2002. Twenty-year follow-up of a randomized trial comparing total mastectomy, lumpectomy, and lumpectomy plus irradiation for the treatment of invasive breast cancer. *N Engl J Med,* 347**,** 1233-41.
FISHER, B., BAUER, M., WICKERHAM, D. L., REDMOND, C. K., FISHER, E. R., CRUZ, A. B.*, et al.* 1983. Relation of number of positive axillary nodes to the prognosis of patients with primary breast cancer. An NSABP update. *Cancer,* 52**,** 1551-7.
FISHER, E. R., ANDERSON, S., REDMOND, C. & FISHER, B. 1993. Pathologic findings from the national surgical adjuvant breast project protocol B-06 10-year pathologic and clinical prognostic discriminants. *Cancer,* 71**,** 2507-2514.
FITZGIBBONS, P. L., PAGE, D. L., WEAVER, D., THOR, A. D., ALLRED, D. C., CLARK, G. M.*, et al.* 2000. Prognostic factors in breast cancer. College of American Pathologists Consensus Statement 1999. *Arch Pathol Lab Med,* 124**,** 966-78.
FITZPATRICK, B., MEHIBEL, M., COWEN, R. L. & STRATFORD, I. J. 2008. iNOS as a therapeutic target for treatment of human tumors. *Nitric Oxide,* 19**,** 217-24.
FLADER, C., LIU, J. & BORCH, R. F. 2000. Development of Novel Quinone Phosphorodiamidate Prodrugs Targeted to DT-Diaphorase. *Journal of Medicinal Chemistry,* 43**,** 3157-3167.
FOK, J. H. L., RAMOS-MONTOYA, A., VAZQUEZ-CHANTADA, M., WIJNHOVEN, P. W. G., FOLLIA, V., JAMES, N.*, et al.* 2019. AZD7648 is a potent and selective DNA-PK inhibitor that enhances radiation, chemotherapy and olaparib activity. *Nature Communications,* 10**,** 5065.
FOKAS, E., PREVO, R., HAMMOND, E. M., BRUNNER, T. B., MCKENNA, W. G. & MUSCHEL, R. J. 2014. Targeting ATR in DNA damage response and cancer therapeutics. *Cancer Treat Rev,* 40**,** 109-17.
FOLKERD, E. J. & DOWSETT, M. 2010. Influence of sex hormones on cancer progression. *J Clin Oncol,* 28**,** 4038-44.
FORMBY, B. & WILEY, T. S. 1999. Bcl-2, survivin and variant CD44 v7-v10 are downregulated and p53 is upregulated in breast cancer cells by progesterone: inhibition of cell growth and induction of apoptosis. *Mol Cell Biochem,* 202**,** 53-61.
FORMENTI, S. C. & DEMARIA, S. 2012. Radiation therapy to convert the tumor into an in situ vaccine. *International journal of radiation oncology, biology, physics,* 84**,** 879-880.
FORTINI, P., PASCUCCI, B., PARLANTI, E., D'ERRICO, M., SIMONELLI, V. & DOGLIOTTI, E. 2003. The base excision repair: mechanisms and its relevance for cancer susceptibility. *Biochimie,* 85**,** 1053-71.

FOWLER, J. F. 1992. Alpha, beta, and surviving fraction. *Int J Radiat Oncol Biol Phys,* 24**,** 188-9.
FRANCESCHINI, G., TERRIBILE, D., MAGNO, S., FABBRI, C., D'ALBA, P. F., CHIESA, F., DI LEONE, A. & MASETTI, R. 2007. Update in the treatment of locally advanced breast cancer: a multidisciplinary approach. *Eur Rev Med Pharmacol Sci,* 11**,** 283-9.
FRANKEN, N. A., RODERMOND, H. M., STAP, J., HAVEMAN, J. & VAN BREE, C. 2006. Clonogenic assay of cells in vitro. *Nat Protoc,* 1**,** 2315-9.
FRANKEN, N. A. P., TEN CATE, R., KRAWCZYK, P. M., STAP, J., HAVEMAN, J., ATEN, J. & BARENDSEN, G. W. 2011. Comparison of RBE values of high-LET α-particles for the induction of DNA-DSBs, chromosome aberrations and cell reproductive death. *Radiation Oncology,* 6**,** 64.
FRASOR, J., DANES, J. M., KOMM, B., CHANG, K. C., LYTTLE, C. R. & KATZENELLENBOGEN, B. S. 2003. Profiling of estrogen up- and down-regulated gene expression in human breast cancer cells: insights into gene networks and pathways underlying estrogenic control of proliferation and cell phenotype. *Endocrinology,* 144**,** 4562-74.
FRIERY, O. P., GALLAGHER, R., MURRAY, M. M., HUGHES, C. M., GALLIGAN, E. S., MCINTYRE, I. A., PATTERSON, L. H., HIRST, D. G. & MCKEOWN, S. R. 2000. Enhancement of the anti-tumour effect of cyclophosphamide by the bioreductive drugs AQ4N and tirapazamine. *British Journal of Cancer,* 82**,** 1469-1473.
FROSINA, G., FORTINI, P., ROSSI, O., CARROZZINO, F., RASPAGLIO, G., COX, L. S., LANE, D. P., ABBONDANDOLO, A. & DOGLIOTTI, E. 1996. Two pathways for base excision repair in mammalian cells. *J Biol Chem,* 271**,** 9573-8.
FUGH-BERMAN, A. & EPSTEIN, S. 1992. Tamoxifen: disease prevention or disease substitution? *Lancet,* 340**,** 1143-5.
FULFORD, L. G., REIS-FILHO, J. S., RYDER, K., JONES, C., GILLETT, C. E., HANBY, A., EASTON, D. & LAKHANI, S. R. 2007. Basal-like grade III invasive ductal carcinoma of the breast: patterns of metastasis and long-term survival. *Breast Cancer Res,* 9**,** R4.
FURGE, L. L. & GUENGERICH, F. P. 2006. Cytochrome P450 enzymes in drug metabolism and chemical toxicology: An introduction. *Biochemistry and Molecular Biology Education,* 34**,** 66-74.
GALEA, M. H., BLAMEY, R. W., ELSTON, C. E. & ELLIS, I. O. 1992. The Nottingham Prognostic Index in primary breast cancer. *Breast Cancer Res Treat,* 22**,** 207-19.
GARG, P. K. & PRAKASH, G. 2015. Current definition of locally advanced breast cancer. *Current oncology (Toronto, Ont.),* 22**,** e409-e410.
GATEI, M., ZHOU, B. B., HOBSON, K., SCOTT, S., YOUNG, D. & KHANNA, K. K. 2001. Ataxia telangiectasia mutated (ATM) kinase and ATM and Rad3 related kinase mediate phosphorylation of Brca1 at distinct and overlapping sites. In vivo assessment using phospho-specific antibodies. *J Biol Chem,* 276**,** 17276-80.
GATENBY, R. A., KESSLER, H. B., ROSENBLUM, J. S., COIA, L. R., MOLDOFSKY, P. J., HARTZ, W. H. & BRODER, G. J. 1988. Oxygen distribution in squamous cell carcinoma metastases and its relationship to outcome of radiation therapy. *Int J Radiat Oncol Biol Phys,* 14**,** 831-8.
GENERALI, D., BERRUTI, A., BRIZZI, M. P., CAMPO, L., BONARDI, S., WIGFIELD, S.*, et al.* 2006. Hypoxia-Inducible Factor-1α Expression Predicts a Poor Response to Primary Chemoendocrine Therapy and Disease-Free Survival in Primary Human Breast Cancer. *Clinical Cancer Research,* 12**,** 4562-4568.
GHOSE, R., MALLICK, P., TANEJA, G., CHU, C. & MOORTHY, B. 2016. In Vitro Approaches to Study Regulation of Hepatic Cytochrome P450 (CYP) 3A Expression by Paclitaxel and Rifampicin. *Methods Mol Biol,* 1395**,** 55-68.
GIATROMANOLAKI, A., KOUKOURAKIS, M. I., SIVRIDIS, E., PASTOREK, J., WYKOFF, C. C., GATTER, K. C. & HARRIS, A. L. 2001. Expression of

hypoxia-inducible carbonic anhydrase-9 relates to angiogenic pathways and independently to poor outcome in non-small cell lung cancer. *Cancer Res,* 61**,** 7992-8.
GIBSON, G. G. & SKETT, P. 2001. *Introduction to Drug Metabolism (3rd ed.),* Hampshire, UK, Nelson Thornes Ltd.
GILKES, D. M. & SEMENZA, G. L. 2013. Role of hypoxia-inducible factors in breast cancer metastasis. *Future Oncol,* 9**,** 1623-36.
GOLDHIRSCH, A., GLICK, J. H., GELBER, R. D., COATES, A. S., THURLIMANN, B. & SENN, H. J. 2005. Meeting highlights: international expert consensus on the primary therapy of early breast cancer 2005. *Ann Oncol,* 16**,** 1569-83.
GOLDHIRSCH, A., WINER, E. P., COATES, A. S., GELBER, R. D., PICCART-GEBHART, M., THÜRLIMANN, B., SENN, H. J. & PANEL, M. 2013. Personalizing the treatment of women with early breast cancer: highlights of the St Gallen International Expert Consensus on the Primary Therapy of Early Breast Cancer 2013. *Annals of oncology : official journal of the European Society for Medical Oncology,* 24**,** 2206-2223.
GOLDHIRSCH, A., WOOD, W. C., COATES, A. S., GELBER, R. D., THURLIMANN, B. & SENN, H. J. 2011. Strategies for subtypes--dealing with the diversity of breast cancer: highlights of the St. Gallen International Expert Consensus on the Primary Therapy of Early Breast Cancer 2011. *Ann Oncol,* 22**,** 1736-47.
GOLDING, S. E., ROSENBERG, E., VALERIE, N., HUSSAINI, I., FRIGERIO, M., COCKCROFT, X. F.*, et al.* 2009. Improved ATM kinase inhibitor KU-60019 radiosensitizes glioma cells, compromises insulin, AKT and ERK prosurvival signaling, and inhibits migration and invasion. *Molecular cancer therapeutics,* 8**,** 2894-2902.
GOMEZ, A., NEKVINDOVA, J., TRAVICA, S., LEE, M. Y., JOHANSSON, I., EDLER, D., MKRTCHIAN, S. & INGELMAN-SUNDBERG, M. 2010. Colorectal cancer-specific cytochrome P450 2W1: intracellular localization, glycosylation, and catalytic activity. *Mol Pharmacol,* 78**,** 1004-11.
GONG, Y., LIU, Y.-R., JI, P., HU, X. & SHAO, Z.-M. 2017. Impact of molecular subtypes on metastatic breast cancer patients: a SEER population-based study. *Scientific Reports,* 7**,** 45411.
GOODARZI, A. A., YU, Y., RIBALLO, E., DOUGLAS, P., WALKER, S. A., YE, R.*, et al.* 2006. DNA-PK autophosphorylation facilitates Artemis endonuclease activity. *The EMBO journal,* 25**,** 3880-3889.
GORDON, L. 2001. Inflammatory breast cancer. *Clin J Oncol Nurs,* 5**,** 175-6.
GRAHAM, K. & UNGER, E. 2018. Overcoming tumor hypoxia as a barrier to radiotherapy, chemotherapy and immunotherapy in cancer treatment. *International journal of nanomedicine,* 13**,** 6049-6058.
GRAY, L. H., CONGER, A. D., EBERT, M., HORNSEY, S. & SCOTT, O. C. 1953. The concentration of oxygen dissolved in tissues at the time of irradiation as a factor in radiotherapy. *Br J Radiol,* 26**,** 638-48.
GREENBAUM, D., COLANGELO, C., WILLIAMS, K. & GERSTEIN, M. 2003. Greenbaum D, Colangelo C, Williams K, Gerstein M. Comparing protein abundance and mRNA expression levels on a genomic scale. Genome Biol 4: 117. *Genome biology,* 4**,** 117.
GREGOIRE, V., HITTELMAN, W. N., ROSIER, J. F. & MILAS, L. 1999. Chemo-radiotherapy: radiosensitizing nucleoside analogues (review). *Oncol Rep,* 6**,** 949-57.
GREIJER, A. E. & VAN DER WALL, E. 2004. The role of hypoxia inducible factor 1 (HIF-1) in hypoxia induced apoptosis. *Journal of clinical pathology,* 57**,** 1009-1014.
GRIMES, D. R., KELLY, C., BLOCH, K. & PARTRIDGE, M. 2014. A method for estimating the oxygen consumption rate in multicellular tumour spheroids. *J R Soc Interface,* 11**,** 20131124.

GRIMES, D. R. & PARTRIDGE, M. 2015. A mechanistic investigation of the oxygen fixation hypothesis and oxygen enhancement ratio. *Biomed Phys Eng Express,* 1**,** 045209.
GROSS, M. W., KARBACH, U., GROEBE, K., FRANKO, A. J. & MUELLER-KLIESER, W. 1995. Calibration of misonidazole labeling by simultaneous measurement of oxygen tension and labeling density in multicellular spheroids. *Int J Cancer,* 61**,** 567-73.
GU, J., LU, H., TIPPIN, B., SHIMAZAKI, N., GOODMAN, M. F. & LIEBER, M. R. 2007. XRCC4:DNA ligase IV can ligate incompatible DNA ends and can ligate across gaps. *Embo j,* 26**,** 1010-23.
GUARINO, M., RUBINO, B. & BALLABIO, G. 2007. The role of epithelial-mesenchymal transition in cancer pathology. *Pathology,* 39**,** 305-18.
GUENGERICH, F. P. 1999. Cytochrome P-450 3A4: regulation and role in drug metabolism. *Annu Rev Pharmacol Toxicol,* 39**,** 1-17.
GUENGERICH, F. P. 2008. Cytochrome p450 and chemical toxicology. *Chem Res Toxicol,* 21**,** 70-83.
GUISE, C. P., MOWDAY, A. M., ASHOORZADEH, A., YUAN, R., LIN, W. H., WU, D. H., SMAILL, J. B., PATTERSON, A. V. & DING, K. 2014. Bioreductive prodrugs as cancer therapeutics: targeting tumor hypoxia. *Chin J Cancer,* 33**,** 80-6.
GUISE, C. P., WANG, A. T., THEIL, A., BRIDEWELL, D. J., WILSON, W. R. & PATTERSON, A. V. 2007. Identification of human reductases that activate the dinitrobenzamide mustard prodrug PR-104A: a role for NADPH:cytochrome P450 oxidoreductase under hypoxia. *Biochem Pharmacol,* 74**,** 810-20.
GULLEDGE, C. J. & DEWHIRST, M. W. 1996. Tumor oxygenation: a matter of supply and demand. *Anticancer Res,* 16**,** 741-9.
GUO, W., LIN, L., HE, X., HE, F., WANG, C., CHEN, N. & WANG, Y. 2017. Biomarkers of DNA Repair and Related Pathways: Significance of Treatment in Triple-Negative Breast Cancer. *Crit Rev Oncog,* 22**,** 427-437.
GUO, Y., TAN, J., MIAO, Y., SUN, Z. & ZHANG, Q. 2019. Effects of Microvesicles on Cell Apoptosis under Hypoxia. *Oxid Med Cell Longev,* 2019**,** 5972152.
GUSTERSON, B. A., GELBER, R. D., GOLDHIRSCH, A., PRICE, K. N., SAVE-SODERBORGH, J., ANBAZHAGAN, R.*, et al.* 1992. Prognostic importance of c-erbB-2 expression in breast cancer. International (Ludwig) Breast Cancer Study Group. *J Clin Oncol,* 10**,** 1049-56.
GUZY, R. D. & SCHUMACKER, P. T. 2006. Oxygen sensing by mitochondria at complex III: the paradox of increased reactive oxygen species during hypoxia. *Exp Physiol,* 91**,** 807-19.
HABASHY, H. O., POWE, D. G., ABDEL-FATAH, T. M., GEE, J. M., NICHOLSON, R. I., GREEN, A. R., RAKHA, E. A. & ELLIS, I. O. 2012. A review of the biological and clinical characteristics of luminal-like oestrogen receptor-positive breast cancer. *Histopathology,* 60**,** 854-63.
HALL, E. & GIACCIA, A. 2012. *Radiobiology for the radiologist,* Philadelphia, Wolters Kluwer Health/Lippincott Williams & Wilkins,.
HALL, E. J. & COX, J. D. 2010. Chapter 1 - Physical and Biologic Basis of Radiation Therapy. *In:* COX, J. D. & ANG, K. K. (eds.) *Radiation Oncology (Ninth Edition).* Philadelphia: Content Repository Only!
HALL, J. S., IYPE, R., SENRA, J., TAYLOR, J., ARMENOULT, L., OGUEJIOFOR, K.*, et al.* 2014. Investigation of radiosensitivity gene signatures in cancer cell lines. *PloS one,* 9**,** e86329-e86329.
HAMAJIMA, N., HIROSE, K., TAJIMA, K., ROHAN, T., CALLE, E. E., HEATH, C. W., JR.*, et al.* 2002. Alcohol, tobacco and breast cancer--collaborative reanalysis of individual data from 53 epidemiological studies, including 58,515 women with breast cancer and 95,067 women without the disease. *Br J Cancer,* 87**,** 1234-45.

HANCE, K. W., ANDERSON, W. F., DEVESA, S. S., YOUNG, H. A. & LEVINE, P. H. 2005. Trends in inflammatory breast carcinoma incidence and survival: the surveillance, epidemiology, and end results program at the National Cancer Institute. *J Natl Cancer Inst,* 97**,** 966-75.

HARRIS, A. L. 2002. Hypoxia--a key regulatory factor in tumour growth. *Nat Rev Cancer,* 2**,** 38-47.

HARTMAN, A. R., KALDATE, R. R., SAILER, L. M., PAINTER, L., GRIER, C. E., ENDSLEY, R. R.*, et al.* 2012. Prevalence of BRCA mutations in an unselected population of triple-negative breast cancer. *Cancer,* 118**,** 2787-95.

HARTMANN, L. C., DEGNIM, A. C., SANTEN, R. J., DUPONT, W. D. & GHOSH, K. 2015. Atypical hyperplasia of the breast--risk assessment and management options. *The New England journal of medicine,* 372**,** 78-89.

HARVEY, J. M., CLARK, G. M., OSBORNE, C. K. & ALLRED, D. C. 1999. Estrogen receptor status by immunohistochemistry is superior to the ligand-binding assay for predicting response to adjuvant endocrine therapy in breast cancer. *J Clin Oncol,* 17**,** 1474-81.

HAVILAND, J. S., OWEN, J. R., DEWAR, J. A., AGRAWAL, R. K., BARRETT, J., BARRETT-LEE, P. J.*, et al.* 2013. The UK Standardisation of Breast Radiotherapy (START) trials of radiotherapy hypofractionation for treatment of early breast cancer: 10-year follow-up results of two randomised controlled trials. *Lancet Oncol,* 14**,** 1086-94.

HAWSAWI, Y. M., AL-NUMAIR, N. S., SOBAHY, T. M., AL-AJMI, A. M., AL-HARBI, R. M., BAGHDADI, M. A., OYOUNI, A. A. & ALAMER, O. M. 2019. The role of BRCA1/2 in hereditary and familial breast and ovarian cancers. *Mol Genet Genomic Med***,** e879.

HAYBITTLE, J. L., BLAMEY, R. W., ELSTON, C. W., JOHNSON, J., DOYLE, P. J., CAMPBELL, F. C., NICHOLSON, R. I. & GRIFFITHS, K. 1982. A prognostic index in primary breast cancer. *Br J Cancer,* 45**,** 361-6.

HAYDAROGLU , A., & OZYIGIT, G 2012. Principles and practice of modern radiotherapy techniques in breast cancer:. *Springer Science & Business Media.*

HAYES, C. L., SPINK, D. C., SPINK, B. C., CAO, J. Q., WALKER, N. J. & SUTTER, T. R. 1996. 17 beta-estradiol hydroxylation catalyzed by human cytochrome P450 1B1. *Proceedings of the National Academy of Sciences,* 93**,** 9776-9781.

HE, L., LV, Y., SONG, Y. & ZHANG, B. 2019. The prognosis comparison of different molecular subtypes of breast tumors after radiotherapy and the intrinsic reasons for their distinct radiosensitivity. *Cancer Manag Res,* 11**,** 5765-5775.

HE, L., YANG, H., ZHOU, S., ZHU, H., MAO, H., MA, Z.*, et al.* 2018. Synergistic antitumor effect of combined paclitaxel with FEN1 inhibitor in cervical cancer cells. *DNA Repair (Amst),* 63**,** 1-9.

HE, L., ZHANG, Y., SUN, H., JIANG, F., YANG, H., WU, H.*, et al.* 2016. Targeting DNA Flap Endonuclease 1 to Impede Breast Cancer Progression. *EBioMedicine,* 14**,** 32-43.

HEGDE, M. L., HAZRA, T. K. & MITRA, S. 2008. Early steps in the DNA base excision/single-strand interruption repair pathway in mammalian cells. *Cell Res,* 18**,** 27-47.

HEIMANN, R., FERGUSON, D., RECANT, W. M. & HELLMAN, S. 1997. Breast cancer metastatic phenotype as predicted by histologic tumor markers. *Cancer J Sci Am,* 3**,** 224-9.

HEJMADI, M. V., MCKEOWN, S. R., FRIERY, O. P., MCINTYRE, I. A., PATTERSON, L. H. & HIRST, D. G. 1996. DNA damage following combination of radiation with the bioreductive drug AQ4N: possible selective toxicity to oxic and hypoxic tumour cells. *Br J Cancer,* 73**,** 499-505.

HELLEDAY, T., PETERMANN, E., LUNDIN, C., HODGSON, B. & SHARMA, R. A. 2008. DNA repair pathways as targets for cancer therapy. *Nat Rev Cancer,* 8**,** 193-204.
HERNANDEZ-AYA, L. F. & GONZALEZ-ANGULO, A. M. 2013. Adjuvant systemic therapies in breast cancer. *Surg Clin North Am,* 93**,** 473-91.
HICKSON, I., ZHAO, Y., RICHARDSON, C. J., GREEN, S. J., MARTIN, N. M., ORR, A. I.*, et al.* 2004. Identification and characterization of a novel and specific inhibitor of the ataxia-telangiectasia mutated kinase ATM. *Cancer Res,* 64**,** 9152-9.
HIGGINS, M. J. & STEARNS, V. 2010. CYP2D6 polymorphisms and tamoxifen metabolism: clinical relevance. *Curr Oncol Rep,* 12**,** 7-15.
HIRSCHHAEUSER, F., MENNE, H., DITTFELD, C., WEST, J., MUELLER-KLIESER, W. & KUNZ-SCHUGHART, L. A. 2010. Multicellular tumor spheroids: an underestimated tool is catching up again. *J Biotechnol,* 148**,** 3-15.
HLAVÁČ, V., BRYNYCHOVÁ, V., VÁCLAVÍKOVÁ, R., EHRLICHOVÁ, M., VRÁNA, D., PECHA, V.*, et al.* 2014. The role of cytochromes p450 and aldo-keto reductases in prognosis of breast carcinoma patients. *Medicine,* 93**,** e255-e255.
HOCKEL, M., SCHLENGER, K., KNOOP, C. & VAUPEL, P. 1991. Oxygenation of carcinomas of the uterine cervix: evaluation by computerized O2 tension measurements. *Cancer Res,* 51**,** 6098-102.
HOEIJMAKERS, J. H. J. 2001. Genome maintenance mechanisms for preventing cancer. *Nature,* 411**,** 366-374.
HOHENBERGER, P., FELGNER, C., HAENSCH, W. & SCHLAG, P. M. 1998. Tumor oxygenation correlates with molecular growth determinants in breast cancer. *Breast Cancer Res Treat,* 48**,** 97-106.
HONTZ, A. E., LI, S. A., LINGLE, W. L., NEGRON, V., BRUZEK, A., SALISBURY, J. L. & LI, J. J. 2007. Aurora a and B overexpression and centrosome amplification in early estrogen-induced tumor foci in the Syrian hamster kidney: implications for chromosomal instability, aneuploidy, and neoplasia. *Cancer Res,* 67**,** 2957-63.
HORSMAN, M. R. & OVERGAARD, J. 2016. The impact of hypoxia and its modification of the outcome of radiotherapy. *Journal of radiation research,* 57 Suppl 1**,** i90-i98.
HORTOBAGYI, G. N., DE LA GARZA SALAZAR, J., PRITCHARD, K., AMADORI, D., HAIDINGER, R., HUDIS, C. A.*, et al.* 2005. The global breast cancer burden: variations in epidemiology and survival. *Clin Breast Cancer,* 6**,** 391-401.
HORTON, J. K., STEFANICK, D. F., KEDAR, P. S. & WILSON, S. H. 2007. ATR signaling mediates an S-phase checkpoint after inhibition of poly(ADP-ribose) polymerase activity. *DNA Repair (Amst),* 6**,** 742-50.
HOWARD-FLANDERS, P. & MOORE, D. 1958. The time interval after pulsed irradiation within which injury to bacteria can be modified by dissolved oxygen. I. A search for an effect of oxygen 0.02 second after pulsed irradiation. *Radiat Res,* 9**,** 422-37.
HUAMBACHANO, O., HERRERA, F., RANCOURT, A. & SATOH, M. S. 2011. Double-stranded DNA binding domain of poly(ADP-ribose) polymerase-1 and molecular insight into the regulation of its activity. *J Biol Chem,* 286**,** 7149-60.
HUANG, Z., LIU, Y., QI, G., BRAND, D. & ZHENG, S. G. 2018. Role of Vitamin A in the Immune System. *Journal of clinical medicine,* 7**,** 258.
HUBALEK, M., CZECH, T. & MÜLLER, H. 2017. Biological Subtypes of Triple-Negative Breast Cancer. *Breast care (Basel, Switzerland),* 12**,** 8-14.
HUBBI, M. E., KSHITIZ, GILKES, D. M., REY, S., WONG, C. C., LUO, W.*, et al.* 2013. A nontranscriptional role for HIF-1α as a direct inhibitor of DNA replication. *Science signaling,* 6**,** ra10-ra10.

HUBBI, M. E. & SEMENZA, G. L. 2015. Regulation of cell proliferation by hypoxia-inducible factors. *American journal of physiology. Cell physiology,* 309**,** C775-C782.
HUDIS, C. A. & GIANNI, L. 2011. Triple-Negative Breast Cancer: An Unmet Medical Need. *The Oncologist,* 16**,** 1-11.
HUNTER, F. W., HSU, H. L., SU, J., PULLEN, S. M., WILSON, W. R. & WANG, J. 2014. Dual targeting of hypoxia and homologous recombination repair dysfunction in triple-negative breast cancer. *Mol Cancer Ther,* 13**,** 2501-14.
HUNTER, F. W., WOUTERS, B. G. & WILSON, W. R. 2016. Hypoxia-activated prodrugs: paths forward in the era of personalised medicine. *British journal of cancer,* 114**,** 1071-1077.
HUNTER, N. & MUIRHEAD, C. R. 2009. Review of relative biological effectiveness dependence on linear energy transfer for low-LET radiations. *J Radiol Prot,* 29**,** 5-21.
HURWITZ, M. D., HANSEN, J. L., PROKOPIOS-DAVOS, S., MANOLA, J., WANG, Q., BORNSTEIN, B. A., HYNYNEN, K. & KAPLAN, I. D. 2011. Hyperthermia combined with radiation for the treatment of locally advanced prostate cancer: long-term results from Dana-Farber Cancer Institute study 94-153. *Cancer,* 117**,** 510-6.
HYPOXYLAB™. 2020. Oxford Optronix. Available: https://www.oxford-optronix.com/ [Accessed 5 January 2020].
IIDA, T., MINE, S., FUJIMOTO, H., SUZUKI, K., MINAMI, Y. & TANAKA, Y. 2002. Hypoxia-inducible factor-1alpha induces cell cycle arrest of endothelial cells. *Genes Cells,* 7**,** 143-9.
INGELMAN-SUNDBERG, M. 2005. The human genome project and novel aspects of cytochrome P450 research. *Toxicol Appl Pharmacol,* 207**,** 52-6.
INIC, Z., ZEGARAC, M., INIC, M., MARKOVIC, I., KOZOMARA, Z., DJURISIC, I., INIC, I., PUPIC, G. & JANCIC, S. 2014. Difference between Luminal A and Luminal B Subtypes According to Ki-67, Tumor Size, and Progesterone Receptor Negativity Providing Prognostic Information. *Clinical Medicine Insights. Oncology,* 8**,** 107-111.
INMAN, M., VISCONTI, A., YAN, C., SIEGEL, D., ROSS, D. & MOODY, C. J. 2014. Antitumour indolequinones: synthesis and activity against human pancreatic cancer cells. *Organic & Biomolecular Chemistry,* 12**,** 4848-4861.
ISKANDER, K., LI, J., HAN, S., ZHENG, B. & JAISWAL, A. K. 2006. NQO1 and NQO2 regulation of humoral immunity and autoimmunity. *J Biol Chem,* 281**,** 30917-24.
IZUMI, T., WIEDERHOLD, L. R., ROY, G., ROY, R., JAISWAL, A., BHAKAT, K. K., MITRA, S. & HAZRA, T. K. 2003. Mammalian DNA base excision repair proteins: their interactions and role in repair of oxidative DNA damage. *Toxicology,* 193**,** 43-65.
JACKSON, R. K., LIEW, L. P. & HAY, M. P. 2019. Overcoming Radioresistance: Small Molecule Radiosensitisers and Hypoxia-activated Prodrugs. *Clin Oncol (R Coll Radiol)*.
JACKSON, S. P. & BARTEK, J. 2009. The DNA-damage response in human biology and disease. *Nature,* 461**,** 1071-8.
JAKOB, B., SPLINTER, J. & TAUCHER-SCHOLZ, G. 2009. Positional stability of damaged chromatin domains along radiation tracks in mammalian cells. *Radiat Res,* 171**,** 405-18.
JAKOVCEVIC, D., DEDIC-PLAVETIC, N., VRBANEC, D., JAKOVCEVIC, A. & JAKIC-RAZUMOVIC, J. 2015. Breast Cancer Molecular Subtypes and Oxidative DNA Damage. *Appl Immunohistochem Mol Morphol,* 23**,** 696-703.
JANG, N. Y., KIM, D. H., CHO, B. J., CHOI, E. J., LEE, J.-S., WU, H.-G., CHIE, E. K. & KIM, I. A. 2015. Radiosensitization with combined use of olaparib and PI-103 in triple-negative breast cancer. *BMC Cancer,* 15**,** 89.

JANSSENS, G. O., RADEMAKERS, S. E., TERHAARD, C. H., DOORNAERT, P. A., BIJL, H. P., VAN DEN ENDE, P.*, et al.* 2012. Accelerated radiotherapy with carbogen and nicotinamide for laryngeal cancer: results of a phase III randomized trial. *J Clin Oncol,* 30**,** 1777-83.

JATOI, I. & PROSCHAN, M. A. 2005. Randomized trials of breast-conserving therapy versus mastectomy for primary breast cancer: a pooled analysis of updated results. *Am J Clin Oncol,* 28**,** 289-94.

JEGGO, P. & LAVIN, M. F. 2009. Cellular radiosensitivity: how much better do we understand it? *Int J Radiat Biol,* 85**,** 1061-81.

JEGGO, P. A., GEUTING, V. & LOBRICH, M. 2011. The role of homologous recombination in radiation-induced double-strand break repair. *Radiother Oncol,* 101**,** 7-12.

JIANG, J., ZHAO, J. H., WANG, X. L., GUO, X. J., YANG, J., BAI, X., JIN, S. Y. & GE, R. L. 2015. Correlation between carbonic anhydrase IX (CA-9), XII (CA-12) and hypoxia inducible factor-2alpha (HIF-2alpha) in breast cancer. *Neoplasma,* 62**,** 456-63.

JIANG, X., LI, W., LI, X., BAI, H. & ZHANG, Z. 2019. Current status and future prospects of PARP inhibitor clinical trials in ovarian cancer. *Cancer management and research,* 11**,** 4371-4390.

JIANG, Y., VERBIEST, T., DEVERY, A. M., BOKOBZA, S. M., WEBER, A. M., LESZCZYNSKA, K. B., HAMMOND, E. M. & RYAN, A. J. 2016. Hypoxia Potentiates the Radiation-Sensitizing Effect of Olaparib in Human Non-Small Cell Lung Cancer Xenografts by Contextual Synthetic Lethality. *Int J Radiat Oncol Biol Phys,* 95**,** 772-81.

JIN, H., TU, D., ZHAO, N., SHEPHERD, L. E. & GOSS, P. E. 2012. Longer-term outcomes of letrozole versus placebo after 5 years of tamoxifen in the NCIC CTG MA.17 trial: analyses adjusting for treatment crossover. *J Clin Oncol,* 30**,** 718-21.

JIN, X. & MU, P. 2015. Targeting Breast Cancer Metastasis. *Breast cancer : basic and clinical research,* 9**,** 23-34.

JOINER, M. C. K., ALBERT 2009. *Quantifying cell kill and cell survival; ,* London.

JONES, M. E., SCHOEMAKER, M. J., WRIGHT, L. B., ASHWORTH, A. & SWERDLOW, A. J. 2017. Smoking and risk of breast cancer in the Generations Study cohort. *Breast Cancer Res,* 19**,** 118.

JONGEN, J. M. J., VAN DER WAALS, L. M., TRUMPI, K., LAOUKILI, J., PETERS, N. A., SCHENNING-VAN SCHELVEN, S. J., GOVAERT, K. M., BOREL RINKES, I. H. M. & KRANENBURG, O. 2017. Downregulation of DNA repair proteins and increased DNA damage in hypoxic colon cancer cells is a therapeutically exploitable vulnerability. *Oncotarget,* 8**,** 86296-86311.

JORDAN, B. F. & SONVEAUX, P. 2012. Targeting tumor perfusion and oxygenation to improve the outcome of anticancer therapy. *Front Pharmacol,* 3**,** 94.

JOY, O., MARIE-THÉRÈSE, R., BELINDA, S. H., KATHERINE, B.-S., MORITZ, V., HUA-LIN, W.*, et al.* 2015. *Spearman's correlation of histopathology/immunohistochemistry scoring*.

KAANDERS, J. H., BUSSINK, J. & VAN DER KOGEL, A. J. 2002. ARCON: a novel biology-based approach in radiotherapy. *Lancet Oncol,* 3**,** 728-37.

KADYK, L. C. & HARTWELL, L. H. 1992. Sister chromatids are preferred over homologs as substrates for recombinational repair in Saccharomyces cerevisiae. *Genetics,* 132**,** 387-402.

KAPAŁCZYŃSKA, M., KOLENDA, T., PRZYBYŁA, W., ZAJĄCZKOWSKA, M., TERESIAK, A., FILAS, V.*, et al.* 2018. 2D and 3D cell cultures - a comparison of different types of cancer cell cultures. *Archives of medical science : AMS,* 14**,** 910-919.

KARASAWA. K., F., M., SHOJI, Y., HORIMOTO,Y., INOUE, T. AND IMAI, T. 2014. Biological Effectiveness of Carbon-Ion Radiation on Various Human Breast Cancer Cell Lines. *Journal of Cell Science & Therapy*.

KARIRI, Y. A., JOSEPH, C., KUROZUMI, S., TOSS, M. S., ALSALEEM, M., RAAFAT, S.*, et al.* 2020. Prognostic significance of KN motif and ankyrin repeat domains 1 (KANK1) in invasive breast cancer. *Breast cancer research and treatment,* 179**,** 349-357.

KARLGREN, M., GOMEZ, A., STARK, K., SVARD, J., RODRIGUEZ-ANTONA, C., OLIW, E.*, et al.* 2006. Tumor-specific expression of the novel cytochrome P450 enzyme, CYP2W1. *Biochem Biophys Res Commun,* 341**,** 451-8.

KARLGREN, M. & INGELMAN-SUNDBERG, M. 2007. Tumour-specific expression of CYP2W1: its potential as a drug target in cancer therapy. *Expert Opin Ther Targets,* 11**,** 61-7.

KARLGREN, M., MIURA, S. & INGELMAN-SUNDBERG, M. 2005. Novel extrahepatic cytochrome P450s. *Toxicol Appl Pharmacol,* 207**,** 57-61.

KASHISHIAN, A., DOUANGPANYA, H., CLARK, D., SCHLACHTER, S. T., EARY, C. T., SCHIRO, J. G.*, et al.* 2003. DNA-dependent protein kinase inhibitors as drug candidates for the treatment of cancer. *Mol Cancer Ther,* 2**,** 1257-64.

KATO, Y., YASHIRO, M., FUYUHIRO, Y., KASHIWAGI, S., MATSUOKA, J., HIRAKAWA, T.*, et al.* 2011. Effects of acute and chronic hypoxia on the radiosensitivity of gastric and esophageal cancer cells. *Anticancer Res,* 31**,** 3369-75.

KAUER-DORNER, D. & BERGER, D. 2018. The Role of Brachytherapy in the Treatment of Breast Cancer. *Breast Care,* 13**,** 157-161.

KEDAR, P. S., STEFANICK, D. F., HORTON, J. K. & WILSON, S. H. 2008. Interaction between PARP-1 and ATR in mouse fibroblasts is blocked by PARP inhibition. *DNA Repair (Amst),* 7**,** 1787-98.

KEDERSHA, N. L., GUPTA, M., LI, W., MILLER, I. & ANDERSON, P. 1999. RNA-binding proteins TIA-1 and TIAR link the phosphorylation of eIF-2 alpha to the assembly of mammalian stress granules. *J Cell Biol,* 147**,** 1431-42.

KELSEY, J. L. & BERNSTEIN, L. 1996. Epidemiology and prevention of breast cancer. *Annu Rev Public Health,* 17**,** 47-67.

KENNECKE, H., YERUSHALMI, R., WOODS, R., CHEANG, M. C., VODUC, D., SPEERS, C. H., NIELSEN, T. O. & GELMON, K. 2010. Metastatic behavior of breast cancer subtypes. *J Clin Oncol,* 28**,** 3271-7.

KENNEDY, D. G., VAN DEN BERG, H. W., CLARKE, R. & MURPHY, R. F. 1985. The effect of the rate of cell proliferation on the synthesis of methotrexate poly-γ-glutamates in two human breast cancer cell lines. *Biochemical Pharmacology,* 34**,** 3087-3090.

KHAITAN, D., CHANDNA, S., ARYA, M. B. & DWARAKANATH, B. S. 2006. Establishment and characterization of multicellular spheroids from a human glioma cell line; Implications for tumor therapy. *J Transl Med,* 4**,** 12.

KIM, G., ISON, G., MCKEE, A. E., ZHANG, H., TANG, S., GWISE, T.*, et al.* 2015. FDA Approval Summary: Olaparib Monotherapy in Patients with Deleterious Germline BRCA-Mutated Advanced Ovarian Cancer Treated with Three or More Lines of Chemotherapy. *Clin Cancer Res,* 21**,** 4257-61.

KIM, J., HO, W. & WU, B. 2011. The Role of the 3D Environment in Hypoxia-induced Drug and Apoptosis Resistance. *Anticancer research,* 31**,** 3237-45.

KIM, J. B. 2005. Three-dimensional tissue culture models in cancer biology. *Semin Cancer Biol,* 15**,** 365-77.

KIM, K.-U., WILSON, S. M., ABAYASIRIWARDANA, K. S., COLLINS, R., FJELLBIRKELAND, L., XU, Z., JABLONS, D. M., NISHIMURA, S. L. & BROADDUS, V. C. 2005. A Novel In Vitro Model of Human Mesothelioma for Studying Tumor Biology and Apoptotic Resistance. *American Journal of Respiratory Cell and Molecular Biology,* 33**,** 541-548.

KIMBUNG, S., LOMAN, N. & HEDENFALK, I. 2015. Clinical and molecular complexity of breast cancer metastases. *Semin Cancer Biol,* 35**,** 85-95.

KINNER, A., WU, W., STAUDT, C. & ILIAKIS, G. 2008. Gamma-H2AX in recognition and signaling of DNA double-strand breaks in the context of chromatin. *Nucleic acids research,* 36**,** 5678-5694.

KINOSHITA, M., JOHNSON, D. L., SHATNEY, C. H., LEE, Y. L. & MOCHIZUKI, H. 2001. Cancer cells surviving hypoxia obtain hypoxia resistance and maintain anti-apoptotic potential under reoxygenation. *Int J Cancer,* 91**,** 322-6.

KLEPPA, L., MARI, P.-O., LARSEN, E., LIEN, G. F., GODON, C., THEIL, A. F.*, et al.* 2012. Kinetics of endogenous mouse FEN1 in base excision repair. *Nucleic Acids Research,* 40**,** 9044-9059.

KOBAYASHI, T., TADA, S., TSUYAMA, T., MUROFUSHI, H., SEKI, M. & ENOMOTO, T. 2002. Focus-formation of replication protein A, activation of checkpoint system and DNA repair synthesis induced by DNA double-strand breaks in Xenopus egg extract. *J Cell Sci,* 115**,** 3159-69.

KOH, J. & KIM, M. J. 2019. Introduction of a New Staging System of Breast Cancer for Radiologists: An Emphasis on the Prognostic Stage. *Korean journal of radiology,* 20**,** 69-82.

KOLLIAS, J., MURPHY, C. A., ELSTON, C. W., ELLIS, I. O., ROBERTSON, J. F. & BLAMEY, R. W. 1999. The prognosis of small primary breast cancers. *Eur J Cancer,* 35**,** 908-12.

KOMOIKE, Y., AKIYAMA, F., IINO, Y., IKEDA, T., TANAKA-AKASHI, S., OHSUMI, S.*, et al.* 2005. Analysis of ipsilateral breast tumor recurrences after breast-conserving treatment based on the classification of true recurrences and new primary tumors. *Breast Cancer,* 12**,** 104-11.

KORENMAN, S. G. 1980. Oestrogen window hypothesis of the aetiology of breast cancer. *Lancet,* 1**,** 700-1.

KORITZINSKY, M. & WOUTERS, B. G. 2013. The roles of reactive oxygen species and autophagy in mediating the tolerance of tumor cells to cycling hypoxia. *Semin Radiat Oncol,* 23**,** 252-61.

KOSHIJI, M., KAGEYAMA, Y., PETE, E. A., HORIKAWA, I., BARRETT, J. C. & HUANG, L. E. 2004. HIF-1alpha induces cell cycle arrest by functionally counteracting Myc. *Embo j,* 23**,** 1949-56.

KOUICHI, K., LUSHENG, Q., MIYUKI, S., MIKI, K., YUUKI, I., KOUSHO, W.*, et al.* 2018. *The FEN1 inhibitor, PTPD, reduces cccDNA production*.

KOUSSOUNADIS, A., LANGDON, S. P., UM, I. H., HARRISON, D. J. & SMITH, V. A. 2015. Relationship between differentially expressed mRNA and mRNA-protein correlations in a xenograft model system. *Scientific reports,* 5**,** 10775-10775.

KROKAN, H. E. & BJORAS, M. 2013. Base excision repair. *Cold Spring Harb Perspect Biol,* 5**,** a012583.

KUCHENBAECKER, K. B., HOPPER, J. L., BARNES, D. R., PHILLIPS, K. A., MOOIJ, T. M., ROOS-BLOM, M. J.*, et al.* 2017. Risks of Breast, Ovarian, and Contralateral Breast Cancer for BRCA1 and BRCA2 Mutation Carriers. *Jama,* 317**,** 2402-2416.

KUCHERLAPATI, M., YANG, K., KURAGUCHI, M., ZHAO, J., LIA, M., HEYER, J.*, et al.* 2002. Haploinsufficiency of Flap endonuclease (Fen1) leads to rapid tumor progression. *Proc Natl Acad Sci U S A,* 99**,** 9924-9.

KUMAR, H. & CHOI, D.-K. 2015. Hypoxia Inducible Factor Pathway and Physiological Adaptation: A Cell Survival Pathway? *Mediators of inflammation,* 2015**,** 584758-584758.

KUMARAKULASINGHAM, M., ROONEY, P. H., DUNDAS, S. R., TELFER, C., MELVIN, W. T., CURRAN, S. & MURRAY, G. I. 2005. Cytochrome p450 profile of colorectal cancer: identification of markers of prognosis. *Clin Cancer Res,* 11**,** 3758-65.

KUREBAYASHI, J., OTSUKI, T., MORIYA, T. & SONOO, H. 2001. Hypoxia reduces hormone responsiveness of human breast cancer cells. *Japanese journal of cancer research : Gann,* 92**,** 1093-1101.

KUROSAWA, A., KOYAMA, H., TAKAYAMA, S., MIKI, K., AYUSAWA, D., FUJII, M., IIIZUMI, S. & ADACHI, N. 2008. The requirement of Artemis in double-

strand break repair depends on the type of DNA damage. *DNA Cell Biol,* 27**,** 55-61.
KYNDI, M., SORENSEN, F. B., KNUDSEN, H., OVERGAARD, M., NIELSEN, H. M. & OVERGAARD, J. 2008. Estrogen receptor, progesterone receptor, HER-2, and response to postmastectomy radiotherapy in high-risk breast cancer: the Danish Breast Cancer Cooperative Group. *J Clin Oncol,* 26**,** 1419-26.
LA, D. K., UPTON, P. B. & SWENBERG, J. A. 2010. 14.05 - Carcinogenic Alkylating Agents*. *In:* MCQUEEN, C. A. (ed.) *Comprehensive Toxicology (Second Edition).* Oxford: Elsevier.
LA VECCHIA, C., GIORDANO, S. H., HORTOBAGYI, G. N. & CHABNER, B. 2011. Overweight, obesity, diabetes, and risk of breast cancer: interlocking pieces of the puzzle. *The oncologist,* 16**,** 726-729.
LAGADEC, C., DEKMEZIAN, C., BAUCHÉ, L. & PAJONK, F. 2012. Oxygen levels do not determine radiation survival of breast cancer stem cells. *PloS one,* 7**,** e34545-e34545.
LAKHANI, N. J., SARKAR, M. A., VENITZ, J. & FIGG, W. D. 2003. 2-Methoxyestradiol, a promising anticancer agent. *Pharmacotherapy,* 23**,** 165-72.
LAM, J. S., SELIGSON, D. B., YU, H., LI, A., EEVA, M., PANTUCK, A. J., ZENG, G., HORVATH, S. & BELLDEGRUN, A. S. 2006. Flap endonuclease 1 is overexpressed in prostate cancer and is associated with a high Gleason score. *BJU Int,* 98**,** 445-51.
LANGHANS, S. A. 2018. Three-Dimensional in Vitro Cell Culture Models in Drug Discovery and Drug Repositioning. *Frontiers in pharmacology,* 9**,** 6-6.
LANKELMA, J., DEKKER, H., LUQUE, F. R., LUYKX, S., HOEKMAN, K., VAN DER VALK, P., VAN DIEST, P. J. & PINEDO, H. M. 1999. Doxorubicin gradients in human breast cancer. *Clin Cancer Res,* 5**,** 1703-7.
LANZEN, J., BRAUN, R. D., KLITZMAN, B., BRIZEL, D., SECOMB, T. W. & DEWHIRST, M. W. 2006. Direct demonstration of instabilities in oxygen concentrations within the extravascular compartment of an experimental tumor. *Cancer Res,* 66**,** 2219-23.
LARSEN, E., GRAN, C., SAETHER, B. E., SEEBERG, E. & KLUNGLAND, A. 2003. Proliferation failure and gamma radiation sensitivity of Fen1 null mutant mice at the blastocyst stage. *Mol Cell Biol,* 23**,** 5346-53.
LE DOUSSAL, V., TUBIANA-HULIN, M., FRIEDMAN, S., HACENE, K., SPYRATOS, F. & BRUNET, M. 1989. Prognostic value of histologic grade nuclear components of Scarff-Bloom-Richardson (SBR). An improved score modification based on a multivariate analysis of 1262 invasive ductal breast carcinomas. *Cancer,* 64**,** 1914-21.
LE, Q. T., MOON, J., REDMAN, M., WILLIAMSON, S. K., LARA, P. N., JR., GOLDBERG, Z.*, et al.* 2009. Phase II study of tirapazamine, cisplatin, and etoposide and concurrent thoracic radiotherapy for limited-stage small-cell lung cancer: SWOG 0222. *J Clin Oncol,* 27**,** 3014-9.
LEE, A. H. & ELLIS, I. O. 2008. The Nottingham prognostic index for invasive carcinoma of the breast. *Pathol Oncol Res,* 14**,** 113-5.
LEE, A. T. J., POLLACK, S. M., HUANG, P. & JONES, R. L. 2017. Phase III Soft Tissue Sarcoma Trials: Success or Failure? *Current treatment options in oncology,* 18**,** 19-19.
LEE, B. I. & WILSON, D. M., 3RD 1999. The RAD2 domain of human exonuclease 1 exhibits 5' to 3' exonuclease and flap structure-specific endonuclease activities. *J Biol Chem,* 274**,** 37763-9.
LEE, J. H., KIM, K. H., MORIO, T. & KIM, H. 2006. Ataxia-telangiectasia-mutated-dependent activation of Ku in human fibroblasts exposed to hydrogen peroxide. *Ann N Y Acad Sci,* 1091**,** 76-82.
LEE, K. J., PIETT, C. G., ANDREWS, J. F., MANN, E., NAGEL, Z. D. & GASSMAN, N. R. 2019a. Defective base excision repair in the response to DNA damaging agents in triple negative breast cancer. *PloS one,* 14**,** e0223725-e0223725.

LEE, Y.-Y., CHO, Y.-J., SHIN, S.-W., CHOI, C., RYU, J.-Y., JEON, H.-K., *et al.* 2019b. Anti-Tumor Effects of Wee1 Kinase Inhibitor with Radiotherapy in Human Cervical Cancer. *Scientific Reports,* 9**,** 15394.

LEEK, R., GRIMES, D. R., HARRIS, A. L. & MCINTYRE, A. 2016. Methods: Using Three-Dimensional Culture (Spheroids) as an In Vitro Model of Tumour Hypoxia. *Adv Exp Med Biol,* 899**,** 167-96.

LEHMANN, B. D., BAUER, J. A., CHEN, X., SANDERS, M. E., CHAKRAVARTHY, A. B., SHYR, Y. & PIETENPOL, J. A. 2011. Identification of human triple-negative breast cancer subtypes and preclinical models for selection of targeted therapies. *J Clin Invest,* 121**,** 2750-67.

LEPORI, D. 2015. Inflammatory breast disease: The radiologist's role. *Diagnostic and Interventional Imaging,* 96**,** 1045-1064.

LESTER, S. C., BOSE, S., CHEN, Y. Y., CONNOLLY, J. L., DE BACA, M. E., FITZGIBBONS, P. L., *et al.* 2009. Protocol for the examination of specimens from patients with invasive carcinoma of the breast. *Arch Pathol Lab Med,* 133**,** 1515-38.

LESUEUR, P., CHEVALIER, F., AUSTRY, J.-B., WAISSI, W., BURCKEL, H., NOËL, G., HABRAND, J.-L., SAINTIGNY, Y. & JOLY, F. 2017. Poly-(ADP-ribose)-polymerase inhibitors as radiosensitizers: a systematic review of pre-clinical and clinical human studies. *Oncotarget,* 8**,** 69105-69124.

LEWIS PHILLIPS, G. D., LI, G., DUGGER, D. L., CROCKER, L. M., PARSONS, K. L., MAI, E., *et al.* 2008. Targeting HER2-positive breast cancer with trastuzumab-DM1, an antibody-cytotoxic drug conjugate. *Cancer Res,* 68**,** 9280-90.

LI, C. I., URIBE, D. J. & DALING, J. R. 2005. Clinical characteristics of different histologic types of breast cancer. *British journal of cancer,* 93**,** 1046-1052.

LI, H., SUN, X., MILLER, E., WANG, Q., TAO, P., LIU, L., *et al.* 2017. BMI, reproductive factors, and breast cancer molecular subtypes: A case-control study and meta-analysis. *J Epidemiol,* 27**,** 143-151.

LI, J., HE, F. & PEI, M. 2011. Creation of an in vitro microenvironment to enhance human fetal synovium-derived stem cell chondrogenesis. *Cell Tissue Res,* 345**,** 357-65.

LI, Y. & YANG, D. Q. 2010. The ATM inhibitor KU-55933 suppresses cell proliferation and induces apoptosis by blocking Akt in cancer cells with overactivated Akt. *Mol Cancer Ther,* 9**,** 113-25.

LIAPIS, V., LABRINIDIS, A., ZINONOS, I., HAY, S., PONOMAREV, V., PANAGOPOULOS, V., *et al.* 2015. Hypoxia-activated pro-drug TH-302 exhibits potent tumor suppressive activity and cooperates with chemotherapy against osteosarcoma. *Cancer Lett,* 357**,** 160-169.

LIAPIS, V., ZINONOS, I., LABRINIDIS, A., HAY, S., PONOMAREV, V., PANAGOPOULOS, V., *et al.* 2016. Anticancer efficacy of the hypoxia-activated prodrug evofosfamide (TH-302) in osteolytic breast cancer murine models. *Cancer Med,* 5**,** 534-45.

LIEBER, M. R. 1997. The FEN-1 family of structure-specific nucleases in eukaryotic DNA replication, recombination and repair. *Bioessays,* 19**,** 233-40.

LIEBER, M. R. 2010. The mechanism of double-strand DNA break repair by the nonhomologous DNA end-joining pathway. *Annu Rev Biochem,* 79**,** 181-211.

LIEDTKE, C., MAZOUNI, C., HESS, K. R., ANDRE, F., TORDAI, A., MEJIA, J. A., *et al.* 2008. Response to neoadjuvant therapy and long-term survival in patients with triple-negative breast cancer. *J Clin Oncol,* 26**,** 1275-81.

LIN, A. & MAITY, A. 2015. Molecular Pathways: A Novel Approach to Targeting Hypoxia and Improving Radiotherapy Efficacy via Reduction in Oxygen Demand. *Clinical cancer research : an official journal of the American Association for Cancer Research,* 21**,** 1995-2000.

LINDSTROM, A., MIDTBO, K., ARNESSON, L. G., GARVIN, S. & SHABO, I. 2017. Fusion between M2-macrophages and cancer cells results in a

subpopulation of radioresistant cells with enhanced DNA-repair capacity. *Oncotarget,* 8**,** 51370-51386.
LISTGARTEN, J., DAMARAJU, S., POULIN, B., COOK, L., DUFOUR, J., DRIGA, A.*, et al.* 2004. Predictive Models for Breast Cancer Susceptibility from Multiple Single Nucleotide Polymorphisms. *Clinical Cancer Research,* 10**,** 2725-2737.
LIU, K., ZHANG, W., DAI, Z., WANG, M., TIAN, T., LIU, X.*, et al.* 2018. Association between body mass index and breast cancer risk: evidence based on a dose-response meta-analysis. *Cancer management and research,* 10**,** 143-151.
LIU, P., QIAN, L., SUNG, J. S., DE SOUZA-PINTO, N. C., ZHENG, L., BOGENHAGEN, D. F.*, et al.* 2008a. Removal of oxidative DNA damage via FEN1-dependent long-patch base excision repair in human cell mitochondria. *Mol Cell Biol,* 28**,** 4975-87.
LIU, S. K., COACKLEY, C., KRAUSE, M., JALALI, F., CHAN, N. & BRISTOW, R. G. 2008b. A novel poly(ADP-ribose) polymerase inhibitor, ABT-888, radiosensitizes malignant human cell lines under hypoxia. *Radiother Oncol,* 88**,** 258-68.
LIU, Y., BEARD, W. A., SHOCK, D. D., PRASAD, R., HOU, E. W. & WILSON, S. H. 2005. DNA polymerase beta and flap endonuclease 1 enzymatic specificities sustain DNA synthesis for long patch base excision repair. *J Biol Chem,* 280**,** 3665-74.
LIU, Y., BEYER, A. & AEBERSOLD, R. 2016. On the Dependency of Cellular Protein Levels on mRNA Abundance. *Cell,* 165**,** 535-550.
LIU, Y., KAO, H. I. & BAMBARA, R. A. 2004. Flap endonuclease 1: a central component of DNA metabolism. *Annu Rev Biochem,* 73**,** 589-615.
LOI, S., SOTIRIOU, C., HAIBE-KAINS, B., LALLEMAND, F., CONUS, N. M., PICCART, M. J., SPEED, T. P. & MCARTHUR, G. A. 2009. Gene expression profiling identifies activated growth factor signaling in poor prognosis (Luminal-B) estrogen receptor positive breast cancer. *BMC Med Genomics,* 2**,** 37.
LOMAX, M. E., FOLKES, L. K. & O'NEILL, P. 2013. Biological consequences of radiation-induced DNA damage: relevance to radiotherapy. *Clin Oncol (R Coll Radiol),* 25**,** 578-85.
LORD, S. J., MARINOVICH, M. L., PATTERSON, J. A., WILCKEN, N., KIELY, B. E., GEBSKI, V.*, et al.* 2012. Incidence of metastatic breast cancer in an Australian population-based cohort of women with non-metastatic breast cancer at diagnosis. *Med J Aust,* 196**,** 688-92.
LOSER, D. A., SHIBATA, A., SHIBATA, A. K., WOODBINE, L. J., JEGGO, P. A. & CHALMERS, A. J. 2010. Sensitization to radiation and alkylating agents by inhibitors of poly(ADP-ribose) polymerase is enhanced in cells deficient in DNA double-strand break repair. *Mol Cancer Ther,* 9**,** 1775-87.
LOWERY, A. J., KELL, M. R., GLYNN, R. W., KERIN, M. J. & SWEENEY, K. J. 2012. Locoregional recurrence after breast cancer surgery: a systematic review by receptor phenotype. *Breast Cancer Res Treat,* 133**,** 831-41.
LUM, D. H., MATSEN, C., WELM, A. L. & WELM, B. E. 2012. Overview of human primary tumorgraft models: comparisons with traditional oncology preclinical models and the clinical relevance and utility of primary tumorgrafts in basic and translational oncology research. *Current protocols in pharmacology,* Chapter 14**,** Unit14.22-14.22.
LV, Y., ZHAO, S., HAN, J., ZHENG, L., YANG, Z. & ZHAO, L. 2015. Hypoxia-inducible factor-1α induces multidrug resistance protein in colon cancer. *OncoTargets and therapy,* 8**,** 1941-1948.
MA, W., HALWEG, C. J., MENENDEZ, D. & RESNICK, M. A. 2012. Differential effects of poly(ADP-ribose) polymerase inhibition on DNA break repair in human cells are revealed with Epstein–Barr virus. *Proceedings of the National Academy of Sciences,* 109**,** 6590-6595.

MAASS, K. F., KULKARNI, C., QUADIR, M. A., HAMMOND, P. T., BETTS, A. M. & WITTRUP, K. D. 2015. A Flow Cytometric Clonogenic Assay Reveals the Single-Cell Potency of Doxorubicin. *Journal of pharmaceutical sciences,* 104**,** 4409-4416.

MACMAHON, B., COLE, P., LIN, T. M., LOWE, C. R., MIRRA, A. P., RAVNIHAR, B., SALBER, E. J., VALAORAS, V. G. & YUASA, S. 1970. Age at first birth and breast cancer risk. *Bull World Health Organ,* 43**,** 209-21.

MADANAYAKE, T. W., FIDLER, T. P., FRESQUEZ, T. M., BAJAJ, N. & ROWLAND, A. M. 2012. Cytochrome P450 2S1 depletion enhances cell proliferation and migration in bronchial epithelial cells, in part, through modulation of prostaglandin E(2) synthesis. *Drug metabolism and disposition: the biological fate of chemicals,* 40**,** 2119-2125.

MAHANEY, B. L., MEEK, K. & LEES-MILLER, S. P. 2009. Repair of ionizing radiation-induced DNA double-strand breaks by non-homologous end-joining. *Biochem J,* 417**,** 639-50.

MALHOTRA, G. K., ZHAO, X., BAND, H. & BAND, V. 2010. Histological, molecular and functional subtypes of breast cancers. *Cancer biology & therapy,* 10**,** 955-960.

MANDILARAS, V., BOUGANIM, N., SPAYNE, J., DENT, R., ARNAOUT, A., BOILEAU, J. F., BRACKSTONE, M., METERISSIAN, S. & CLEMONS, M. 2015. Concurrent chemoradiotherapy for locally advanced breast cancer-time for a new paradigm? *Curr Oncol,* 22**,** 25-32.

MANLEY, E., JR. & WAXMAN, D. J. 2013. Impact of tumor blood flow modulation on tumor sensitivity to the bioreductive drug banoxantrone. *J Pharmacol Exp Ther,* 344**,** 368-77.

MAO, X., MCMANAWAY, S., JAISWAL, J. K., HONG, C. R., WILSON, W. R. & HICKS, K. O. 2019. Schedule-dependent potentiation of chemotherapy drugs by the hypoxia-activated prodrug SN30000. *Cancer Biol Ther,* 20**,** 1258-1269.

MAO, X., MCMANAWAY, S., JAISWAL, J. K., PATEL, P. B., WILSON, W. R., HICKS, K. O. & BOGLE, G. 2018. An agent-based model for drug-radiation interactions in the tumour microenvironment: Hypoxia-activated prodrug SN30000 in multicellular tumour spheroids. *PLoS Comput Biol,* 14**,** e1006469.

MARECHAL, A. & ZOU, L. 2015. RPA-coated single-stranded DNA as a platform for post-translational modifications in the DNA damage response. *Cell Res,* 25**,** 9-23.

MARTIN, T. A. & JIANG, W. G. 2009. Loss of tight junction barrier function and its role in cancer metastasis. *Biochimica et Biophysica Acta (BBA) - Biomembranes,* 1788**,** 872-891.

MASAOKA, A., GASSMAN, N. R., HORTON, J. K., KEDAR, P. S., WITT, K. L., HOBBS, C. A.*, et al.* 2013. Interaction between DNA Polymerase beta and BRCA1. *PLoS One,* 8**,** e66801.

MATTHEWS, J. H., MEEKER, B. E. & CHAPMAN, J. D. 1989. Response of human tumor cell lines in vitro to fractionated irradiation. *Int J Radiat Oncol Biol Phys,* 16**,** 133-8.

MAYER, R., HAMILTON-FARRELL, M. R., VAN DER KLEIJ, A. J., SCHMUTZ, J., GRANSTROM, G., SICKO, Z.*, et al.* 2005. Hyperbaric oxygen and radiotherapy. *Strahlenther Onkol,* 181**,** 113-23.

MCCLENDON, A. K. & OSHEROFF, N. 2007. DNA topoisomerase II, genotoxicity, and cancer. *Mutation research,* 623**,** 83-97.

MCDONNELL, A. M. & DANG, C. H. 2013. Basic review of the cytochrome p450 system. *Journal of the advanced practitioner in oncology,* 4**,** 263-268.

MCERLANE, V., YAKKUNDI, A., MCCARTHY, H. O., HUGHES, C. M., PATTERSON, L. H., HIRST, D. G., ROBSON, T. & MCKEOWN, S. R. 2005. A cytochrome P450 2B6 meditated gene therapy strategy to enhance the effects of radiation or cyclophosphamide when combined with the bioreductive drug AQ4N. *J Gene Med,* 7**,** 851-9.

MCGOWAN, D. R., SKWARSKI, M., BRADLEY, K. M., CAMPO, L., FENWICK, J. D., GLEESON, F. V.*, et al.* 2019. Buparlisib with thoracic radiotherapy and its effect on tumour hypoxia: A phase I study in patients with advanced non-small cell lung carcinoma. *Eur J Cancer,* 113**,** 87-95.

MCINTYRE, A., PATIAR, S., WIGFIELD, S., LI, J. L., LEDAKI, I., TURLEY, H.*, et al.* 2012. Carbonic anhydrase IX promotes tumor growth and necrosis in vivo and inhibition enhances anti-VEGF therapy. *Clin Cancer Res,* 18**,** 3100-11.

MCKEAGE, M. J., JAMESON, M. B., RAMANATHAN, R. K., RAJENDRAN, J., GU, Y., WILSON, W. R., MELINK, T. J. & TCHEKMEDYIAN, N. S. 2012. PR-104 a bioreductive pre-prodrug combined with gemcitabine or docetaxel in a phase Ib study of patients with advanced solid tumours. *BMC Cancer,* 12**,** 496.

MCKENNA, D. J., ERRINGTON, R. & PORS, K. 2018. Current challenges and opportunities in treating hypoxic prostate tumors. *J Cancer Metastasis Treat* 4:11.

MCKEOWN, S. R. 2014. Defining normoxia, physoxia and hypoxia in tumours-implications for treatment response. *The British journal of radiology,* 87**,** 20130676-20130676.

MCKEOWN, S. R., COWEN, R. L. & WILLIAMS, K. J. 2007. Bioreductive drugs: from concept to clinic. *Clin Oncol (R Coll Radiol),* 19**,** 427-42.

MCKEOWN, S. R., FRIERY, O. P., MCINTYRE, I. A., HEJMADI, M. V., PATTERSON, L. H. & HIRST, D. G. 1996. Evidence for a therapeutic gain when AQ4N or tirapazamine is combined with radiation. *Br J Cancer Suppl,* 27**,** S39-42.

MCKEOWN, S. R., HEJMADI, M. V., MCINTYRE, I. A., MCALEER, J. J. & PATTERSON, L. H. 1995. AQ4N: an alkylaminoanthraquinone N-oxide showing bioreductive potential and positive interaction with radiation in vivo. *British journal of cancer,* 72**,** 76-81.

MCSHANE, L. M., ALTMAN, D. G., SAUERBREI, W., TAUBE, S. E., GION, M., CLARK, G. M. & STATISTICS SUBCOMMITTEE OF THE, N. C. I. E. W. G. O. C. D. 2005. REporting recommendations for tumour MARKer prognostic studies (REMARK). *British journal of cancer,* 93**,** 387-391.

MCTIERNAN, A. 2003. Behavioral risk factors in breast cancer: can risk be modified? *Oncologist,* 8**,** 326-34.

MEDINA, D., KITTRELL, F. S., TSIMELZON, A. & FUQUA, S. A. 2007. Inhibition of mammary tumorigenesis by estrogen and progesterone in genetically engineered mice. *Ernst Schering Found Symp Proc***,** 109-26.

MEDRI, L., VOLPI, A., NANNI, O., VECCI, A. M., MANGIA, A., SCHITTULLI, F.*, et al.* 2003. Prognostic relevance of mitotic activity in patients with node-negative breast cancer. *Mod Pathol,* 16**,** 1067-75.

MEHIBEL, M., SINGH, S., CHINJE, E. C., COWEN, R. L. & STRATFORD, I. J. 2009. Effects of cytokine-induced macrophages on the response of tumor cells to banoxantrone (AQ4N). *Mol Cancer Ther,* 8**,** 1261-9.

MEHIBEL, M., SINGH, S., COWEN, R. L., WILLIAMS, K. J. & STRATFORD, I. J. 2016. Radiation enhances the therapeutic effect of Banoxantrone in hypoxic tumour cells with elevated levels of nitric oxide synthase. *Oncol Rep,* 35**,** 1925-32.

MEHRGOU, A. & AKOUCHEKIAN, M. 2016. The importance of BRCA1 and BRCA2 genes mutations in breast cancer development. *Medical journal of the Islamic Republic of Iran,* 30**,** 369-369.

MEHTA, G., HSIAO, A. Y., INGRAM, M., LUKER, G. D. & TAKAYAMA, S. 2012. Opportunities and challenges for use of tumor spheroids as models to test drug delivery and efficacy. *J Control Release,* 164**,** 192-204.

MEHTA, M., BASALINGAPPA, K., GRIFFITH, J. N., ANDRADE, D., BABU, A., AMREDDY, N.*, et al.* 2016. HuR silencing elicits oxidative stress and DNA damage and sensitizes human triple-negative breast cancer cells to radiotherapy. *Oncotarget,* 7**,** 64820-64835.

MEIBOHM, B. & DERENDORF, H. 1997. Basic concepts of pharmacokinetic/pharmacodynamic (PK/PD) modeling. *International journal of clinical pharmacology and therapeutics,* 35**,** 401-13.
MEIJER, T. W., KAANDERS, J. H., SPAN, P. N. & BUSSINK, J. 2012. Targeting hypoxia, HIF-1, and tumor glucose metabolism to improve radiotherapy efficacy. *Clin Cancer Res,* 18**,** 5585-94.
MENEAR, K. A., ADCOCK, C., BOULTER, R., COCKCROFT, X. L., COPSEY, L., CRANSTON, A.*, et al.* 2008. 4-[3-(4-cyclopropanecarbonylpiperazine-1-carbonyl)-4-fluorobenzyl]-2H-phthalazin- 1-one: a novel bioavailable inhibitor of poly(ADP-ribose) polymerase-1. *J Med Chem,* 51**,** 6581-91.
MENG, F., EVANS, J. W., BHUPATHI, D., BANICA, M., LAN, L., LORENTE, G.*, et al.* 2012. Molecular and cellular pharmacology of the hypoxia-activated prodrug TH-302. *Mol Cancer Ther,* 11**,** 740-51.
MENGWASSER, K. E., ADEYEMI, R. O., LENG, Y., CHOI, M. Y., CLAIRMONT, C., D'ANDREA, A. D. & ELLEDGE, S. J. 2019. Genetic Screens Reveal FEN1 and APEX2 as BRCA2 Synthetic Lethal Targets. *Mol Cell,* 73**,** 885-899.e6.
METSÄLÄ, O., KREUTZER, J., HÖGEL, H., MIIKKULAINEN, P., KALLIO, P. & JAAKKOLA, P. M. 2018. Transportable system enabling multiple irradiation studies under simultaneous hypoxia in vitro. *Radiation Oncology,* 13**,** 220.
MICHMERHUIZEN, A. R., PESCH, A. M., MOUBADDER, L., CHANDLER, B. C., WILDER-ROMANS, K., CAMERON, M.*, et al.* 2019. PARP1 Inhibition Radiosensitizes Models of Inflammatory Breast Cancer to Ionizing Radiation. *Molecular Cancer Therapeutics***,** molcanther.0520.2019.
MILLER, V. A., NG, K. K., GRANT, S. C., KINDLER, H., PIZZO, B., HEELAN, R. T., VON ROEMELING, R. & KRIS, M. G. 1997. Phase II study of the combination of the novel bioreductive agent, tirapazamine, with cisplatin in patients with advanced non-small-cell lung cancer. *Ann Oncol,* 8**,** 1269-71.
MILLIGAN, J. R., AGUILERA, J. A., NGUYEN, T. T., PAGLINAWAN, R. A. & WARD, J. F. 2000. DNA strand-break yields after post-irradiation incubation with base excision repair endonucleases implicate hydroxyl radical pairs in double-strand break formation. *Int J Radiat Biol,* 76**,** 1475-83.
MILOTTI, E., STELLA, S. & CHIGNOLA, R. 2017. Pulsation-limited oxygen diffusion in the tumour microenvironment. *Sci Rep,* 7**,** 39762.
MIN, S. Y., LEE, S. J., SHIN, K. H., PARK, I. H., JUNG, S. Y., LEE, K. S.*, et al.* 2011. Locoregional recurrence of breast cancer in patients treated with breast conservation surgery and radiotherapy following neoadjuvant chemotherapy. *Int J Radiat Oncol Biol Phys,* 81**,** e697-705.
MISTRY, I. N., THOMAS, M., CALDER, E. D. D., CONWAY, S. J. & HAMMOND, E. M. 2017. Clinical Advances of Hypoxia-Activated Prodrugs in Combination With Radiation Therapy. *Int J Radiat Oncol Biol Phys,* 98**,** 1183-1196.
MIYOSHI, Y., ANDO, A., TAKAMURA, Y., TAGUCHI, T., TAMAKI, Y. & NOGUCHI, S. 2002. Prediction of response to docetaxel by CYP3A4 mRNA expression in breast cancer tissues. *Int J Cancer,* 97**,** 129-32.
MIYOSHI, Y., TAGUCHI, T., KIM, S. J., TAMAKI, Y. & NOGUCHI, S. 2005. Prediction of response to docetaxel by immunohistochemical analysis of CYP3A4 expression in human breast cancers. *Breast Cancer,* 12**,** 11-5.
MLADENOV, E., MAGIN, S., SONI, A. & ILIAKIS, G. 2013. DNA double-strand break repair as determinant of cellular radiosensitivity to killing and target in radiation therapy. *Front Oncol,* 3**,** 113.
MODUGNO, F., KNOLL, C., KANBOUR-SHAKIR, A. & ROMKES, M. 2003. A potential role for the estrogen-metabolizing cytochrome P450 enzymes in human breast carcinogenesis. *Breast Cancer Res Treat,* 82**,** 191-7.
MOELLER, B. J., CAO, Y., LI, C. Y. & DEWHIRST, M. W. 2004. Radiation activates HIF-1 to regulate vascular radiosensitivity in tumors: role of reoxygenation, free radicals, and stress granules. *Cancer Cell,* 5**,** 429-41.
MOELLER, B. J. & DEWHIRST, M. W. 2006. HIF-1 and tumour radiosensitivity. *Br J Cancer,* 95**,** 1-5.

MOGGS, J. G., MURPHY, T. C., LIM, F. L., MOORE, D. J., STUCKEY, R., ANTROBUS, K., KIMBER, I. & ORPHANIDES, G. 2005. Anti-proliferative effect of estrogen in breast cancer cells that re-express ERalpha is mediated by aberrant regulation of cell cycle genes. *J Mol Endocrinol,* 34**,** 535-51.

MOHAMMED, R. A. A., MARTIN, S. G., MAHMMOD, A. M., MACMILLAN, R. D., GREEN, A. R., PAISH, E. C. & ELLIS, I. O. 2011. Objective assessment of lymphatic and blood vascular invasion in lymph node-negative breast carcinoma: findings from a large case series with long-term follow-up. *The Journal of Pathology,* 223**,** 358-365.

MOLINA-ORTIZ, D., CAMACHO-CARRANZA, R., GONZÁLEZ-ZAMORA, J. F., SHALKOW-KALINCOVSTEIN, J., CÁRDENAS-CARDÓS, R., NOSTÍ-PALACIOS, R. & VENCES-MEJÍA, A. 2014. Differential expression of cytochrome P450 enzymes in normal and tumor tissues from childhood rhabdomyosarcoma. *PloS one,* 9**,** e93261-e93261.

MONGAN, N. P. & GUDAS, L. J. 2007. Diverse actions of retinoid receptors in cancer prevention and treatment. *Differentiation,* 75**,** 853-70.

MUELLER-KLIESER, W., FREYER, J. P. & SUTHERLAND, R. M. 1986. Influence of glucose and oxygen supply conditions on the oxygenation of multicellular spheroids. *British journal of cancer,* 53**,** 345-353.

MUKHERJEE, A., HUBER, K., EVANS, H., LAKHANI, N. & MARTIN, S. 2007. A cellular and molecular investigation of the action of PMX464, a putative thioredoxin inhibitor, in normal and colorectal cancer cell lines. *Br J Pharmacol,* 151**,** 1167-75.

MUNSHI, A. H., M. MEYN, R. E. 2005. Clonogenic cell survival assay. *Methods Mol Med,* 110**,** 21-8.

MURANTE, R. S., RUMBAUGH, J. A., BARNES, C. J., NORTON, J. R. & BAMBARA, R. A. 1996. Calf RTH-1 nuclease can remove the initiator RNAs of Okazaki fragments by endonuclease activity. *J Biol Chem,* 271**,** 25888-97.

MUREDDA, M., NUNOYA, K., BURTCH-WRIGHT, R. A., KURZ, E. U., COLE, S. P. & DEELEY, R. G. 2003. Cloning and Characterization of the Murine and Rat mrp1 Promoter Regions. *Mol Pharmacol,* 64**,** 1259-69.

MURRAY, G. I. 2000. The role of cytochrome P450 in tumour development and progression and its potential in therapy. *J Pathol,* 192**,** 419-26.

MURRAY, G. I., PATIMALLA, S., STEWART, K. N., MILLER, I. D. & HEYS, S. D. 2010. Profiling the expression of cytochrome P450 in breast cancer. *Histopathology,* 57**,** 202-211.

MURRAY, G. I., TAYLOR, M. C., MCFADYEN, M. C. E., MCKAY, J. A., GREENLEE, W. F., BURKE, M. D. & MELVIN, W. T. 1997. Tumor-specific Expression of Cytochrome P450 CYP1B1. *Cancer Research,* 57**,** 3026-3031.

MUSKHELISHVILI, L., THOMPSON, P. A., KUSEWITT, D. F., WANG, C. & KADLUBAR, F. F. 2001. In situ hybridization and immunohistochemical analysis of cytochrome P450 1B1 expression in human normal tissues. *J Histochem Cytochem,* 49**,** 229-36.

MUSS, H. B., THOR, A. D., BERRY, D. A., KUTE, T., LIU, E. T., KOERNER, F.*, et al.* 1994. c-erbB-2 expression and response to adjuvant therapy in women with node-positive early breast cancer. *N Engl J Med,* 330**,** 1260-6.

MUSTACCHI, G., BIGANZOLI, L., PRONZATO, P., MONTEMURRO, F., DAMBROSIO, M., MINELLI, M., MOLTENI, L. & SCALTRITI, L. 2015. HER2-positive metastatic breast cancer: a changing scenario. *Crit Rev Oncol Hematol,* 95**,** 78-87.

NAKAMURA, A., SEDELNIKOVA, O. A., REDON, C., PILCH, D. R., SINOGEEVA, N. I., SHROFF, R., LICHTEN, M. & BONNER, W. M. 2006. Techniques for gamma-H2AX detection. *Methods Enzymol,* 409**,** 236-50.

NAKAMURA, J., PURVIS, E. R. & SWENBERG, J. A. 2003. Micromolar concentrations of hydrogen peroxide induce oxidative DNA lesions more efficiently than millimolar concentrations in mammalian cells. *Nucleic Acids Res,* 31**,** 1790-5.

NAKAMURA, N., KAWAMORI, J., TAKAHASHI, O., SHIKAMA, N., SEKIGUCHI, K., TAKAHASHI, T.*, et al.* 2018. Palliative radiotherapy for breast cancer patients with skin invasion: a multi-institutional prospective observational study. *Japanese Journal of Clinical Oncology,* 48**,** 555-558.

NAM, E. A. & CORTEZ, D. 2011. ATR signalling: more than meeting at the fork. *The Biochemical journal,* 436**,** 527-536.

NAMIKI, Y. & ZOU, L. 2006. ATRIP associates with replication protein A-coated ssDNA through multiple interactions. *Proceedings of the National Academy of Sciences of the United States of America,* 103**,** 580-585.

NARDULLI, A. M. & KATZENELLENBOGEN, B. S. 1988. Progesterone receptor regulation in T47D human breast cancer cells: analysis by density labeling of progesterone receptor synthesis and degradation and their modulation by progestin. *Endocrinology,* 122**,** 1532-40.

NAROD, S. A., TUNG, N., LUBINSKI, J., HUZARSKI, T., ROBSON, M., LYNCH, H. T.*, et al.* 2014. A prior diagnosis of breast cancer is a risk factor for breast cancer in BRCA1 and BRCA2 carriers. *Current oncology (Toronto, Ont.),* 21**,** 64-68.

NEMEIKAITĖ-ČĖNIENĖ, A., ŠARLAUSKAS, J., JONUŠIENĖ, V., MAROZIENĖ, A., MISEVIČIENĖ, L., YANTSEVICH, A. V. & ČĖNAS, N. 2019. Kinetics of Flavoenzyme-Catalyzed Reduction of Tirapazamine Derivatives: Implications for Their Prooxidant Cytotoxicity. *International journal of molecular sciences,* 20**,** 4602.

NESBITT, H., BYRNE, N. M., WILLIAMS, S. N., MING, L., WORTHINGTON, J., ERRINGTON, R. J.*, et al.* 2017a. Targeting Hypoxic Prostate Tumors Using the Novel Hypoxia-Activated Prodrug OCT1002 Inhibits Expression of Genes Associated with Malignant Progression. *Clin Cancer Res,* 23**,** 1797-1808.

NESBITT, H., WORTHINGTON, J., ERRINGTON, R. J., PATTERSON, L. H., SMITH, P. J., MCKEOWN, S. R. & MCKENNA, D. J. 2017b. The unidirectional hypoxia-activated prodrug OCT1002 inhibits growth and vascular development in castrate-resistant prostate tumors. *Prostate,* 77**,** 1539-1547.

NEVE, R. M., CHIN, K., FRIDLYAND, J., YEH, J., BAEHNER, F. L., FEVR, T.*, et al.* 2006. A collection of breast cancer cell lines for the study of functionally distinct cancer subtypes. *Cancer Cell,* 10**,** 515-27.

NGUYEN, P. L., TAGHIAN, A. G., KATZ, M. S., NIEMIERKO, A., ABI RAAD, R. F., BOON, W. L.*, et al.* 2008. Breast cancer subtype approximated by estrogen receptor, progesterone receptor, and HER-2 is associated with local and distant recurrence after breast-conserving therapy. *J Clin Oncol,* 26**,** 2373-8.

NICE. 2018. *Clinical Guidelines for Early and locally advanced breast cancer: diagnosis and management* [Online]. London: National Institute for Health and Care Excellence (UK)

Available: https://www.nice.org.uk/guidance/ng101 [Accessed 25 November 2019].

NIEMANS, R., YAROMINA, A., THEYS, J., MARCUS, D., ASHOORZADEH, A., ABBATTISTA, M.*, et al.* 2018. EP-2327: Hypoxic cell killing by CP-506, a novel hypoxia-activated prodrug. *Radiotherapy and Oncology,* 127**,** S1283-S1284.

NIKJOO, H., UEHARA, S., WILSON, W. E., HOSHI, M. & GOODHEAD, D. T. 1998. Track structure in radiation biology: theory and applications. *Int J Radiat Biol,* 73**,** 355-64.

NISHIDA, C. R., LEE, M. & DE MONTELLANO, P. R. 2010. Efficient hypoxic activation of the anticancer agent AQ4N by CYP2S1 and CYP2W1. *Mol Pharmacol,* 78**,** 497-502.

NISHIDA, C. R. & ORTIZ DE MONTELLANO, P. R. 2008. Reductive Heme-Dependent Activation of the N-Oxide Prodrug AQ4N by Nitric Oxide Synthase. *Journal of Medicinal Chemistry,* 51**,** 5118-5120.
NISHIMURA, R., OSAKO, T., OKUMURA, Y., HAYASHI, M., TOYOZUMI, Y. & ARIMA, N. 2010. Ki-67 as a prognostic marker according to breast cancer subtype and a predictor of recurrence time in primary breast cancer. *Exp Ther Med,* 1**,** 747-754.
NIWA, T., MURAYAMA, N., IMAGAWA, Y. & YAMAZAKI, H. 2015. Regioselective hydroxylation of steroid hormones by human cytochromes P450. *Drug Metab Rev,* 47**,** 89-110.
NIXON, A. J., NEUBERG, D., HAYES, D. F., GELMAN, R., CONNOLLY, J. L., SCHNITT, S.*, et al.* 1994. Relationship of patient age to pathologic features of the tumor and prognosis for patients with stage I or II breast cancer. *Journal of Clinical Oncology,* 12**,** 888-894.
NOEL, G., GODON, C., FERNET, M., GIOCANTI, N., MEGNIN-CHANET, F. & FAVAUDON, V. 2006. Radiosensitization by the poly(ADP-ribose) polymerase inhibitor 4-amino-1,8-naphthalimide is specific of the S phase of the cell cycle and involves arrest of DNA synthesis. *Mol Cancer Ther,* 5**,** 564-74.
NOTTE, A., NINANE, N., ARNOULD, T. & MICHIELS, C. 2013. Hypoxia counteracts taxol-induced apoptosis in MDA-MB-231 breast cancer cells: role of autophagy and JNK activation. *Cell Death Dis,* 4**,** e638.
NUNES, A. S., BARROS, A. S., COSTA, E. C., MOREIRA, A. F. & CORREIA, I. J. 2019. 3D tumor spheroids as in vitro models to mimic in vivo human solid tumors resistance to therapeutic drugs. *Biotechnology and Bioengineering,* 116**,** 206-226.
NYSTROM, L., ANDERSSON, I., BJURSTAM, N., FRISELL, J., NORDENSKJOLD, B. & RUTQVIST, L. E. 2002. Long-term effects of mammography screening: updated overview of the Swedish randomised trials. *Lancet,* 359**,** 909-19.
O'CONNOR, L. J., CAZARES-KORNER, C., SAHA, J., EVANS, C. N., STRATFORD, M. R., HAMMOND, E. M. & CONWAY, S. J. 2016. Design, synthesis and evaluation of molecularly targeted hypoxia-activated prodrugs. *Nat Protoc,* 11**,** 781-94.
O'SHAUGHNESSY, J. 2005. Extending survival with chemotherapy in metastatic breast cancer. *Oncologist,* 10 Suppl 3**,** 20-9.
OLIVE, P. L., AQUINO-PARSONS, C., MACPHAIL, S. H., LIAO, S. Y., RALEIGH, J. A., LERMAN, M. I. & STANBRIDGE, E. J. 2001. Carbonic anhydrase 9 as an endogenous marker for hypoxic cells in cervical cancer. *Cancer Res,* 61**,** 8924-9.
OLIVE, P. L., VIKSE, C. & TROTTER, M. J. 1992. Measurement of oxygen diffusion distance in tumor cubes using a fluorescent hypoxia probe. *Int J Radiat Oncol Biol Phys,* 22**,** 397-402.
OLIVOTTO, I. A., BAJDIK, C. D., RAVDIN, P. M., SPEERS, C. H., COLDMAN, A. J., NORRIS, B. D., DAVIS, G. J., CHIA, S. K. & GELMON, K. A. 2005. Population-based validation of the prognostic model ADJUVANT! for early breast cancer. *J Clin Oncol,* 23**,** 2716-25.
ONS. 2019. *Cancer survival by stage at diagnosis for England* [Online]. Available: https://www.ons.gov.uk/peoplepopulationandcommunity/healthandsocialcare/conditionsanddiseases/datasets/cancersurvivalratescancersurvivalinenglandadultsdiagnosed [Accessed 7 January 2020].
OPLUSTIL O'CONNOR, L., RULTEN, S. L., CRANSTON, A. N., ODEDRA, R., BROWN, H., JASPERS, J. E.*, et al.* 2016. The PARP Inhibitor AZD2461 Provides Insights into the Role of PARP3 Inhibition for Both Synthetic Lethality and Tolerability with Chemotherapy in Preclinical Models. *Cancer Res,* 76**,** 6084-6094.
ORAIOPOULOU, M. E., TZAMALI, E., TZEDAKIS, G., VAKIS, A., PAPAMATHEAKIS, J. & SAKKALIS, V. 2017. In Vitro/In Silico Study on the Role of Doubling

Time Heterogeneity among Primary Glioblastoma Cell Lines. *BioMed research international,* 2017**,** 8569328-8569328.
ORONSKY, B. T., KNOX, S. J. & SCICINSKI, J. 2011. Six degrees of separation: the oxygen effect in the development of radiosensitizers. *Translational oncology,* 4**,** 189-198.
ORTMANN, B., DRUKER, J. & ROCHA, S. 2014. Cell cycle progression in response to oxygen levels. *Cellular and molecular life sciences : CMLS,* 71**,** 3569-3582.
OTAKE, S. & GOTO, T. 2019. Stereotactic Radiotherapy for Oligometastasis. *Cancers,* 11**,** 133.
OVERGAARD, J. 2007. Hypoxic radiosensitization: adored and ignored. *J Clin Oncol,* 25**,** 4066-74.
OVERGAARD, J. & HORSMAN, M. R. 1996. Modification of hypoxia-induced radioresistance in tumors by the use of oxygen and sensitizers. *Seminars in Radiation Oncology,* 6**,** 10-21.
OVERGAARD, J., SAND HANSEN, H., OVERGAARD, M., BASTHOLT, L., BERTHELSEN, A., SPECHT, L., LINDELØV, B. & JØRGENSEN, K. 1998. A randomized double-blind phase III study of nimorazole as a hypoxic radiosensitizer of primary radiotherapy in supraglottic larynx and pharynx carcinoma. Results of the Danish Head and Neck Cancer Study (DAHANCA) Protocol 5-85. *Radiotherapy and Oncology,* 46**,** 135-146.
PAIK, S., BRYANT, J., PARK, C., FISHER, B., TAN-CHIU, E., HYAMS, D.*, et al.* 1998. erbB-2 and response to doxorubicin in patients with axillary lymph node-positive, hormone receptor-negative breast cancer. *J Natl Cancer Inst,* 90**,** 1361-70.
PAIK, S., SHAK, S., TANG, G., KIM, C., BAKER, J., CRONIN, M.*, et al.* 2004. A multigene assay to predict recurrence of tamoxifen-treated, node-negative breast cancer. *N Engl J Med,* 351**,** 2817-26.
PALCIC, B. & SKARSGARD, L. D. 1984. Reduced oxygen enhancement ratio at low doses of ionizing radiation. *Radiat Res,* 100**,** 328-39.
PAMPALONI, F., REYNAUD, E. G. & STELZER, E. H. 2007. The third dimension bridges the gap between cell culture and live tissue. *Nat Rev Mol Cell Biol,* 8**,** 839-45.
PAPADOPOULOS, K. P., GOEL, S., BEERAM, M., WONG, A., DESAI, K., HAIGENTZ, M.*, et al.* 2008. A Phase 1 Open-Label, Accelerated Dose-Escalation Study of the Hypoxia-Activated Prodrug AQ4N in Patients with Advanced Malignancies. *Clinical Cancer Research,* 14**,** 7110-7115.
PAPANDREOU, I., KRISHNA, C., KAPER, F., CAI, D., GIACCIA, A. J. & DENKO, N. C. 2005. Anoxia is necessary for tumor cell toxicity caused by a low-oxygen environment. *Cancer Res,* 65**,** 3171-8.
PARDO, B., GOMEZ-GONZALEZ, B. & AGUILERA, A. 2009. DNA repair in mammalian cells: DNA double-strand break repair: how to fix a broken relationship. *Cell Mol Life Sci,* 66**,** 1039-56.
PARK, H. J., BAE, J. S., KIM, K. M., MOON, Y. J., PARK, S.-H., HA, S. H.*, et al.* 2018. The PARP inhibitor olaparib potentiates the effect of the DNA damaging agent doxorubicin in osteosarcoma. *Journal of Experimental & Clinical Cancer Research,* 37**,** 107.
PARK, S.-Y., CHOI, J.-H. & NAM, J.-S. 2019. Targeting Cancer Stem Cells in Triple-Negative Breast Cancer. *Cancers,* 11**,** 965.
PARSELS, L. A., KARNAK, D., PARSELS, J. D., ZHANG, Q., VELEZ-PADILLA, J., REICHERT, Z. R.*, et al.* 2018. PARP1 Trapping and DNA Replication Stress Enhance Radiosensitization with Combined WEE1 and PARP Inhibitors. *Mol Cancer Res,* 16**,** 222-232.
PARTRIDGE, A. H., HUGHES, M. E., WARNER, E. T., OTTESEN, R. A., WONG, Y. N., EDGE, S. B.*, et al.* 2016. Subtype-Dependent Relationship Between Young Age at Diagnosis and Breast Cancer Survival. *J Clin Oncol,* 34**,** 3308-14.

PASCUCCI, B., STUCKI, M., JONSSON, Z. O., DOGLIOTTI, E. & HUBSCHER, U. 1999. Long patch base excision repair with purified human proteins. DNA ligase I as patch size mediator for DNA polymerases delta and epsilon. *J Biol Chem,* 274**,** 33696-702.

PASTOREKOVA, S. & GILLIES, R. J. 2019. The role of carbonic anhydrase IX in cancer development: links to hypoxia, acidosis, and beyond. *Cancer and Metastasis Reviews,* 38**,** 65-77.

PATEL, K. J. & TANNOCK, I. F. 2009. The influence of P-glycoprotein expression and its inhibitors on the distribution of doxorubicin in breast tumors. *BMC cancer,* 9**,** 356-356.

PATTERSON, A. V., FERRY, D. M., EDMUNDS, S. J., GU, Y., SINGLETON, R. S., PATEL, K.*, et al.* 2007. Mechanism of action and preclinical antitumor activity of the novel hypoxia-activated DNA cross-linking agent PR-104. *Clin Cancer Res,* 13**,** 3922-32.

PATTERSON, A. V., ROBERTSON, N., HOULBROOK, S., STEPHENS, M. A., ADAMS, G. E., HARRIS, A. L., STRATFORD, I. J. & CARMICHAEL, J. 1994. The role of DT-diaphorase in determining the sensitivity of human tumor cells to tirapazamine (SR 4233). *Int J Radiat Oncol Biol Phys,* 29**,** 369-72.

PATTERSON, L. H. 1993. Rationale for the use of aliphatic N-oxides of cytotoxic anthraquinones as prodrug DNA binding agents: a new class of bioreductive agent. *Cancer and Metastasis Reviews,* 12**,** 119-134.

PATTERSON, L. H. 2002. Bioreductively activated antitumor N-oxides: the case of AQ4N, a unique approach to hypoxia-activated cancer chemotherapy. *Drug Metab Rev,* 34**,** 581-92.

PATTERSON, L. H. & MCKEOWN, S. R. 2000. AQ4N: a new approach to hypoxia-activated cancer chemotherapy. *British journal of cancer,* 83**,** 1589-1593.

PATTERSON, L. H., MCKEOWN, S. R., RUPARELIA, K., DOUBLE, J. A., BIBBY, M. C., COLE, S. & STRATFORD, I. J. 2000. Enhancement of chemotherapy and radiotherapy of murine tumours by AQ4N, a bioreductively activated anti-tumour agent. *Br J Cancer,* 82**,** 1984-90.

PAULL, T. T., ROGAKOU, E. P., YAMAZAKI, V., KIRCHGESSNER, C. U., GELLERT, M. & BONNER, W. M. 2000. A critical role for histone H2AX in recruitment of repair factors to nuclear foci after DNA damage. *Curr Biol,* 10**,** 886-95.

PEEKEN, J. C., VAUPEL, P. & COMBS, S. E. 2017. Integrating Hyperthermia into Modern Radiation Oncology: What Evidence Is Necessary? *Frontiers in oncology,* 7**,** 132-132.

PELKONEN, O. & RAUNIO, H. 1997. Metabolic activation of toxins: tissue-specific expression and metabolism in target organs. *Environ Health Perspect,* 105 Suppl 4**,** 767-74.

PEREIRA, H., PINDER, S. E., SIBBERING, D. M., GALEA, M. H., ELSTON, C. W., BLAMEY, R. W., ROBERTSON, J. F. & ELLIS, I. O. 1995. Pathological prognostic factors in breast cancer. IV: Should you be a typer or a grader? A comparative study of two histological prognostic features in operable breast carcinoma. *Histopathology,* 27**,** 219-26.

PEROU, C. M. 2011. Molecular stratification of triple-negative breast cancers. *Oncologist,* 16 Suppl 1**,** 61-70.

PEROU, C. M., SORLIE, T., EISEN, M. B., VAN DE RIJN, M., JEFFREY, S. S., REES, C. A.*, et al.* 2000. Molecular portraits of human breast tumours. *Nature,* 406**,** 747-52.

PETO, R., DAVIES, C., GODWIN, J., GRAY, R., PAN, H. C., CLARKE, M.*, et al.* 2012. Comparisons between different polychemotherapy regimens for early breast cancer: meta-analyses of long-term outcome among 100,000 women in 123 randomised trials. *Lancet,* 379**,** 432-44.

PHILLIPS, R. M. 2016. Targeting the hypoxic fraction of tumours using hypoxia-activated prodrugs. *Cancer Chemother Pharmacol,* 77**,** 441-57.

PHILLIPS, R. M., HENDRIKS, H. R. & PETERS, G. J. 2013. EO9 (Apaziquone): from the clinic to the laboratory and back again. *Br J Pharmacol,* 168**,** 11-8.

PICCART-GEBHART, M. J., PROCTER, M., LEYLAND-JONES, B., GOLDHIRSCH, A., UNTCH, M., SMITH, I., *et al.* 2005. Trastuzumab after adjuvant chemotherapy in HER2-positive breast cancer. *N Engl J Med,* 353**,** 1659-72.

PICON-RUIZ, M., MORATA-TARIFA, C., VALLE-GOFFIN, J. J., FRIEDMAN, E. R. & SLINGERLAND, J. M. 2017. Obesity and adverse breast cancer risk and outcome: Mechanistic insights and strategies for intervention. *CA: a cancer journal for clinicians,* 67**,** 378-397.

PIERCE, A., MCGOWAN, P. M., COTTER, M., MULLOOLY, M., O'DONOVAN, N., RANI, S., O'DRISCOLL, L., CROWN, J. & DUFFY, M. J. 2013. Comparative antiproliferative effects of iniparib and olaparib on a panel of triple-negative and non-triple-negative breast cancer cell lines. *Cancer biology & therapy,* 14**,** 537-545.

PINTO, M., PRISE, K. M. & MICHAEL, B. D. 2005. Evidence for complexity at the nanometer scale of radiation-induced DNA DSBs as a determinant of rejoining kinetics. *Radiat Res,* 164**,** 73-85.

PLUMB, J. A. & WORKMAN, P. 1994. Unusually marked hypoxic sensitization to indoloquinone EO9 and mitomycin C in a human colon-tumour cell line that lacks DT-diaphorase activity. *Int J Cancer,* 56**,** 134-9.

POLESZCZUK, J., LUDDY, K., CHEN, L., LEE, J. K., HARRISON, L. B., CZERNIECKI, B. J., SOLIMAN, H. & ENDERLING, H. 2017. Neoadjuvant radiotherapy of early-stage breast cancer and long-term disease-free survival. *Breast Cancer Research,* 19**,** 75.

POMMIER, Y., O'CONNOR, M. J. & DE BONO, J. 2016. Laying a trap to kill cancer cells: PARP inhibitors and their mechanisms of action. *Sci Transl Med,* 8**,** 362ps17.

POMP, J., WIKE, J. L., OUWERKERK, I. J., HOOGSTRATEN, C., DAVELAAR, J., SCHRIER, P. I., LEER, J. W., THAMES, H. D. & BROCK, W. A. 1996. Cell density dependent plating efficiency affects outcome and interpretation of colony forming assays. *Radiother Oncol,* 40**,** 121-5.

POTTER, C. & HARRIS, A. L. 2004. Hypoxia inducible carbonic anhydrase IX, marker of tumour hypoxia, survival pathway and therapy target. *Cell Cycle,* 3**,** 164-7.

PRASAD, C. B., PRASAD, S. B., YADAV, S. S., PANDEY, L. K., SINGH, S., PRADHAN, S. & NARAYAN, G. 2017. Olaparib modulates DNA repair efficiency, sensitizes cervical cancer cells to cisplatin and exhibits anti-metastatic property. *Scientific reports,* 7**,** 12876-12876.

PRAT, A., CAREY, L. A., ADAMO, B., VIDAL, M., TABERNERO, J., CORTES, J., PARKER, J. S., PEROU, C. M. & BASELGA, J. 2014. Molecular features and survival outcomes of the intrinsic subtypes within HER2-positive breast cancer. *J Natl Cancer Inst,* 106.

PRAT, A. & PEROU, C. M. 2011. Deconstructing the molecular portraits of breast cancer. *Mol Oncol,* 5**,** 5-23.

PREDICT, N. 2011. *NHS Breast cancer Predict* [Online]. Available: https://breast.predict.nhs.uk/ [Accessed 26 Nov 2019 2019].

PRGOMET, Z., ANDERSSON, T. & LINDBERG, P. 2017. Optimization, validation, and identification of two reliable antibodies for immunodetection of WNT5A. *Biotechnic & Histochemistry,* 92**,** 46-58.

PRISE, K. M., DAVIES, S. & MICHAEL, B. D. 1993. Evidence for induction of DNA double-strand breaks at paired radical sites. *Radiat Res,* 134**,** 102-6.

PUCK, T. T. & MARCUS, P. I. 1955. A RAPID METHOD FOR VIABLE CELL TITRATION AND CLONE PRODUCTION WITH HELA CELLS IN TISSUE CULTURE: THE USE OF X-IRRADIATED CELLS TO SUPPLY CONDITIONING FACTORS. *Proc Natl Acad Sci U S A,* 41**,** 432-7.

PUCK, T. T. & MARCUS, P. I. 1956. Action of x-rays on mammalian cells. *J Exp Med,* 103**,** 653-66.

PURI, R., PALIT, V., LOADMAN, P. M., FLANNIGAN, M., SHAH, T., CHOUDRY, G. A.*, et al.* 2006. Phase I/II pilot study of intravesical apaziquone (EO9) for superficial bladder cancer. *J Urol,* 176**,** 1344-8.

QIAN, C., LI, M., SUI, J., REN, T., LI, Z., ZHANG, L., ZHOU, L., CHENG, Y. & WANG, D. 2014. Identification of a novel potential antitumor activity of gossypol as an APE1/Ref-1 inhibitor. *Drug design, development and therapy,* 8**,** 485-496.

QU, Y., HAN, B., YU, Y., YAO, W., BOSE, S., KARLAN, B. Y., GIULIANO, A. E. & CUI, X. 2015. Evaluation of MCF10A as a Reliable Model for Normal Human Mammary Epithelial Cells. *PLoS One,* 10**,** e0131285.

RAFEHI, H., ORLOWSKI, C., GEORGIADIS, G. T., VERVERIS, K., EL-OSTA, A. & KARAGIANNIS, T. C. 2011. Clonogenic assay: adherent cells. *Journal of visualized experiments : JoVE***,** 2573.

RAINEY, M. D., CHARLTON, M. E., STANTON, R. V. & KASTAN, M. B. 2008. Transient inhibition of ATM kinase is sufficient to enhance cellular sensitivity to ionizing radiation. *Cancer research,* 68**,** 7466-7474.

RAKHA, E. A., EL-SAYED, M. E., GREEN, A. R., PAISH, E. C., POWE, D. G., GEE, J.*, et al.* 2007. Biologic and clinical characteristics of breast cancer with single hormone receptor positive phenotype. *J Clin Oncol,* 25**,** 4772-8.

RAKHA, E. A., EL-SAYED, M. E., LEE, A. H., ELSTON, C. W., GRAINGE, M. J., HODI, Z., BLAMEY, R. W. & ELLIS, I. O. 2008. Prognostic significance of Nottingham histologic grade in invasive breast carcinoma. *J Clin Oncol,* 26**,** 3153-8.

RAKHA, E. A., REIS-FILHO, J. S., BAEHNER, F., DABBS, D. J., DECKER, T., EUSEBI, V.*, et al.* 2010. Breast cancer prognostic classification in the molecular era: the role of histological grade. *Breast Cancer Res,* 12**,** 207.

RAKHA, E. A., SORIA, D., GREEN, A. R., LEMETRE, C., POWE, D. G., NOLAN, C. C., GARIBALDI, J. M., BALL, G. & ELLIS, I. O. 2014. Nottingham Prognostic Index Plus (NPI+): a modern clinical decision making tool in breast cancer. *Br J Cancer,* 110**,** 1688-97.

RALEIGH, D. R. & HAAS-KOGAN, D. A. 2013. Molecular targets and mechanisms of radiosensitization using DNA damage response pathways. *Future oncology (London, England),* 9**,** 219-233.

RALEIGH, S. M., WANOGHO, E., BURKE, M. D., MCKEOWN, S. R. & PATTERSON, L. H. 1998. Involvement of human cytochromes P450 (CYP) in the reductive metabolism of AQ4N, a hypoxia activated anthraquinone di-N-oxide prodrug. *Int J Radiat Oncol Biol Phys,* 42**,** 763-7.

RAMÓN Y CAJAL, T., ALTÉS, A., PARÉ, L., DEL RIO, E., ALONSO, C., BARNADAS, A. & BAIGET, M. 2010. Impact of CYP2D6 polymorphisms in tamoxifen adjuvant breast cancer treatment. *Breast Cancer Res Treat,* 119**,** 33-8.

RANKIN, E. B., NAM, J. M. & GIACCIA, A. J. 2016. Hypoxia: Signaling the Metastatic Cascade. *Trends Cancer,* 2**,** 295-304.

RAVDIN, P. M., GREEN, S., DORR, T. M., MCGUIRE, W. L., FABIAN, C., PUGH, R. P.*, et al.* 1992. Prognostic significance of progesterone receptor levels in estrogen receptor-positive patients with metastatic breast cancer treated with tamoxifen: results of a prospective Southwest Oncology Group study. *J Clin Oncol,* 10**,** 1284-91.

RAVIRAJ, J., BOKKASAM, V. K., KUMAR, V. S., REDDY, U. S. & SUMAN, V. 2014. Radiosensitizers, radioprotectors, and radiation mitigators. *Indian J Dent Res,* 25**,** 83-90.

REA, D., FRANCIS, A., HANBY, A. M., SPEIRS, V., RAKHA, E., SHAABAN, A.*, et al.* 2015. Inflammatory breast cancer: time to standardise diagnosis assessment and management, and for the joining of forces to facilitate effective research. *British Journal of Cancer,* 112**,** 1613-1615.

REAPER, P. M., GRIFFITHS, M. R., LONG, J. M., CHARRIER, J. D., MACCORMICK, S., CHARLTON, P. A., GOLEC, J. M. & POLLARD, J. R. 2011. Selective killing

of ATM- or p53-deficient cancer cells through inhibition of ATR. *Nat Chem Biol,* 7**,** 428-30.
REBBECK, T. R., COUCH, F. J., KANT, J., CALZONE, K., DESHANO, M., PENG, Y., CHEN, K., GARBER, J. E. & WEBER, B. L. 1996. Genetic heterogeneity in hereditary breast cancer: role of BRCA1 and BRCA2. *Am J Hum Genet,* 59**,** 547-53.
REINBOLT, R. E., MANGINI, N., HILL, J. L., LEVINE, L. B., DEMPSEY, J. L., SINGARAVELU, J., KOEHLER, K. A., TALLEY, A. & LUSTBERG, M. B. 2015. Endocrine therapy in breast cancer: the neoadjuvant, adjuvant, and metastatic approach. *Semin Oncol Nurs,* 31**,** 146-55.
RICHARDSON, R. B. & HARPER, M. E. 2016. Mitochondrial stress controls the radiosensitivity of the oxygen effect: Implications for radiotherapy. *Oncotarget,* 7**,** 21469-83.
RIFFLE, S. & HEGDE, R. S. 2017. Modeling tumor cell adaptations to hypoxia in multicellular tumor spheroids. *J Exp Clin Cancer Res,* 36**,** 102.
RIFFLE, S., PANDEY, R. N., ALBERT, M. & HEGDE, R. S. 2017. Linking hypoxia, DNA damage and proliferation in multicellular tumor spheroids. *BMC cancer,* 17**,** 338-338.
RISCHIN, D., HICKS, R. J., FISHER, R., BINNS, D., CORRY, J., PORCEDDU, S. & PETERS, L. J. 2006. Prognostic significance of [18F]-misonidazole positron emission tomography-detected tumor hypoxia in patients with advanced head and neck cancer randomly assigned to chemoradiation with or without tirapazamine: a substudy of Trans-Tasman Radiation Oncology Group Study 98.02. *J Clin Oncol,* 24**,** 2098-104.
RISCHIN, D., PETERS, L. J., O'SULLIVAN, B., GIRALT, J., FISHER, R., YUEN, K.*, et al.* 2010. Tirapazamine, cisplatin, and radiation versus cisplatin and radiation for advanced squamous cell carcinoma of the head and neck (TROG 02.02, HeadSTART): a phase III trial of the Trans-Tasman Radiation Oncology Group. *J Clin Oncol,* 28**,** 2989-95.
RITTE, R., TIKK, K., LUKANOVA, A., TJONNELAND, A., OLSEN, A., OVERVAD, K.*, et al.* 2013. Reproductive factors and risk of hormone receptor positive and negative breast cancer: a cohort study. *BMC Cancer,* 13**,** 584.
RIVERA, S. P., WANG, F., SAARIKOSKI, S. T., TAYLOR, R. T., CHAPMAN, B., ZHANG, R. & HANKINSON, O. 2007. A novel promoter element containing multiple overlapping xenobiotic and hypoxia response elements mediates induction of cytochrome P4502S1 by both dioxin and hypoxia. *J Biol Chem,* 282**,** 10881-93.
ROBERTSON, A. B., KLUNGLAND, A., ROGNES, T. & LEIROS, I. 2009. DNA repair in mammalian cells: Base excision repair: the long and short of it. *Cell Mol Life Sci,* 66**,** 981-93.
ROBERTSON, F. M., BONDY, M., YANG, W., YAMAUCHI, H., WIGGINS, S., KAMRUDIN, S.*, et al.* 2010. Inflammatory breast cancer: the disease, the biology, the treatment. *CA Cancer J Clin,* 60**,** 351-75.
ROBERTSON, N., HAIGH, A., ADAMS, G. E. & STRATFORD, I. J. 1994. Factors affecting sensitivity to EO9 in rodent and human tumour cells in vitro: DT-diaphorase activity and hypoxia. *Eur J Cancer,* 30a**,** 1013-9.
ROBSON, M., IM, S. A., SENKUS, E., XU, B., DOMCHEK, S. M., MASUDA, N.*, et al.* 2017. Olaparib for Metastatic Breast Cancer in Patients with a Germline BRCA Mutation. *N Engl J Med,* 377**,** 523-533.
ROCKWELL, S., DOBRUCKI, I. T., KIM, E. Y., MARRISON, S. T. & VU, V. T. 2009. Hypoxia and radiation therapy: past history, ongoing research, and future promise. *Curr Mol Med,* 9**,** 442-58.
RODRIGUEZ, M. & POTTER, D. A. 2013. CYP1A1 regulates breast cancer proliferation and survival. *Molecular cancer research : MCR,* 11**,** 780-792.
ROFSTAD, E. K. 2000. Microenvironment-induced cancer metastasis. *Int J Radiat Biol,* 76**,** 589-605.

ROGAKOU, E. P., PILCH, D. R., ORR, A. H., IVANOVA, V. S. & BONNER, W. M. 1998. DNA double-stranded breaks induce histone H2AX phosphorylation on serine 139. *J Biol Chem,* 273**,** 5858-68.
ROJAS, K. & STUCKEY, A. 2016. Breast Cancer Epidemiology and Risk Factors. *Clin Obstet Gynecol,* 59**,** 651-672.
RONCHI, C. L., SBIERA, S., VOLANTE, M., STEINHAUER, S., SCOTT-WILD, V., ALTIERI, B.*, et al.* 2014. CYP2W1 is highly expressed in adrenal glands and is positively associated with the response to mitotane in adrenocortical carcinoma. *PloS one,* 9**,** e105855-e105855.
ROOTS, R. & SMITH, K. C. 1974. On the nature of the oxygen effect on x-ray-induced DNA single-strand breaks in mammalian cells. *Int J Radiat Biol Relat Stud Phys Chem Med,* 26**,** 467-80.
ROSEN, P. P., GROSHEN, S., KINNE, D. W. & NORTON, L. 1993. Factors influencing prognosis in node-negative breast carcinoma: analysis of 767 T1N0M0/T2N0M0 patients with long-term follow-up. *J Clin Oncol,* 11**,** 2090-100.
ROSS, J. S. & FLETCHER, J. A. 1998. The HER-2/neu oncogene in breast cancer: prognostic factor, predictive factor, and target for therapy. *Stem Cells,* 16**,** 413-28.
ROY, R., CHUN, J. & POWELL, S. N. 2011. BRCA1 and BRCA2: different roles in a common pathway of genome protection. *Nature reviews. Cancer,* 12**,** 68-78.
RUBOVSZKY, G. & HORVATH, Z. 2017. Recent Advances in the Neoadjuvant Treatment of Breast Cancer. *J Breast Cancer,* 20**,** 119-131.
RUGO, H. S., OLOPADE, O. I., DEMICHELE, A., YAU, C., VAN 'T VEER, L. J., BUXTON, M. B.*, et al.* 2016. Adaptive Randomization of Veliparib-Carboplatin Treatment in Breast Cancer. *The New England journal of medicine,* 375**,** 23-34.
RUNDQVIST, H. & JOHNSON, R. S. 2013. Tumour oxygenation: implications for breast cancer prognosis. *J Intern Med,* 274**,** 105-12.
RUSSO, J., HASAN LAREEF, M., BALOGH, G., GUO, S. & RUSSO, I. H. 2003. Estrogen and its metabolites are carcinogenic agents in human breast epithelial cells. *J Steroid Biochem Mol Biol,* 87**,** 1-25.
RYU, Y. J., KANG, S. J., CHO, J. S., YOON, J. H. & PARK, M. H. 2018. Lymphovascular invasion can be better than pathologic complete response to predict prognosis in breast cancer treated with neoadjuvant chemotherapy. *Medicine,* 97**,** e11647-e11647.
SAARIKOSKI, S. T., RIVERA, S. P., HANKINSON, O. & HUSGAFVEL-PURSIAINEN, K. 2005a. CYP2S1: a short review. *Toxicol Appl Pharmacol,* 207**,** 62-9.
SAARIKOSKI, S. T., WIKMAN, H. A., SMITH, G., WOLFF, C. H. & HUSGAFVEL-PURSIAINEN, K. 2005b. Localization of cytochrome P450 CYP2S1 expression in human tissues by in situ hybridization and immunohistochemistry. *J Histochem Cytochem,* 53**,** 549-56.
SAIDY, B., RAKHA, E. A., GREEN, A. R., ELLIS, I. O., MARTIN, S. G. & STORR, S. J. 2020. Retrospective assessment of cyclin-dependent kinase 5 mRNA and protein expression and its association with patient survival in breast cancer. *Journal of Cellular and Molecular Medicine,* 24**,** 6263-6271.
SALCEDA, J., FERNÁNDEZ, X. & ROCA, J. 2006. Topoisomerase II, not topoisomerase I, is the proficient relaxase of nucleosomal DNA. *The EMBO journal,* 25**,** 2575-2583.
SARRIO, D., RODRIGUEZ-PINILLA, S. M., HARDISSON, D., CANO, A., MORENO-BUENO, G. & PALACIOS, J. 2008. Epithelial-mesenchymal transition in breast cancer relates to the basal-like phenotype. *Cancer Res,* 68**,** 989-97.
SARTORI, A. A., LUKAS, C., COATES, J., MISTRIK, M., FU, S., BARTEK, J., BAER, R., LUKAS, J. & JACKSON, S. P. 2007. Human CtIP promotes DNA end resection. *Nature,* 450**,** 509-14.

SCANLON, S. E. & GLAZER, P. M. 2015. Multifaceted control of DNA repair pathways by the hypoxic tumor microenvironment. *DNA Repair (Amst),* 32**,** 180-189.
SCHMID, T. E., DOLLINGER, G., BEISKER, W., HABLE, V., GREUBEL, C., AUER, S.*, et al.* 2010. Differences in the kinetics of γ-H2AX fluorescence decay after exposure to low and high LET radiation. *International Journal of Radiation Biology,* 86**,** 682-691.
SCHMIDT, M., GEHRMANN, M., HENGSTLER, J. G. & KOELBL, H. 2010. New prognostic and predictive factors in breast cancer. *Minerva Ginecol,* 62**,** 599-611.
SCHMIDT, M., SCHOLZ, C. J., POLEDNIK, C. & ROLLER, J. 2016. Spheroid-based 3-dimensional culture models: Gene expression and functionality in head and neck cancer. *Oncol Rep,* 35**,** 2431-40.
SCHROTH, W., ANTONIADOU, L., FRITZ, P., SCHWAB, M., MUERDTER, T., ZANGER, U. M., SIMON, W., EICHELBAUM, M. & BRAUCH, H. 2007. Breast cancer treatment outcome with adjuvant tamoxifen relative to patient CYP2D6 and CYP2C19 genotypes. *J Clin Oncol,* 25**,** 5187-93.
SCOTT, S. P. & PANDITA, T. K. 2006. The Cellular Control of DNA Double-Strand Breaks. *Journal of cellular biochemistry,* 99**,** 1463-1475.
SEBENS, S. & SCHAFER, H. 2012. The tumor stroma as mediator of drug resistance--a potential target to improve cancer therapy? *Curr Pharm Biotechnol,* 13**,** 2259-72.
SEMENZA, G. L. 2003. Targeting HIF-1 for cancer therapy. *Nat Rev Cancer,* 3**,** 721-32.
SEMENZA, G. L. 2010. Defining the role of hypoxia-inducible factor 1 in cancer biology and therapeutics. *Oncogene,* 29**,** 625-634.
SEMENZA, G. L. 2012. Hypoxia-inducible factors in physiology and medicine. *Cell,* 148**,** 399-408.
SEMENZA, G. L. 2016. The hypoxic tumor microenvironment: A driving force for breast cancer progression. *Biochimica et biophysica acta,* 1863**,** 382-391.
SENKUS, E., KYRIAKIDES, S., OHNO, S., PENAULT-LLORCA, F., POORTMANS, P., RUTGERS, E., ZACKRISSON, S. & CARDOSO, F. 2015. Primary breast cancer: ESMO Clinical Practice Guidelines for diagnosis, treatment and follow-up. *Ann Oncol,* 26 Suppl 5**,** v8-30.
SERMEUS, A., GENIN, M., MAINCENT, A., FRANSOLET, M., NOTTE, A., LECLERE, L., RIQUIER, H., ARNOULD, T. & MICHIELS, C. 2012. Hypoxia-induced modulation of apoptosis and BCL-2 family proteins in different cancer cell types. *PloS one,* 7**,** e47519-e47519.
SHAH, R., ROSSO, K. & NATHANSON, S. D. 2014. Pathogenesis, prevention, diagnosis and treatment of breast cancer. *World journal of clinical oncology,* 5**,** 283-298.
SHAO, N., SHI, Y., YU, L., YE, R., SHAN, Z., ZHANG, Z., ZHANG, Y. & LIN, Y. 2019. Prospect for Application of PARP Inhibitor in Patients with HER2 Negative Breast Cancer. *International journal of biological sciences,* 15**,** 962-972.
SHARBEEN, G., MCCARROLL, J., GOLDSTEIN, D. & PHILLIPS, P. A. 2015. Exploiting base excision repair to improve therapeutic approaches for pancreatic cancer. *Frontiers in nutrition,* 2**,** 10-10.
SHARMA, A., ARAMBULA, J. F., KOO, S., KUMAR, R., SINGH, H., SESSLER, J. L. & KIM, J. S. 2019. Hypoxia-targeted drug delivery. *Chemical Society Reviews,* 48**,** 771-813.
SHARMA, A., SINGH, K. & ALMASAN, A. 2012. Histone H2AX phosphorylation: a marker for DNA damage. *Methods Mol Biol,* 920**,** 613-26.
SHAW, P. M., HOSEA, N. A., THOMPSON, D. V., LENIUS, J. M. & GUENGERICH, F. P. 1997. Reconstitution premixes for assays using purified recombinant human cytochrome P450, NADPH-cytochrome P450 reductase, and cytochrome b5. *Arch Biochem Biophys,* 348**,** 107-15.

SHEN, B., SINGH, P., LIU, R., QIU, J., ZHENG, L., FINGER, L. D. & ALAS, S. 2005. Multiple but dissectible functions of FEN-1 nucleases in nucleic acid processing, genome stability and diseases. *Bioessays,* 27**,** 717-29.
SHENG, H., SHAO, J., WASHINGTON, M. K. & DUBOIS, R. N. 2001. Prostaglandin E2 increases growth and motility of colorectal carcinoma cells. *J Biol Chem,* 276**,** 18075-81.
SHILOH, Y. 2001. ATM and ATR: networking cellular responses to DNA damage. *Curr Opin Genet Dev,* 11**,** 71-7.
SHIMADA, T., HAYES, C. L., YAMAZAKI, H., AMIN, S., HECHT, S. S., GUENGERICH, F. P. & SUTTER, T. R. 1996. Activation of Chemically Diverse Procarcinogens by Human Cytochrome P-450 1B1. *Cancer Research,* 56**,** 2979-2984.
SIEGEL, R. L., MILLER, K. D. & JEMAL, A. 2018. Cancer statistics, 2018. *CA Cancer J Clin,* 68**,** 7-30.
SIGLIN, J., CHAMP, C. E., VAKHNENKO, Y., ANNE, P. R. & SIMONE, N. L. 2012. Radiation Therapy for Locally Recurrent Breast Cancer. *International Journal of Breast Cancer,* 2012**,** 7.
SILVER, D. P., RICHARDSON, A. L., EKLUND, A. C., WANG, Z. C., SZALLASI, Z., LI, Q.*, et al.* 2010. Efficacy of Neoadjuvant Cisplatin in Triple-Negative Breast Cancer. *Journal of Clinical Oncology,* 28**,** 1145-1153.
SIMPSON, J. F. 2009. Update on atypical epithelial hyperplasia and ductal carcinoma in situ. *Pathology,* 41**,** 36-9.
SIMPSON, J. F., GRAY, R., DRESSLER, L. G., COBAU, C. D., FALKSON, C. I., GILCHRIST, K. W., PANDYA, K. J., PAGE, D. L. & ROBERT, N. J. 2000. Prognostic value of histologic grade and proliferative activity in axillary node-positive breast cancer: results from the Eastern Cooperative Oncology Group Companion Study, EST 4189. *J Clin Oncol,* 18**,** 2059-69.
SINGH, M. S., FRANCIS, P. A. & MICHAEL, M. 2011. Tamoxifen, cytochrome P450 genes and breast cancer clinical outcomes. *Breast,* 20**,** 111-8.
SINGH, P., YANG, M., DAI, H., YU, D., HUANG, Q., TAN, W., KERNSTINE, K. H., LIN, D. & SHEN, B. 2008. Overexpression and hypomethylation of flap endonuclease 1 gene in breast and other cancers. *Mol Cancer Res,* 6**,** 1710-7.
SINN, H.-P. & KREIPE, H. 2013. A Brief Overview of the WHO Classification of Breast Tumors, 4th Edition, Focusing on Issues and Updates from the 3rd Edition. *Breast care (Basel, Switzerland),* 8**,** 149-154.
SJÖSTRÖM, M., LUNDSTEDT, D., HARTMAN, L., HOLMBERG, E., KILLANDER, F., KOVÁCS, A.*, et al.* 2017. Response to Radiotherapy After Breast-Conserving Surgery in Different Breast Cancer Subtypes in the Swedish Breast Cancer Group 91 Radiotherapy Randomized Clinical Trial. *J Clin Oncol,* 35**,** 3222-3229.
SKARSGARD, L. D. & HARRISON, I. 1991. Dose Dependence of the Oxygen Enhancement Ratio (OER) in Radiation Inactivation of Chinese Hamster V79-171 Cells. *Radiation Research,* 127**,** 243-247.
SKOWRONEK, J. & CHICHEŁ, A. 2014. Brachytherapy in breast cancer: an effective alternative. *Przeglad menopauzalny = Menopause review,* 13**,** 48-55.
SKOWRONEK, J., WAWRZYNIAK-HOJCZYK, M. & AMBROCHOWICZ, K. 2012. Brachytherapy in accelerated partial breast irradiation (APBI) - review of treatment methods. *J Contemp Brachytherapy,* 4**,** 152-64.
SLAMON, D., EIERMANN, W., ROBERT, N., PIENKOWSKI, T., MARTIN, M., PRESS, M.*, et al.* 2011. Adjuvant trastuzumab in HER2-positive breast cancer. *N Engl J Med,* 365**,** 1273-83.
SLAUGHTER, R. L. & EDWARDS, D. J. 1995. Recent advances: the cytochrome P450 enzymes. *Ann Pharmacother,* 29**,** 619-24.
SMITH-WARNER, S. A., SPIEGELMAN, D., YAUN, S. S., VAN DEN BRANDT, P. A., FOLSOM, A. R., GOLDBOHM, R. A.*, et al.* 1998. Alcohol and breast cancer in women: a pooled analysis of cohort studies. *Jama,* 279**,** 535-40.

SMITH, G., WOLF, C., DEENI, Y., DAWE, R., EVANS, A., COMRIE, M., FERGUSON, J. & IBBOTSON, S. 2003. Cutaneous expression of cytochrome P450 CYP2S1: Individuality in regulation by therapeutic agents for psoriasis and other skin diseases. *Lancet,* 361**,** 1336-43.

SMITH, I., PROCTER, M., GELBER, R. D., GUILLAUME, S., FEYEREISLOVA, A., DOWSETT, M.*, et al.* 2007. 2-year follow-up of trastuzumab after adjuvant chemotherapy in HER2-positive breast cancer: a randomised controlled trial. *Lancet,* 369**,** 29-36.

SMITH, J., THO, L. M., XU, N. & GILLESPIE, D. A. 2010. The ATM-Chk2 and ATR-Chk1 pathways in DNA damage signaling and cancer. *Adv Cancer Res,* 108**,** 73-112.

SMITH, P. J., DESNOYERS, R., BLUNT, N., GILES, Y., PATTERSON, L. H. & WATSON, J. V. 1997. Flow cytometric analysis and confocal imaging of anticancer alkylaminoanthraquinones and their N-oxides in intact human cells using 647-nm krypton laser excitation. *Cytometry,* 27**,** 43-53.

SMITTENAAR, C. R., PETERSEN, K. A., STEWART, K. & MOITT, N. 2016. Cancer incidence and mortality projections in the UK until 2035. *Br J Cancer,* 115**,** 1147-1155.

SOMALI, I., USTAOGLU, B. Y., TARHAN, M. O., YIGIT, S. C., DEMIR, L., ELLIDOKUZ, H., ERTEN, C. & ALACACIOGLU, A. 2013. Clinicopathologic and demographic evaluation of triple- negative breast cancer patients among a turkish patient population: a single center experience. *Asian Pac J Cancer Prev,* 14**,** 6013-7.

SON, B. H., KWAK, B. S., KIM, J. K., KIM, H. J., HONG, S. J., LEE, J. S., HWANG, U. K., YOON, H. S. & AHN, S. H. 2006. Changing patterns in the clinical characteristics of Korean patients with breast cancer during the last 15 years. *Arch Surg,* 141**,** 155-60.

SONG, C. W., PARK, H. & GRIFFIN, R. J. 2001. Improvement of tumor oxygenation by mild hyperthermia. *Radiat Res,* 155**,** 515-28.

SONG, H., HEDAYATI, M., HOBBS, R. F., SHAO, C., BRUCHERTSEIFER, F., MORGENSTERN, A., DEWEESE, T. L. & SGOUROS, G. 2013. Targeting aberrant DNA double-strand break repair in triple-negative breast cancer with alpha-particle emitter radiolabeled anti-EGFR antibody. *Mol Cancer Ther,* 12**,** 2043-54.

SONG, J., MIERMONT, A., LIM, C. T. & KAMM, R. D. 2018. A 3D microvascular network model to study the impact of hypoxia on the extravasation potential of breast cell lines. *Sci Rep,* 8**,** 17949.

SONG, Y. J., SHIN, S. H., CHO, J. S., PARK, M. H., YOON, J. H. & JEGAL, Y. J. 2011. The role of lymphovascular invasion as a prognostic factor in patients with lymph node-positive operable invasive breast cancer. *J Breast Cancer,* 14**,** 198-203.

SONG, Y. P., MISTRY, H., CHOUDHURY, A. & HOSKIN, P. 2019. Long-term outcomes of hypoxia modification in bladder preservation: Update from BCON trial. *Journal of Clinical Oncology,* 37**,** 356-356.

SONVEAUX, P. 2017. ROS and radiotherapy: more we care. *Oncotarget,* 8**,** 35482-35483.

SORLIE, T., PEROU, C. M., TIBSHIRANI, R., AAS, T., GEISLER, S., JOHNSEN, H.*, et al.* 2001. Gene expression patterns of breast carcinomas distinguish tumor subclasses with clinical implications. *Proc Natl Acad Sci U S A,* 98**,** 10869-74.

SOULE, H. D., MALONEY, T. M., WOLMAN, S. R., PETERSON, W. D., JR., BRENZ, R., MCGRATH, C. M.*, et al.* 1990. Isolation and characterization of a spontaneously immortalized human breast epithelial cell line, MCF-10. *Cancer Res,* 50**,** 6075-86.

SPEERS, C., ZHAO, S., LIU, M., BARTELINK, H., PIERCE, L. J. & FENG, F. Y. 2015. Development and Validation of a Novel Radiosensitivity Signature in Human Breast Cancer. *Clin Cancer Res,* 21**,** 3667-77.

SPENCER, J. A., FERRARO, F., ROUSSAKIS, E., KLEIN, A., WU, J., RUNNELS, J. M., *et al.* 2014. Direct measurement of local oxygen concentration in the bone marrow of live animals. *Nature,* 508**,** 269-73.
SPIRO, I. J., RICE, G. C., DURAND, R. E., STICKLER, R. & LING, C. C. 1984. Cell killing, radiosensitization and cell cycle redistribution induced by chronic hypoxia. *Int J Radiat Oncol Biol Phys,* 10**,** 1275-80.
STEEL, G. G. 1996. From targets to genes: a brief history of radiosensitivity. *Phys Med Biol,* 41**,** 205-22.
STENSTEDT, K., HALLSTROM, M., JOHANSSON, I., INGELMAN-SUNDBERG, M., RAGNHAMMAR, P. & EDLER, D. 2012. The expression of CYP2W1: a prognostic marker in colon cancer. *Anticancer Res,* 32**,** 3869-74.
STEPHAN, H., CONCANNON, C., KREMMER, E., CARTY, M. P. & NASHEUER, H.-P. 2009. Ionizing radiation-dependent and independent phosphorylation of the 32-kDa subunit of replication protein A during mitosis. *Nucleic Acids Research,* 37**,** 6028-6041.
STEWARD, W. P., MIDDLETON, M., BENGHIAT, A., LOADMAN, P. M., HAYWARD, C., WALLER, S., *et al.* 2007. The use of pharmacokinetic and pharmacodynamic end points to determine the dose of AQ4N, a novel hypoxic cell cytotoxin, given with fractionated radiotherapy in a phase I study. *Ann Oncol,* 18**,** 1098-103.
STORR, S. J., ZHANG, S., PERREN, T., LANSDOWN, M., FATAYER, H., SHARMA, N., GAHLAUT, R., SHAABAN, A. & MARTIN, S. G. 2016. The calpain system is associated with survival of breast cancer patients with large but operable inflammatory and non-inflammatory tumours treated with neoadjuvant chemotherapy. *Oncotarget,* 7**,** 47927-47937.
SU, Y.-J., HUANG, S.-Y., NI, Y.-H., LIAO, K.-F. & CHIU, S.-C. 2018. Anti-Tumor and Radiosensitization Effects of N-Butylidenephthalide on Human Breast Cancer Cells. *Molecules (Basel, Switzerland),* 23**,** 240.
SUGIYAMA, T., ZAITSEVA, E. M. & KOWALCZYKOWSKI, S. C. 1997. A single-stranded DNA-binding protein is needed for efficient presynaptic complex formation by the Saccharomyces cerevisiae Rad51 protein. *J Biol Chem,* 272**,** 7940-5.
SUN, H., HE, L., WU, H., PAN, F., WU, X., ZHAO, J., *et al.* 2017. The FEN1 L209P mutation interferes with long-patch base excision repair and induces cellular transformation. *Oncogene,* 36**,** 194-207.
SUTHERLAND, R. M., MCCREDIE, J. A. & INCH, W. R. 1971. Growth of multicell spheroids in tissue culture as a model of nodular carcinomas. *J Natl Cancer Inst,* 46**,** 113-20.
SWAIN, S. M., BASELGA, J., KIM, S. B., RO, J., SEMIGLAZOV, V., CAMPONE, M., *et al.* 2015. Pertuzumab, trastuzumab, and docetaxel in HER2-positive metastatic breast cancer. *N Engl J Med,* 372**,** 724-34.
SWEDE, H., MOYSICH, K. B., FREUDENHEIM, J. L., QUIRK, J. T., MUTI, P. C., HURD, T. C., EDGE, S. B., WINSTON, J. S. & MICHALEK, A. M. 2001. Breast cancer risk factors and HER2 over-expression in tumors. *Cancer Detect Prev,* 25**,** 511-9.
SWINSON, D. E., JONES, J. L., RICHARDSON, D., WYKOFF, C., TURLEY, H., PASTOREK, J., TAUB, N., HARRIS, A. L. & O'BYRNE, K. J. 2003. Carbonic anhydrase IX expression, a novel surrogate marker of tumor hypoxia, is associated with a poor prognosis in non-small-cell lung cancer. *J Clin Oncol,* 21**,** 473-82.
SZAEFER, H., LICZNERSKA, B., CYKOWIAK, M. & BAER-DUBOWSKA, W. 2019. Expression of CYP2S1 and CYP2W1 in breast cancer epithelial cells and modulation of their expression by synthetic methoxy stilbenes. *Pharmacological Reports,* 71**,** 1001-1005.
TAKASAKI, C., KOBAYASHI, M., ISHIBASHI, H., AKASHI, T. & OKUBO, K. 2016. Expression of hypoxia-inducible factor-1alpha affects tumor proliferation

and antiapoptosis in surgically resected lung cancer. *Mol Clin Oncol,* 5**,** 295-300.
TAN, B. S., TIONG, K. H., MURUHADAS, A., RANDHAWA, N., CHOO, H. L., BRADSHAW, T. D., STEVENS, M. F. G. & LEONG, C.-O. 2011. CYP2S1 and CYP2W1 Mediate 2-(3,4-Dimethoxyphenyl)-5-Fluorobenzothiazole (GW-610, NSC 721648) Sensitivity in Breast and Colorectal Cancer Cells. *Molecular Cancer Therapeutics,* 10**,** 1982-1992.
TANG, X. H. & GUDAS, L. J. 2011. Retinoids, retinoic acid receptors, and cancer. *Annu Rev Pathol,* 6**,** 345-64.
TASSONE, P., BLOTTA, S., PALMIERI, C., MASCIARI, S., QUARESIMA, B., MONTAGNA, M.*, et al.* 2005. Differential sensitivity of BRCA1-mutated HCC1937 human breast cancer cells to microtubule-interfering agents. *Int J Oncol,* 26**,** 1257-63.
TCGA 2012. Comprehensive molecular portraits of human breast tumours. *Nature,* 490**,** 61-70.
TEICHER, B. A. 1994. Hypoxia and drug resistance. *Cancer Metastasis Rev,* 13**,** 139-68.
TEICHER, B. A., LAZO, J. S. & SARTORELLI, A. C. 1981. Classification of antineoplastic agents by their selective toxicities toward oxygenated and hypoxic tumor cells. *Cancer Res,* 41**,** 73-81.
TELLI, M. L., TIMMS, K. M., REID, J., HENNESSY, B., MILLS, G. B., JENSEN, K. C.*, et al.* 2016. Homologous Recombination Deficiency (HRD) Score Predicts Response to Platinum-Containing Neoadjuvant Chemotherapy in Patients with Triple-Negative Breast Cancer. *Clin Cancer Res,* 22**,** 3764-73.
TEVIS, K. M., COLSON, Y. L. & GRINSTAFF, M. W. 2017. Embedded Spheroids as Models of the Cancer Microenvironment. *Advanced biosystems,* 1**,** 1700083.
THAKUR, P., SEAM, R. K., GUPTA, M. K., GUPTA, M., SHARMA, M. & FOTEDAR, V. 2017. Breast cancer risk factor evaluation in a Western Himalayan state: A case-control study and comparison with the Western World. *South Asian J Cancer,* 6**,** 106-109.
THIOLLOY, S., DESCHOEMAEKER, S., ONGENAE, N., GILISSEN, J., DUBOIS, L., YAROMINA, A.*, et al.* 2018. Abstract 4959: CP-506, a next generation hypoxia-activated prodrug, as promising novel anti-cancer therapeutic. *Cancer Research,* 78**,** 4959-4959.
THODAY, J. M. & READ, J. 1947. Effect of oxygen on the frequency of chromosome aberrations produced by X-rays. *Nature,* 160**,** 608.
THOMAS, R. D., GREEN, M. R., WILSON, C., WECKLE, A. L., DUANMU, Z., KOCAREK, T. A. & RUNGE-MORRIS, M. 2006. Cytochrome P450 expression and metabolic activation of cooked food mutagen 2-amino-1-methyl-6-phenylimidazo[4,5-b]pyridine (PhIP) in MCF10A breast epithelial cells. *Chem Biol Interact,* 160**,** 204-16.
THORBJARNARDOTTIR, T., OLAFSDOTTIR, E. J., VALDIMARSDOTTIR, U. A., OLAFSSON, O. & TRYGGVADOTTIR, L. 2014. Oral contraceptives, hormone replacement therapy and breast cancer risk: a cohort study of 16 928 women 48 years and older. *Acta Oncol,* 53**,** 752-8.
TIAN, X., LARA, H., WAGNER, K. T., SARIPALLI, S., HYDER, S. N., FOOTE, M.*, et al.* 2015. Improving DNA double-strand repair inhibitor KU55933 therapeutic index in cancer radiotherapy using nanoparticle drug delivery. *Nanoscale,* 7**,** 20211-20219.
TIMOTHY, A. R., OVERGAARD, J. & OVERGAARD, M. 1984. A phase I clinical study of nimorazole as a hypoxic radiosensitizer. *International Journal of Radiation Oncology*Biology*Physics,* 10**,** 1765-1768.
TORRES-ROCA, J. F., ESCHRICH, S., ZHAO, H., BLOOM, G., SUNG, J., MCCARTHY, S.*, et al.* 2005. Prediction of Radiation Sensitivity Using a Gene Expression Classifier. *Cancer Research,* 65**,** 7169-7176.

TOUSTRUP, K., SORENSEN, B. S., LASSEN, P., WIUF, C., ALSNER, J. & OVERGAARD, J. 2012. Gene expression classifier predicts for hypoxic modification of radiotherapy with nimorazole in squamous cell carcinomas of the head and neck. *Radiother Oncol,* 102**,** 122-9.

TOUSTRUP, K., SORENSEN, B. S., NORDSMARK, M., BUSK, M., WIUF, C., ALSNER, J. & OVERGAARD, J. 2011. Development of a hypoxia gene expression classifier with predictive impact for hypoxic modification of radiotherapy in head and neck cancer. *Cancer Res,* 71**,** 5923-31.

TRAMM, T., KYNDI, M., MYHRE, S., NORD, S., ALSNER, J., SØRENSEN, F. B., SØRLIE, T. & OVERGAARD, J. 2014. Relationship between the prognostic and predictive value of the intrinsic subtypes and a validated gene profile predictive of loco-regional control and benefit from post-mastectomy radiotherapy in patients with high-risk breast cancer. *Acta Oncol,* 53**,** 1337-46.

TREDAN, O., GARBENS, A. B., LALANI, A. S. & TANNOCK, I. F. 2009. The hypoxia-activated ProDrug AQ4N penetrates deeply in tumor tissues and complements the limited distribution of mitoxantrone. *Cancer Res,* 69**,** 940-7.

TRESZEZAMSKY, A. D., KACHNIC, L. A., FENG, Z., ZHANG, J., TOKADJIAN, C. & POWELL, S. N. 2007. BRCA1- and BRCA2-Deficient Cells Are Sensitive to Etoposide-Induced DNA Double-Strand Breaks via Topoisomerase II. *Cancer Research,* 67**,** 7078-7081.

TSUCHIYA, Y., NAKAJIMA, M. & YOKOI, T. 2005. Cytochrome P450-mediated metabolism of estrogens and its regulation in human. *Cancer Lett,* 227**,** 115-24.

TU, L. C., MELENDY, T. & BEERMAN, T. A. 2004. DNA damage responses triggered by a highly cytotoxic monofunctional DNA alkylator, hedamycin, a pluramycin antitumor antibiotic. *Mol Cancer Ther,* 3**,** 577-85.

TU, W. Z., LI, B., HUANG, B., WANG, Y., LIU, X. D., GUAN, H.*, et al.* 2013. gammaH2AX foci formation in the absence of DNA damage: mitotic H2AX phosphorylation is mediated by the DNA-PKcs/CHK2 pathway. *FEBS Lett,* 587**,** 3437-43.

TU, X., KAHILA, M. M., ZHOU, Q., YU, J., KALARI, K. R., WANG, L.*, et al.* 2018. ATR Inhibition Is a Promising Radiosensitizing Strategy for Triple-Negative Breast Cancer. *Mol Cancer Ther,* 17**,** 2462-2472.

TUMEY, L. N., BOM, D., HUCK, B., GLEASON, E., WANG, J., SILVER, D.*, et al.* 2005. The identification and optimization of a N-hydroxy urea series of flap endonuclease 1 inhibitors. *Bioorg Med Chem Lett,* 15**,** 277-81.

TURNER, N., TUTT, A. & ASHWORTH, A. 2004. Hallmarks of 'BRCAness' in sporadic cancers. *Nat Rev Cancer,* 4**,** 814-9.

TUTT, A., ROBSON, M., GARBER, J. E., DOMCHEK, S. M., AUDEH, M. W., WEITZEL, J. N.*, et al.* 2010. Oral poly(ADP-ribose) polymerase inhibitor olaparib in patients with BRCA1 or BRCA2 mutations and advanced breast cancer: a proof-of-concept trial. *Lancet,* 376**,** 235-44.

UNRUH, A., RESSEL, A., MOHAMED, H. G., JOHNSON, R. S., NADROWITZ, R., RICHTER, E., KATSCHINSKI, D. M. & WENGER, R. H. 2003. The hypoxia-inducible factor-1 alpha is a negative factor for tumor therapy. *Oncogene,* 22**,** 3213-20.

URSIN, G., BERNSTEIN, L., LORD, S. J., KARIM, R., DEAPEN, D., PRESS, M. F.*, et al.* 2005. Reproductive factors and subtypes of breast cancer defined by hormone receptor and histology. *British journal of cancer,* 93**,** 364-371.

UZIEL, T., LERENTHAL, Y., MOYAL, L., ANDEGEKO, Y., MITTELMAN, L. & SHILOH, Y. 2003. Requirement of the MRN complex for ATM activation by DNA damage. *Embo j,* 22**,** 5612-21.

VACHON, C. M., VAN GILS, C. H., SELLERS, T. A., GHOSH, K., PRUTHI, S., BRANDT, K. R. & PANKRATZ, V. S. 2007. Mammographic density, breast cancer risk and risk prediction. *Breast cancer research : BCR,* 9**,** 217-217.

VAIDYA, J. S., JOSEPH, D. J., TOBIAS, J. S., BULSARA, M., WENZ, F., SAUNDERS, C.*, et al.* 2010. Targeted intraoperative radiotherapy versus whole breast radiotherapy for breast cancer (TARGIT-A trial): an international, prospective, randomised, non-inferiority phase 3 trial. *Lancet,* 376**,** 91-102.

VAIDYA, J. S., WENZ, F., BULSARA, M., TOBIAS, J. S., JOSEPH, D. J., KESHTGAR, M.*, et al.* 2014. Risk-adapted targeted intraoperative radiotherapy versus whole-breast radiotherapy for breast cancer: 5-year results for local control and overall survival from the TARGIT-A randomised trial. *Lancet,* 383**,** 603-13.

VALDIGLESIAS, V., GIUNTA, S., FENECH, M., NERI, M. & BONASSI, S. 2013. gammaH2AX as a marker of DNA double strand breaks and genomic instability in human population studies. *Mutat Res,* 753**,** 24-40.

VALDIMARSSON, H., BAKE, B. S., JÓNSDÓTDR, I. & FRY, L. 1986. Psoriasis: a disease of abnormal Keratinocyte proliferation induced by T lymphocytes. *Immunol Today,* 7**,** 256-9.

VAN DE VIJVER, M. J., HE, Y. D., VAN'T VEER, L. J., DAI, H., HART, A. A., VOSKUIL, D. W.*, et al.* 2002. A gene-expression signature as a predictor of survival in breast cancer. *N Engl J Med,* 347**,** 1999-2009.

VAN DEN EYNDEN, G. G., VAN DER AUWERA, I., VAN LAERE, S. J., COLPAERT, C. G., TURLEY, H., HARRIS, A. L.*, et al.* 2005. Angiogenesis and hypoxia in lymph node metastases is predicted by the angiogenesis and hypoxia in the primary tumour in patients with breast cancer. *Br J Cancer,* 93**,** 1128-36.

VAN DER LEIJ, F., BOSMA, S. C. J., VAN DE VIJVER, M. J., WESSELING, J., VREESWIJK, S., RIVERA, S.*, et al.* 2015. First results of the preoperative accelerated partial breast irradiation (PAPBI) trial. *Radiotherapy and Oncology,* 114**,** 322-327.

VAN DER ZEE, J., GONZÁLEZ GONZÁLEZ, D., VAN RHOON, G. C., VAN DIJK, J. D., VAN PUTTEN, W. L. & HART, A. A. 2000. Comparison of radiotherapy alone with radiotherapy plus hyperthermia in locally advanced pelvic tumours: a prospective, randomised, multicentre trial. Dutch Deep Hyperthermia Group. *Lancet,* 355**,** 1119-25.

VAN DONGEN, J. A., VOOGD, A. C., FENTIMAN, I. S., LEGRAND, C., SYLVESTER, R. J., TONG, D.*, et al.* 2000. Long-term results of a randomized trial comparing breast-conserving therapy with mastectomy: European Organization for Research and Treatment of Cancer 10801 trial. *J Natl Cancer Inst,* 92**,** 1143-50.

VAN GILS, C. H., OTTEN, J. D., VERBEEK, A. L. & HENDRIKS, J. H. 1998. Mammographic breast density and risk of breast cancer: masking bias or causality? *Eur J Epidemiol,* 14**,** 315-20.

VAN LEEUWEN, C. M., OEI, A. L., CREZEE, J., BEL, A., FRANKEN, N. A. P., STALPERS, L. J. A. & KOK, H. P. 2018. The alfa and beta of tumours: a review of parameters of the linear-quadratic model, derived from clinical radiotherapy studies. *Radiation oncology (London, England),* 13**,** 96-96.

VAN VEELEN, L. R., CERVELLI, T., VAN DE RAKT, M. W., THEIL, A. F., ESSERS, J. & KANAAR, R. 2005. Analysis of ionizing radiation-induced foci of DNA damage repair proteins. *Mutat Res,* 574**,** 22-33.

VAUPEL, P., HOCKEL, M. & MAYER, A. 2007. Detection and characterization of tumor hypoxia using pO2 histography. *Antioxid Redox Signal,* 9**,** 1221-35.

VAUPEL, P. & MAYER, A. 2007. Hypoxia in cancer: significance and impact on clinical outcome. *Cancer Metastasis Rev,* 26**,** 225-39.

VAUPEL, P., MAYER, A., BRIEST, S. & HOCKEL, M. 2003. Oxygenation gain factor: a novel parameter characterizing the association between hemoglobin level and the oxygenation status of breast cancers. *Cancer Res,* 63**,** 7634-7.

VAUPEL, P., MAYER, A., BRIEST, S. & HOCKEL, M. 2005. Hypoxia in breast cancer: role of blood flow, oxygen diffusion distances, and anemia in the development of oxygen depletion. *Adv Exp Med Biol,* 566**,** 333-42.
VAUPEL, P., MAYER, A. & HÖCKEL, M. 2004. Tumor hypoxia and malignant progression. *Methods Enzymol,* 381**,** 335-54.
VAUPEL, P., SCHLENGER, K., KNOOP, C. & HOCKEL, M. 1991. Oxygenation of human tumors: evaluation of tissue oxygen distribution in breast cancers by computerized O2 tension measurements. *Cancer Res,* 51**,** 3316-22.
VAVROVA, J., ZARYBNICKA, L., JOST, P., TICHY, A., REZACOVA, M., SINKOROVA, Z. & PEJCHAL, J. 2016. Comparison of the Radiosensitizing Effect of ATR, ATM and DNA-PK Kinase Inhibitors on Cervical Carcinoma Cells. *Folia Biol (Praha),* 62**,** 167-74.
VELDWIJK, M. R., ZHANG, B., WENZ, F. & HERSKIND, C. 2014. The biological effect of large single doses: a possible role for non-targeted effects in cell inactivation. *PLoS One,* 9**,** e84991.
VELIC, D., COUTURIER, A. M., FERREIRA, M. T., RODRIGUE, A., POIRIER, G. G., FLEURY, F. & MASSON, J.-Y. 2015. DNA Damage Signalling and Repair Inhibitors: The Long-Sought-After Achilles' Heel of Cancer. *Biomolecules,* 5**,** 3204-3259.
VENS, C. & BEGG, A. C. 2010. Targeting base excision repair as a sensitization strategy in radiotherapy. *Semin Radiat Oncol,* 20**,** 241-9.
VERHAGEN, C. V., DE HAAN, R., HAGEMAN, F., OOSTENDORP, T. P., CARLI, A. L., O'CONNOR, M. J.*, et al.* 2015. Extent of radiosensitization by the PARP inhibitor olaparib depends on its dose, the radiation dose and the integrity of the homologous recombination pathway of tumor cells. *Radiother Oncol,* 116**,** 358-65.
VERMA, S., MILES, D., GIANNI, L., KROP, I. E., WELSLAU, M., BASELGA, J.*, et al.* 2012. Trastuzumab emtansine for HER2-positive advanced breast cancer. *N Engl J Med,* 367**,** 1783-91.
VERNON, C. C., HAND, J. W., FIELD, S. B., MACHIN, D., WHALEY, J. B., VAN DER ZEE, J.*, et al.* 1996. Radiotherapy with or without hyperthermia in the treatment of superficial localized breast cancer: results from five randomized controlled trials. International Collaborative Hyperthermia Group. *Int J Radiat Oncol Biol Phys,* 35**,** 731-44.
VERONESI, U., CASCINELLI, N., MARIANI, L., GRECO, M., SACCOZZI, R., LUINI, A., AGUILAR, M. & MARUBINI, E. 2002. Twenty-year follow-up of a randomized study comparing breast-conserving surgery with radical mastectomy for early breast cancer. *N Engl J Med,* 347**,** 1227-32.
VEUGER, S. J. & DURKACZ, B. W. 2011. Persistence of unrepaired DNA double strand breaks caused by inhibition of ATM does not lead to radio-sensitisation in the absence of NF-kappaB activation. *DNA Repair (Amst),* 10**,** 235-44.
VICINI, F., KINI, V. R., CHEN, P., HORWITZ, E., GUSTAFSON, G., BENITEZ, P.*, et al.* 1999. Irradiation of the tumor bed alone after lumpectomy in selected patients with early-stage breast cancer treated with breast conserving therapy. *J Surg Oncol,* 70**,** 33-40.
VINCI, M., GOWAN, S., BOXALL, F., PATTERSON, L., ZIMMERMANN, M., COURT, W.*, et al.* 2012. Advances in establishment and analysis of three-dimensional tumor spheroid-based functional assays for target validation and drug evaluation. *BMC Biol,* 10**,** 29.
VODUC, K. D., CHEANG, M. C., TYLDESLEY, S., GELMON, K., NIELSEN, T. O. & KENNECKE, H. 2010. Breast cancer subtypes and the risk of local and regional relapse. *J Clin Oncol,* 28**,** 1684-91.
VOISSIERE, A., JOUBERTON, E., MAUBERT, E., DEGOUL, F., PEYRODE, C., CHEZAL, J.-M. & MIOT-NOIRAULT, E. 2017. Development and characterization of a human three-dimensional chondrosarcoma culture for in vitro drug testing. *PloS one,* 12**,** e0181340-e0181340.

VOLPI, A., BACCI, F., PARADISO, A., SARAGONI, L., SCARPI, E., RICCI, M.*, et al.* 2004. Prognostic relevance of histological grade and its components in node-negative breast cancer patients. *Mod Pathol,* 17**,** 1038-44.
WALKER, R. A. 2005. World Health Organization Classification of Tumours. Pathology and Genetics of Tumours of the Breast and Female Genital Organs. *Histopathology,* 46**,** 229-229.
WANG, H., JIANG, H., VAN DE GUCHT, M. & DE RIDDER, M. 2019. Hypoxic Radioresistance: Can ROS Be the Key to Overcome It? *Cancers,* 11**,** 112.
WANG, J., ZHOU, L., LI, Z., ZHANG, T., LIU, W., LIU, Z.*, et al.* 2015. YY1 suppresses FEN1 over-expression and drug resistance in breast cancer. *BMC Cancer,* 15**,** 50.
WANG, K. & GUENGERICH, F. P. 2012. Bioactivation of fluorinated 2-aryl-benzothiazole antitumor molecules by human cytochrome P450s 1A1 and 2W1 and deactivation by cytochrome P450 2S1. *Chemical research in toxicology,* 25**,** 1740-1751.
WANG, M., HOU, L., CHEN, M., ZHOU, Y., LIANG, Y., WANG, S., JIANG, J. & ZHANG, Y. 2017. Neoadjuvant Chemotherapy Creates Surgery Opportunities For Inoperable Locally Advanced Breast Cancer. *Scientific Reports,* 7**,** 44673.
WANG, Y., LIU, Y., TANG, T., LUO, Y., STEVENS, M. F. G., CHENG, X.*, et al.* 2020. The antitumour activity of 2-(4-amino-3-methylphenyl)-5-fluorobenzothiazole in human gastric cancer models is mediated by AhR signalling. *Journal of cellular and molecular medicine,* 24**,** 1750-1759.
WANG, Y., YIN, Q., YU, Q., ZHANG, J., LIU, Z., WANG, S., LV, S. & NIU, Y. 2011. A retrospective study of breast cancer subtypes: the risk of relapse and the relations with treatments. *Breast Cancer Res Treat,* 130**,** 489-98.
WARBRICK, E., COATES, P. J. & HALL, P. A. 1998. Fen1 expression: a novel marker for cell proliferation. *J Pathol,* 186**,** 319-24.
WARD, E. M., DESANTIS, C. E., LIN, C. C., KRAMER, J. L., JEMAL, A., KOHLER, B., BRAWLEY, O. W. & GANSLER, T. 2015. Cancer statistics: Breast cancer in situ. *CA Cancer J Clin,* 65**,** 481-95.
WARD, J. F. 1985. Biochemistry of DNA lesions. *Radiat Res Suppl,* 8**,** S103-11.
WARD, J. F. 1988. DNA damage produced by ionizing radiation in mammalian cells: identities, mechanisms of formation, and reparability. *Prog Nucleic Acid Res Mol Biol,* 35**,** 95-125.
WARD, J. F., EVANS, J. W., LIMOLI, C. L. & CALABRO-JONES, P. M. 1987. Radiation and hydrogen peroxide induced free radical damage to DNA. *Br J Cancer Suppl,* 8**,** 105-12.
WARD, T. A., MCHUGH, P. J. & DURANT, S. T. 2017. Small molecule inhibitors uncover synthetic genetic interactions of human flap endonuclease 1 (FEN1) with DNA damage response genes. *PLoS One,* 12**,** e0179278.
WARE, J. H., ZHOU, Z., GUAN, J., KENNEDY, A. R. & KOPELOVICH, L. 2007. Establishment of human cancer cell clones with different characteristics: a model for screening chemopreventive agents. *Anticancer Res,* 27**,** 1-16.
WATANABE, N., OKOCHI, E., MOCHIZUKI, M., SUGIMURA, T. & USHIJIMA, T. 2001. The Presence of Single Nucleotide Instability in Human Breast Cancer Cell Lines. *Cancer Research,* 61**,** 7739-7742.
WAZIR, U., MOKBEL, K., CARMICHAEL, A. & MOKBEL, K. 2017. Are online prediction tools a valid alternative to genomic profiling in the context of systemic treatment of ER-positive breast cancer? *Cellular & molecular biology letters,* 22**,** 20-20.
WEIGELT, B., GEYER, F. C. & REIS-FILHO, J. S. 2010. Histological types of breast cancer: how special are they? *Molecular oncology,* 4**,** 192-208.
WEIGELT, B. & REIS-FILHO, J. S. 2009. Histological and molecular types of breast cancer: is there a unifying taxonomy? *Nat Rev Clin Oncol,* 6**,** 718-30.
WELLINGS, S. R. & JENSEN, H. M. 1973. On the origin and progression of ductal carcinoma in the human breast. *J Natl Cancer Inst,* 50**,** 1111-8.

WEN, S.-H., SU, S.-C., LIOU, B.-H., LIN, C.-H. & LEE, K.-R. 2018. Sulbactam-enhanced cytotoxicity of doxorubicin in breast cancer cells. *Cancer cell international,* 18**,** 128-128.
WHEATON, W. W., WEINBERG, S. E., HAMANAKA, R. B., SOBERANES, S., SULLIVAN, L. B., ANSO, E.*, et al.* 2014. Metformin inhibits mitochondrial complex I of cancer cells to reduce tumorigenesis. *eLife,* 3**,** e02242-e02242.
WILLERS, H., DAHM-DAPHI, J. & POWELL, S. N. 2004. Repair of radiation damage to DNA. *Br J Cancer,* 90**,** 1297-301.
WILLIAMS, K. J., ALBERTELLA, M. R., FITZPATRICK, B., LOADMAN, P. M., SHNYDER, S. D., CHINJE, E. C.*, et al.* 2009. In vivo activation of the hypoxia-targeted cytotoxin AQ4N in human tumor xenografts. *Mol Cancer Ther,* 8**,** 3266-75.
WILLIAMS, K. J., TELFER, B. A., XENAKI, D., SHERIDAN, M. R., DESBAILLETS, I., PETERS, H. J.*, et al.* 2005. Enhanced response to radiotherapy in tumours deficient in the function of hypoxia-inducible factor-1. *Radiother Oncol,* 75**,** 89-98.
WILLIAMSON, S. K., CROWLEY, J. J., LARA, P. N., JR., MCCOY, J., LAU, D. H., TUCKER, R. W., MILLS, G. M. & GANDARA, D. R. 2005. Phase III trial of paclitaxel plus carboplatin with or without tirapazamine in advanced non-small-cell lung cancer: Southwest Oncology Group Trial S0003. *J Clin Oncol,* 23**,** 9097-104.
WILSON, W. R., DENNY, W. A., PULLEN, S. M., THOMPSON, K. M., LI, A. E., PATTERSON, L. H. & LEE, H. H. 1996. Tertiary amine N-oxides as bioreductive drugs: DACA N-oxide, nitracrine N-oxide and AQ4N. *Br J Cancer Suppl,* 27**,** S43-7.
WILSON, W. R. & HAY, M. P. 2011. Targeting hypoxia in cancer therapy. *Nature Reviews Cancer,* 11**,** 393.
WIRAPATI, P., SOTIRIOU, C., KUNKEL, S., FARMER, P., PRADERVAND, S., HAIBE-KAINS, B.*, et al.* 2008. Meta-analysis of gene expression profiles in breast cancer: toward a unified understanding of breast cancer subtyping and prognosis signatures. *Breast Cancer Res,* 10**,** R65.
WISHART, G. C., AZZATO, E. M., GREENBERG, D. C., RASHBASS, J., KEARINS, O., LAWRENCE, G., CALDAS, C. & PHAROAH, P. D. 2010. PREDICT: a new UK prognostic model that predicts survival following surgery for invasive breast cancer. *Breast Cancer Res,* 12**,** R1.
WITHERBY, S., RIZACK, T., SAKR, B. J., LEGARE, R. D. & SIKOV, W. M. 2016. Advances in Medical Management of Early Stage and Advanced Breast Cancer: 2015. *Seminars in Radiation Oncology,* 26**,** 59-70.
WITHERS, H. R. 1987. *Biologic basis of radiation therapy,* United States, JP Lippincott Co.
WONG, C. C., GILKES, D. M., ZHANG, H., CHEN, J., WEI, H., CHATURVEDI, P.*, et al.* 2011. Hypoxia-inducible factor 1 is a master regulator of breast cancer metastatic niche formation. *Proc Natl Acad Sci U S A,* 108**,** 16369-74.
WOOLSTON, C. & MARTIN, S. 2011. Analysis of tumor and endothelial cell viability and survival using sulforhodamine B and clonogenic assays. *Methods Mol Biol,* 740**,** 45-56.
WOOLSTON, C. M., ZHANG, L., STORR, S. J., AL-ATTAR, A., SHEHATA, M., ELLIS, I. O., CHAN, S. Y. & MARTIN, S. G. 2012. The prognostic and predictive power of redox protein expression for anthracycline-based chemotherapy response in locally advanced breast cancer. *Modern pathology : an official journal of the United States and Canadian Academy of Pathology, Inc,* 25**,** 1106-1116.
WORKMAN, P. 1994. Enzyme-directed bioreductive drug development revisited: a commentary on recent progress and future prospects with emphasis on quinone anticancer agents and quinone metabolizing enzymes, particularly DT-diaphorase. *Oncol Res,* 6**,** 461-75.

WOUTERS, A., PAUWELS, B., LARDON, F. & VERMORKEN, J. B. 2007. Review: implications of in vitro research on the effect of radiotherapy and chemotherapy under hypoxic conditions. *Oncologist,* 12**,** 690-712.
WRANN, S., KAUFMANN, M. R., WIRTHNER, R., STIEHL, D. P. & WENGER, R. H. 2013. HIF mediated and DNA damage independent histone H2AX phosphorylation in chronic hypoxia. *Biol Chem,* 394**,** 519-28.
WRIGHT, W. D., SHAH, S. S. & HEYER, W. D. 2018. Homologous recombination and the repair of DNA double-strand breaks. *J Biol Chem,* 293**,** 10524-10535.
WU, D. & YOTNDA, P. 2011. Induction and testing of hypoxia in cell culture. *Journal of visualized experiments : JoVE***,** 2899.
WU, S. B. & WEI, Y. H. 2012. AMPK-mediated increase of glycolysis as an adaptive response to oxidative stress in human cells: implication of the cell survival in mitochondrial diseases. *Biochim Biophys Acta,* 1822**,** 233-47.
WU, Z. L., SOHL, C. D., SHIMADA, T. & GUENGERICH, F. P. 2006. Recombinant enzymes overexpressed in bacteria show broad catalytic specificity of human cytochrome P450 2W1 and limited activity of human cytochrome P450 2S1. *Mol Pharmacol,* 69**,** 2007-14.
WUST, P., HILDEBRANDT, B., SREENIVASA, G., RAU, B., GELLERMANN, J., RIESS, H., FELIX, R. & SCHLAG, P. M. 2002. Hyperthermia in combined treatment of cancer. *Lancet Oncol,* 3**,** 487-97.
WYKOFF, C. C., BEASLEY, N. J., WATSON, P. H., TURNER, K. J., PASTOREK, J., SIBTAIN, A.*, et al.* 2000. Hypoxia-inducible expression of tumor-associated carbonic anhydrases. *Cancer Res,* 60**,** 7075-83.
XIAO, W., ZHENG, S., YANG, A., ZHANG, X., ZOU, Y., TANG, H. & XIE, X. 2018. Breast cancer subtypes and the risk of distant metastasis at initial diagnosis: a population-based study. *Cancer management and research,* 10**,** 5329-5338.
XIN, L., LIU, Y.-H., MARTIN, T. A. & JIANG, W. G. 2017. The Era of Multigene Panels Comes? The Clinical Utility of Oncotype DX and MammaPrint. *World journal of oncology,* 8**,** 34-40.
YAKKUNDI, A., MCERLANE, V., MURRAY, M., MCCARTHY, H. O., WARD, C., HUGHES, C. M.*, et al.* 2006. Tumor-selective drug activation: a GDEPT approach utilizing cytochrome P450 1A1 and AQ4N. *Cancer Gene Ther,* 13**,** 598-605.
YEO, B., TURNER, N. C. & JONES, A. 2014. An update on the medical management of breast cancer. *Bmj,* 348**,** g3608.
YERSAL, O. & BARUTCA, S. 2014. Biological subtypes of breast cancer: Prognostic and therapeutic implications. *World journal of clinical oncology,* 5**,** 412-424.
YILDIRIM, E., DALGIC, T. & BERBEROGLU, U. 2000. Prognostic significance of young age in breast cancer. *J Surg Oncol,* 74**,** 267-72.
YOSHIOKA, H., KASAI, N., IKUSHIRO, S., SHINKYO, R., KAMAKURA, M., OHTA, M., INOUYE, K. & SAKAKI, T. 2006. Enzymatic properties of human CYP2W1 expressed in Escherichia coli. *Biochem Biophys Res Commun,* 345**,** 169-74.
YOU, Z., BAILIS, J. M., JOHNSON, S. A., DILWORTH, S. M. & HUNTER, T. 2007. Rapid activation of ATM on DNA flanking double-strand breaks. *Nat Cell Biol,* 9**,** 1311-8.
YOULDEN, D. R., CRAMB, S. M., DUNN, N. A. M., MULLER, J. M., PYKE, C. M. & BAADE, P. D. 2012. The descriptive epidemiology of female breast cancer: An international comparison of screening, incidence, survival and mortality. *Cancer Epidemiology,* 36**,** 237-248.
YU, B., SHAH, A., WANG, B., RAJARAM, N., WANG, Q., RAMANUJAM, N., PALMER, G. M. & DEWHIRST, M. W. 2014. Measuring tumor cycling hypoxia and angiogenesis using a side-firing fiber optic probe. *Journal of biophotonics,* 7**,** 552-564.

ZABICKI, K., COLBERT, J. A., DOMINGUEZ, F. J., GADD, M. A., HUGHES, K. S., JONES, J. L., SPECHT, M. C., MICHAELSON, J. S. & SMITH, B. L. 2006. Breast cancer diagnosis in women < or = 40 versus 50 to 60 years: increasing size and stage disparity compared with older women over time. *Ann Surg Oncol,* 13**,** 1072-7.

ZANGER, U. M. & SCHWAB, M. 2013. Cytochrome P450 enzymes in drug metabolism: Regulation of gene expression, enzyme activities, and impact of genetic variation. *Pharmacology & Therapeutics,* 138**,** 103-141.

ZANGER, U. M., TURPEINEN, M., KLEIN, K. & SCHWAB, M. 2008. Functional pharmacogenetics/genomics of human cytochromes P450 involved in drug biotransformation. *Anal Bioanal Chem,* 392**,** 1093-108.

ZANNELLA, V. E., DAL PRA, A., MUADDI, H., MCKEE, T. D., STAPLETON, S., SYKES, J.*, et al.* 2013. Reprogramming metabolism with metformin improves tumor oxygenation and radiotherapy response. *Clin Cancer Res,* 19**,** 6741-50.

ZANOTTI, L., BOTTINI, A., ROSSI, C., GENERALI, D. & CAPPELLETTI, M. R. 2014. Diagnostic tests based on gene expression profile in breast cancer: from background to clinical use. *Tumour Biol,* 35**,** 8461-70.

ZARDAVAS, D. & PICCART, M. 2015. Neoadjuvant therapy for breast cancer. *Annu Rev Med,* 66**,** 31-48.

ZHANG, C., WANG, S., ISRAEL, H. P., YAN, S. X., HOROWITZ, D. P., CROCKFORD, S.*, et al.* 2015a. Higher locoregional recurrence rate for triple-negative breast cancer following neoadjuvant chemotherapy, surgery and radiotherapy. *SpringerPlus,* 4**,** 386-386.

ZHANG, K., KEYMEULEN, S., NELSON, R., TONG, T. R., YUAN, Y.-C., YUN, X.*, et al.* 2018. Overexpression of Flap Endonuclease 1 Correlates with Enhanced Proliferation and Poor Prognosis of Non–Small-Cell Lung Cancer. *The American Journal of Pathology,* 188**,** 242-251.

ZHANG, Q., GU, J., LI, L., LIU, J., LUO, B., CHEUNG, H. W.*, et al.* 2009. Control of cyclin D1 and breast tumorigenesis by the EglN2 prolyl hydroxylase. *Cancer Cell,* 16**,** 413-24.

ZHANG, S. M., LEE, I. M., MANSON, J. E., COOK, N. R., WILLETT, W. C. & BURING, J. E. 2007. Alcohol consumption and breast cancer risk in the Women's Health Study. *Am J Epidemiol,* 165**,** 667-76.

ZHANG, T., SHEN, Y., CHEN, Y., HSIEH, J. T. & KONG, Z. 2015b. The ATM inhibitor KU55933 sensitizes radioresistant bladder cancer cells with DAB2IP gene defect. *Int J Radiat Biol,* 91**,** 368-78.

ZHANG, X., WU, X., SU, P., GAO, Y., MENG, B., SUN, Y., LI, L., ZHOU, Z. & ZHOU, G. 2012. Doxorubicin Influences the Expression of Glucosylceramide Synthase in Invasive Ductal Breast Cancer. *PLOS ONE,* 7**,** e48492.

ZHANG, Y., STORR, S. J., JOHNSON, K., GREEN, A. R., RAKHA, E. A., ELLIS, I. O., MORGAN, D. A. & MARTIN, S. G. 2014. Involvement of metformin and AMPK in the radioresponse and prognosis of luminal versus basal-like breast cancer treated with radiotherapy. *Oncotarget,* 5**,** 12936-49.

ZHAO, Y., WAN, D., YANG, J., HAMMOCK, B. D. & ORTIZ DE MONTELLANO, P. R. 2016. Catalytic Activities of Tumor-Specific Human Cytochrome P450 CYP2W1 Toward Endogenous Substrates. *Drug Metabolism and Disposition,* 44**,** 771-780.

ZOU, L. & ELLEDGE, S. J. 2003. Sensing DNA damage through ATRIP recognition of RPA-ssDNA complexes. *Science,* 300**,** 1542-8.

ZOU, Y., LIU, Y., WU, X. & SHELL, S. M. 2006. Functions of human replication protein A (RPA): from DNA replication to DNA damage and stress responses. *Journal of cellular physiology,* 208**,** 267-273.

ZUO, T., ZENG, H., LI, H., LIU, S., YANG, L., XIA, C.*, et al.* 2017. The influence of stage at diagnosis and molecular subtype on breast cancer patient survival: a hospital-based multi-center study. *Chinese journal of cancer,* 36**,** 84-84.

Appendix A: Supplementary information for Chapter 2

Table A1 Pathological and molecular features of breast cancer cell lines.

Cell line	Cell type	Pathology	P53 status	BRCA-1 status	ER	PgR	HER-2	Molecular Classification
MCF-7	Epithelial	Ductal Carcinoma	WT	WT	+	+	-	Luminal
T47D	Epithelial	Ductal Carcinoma	Mutated	WT	+	+	-	Luminal
MDAMB-231	Epithelial	Adeno-Carcinoma	Mutated	WT	-	-	-	Basal-like/ triple-negative
MDAMB-468	Epithelial	Adeno-Carcinoma	Mutated	WT	-	-	-	Basal-like/ triple-negative
MDAMB-436	Pleomorphic, multinucleated	Adeno-Carcinoma	Mutated	Mutated	-	-	-	Basal-like/ triple-negative

Abbreviations: WT, wild-type; +, positive; -, negative; ER, estrogen receptor; PgR, progesterone receptor; HER-2, human epidermal growth factor receptor - 2. Data adapted from (Dai et al., 2017).

Table A2 Cell culture media formulations for cell lines.

Cell line	Reagent	Source	Volume
MCF7	RPMI-1640 medium	R8758, Sigma, UK	500 ml
	Heat Inactivated Iron Supplemented Donor Calf Serum	Gibco, Life Technologies, UK	50 ml
	Penicillin/Streptomycin (with 10,000 units penicillin and 10 mg streptomycin/mL)	P4333, Sigma, UK	5 ml
T47D	Dulbecco's Modified Eagle's Medium - high glucose (with 4500 mg/L glucose, L-glutamine, and sodium bicarbonate, without sodium pyruvate)	D5796, Sigma, UK	500 ml
	Heat Inactivated Iron Supplemented Donor Calf Serum	Gibco, Life Technologies, UK	50 ml
	Penicillin/Streptomycin (with 10,000 units penicillin and 10 mg streptomycin/mL)	P4333, Sigma, UK	5 ml
MDAMB-231 & MDAMB-468	Minimum essential medium eagle (MEM) (with Earle's salts, nonessential amino acids and sodium bicarbonate, without L-glutamine)	M2279, Sigma, UK	500 ml
	Heat Inactivated Iron Supplemented Donor Calf Serum	Gibco, Life Technologies, UK	50 ml
	Penicillin/Streptomycin (with 10,000 units penicillin and 10 mg streptomycin/mL)	P4333, Sigma, UK	5 ml
	L-Glutamine (200 mM)	G7513, Sigma, UK	5 ml
	MEM Non-essential amino acids solution (100x)	M7145, Sigma, UK	5 ml
MDAMB-436	DMEM/F12 HEPES (with L-Glutamine and 15mM HEPES)	31330, Invitrogen, UK	500 ml
	Heat Inactivated Iron Supplemented Donor Calf Serum	Gibco, Life Technologies, UK	5 ml
	Penicillin/Streptomycin (with 10,000 units penicillin and 10 mg streptomycin/mL)	P4333, Sigma, UK	5 ml

Abbreviations: ml - millilitres.

A1 Optimisation experiments for RPA assessment by immunofluorescence

In order to assess the optimum ionising radiation dose for RPA expression, MDAMB-231 and T47D cells were trypsinized, and seeded at a density of $2x10^4$ cells onto coated sterile coverslips (Corning™ BioCoat™) in 6-well plates and allowed to adhere overnight. The following day, cells were irradiated at 0.5, 1 or 1.5 Gy of IR. At 1 hour post-radiation exposure, cells were fixed with 4% paraformaldehyde for 10-20 minutes. Following which, cells were permeabilized and blocked in 0.3% Triton X-100 with 2% serum for 30 minutes at room temperature. Cells were stained with the primary anti-RPA (1:200, Abcam) and incubated overnight at 4°C. The following day, cells were treated with Alexa 488-conjugated goat anti-mouse secondary antibody (1:200 dilution, Abcam) for 1 hour in the dark, followed by 2-3 washes in 0.05% PBS-Tween-20 buffer. Nuclei were counterstained with Vectashield containing DAPI (Vector). Imaging was performed at x63 magnification on a confocal microscope (Leica TCS SPE). The number of RPA or γ-H2AX foci per nuclei was counted using ImageJ software and 100 nuclei were analysed for each treatment condition.

As shown in Figure A1, exposure to ionising radiation significantly increased RPA expression in both T47D and MDAMB-231 cells. A dose of 1 Gy resulted in average RPA foci of 51±9.3/nucleus in T47D (P=0.052) and 53±0.8/nucleus in MDAMB-231 (P=0.0009) cells. At 1.5 Gy, T47D cells demonstrated average RPA foci of 52±8.4/nucleus (P=0.041) and MDAMB-231 cells with 95±13.2/nucleus (P=0.020). Based on data obtained, a dose of 1 Gy was considered suitable to assess RPA expression for ease of counting since higher doses would increase the number of RPA foci.

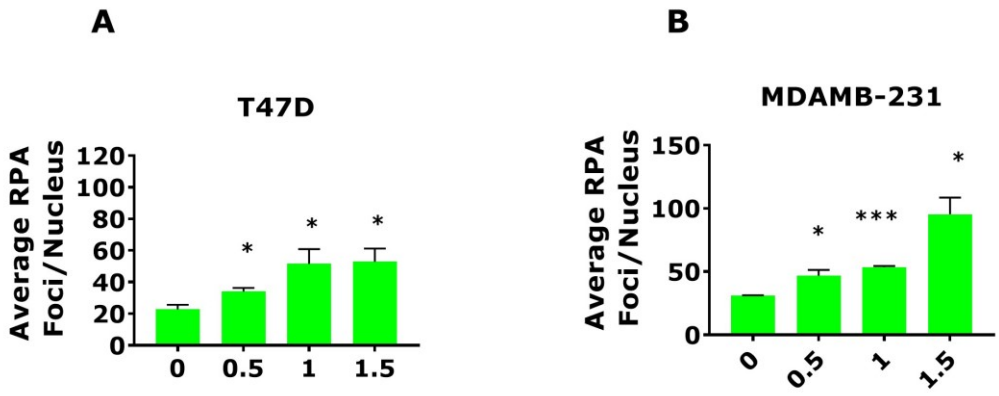


Figure A1 Quantification of RPA foci in irradiated breast cancer cells. (A) T47D and (B) MDAMB-231 cells were treated with (0.5, 1 or 1.5) Gy of IR prior to assessing RPA expression by immunofluorescence. Figures show the average number of RPA foci/nucleus after 1 Gy irradiation. 100 cells were analysed for each case. Data represent the mean ± SD of two independent experiments. One-way ANOVA test was used to calculate statistics. **P*<0.05, ***P*<0.01, ****P*<0.001.

After dose selection of 1Gy, RPA expression was assessed at various time-points to assess time-post irradiation at which RPA expression was maximum. Cells were treated as mentioned above and fixed at required time points of (0, 0.5, 2, 4, 6 and 24) hours. As seen in Figure A2, both T47D and MDAMB-231 cells expressed highest levels in RPA expression at 0.5 hours post-IR exposure.

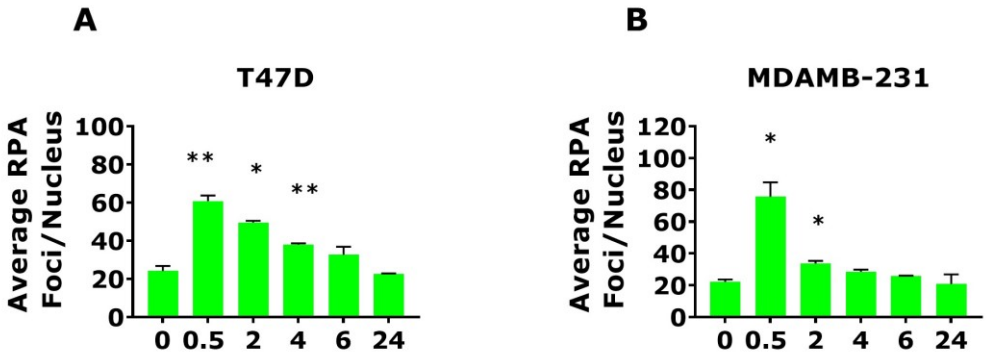


Figure A2 Quantification of RPA foci at various time-points. (A) T47D and (B) MDAMB-231 cells were irradiated at 1Gy ionising radiation prior to assessing RPA expression at 0.5, 2, 4, 6 and 24 hours. Figures show the average number of RPA foci/nucleus after 1 Gy irradiation. 100 cells were analysed for each case. Data represent the mean ± SD of two independent experiments. One-way ANOVA test was used to calculate statistics. **P*<0.05, ***P*<0.01, ****P*<0.001.

The average foci/nucleus at 0.5 hours, were 60±2.9 in T47D (*P*=0.005) and 75±9.1 in MDAMB-231 (*P*=0.023) cells. Therefore all PTPD radiation

combination experiments were carried out at 1 Gy of IR, after which RPA expression was assessed at 0.5 hours post-IR exposure.

A2 Optimisation experiment for γH2AX expression by flow cytometry

In order to identify the optimal dose of IR for γH2AX expression, MDAMB-231 cells were irradiated with various doses of IR and levels of γH2AX was assessed at various time-points using flow cytometry analysis. 1×10^5 cells were plated in 6-well plates and incubated overnight to allow cell adherence. The following day, cells were irradiated at different doses (1, 2 or 4 Gy), or sham irradiated, and harvested at required time points of (0, 0.5, 1, 2, 4, 6 and 24) hours. Cells were trypsinized and pelleted by centrifugation at 200 x g for 5 minutes. Following wash with PBS for 2 x 5 minutes, cells were treated according to manufacturer's instructions for γH2AX detection (H2AX phosphorylation kit – 17-344, Merck Millipore). Briefly, cells were fixed in fixation buffer for 20 minutes, followed by permeabilization with kit supplied buffer. γH2AX antibody conjugated with FITC was added to test samples and incubated for 20 minutes on ice. Kit supplied normal mouse antibody conjugated with FITC was used as the isotype control. Following wash, cells were resuspended in 500 µl PBS and transferred to FACS tubes for analysis. For all flow cytometry assays, acquisition of >20,000 events was performed using a MACSQuant Analyser Miltenyi Biotech. Data for FACS was analysed using FlowJo 7.6.1 (Tree Star, Ashland, USA). Data presented graphically in Figure A3 represents mean fluorescence intensity (MFI) of 2 independent experiments.

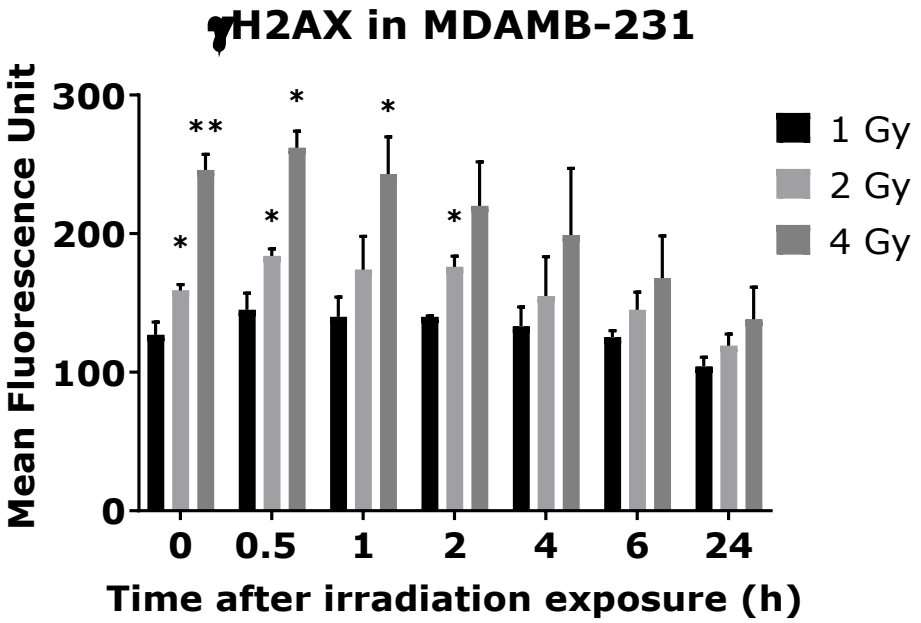


Figure A3. Quantification of γH2AX expression induced by ionising radiation. Bar graphs depicting γ-H2AX expression in MDAMB-231 cells at various time-points (0, 0.5, 1, 2, 4, 6 and 24) hours post-ionising radiation exposure of 1, 2 and 4 Gy. Acquisition of 20,000 events was recorded by the MACSQuant flow cytometer. Data represent the MFI ± standard deviation (SD) of two independent experiments. One-way ANOVA test was used to calculate statistics. *P<0.05, **P<0.01, ***P<0.001.

As shown in Figure A3, all 3 doses of IR induced γH2AX expression with highest expression observed at 4 Gy. Cells irradiated with 4 Gy of IR showed higher mean levels of γH2AX fluorescence of 262 (P=0.010) at 0.5 hours compared to 125 and 184 observed in cells irradiated with 1 and 2 Gy respectively. In all 3 doses, maximum DNA damage was observed at 0-0.5 hour post-irradiation exposure. A rapid decline in DNA double strand break as assessed by γH2AX fluorescence was noted post-1 hour and at 24 hours the levels of γH2AX had declined to levels of untreated control cells (MFI of 138). Therefore, for PTPD radiation combination experiments, cells were irradiated at 4 Gy after which γH2AX expression was assessed at 0.5 hours post-IR exposure.

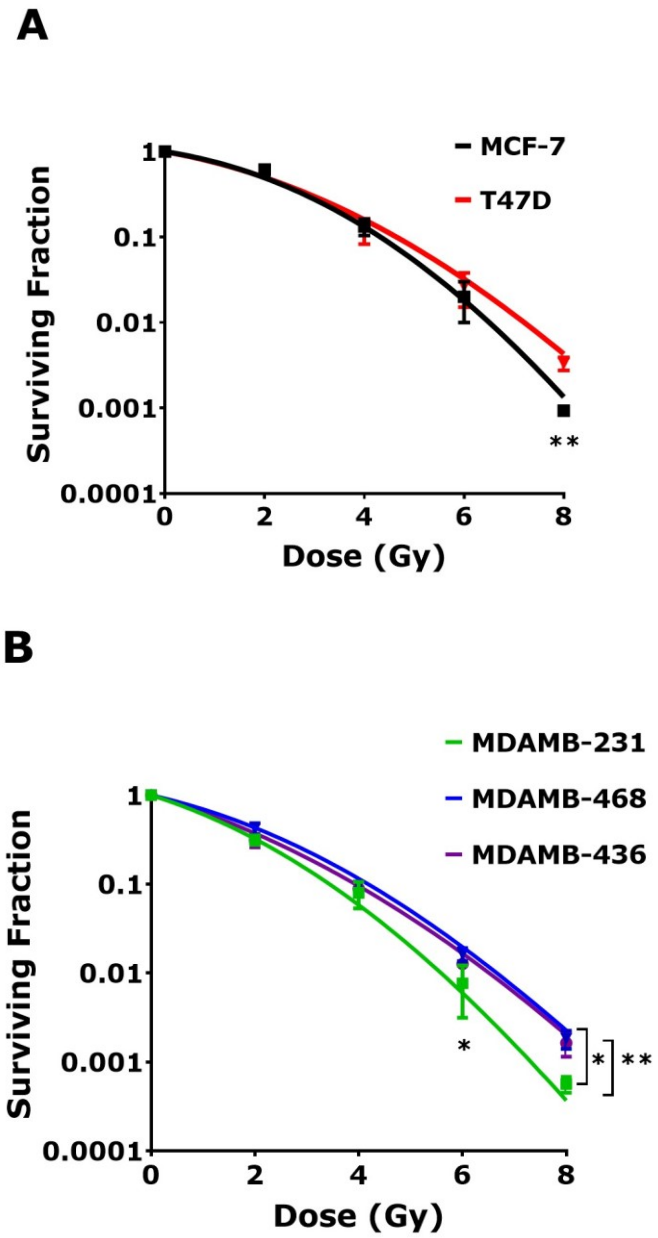


Figure A4 Survival curves of breast cancer cells after single dose irradiation. (A) Luminal breast cancer cells. (B) Triple negative breast cancer cells. The PEs of individual cell lines were: MCF-7 - 45±4.72%; T47D - 15±2.64%; MDAMB-231 - 49±4.72%; MDAMB-468 - 44±2.08%; MDAMB-436 - 19±2.51%. Data represent the mean SF ± SD of three independent experiments, with each experiment containing six parallel data sets, which are analysed using the Student's t-test. *P<0.05, ** P<0.01 and ***P<0.001 for MCF-7 v T47D and MDAMB-231 v MDAMB-468 and MDAMB-436 cells.

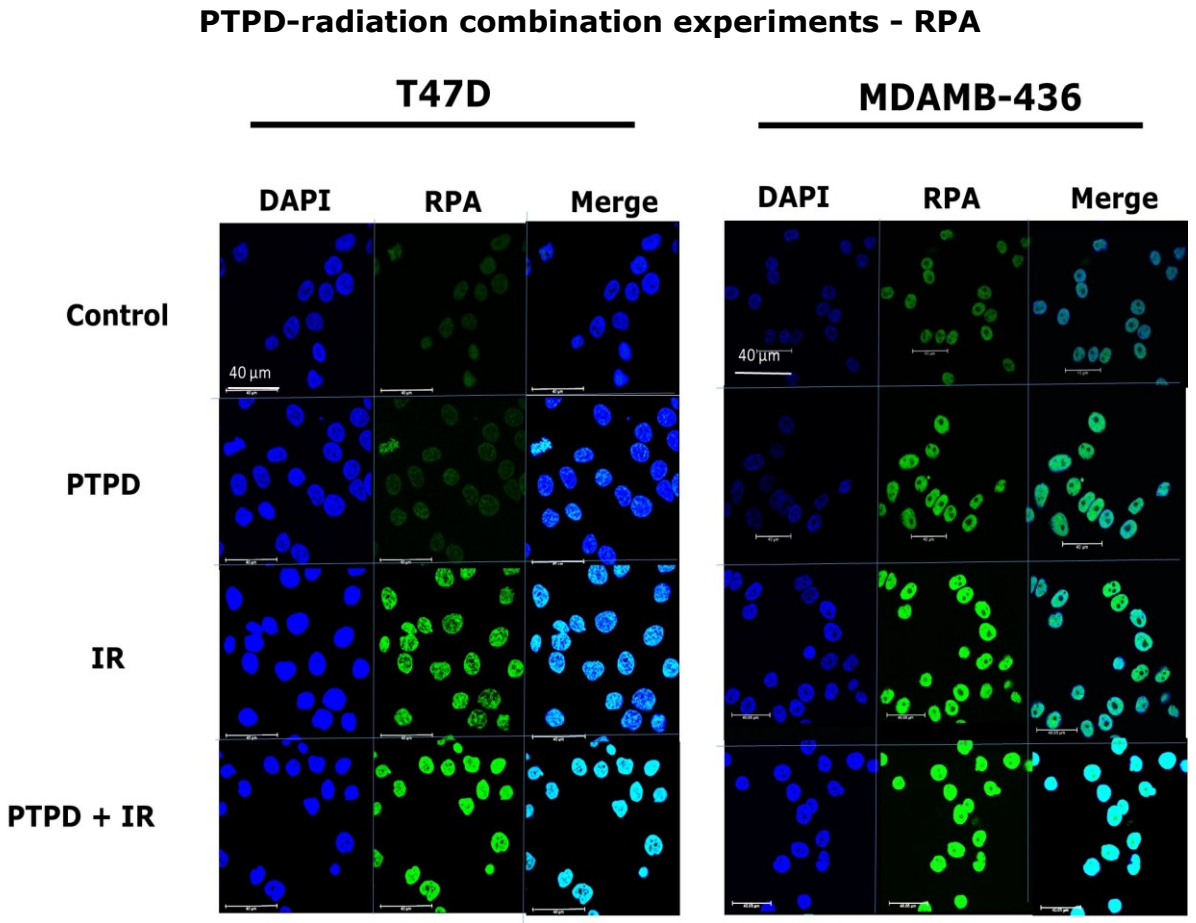


Figure A5. RPA foci formation in breast cancer cells following treatment with PTPD and/or radiation. Representative images of RPA immunofluorescent staining in T47D, MDAMB-436, MDAMB-231 and MDAMB-468 cells. 63x magnification. Blue-DAPI fluorescent stain. Green-RPA; Scale bar represents 40 µm.

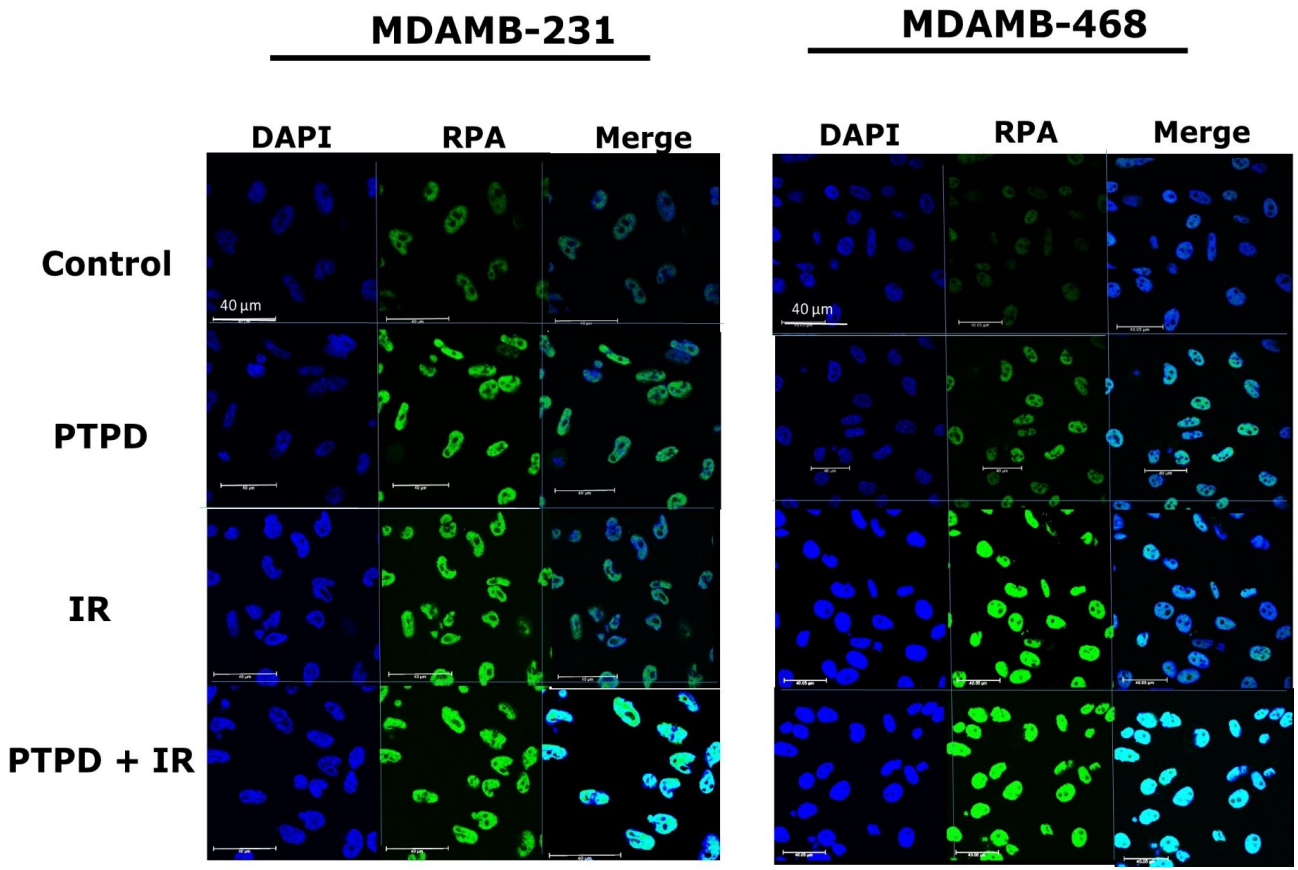


Figure A5. RPA foci formation in breast cancer cells following treatment with PTPD and/or radiation. Representative images of RPA immunofluorescent staining in T47D, MDAMB-436, MDAMB-231 and MDAMB-468 cells. 63x magnification. Blue-DAPI fluorescent stain. Green-RPA; Scale bar represents 40 µm.

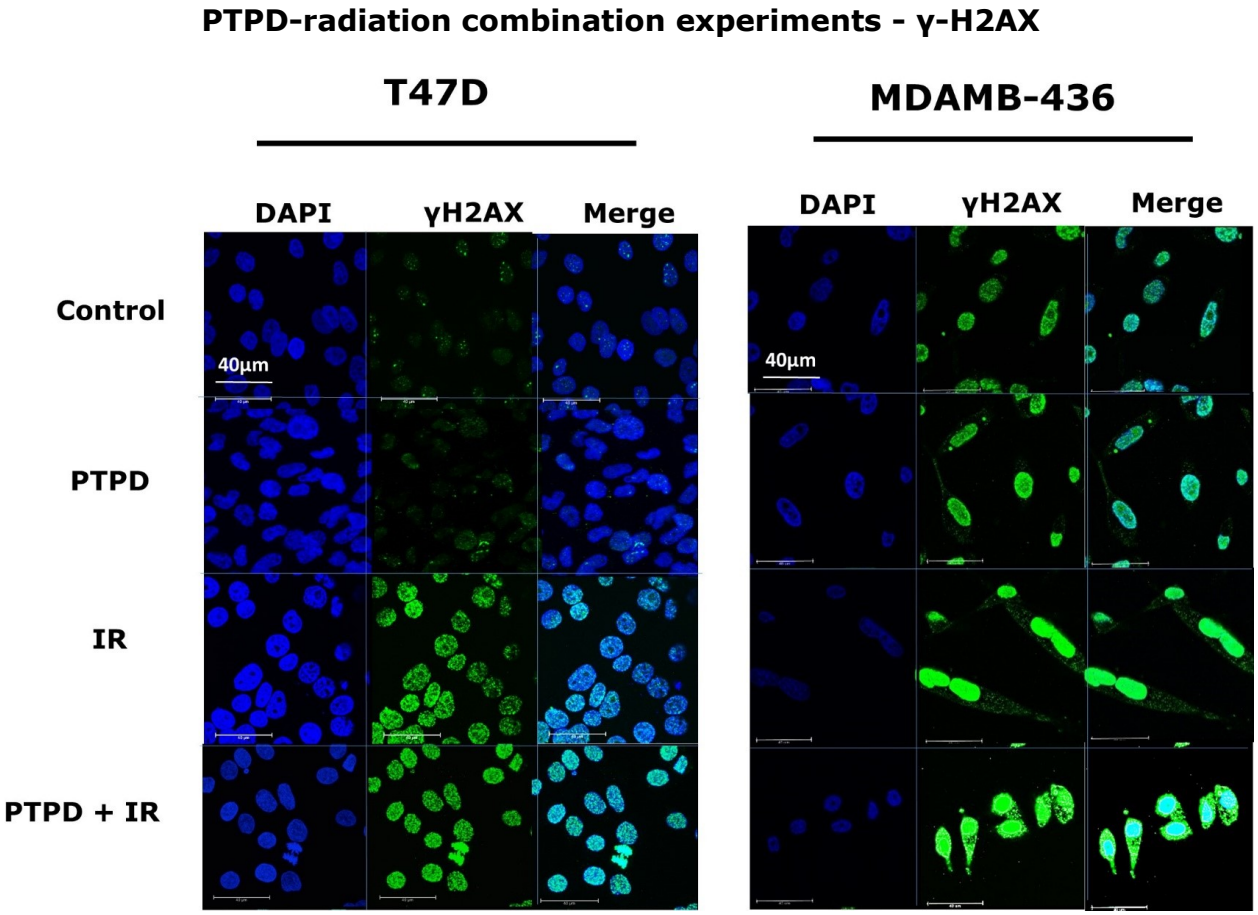


Figure A6. γ-H2AX foci formation in breast cancer cells following treatment with PTPD and/or radiation. Representative images of γ-H2AX immunofluorescent staining in T47D, MDAMB-436, MDAMB-231 and MDAMB-468 cells. 63x magnification. Blue-DAPI fluorescent stain. Green - γ-H2AX; Scale bar represents 40 µm.

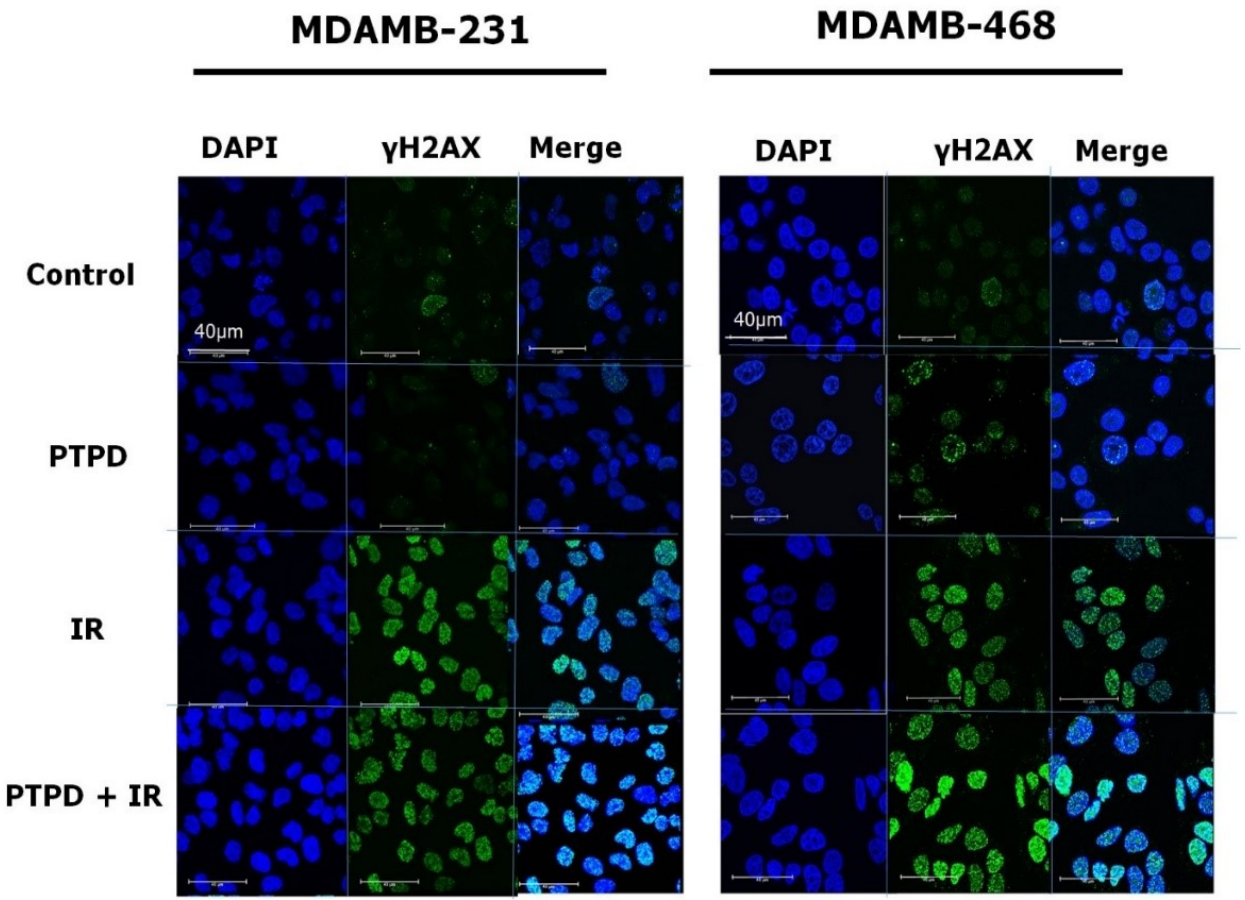


Figure A6. γ-H2AX foci formation in breast cancer cells following treatment with PTPD and/or radiation. Representative images of γ-H2AX immunofluorescent staining in T47D, MDAMB-436, MDAMB-231 and MDAMB-468 cells. 63x magnification. Blue-DAPI fluorescent stain. Green - γ-H2AX; Scale bar represents 40 μm.

Appendix B: Supplementary information for Chapter 3

Table B1 Pathological and molecular features of MCF-10A cells.

Cell line	Cell types	Pathology	P53 status	BRCA-1 status	ER	PgR	HER-2	Molecular Classification
MCF-10A	Epithelial	Fibrocystic disease Non-tumorigenic	WT	WT	-	-	-	Basal-like/ triple negative

Abbreviations: WT, wild-type; -, negative; ER, estrogen receptor; PgR, progesterone receptor; HER -2, human epidermal growth factor receptor - 2.

Table B2 Cell culture media formulation for MCF-10A cells.

Cell line	Reagent	Source	Volume
MCF-10A	DMEM/F12 HEPES (with L-Glutamine and 15mM HEPES)	31330, Invitrogen, UK	500 ml
	Heat Inactivated Horse Serum	H1138, Sigma, UK	12.5 ml
	Penicillin/Streptomycin (with 10,000 units penicillin and 10 mg streptomycin/mL)	P4333, Sigma, UK	5 ml
	Hydrocortisone (5mg/ml)	H0888, Sigma, UK	50 µl
	Cholera Toxin (1mg/ml)	C8052, Sigma, UK	50 µl
	Insulin bovine pancreas (5mg/ml)	16634, Sigma, UK	1 ml
	EGF (100µg/ml)	E1257, Sigma, UK	100 µl

Abbreviations: µl – microliters, ml - millilitres.

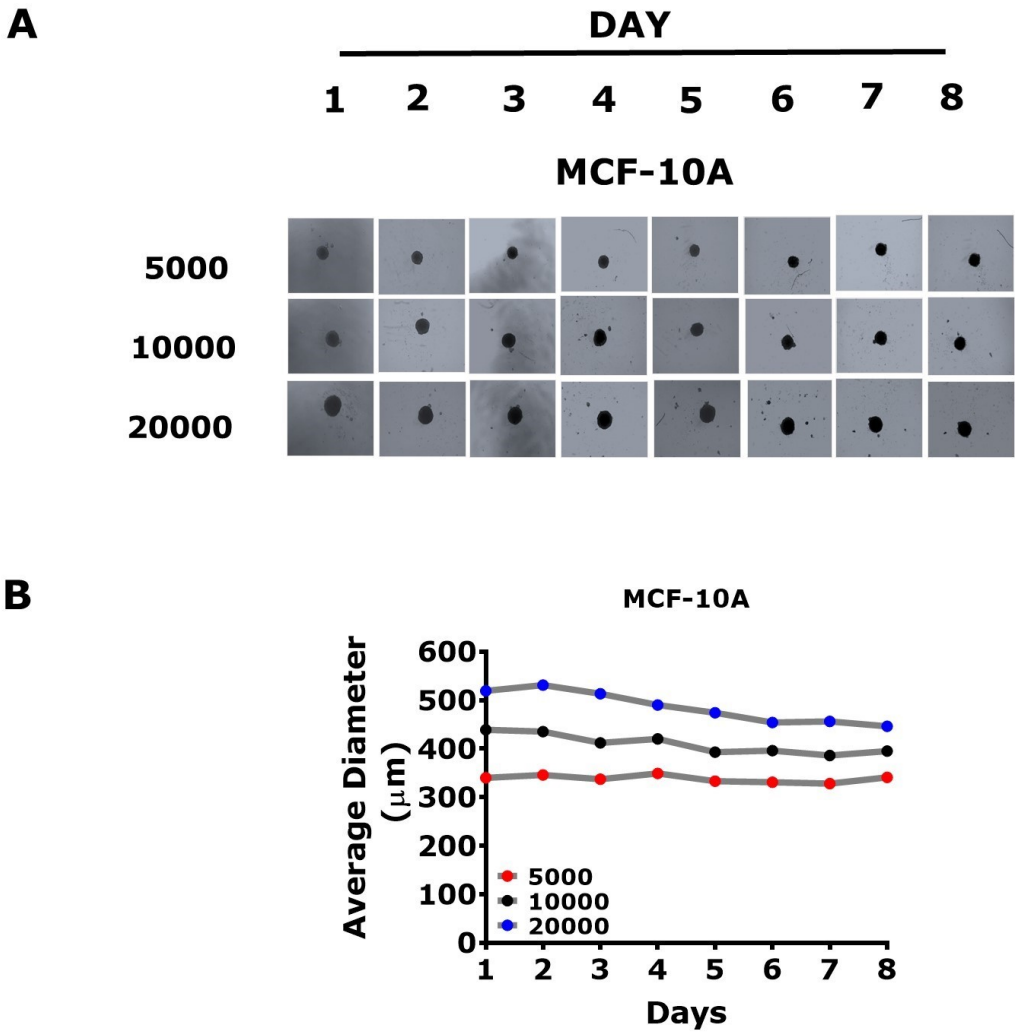


Figure B1 Morphology of MCF-10A spheroids. (A) Representative phase contrast micrographs from Day 1 to 8 with seeding density of 5000, 10,000 and 20,000 cells/well in 96-well ultra-low attachment plates (10x magnification). (B) Measurement of spheroid diameter over an 8-day culture. Each point represents the average diameter calculated from measurements of 6 spheroids of one experiment.

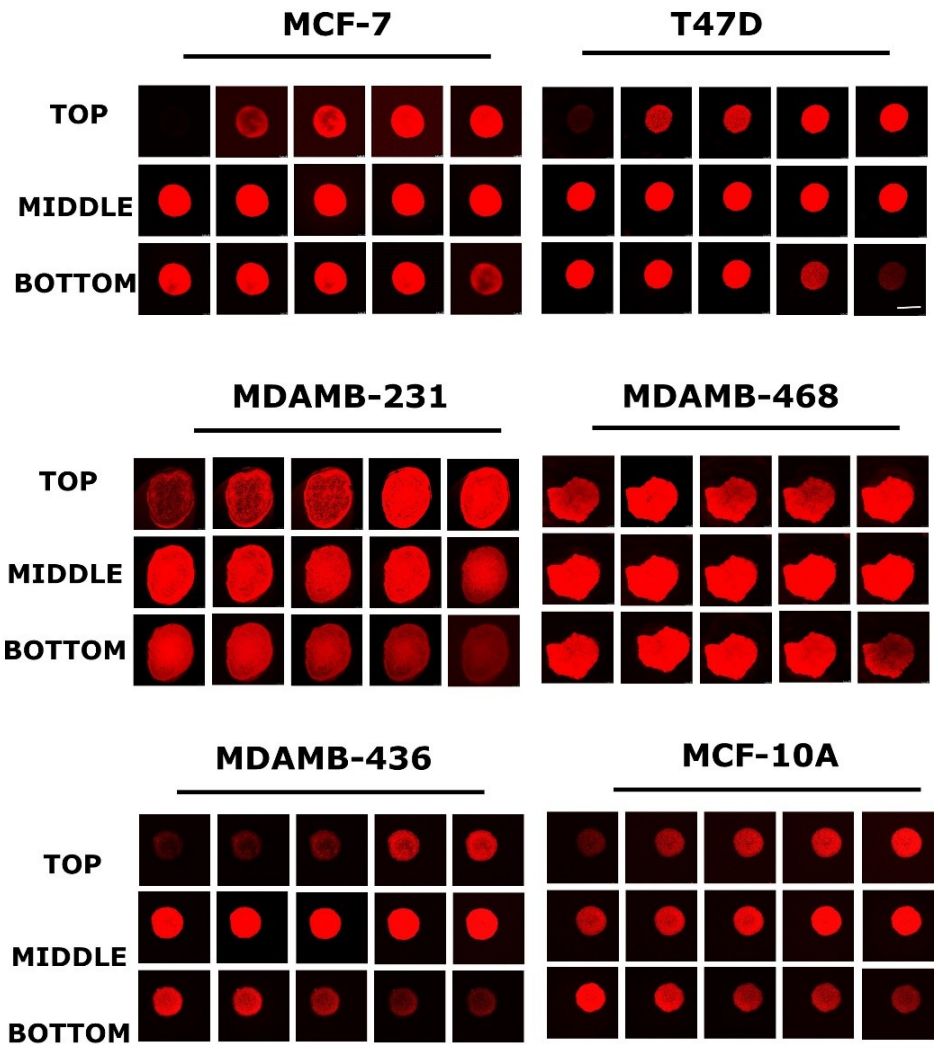


Figure B2 Doxorubicin penetration in breast cancer spheroids. Confocal microscope representative images of spheroid cross-sections (10x magnification, step size 15 μm) are shown above. Experiment was conducted once, containing 30 spheroids. Scale bar represents 200 μm.

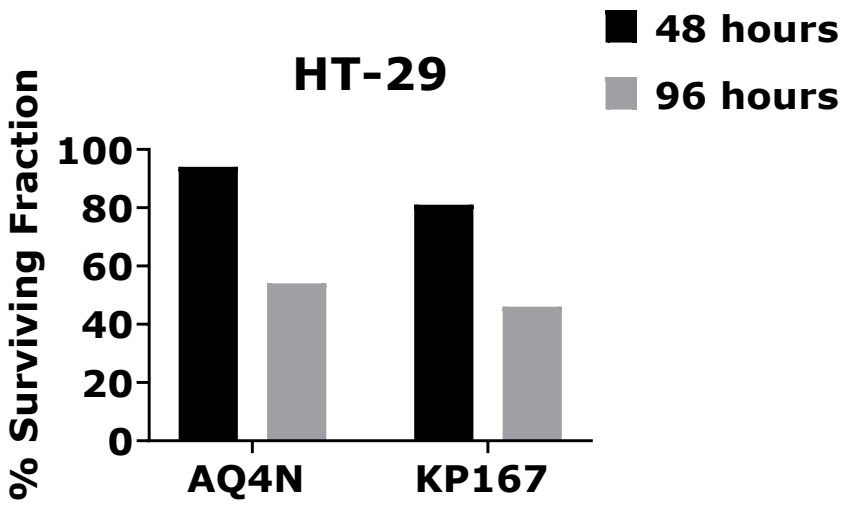


Figure B3 Effect of AQ4N and KP167 on clonogenic survival of HT-29 cells. SF obtained after treatment is shown against the corresponding treatment. PEs of HT-29 cells were 53±4.35%. Data obtained from one independent experiment performed in triplicate.

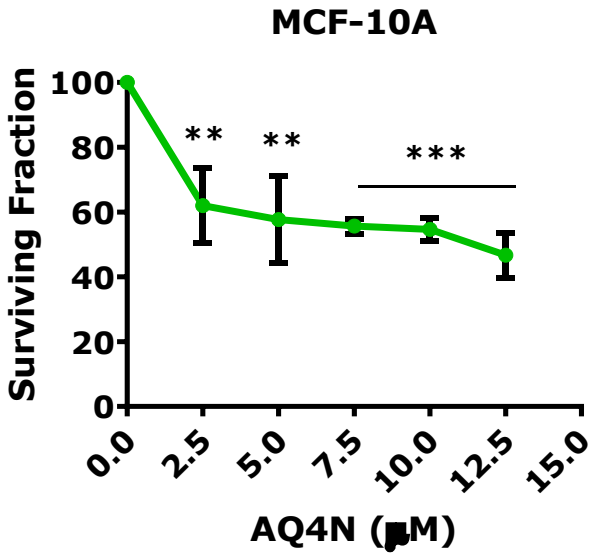


Figure B4 Effect of AQ4N on clonogenic survival of MCF-10A spheroids. PE - 65 ± 4.44%. Data represent the mean ± SD of three independent experiments, with each experiment containing six parallel data sets which are analysed using the Student's *t*-test. **P*<0.05, ***P*<0.01, ****P*<0.001 for control v AQ4N.

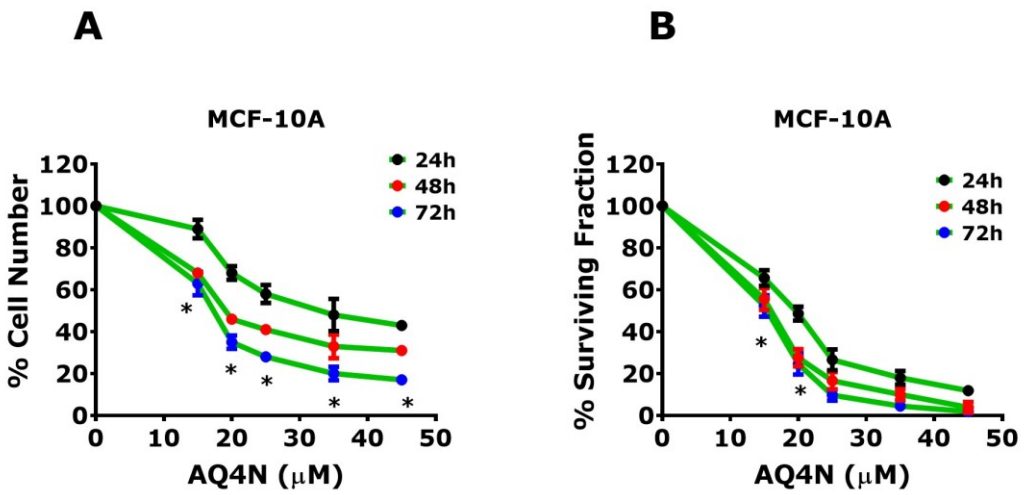


Figure B5 Effect of AQ4N on cell proliferation and clonogenic survival of MCF-10A cells in 2D normoxia. PE of cells were 65±4.44%. Data represent the mean ± SD of three independent experiments, with each experiment containing six parallel data sets, which are analysed using Student's *t*-test. **P*<0.05 for 24 hours v 48 and 72 hours.

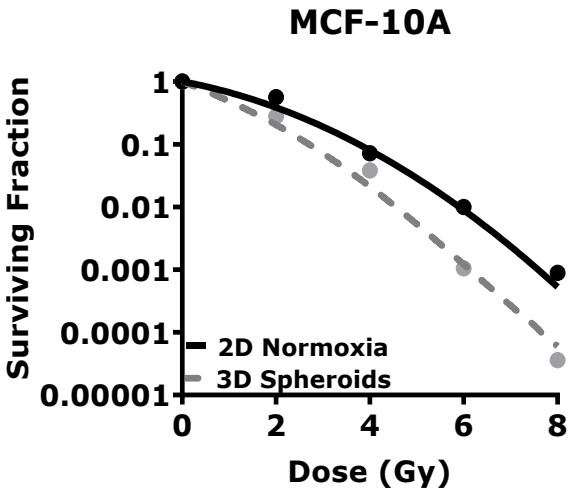


Figure B6 Radiation response of MCF-10A cells in 2D V 3D culture. PE for 2D and 3D cultures was 23±0.28% and 36% respectively. Data represent one independent experiment, containing six parallel data sets.

Table B3 Radiobiologic parameters of MCF-10A cells in 2D normoxia and 3D spheroid cultures.

Cell line	α (Gy^{-1})	β (Gy^{-2})	α/β (Gy)	SF2
MCF-10A				
2D Normoxia	0.31	0.07	4.07	0.38
3D Spheroids	0.65	0.07	16.79	0.20

Parameters were calculated from clonogenic data fitted to a linear quadratic model. Data represent one independent experiment. Abbreviations: IR, irradiation; SF2, surviving fraction at 2Gy.

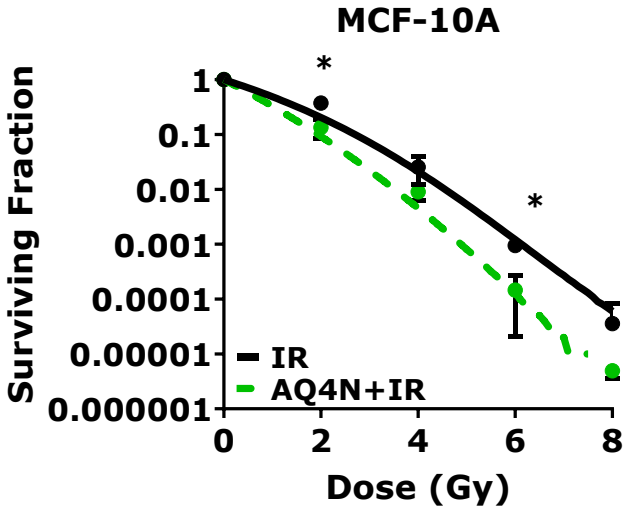


Figure B7 Effect of AQ4N on radiosensitivity of MCF-10A spheroids. PEs of cells were 36%. Data represent the mean SF ± SD of two independent experiments, with each experiment containing six parallel data sets, which are analysed using the Student's *t*-test. *P<0.05.

Table B4 Radiobiologic parameters of MCF-10A cells treated with IR and/or AQ4N.

Cell line Spheroids	α (Gy^{-1})	β (Gy^{-2})	α/β (Gy)	SF2	$SER_{(0.01)}$
MCF-10A					
IR	0.65±0.34	0.07±0.06	16.79±19.04	0.20±0.08	
AQ4N+IR	1.02±0.05	0.04±0.03	27.73±20.01	0.05±0.05	1.36±0.12
t test	*P*=0.273	*P*=0.650	*P*=0.631	*P*=0.163	

Statistical significance was determined by Student's *t*-test. The *P*-values are bold where they are ≤ 0.05. Abbreviations: IR, irradiation; $SER_{0.01}$, sensitiser enhancement ratio at 1% survival; SF2, surviving fraction at 2Gy.

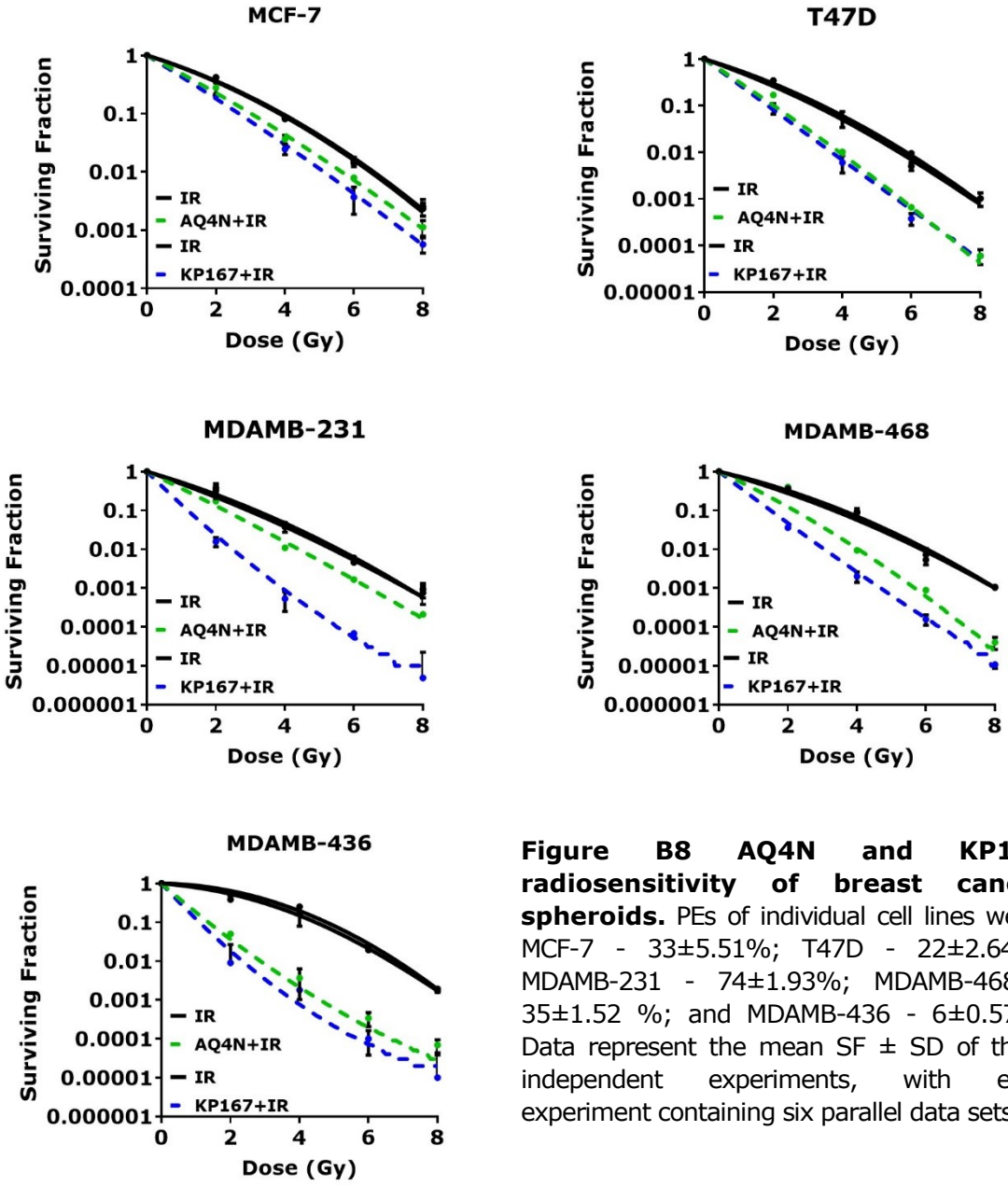


Figure B8 AQ4N and KP167 radiosensitivity of breast cancer spheroids. PEs of individual cell lines were: MCF-7 - 33±5.51%; T47D - 22±2.64%; MDAMB-231 - 74±1.93%; MDAMB-468 - 35±1.52 %; and MDAMB-436 - 6±0.57%. Data represent the mean SF ± SD of three independent experiments, with each experiment containing six parallel data sets.

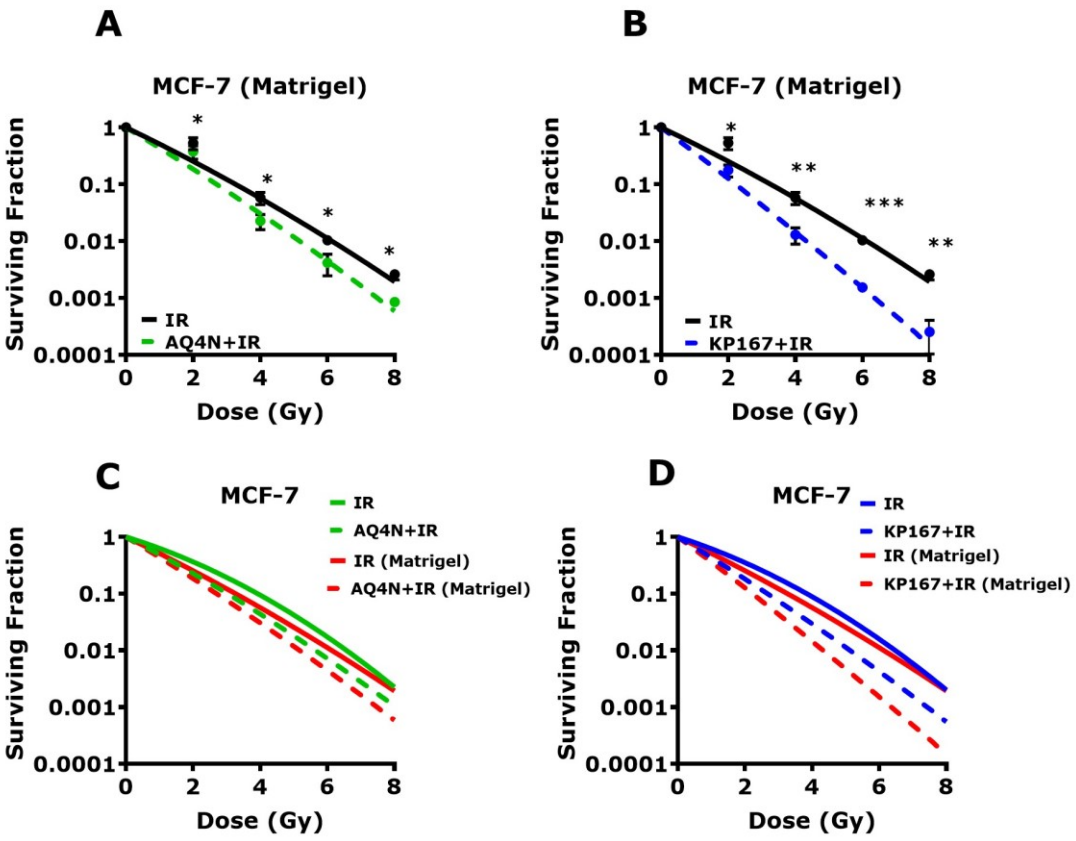


Figure B9 AQ4N and KP167 radiosensitivity of MCF-7 spheroids formed with matrigel. A) Effect of AQ4N on MCF-7+M. B) Effect of KP167 on MCF-7+M. C) Overlay of +/- Matrigel (AQ4N). D) Overlay of +/- Matrigel (KP167). PEs of MCF-7 cells were 30±1.52%. Data represent the mean SF ± SD of three independent experiments, with each experiment containing six parallel data sets, which are analysed using the Student's *t*-test. **P*<0.05, ***P*<0.01 and ****P*<0.001 for IR v AQ4N+IR or IR v KP167+IR.

Table B5 Radiobiologic parameters of MCF-7 (+ matrigel) cells treated with IR and AQ4N/KP167.

Cell line Spheroids	α (Gy^{-1})	β (Gy^{-2})	α/β (Gy)	SF2	SER (0.01)
MCF-7					
IR	0.65±0.05	0.01±0.01	44.15±17.91	0.25±0.02	
AQ4N+IR	0.81±0.09	0.01±0.01	117.34±140.66	0.18±0.02	1.20±0.06
t test	**P=0.05**	*P*=0.924	*P*=0.421	**P=0.029**	
MCF-7					
IR	0.65±0.05	0.01±0.01	44.15±17.91	0.25±0.02	
KP167+IR	1.01±0.04	0.01±0.01	184.16±187.05	0.12±0.01	1.47±0.10
t test	**P<0.001**	*P*=0.706	*P*=0.266	**P<0.001**	

Statistical significance was determined by Student's *t*-test. The *P*-values are bold where they are ≤ 0.05. Abbreviations: IR, irradiation; SF2, surviving fraction at 2Gy.

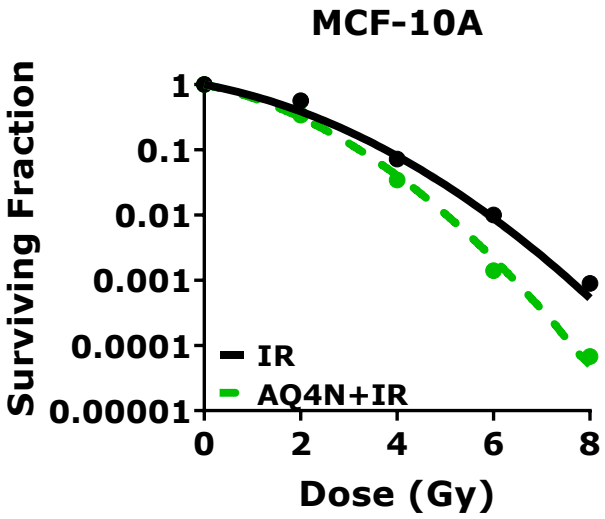


Figure B10 Effect of AQ4N radiosensitivity of MCF-10A in 2D normoxia. PE 23±0.28%. Data represent one experiment, with six parallel data sets.

Table B6 Radiobiologic parameters of MCF-10A cells treated with IR and/or AQ4N.

Cell line Normoxia	α (Gy^{-1})	β (Gy^{-2})	α/β (Gy)	SF2	$SER_{(0.01)}$
MCF-10A					
IR	0.31	0.07	4.07	0.38	1.15
AQ4N+IR	0.35	0.11	3.22	0.31	

Data represent one independent experiment. Abbreviations: IR, irradiation; $SER_{0.01}$, sensitiser enhancement ratio at 1% survival; SF2, surviving fraction at 2Gy.

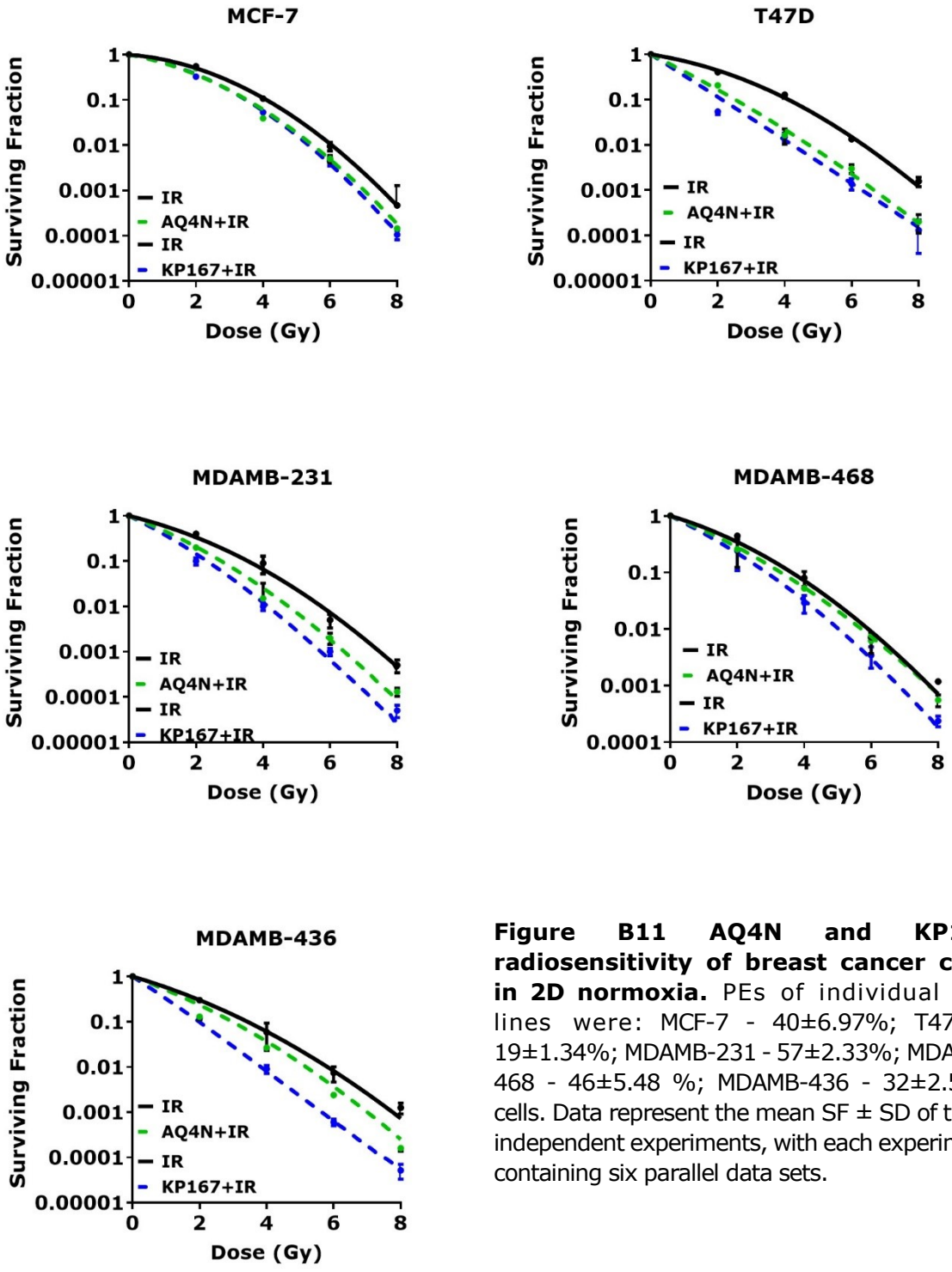


Figure B11 AQ4N and KP167 radiosensitivity of breast cancer cells in 2D normoxia. PEs of individual cell lines were: MCF-7 - 40±6.97%; T47D - 19±1.34%; MDAMB-231 - 57±2.33%; MDAMB-468 - 46±5.48 %; MDAMB-436 - 32±2.55% cells. Data represent the mean SF ± SD of three independent experiments, with each experiment containing six parallel data sets.

Appendix C: Supplementary information for Chapter 4

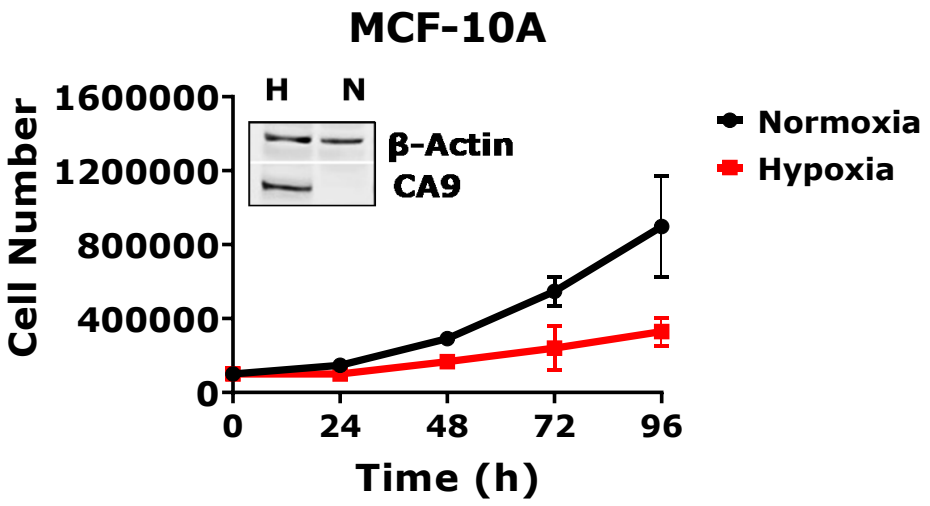


Figure C1 Effect of normoxia and hypoxia (1% O_2) on proliferation of MCF-10A cells. Inset image show representative blot for the expression of CA9 in normoxia (N) and hypoxia (H) cells with β-Actin used as a loading control. Data presented graphically represent the mean cell number/well ± SD of three independent experiments, with each experiment conducted in triplicate, which are analysed using the Student's t-test. P>0.05 for normoxia v hypoxia (not significant).

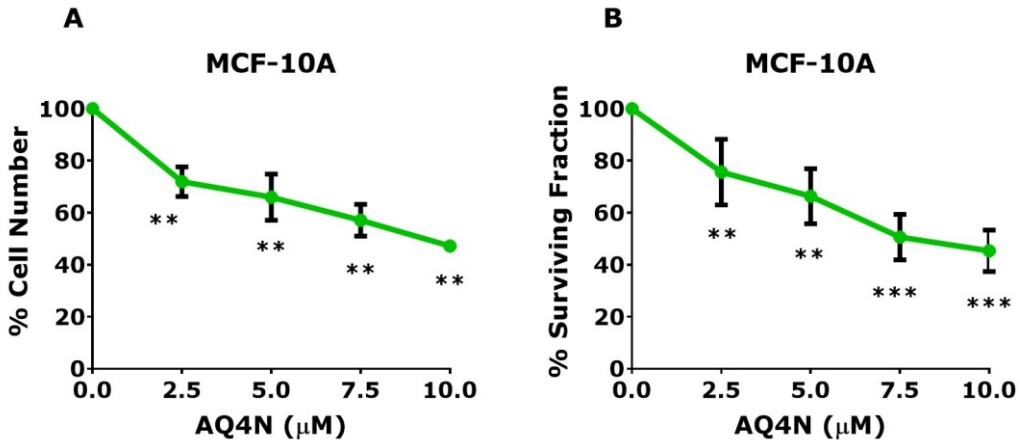


Figure C2 Effect of AQ4N on cell proliferation and clonogenic survival of MCF-10A cells (1% O_2). A) Effect on proliferation. B) Effect on clonogenic survival. PE was 30±2.24%. Data represent the mean ± SD of three independent experiments, with each experiment performed in triplicate.

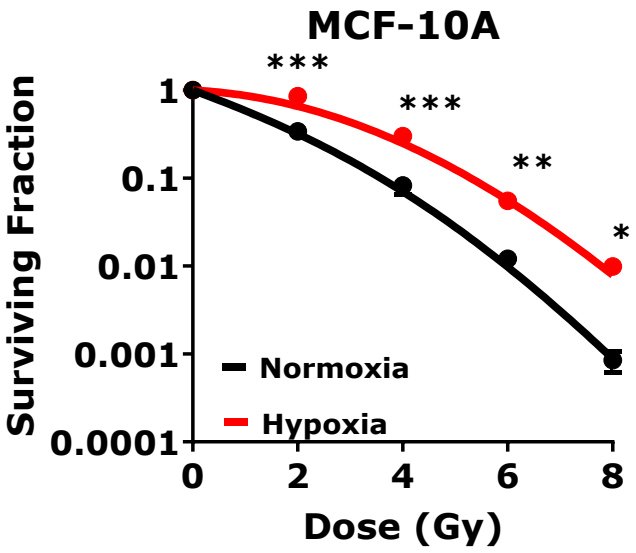


Figure C3 Radiation response of MCF-10A cells in 2D normoxia and hypoxia (1% O_2) culture conditions. PE under normoxia and hypoxia were 49±7.07% and 27±1.41% respectively. Data represent the mean SF ± SD of three independent experiments, with each experiment containing six parallel data sets, which are analysed using the Student's *t*-test. **P*<0.05, ***P*<0.01, ****P*<0.001 normoxia v hypoxia.

Table C1 Radiobiologic parameters of breast cancer cells in 2D normoxia and hypoxia cultures.

Cell line	α (Gy^{-1})	β (Gy^{-2})	α/β (Gy)	SF2	$OER_{(0.01)}$
MCF-10A					
2D Normoxia	0.50±0.26	0.04±0.03	15.9±11.72	0.31±0.14	
2D Hypoxia	0.06±0.03	0.07±0.01	1.04±0.48	0.65±0.04	1.55±0.16
t test	***P*=0.046**	*P*=0.281	*P*=0.092	***P*=0.016**	

Statistical significance was determined by Student's *t*-test. The *P*-values are bold where they are ≤ 0.05. Abbreviations: IR, irradiation; $OER_{0.01}$, oxygen enhancement ratio at 1% survival; SF2, surviving fraction at 2Gy.

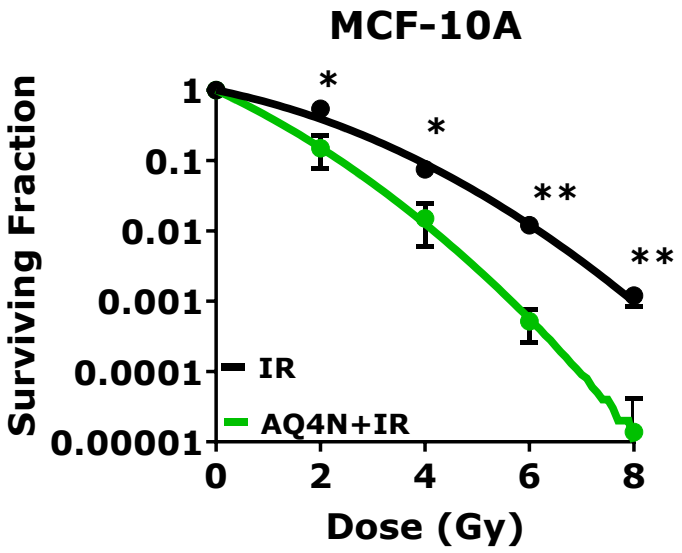


Figure C4 Effect of AQ4N on radiosensitivity of MCF-10A cells in 2D hypoxia (1% O_2). PE of MCF-10A was – 53±5.65%. Data represent the mean SF ± SD of three independent experiments, with each experiment containing six parallel data sets, which are analysed using the Student's *t*-test. **P*<0.05, ***P*<0.01 and ****P*<0.001 for IR v AQ4N+IR.

Table C2 Radiobiologic parameters of breast cancer cells in 2D hypoxia treated with IR and/or AQ4N.

Cell line	α (Gy^{-1})	β (Gy^{-2})	α/β (Gy)	SF2	$SER_{(0.01)}$
MCF-10A					
IR	0.34±0.06	0.06±0.01	5.20±1.35	0.39±0.04	
AQ4N+IR	0.78±0.25	0.09±0.01	8.37±2.91	0.15±0.07	1.71±0.32
t test	*P*=0.134	***P*=0.035**	*P*=0.224	*P*=0.063	

Statistical significance was determined by Student's *t*-test. The *P*-values are bold where they are ≤ 0.05. Abbreviations: IR, irradiation; $SER_{0.01}$, sensitiser enhancement ratio at 1% survival; SF2, surviving fraction at 2Gy.

Appendix D: Supplementary information for Chapter 5

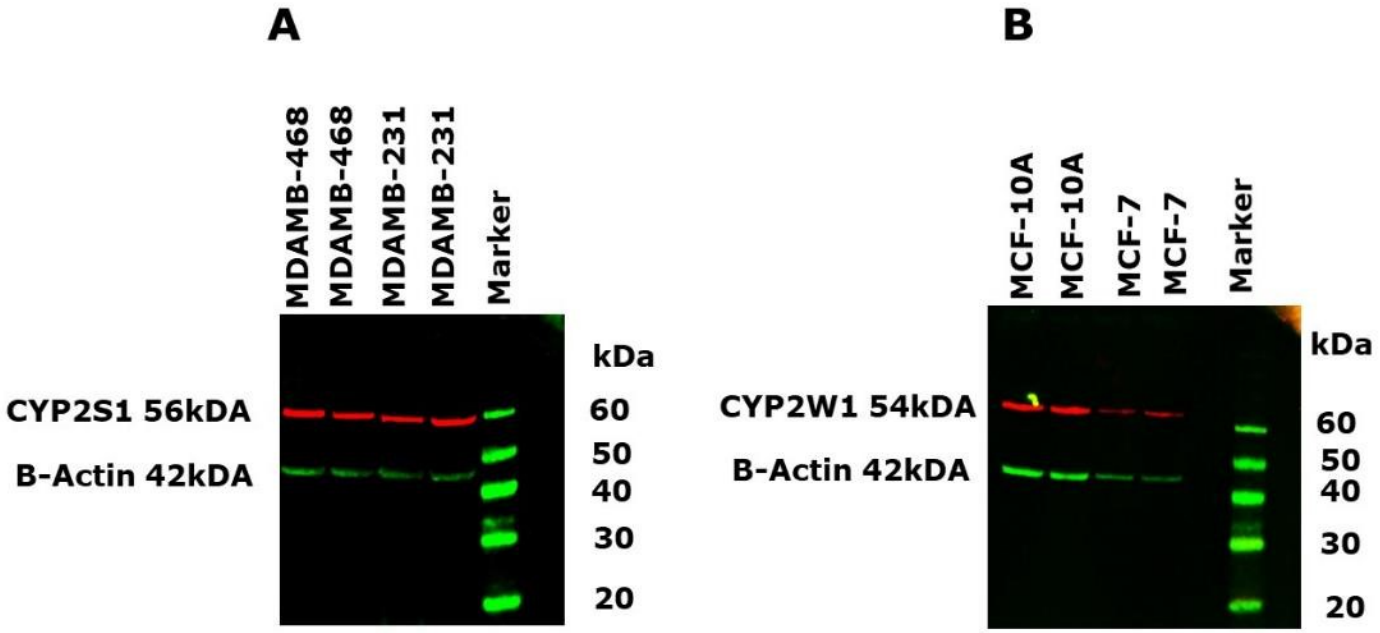


Figure D1 Representative Western blot images showing specific CYP2S1 and CYP2W1 expression in breast cancer cells. Breast cancer cell lysates were subjected to Western blot to assess specificity of (A) CYP2S1 and (B) CYP2W1 primary antibodies. Representative blots are of 3 independent experiments with lysates from cells with different passage numbers.

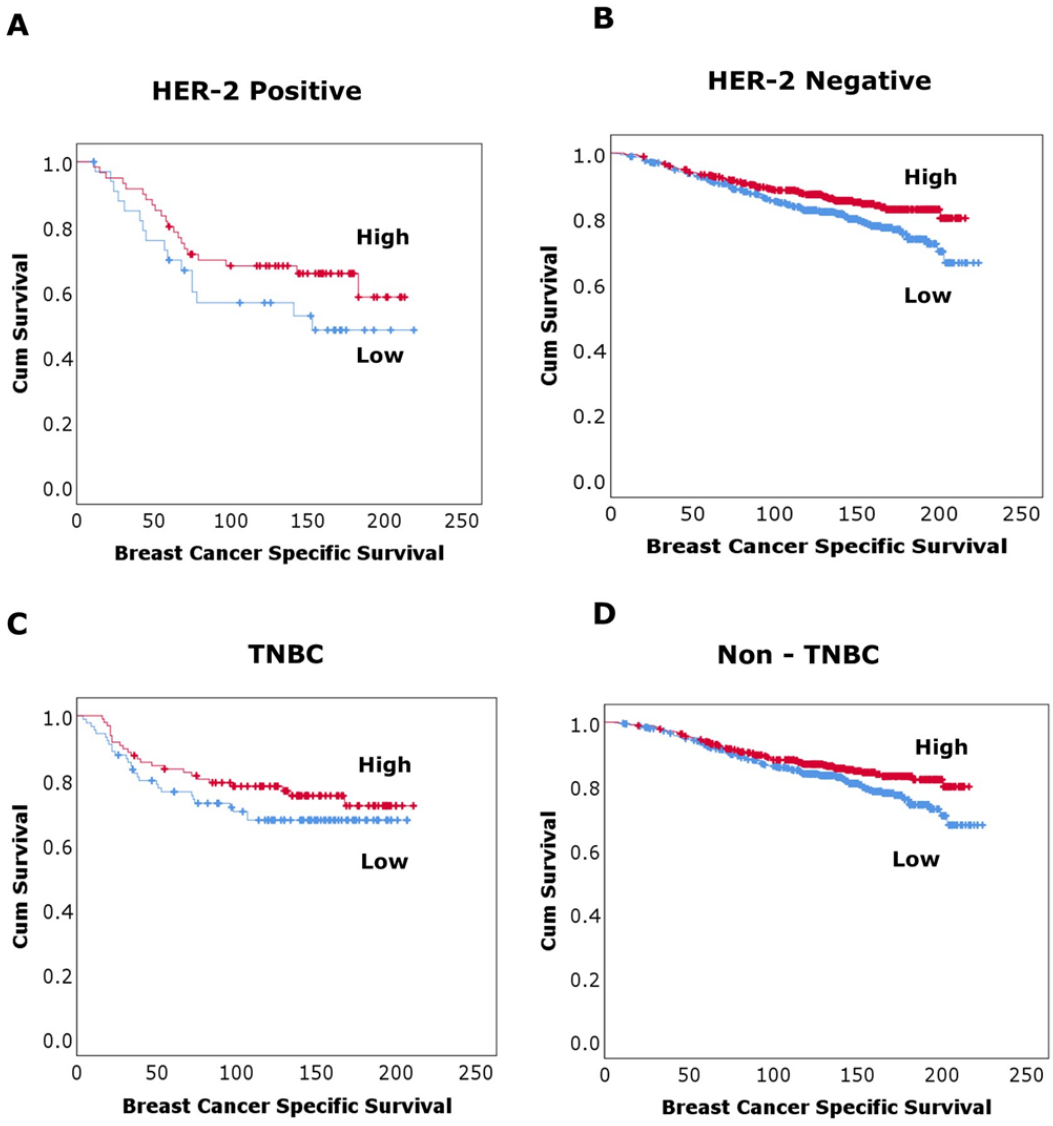


Figure D2 Kaplan-Meier survival curves of cytoplasmic CYP2S1 and breast cancer specific survival in (A) HER-2 positive (B) HER-2 negative (C) Triple negative and (D) Non-triple negative patients.

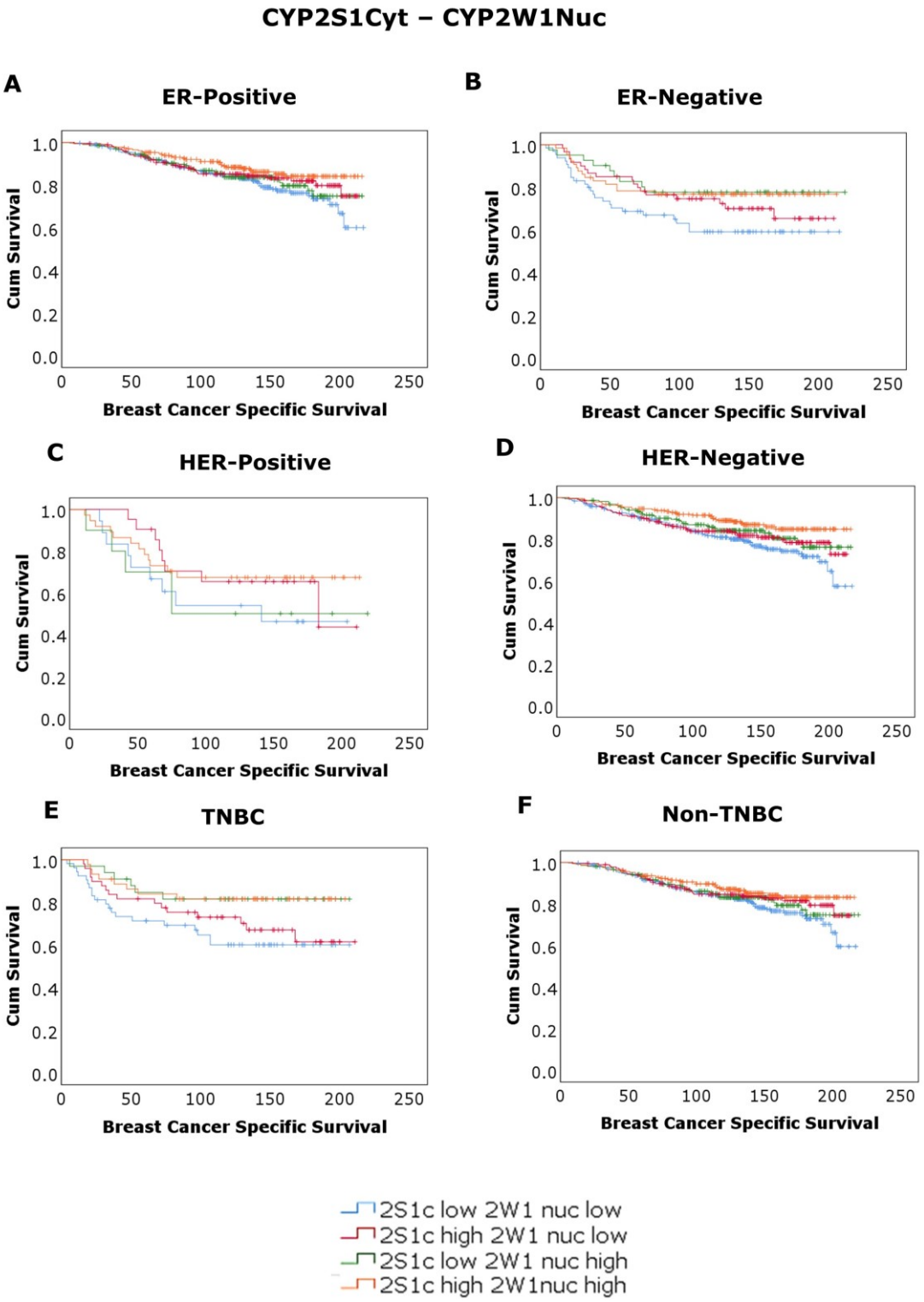


Figure D3 Kaplan-Meier survival curves of combined cytoplasmic CYP2S1/nuclear CYP2W1 and breast cancer specific survival in (A) ER-positive (B) ER-negative (C) HER-2 positive (D) HER-2 negative breast cancers (E) TNBC and (B) (F) Non-TNBC's.

Table D1 Correlation of CYP2S1 mRNA with clinicopathological parameters in the METABRIC cohort.

Clinicopathological parameters	CYP2S1 mRNA expression		
	Low	High	P-value
Grade			
1	167 (8.8%)	3 (0.2%)	0.062
2	733 (38.7%)	37 (2.0%)	
3	895 (47.3%)	57 (3.0%)	
Size			
<20cm	809 (41.4%)	49 (2.5%)	0.69
≥20cm	1037 (53.1%)	58 (3.0%)	
Nodal stage			
1	972 (49.3%)	63 (3.2%)	0.315
2	595 (30.2%)	27 (1.4%)	
3	299 (15.2%)	17 (0.9%)	
ER status			
Negative	442 (22.3%)	32 (1.6%)	0.137
Positive	1431 (72.3%)	75 (3.8%)	
PgR status			
Negative	873(44.1%)	67 (3.4%)	**0.001**
Positive	1000 (50.5%)	40 (2.0%)	
HER-2 status			
Negative	1628 (82.2%)	105 (5.3%)	**0.001**
Positive	245 (12.4%)	2 (0.1%)	
Pam50 subtype			
Basal	298 (15.1%)	31 (1.6%)	**0.009**
HER-2	226 (11.4%)	14 (0.7%)	
Luminal A	691 (34.9%)	27 (1.4%)	
Luminal B	461 (23.3%)	27 (1.4%)	
NC	6 (0.3%)	0	
Normal	191 (9.6%)	8 (0.4%)	

Abbreviations: ER, estrogen receptor; PgR, progesterone receptor; HER2, human epidermal growth factor receptor-2. The P values are resultant from the Pearson χ^2 test of association or Fisher's Exact test if a cell count was less than five. Significant *P*-values are indicated in bold. The number and percentage of observations for cohort is shown for each clinicopathological variable.

Table D2 Correlation of CYP2W1 mRNA with clinicopathological parameters in the METABRIC cohort.

Clinicopathological parameters	CYP2W1 mRNA expression		
	Low	High	P-value
Grade			
1	60 (5.2%)	51 (4.4%)	0.598
2	245 (21.1%)	221 (19.1%)	
3	291 (25.1%)	291 (25.1%)	
Size			
<20cm	294 (24.6%)	233 (19.5%)	**0.009**
≥20cm	321 (26.9%)	346 (29.0%)	
Nodal stage			
1	338 (28.0%)	298 (24.7%)	0.179
2	196 (16.3%)	180 (14.9%)	
3	88 (7.3%)	105 (8.7%)	
ER status			
Negative	139 (11.5%)	153 (12.6%)	0.136
Positive	484 (39.9%)	436 (36.0%)	
PgR status			
Negative	300 (24.8%)	295 (24.3%)	0.502
Positive	323 (26.7%)	294 (24.3%)	
HER-2 status			
Negative	540 (44.6%)	518 (42.7%)	0.508
Positive	83 (6.8%)	71 (5.9%)	
Pam50 subtype			
Basal	88 (7.3%)	112 (9.2%)	**0.02**
HER-2	94 (7.8%)	62 (5.1%)	
Luminal A	228 (18.8%)	198 (16.3%)	
Luminal B	149 (12.3%)	151 (13.1%)	
NC	1 (0.1%)	4 (0.3%)	
Normal	63 (5.2%)	54 (4.5%)	

Abbreviations: ER, estrogen receptor; PgR, progesterone receptor; HER2, human epidermal growth factor receptor-2. The P values are resultant from the Pearson χ^2 test of association or Fisher's Exact test if a cell count was less than five. Significant *P*-values are indicated in bold. The number and percentage of observations for cohort is shown for each clinicopathological variable.

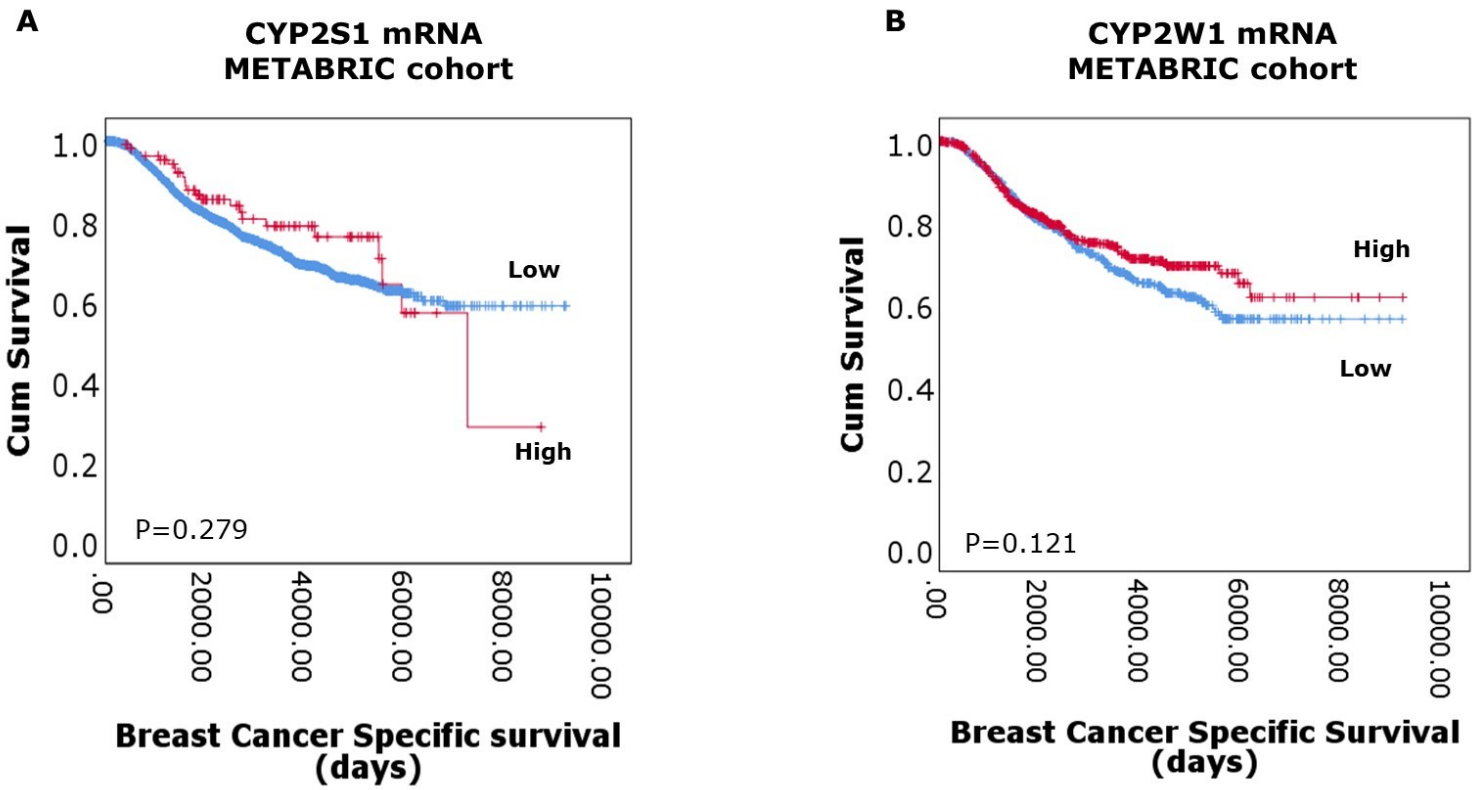


Figure D4 Kaplan-Meier analysis of CYP2S1 and CYP2W1 mRNA on breast cancer specific survival in the METABRIC cohort. Survival curves showing the impact of low (blue line) and high (red line) (A) CYP2S1 and (B) CYP2W1 expression on breast cancer specific survival. Significance was determined using the log-rank test. $P<0.05$ (not significant).